

**Defining the mechanisms of
multi-target tyrosine kinase
inhibitor resistance in
soft tissue sarcoma**



Mark L. Elms

A thesis submitted for the degree of
Doctor of Philosophy

The Institute of Cancer Research
University of London

Declaration

The work presented in this thesis was completed under the supervision of Dr. Paul Huang in the Molecular and Systems Oncology team at the Institute of Cancer Research, London, United Kingdom.

I, Mark Elms, confirm that the work presented within this thesis is my own. Information that has been derived from other sources is clearly indicated within the thesis.

Abstract

Soft tissue sarcomas (STS) are a rare, heterogeneous, and challenging group of cancers to treat effectively. The approval of pazopanib, as well as promising clinical trial data for a number of other multi-target tyrosine kinase inhibitors (TKI), has demonstrated that this family of drug could be employed in the effective treatment of a number of advanced STS subtypes. However, treatment of advanced STS patients with multi-target TKIs has been shown to universally result in drug resistance, either through an intrinsic resistance or an acquired resistance after an initial response. The mechanisms of multi-target TKI resistance in STS are currently poorly understood and, as a result, STS patients currently lack effective salvage therapies. There is therefore a clinically unmet need to better understand mechanisms of multi-target TKI resistance in STS. This increased knowledge will allow for the development of novel treatment strategies to combat the emergence of TKI resistance, as well as salvage therapies that could be employed to treat TKI-resistant disease.

In order to answer these questions, this project employed patient-derived xenograft (PDX)-derived STS cells as models of acquired and intrinsic pazopanib resistance and these were subjected to small molecule inhibitor screens. The multi-target TKI dasatinib was found to be an effective salvage therapy in pazopanib-resistant STS cells, mediated through inhibition of the Src signalling pathway. Building on this, I attempted to establish upstream mediators of Src signalling activity in Src-dependent, pazopanib-resistant STS and subsequently identified integrin signalling as a potential upstream regulator.

Additionally, I determined that the TKIs erdafitinib and ponatinib were effective in the first-line treatment of the A204 and G402 malignant rhabdoid tumour (MRT) cell lines characterised by co-activation of PDGFR α and FGFR1. Further to this, in A204 models harbouring multi-target TKI resistance towards pazopanib, regorafenib, sitravatinib, and anlotinib, erdafitinib and ponatinib were also found to be effective salvage therapies. Interestingly, the acquisition of sitravatinib resistance resulted in the emergence of collateral sensitivity to selective FGFR inhibition by infigratinib. Upon re-acquisition of resistance to infigratinib, I have also elucidated further-line strategies that can be utilised to control disease progression. Through these means, I have nominated a number of treatment strategies that could be employed in order to control disease progression and resistance in MRT, an aggressive paediatric STS subtype.

COVID-19 impact statement

The Institute of Cancer Research (ICR) laboratories were closed on 23/03/20. Following the government “Stay at Home” order, I met with my primary supervisor (Paul Huang) on 20/03/20 and planned to immediately stop experiments.

The initial lockdown resulted in having to cease all experiments, the majority of which were being undertaken in A204 and G402 resistant models that required long-term culturing before utilisation in experiments. Unfortunately, they had not yet reached the stage of utility and had to be discarded. There was therefore a need to re-derive A204 resistant cells (~2/3 months of work lost) post-lockdown whilst work on G402 resistant cells had to be postponed indefinitely due to time constraints.

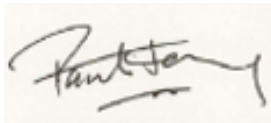
ICR laboratories were reopened on 08/06/20. Between 08/06/20 to 16/08/21, further disruption has occurred in terms of working shift-work due to social distancing rules, thereby limiting the number of personnel allowed within the laboratory and the ICR as a whole. The laboratory was operating at ~30% capacity due to shift work arrangements. Furthermore, the tissue culture laboratory was operating at ~25% capacity between June and July 2020. Rearrangement of the tissue culture laboratory increased capacity to ~50% from August 2020 onwards. These restrictions significantly impacted productivity.

Due to the initial laboratory closure and subsequent social distancing restrictions, a deadline extension was granted from 01/10/21 to 01/12/21.

Mark Elms

Mark Elms

Dr. Paul Huang

A handwritten signature in black ink on a light-colored background, appearing to read "Paul Huang".

Acknowledgements

I would firstly like to thank Dr. Paul Huang for giving me the opportunity to work and study within his lab at the ICR. His continuous support, expertise, and encouragement have been invaluable throughout the duration of my PhD.

Further to this, I would like to thank the entire Molecular and Systems Oncology team, both past and present, who have been extremely helpful in their advice and guidance throughout the project. Most importantly, they have been (and will continue to be) excellent friends, both inside and outside of work, and have made the lab a wonderfully nice and enjoyable place to work. I would especially like to thank Yiannis Assiotis, an honorary member of the lab, for his friendship, advice, and guidance throughout my time at the ICR.

Outside of work, I would like to thank all my friends that have helped support and encourage me during my time in London, especially Josh De Lyon, who has been my flatmate for the majority of my PhD.

Importantly, I would like to thank my parents, Mum and Darrell, for their unwavering support throughout my PhD and beyond. They have always been there for me throughout the good times and the (occasional) bad.

Finally, but by no means least, I would like to thank Lana Archer for sticking with me throughout the months of writing and re-writing, my moods following failed experiments, several months in quarantines and lockdowns, and her continuous support and encouragement.

Table of contents

Title page	1
Declaration	2
Abstract	2
COVID-19 impact statement	3
Acknowledgements	4
Table of contents	5
List of figures	8
List of tables and equations	10
Abbreviations and acronyms	12
1 Introduction	20
1.1 Sarcoma	21
1.1.1 Sarcoma overview	21
1.1.2 Soft tissue sarcoma	23
1.1.2.1 Epidemiology and aetiology	25
1.1.2.1.1 Viral aetiological factors	26
1.1.2.1.2 Genetic aetiological factors	27
1.1.2.1.3 Chemical and radiation aetiological factors	29
1.1.2.2 Classifications of soft tissue sarcomas	30
1.1.2.2.1 “Simple” soft tissue sarcomas	33
1.1.2.2.2 “Complex” soft tissue sarcomas	37
1.2 Receptor tyrosine kinase signalling	38
1.2.1 Mitogen-activated protein kinase signalling	43
1.2.2 Phosphoinositide 3-kinase/Akt signalling	44
1.2.3 Src signalling	46
1.2.4 RTK-associated signalling cascade crosstalk	47
1.2.5 RTK signalling in cancer	48
1.2.6 Targeting RTKs for cancer therapy with tyrosine kinase inhibitors	51
1.3 Cancer therapeutics in soft tissue sarcoma	53
1.3.1 Chemotherapeutic landscape in soft tissue sarcoma	53
1.3.2 Current perspectives of targeted therapies in soft tissue sarcoma	55
1.3.3 Multi-target tyrosine kinase inhibitors in soft tissue sarcoma	61

1.3.3.1	Preclinical characterisation of multi-target tyrosine kinase inhibitors	64
1.3.3.2	Pazopanib	65
1.3.3.2.1	Preclinical characterisation of pazopanib in soft tissue sarcoma	66
1.3.3.2.2	Clinical evaluation of pazopanib in soft tissue sarcoma	67
1.3.3.3	Regorafenib	76
1.3.3.4	Sitravatinib	79
1.3.3.5	Anlotinib	81
1.3.3.6	Landscape of multi-target tyrosine kinase inhibitors in soft tissue sarcoma	86
1.3.3.7	Tyrosine kinase inhibitor resistance mechanisms in cancer	92
1.3.3.7.1	Current literature of multi-target TKI resistance specific to non-GIST soft tissue sarcoma	96
1.3.3.7.1.1	Acquired multi-target TKI resistance in soft tissue sarcoma	96
1.3.3.7.1.2	Intrinsic multi-target TKI resistance in soft tissue sarcoma	97
1.4	Hypothesis and aims	98
2	Materials and methods	100
2.1	Mammalian cell culture and phenotypic assays	101
2.1.1	Cell culture and derivation of acquired resistance sublines	101
2.1.2	Cell viability assay	103
2.1.3	Temporal (27 day) cell viability assay	103
2.1.4	Apoptosis assay	104
2.1.5	Small molecule inhibitor screen	104
2.1.6	Tyrosine kinase inhibitor sequential treatment assay	105
2.1.7	Growth curve assay	107
2.1.8	Colony formation assay	107
2.1.9	Xenograft assay	107
2.2	Molecular biology techniques	108
2.2.1	Retroviral plasmid production and transduction	108
2.2.2	Quantitative polymerase chain reaction	110
2.2.3	SS18-SSX fusion polymerase chain reaction	111
2.2.4	Short tandem repeat analysis	112
2.3	Protein analysis techniques	113
2.3.1	Immunoblotting	113
2.3.2	Temporal (27 day) immunoblotting	114
2.3.3	Temporal (14 day) immunoblotting	115
2.3.4	Phospho-receptor tyrosine kinase array	115
2.3.5	Mass spectrometry	116
3	Pazopanib-resistant soft tissue sarcomas are vulnerable to targeting of the Src pathway	119
3.1	Introduction	120
3.2	Results	121
3.2.1	Generation of PDX-derived cell models of soft tissue sarcoma	121

3.2.2	SARC-209 and J000104314 PDX-derived cell models are resistant to pazopanib <i>in vitro</i>	125
3.2.3	A small molecule inhibitor screen identifies dasatinib as an effective salvage therapy for pazopanib-resistant soft tissue sarcomas	126
3.2.4	Pazopanib-resistant soft tissue sarcomas are sensitive to inhibition of the Src pathway by dasatinib	129
3.3	Discussion	138
4	Understanding the mechanistic basis of Src dependency in pazopanib-resistant soft tissue sarcoma	142
4.1	Introduction	143
4.2	Results	144
4.2.1	IL-8 signalling does not confer pazopanib resistance through autocrine signalling in soft tissue sarcoma models of pazopanib resistance	144
4.2.2	IL-8 stimulation does not affect Src pathway activity in pazopanib-resistant soft tissue sarcoma	150
4.2.3	Integrin signalling is a potential upstream receptor of Src signalling in pazopanib-resistant soft tissue sarcoma	151
4.3	Discussion	156
5	Characterisation of multi-target tyrosine kinase inhibitor sensitivity in cell line models of soft tissue sarcoma	161
5.1	Introduction	162
5.2	Results	163
5.2.1	The malignant rhabdoid tumour cell lines A204 and G402 are sensitive to multi-target tyrosine kinase inhibitors	163
5.2.2	Multi-target tyrosine kinase inhibitors have antiproliferative and pro-apoptotic activity in malignant rhabdoid tumour cell line models	166
5.2.3	Evaluation of combination therapy with multi-target TKIs	170
5.2.4	Multi-target TKIs potently reduce Akt phosphorylation in malignant rhabdoid tumour cell line models	172
5.2.5	Investigation into combinatorial multi-target TKI plus FGFR inhibitor treatment strategies to provide enhanced antitumour activity	173
5.2.6	Treatment of malignant rhabdoid tumour cells with first-line erdafitinib, ponatinib, or combination therapy suppresses the emergence of drug resistance	182
5.3	Discussion	183
6	Determination of effective salvage therapy regimens for multi-target TKI-resistant malignant rhabdoid tumour	190
6.1	Introduction	191
6.2	Results	193
6.2.1	Derivation of multi-target TKI acquired resistance in the A204 cell line	193
6.2.2	Multi-target TKI-resistant A204 cells harbour reduced PDGFR α expression and Akt signalling activity	198
6.2.3	Proteomic analysis of A204 TKI-resistant sublines reveal common alterations correlated with multi-target TKI resistance	199
6.2.4	A small molecule inhibitor screen identifies salvage therapies for TKI-resistant malignant rhabdoid tumour	204
6.2.5	Confirmation of erdafitinib and ponatinib activity in multi-target TKI-resistant A204 sublines	209
6.2.6	Assessment of infigratinib collateral sensitivity in multi-target TKI-resistant A204 sublines	213
6.2.7	Determining the reproducibility and characteristics of selective infigratinib collateral sensitivity	215

6.2.8 Investigation into the causal factors of selective infigratinib collateral sensitivity in sitravatinib-resistant cells	221
6.2.9 Sitravatinib pre-treated A204 cells and the A204SitR subline re-acquire resistance to infigratinib following longer-term and chronic infigratinib exposure	226
6.2.10 Second-line treatment with erdafitinib and ponatinib suppresses cellular proliferation following progression on first-line multi-target TKI treatment	227
6.3 Discussion	230
7 Discussion	237
7.1 Introduction	238
7.2 Outstanding challenges for increasing the efficacy of multi-target TKI therapy in soft tissue sarcoma	238
7.2.1 Predictive biomarkers of multi-target TKI response in soft tissue sarcoma	239
7.2.2 Intratumoural heterogeneity and liquid biopsies	242
7.3 Emerging therapies for the treatment of soft tissue sarcoma	246
7.3.1 Adaptive sequential therapy and collateral sensitivity	246
7.3.2 Immunotherapy	251
7.3.2.1 Vaccine therapy	256
7.3.2.2 Adoptive T cell immunotherapy	257
7.3.2.2.1 T cell receptor therapy	258
7.3.2.2.2 Chimeric antigen receptor T cell therapy	259
7.3.2.3 Immunotherapy and IL-8 signalling	260
7.3.3 Personalised medicine and MULTISARC	262
7.4 Concluding remarks and future directions	264
8 Appendix	270
9 References	277

List of figures

- 1.1 Incidence of sarcomas in adult and paediatric malignancies per annum.
- 1.2 Mesenchymal cell differentiation and associated sarcomas.
- 1.3 Dendrogram of STS subtypes based on cell lineage.
- 1.4 Spectrum of genetic characteristics and complexity in STS.
- 1.5 Examples of genetically “simple” STS subtypes.
- 1.6 Canonical RTK activation and signalling.
- 1.7 Prototypical RTK kinase domain architecture.
- 1.8 Recommended treatment paradigms for advanced STS.
- 1.9 Kinase selectivity maps.
- 1.10 Skeletal formula structure of pazopanib.
- 1.11 Skeletal formula structure of regorafenib.
- 1.12 Skeletal formula structure of sitravatinib.
- 1.13 Skeletal formula structure of anlotinib.

- 3.1 Generation of SARC-209 and J000104314 PDX-derived cell models.
- 3.2 Patient clinical history and histopathological evaluation of STS subtypes.
- 3.3 Molecular diagnosis of synovial sarcoma in the J000104314 PDX-derived cell model.
- 3.4 Cell viability assays to determine pazopanib sensitivity in SARC-209 and J000104314 PDX-derived cell models.
- 3.5 Small molecule inhibitor screens of SARC-209 and J000104314 PDX-derived cell models
- 3.6 Analysis of small molecule inhibitor screens of SARC-209 and J000104314 PDX-derived cell models.
- 3.7 Cell viability and colony formation assays of SARC-209 and J000104314 PDX-derived cell models treated with pazopanib and dasatinib.
- 3.8 Apoptosis assays of SARC-209 and J000104314 PDX-derived cell models treated with pazopanib and dasatinib.
- 3.9 Immunoblots of SARC-209 and J000104314 PDX-derived cell models treated with pazopanib and dasatinib.
- 3.10 Generation of Src construct-expressing SARC-209 cells.
- 3.11 Src^{T338I} expression rescues the phenotype of dasatinib sensitivity in SARC-209 cells.
- 3.12 Src^{K295M} expression reduces the proliferation of SARC-209 cells.
- 3.13 *In vivo* evaluation of dasatinib in mouse xenograft models of STS.
- 4.1 Clinical history of a STS patient with acquired pazopanib resistance and significant gene expression changes between biopsies.
- 4.2 *CXCL8* (IL-8) expression levels in a panel of sarcoma cell lines and PDX-derived models.
- 4.3 Generation of *CXCR1*- and *CXCR2*-expressing SARC-209 cells.
- 4.4 *CXCR1* and *CXCR2* expression levels in a panel of sarcoma cell lines and PDX-derived models.
- 4.5 Immunoblot of exogenous IL-8 stimulation of SARC-209 *CXCR1*- and *CXCR2*-expressing cells.
- 4.6 The integrin inhibitor cilengitide trifluoroacetate decreases Src phosphorylation.
- 4.7 Evaluating the expression of a panel of integrin subunits in pazopanib-resistant STS models.
- 5.1 Cell viability assays of a panel of sarcoma cell lines to determine sensitivities to pazopanib, regorafenib, sitravatinib, and anlotinib.
- 5.2 Statistical significance grids of the sarcoma cell line panel evaluating sensitivity to pazopanib, regorafenib, sitravatinib, and anlotinib.
- 5.3 Evaluation of PDGFR α and FGFR1 expression levels in the sarcoma cell line panel.
- 5.4 Evaluation of long-term sensitivity of A204 and G402 cells to pazopanib, regorafenib, sitravatinib, and anlotinib treatment.
- 5.5 Evaluation of A204 and G402 proliferation in response to treatment by pazopanib, regorafenib, sitravatinib, and anlotinib for 6 weeks.
- 5.6 Evaluation of apoptosis levels in A204 and G402 cells in response to treatment by pazopanib, regorafenib, sitravatinib, and anlotinib.
- 5.7 Cell viability assays evaluating the combinatorial effect of pazopanib, regorafenib, sitravatinib, and anlotinib dual treatment in A204 and G402 cells.
- 5.8 Immunoblots of A204 and G402 cells treated with two concentrations of pazopanib, regorafenib, sitravatinib, and anlotinib.
- 5.9 Cell viability assays evaluating the synergistic, combinatorial effect of multi-target TKI plus FGFR inhibitor treatment in A204 and G402 cells.
- 5.10 Assays evaluating changes in apoptosis levels in A204 and G402 cells upon combination therapy of multi-target TKIs plus FGFR inhibitors.
- 5.11 Apoptosis assays evaluating the pro-apoptotic effects of ponatinib therapy in A204 and G402 cells.
- 5.12 Immunoblots of A204 and G402 cells treated with monotherapies or dual therapies to assess for dual Akt and ERK1/2 signalling blockade.
- 5.13 Erdafitinib, ponatinib, and combination therapies suppress the growth of TKI-resistant cells in the first-line setting.
- 5.14 Hypothesised mechanism of action of the discussed TKIs in MRT cell line models.

- 6.1 Schematic outlining the experimental process of deriving acquired multi-target TKI resistant sublines from the sensitive, parental A204 cells.
- 6.2 Confirmation of multi-target TKI acquired resistance in derived A204 TKI-resistant sublines.
- 6.3 Evaluation of cross-resistance in the A204 multi-target TKI-resistant sublines.
- 6.4 Immunoblots of A204 parental and TKI-resistant sublines to evaluate PDGFR α and FGFR1 expression and downstream effector phosphorylation profiles.
- 6.5 Heatmap of global proteomic analysis of A204 parental cells and TKI-resistant sublines.
- 6.6 Pearson's correlation of proteomic A204 parental and TKI-resistant subline biological replicates.
- 6.7 Heatmap of proteins found to be differentially expressed in multi-target TKI-resistant sublines compared to A204 parental cells.
- 6.8 Small molecule inhibitor screens of parental A204 cells and TKI-resistant sublines.
- 6.9 Confirmation of A204 multi-target TKI-resistant subline sensitivities to erdafitinib and ponatinib.
- 6.10 Apoptotic and signalling modulations in response to erdafitinib and ponatinib treatment of A204 TKI-resistant sublines.
- 6.11 Evaluation of infigratinib activity in A204 TKI-resistant sublines.
- 6.12 Schematic outlining methodology for sequential TKI treatment experiments.
- 6.13 Growth curve assays evaluating infigratinib as a second-line therapy in multi-target TKI pre-treated A204 cells.
- 6.14 Immunoblot of A204 cells pre-treated with either DMSO or sitravatinib.
- 6.15 Temporal assessment of infigratinib collateral sensitivity in A204 sitravatinib pre-treated cells.
- 6.16 *FGFR1/3/4* and *PDGFRA* expression levels in A204 parental and TKI-resistant sublines.
- 6.17 Schematic outlining the experimental protocol employed for the phospho-RTK array.
- 6.18 Phospho-RTK antibody array of DMSO or sitravatinib pre-treated cells.
- 6.19 Collateral sensitivity to infigratinib is temporary and cells re-acquire resistance after prolonged exposure.
- 6.20 Erdafitinib is an effective second-line therapy in controlling cell growth of A204SitR and sitravatinib pre-treated A204 cells
- 6.21 Second-line treatment with erdafitinib and ponatinib suppresses cellular proliferation following progression on first-line multi-target TKI treatment.
- 6.22 Drug cycling and sequential strategies to control disease progression through the targeting of collateral sensitivities.
- 6.23 Nominated sequential treatment strategies outlined in Chapter 6 as effective long-term treatment regimens for disease control in MRT, and potentially other STS driven by PDGFR and FGFR signalling.
- 7.1 Candidate model of Src activity within the SARC-209 pazopanib-resistant STS model.
- 7.2 Candidate model of multi-target TKI resistance in the A204 TKI-resistant sublines.
- S1 Genomic sequencing results of SARC-209 *CXCR1*-expressing cells.
- S2 Genomic sequencing results of SARC-209 *CXCR2*-expressing cells.

List of tables and equations

- 1.1 Examples of STS subtypes with subtype-associated, recurrent genetic aberrations and oncogenic consequences.
- 1.2 Currently approved targeted therapies for use in STS with given clinical indications and molecular targets.
- 1.3 Selectivity profiles of commonly targeted tyrosine kinases by multi-target TKIs that are currently undergoing clinical evaluation in STS, with either known or proposed binding mode type.
- 1.4 Clinical evaluations of pazopanib activity in non-GIST STS.
- 1.5 Clinical evaluations of regorafenib, sitravatinib, and anlotinib activity in non-GIST STS.

- 1.6 Notable clinical evaluations of other multi-target TKIs in non-GIST STS.
- 2.1 Small molecule inhibitors utilised within the small molecule inhibitor screens with primary target(s) and supplier.
- 2.2 Protocol schedule for 6-week TKI sequential treatment assay.
- 2.3 Plasmids utilised for retroviral transductions with Addgene repository plasmid identifiers.
- 2.4 Site-directed mutagenesis and cloning primers.
- 2.5 qPCR primers and conditions.
- 2.6 SS18-SSX fusion PCR primers and conditions.
- 2.7 Primary and secondary antibodies utilised for immunoblotting with associated dilutions.
- 3.1 STR analysis of the SARC-209 PDX-derived cell model.
- 4.1 Panel of 14 sarcoma cell lines with subtype, Cellosaurus accession codes, and additional comments.
- 4.2 Reference table displaying small molecule inhibitors utilised within the Src phosphorylation screen with primary target(s) and rationale for inclusion.
- 4.3 Panel of assessed integrin subunits.
- 5.1 Panel of 14 sarcoma cell lines that were subjected to cell viability assays with pazopanib, regorafenib, sitravatinib, and anlotinib.
- 5.2 A204 and G402 cells treated with combinations of the TKIs pazopanib (Paz), regorafenib (Reg), sitravatinib (Sit), anlotinib (Anlo), infigratinib (Inf), and erdafitinib (Erda), with associated combination indices.
- 5.3 A204 and G402 cells treated with combinations of the TKIs pazopanib (Paz), regorafenib (Reg), sitravatinib (Sit), anlotinib (Anlo), infigratinib (Inf), erdafitinib (Erda) and ponatinib, with associated IC₅₀ values (µM)
- 6.1 Differentially expressed proteins in TKI-resistant sublines compared to parental cells, with protein names, general function, and gene ontology annotations.
- 6.2 Small molecule inhibitors utilised within the A204 parental and TKI-resistant subline screens.
- 7.1 Immune checkpoint inhibitor regimens currently undergoing clinical evaluation in STS.
- 7.2 Treatment paradigms employed in the MULTISARC trial based on targetable genomic alterations determined via NGS.
- S1 A204, SARC-209, and J000104314 cells treated with pazopanib (Paz), with associated IC₅₀ (µM).
- S2 Inhibitors with ≤ 60% cell viability (compared to DMSO control) in small molecule inhibitor screens of SARC-209 and J000104314 cells.
- S3 SARC-209 and J000104314 cells treated with the TKIs pazopanib (Paz) and dasatinib (Das), with associated IC₅₀ values (µM).
- S4 EV, Src^{WT}, and Src^{T338I} cells treated with dasatinib (Das), with associated IC₅₀ values (µM).
- S5 Panel of 14 sarcoma cell lines treated with the TKIs pazopanib (Paz), regorafenib (Reg), sitravatinib (Sit), and anlotinib (Anlo), with associated IC₅₀ values (µM).
- S6 A204 and G402 cells treated with combinations of the TKIs pazopanib (Paz), regorafenib (Reg), sitravatinib (Sit), and anlotinib (Anlo), with associated IC₅₀ values (µM).
- S7 A204 and G402 cells treated with combinations of the TKIs pazopanib (Paz), regorafenib (Reg), sitravatinib (Sit), anlotinib (Anlo), infigratinib (Inf), erdafitinib (Erda), and ponatinib (Pon), with associated IC₅₀ values (µM).
- S8 A204 parental cells and TKI-resistant sublines treated with the TKIs pazopanib (Paz), regorafenib (Reg), sitravatinib (Sit), or anlotinib (Anlo), with associated IC₅₀ values (µM).
- S9 A204 parental cells and TKI-resistant sublines treated with the TKIs pazopanib (Paz), regorafenib (Reg), sitravatinib (Sit), and anlotinib (Anlo) to assess cross-resistance, with associated IC₅₀ values (µM).
- S10 Inhibitors with ≤ 60% cell viability (compared to DMSO control) in small molecule inhibitor screens of A204 and A204 TKI-resistant sublines.
- S11 A204 TKI-resistant sublines treated with combinations of the TKIs pazopanib (Paz), regorafenib (Reg), sitravatinib (Sit), anlotinib (Anlo), erdafitinib (Erda) and ponatinib (Pon), with associated IC₅₀ values (µM).
- S12 A204 parental cells and TKI-resistant sublines treated with infigratinib (Inf), with associated IC₅₀ values (µM).
- E1 Combination index calculation.

Abbreviations and acronyms

ACTB	β-actin
ADP	Adenosine diphosphate
Adv	Advanced
AGC	Protein kinases A, G, and C
AIDS	Acquired immune deficiency syndrome
ALK	Anaplastic lymphoma kinase
AMEL	Amelogenin
Anlo	Anlotinib
ANOVA	Analysis of variance
aRMS	Alveolar rhabdomyosarcoma
AS	Angiosarcoma
ASPA	Animals (Scientific Procedures) Act 1986
ASPS	Alveolar soft part sarcoma
ATCC	American Type Culture Collection
ATP(ase)	Adenosine triphosphate (hydrolase)
BCA	Bicinchoninic acid
Bcl-(2/6/xL)	B-cell lymphoma (2/6/xL) protein
Bcl-w	Bcl-2-like protein 2
BCOR	Bcl-6 corepressor
Bcr	Breakpoint cluster region protein
BD	Bis die
BET	Bromo- and extra-terminal domain
bNGF	Basic nerve growth factor
bp	Base pairs
BSA	Bovine serum albumin
BSU	Biological services unit
Bx	Biopsy
CAMK	Ca ²⁺ /calmodulin-dependent protein kinase
CAR-T	Chimeric antigen receptor T
CBR	Clinical benefit rate
CCS	Clear cell sarcoma
CDK(4/6)	Cyclin-dependent kinase (4/6)

CDKN2A	Cyclin-dependent kinase inhibitor 2A
cDNA	Complementary DNA
Chk1	Checkpoint kinase 1
CI	Confidence interval
CIC	Capicua transcriptional repressor
CK(1/2)	Casein kinase (1/2)
CMGC	Cyclin-dependent kinase, mitogen-activated protein kinase, glycogen synthase kinase, and cyclin-dependent-kinase-like kinase
CNS	Central nervous system
CO ₂	Carbon dioxide
COL1A1	Collagen type I α 1 chain
COL6A3	Collage type VI α 3 chain
CR	Complete response
CRISPR	Clustered regularly interspaced short palindromic repeats
CRL4	Cullin 4 ring E3 ubiquitin ligase complex
CSF1PO	Colony stimulating factor 1 receptor proto-oncogene
CSF1(R)	Colony stimulating factor 1 (receptor)
Ct	Cycle threshold
CT	Computerised tomography
CTC	Circulating tumour cell
ctDNA/RNA	Circulating tumour DNA/RNA
C-terminal	Carboxyl-terminal
CTLA-4	Cytotoxic T-lymphocyte-associated protein 4
CTNNB1	β -catenin
CXCL8	Chemokine C-X-C motif ligand 8
CXCR(1/2)	C-X-C motif chemokine receptor (1/2)
CVCL	Cellosaurus accession code
CYP450	Cytochrome P450
Dac	Dacarbazine
Das	Dasatinib
DCR	Disease control rate
DDLPS	Dedifferentiated liposarcoma
DDR2	Discoidin domain receptor 2
DFG	Asp-Phe-Gly
DFSP	Dermatofibrosarcoma protuberans
DMEM	Dulbecco's modified Eagle medium

DMSO	Dimethyl sulfoxide
DNA	Deoxyribonucleic acid
DNase	Deoxyribonuclease
Dox	Doxorubicin
DSRCT	Desmoplastic small round cell tumour
DT	Desmoid tumour
DUSP6	Dual specificity phosphate 6
EBV	Epstein-Barr virus
ECM	Extracellular matrix
EDTA	Ethylenediaminetetraacetic acid
EGF(R)	Epidermal growth factor (receptor)
EHE	Epithelioid haemangioendothelioma
EORTC	European Organisation for Research and Treatment of Cancer
Eph(A2/4/7)	Ephrin (A2/4/7)
ER	Endoplasmic reticulum
Erda	Erdafitinib
ERK(1/2)	Extracellular signal-regulated kinase (1/2)
eRMS	Embryonal rhabdomyosarcoma
ES	Epithelioid sarcoma
ESMC	Extraskelatal myxoid chondrosarcoma
ETS	E26 transformation-specific
EV	Empty vector
EWSR1	Ewing RNA binding protein 1
EZH2	Enhancer of zeste homolog 2
FAK	Focal adhesion kinase
FBS	Foetal bovine serum
FDA	Food and Drug Administration
FDG-PET CT	Fluorodeoxyglucose (¹⁸ F)-positron emission tomography computerised tomography
FDR	False discovery rate
FGA	Fibrinogen α chain
FGF(R)(1/2/3/4)	Fibroblast growth factor (receptor) (1/2/3/4)
FGFRI	Fibroblast growth factor receptor inhibitor
FOXO	Forkhead box O
FRS2	Fibroblast growth factor receptor substrate 2
GAB1	GRB2-associated-binding protein 1

GAP	GTPase-activating proteins
GDP	Guanosine diphosphate
GEF	Guanine nucleotide-exchange factor
Gem	Gemcitabine
GIMP	GNU image manipulation program
GIST	Gastrointestinal stromal tumour
GPCR	G-protein coupled receptor
GRB2	Growth factor receptor-bound protein 2
GSK3	Glycogen synthase kinase 3
GTP(ase)	Guanosine triphosphate (hydrolase)
H & E	Haematoxylin & eosin
HAART	Highly active antiretroviral therapy
HDAC	Histone deacetylase
HEPES	4-(2-hydroxyethyl)-1-piperazineethanesulfonic acid
HER(2/3)	Human epidermal growth factor receptor 2
HGF	Hepatocyte growth factor
HHV8	Human herpesvirus 8
HIF	Hypoxia inducible factor
HIV	Human immunodeficiency virus
HMVEC	Human microvascular endothelial cell
HR	Hazard ratio
HRP	Horseradish peroxidase
Hsp90	Heat shock protein 90
HUVEC	Human umbilical vein endothelial cell
IACR	International Association of Cancer Registries
IC ₅₀	Inhibitory constant
ICAM-1	Intercellular adhesion molecule 1
ICI	Immune checkpoint inhibitor
ICR	Institute of Cancer Research
IGF1R	Insulin-like growth factor 1 receptor
IKK(1/2)	IκB kinase (1/2)
IL-(2(ra)/6/8/12p40)	Interleukin-(2(receptor α)/6/8/12 subunit p40)
IMT	Inflammatory myofibroblastic tumour
Inf	Infigratinib
InsR	Insulin receptor
Inv	Inversion

IRS(1/2/3/4)	Insulin receptor substrates (1/2/3/4)
ITG(A2/3/6/7/10/V)(B1/3/4)	Integrin (α 2/3/6/7/10/V)(β 1/3/4)
JAK(1/2)	Janus kinase (1/2)
JNK(1/2/3)	c-Jun N-terminal kinase (1/2/3)
K _d	Dissociation constant
LAG3	Lymphocyte-activation gene 3
LFS	Li-Fraumeni syndrome
LIF	Leukaemia inhibitory factor
LMB	Leiomyoblastoma
LMS	Leiomyosarcoma
LPS	Liposarcoma
MACS	Magnetic-activated cell sorting
MAPK	Mitogen-activated protein kinase
MEK	Mitogen-activated protein kinase kinase
MHC	Major histocompatibility complex
miRNA	MicroRNA
MLPS	Myxoid liposarcoma
(m)OS	(Median) overall survival
MPC3	Mitochondrial pyruvate carrier 3
(m)PFS	(Median) progression-free survival
MPNST	Malignant peripheral nerve sheath tumour
mRNA	Messenger RNA
MRT	Malignant rhabdoid tumour
MSC	Mesenchymal stem cells
MSKCC	Memorial Sloan Kettering Cancer Center
mTOR	Mechanistic target of rapamycin
n/a	Not available
NCT	National Clinical Trial
NF-1	Neurofibromatosis type 1
NF1	Neurofibromin 1
NGS	Next-generation sequencing
NHS	National Health Service
NOS	Not otherwise specified
NSCLC	Non-small cell lung cancer
N-terminal	Amino-terminal
NTRK(1/2/3)	Neurotrophic tyrosine kinase receptor (1/2/3)

OD	Omni die (once daily)
ORR	Objective/overall response rate
OSR	Overall survival rate
p	p (short) arm of chromosome
P(0/1)	Passage number (0/1)
PARP	Poly (ADP-ribose) polymerase
Paz	Pazopanib
PBS	Phosphate-buffered saline
PCR	Polymerase chain reaction
PD	Progressive disease
PD-1	Programmed cell death protein 1
PDGF(R)((A/α)/(B/β))	Platelet-derived growth factor (receptor) (α/β)
PD-L1	Programmed death-ligand 1
PDPK1	Phosphoinositide-dependent protein kinase 1
PDX	Patient-derived xenograft
PEComa	Perivascular epithelioid cell sarcoma
PFR	Progression-free rate
PI3K	Phosphoinositide 3-kinase
PIK3CA	Phosphoinositide 3-kinase, catalytic, α polypeptide
PIP ₂	Phosphatidylinositol (4,5)-biphosphate
PIP ₃	Phosphatidylinositol (3,4,5)-triphosphate
PLK1	Polo-like kinase 1
PMID	PubMed Identifier
PNET	Primitive neuroectodermal tumour
PNS	Peripheral nerve system
p.o.	Per os (by mouth)
Pon	Ponatinib
PR	Partial response
PRC2	Polycomb repressive complex 2
PRSA	Pazopanib, regorafenib, sitravatinib, and anlotinib
P/R/S/A	Pazopanib, regorafenib, sitravatinib, or anlotinib
PT	Previously treated with
PTB	Phosphotyrosine-binding
PTEN	Phosphatase and tensin homolog
PTK2B	Protein tyrosine kinase 2β
PTPN11	Phosphatase non-receptor type 11

PVDF	Polyvinylidene fluoride
q	q (long) arm of chromosome
qPCR	Quantitative polymerase chain reaction
Raf	Rapidly accelerated fibrosarcoma
Ras	Rat sarcoma
RB1	Retinoblastoma protein 1
RBC	Red blood cell
RCOG	Royal College of Obstetricians and Gynaecologists
RECIST	Response evaluation criteria in solid tumours
Reg	Regorafenib
RET	Rearranged during transfection
RGC	Receptor guanylate cyclase
RIP	Rest in peace
RIPA	Radioimmunoprecipitation assay
Rn	Reporter signal
RNA	Ribonucleic acid
RNase	Ribonuclease
RPMI	Roswell Park Memorial Institute
RRID	Research Resource Identifiers
RTK(I)	Receptor tyrosine kinase (inhibitor)
SAM	Significance analysis of microarrays
S.D.	Standard deviation
SCF	Stem cell factor
SD	Stable disease
SDH(A/B/C/D)	Succinate dehydrogenase (A/B/C/D)
SDS	Sodium dodecyl sulfate
SFT	Solitary fibrous tumour
SH(1/2/3/4)	Src homology (1/2/3/4)
SHC	Src homology 2 domain-containing
SHH	Sonic hedgehog
shRNA	Short hairpin RNA
siRNA	Small interfering RNA
Sit	Sitravatinib
SMARCB1	SWI/SNF-related matrix-associated actin-dependent regulator of chromatin subfamily B member 1
SNS	Sympathetic nervous system
SOS	Son of sevenless

Src ^{K295M}	Dominant-negative Src
Src ^{T338I}	Dasatinib-resistant Src
Src ^{WT}	Wild-type Src
SS	Synovial sarcoma
SS18	Synovial sarcoma translocation, chromosome 18
SSX1/2/4	Synovial sarcoma X 1/2/4 breakpoint proteins
STAT(3)	Signal transducer and activator of transcription (3)
STE	Sterile kinase
STR	Short tandem repeats
STS	Soft tissue sarcoma
SWI/SNF	Switch/sucrose non-fermentable
t	Translocation
TBS(T)	Tris-buffered saline (with 0.1% Tween 20)
TCR	T cell receptor
TGCT	Tenosynovial giant cell tumour
TGF(α/β)(R)(1)	Transforming growth factor (α/β)(receptor)(1)
TH01	Tyrosine hydroxylase intron 1
TK(D)	Tyrosine kinase (domain)
TKI	Tyrosine kinase inhibitor
TKL	Tyrosine kinase-like
TLS	Tertiary lymphoid structure
TME	Tumour microenvironment
TMT	Tandem mass tag
TMZ	Temozolamide
TP53	Tumour protein 53
TPOX	Thyroid peroxidase intron 10
TSC(1/2)	Tuberous sclerosis complex (1/2)
UK	United Kingdom
UPS	Undifferentiated pleomorphic sarcoma
VEGF(R)(1/2/3)	Vascular endothelial growth factor (receptor)(1/2/3)
Veh	Vehicle
vWA	Von Willebrand factor type A domain protein
WDLPS	Well-differentiated liposarcoma
WHO	World Health Organization

Chapter 1

Introduction

1.1 Sarcoma

1.1.1 Sarcoma overview

Sarcomas are a rare and heterogeneous group of cancers that comprise approximately 1% of all adult malignancies diagnosed annually and currently consist of approximately 160 different histological subtype classifications (**Figure 1.1**) (Blay *et al.*, 2019; Cancer Research UK, 2010; Cancer Research UK, 2017; WHO, 2020). The incidence increases to approximately 10% within paediatric (0-14 years) malignancies (**Figure 1.1**) (Cancer Research UK, 2006-2008).

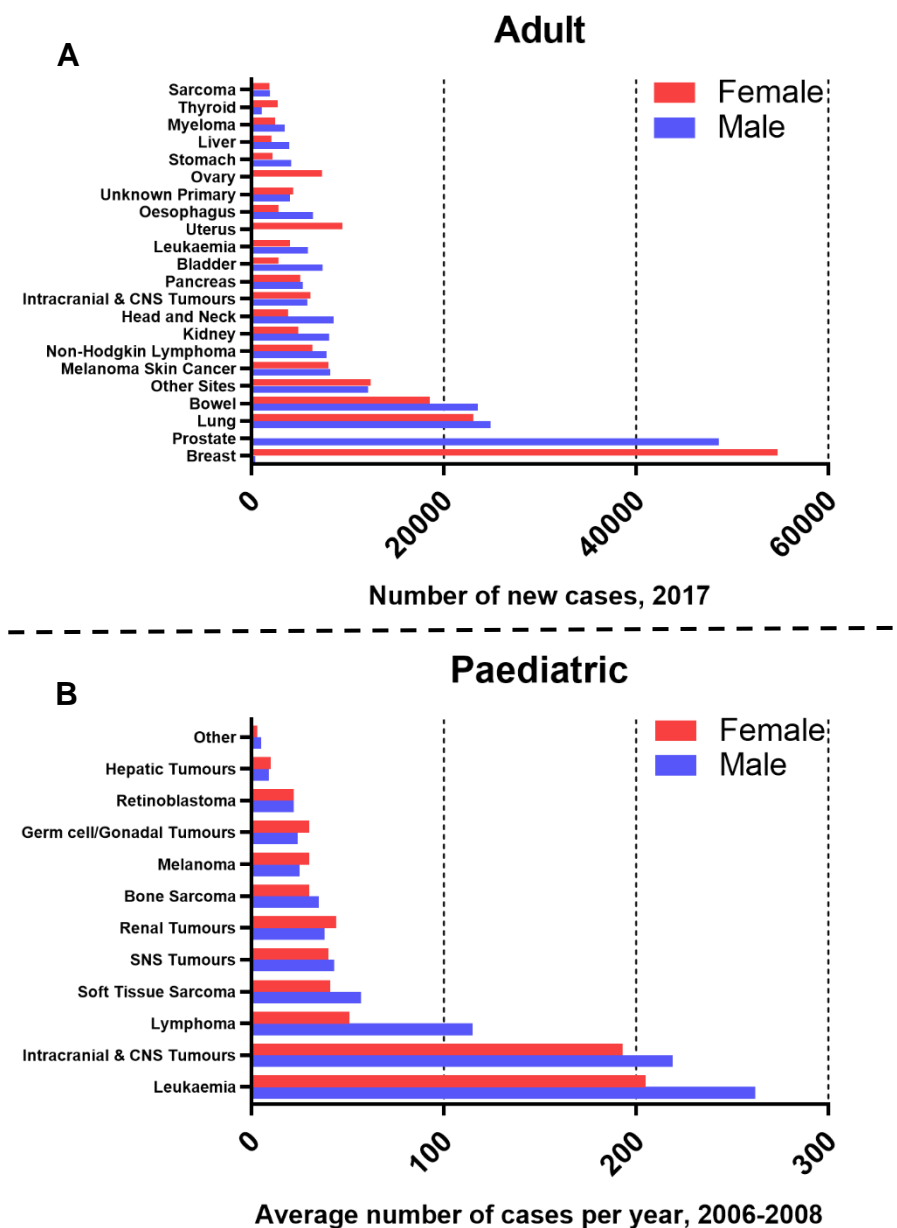


Figure 1.1: Incidence of sarcomas in adult and paediatric malignancies per annum. (A) Annual incidence of sarcoma and the 20 most commonly diagnosed adult cancers in the United Kingdom (UK) for 2017 (Cancer Research UK, 2017). Sarcoma data are an amalgamation of newest available data for the UK from 2010 (for soft tissue sarcoma)

and 2017 (for bone/cartilage sarcoma) (Cancer Research UK, 2010; Cancer Research UK, 2017). These data exclude non-melanoma skin cancer because of known under-reporting. **(B)** Average annual incidence of the 12 most commonly diagnosed paediatric cancers (0-14 years) in the UK for the years 2006-2008 (Cancer Research UK, 2006-2008). CNS; Central Nervous System, SNS; Sympathetic nervous system.

Sarcomas are classified as malignant tumours that arise in tissues derived from cells of the embryonic mesenchyme (Sannino *et al.*, 2017). During the early stages of embryogenesis, gastrulation of the blastula results in triploblasty where the embryo is separated into three distinct germ layers: an outer ectoderm, an inner endoderm, and a central mesoderm (Ferretti & Hadjantonakis, 2019). Whilst the ectoderm and endoderm form layers of epithelial cells, the mesoderm forms the majority of a type of early connective tissue called the mesenchyme, with a small contribution being derived from the neuroectoderm (Clark *et al.*, 2005; Hay, 2005; Linch *et al.*, 2014; MacCord, 2012). The mesenchyme consists of a loose network of motile mesenchymal cells embedded in a fluid extracellular matrix (ECM). A main characteristic of these mesenchymal cells is their ability to migrate and invade throughout the epithelial layers of the developing embryo. The mesenchyme is primarily a transient tissue existing during embryogenesis and early development, however mesenchymal stem cells (MSC) are present in various adult tissues such as bone marrow, adipose tissue, and dental tissues (Hay, 2005; Lamouille *et al.*, 2014; MacCord, 2012; Ullah *et al.*, 2015). Embryonic mesenchymal cells and MSC are multipotent and differentiate into a variety of discrete cell types comprising connective tissue structures such as bone, cartilage, muscle, fat, vasculature, stroma, and others (**Figure 1.2**) (Gaebler *et al.*, 2017). Cancerous growth within these tissues results in the formation of sarcomas and, therefore, sarcomas can occur in any anatomical location throughout the body; most commonly in the extremities (WHO, 2020). As sarcomas originate from a variety of differing cell types, with the only common denominator being their mesenchymal ancestry, sarcomas are characterised by extreme clinical, molecular, and histological heterogeneity (Linch *et al.*, 2014; Schaefer *et al.*, 2018).

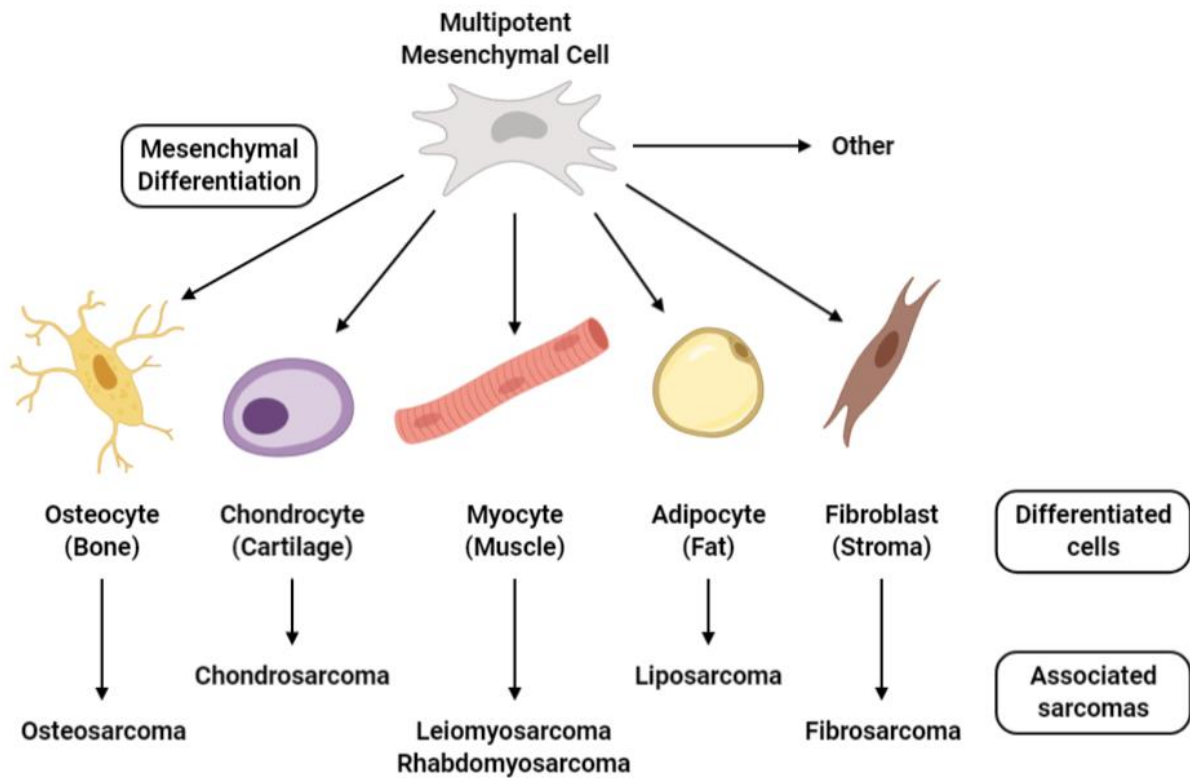


Figure 1.2: Mesenchymal cell differentiation and associated sarcomas. Schematic of mesenchymal cell differentiation and associated sarcomas that arise from these differentiated cells (adapted from Gaebler *et al.*, 2017). Image was created using BioRender.

Sarcomas are classified into two distinct sub-divisions (National Cancer Intelligence Network, 2013):

- osteo/chondrosarcomas of bone and cartilage
- soft tissue sarcomas (STS) of soft tissues such as muscles, fat, stroma, etc.

There is a further, less distinct classification of sarcomas that arise from cells of both bone/cartilage and soft tissues, such as Ewing sarcoma (WHO, 2020). The vast majority of sarcomas are STS, which comprise approximately 85% of sarcoma diagnoses per annum (Cancer Research UK, 2010; Cancer Research UK, 2017).

1.1.2 Soft tissue sarcoma

STS are malignancies of the soft connective tissues of the body such as smooth muscle (leiomyosarcoma), skeletal muscle (rhabdomyosarcoma), fat (liposarcoma), blood vessels (angiosarcoma), and stroma (fibrosarcoma), among many others (**Figure 1.3**) (Clark *et al.*, 2005; WHO, 2020). The latest classifications from the World

Health Organisation (WHO) have identified approximately 80 differing histological subtypes and, therefore, STS are highly heterogeneous in their pathology, disease presentation, and clinical response (WHO, 2020).

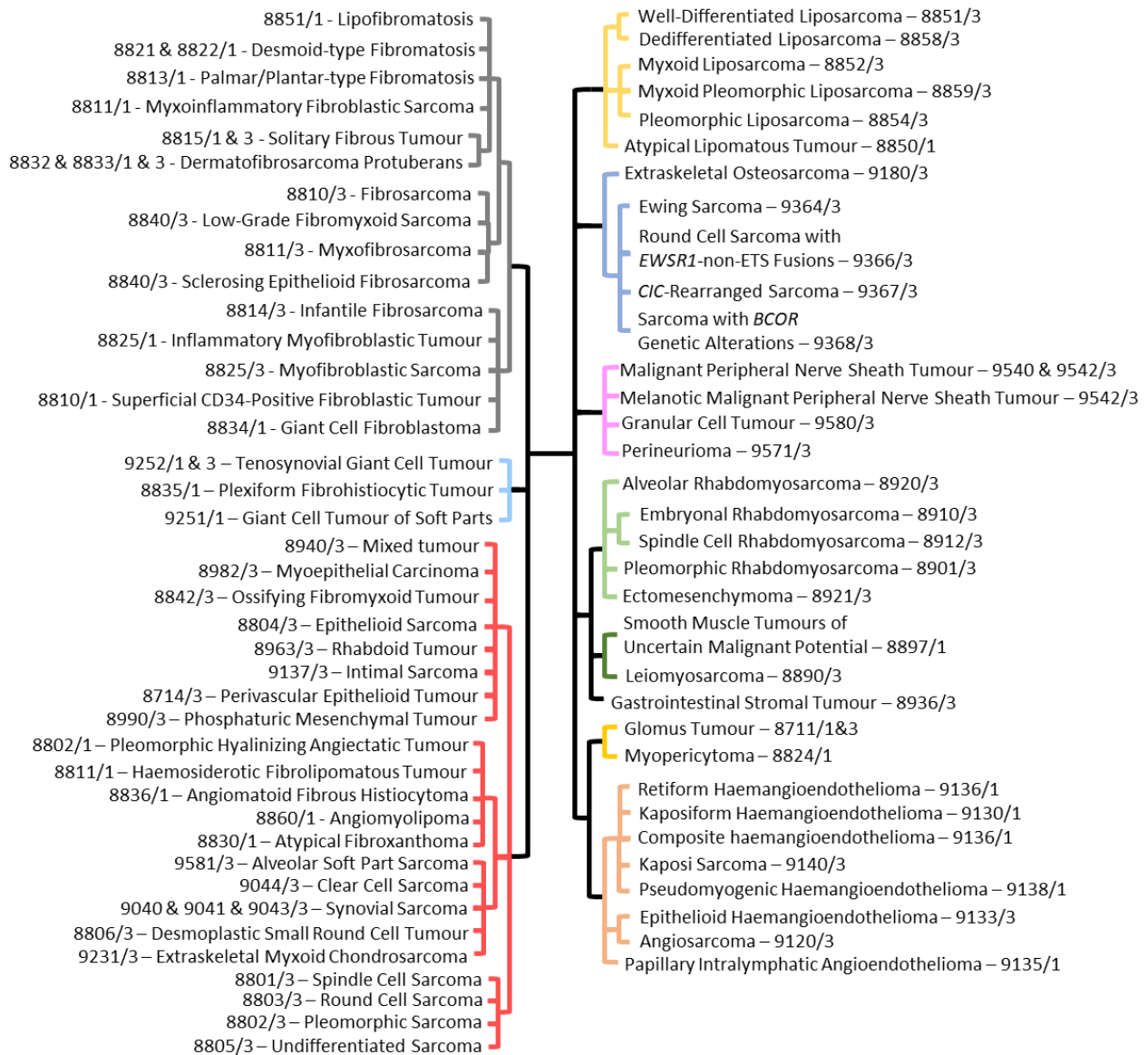


Figure 1.3: Dendrogram of STS subtypes based on cell lineage. Dendrogram displays ~80 STS subtypes, as defined by WHO classifications (WHO, 2020). Figure excludes benign tumours. Dendrogram is ordered based on cell lineage, as well as prognostic and genetic similarities (anticlockwise from top left); fibroblastic/myofibroblastic (grey), fibrohistiocytic (cyan), uncertain differentiation (red), vascular (peach), pericytic (orange), GIST (black), smooth muscle (dark green), skeletal muscle (light green), peripheral nerve sheath (pink), chondro-osseous (blue), and adipocytic (yellow) (adapted from Taylor *et al.*, 2011). Morphology codes are from the International Classification of Diseases for Oncology, third edition, second revision (IACR, 2019). Behaviour is coded /1 for unspecified, borderline, or uncertain behaviour, and /3 for malignant tumours (WHO, 2020). Bcl-6; B-cell lymphoma 6 protein, BCOR; Bcl-6 corepressor, CIC; Capicua transcriptional repressor, ETS; E26 transformation-specific, EWSR1; Ewing RNA binding protein 1, GIST; Gastrointestinal stromal tumour, RNA; Ribonucleic acid, STS; Soft tissue sarcoma, WHO; World Health Organization.

The approximation of 80 subtypes of STS excludes benign soft tissue tumours, which are 100 times more common than their malignant counterparts (Clark *et al.*, 2005; WHO, 2020). For example, lipomas – benign tumours of mature adipocytes – are relatively common and occur in around 1% of the general population, with this incidence increasing in the elderly and obese populations (Cancer Research UK, 2020; Johnson *et al.*, 2018; WHO, 2020). Although frequently painless, harmless, and extremely unlikely to develop into malignant disease, benign soft tissue tumours can still have profound effects on patient health and wellbeing. For instance, fibroids (also known as uterine leiomyomas or myomas) are benign tumours that occur in the smooth muscle wall of the uterus and occur in around 50-60% of women (Donnez *et al.*, 2018). A surgical technique called morcellation can be used to treat fibroids by cutting the uterine tumour tissue into smaller pieces that can be removed laparoscopically (RCOG, 2019). However, fibroids can harbour unexpected and undiagnosed malignant uterine leiomyosarcoma – a risk which increases with age – and morcellation of malignant tissue can result in the dissemination of the disease, thereby increasing patient mortality (Chen *et al.*, 2018; George *et al.*, 2014; Nobre *et al.*, 2021; RCOG, 2019). Furthermore, due to the relative rarity of STS compared to the frequency of benign soft tissue tumours, as well as the extensive clinical, histological, and molecular similarities in benign and malignant tissues, STS are often initially misdiagnosed as benign tumours (Chen *et al.*, 2018; Clark *et al.*, 2005; Johnson *et al.* 2018; O'Donnell *et al.*, 2013; WHO, 2020). Additionally, although exceptionally rare, benign tumours can develop into malignancies as is observed in the infrequent transformation (~9-15%) of benign plexiform neurofibromas of the peripheral nervous system (PNS) into malignant peripheral nerve sheath tumour (Evans *et al.*, 2012; Uusitalo *et al.*, 2016; WHO, 2020; Widemann, 2009). Misdiagnosis can therefore result in delays in proper diagnosis and specialist management, harmful and/or inappropriate surgeries, and the progression of undetected STS resulting in increased mortality.

1.1.2.1 Epidemiology and aetiology

As with sarcomas in general, STS are extremely rare, making up <1% of all adult malignancies diagnosed annually (Clark *et al.*, 2005; WHO, 2020). This incidence

once again increases in children, with STS constituting ~6-8% of all paediatric (0-14 years) cancers, with certain histologies occurring almost exclusively at this stage of development, such as embryonal rhabdomyosarcoma (Cancer Research UK, 2006-2008; Sangkhathat, 2015; Skapek *et al.*, 2019; WHO, 2020). As with almost all cancers, STS become more common with age however age-related incidences vary markedly dependent on subtype (Cancer Research UK, 2008-2010; White *et al.*, 2015; WHO, 2020). For instance, liposarcoma, leiomyosarcoma, and undifferentiated pleomorphic sarcoma comprise the majority of geriatric malignancies, synovial sarcoma predominantly affects young adults, and approximately half of paediatric STS diagnoses are rhabdomyosarcomas (Jones *et al.*, 2017; Parikh *et al.*, 2018; Skapek *et al.*, 2019; WHO, 2020).

STS can arise throughout the body but most commonly (~75%) occur in the extremities, especially in the thigh, and ~20% are located in the trunk and retroperitoneum (Clark *et al.*, 2005; Hoefkens *et al.*, 2016; WHO, 2020). The aetiology of most STS are unknown and the majority of these malignancies are believed to arise *de novo*, without an apparent causative factor such as genetics, smoking/diet, or environmental factors (American Cancer Society, 2018; Clark *et al.*, 2005; WHO, 2020). Despite this, around 10% of STS are known to be associated with specific aetiologic agents such as viruses, genomic alterations, chemical carcinogens, and radiation (American Cancer Society, 2018; Cancer Research UK, 2015; Dow *et al.*, 2014; WHO, 2020).

1.1.2.1.1 Viral aetiological factors

One of the most well studied STS of this minority of aetiologically-certain malignancies is Kaposi sarcoma - caused by the infection of immunocompromised persons by human herpesvirus 8 (HHV8) - which gained widespread public attention during the height of the acquired immune deficiency syndrome (AIDS) epidemic in the early 1980s (Cesarman *et al.*, 2019; Dow *et al.*, 2014). This notoriety is due to the opportunistic nature of HHV8 infection and subsequent Kaposi sarcoma incidence in human immunodeficiency virus (HIV)-positive immunocompromised populations (Cesarman *et al.*, 2015; Dow *et al.*, 2014). Kaposi sarcoma manifests as locally aggressive neoplasms of endothelial cells resulting in cutaneous lesions and nodules

that were, and continue to be, a highly stigmatising symptom of HIV infection (Cesarman *et al.*, 2019; WHO, 2020). As the AIDS epidemic continues to rage throughout sub-Saharan Africa, Kaposi sarcoma remains the most common cancer in men, and second most common in woman, in countries such as Uganda, Malawi, and Zimbabwe (Cesarman *et al.*, 2019; Harris, 2016; Jamison *et al.*, 2006). Similarly, the Epstein-Barr virus (EBV) – another member of the herpesvirus family – has been associated as an opportunistic aetiological factor in leiomyosarcoma of the immunocompromised (Cancer Research UK, 2015; Deyrup *et al.*, 2006; Shannon-Lowe & Rickinson, 2019; WHO, 2020). It is important to differentiate virus-associated sarcomas from the majority of ‘normal’ STS as they usually require substantially different therapies (Cancer Research UK, 2018; Schneider & Dittmer, 2017).

1.1.2.1.2 Genetic aetiological factors

Although infrequent, a fraction of STS cases are notably associated with heritable cancer predisposition syndromes (Farid & Ngeow, 2016). These disorders are caused by inherited genetic mutations in one or more genes that result in the predisposition of the afflicted individual to the development of cancer, particularly early-onset cancers (Farid & Ngeow, 2016; Garber & Offit, 2005). An example of such a syndrome that is associated with the development of STS is Li-Fraumeni syndrome (LFS) (Farid & Ngeow, 2016; Gonzalez *et al.*, 2009). LFS is a rare autosomal dominant disease caused by germline mutations in the tumour protein 53 (*TP53*) tumour suppressor gene (Gonzalez *et al.*, 2009; Malkin, 2011). These mutations result in the aberrant activity of the *TP53*-encoded transcription factor p53, resulting in dysregulation of DNA repair, cell cycle, senescence, and apoptosis mechanisms, potentially leading to tumorigenesis (Mello & Attardi, 2018; Ognjanovic *et al.*, 2012). LFS sufferers are therefore characterised by an increased predisposition towards early-onset cancer and an extremely high lifetime cancer risk, with STS making up the second most common (~11.6-17.8%) LFS-associated malignancy, behind only breast cancer (Bougeard *et al.*, 2015; Farid & Ngeow, 2016; Nichols *et al.*, 2001; WHO, 2020).

Another cancer predisposition syndrome associated with the development of STS is neurofibromatosis type 1 (NF-1). Similarly to LFS, NF-1 is an autosomal dominant disorder caused by inactivating germline mutations in the tumour suppressing *NF1*

gene encoding neurofibromin 1 (Emmerich *et al.*, 2015; Farid & Ngeow, 2016; Gutmann *et al.*, 2017). Neurofibromin 1 acts as a tumour suppressor through its activity as a negative regulator of the mitogen-activated protein kinase (MAPK) pathway – a pathway integral to physiological, as well as tumourigenic, cellular phenotypes such as growth, proliferation, and survival (Emmerich *et al.*, 2015; Ratner & Miller, 2015; Yap *et al.*, 2014; Zhang & Liu, 2002). Neurofibromin 1 is highly expressed in the PNS (Ryu *et al.*, 2019). Therefore, NF-1 results in the development of multiple neurofibromas of peripheral nerve sheaths and significantly increases (≥ 2 -fold increase) the risk of developing malignant peripheral nerve sheath tumour, with ~5-13% of NF-1 patients developing these malignancies (De Raedt *et al.*, 2003; Farid & Ngeow, 2016; Widemann, 2009). Furthermore, ~5-7% of NF-1 patients develop gastrointestinal stromal tumours (GIST), which are malignancies of the interstitial cells of Cajal that line the gastrointestinal tract (Corless *et al.*, 2011; Farid & Ngeow, 2016; Nishida *et al.*, 2016; WHO, 2020). In addition, a variety of other heritable syndromes are associated with the development and increased lifetime risk of GIST, such as Carney-Stratakis syndrome and familial GIST syndrome, which are caused by germline succinate dehydrogenase (*SDH*) and platelet-derived growth factor receptor α (*PDGFRA*)/*KIT* mutations, respectively (Farid & Ngeow, 2016; Li *et al.*, 2005; Stratakis & Carney, 2009; WHO, 2020). In addition to the various cancer predisposition syndromes described, there are multiple other heritable disorders that have also been reported as being associated with an increased risk of developing STS, such as hereditary retinoblastoma, Gardner, and Werner syndromes, among many others (Cancer Research UK, 2015; Farid & Ngeow, 2016; Hatzimarkou *et al.*, 2006; Lauper *et al.*, 2013; WHO, 2020).

These rare, inherited cancer predisposition syndromes account for a minute number of overall STS incident cases, however, a large, multicentre study has recently reported that potentially up to 50% of STS patients harbour inherited, putatively pathogenic and aetiological germline variants of known or novel cancer-associated genes (Ballinger *et al.*, 2016). These results, if validated, suggest that a large proportion of sarcomas actually develop due to underlying genomic aberrations, contrary to the prior belief that the majority of STS develop *de novo*, which could have wide ranging implications in terms of familial genetic testing, screening, and therapy (Ballinger *et al.*, 2016; Benjamin & Futreal, 2016; Thomas *et al.*, 2012).

1.1.2.1.3 Chemical and radiation aetiological factors

Chemical substances and radiation have long been known as causative factors in a wide range of cancers, especially in occupations highly exposed to such carcinogens (Cancer Research UK, 2015; Goodson 3rd *et al.*, 2015). Numerous studies have highlighted the association between excess occupational exposure to chemical carcinogens, such as vinyl chloride, phenoxy herbicides, and dioxins, with an increased risk of developing STS (Eriksson *et al.*, 1990; Hardell & Eriksson, 1988; NHS, 2019; Rhomberg, 1998; Zahm & Fraumeni Jr, 1997). However, more recent studies on phenoxy herbicides have not found a significant association and therefore the absolute risk of these chemicals in the development of STS is disputed and uncertain (Jayakody *et al.*, 2015). These contemporary studies hypothesise that this loss of association could be due to the decrease of dioxin contamination in modern phenoxy herbicides (Jayakody *et al.*, 2015; Zambon *et al.*, 2007; WHO, 2020).

Approximately 5% of all diagnosed STS are radiation-associated; most commonly as a result of prior radiotherapeutic irradiation in the management of other malignancies such as breast cancer and lymphoma (Brady *et al.*, 1992; Clark *et al.*, 2005; Karlsson *et al.*, 1998; Mito *et al.*, 2019; WHO, 2020). The risk of developing radiation-induced STS increases linearly with administered dose (to at least 40-50 Gy), with children being the demographic most at risk (Berrington de Gonzalez *et al.*, 2012; Karlsson *et al.*, 1998; WHO, 2020). Furthermore, there is also evidence that individuals suffering from hereditary cancer predisposition syndromes are more susceptible to developing radiation-induced STS (Berrington de Gonzalez *et al.*, 2012). The most commonly diagnosed radiation-induced STS subtype is undifferentiated pleomorphic sarcoma, and the association with radiation frequently results in a more aggressive disease phenotype and a worse prognosis (Brady *et al.*, 1992; Dineen *et al.*, 2015; Gladdy *et al.*, 2010; WHO, 2020). Despite the known association, radiation-associated STS occur in fewer than 1% of patients who receive radiation therapy and therefore the overall benefits of radiotherapy outweigh the minimally increased risk of sarcoma (Clark *et al.*, 2005; Mito *et al.*, 2019).

1.1.2.2 Classifications of soft tissue sarcomas

The heterogeneity of STS can be broadly classified into two distinct subgroups based on their underlying genetic profiles and characteristics (**Figure 1.4**) (Bovée & Hogendoorn, 2010; Linch *et al.*, 2014):

1. Genetically “Simple” STS – comprise tumours with specific pathognomonic genetic alterations, recurrent aberrations, and relatively simple karyotypes (**Table 1.1**)
2. Genetically “Complex” STS – comprise tumours with non-recurrent genetic alterations and relatively complex karyotypes.

Despite this apparently simple distinction between subgroups, classification of STS can be more accurately based upon a spectrum of genomic characteristics and complexity (**Figure 1.4**) (Lim *et al.*, 2015). Additionally, advanced and progressing tumours tend to display higher degrees of genomic complexity and mutational burden than the originating primary tumour (Bovée & Hogendoorn, 2010; Lim *et al.*, 2015; Mariño-Enriquez & Bovée, 2016). Our ever-increasing understanding of the differences in genomic characteristics and complexities present in specific STS subtypes has and will continue to advance our ability to accurately diagnose patients, with the overall clinical aim being to provide and develop the most effective treatments based on underlying genetics and biology, as opposed to histology and morphology. Therefore, a continued advancement of our understanding of the genetic and biological processes underpinning STS subtypes will allow sarcoma clinicians to treat specific subtypes with effective biology-driven therapies, as opposed to a one-size-fits-all treatment approach for the molecularly and clinically heterogeneous group of malignancies falling under the diagnostic umbrella of STS (Lim *et al.*, 2015).

Table 1.1: Examples of STS subtypes with subtype-associated, recurrent genetic aberrations and oncogenic consequences.			
Subtype	Subtype-associated, recurrent genetic aberration(s)	Affected genes	Oncogenic consequence
Chromosomal translocations, inversions, & rearrangements (~15-20%)			
Alveolar rhabdomyosarcoma	t(2;13)(q35;q14)	PAX3-FOXO1 fusion	Aberrant transcription
Alveolar soft part sarcoma	t(1;13)(p36;q14)	PAX7-FOXO1 fusion	Aberrant transcription
BCOR-rearranged sarcoma	t(X;17)(p11;q25)	TFE3-ASPSCR1 fusion	Aberrant transcription
CIC-rearranged sarcoma	Inv(X)(p11p11)	BCOR-CCNB3 fusion	Aberrant transcription
Clear cell sarcoma	t(4;19)(q35;q13)	CIC-DUX4 fusion	Aberrant transcription
Desmoplastic small round cell tumour	t(10;19)(q26;q13)	EWSR1-ATF1 fusion	Aberrant transcription
Dermatofibrosarcoma protuberans	t(12;22)(q13;q12)	EWSR1-WT1 fusion	Aberrant transcription
Epithelioid haemangiioendothelioma	Supernumerary ring chromosomes; 17 & 22	COL1A1-PDGFB fusion	Oncogenic PDGFR signalling
Ewing sarcoma (Primitive neuroectodermal tumour)	t(17;22)(q22;q13)	WWTR1-CAMTA1 fusion	Aberrant transcription
Extraskelatal myxoid chondrosarcoma	t(1;3)(p36;q25)	YAP1-TFE3 fusion	Aberrant transcription
Infantile fibrosarcoma	t(X;11)(p11;q22)	EWSR1-FLI1 fusion	Aberrant transcription
Inflammatory myofibroblastic tumour	t(11;22)(q24;q12)	EWSR1-ERG fusion	Aberrant transcription
Low-grade fibromyxoid sarcoma	t(21;22)(q22;q12)	EWSR1-NR4A3 fusion	Aberrant transcription
Mesenchymal chondrosarcoma	t(9;22)(q22;q12)	TAF15-NR4A3 fusion	Aberrant transcription
Myxoid liposarcoma	t(9;17)(q22;q11)	TCF12-NR4A3 fusion	Oncogenic NTRK signalling
Pseudomyogenic haemangiioendothelioma	t(12;15)(p13;q25)	ETV6-NTRK3 fusion	Oncogenic ALK signalling
Sclerosing epithelioid fibrosarcoma	t(1;2)(q22;p23)	TPM3-ALK fusion	Oncogenic ALK signalling
Solitary fibrous tumour	t(2;19)(p23;p13)	TPM4-ALK fusion	Oncogenic ALK signalling
Synovial sarcoma (Figure 1.5)	t(2;17)(p23;q23)	CLTC-ALK fusion	Oncogenic ALK signalling
Oncogenic mutations (~20%)			
Epithelioid sarcoma (Figure 1.5)	Supernumerary ring chromosomes; 7 & 16	FUS-CREB3L2 fusion	Aberrant transcription
Gastrointestinal stromal tumour (Figure 1.5)	t(7;16)(q33;p11)	FUS-CREB3L1 fusion	Aberrant transcription
Malignant peripheral nerve sheath tumour	t(8;8)(q13;q21)	HEY1-NCOA2 fusion	Aberrant transcription
Malignant rhabdoid tumour (Figure 1.5)	t(12;16)(q13;p11)	FUS-DDIT3 fusion	Aberrant transcription
PEComa	t(12;22)(q13;q12)	EWSR1-DDIT3 fusion	Aberrant transcription
PEComa	t(7;19)(q22;q13)	SERPINE1-FOSB fusion	Aberrant transcription
PEComa	t(11;22)(p11;q12)	EWSR1-CREB3L1 fusion	Aberrant transcription
PEComa	Inv(12)(q13q13)	NAB2-STAT6 fusion	Aberrant transcription
PEComa	t(X;18)(p11;q11)	SS18-SSX1/SSX2 fusion	Aberrant transcription
Gene amplifications (~10-15%)			
Dedifferentiated liposarcoma	Deletions/inactivating mutations/epigenetic silencing; 22q11	SMARCB1 loss-of-function	Tumour suppressor deactivation
Intimal sarcoma	Activating mutations; 4q12	KIT, PDGFRA gain-of-function (~85%)	Oncogenic PDGFR/KIT signalling
Well-differentiated liposarcoma	Inactivating mutations/epigenetic silencing; 5p15/1p36/1q23/11q23	SDH loss-of-function/dysfunction (~5-10%)	Oncogenic succinate accumulation
Well-differentiated liposarcoma	Deletions/inactivating mutations; 17q11 & 11q14	NF1, SUZ12, EED loss-of-function	Tumour suppressor deactivation
Well-differentiated liposarcoma	Deletions/inactivating mutations/epigenetic silencing; 22q11	SMARCB1 loss-of-function	Tumour suppressor deactivation
Well-differentiated liposarcoma	Deletions/inactivating mutations; 9q34 or 16p13	TSC1, TSC2 loss-of-function	Tumour suppressor deactivation
Dedifferentiated liposarcoma	Amplifications; 12q14-q15 & 1p32	MDM2, CDK4, JUN amplification	Oncogene activation
Intimal sarcoma	Amplifications; 12q13-q15 & 4q12	MDM2, CDK4, TSPAN31, GLI1, PDGFRA, KIT amplification	Oncogene activation
Well-differentiated liposarcoma	Amplifications; 12q14-q15	MDM2, CDK4 amplification	Oncogene activation

Table displays the most common, recurrent, and characteristic genetic aberrations observed in specific STS subtypes and is not an exhaustive list of all known subtype-associated genetic abnormalities. Translocations with a prevalence of >5% are included. The approximate percentages shown are in the context of all STS. Bcl-6; B-cell lymphoma 6 protein, BCOR; Bcl-6 corepressor, CIC; Capicua transcriptional corepressor, Inv; Inversion, NTRK; Neurotrophic tyrosine kinase receptor, p; p (short) arm of chromosome, PDGFR; Platelet-derived growth factor receptor, PEComa; Perivascular epithelioid cell sarcoma, q; q (long) arm of chromosome, STS; Soft tissue sarcoma, t; Translocation (Bovée & Hogendoorn, 2010; Guillou & Aurias, 2010; Linch et al., 2014; Schaefer et al., 2018; WHO, 2020).

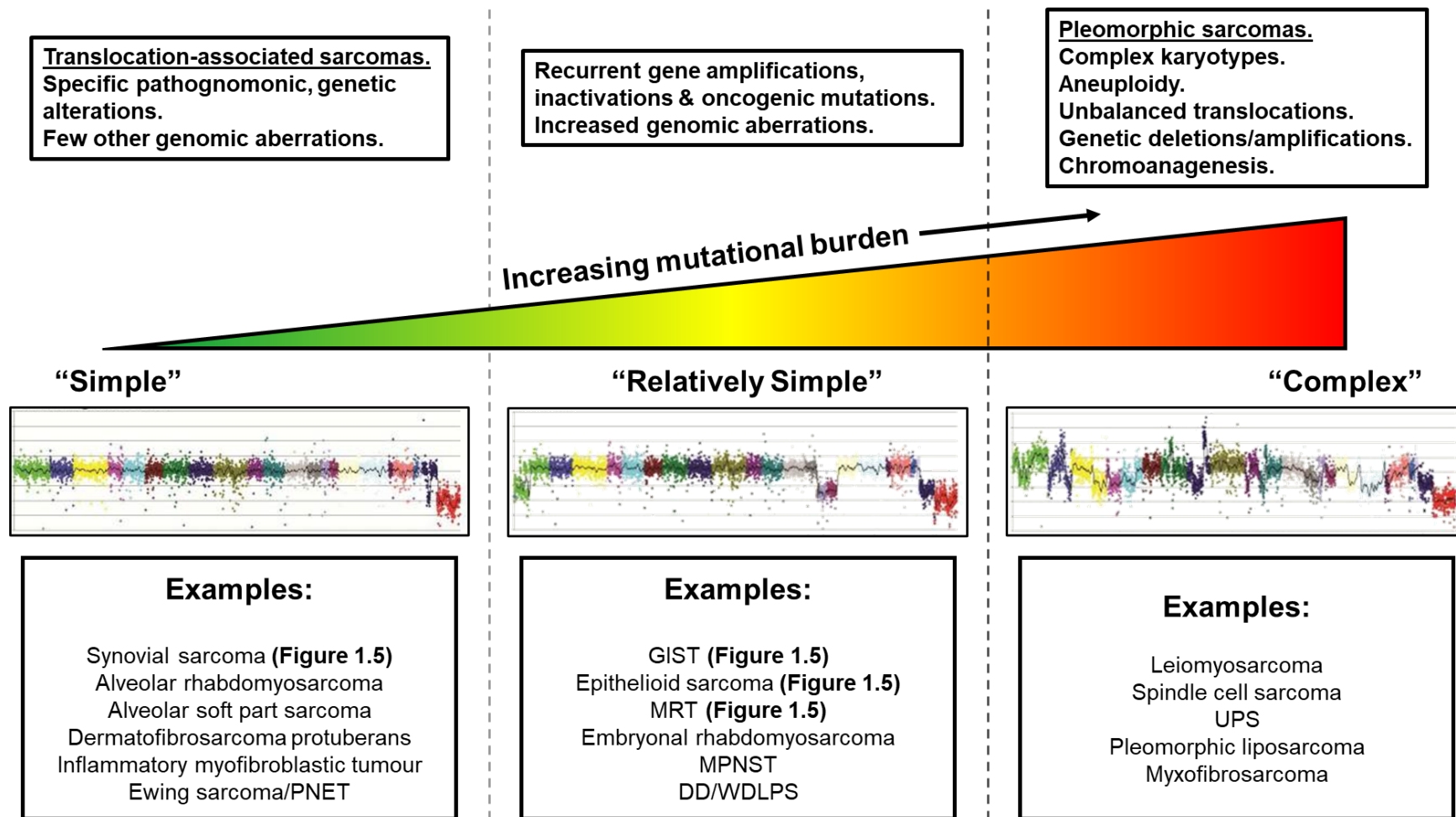


Figure 1.4: Spectrum of genetic characteristics and complexity in STS. Translocation-associated STS typically display a simple genetic profile and stable genome with low mutational burden and normal diploid karyotype. "Relatively simple" STS display recurrent genetic aberrations and oncogenic driver mutations with increased mutational burden and background genome complexity. Pleomorphic STS are characterised by complex genomic profiles, numerous chromosomal abnormalities, and high mutational load. These STS lack recurrent or consistent genetic alterations. (Guillou & Aurias, 2010; Holland & Cleveland, 2012; Lim *et al.*, 2015; Linch *et al.*, 2014; Mariño-Enriquez & Bovée, 2016; Setty *et al.*, 2020). Examples of copy number profiles from Ewing sarcoma/PNET ("simple"), GIST ("relatively simple"), and UPS ("complex") (adapted from Mariño-Enriquez & Bovée, 2016). DDLPS; Dedifferentiated liposarcoma, GIST; Gastrointestinal stromal tumour, MPNST; Malignant peripheral nerve sheath tumour, MRT; Malignant rhabdoid tumour, PNET; Primitive neuroectodermal tumour, UPS; Undifferentiated liposarcoma, WDLPS; Well-differentiated liposarcoma.

1.1.2.2.1 “Simple” soft tissue sarcomas

The first group of STS comprise tumours with specific pathognomonic genetic alterations or oncogenic mutations with relatively simple karyotypes (~45-55% of STS) (Bovée & Hogendoorn, 2010; Guillou & Aurias, 2010; Linch *et al.*, 2014) (**Figure 1.5; Table 1**). Approximately 15-20% of sarcomas are characterised by chromosomal translocations that produce fusion or chimeric genes. Most often, these genes encode aberrant transcription factors, such as is observed in synovial sarcoma, alveolar soft part sarcoma, alveolar rhabdomyosarcoma, and many others (**Table 1.1**) (Linch *et al.*, 2014; Schaefer *et al.*, 2018).

For example, >95% of synovial sarcomas are characterised by the t(X;18)(p11;q11) translocation which fuses the *SS18* gene on chromosome 18 to one of the three *SSX* genes (*SSX1/2/4*) on the X chromosome (**Figure 1.5A**) (Stacchiotti & Van Tine, 2018; WHO, 2020). Of these translocations, the *SS18-SSX1* fusion represents approximately two thirds of synovial sarcomas and *SS18-SSX2* constitutes the remaining third, with the *SS18-SSX4* presenting very rarely (Przybyl *et al.*, 2012; WHO, 2020). Expression of these gene fusions synthesise the chimeric *SS18-SSX* protein that competes with wild-type *SS18* for binding to switch/sucrose non-fermentable (SWI/SNF) chromatin remodelling complexes (Kadoch & Crabtree, 2013; Svejstrup, 2013). Binding of the *SS18-SSX1* fusion protein results in pathological alterations of SWI/SNF complexes, such as changes in subtype expression levels, molecular subunit constitution, and genomic distribution (Li *et al.*, 2021). The tumourigenic SWI/SNF complexes subsequently bind DNA resulting in nucleosome and chromatin remodelling, as well as the recruitment of transcriptional machinery, in order to activate aberrant expression of oncogenes, such as *SOX2*, that result in oncogenic synovial sarcoma proliferation (**Figure 1.5A**) (Kadoch & Crabtree, 2013; Mittal & Roberts, 2020; Stacchiotti & Van Tine, 2018; Svejstrup, 2013).

The remaining ~30-35% of “simple” STS are characterised by recurrent genetic alterations such gene amplifications, activating/inactivating/deleterious mutations, as well as epigenetic silencing, that additionally also tend to display more complex background genomic aberrations than translocation-associated STS (**Table 1.1; Figure 1.4**) (Linch *et al.*, 2014; Schaefer *et al.*, 2018).

An example of this subset of STS is GIST, which are characterised in ~85% of cases by activating mutations of the 4q12 locus that encodes the receptor tyrosine kinases (RTK) KIT and platelet-derived growth factor receptor α (PDGFR α) (**Table 1.1; Figure 1.4; Figure 1.5B**) (Corless *et al.*, 2014; WHO, 2020). The vast majority of GIST-inducing RTK mutational events are mutually exclusive and lead to constitutive, ligand-independent activity of the associated RTK resulting in oncogenic intracellular activity and tumourigenesis (**Figure 1.5B**) (Braconi *et al.*, 2008; Corless *et al.*, 2014; Schaefer *et al.*, 2017). Most GISTs harbour mutations in *KIT* (~75%) with the primary site of mutation existing within the autoinhibitory juxtamembrane domain-encoding exon 11 (~65%) (**Figure 1.5B**) (Corless *et al.*, 2004; Corless *et al.*, 2014). Less common mutation sites on *KIT* include exon 9 (~8%), 13 (~1%), 17 (~1%), and in extremely rare cases, exon 8 (**Figure 1.5B**) (Corless *et al.*, 2014; Ito *et al.*, 2014). Moreover, ~10% of GISTs are distinguished by *PDGFRA* mutations; most commonly in exon 18 (~8%), with rarer cases in exon 12 (~2%) and 14 (<1%) (**Figure 1.5B**) (Corless *et al.*, 2014). These *PDGFRA*-mutant GISTs are characterised as far less aggressive cancers than their *KIT*-mutated counterparts due to their reduced metastatic potential, resulting in a stark disparity in harboured mutations in advanced-setting GIST (~83% for *KIT* vs. ~2% for *PDGFRA*) (Emile *et al.*, 2012; Joensuu *et al.*, 2015; WHO, 2020). The remaining ~15% of wild-type *KIT* and *PDGFRA* GIST most commonly harbour inactivating mutations or promoter methylation epimutations of SDH subunit genes (*SDHA-D*) (~5-10%) (**Table 1.1**) (Ibrahim & Chopra, 2020; Killian *et al.*, 2014; WHO, 2020). These aberrations result in the loss-of-function/dysfunction of SDH, which is an essential component of several critical metabolic processes such as the respiratory electron transport chain and the citric acid cycle (Rutter *et al.*, 2010). Physiological SDH functions by oxidising succinate to fumarate and, therefore, loss of SDH function results in oncogenic succinate accumulation (Ibrahim & Chopra, 2020; Rutter *et al.*, 2010). The presence of excess cellular succinate results in the overexpression of hypoxia-inducible factor (HIF) proteins and subsequent increased transcription of HIF-regulated oncogenes resulting in GIST tumourigenesis (Ibrahim & Chopra, 2020). Additionally, in exceedingly rare instances of GIST (<5%), oncogenic mutations have also been reported in the oncogenes *NF1* (inactivating), *KRAS*, and *BRAF* (activating) (Gasparotto *et al.*, 2017; Miranda *et al.*, 2012; WHO, 2020).

Furthermore, inactivating/deleterious mutations and epigenetic silencing epimutations are the most common aberrations presented in epithelioid sarcoma and malignant rhabdoid tumours (Kalimuthu & Chetty, 2016; Linch *et al.*, 2014; Schaefer *et al.*, 2018).

For both of these subtypes, the pathognomonic genetic abnormality is the loss-of-function of the SMARCB1 tumour suppressor; an occurrence that is observed in >90% of epithelioid sarcomas and ~95-98% of malignant rhabdoid tumours (**Table 1.1; Figure 1.5**) (Hornick *et al.*, 2009; Kalimuthu & Chetty, 2016; Wang *et al.*, 2019; WHO, 2020). The loss of SMARCB1 function has been reported to be caused by a variety of mutational events such as point mutations, partial or whole gene deletions, and loss of heterozygosity (Brennan *et al.*, 2013; Eaton *et al.*, 2011; Sullivan *et al.*, 2013; WHO, 2020). Additionally, epigenetic miRNA silencing has been implicated in repressing *SMARCB1* expression, especially in the context of epithelioid sarcoma (Papp *et al.*, 2014; Kia *et al.*, 2008; Kohashi *et al.*, 2014; Sapi *et al.*, 2016). As described previously with synovial sarcoma, SMARCB1-deficient SWI/SNF complexes pathologically bind DNA and remodel the chromatin and nucleosome environment, thereby allowing for access of the relevant transcriptional machinery to the DNA, resulting in aberrant gene expression. Importantly, SMARCB1 loss leads to the increased expression and recruitment of enhancer of zeste homolog 2 (EZH2) - the critical enzymatic component of the polycomb repressive complex 2 (PRC2) - that has been shown to be an actionable target in the treatment of SMARCB1-deficient cancers (Bracken *et al.*, 2007; Gounder *et al.*, 2017; Italiano, 2020). EZH2 operates by trimethylating histones which results in the transcriptional repression of a number of tumour suppressor genes, such as cyclin-dependent kinase inhibitor 2A (*CDKN2A*) at the *INK4a/ARF* locus, and the subsequent upregulation of oncogenic genes, such as *MYC*, β -catenin (*CTNNB1*), and sonic hedgehog (*SHH*) (Bracken *et al.*, 2007; Italiano, 2020).

The increased recognition and research into understanding the underlying and consistent molecular features and biology that underpin specific, “simple” STS subtypes, as opposed to attempting to solve the chaotic and extremely diverse biology of monolithic STS as a whole, has resulted in a number of advancements in the clinical setting. Importantly, it allows for the design and development of effective and novel therapies for patients with specific STS subtypes that target the pathobiology initiating and driving the specific disease. Additionally, this increased biological understanding

increases diagnostic and prognostic accuracy in the clinic, which is essential for determining the most effective treatment regimen for a specific patient.

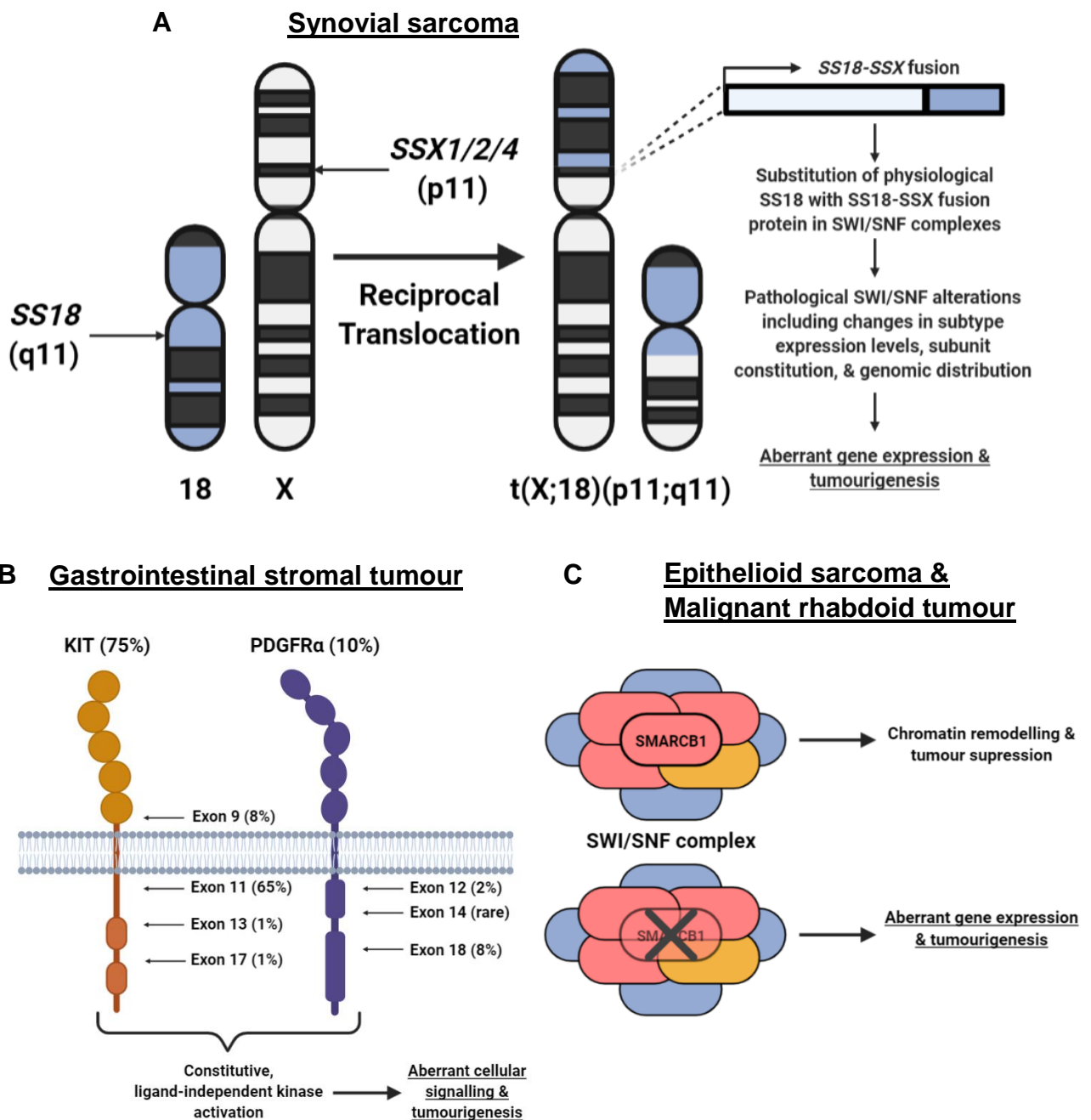


Figure 1.5 Examples of genetically “simple” STS subtypes. **(A) Synovial Sarcoma (SS)**. Chromosomal t(X;18)(p11.2;q11.2) translocation resulting in the fusion of the *SS18* gene (chromosome 18) to the *SSX1/2/4* (X chromosome) gene and subsequent downstream effects which lead to SS tumourigenesis (adapted from Kadoch & Crabtree, 2013; Li *et al.*, 2021; Svejstrup, 2013). **(B) Gastrointestinal Stromal Tumour (GIST)**. Distribution and prevalence of KIT or PDGFRα point mutations (by exon) which lead to aberrant intracellular signalling and the tumourigenesis of GIST (adapted from Corless, 2014; Oppelt *et al.*, 2017). **(C) Epithelioid Sarcoma (ES) & Malignant Rhabdoid Tumour (MRT)** Loss, inactivation and/or epigenetic silencing of SMARCB1 subunit of the SWI/SNF chromatin remodelling complex leading to ES and MRT tumourigenesis (Le Loarer *et al.*, 2014; Kalimuthu & Chetty, 2016; Kim & Roberts, 2015; WHO, 2020). Images were created using BioRender. PDGFRα; Platelet-derived growth

factor receptor α , p; short (p) arm, q; long (q) arm, SMARCB1; SWI/SNF-related matrix-associated actin-dependent regulator of chromatin subfamily B member 1, SS18; Synovial sarcoma translocation, chromosome 18, SSX1/2/4; Synovial sarcoma X 1/2/4 breakpoint proteins, SWI/SNF; Switch/Sucrose non-fermentable, t; Translocation.

1.1.2.2.2 “Complex” soft tissue sarcomas

The second group of STS is associated with relatively complex karyotypes and display no specific or recurrent genetic aberrations within subtypes (~45-55% of STS) (**Figure 1.4**) (Guillou & Aurias, 2010; Linch *et al.*, 2014). The karyotypic complexity of these STS are characterised by high genomic instability with inconsistent aberrations such as aneuploidy, unbalanced translocations, chromosomal segment amplifications and deletions, and chromoanagenesis (**Figure 1.4**) (Guillou & Aurias, 2010; Holland & Cleveland, 2012; Linch *et al.*, 2014; Mariño-Enriquez & Bovée, 2016). Despite the erratic and chaotic nature of these tumours, “complex” STS frequently harbour loss of tumour suppressor genes such as *TP53*, retinoblastoma protein (*RB1*), and *CDKN2A*; with these events postulated to occur early within sarcomagenesis (Bui *et al.*, 2019; Chudasama *et al.*, 2018; Mariño-Enriquez & Bovée, 2016; Schaefer *et al.*, 2018). Furthermore, although relatively low compared to other cancers, the mutational burden within this subgroup of STS is much higher and far more varied than is observed in the genetically “simple” STS (Petitprez *et al.*, 2020). The higher mutational load, and resultant increase in tumour cell neoantigen expression, could potentially make these group of “complex” sarcomas a promising candidate for immune checkpoint immunotherapy (Lim *et al.*, 2015; Petitprez *et al.*, 2020).

This subgroup of STS consists of some of the most frequently diagnosed STS subtypes; most notably leiomyosarcoma, liposarcoma, and undifferentiated pleomorphic sarcoma, with these three subtypes making up to approximately 40-50% of STS diagnoses per annum on their own (Ducimetière *et al.*, 2011; Guillou & Aurias, 2010; Hung *et al.*, 2015; Linch *et al.*, 2014; Parikh *et al.*, 2018). Other rarer subtypes within this group including spindle cell sarcoma, myxofibrosarcoma, and angiosarcoma (Guillou & Aurias, 2010; Linch *et al.*, 2014; WHO, 2020). Due to the great amount of heterogeneity and genomic complexity inherent within members of the “complex” subset of STS, there are currently no specific or recurrent molecular diagnostic markers for these malignancies (Mariño-Enriquez & Bovée, 2016). Therefore, diagnosis of these malignancies remains through standard

clinicopathological routes such as histopathological examination in order to identify tissue differentiation and evaluate morphology (Mariño-Enríquez & Bovée, 2016; Schaefer *et al.*, 2018).

As opposed to “simple” sarcomas that harbour recurrent, specific alterations that give rise to potentially targetable tumourigenic processes, genomically “complex” STS pose a greater challenge in terms of developing novel and effective therapies due to the vast heterogeneity displayed in terms of underlying biology and clinical response. Therefore, there is currently a push to develop efficient patient stratification techniques that are based on molecular signatures such as gene expression, tumour microenvironment, and mutational status. Not only would this allow for the stratification and identification of patients most likely to benefit from a currently available therapies, but it would also give insights into potentially actionable molecular targets for the discovery and development of novel therapies for “complex” STS.

1.2 Receptor tyrosine kinase signalling

The transduction of biological signals through reversible phosphorylation cascades is integral to the physiological molecular processes that mediate cellular survival, proliferation, growth, migration, differentiation, and many others (Ardito *et al.*, 2017; Humphrey *et al.*, 2015). Phosphorylation is catalysed by a family of enzymes known as kinases that facilitate the transfer of phosphate groups from high-energy, donor molecules (such as adenosine triphosphate (ATP) or guanosine triphosphate (GTP)) to substrates such as proteins, lipids, and carbohydrates (Duong-Ly & Peterson, 2014; Roy *et al.*, 2019). Although both mediate phosphorylation, kinases are distinct from phosphorylases, which catalyse the addition of a phosphate group from an inorganic phosphate to a substrate (Pergolizzi *et al.*, 2017). The human genome contains 538 known protein kinases, making up approximately 2% of all human genes (Berndt *et al.*, 2017; Schwartz & Murray, 2011).

Protein kinases operate by phosphorylating substrate proteins at specific amino acid residues that contain free hydroxyl groups, namely serine, threonine, and tyrosine (although phosphorylation at other amino acid residues such as histidine and aspartate is also known) (Ardito *et al.*, 2017; Schwartz & Murray, 2011). The majority

of human protein kinases are serine/threonine kinases and phosphorylation of these amino acid residues occurs far more commonly than is observed with tyrosine phosphorylation. In fact, tyrosine phosphorylation is estimated to occur in as low as ~1-2% in the context of the whole phosphoproteome, compared to ~85% for serine and ~12% for threonine (Ardito *et al.*, 2017; Fabbro *et al.*, 2015; Nishi *et al.*, 2014; Tan & Huang, 2017).

Despite tyrosine phosphorylation being a relatively rare post-translational modification, tyrosine kinases constitute a large family of 90 known kinases and are an essential component in a variety of biochemical processes that maintain cellular homeostasis (Paul & Mukhopadhyay, 2004; Robinson *et al.*, 2000). Of these 90 tyrosine kinases, RTKs constitute the vast majority with 58 currently known and which all share similar molecular architectures and structures (Lemmon & Schlessinger, 2010).

RTKs are transmembrane, cell surface receptors that consist of an extracellular ligand-binding domain, a transmembrane α -helix domain, and a cytoplasmic tyrosine kinase domain (TKD) (**Figure 1.6**) (Lemmon & Schlessinger, 2010). The majority of RTKs are expressed on the cell surface as inactive monomers with a few exceptions such as insulin-like growth factor 1 receptor (IGF1R) and insulin receptor (InsR) that pre-exist as inactive dimers (Lemmon & Schlessinger, 2010; Ward *et al.*, 2007). In order to activate RTKs, receptor-specific ligands bind to the extracellular ligand-binding domains of monomeric RTKs, inducing them to form active dimers (and/or oligomers) with other ligand-bound RTK monomers (**Figure 1.6**) (Lemmon & Schlessinger, 2010). This ligand-induced dimerisation causes conformational changes to occur within the cytoplasmic TKDs, thereby initiating the kinase activity of the receptor.

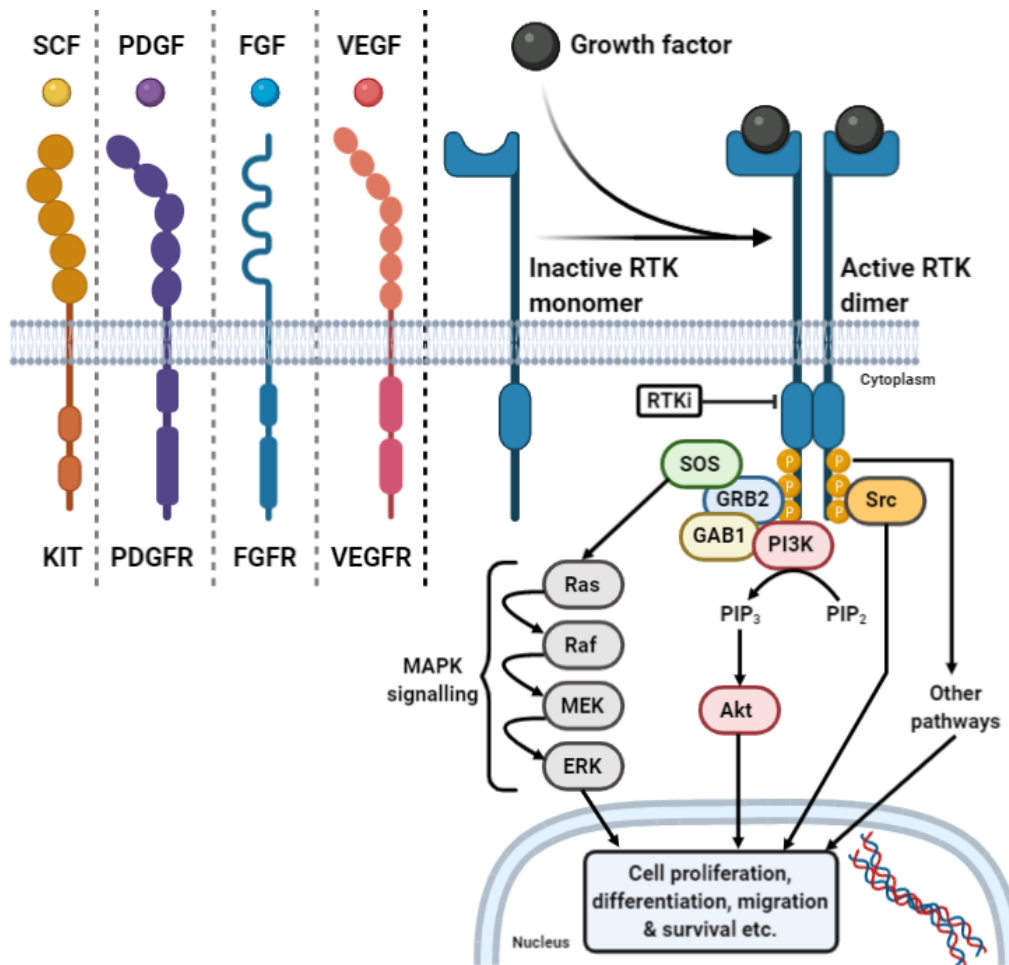


Figure 1.6: Canonical RTK activation and signalling. Archetypal RTK examples including KIT, platelet-derived growth factor receptor (PDGFR), fibroblast growth factor receptor (FGFR), and vascular endothelial growth factor receptor (VEGFR) shown with associated extracellular ligands, namely stem cell factor (SCF), PDGF, FGF, and VEGF, respectively. Ligand-induced dimerisation activates RTK autophosphorylation resulting in the recruitment of cytoplasmic effector proteins and activation of downstream signalling pathways MAPK, PI3K/Akt, Src, and others. Receptor tyrosine kinase inhibitors (RTKi) inhibit RTK phosphorylation through blockade of the ATP binding site in the tyrosine kinase domain (TKD) (Guo *et al.*, 2020; Lemmon & Schlessinger, 2010; Sugiyama *et al.*, 2019; Zhang & Yu, 2012). Image was created using BioRender. ERK; Extracellular signal-regulated kinase, GAB1: GRB2-associated-binding protein 1, GRB2; Growth factor receptor-bound protein 2, MAPK; Mitogen-activated protein kinase, MEK; Mitogen-activated protein kinase kinase, PI3K; Phosphoinositide 3-kinase, PIP₂; Phosphatidylinositol (4,5)-biphosphate, PIP₃; Phosphatidylinositol (3,4,5)-triphosphate, Raf; Rapidly accelerated fibrosarcoma, Ras; Rat sarcoma, RTK; Receptor tyrosine kinase, SOS; Son of sevenless.

The structure of TKDs are highly conserved within the RTK family however the activation mechanisms between family members differ significantly (Lemmon & Schlessinger, 2010; Roskoski Jr., 2005). TKDs consist of a bilobed architecture, composed of a smaller N-terminal lobe and a larger C-terminal lobe with a catalytic, ATP-binding site existing within the cleft of these lobes (**Figure 1.7**) (Roskoski Jr., 2005). In an inactive state, conserved regulatory structures within the TKDs, such as the activation loop and the α -C-helix, are configured in such a way that ATP and/or

protein substrate binding is obstructed (**Figure 1.7**) (Lemmon & Schlessinger, 2005; Roskoski Jr., 2005). Additionally, in a subset of RTKs, regulatory elements exist within the juxtamembrane and C-terminal tail regions that significantly interact with TKD configuration in order to stabilise the inactive conformation (Lemmon & Schlessinger, 2010; Roskoski Jr., 2005). These mechanisms of catalytic retardation are known as *cis*-inhibition and the specific mechanistic nature of this inhibition differs between RTK family members. However, in general, ligand binding and subsequent dimerisation results in rotation of the N- and C-terminal lobes and re-orientation of the α -C-helix and activation loop; opening the active site cleft for ATP to enter and bind for phosphate transfer (**Figure 1.7**) (Lemmon & Schlessinger, 2010; Roskoski Jr., 2005; Ségaliny, 2015). This initiates *trans*-autophosphorylation of activation loop tyrosine residues (and/or juxtamembrane/C-terminal tail regulatory tyrosine residues) and release of *cis*-autoinhibition, thereby stabilising the ATP-binding site and maintaining the TKD in its most catalytically active configuration (Lemmon & Schlessinger, 2010; Roskoski Jr., 2005).

Further *trans*-autophosphorylation events occur, firstly to fully stabilise the active conformation and enhance catalytic activity, before creating C-terminal phosphotyrosine “docking” sites for downstream effectors proteins harbouring Src homology (SH) 2 and phosphotyrosine-binding (PTB) domains, such as Src, phosphoinositide 3-kinase (PI3K), and growth factor receptor-bound protein 2 (GRB2) (**Figure 1.7**) (Lemmon & Schlessinger, 2010; Roskoski Jr., 2005; Wagner *et al.*, 2013). Recruitment of these signalling molecules results in the initiation of various downstream signal transduction pathways such as MAPK, PI3K/Akt, and Src pathways; signalling axes which are essential for many cellular phenotypes such as proliferation, differentiation, migration, and survival (**Figure 1.7**) (Mendoza *et al.*, 2011; Vyse & Huang, 2019; Zhang & Yu, 2012).

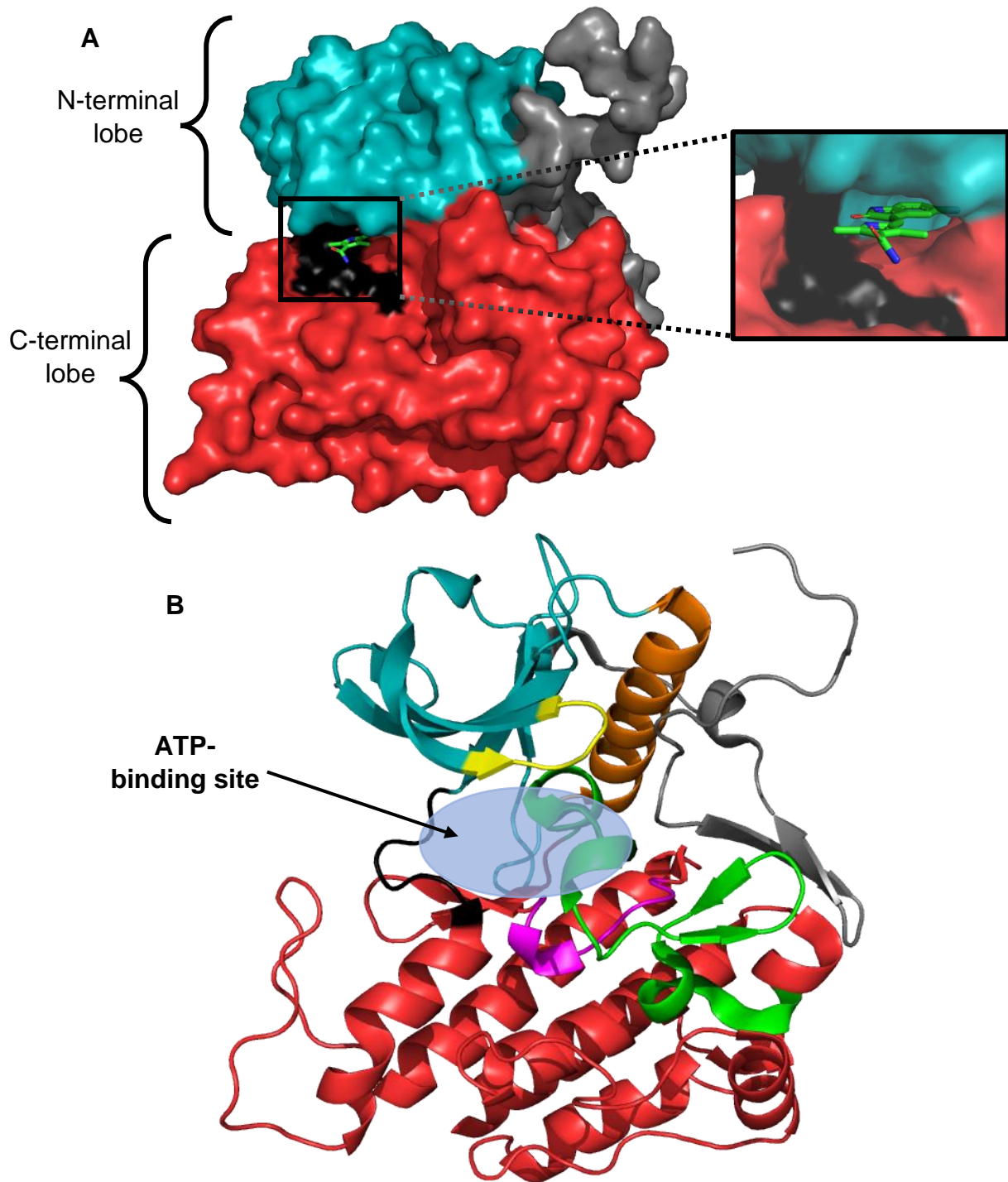


Figure 1.7: Prototypical RTK kinase domain architecture. (A) Structure of a prototypical RTK (KIT) tyrosine kinase domain (TKD) showing N-terminal lobe (blue), C-terminal lobe (red), juxtamembrane region (grey), and central bilobular cleft allowing for access to ATP-binding site (black). Inset: Zoomed image of ATP-binding site cleft showing blockade of ATP access to catalytic site by a receptor tyrosine kinase inhibitor (RTKI) (sunitinib). (B) Cartoon ribbon representation of the secondary structure, catalytic sites, and regulatory elements of a prototypical TKD (KIT). The catalytically important ATP-binding loop (yellow) and catalytic loop (pink) are shown to surround the central ATP-binding site. The regulatory C- α -helix (orange) and activation loop (green) are intrinsic to the activation and regulation of kinase activity. Images were created using PyMol 1.4 using the Protein Data Bank accession code 3G0E (KIT kinase domain in complex with sunitinib) (Gajiwala *et al.*, 2009; Roskoski Jr., 2005). ATP; Adenosine triphosphate, C-terminal; Carboxyl-terminal, N-terminal; Amino-terminal, RTK; Receptor tyrosine kinase.

1.2.1 Mitogen-activated protein kinase signalling

One of the most important signalling pathway cascades mediated by RTK activity is the MAPK signalling axis consisting of Ras, Raf, mitogen-activated protein kinase kinase (MEK), and extracellular signal-regulated kinase (ERK) (**Figure 1.6**) (McKay & Morrison, 2007; Mendoza *et al.*, 2011). As described above, canonical RTK activation creates phosphotyrosine docking sites for adaptor molecules such as GRB2 that, in turn, recruits Son of sevenless (SOS) to the receptor interface (Mendoza *et al.*, 2011; McKay & Morrison, 2007). To note, certain RTKs require additional unique docking proteins that bind and recruit GRB2 to propagate signals to the cell interior including the fibroblast growth factor receptor substrate 2 (FRS2) for fibroblast growth factor receptor (FGFR) signalling and insulin receptor substrates 1-4 (IRS1-4) for IGF1R/InsR signalling (Boucher *et al.*, 2014; Lemmon & Schlessinger, 2010; Mendoza *et al.*, 2011; Ornitz & Itoh, 2015). Furthermore, in certain RTK signalling contexts, the Src homology 2 domain-containing (SHC) family of docking proteins are utilised to localise GRB2 to the receptor interface (Ahmed & Prigent, 2017). SOS functions as a Ras-guanine nucleotide-exchange factor (GEF) which are proteins that catalyse the substitution of guanosine diphosphate (GDP) for GTP in order to activate GTPases, in this case Ras-GTPase (Mendoza *et al.*, 2011; Roberts & Der, 2007).

Ras GTPases are critical membrane-anchored signalling proteins that exist either in an inactive GDP-bound state or an active GTP-bound state (Gorfe, 2010; Mendoza *et al.*, 2011). RTK-complex bound SOS activates Ras by catalysing the release of bound GDP and facilitating the binding of GTP. Conversely, and counter-intuitively, GTPase-activating proteins (GAP) inactivate GTPases, such as Ras, by actuating the GTPases to hydrolyse their bound GTP to GDP and become inactive (Mendoza *et al.*, 2011). Activated Ras recruits cytosolic Raf serine/threonine kinase and localises it to the plasma membrane. Ras-induced activation of Raf is highly complex and consists of a number of biological mechanisms, including cycles of phosphorylation/dephosphorylation, dimerisation, intra- and inter-protein interactions, and membrane localisation (McKay & Morrison, 2007; Terrell & Morrison, 2019). Once activated, Raf phosphorylates and activates the MEK dual-specificity kinases that, in turn, phosphorylates and activates the ERK serine/threonine kinases (Roberts & Der, 2007). Finally, ERK phosphorylates and activates a large number of protein substrates (>160-~200) throughout the cell resulting in a wide array of cellular responses (McKay

& Morrison, 2007; Roberts & Der, 2007; Wortzel & Seger, 2011). However, the majority of ERK substrates are nuclear, such as transcription factors, owing to the ability of ERK to translocate to the nucleus. This therefore results in the modulation of gene expression, including critical genes regulating cellular proliferation, growth, and survival such as *JUN*, *MYC*, and *BCL2* (Lavoie *et al.*, 2020; Roberts & Der, 2007).

Aberrant signalling within the MAPK pathway can therefore have neoplastic consequences. For instance, oncogenic mutations in both Ras and Raf are commonly implicated in a range of cancers. Although sources vary, a common consensus of between ~15-30% of all human cancers harbour mutations in one of the three major isoforms of Ras (*KRAS*, *NRAS*, and *HRAS*) (Davies *et al.*, 2002; Downward, 2003; Hobbs *et al.*, 2016; Prior *et al.*, 2012; Roberts & Der, 2007). Similarly, activating mutations in the Raf isoform, *BRAF*, are also extremely common in cancers, especially melanomas (~50-60%), thyroid (~50-60%) and colorectal cancers (~8-15%) (Ascierto *et al.*, 2012; Fanelli *et al.*, 2020; Fukushima *et al.*, 2003; Holderfield *et al.*, 2014; Maurer *et al.*, 2011). This therefore highlights the importance of physiological RTK-MAPK signalling axis activity and regulation in order to maintain healthy cellular processes and avoid tumourigenic phenotypes.

1.2.2 Phosphoinositide 3-kinase/Akt signalling

Another major downstream signalling pathway initiated by RTK activation is the PI3K/Akt signalling axis (**Figure 1.7**). Canonical RTK activation recruits the GRB2 adaptor protein to the receptor complex (Lemmon & Schlessinger, 2010; Ornitz & Itoh, 2015; Sugiyama *et al.*, 2019). Following this, GRB2 recruits the docking protein GRB2-associated binder 1 (GAB1) which then becomes phosphorylated by cytosolic kinases (Ornitz & Itoh, 2015; Sugiyama *et al.*, 2019; Wang *et al.*, 2015). This provides phosphorylated docking sites for PI3K recruitment to the signalling complex, thereby activating it. Similar to MAPK signalling, certain RTK members harbour subtle differences in their signal propagation to PI3K such as SHC docking protein utilisation, FGFR signalling requiring FRS2 to recruit GRB2, and IGFR1R/InsR signalling completely replacing the GRB2/GAB1 complex with IRS1-4 (Ahmed & Prigent, 2017; Boucher *et al.*, 2014; Lemmon & Schlessinger, 2010; Ornitz & Itoh, 2015). In addition to indirect binding, PI3K can also bind directly to phosphotyrosine residues on RTKs

(Mendoza *et al.*, 2011; Sugiyama *et al.*, 2019). Activated PI3K acts as a lipid kinase that converts the phospholipid secondary messenger phosphatidylinositol 4,5-bisphosphate (PIP₂) to phosphatidylinositol (3,4,5)-triphosphate (PIP₃) on the inner cell membrane (Guo *et al.*, 2015; Manning & Toker, 2017; Yang *et al.*, 2019). Synthesis of PIP₃ recruits the serine/threonine kinase Akt and phosphoinositide-dependent protein kinase 1 (PDK1) to the cell membrane where Akt is phosphorylated and activated by PDK1 (Guo *et al.*, 2015; Mendoza *et al.*, 2011; Yang *et al.*, 2019). Activated Akt is then released from the cell membrane and travels to other subcellular locations to phosphorylate a wide array of substrates (~150) including mechanistic target of rapamycin (mTOR), glycogen synthase kinase 3 (GSK3), and forkhead box O (FOXO) (Agarwal, 2018; Guo *et al.*, 2015; Manning & Toker, 2017). PI3K/Akt signalling is therefore a crucial component in mediating important cellular processes, such as proliferation, metabolism, and survival, and dysregulation of this pathway is one of the most common oncogenic occurrences in cancer (Janku *et al.*, 2018; Madsen *et al.*, 2018; Manning & Toker, 2017).

In fact, recent studies have shown that mutations/alterations in two core genes of the PI3K/Akt signalling axis, phosphoinositide 3-kinase, catalytic, α polypeptide (*PIK3CA*) and phosphatase and tensin homolog (*PTEN*), are the most frequently mutated genes in more than 12 different solid tumour types, behind only *TP53* (Madsen *et al.*, 2018). In an oncogenic capacity, activating mutations in the *PIK3CA* gene, which encodes the catalytic subunit of PI3K, have been shown to be highly prevalent in a range of cancers, especially endometrial (~10-53%), breast (~7-35%), ovarian (~33%), and colorectal (~17-30%) (Madsen *et al.*, 2018; Thorpe *et al.*, 2015). Conversely, inactivation, suppression, or deletion of the tumour suppressor *PTEN* gene, also highly prevalent in many cancers (especially endometrial (~35%) and glioblastoma (~29%)), results in dysregulated and hyperactive PI3K/Akt signalling (Yin & Shen, 2008). This is due to the role of PTEN as a lipid phosphatase that dephosphorylates PIP₃ to PIP₂, thereby reversing PI3K activity and negatively regulating the PI3K/Akt signalling pathway (Milella *et al.*, 2015; Sugiyama *et al.*, 2019). Therefore, RTK signalling propagation via the PI3K/Akt signalling axis is an extremely important and tightly regulated signal transduction pathway in maintaining cellular homeostasis, with pathway dysregulation having potent oncogenic consequences.

1.2.3 Src signalling

Src kinase is a critical cellular signalling node that belongs to the eponymous Src family kinase group of non-receptor tyrosine kinases (Zhang & Yu, 2012). Prior to activation, Src exists as a membrane-anchored kinase consisting of four SH domains (SH1-4) that interact with one another to autoinhibit kinase activity and hold Src in a kinase-inactive state (Fajer *et al.*, 2017). In response to RTK activation, Src binds directly with RTK phosphotyrosine residues via its SH2 domain, thereby converting Src into a kinase-active conformation (**Figure 1.7**). This results in Src autophosphorylation and full activation of the kinase (Boczek *et al.*, 2019). Activation of Src then results in the regulation of a wide variety of downstream signalling molecules such as Akt, MAPKs, signal transducer and activator of transcription 3 (STAT3), and focal adhesion kinase (FAK) (Bromann *et al.*, 2004; Yeatman, 2004). Therefore, Src signalling is integral in mediating numerous, disparate cellular phenotypes that are regularly hijacked by cancers to promote oncogenic progression and metastasis such as cellular proliferation, adhesion, and migration/invasion. For instance, Src phosphorylates and regulates FAK activity, an integral component of focal adhesion complexes that regulate cellular motility and is, therefore, a major driver of metastasis in cancer (Martínez *et al.*, 2020; Yeatman, 2004). Additionally, Src-mediated modulation of Akt, MAPK, and STAT3 signalling pathways induces cellular responses relating to proliferation and survival (Zhang & Yu, 2012).

Therefore, Src overexpression and overactivity has been reported in many tumour types including colorectal, lung, and breast cancer (Chen *et al.*, 2014; Finn, 2008; Irby & Yeatman, 2000). Interestingly, activating *SRC* mutations are exceptionally rare in human cancers and oncogenic Src overactivity is primarily caused by increased gene expression (Wheeler *et al.*, 2009). Therefore, due to the role of Src as an important central signalling hub controlling a diverse array of cellular processes and the potent tumourigenic progression and metastatic dissemination that can occur due to Src pathway dysregulation, Src kinase is an extremely attractive target for targeted cancer therapeutics.

1.2.4 RTK-associated signalling cascade crosstalk

Although commonly modelled simplistically as linear signalling pathways downstream of RTKs, the MAPK, PI3K/Akt, and Src pathways have frequently been shown to engage in significant crosstalk. This crosstalk results in the signalling pathways co-regulating one another as well as various, critical biological processes. For instance, it is well established that the MAPK and PI3K/Akt signalling pathways participate in extensive crosstalk and pathway integration downstream of RTK signalling (Manning & Toker, 2017; Mendoza *et al.*, 2011). For example, ERK is known to phosphorylate the docking protein GAB1 at inhibitory phosphosites, thereby inhibiting GAB1-mediated recruitment of PI3K. Conversely, activated Akt has been shown to phosphorylate and inhibit Raf resulting in negative regulation of the MAPK signalling pathway. In contrast to negative regulation, components of the MAPK signalling pathway can also activate PI3K/Akt constituents such as the allosteric activation of PI3K by GTP-bound, active Ras. Similarly, activated ERK has been shown to induce mTOR activity through phosphorylation and disassociation of the tuberous sclerosis complex 1/2 (TSC1/2) complex, an inhibitory complex of mTOR signalling (Manning & Toker, 2017; Mendoza *et al.*, 2011). In addition to extensive crosstalk, many of the latter kinase components of the MAPK and PI3K/Akt pathway (e.g., ERK, Akt) have very broad substrate specificity resulting in significant overlap between target substrates. Therefore, ERK and Akt have often been reported to act upon the same substrate protein, such as FOXO, c-Myc, and GSK3, sometimes concurrently, to promote cell survival, proliferation, differentiation, and migration (Manning & Toker, 2017; Mendoza *et al.*, 2011).

As discussed previously, Src is a critical cellular signalling node that transduces RTK-associated signals to intracellular processes such as MAPK and PI3K/Akt signalling. Therefore, significant crosstalk exists between Src, MAPK and PI3K/Akt signalling pathways (Jiao *et al.*, 2018; Zhang & Yu, 2012). For instance, extensive studies have shown that Src signalling has been shown to activate the PI3K/Akt pathway through various means such as direct Akt phosphorylation, PTEN inhibition, and indirect PI3K p85 subunit activation (Beadnell *et al.*, 2018; Chen *et al.*, 2001; Lu *et al.*, 2003; Riggins *et al.*, 2003; Zhang & Yu, 2012). Similarly, Src activation of Ras is very well established and Src phosphorylation of Raf has also been reported – both of which activate the

MAPK signalling cascade (Kim *et al.*, 2009; Van der Geer *et al.*, 1996, Williams *et al.*, 1992; Zhang & Yu, 2012).

The MAPK, PI3K/Akt, and Src pathways represent critical biological processes that function to propagate biological signals from RTKs to the cell interior and nucleus, thereby regulating cell survival, proliferation, differentiation, and growth. In addition to their exclusive and independent processes, these signalling pathways extensively partake in inter-pathway crosstalk and signal convergence. In the context of cancer, these factors are important aspects to consider in the research of novel treatments and therapeutic resistance. This is because malignant cancer cells can evade therapeutic efficiency by co-opting and/or activating compensatory signalling networks in order to survive, proliferate, and grow (Grünewald *et al.*, 2020; Logue & Morrison, 2012; Trusolino & Bertotti, 2012; Von Manstein *et al.*, 2013).

1.2.5 RTK signalling in cancer

Due to their intrinsic role in signal transduction to induce a variety of cellular processes, aberrant RTK signalling is often observed in a wide range of cancers. Within cancers, RTK signalling is primarily dysregulated via one of four mechanisms: overexpression/amplification, activating mutations, chromosomal translocations, or autocrine activation (Du & Lovly, 2018; Lemmon & Schlessinger, 2010).

Genomic amplification and subsequent RTK overexpression are pathological events that lead to the accumulation of excessive RTK expression at the cell membrane. This, therefore, results in increased receptor dimerisation, dilution of negative regulatory mechanisms, and oncogenic signalling cascade overactivity (Du & Lovly, 2018). Consequently, RTK overexpression has been reported in a wide range of malignancies including PDGFR α in gliomas, epidermal growth factor (EGFR) in glioblastomas, FGFR1/3 in breast cancers, and human epidermal growth factor receptor 2 (HER2), MET, and EGFR in lung cancers (Alentorn *et al.*, 2012; An *et al.*, 2018; Du & Lovly, 2018; Helsten *et al.*, 2016; Hirsch *et al.*, 2009; Lemmon & Schlessinger, 2010; Navid *et al.*, 2020; Rosell *et al.*, 2020; Selvaggi *et al.*, 2004).

The emergence of a gain-of-function mutation in RTKs results in unregulated receptor activation and subsequent aberrant signal transduction to the cell interior. As such,

activating RTK mutations are functional drivers in a variety of cancers, with notable examples including *EGFR* and *KIT* mutations in non-small cell lung cancer (NSCLC) and GIST, respectively (Du & Lovly, 2018; Harrison *et al.*, 2020). In the case of *EGFR*, approximately 85-90% of *EGFR* mutations are described by the L858R point mutation or exon 19 deletions. These activating mutations destabilise the inactive receptor conformation resulting in increased receptor dimerisation and oncogenic activity (Du & Lovly, 2018; Harrison *et al.*, 2020). For GIST, the majority of mutations (~65%) occur in exon 11 of *KIT*, which encodes the receptor's autoinhibitory juxtamembrane domain (Corless *et al.*, 2004; Corless *et al.*, 2014). Therefore, mutations within this domain relieve the *cis*-autoinhibitory function, allowing for ligand-independent receptor dimerisation and activation (Corless *et al.*, 2004; Lemmon & Schlessinger, 2010). Other rarer, gain-of-function mutational sites for both these receptors exist such as *EGFR* exon 20 mutations in NSCLC, *EGFR* VIII extracellular domain mutations in glioblastoma, and extracellular/TKD *KIT* mutations, as well as *PDGFRA* mutations, in GIST (An *et al.*, 2018; Corless *et al.*, 2004; Corless *et al.*, 2014; Vyse & Huang, 2019). Activating mutations in other RTKs such as *FGFR* (e.g., *FGFR3* S249C) and *RET* (e.g., M918T) have also been extensively reported in cancers such as urothelial carcinomas and thyroid cancers, respectively (Garje *et al.*, 2020; Helsten *et al.*, 2016; Lima *et al.*, 2020; Romei *et al.*, 2018).

Chromosomal rearrangements that occur at RTK gene loci can lead to the formation of oncogenic RTK fusion proteins (Du & Lovly, 2018). Most often, these RTK fusion proteins consist of the TKD of the RTK fused to a section of another protein, thereby removing the regulatory RTK domains and resulting in a constitutively-active kinase (Du & Lovly, 2018; Medves & Demoulin, 2012). Therefore, RTK fusion proteins have commonly been identified as tumourigenic drivers in various cancer types including certain STS subtypes such as infantile fibrosarcoma and inflammatory myofibroblastic tumour (Antonescu *et al.*, 2015; Church *et al.*, 2018; Du & Lovly, 2018; Linch *et al.*, 2014; Schaefer *et al.*, 2018). Within these STS subtypes, the gene fusions of *ETV6-NTRK3* and *TPM3/TPM4/CLTC*-anaplastic lymphoma kinase (*ALK*) are pathognomonic for infantile fibrosarcoma and inflammatory myofibroblastic tumour, respectively, and result in constitutive and oncogenic RTK signalling (**Table 1.1**) (Linch *et al.*, 2014; Schaefer *et al.*, 2018; WHO, 2020). Oncogenic RTK signalling also occurs in dermatofibrosarcoma protuberans as a consequence of a chromosomal

rearrangement, however this occurs within the PDGFB ligand rather than the receptor itself. The collagen type I α 1 chain (COL1A1)-PDGFB fusion protein causes the constitutive transcription and expression of the PDGFB ligand, resulting in continuous receptor activation and subsequent oncogenic signal transduction (Noujaim *et al.*, 2015; Simon *et al.*, 2001; Thway *et al.*, 2016; WHO, 2020). Outside of sarcoma, chromosomal rearrangements of *ALK*, *RET*, and neurotrophic tyrosine kinase receptor (*NTRK*) RTKs have recurrently been detected in NSCLC and thyroid cancers, with *ALK* alterations being extremely common in anaplastic large cell lymphoma patients (Cocco *et al.*, 2018; Corte *et al.*, 2018; Du & Lovly, 2018; Pérot *et al.*, 2014; Santoro *et al.*, 2020; Solomon *et al.*, 2009).

The final principal mechanism of aberrant RTK signalling results from autocrine signalling (Du & Lovly, 2018; Lemmon & Schlessinger, 2010). RTK autocrine activation occurs when secreted growth factors and cytokines act upon the secretory cell itself rather than another target cell (Dođaner *et al.*, 2016). Dysregulated autocrine signalling in this manner creates constitutively activated signalling loops resulting in continuous RTK activation and subsequent tumourigenic intracellular signalling (Dođaner *et al.*, 2016). Furthermore, the intracellular signalling cascades often result in promoting expression of further growth factors or cytokines, thereby continuing the autocrine activation loop (Du & Lovly, 2018; Walsh *et al.*, 1991). Oncogenic autocrine signalling loops have been reported in a variety of cancers but notable examples include transforming growth factor α (TGF α)-EGF and stem cell factor (SCF)-KIT in lung cancers, as well as hepatocyte growth factor (HGF)-MET in haematological malignancies (Ciardiello & Tortora, 2001; Du & Lovly, 2018; Hibi *et al.*, 1991; Kentsis *et al.*, 2012; Krystal *et al.*, 1996).

Although these four processes represent the principal pathological mechanisms, research into the emerging mechanisms that aberrantly activate RTKs such as miRNA modulation, tumour microenvironment alterations, and signal attenuation by negative regulators is ongoing (Du & Lovly, 2018; Ledda & Paratcha, 2007; Tan *et al.*, 2018; Xu *et al.*, 2021).

1.2.6 Targeting RTKs for cancer therapy with tyrosine kinase inhibitors

Due to their critical role in the development and progression of many cancer types through various well-known and emerging mechanisms, RTKs represent an attractive target for cancer therapeutics. Therefore, developing tyrosine kinase inhibitors (TKIs) that target aberrant RTK signalling is a key goal in contemporary cancer research. In fact, there are now over 30 TKIs targeting RTKs (also termed RTKI) that have been approved for clinical use in cancer therapy (Thomson *et al.*, 2021). TKIs can be classified in a number of ways, either through their selectivity or binding mechanism. Firstly, TKIs can either be multi-target or selective (Guo & Ma, 2020; Thomson *et al.*, 2021). The first class describes TKIs that target a broad range of kinases non-specifically. Therefore, their inhibitory activity can have an effect on multiple intracellular signalling axes thereby increasing the potency of the inhibitor towards arresting cancer cell proliferation and/or survival. Additionally, the targeting of multiple pathways can aid to prevent signalling rewiring through compensatory signalling pathways, thereby helping to delay therapy resistance. However, this increased inhibition of multiple targets can also result in off-target effects and heightened toxicity in patients (Broekman *et al.*, 2011). The second class consists of TKIs that target a specific kinase or a kinase family with highly conserved structures (e.g., FGFR1/2/3/4) (Nakamura *et al.*, 2021). Although associated with reduced off-target effects, use of single-target TKIs often falls short of clinically meaningful activity in patients with cancers that are driven by multifactorial elements (Talevi, 2015).

TKIs can also be categorised based on their mechanism of binding kinases such as RTKs; irreversible or reversible. Irreversible TKIs, as the name suggests, form a strong, irreversible covalent bond with the kinase active site, most frequently with a nucleophilic cysteine residue located adjacent to the ATP-binding pocket (Garuti *et al.*, 2011; Wu *et al.*, 2015). This covalent bond holds the inhibitor in place and irreversibly blocks the binding of ATP to the kinase, thereby rendering the kinase inactive (Garuti *et al.*, 2011; Wu *et al.*, 2015). On the other hand, reversible TKIs form weaker intermolecular bonds, such as hydrogen bonds, with the kinase to elicit their inhibitory activity. These reversible TKIs can be further sub-divided into six different classes (Type I, I ½, II, III, IV, V) dependent on their mechanism and location of binding, as well as their inhibitor-bound kinase structure (Roskoski Jr., 2016; Thomson *et al.*, 2021; Wu *et al.*, 2015). For this final point about inhibitor-bound kinase structures, an

important detail in the classification of TKIs, especially I, I ½, and II, is the orientation of the highly conserved DFG (Asp-Phe-Gly) motif within the activation loop of the TKD (Thomson *et al.*, 2021; Roskoski Jr., 2016). As discussed previously, the activation loop controls access to the active site and ATP-binding pocket and the DFG component is an integral component of substrate binding and subsequent catalysis (Thomson *et al.*, 2021; Roskoski Jr., 2016).

Type I, I ½, and II TKIs are competitive inhibitors that bind to the ATP-binding site within the TKD of kinases. These TKIs compete with ATP molecules for binding into the adenine-binding pocket via hydrogen bonds to amino acid residues that exist within the active site cleft (Roskoski Jr., 2016; Thomson *et al.*, 2021; Wu *et al.*, 2015). Type I inhibitors bind to the active conformation of the TKD with the DFG motif-aspartate facing inwards towards the catalytic site. Similarly, type I ½ inhibitors also bind to the TKD with the DFG-aspartate facing inwards, however this class of inhibitor binds to the TKD in an inactive conformation. Type II inhibitors also bind to the inactive TKD conformation but with the DFG-aspartate protruding away from the catalytic, ATP-binding site (Roskoski Jr., 2016; Thomson *et al.*, 2021; Wu *et al.*, 2015). These three types are further classified as either “A” or “B” subtypes depending on where exactly the inhibitor binds within the ATP-binding site (Roskoski Jr., 2016). “A” subtypes bind to both the front and back cleft, as well as near the gatekeeper residue, whilst “B” subtypes do not bind to the back cleft (Roskoski Jr., 2016). As opposed to competitive inhibitors, Type III and IV TKIs are allosteric inhibitors that do not interact with the ATP-binding pocket. Type III inhibitors bind exclusively to proximal allosteric sites which are adjacent to the ATP-binding site. Conversely, type IV inhibitors bind to distal allosteric sites that are remote from the ATP-binding site (Roskoski Jr., 2016; Thomson *et al.*, 2021; Wu *et al.*, 2015). Finally, type V inhibitors refer to bisubstrate or bivalent inhibitors that can concurrently bind to two differing regions of the TKD (Gower *et al.*, 2014; Roskoski Jr., 2016).

In spite of these differences, the ultimate objective of utilising TKIs to inhibit kinases, including RTKs, is to block survival, migratory, and proliferation signalling pathways in cancer. However, although targeted TKI treatments are becoming increasingly widespread within contemporary cancer therapy, treatment with TKIs is susceptible to the acquisition of drug resistance in patients leading to disease relapse and progression. Additionally, patients can also harbour intrinsic resistance to treatment

and show no initial response at all (Lovly & Shaw, 2014). There is therefore a clinical need to understand the resistance mechanisms in response to TKI treatment in order to determine and develop salvage therapies that can be used to effectively treat TKI-resistant cancers.

1.3 Cancer therapeutics in soft tissue sarcoma

1.3.1 Chemotherapeutic landscape in soft tissue sarcoma

A subset of STS comprise aggressive cancers, with up to 50% of patients developing recurrent or metastatic disease despite optimal management of primary disease. At this advanced stage, STS are almost universally fatal with a median overall survival (mOS) of ~12-19 months (In *et al.*, 2017; Kasper *et al.*, 2014; Linch *et al.*, 2014). The treatment of localised and primary disease is surgical resection with curative intent with or without adjuvant or neoadjuvant radio/chemotherapy (Dangoor *et al.*, 2016). Unfortunately, STS are often primarily presented or frequently recur as inoperable and metastatic disease (Kasper *et al.*, 2014; Linch *et al.*, 2014). At this advanced stage, the cornerstone of first-line therapy remains cytotoxic anthracycline chemotherapy, most notably doxorubicin (Adriamycin[®]), with or without concomitant ifosfamide (Ifex[®]) (**Figure 1.8**) (D'Ambrosio *et al.*, 2020; Martín-Broto *et al.*, 2020). Although this treatment regimen remains the gold-standard for first-line therapy in advanced STS, certain histology-driven treatment paradigms are recommended (Linch *et al.*, 2014). For instance, recent studies have shown that leiomyosarcoma and solitary fibrous tumour may benefit from doxorubicin plus dacarbazine (DTIC[®]) in the first-line advanced setting (D'Ambrosio *et al.*, 2020; Martín-Broto *et al.*, 2020; Martín-Broto *et al.*, 2021; Smrke *et al.*, 2021). Similarly, chemotherapeutic regimens involving taxanes, gemcitabine (Gemzar[®]), and liposomal doxorubicin (Caelyx[®]) have been indicated for use in patients diagnosed with angiosarcoma (**Figure 1.8**) (Blay *et al.*, 2014; Linch *et al.*, 2014; Martín-Broto *et al.*, 2020). Differences in histological subtypes remain an important consideration for chemotherapeutic treatment decision making due to contrasting chemosensitivities. For example, Ewing sarcoma and embryonal rhabdomyosarcoma display very high chemosensitivity, synovial sarcoma and myxoid liposarcoma show potent, selective chemosensitivities to ifosfamide and trabectedin (Yondelis[®]), respectively, whilst certain sarcomas such as clear cell sarcoma,

dermatofibrosarcoma, and extraskelatal myxoid chondrosarcoma are highly chemoresistant (Blay *et al.*, 2014; Ward & Odili, 2018). As treatment proceeds through second and later lines of therapy following anthracycline failure, chemotherapeutics commonly utilised to treat STS include trabectedin, eribulin (Halaven®), and gemcitabine-based regimens (**Figure 1.8**) (Linch *et al.*, 2014; Martín-Broto *et al.*, 2020). Other considerations for chemotherapeutic selection are clinicopathological factors such as age and low performance status, where standard doxorubicin and ifosfamide-based chemotherapy would not be suitable due to cardiac toxicity and tolerability issues. In these cases, other chemotherapeutic tactics such as cyclophosphamide (Cytoxan®) plus prednisolone (Orapred®), or gemcitabine, would be more suitable (**Figure 1.8**) (Linch *et al.*, 2014; Mir *et al.*, 2011).

Despite these various treatment paradigms for STS patients, marginal progress has been made over the past two decades to increase the survival rates of patients, thereby highlighting the urgent need for novel therapies and treatment regimens (In *et al.*, 2017; Kasper *et al.*, 2014; Linch *et al.*, 2014).

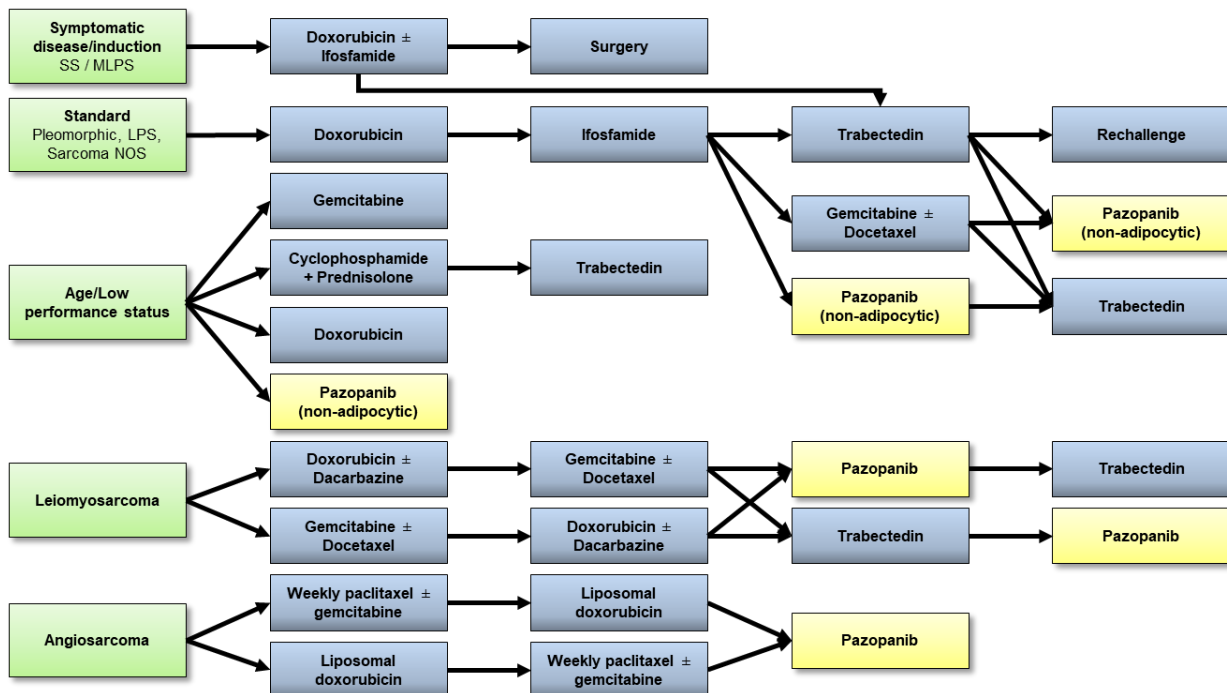


Figure 1.8: Recommended treatment paradigms for advanced STS. Recommended treatment pathways for advanced STS driven by disease aspects such as histology, presentation, and clinicopathological factors. Vertical columns do not display hierarchy of which agents should be used in preference to another (adapted from Linch *et al.*, 2014). LPS; Liposarcoma, MLPS; Myxoid liposarcoma, NOS; Not otherwise specified, SFT; Solitary fibrous tumour, SS; Synovial sarcoma.

1.3.2 Current perspectives of targeted therapies in soft tissue sarcoma

The heterogeneity of STS subtypes in terms of underlying biology and clinical response makes this group of neoplasms inherently difficult to treat effectively. The additional aspect of the rarity of the incorporated subtypes within the “STS” umbrella term results in difficulty in undertaking adequately powered phase III clinical trials in order to uncover novel treatments that can be used effectively in certain subtypes. As such, many clinical trials of potential therapies in STS are undertaken on a heterogeneous cohort that are made up of many differing subtypes, thereby resulting in a “one size fits all” paradigm where patients diagnosed with STS are given an identical treatment, regardless of the actual STS subtype presented (Mir *et al.*, 2016; Van der Graaf *et al.*, 2012).

One important exception to this is within the subtype of GIST, the most common STS subtype (~20% of annual STS diagnoses) (Ducimetière *et al.*, 2011; Judson *et al.*, 2017; Menge *et al.*, 2018). The underlying pathology, treatment response, and resistance mechanisms of GIST are far better understood than other STS and the current gold-standard treatment paradigm and search for novel therapies are guided by this understanding. Due to the characteristic presence of activating mutations in KIT and PDGFR α RTKs (seen in ~85% of GISTs) (**Table 1.1; Figure 1.5**), the TKI imatinib (Glivec[®]) is indicated as the primary treatment of patients with advanced or inoperable GIST (**Table 1.2**). Following disease relapse and progression with imatinib therapy, patients are subsequently treated with second- and third-line therapies which utilise the multi-target TKIs sunitinib (Sutent[®]) and regorafenib (Stivarga[®]), respectively (**Table 1.2**) (Corless *et al.*, 2011; Judson *et al.*, 2017; Wilding *et al.*, 2019). Recently, a fourth line therapy for GIST patients that have progressed on imatinib, sunitinib, and regorafenib, called ripretinib (Qinlock[®]), has been approved for clinical use (**Table 1.2**). Ripretinib is a switch control TKI that inhibits both KIT and PDGFR α through binding of both the kinase switch pocket and activation loop, forcing the RTK into an inactive conformation. This unique mechanism of TKI inhibition allows ripretinib to broadly inhibit all known clinically relevant KIT and PDGFR α primary and secondary mutations, including drug-resistance mutations that have arisen in response to previous multi-target TKI therapy (Smith *et al.*, 2019; Blay *et al.*, 2020). Additionally, in patients harbouring imatinib/sunitinib/regorafenib-resistant PDGFRA exon 18 mutations, including the D842V mutation (the primary driver mutation in ~5-6% of

GIST), a new TKI therapy called avapritinib (Ayvakyt[®]) has been approved for use in these patients (**Table 1.2**) (Heinrich *et al.*, 2020; Indio *et al.*, 2018).

In contrast, the mechanisms of targeted therapy response and resistance in non-GIST STS subtypes are currently not as well understood and approved targeted therapies for this broad range of malignancies are limited. Currently, there is only one TKI which has been approved for use in multiple subtypes of non-adipocytic, non-GIST STS and this is the orally bioavailable, multi-target kinase inhibitor pazopanib (Votrient[®]) (**Table 1.2**) (Lee *et al.*, 2019). Of note, there are targeted therapies that have been approved for a limited set of specific STS subtypes (**Table 1.2**). These subtypes of STS are in the first class of sarcomas that are characterised by specific pathognomonic genetic alterations but otherwise have relatively simple karyotypes (**Table 1.1**; **Figure 1.4 & 1.5**).

For instance, the multi-target TKI imatinib is approved for use in advanced and metastatic dermatofibrosarcoma protuberans (**Table 1.2**), a chemoresistant STS subtype that is one of the most common sarcomas of the dermis (McArthur *et al.*, 2005; Noujaim *et al.*, 2015). Dermatofibrosarcoma protuberans, in the majority of cases (>95%), is diagnosed via the presence of the *COL1A1-PDGFB* chimeric gene that fuses variable segments of the *COL1A1* gene to all of the *PDGFB* gene except for exon 1, which is known to contain transcription/translation repressor elements for *PDGFB* expression (Simon *et al.*, 2001; WHO, 2020). This, therefore, results in constitutive processing of the fusion gene that leads to synthesis of the COL1A1-PDGFB fusion protein. This fusion protein is then proteolytically modified to create mature, wild-type PDGFB ligand that subsequently binds and activates PDGFR β RTK in a constitutive and autocrine manner (Noujaim *et al.*, 2015; Simon *et al.*, 2001; Thway *et al.*, 2016; WHO, 2020). Constitutive PDGFR β activity results in overactivity of downstream intracellular, signalling cascades leading to oncogenic phenotypes such as unregulated cellular proliferation (Noujaim *et al.*, 2015; Thway *et al.*, 2016). Therefore, this dermatofibrosarcoma protuberans tumourigenesis pathway provides a rationale for targeting PDGFR β via imatinib therapy, which has subsequently shown preclinical and clinical utility leading to regulatory approval of imatinib in this disease (Greco *et al.*, 2001; McArthur *et al.*, 2005; Rutkowski *et al.*, 2010; Sjöblom *et al.*, 2001; Wilding *et al.*, 2019). However, translocation-negative dermatofibrosarcoma

protuberans remain resistant to imatinib therapy and further investigation into new therapies and regimens is needed for these tumours (Noujaim *et al.*, 2015).

Furthermore, the selective colony stimulating factor 1 receptor (CSF1R) inhibitor pexidartinib (Turalio®) has been approved for use in adult patients with symptomatic and unresectable tenosynovial giant cell tumours associated with severe morbidity and/or disabilities (**Table 1.2**) (Tap *et al.*, 2019). Tenosynovial giant cell tumours are neoplasms that most often arise from synovial tissue of the joints and tendon sheaths and are characterised by the collagen type VI α 3 chain (*COL6A3*)-*CSF1* translocation (Mastboom *et al.*, 2019; Tap *et al.*, 2019; West *et al.*, 2006; WHO, 2020). Similarly to dermatofibrosarcoma protuberans, this translocation results in the *COL6A3* promoter region being fused to the *CSF1* gene, thereby giving rise to aberrant CSF1 ligand overexpression. Chronic CSF1 secretion by tenosynovial giant cell tumour cells recruits CSF1R-expressing inflammatory cells such as monocytes and macrophages, leading to an abnormal accumulation of cells to form the tumour mass. Therefore, the majority of cells within these lesions (~84-98%) are not neoplastic and do not harbour the pathognomonic fusion but do highly express the CSF1R RTK (Mastboom *et al.*, 2019; West *et al.*, 2006). Therefore, pexidartinib is utilised to inhibit CSF1R activity in the recruited inflammatory cells thereby disrupting the neoplastic paracrine signalling events driving tenosynovial giant cell tumour progression (Palmerini *et al.*, 2020; West *et al.*, 2006).

Additionally, the EZH2 inhibitor tazemetostat (Tazverik®) has been approved for metastatic, unresectable, and/or locally advanced epithelioid sarcoma after the findings of a phase II multicentre trial (**Table 1.2**) (Gounder *et al.*, 2017; Stacchiotti *et al.*, 2019). As described previously, the vast majority of epithelioid sarcomas are characterised by the loss of tumour suppressor SMARCB1 function (**Table 1.1; Figure 1.5**). This results in destabilisation and pathological activity of the SWI/SNF remodelling complex and unregulated EZH2 histone methylation that, in turn, results in the transcriptional repression of a broad range of tumour suppressor genes (Bracken *et al.*, 2007; Gounder *et al.*, 2019). This understanding of the biology underpinning epithelioid sarcoma has resulted in the clinical evaluation and utilisation of tazemetostat in this rare disease. A 2019 clinical study of tazemetostat in epithelioid sarcoma showed complete (CR) (1.6%) or partial responses (PR) (13%) in a small subset of epithelioid sarcoma patients (objective response rate (ORR): 15%, according

to the response evaluation criteria in solid tumours (RECIST)) and a disease control rate (DCR) of 26% (Stacchiotti *et al.*, 2019).

In the distinct case of the virally induced Kaposi sarcoma, the immunomodulatory, thalidomide-analogue pomalidomide (Imnovid®) has recently been approved for use (**Table 1.2**). This indication is limited to AIDS-related Kaposi sarcoma patients that have previously been treated with highly active antiretroviral therapy (HAART), as well as HIV-negative patients (Gandhi *et al.*, 2014; Polizzotto *et al.*, 2016). Pomalidomide acts by binding and modulating the activity of cereblon; the substrate receptor of the cullin 4 ring E3 ubiquitin ligase complex (CRL4) (Davis *et al.*, 2017; Gandhi *et al.*, 2014; Lee *et al.*, 2017). An integral component of ubiquitination, E3 ubiquitin ligases catalyse the transfer of ubiquitin molecules from E2 ubiquitin-conjugating enzymes to protein substrates, targeting the protein for proteasomal degradation. As a result of pomalidomide treatment, cereblon activity is modulated to recruit, ubiquitinate, and subsequently destroy the transcription factors Ikaros and Aiolos (Davis *et al.*, 2017; Gandhi *et al.*, 2014; Lee *et al.*, 2017). Degradation of these substrates results in increased expression of interleukin-2 (IL-2) and other cytokines that are known to activate T cell function and immune response (Davis *et al.*, 2017; Gandhi *et al.*, 2014; Lee *et al.*, 2017). These immunomodulatory effects of pomalidomide, in conjunction with observed antiangiogenic and antiproliferative properties, has resulted in effective antineoplastic responses in Kaposi sarcoma patients, regardless of HIV status (Polizzotto *et al.*, 2016).

Although not specific to STS, two tissue-agnostic small molecule inhibitors for the treatment of adult and paediatric patients with metastatic, advanced, and/or unresectable solid tumours harbouring *NTRK* gene fusions has recently been approved for use (**Table 1.2**). These inhibitors are larotrectinib (Viktrakvi®) and entrectinib (Rozlytrek®) which bind to and inhibit the activity of NTRK RTKs. NTRKs are receptors that are most commonly expressed on the surface of neural cells and bind neurotrophic growth factors to transduce biological signals. They are therefore an essential component of neuron cell survival, differentiation, and innervation (Marlin & Li, 2015). *NTRK* translocations and genetic aberrations can lead to the formation of oncogenic *NTRK* gene fusions that are aberrantly expressed. In addition to pathological overexpression, the resultant fusion protein is constitutively activated independent of ligand binding (Cocco *et al.*, 2018; Wilding *et al.*, 2020). *NTRK* fusions

have been found to occur in a diverse range of malignancies, with up to 1% of cancers postulated to harbour such mutations (Cocco *et al.*, 2018; Drilon *et al.*, 2018; Wilding *et al.*, 2020). Within STS, *NTRK* fusions have been reported in various STS subtypes including uterine leiomyosarcoma, spindle cell sarcomas, and *KIT/PDGFR*A-mutation-negative GIST. Importantly, the *ETV6-NTRK3* fusion is the pathognomonic (~70% of cases), oncogenic driver of infantile fibrosarcoma, a locally aggressive malignancy occurring most commonly during infancy, with the remainder of cases primarily consisting of *NTRK1/2/3* fused to other gene partners (Church *et al.*, 2018; WHO, 2020; Wilding *et al.*, 2020). Approval of larotrectinib and entrectinib was based on the findings of multiple, multicentre clinical trials which enrolled patients with a variety of differing solid tumour types, including a relatively large proportion of STS, that harboured *NTRK* alterations (Drilon *et al.*, 2017; Drilon *et al.*, 2018; Wilding *et al.*, 2019). The findings of these trials displayed a significant antitumour effect in *NTRK*-gene fusion tumours upon treatment with larotrectinib and entrectinib and therefore supports the use of these inhibitors in the treatment of *NTRK*-gene fusion positive STS (Doebele *et al.*, 2015; Wilding *et al.*, 2019; Wilding *et al.*, 2020). Further work is currently ongoing for patients that progress on larotrectinib or entrectinib treatment due to the acquirement of drug resistance mutations, with the commencement of clinical phase I-II trials of selitrectinib (LOXO-195) (NCT03215511) (Hyman *et al.*, 2019).

Similar to the tissue-agnostic approval of the *NTRK* inhibitors, the immunotherapy, humanised antibody pembrolizumab (Keytruda®) has been approved for use in advanced, unresectable solid tumours that are microsatellite instability-high, mismatch repair deficient, or tumour mutational burden-high (as determined by an FDA-approved test), which have progressed on previous therapies and with no alternative satisfactory treatment (**Table 1.2**) (Le *et al.*, 2015; Le *et al.*, 2017; Marabelle *et al.*, 2020). Pembrolizumab is an immune checkpoint inhibitor that binds and inhibits programmed cell death protein 1 (PD-1) (Marabelle *et al.*, 2020). In a physiologically healthy system, PD-1 is expressed on the surface of T lymphocytes (as well as other immune cells) and binds to programmed death-ligand 1 (PD-L1) on the surface of normal, healthy tissue, thus preventing T cell-mediated cell death of the PD-L1-presenting cells (Vaddepally *et al.*, 2020). Highly immunogenic cancer cells often overexpress PD-L1 to escape destruction by the immune system through binding PD-

1 and inhibiting the T cell immune response. Pembrolizumab functions by blocking the binding of PD-1 to PD-L1, thereby activating and enhancing the T cell immune response in order to destroy the cancer cells (Vaddepally *et al.*, 2020).

Table 1.2: Currently approved targeted therapies for use in STS with given clinical indications and molecular targets.					
Approved targeted therapies	Trade name	Indication	FDA approval date	Molecular target(s)	Clinical trial(s) leading to regulatory approval
Pazopanib	Votrient®	Adv. non-adipocytic/GIST STS PT. chemotherapy	2012	Multiple RTKs including PDGFRs, VEGFRs, and KIT	NCT00753688; Van der Graaf <i>et al.</i> , 2012
Imatinib	Glivec®	Adv. GIST	2002	Multiple kinases including Abl1, Bcr-Abl1, PDGFRs, and KIT	Demetri <i>et al.</i> , 2002
		Adv. DFSP	2006		NCT00122473; McArthur <i>et al.</i> , 2005
Sunitinib	Sutent®	Adv. GIST PT. imatinib	2006	Multiple RTKs including PDGFRs, VEGFRs, and KIT	NCT00075218; Demetri <i>et al.</i> , 2006
Regorafenib	Stivarga®	Adv. GIST PT. imatinib/sunitinib	2013	Multiple RTKs including PDGFRs, VEGFRs, and KIT	NCT01271712; Demetri <i>et al.</i> , 2013
Avapritinib	Ayvakyt®	Adv. GIST with <i>PDGFRA</i> exon 18 mutations, including D842V mutations	2020	KIT/PDGFR α , including PDGFR α D842V & KIT D816V mutations	NCT02508532; Heinrich <i>et al.</i> , 2020
Ripretinib	Qinlock®	Adv. GIST PT. imatinib/sunitinib/regorafenib	2020	KIT/PDGFR α	NCT03353753; Blay <i>et al.</i> , 2020
Tazemetostat	Tazverik®	Adv. Epithelioid sarcoma not eligible for complete resection	2020	EZH2	NCT02601950; Stacchiotti <i>et al.</i> , 2019
Larotrectinib	Viktrakvi®	Adv. solid tumours harbouring NTRK fusions , with no known acquired resistance mutations or alternative satisfactory treatment	2018	NTRKs	NCT02122913; NCT02637687; NCT02576431; Drilon <i>et al.</i> , 2018
Entrectinib	Rozlytrek®	Adv. solid tumours harbouring NTRK fusions , with no known acquired resistance mutations or alternative satisfactory treatment	2019	NTRKs	NCT02097810; NCT02568267; Drilon <i>et al.</i> , 2017
Pexidartinib	Turalio®	Adv. symptomatic TGCT with severe morbidity/functional limitations and surgically unresponsive	2019	CSF1R	NCT02371369; Tap <i>et al.</i> , 2019
Pomalidomide	Imnovid®	AIDS-related Kaposi sarcoma PT. HAART and HIV-negative Kaposi sarcoma	2020	Cereblon	NCT01495598; Polizzotto <i>et al.</i> , 2016
Pembrolizumab	Keytruda®	Adv. unresectable solid tumours that are microsatellite instability-high or mismatch repair deficient , with no alternative satisfactory treatment	2017	PD-1	NCT01876511; Le <i>et al.</i> , 2015; Le <i>et al.</i> , 2017
		Adv. unresectable solid tumours that are tumour mutational burden-high (as determined by an FDA-approved test), with no alternative satisfactory treatment	2020		NCT02628067; Marabelle <i>et al.</i> , 2020

Adv.; Advanced, AIDS; Acquired immunodeficiency syndrome, Bcr; Breakpoint cluster region protein, CSF1R; Colony stimulating factor 1 receptor, DFSP; Dermatofibrosarcoma protuberans, EZH2; Enhancer of zeste homolog 2, FDA; Food & Drug Administration, GIST; Gastrointestinal stromal tumour, HAART; Highly active antiretroviral therapy, NTRK; Neurotrophic tyrosine kinase receptor, PD-1; Programmed cell death protein 1, PDGFR(A α); Platelet-derived growth factor receptor (A α), PT; Previously treated with, RTK; Receptor tyrosine kinase, STS; Soft tissue sarcoma, TGCT; Tenosynovial giant cell tumour, VEGFR; Vascular endothelial growth factor receptor.

Broadly speaking, STS are considered relatively non-immunogenic with low tumour mutational burden compared to other cancer types and therefore the utility of immune checkpoint inhibitors in STS may be limited (Petitprez *et al.*, 2020; Vyse *et al.*, 2021). Despite this, a recent study has reported that within the genetically “complex” STS subgroup exists a subset of relatively immunogenic STS that harbour high levels of tumour mutational burden, immune infiltrate, and tertiary lymphoid structures (TLS)

(Petitprez *et al.*, 2020). Petitprez *et al.* reported that these immunogenic STS had improved survival and high response rate to pembrolizumab therapy compared to the remainder of the evaluated STS cohort. Although further investigation into predictive biomarkers and patient stratification techniques is warranted, this study provides compelling, preliminary evidence to the existence of a group of immunogenic STS patients that may be more likely to significantly benefit from immune checkpoint immunotherapy (Petitprez *et al.*, 2020; Vyse *et al.*, 2021).

Despite the progress made in developing approved therapies for specific, genomically “simple” STS (as well as tissue-agnostic therapies selective for particular molecular signatures and genotypes), limited approved targeted therapies exist for a broad range of STS subtypes, especially the more genetically “complex” sarcomas such as liposarcoma, leiomyosarcoma, and undifferentiated pleomorphic sarcoma. Additionally, there are currently no targeted therapy treatment options to combat first-line targeted therapy resistance for non-GIST STS. There is therefore an unmet clinical need to develop further novel and effective targeted therapies for a broader range of STS subtypes.

1.3.3 Multi-target tyrosine kinase inhibitors in soft tissue sarcoma

As shown in **Table 1.2**, the majority of approved targeted therapies for clinical use in STS are multi-target TKIs that primarily target angiogenic and growth-promoting RTKs such as VEGFRs, PDGFRs, FGFRs, and KIT (Davis *et al.*, 2011; Zopf *et al.*, 2016; Patwardhan *et al.*, 2016; Wilding *et al.*, 2019; Xie *et al.*, 2018). Despite this, there is currently only one TKI - pazopanib - that is approved for a broad range of STS subtype and this therapy has well-described issues with clinical efficacy and drug resistance (Lee *et al.*, 2019). In order to develop more treatment options for patients with STS, investigation into the preclinical and clinical efficacy of further multi-target TKIs in STS remains a cornerstone of contemporary sarcoma research. There are currently a wide variety of multi-target TKIs that are undergoing various stages of clinical evaluation in STS including regorafenib, sitravatinib, anlotinib, sunitinib, sorafenib (Nexavar®), axitinib (Inlyta®), cediranib (Recentin®), dasatinib (Sprycel®), imatinib, crizotinib (Xalkori®), and nintedanib (Ofev®/Vargatef®) (**Table 1.3; Figure 1.9**). These TKIs primarily target multiple RTKs (**Table 1.3; Figure 1.9**) and elicit their inhibition through

reversible blockade of the TKD ATP-binding pocket, thereby inhibiting *trans*-autophosphorylation and activation of downstream signalling cascades (Jiao *et al.*, 2018).

Table 1.3: Selectivity profiles of commonly targeted tyrosine kinases by multi-target TKIs that are currently undergoing clinical evaluation in STS, with either known or proposed binding mode type.		
TKIs (type)	Commonly targeted tyrosine kinases in order of selectivity	References
Pazopanib (I)	PDGFRβ < KIT < PDGFRα < CSF1R < VEGFR1 = VEGFR2 < VEGFR3 << FGFR2 < RET < Abl1 < FGFR3 < FGFR1 << MET < ALK < FGFR4 = Src (K_d)	Davis <i>et al.</i> , 2011
Regorafenib (II)	RET < PDGFRβ < PDGFRα < VEGFR1 < Abl1 < KIT < VEGFR3 < CSF1R < VEGFR2 << NTRK3 (K_d)	Zopf <i>et al.</i> , 2016
Sitravatinib (II)	VEGFR3 < VEGFR2 = NTRK1 < VEGFR1 = KIT < NTRK2 < MET < PDGFRα < RET << Src << CSF1R < Abl1 (IC_{50})	Patwardhan <i>et al.</i> , 2016
Anlotinib (II)	VEGFR2 < VEGFR3 < KIT < VEGFR1 << PDGFRβ (IC_{50})	Xie <i>et al.</i> , 2018
Sunitinib (I $\frac{1}{2}$ - II)	PDGFRβ < KIT < PDGFRα < VEGFR2 < VEGFR1 < CSF1R < RET << VEGFR3 << NTRK1 << ALK << Abl1 < FGFR3 << FGFR1/2 < NTRK2 << FGFR4 = Src << NTRK3 << MET (K_d)	Davis <i>et al.</i> , 2011
Sorafenib (II)	RET < CSF1R = KIT < VEGFR1 < PDGFRβ < VEGFR2 < PDGFRα < VEGFR3 < Abl1 << NTRK3 << NTRK2 << FGFR2 < FGFR1 << FGFR3 << FGFR4 < NTRK1 (K_d)	Davis <i>et al.</i> , 2011
Axitinib (II)	PDGFRα < PDGFRβ < KIT < VEGFR1 < VEGFR2 < CSF1R < Abl1 < FGFR2 < RET < VEGFR3 < FGFR3 < FGFR1 << MET << NTRK1 (K_d)	Davis <i>et al.</i> , 2011
Cediranib (I or II)	PDGFRβ < KIT < PDGFRα < VEGFR1 < VEGFR2 < VEGFR3 < RET < RET < FGFR3 < FGFR2 < FGFR1 < Src < Abl1 << EGFR << MET << FGFR4 << ALK (K_d)	Davis <i>et al.</i> , 2011
Dasatinib (I – I $\frac{1}{2}$)	Abl1 < Src < PDGFRα < CSF1R < PDGFRβ < KIT << EGFR << RET << FGFR2 << VEGFR2 << FGFR1 < FGFR3 << VEGFR1 (K_d)	Davis <i>et al.</i> , 2011
Imatinib (II)	Abl1 < CSF1R < KIT < PDGFRβ < PDGFRα (K_d)	Davis <i>et al.</i> , 2011
Crizotinib (I – I $\frac{1}{2}$)	MET < ALK < NTRK2 << Abl1 < NTRK3 < NTRK1 << CSF1R << Src << RET < VEGFR1 < EGFR < FGFR3 (K_d)	Davis <i>et al.</i> , 2011
Nintedanib (II)	VEGFR2 < NTRK1 < KIT < PDGFRβ < PDGFRα < NTRK2 < ALK < RET < NTRK3 < CSF1R < VEGFR1 < FGFR1 < FGFR3 < VEGFR3 << MET < Abl1 << FGFR2 << Src << FGFR4 (K_d)	Davis <i>et al.</i> , 2011

Key: K_d or IC_{50} (x) of; $x \leq 1$ nM, $1 < x < 10$ nM, $10 \leq x < 50$ nM, $50 \leq x < 100$ nM, $x \geq 100$ nM

ALK; Anaplastic lymphoma kinase, CSF1R: Colony stimulation factor 1 receptor, FGFR(1/2/3/4); Fibroblast growth factor receptor (1/2/3/4), IC_{50} ; Inhibitory constant, K_d ; Dissociation constant, NTRK(1/2/3); Neurotrophic tyrosine kinase receptor (1/2/3), PDGFR(α/β); Platelet-derived growth factor receptor (α/β), RET; Rearranged during transfection, TKI; Tyrosine kinase inhibitor, VEGFR(1/2/3); Vascular endothelial growth factor receptor (1/2/3) (adapted from Wilding *et al.*, 2019) (Jiang *et al.*, 2021; Roskoski Jr. *et al.*, 2016; Wedge *et al.*, 2005; Xie *et al.*, 2018).

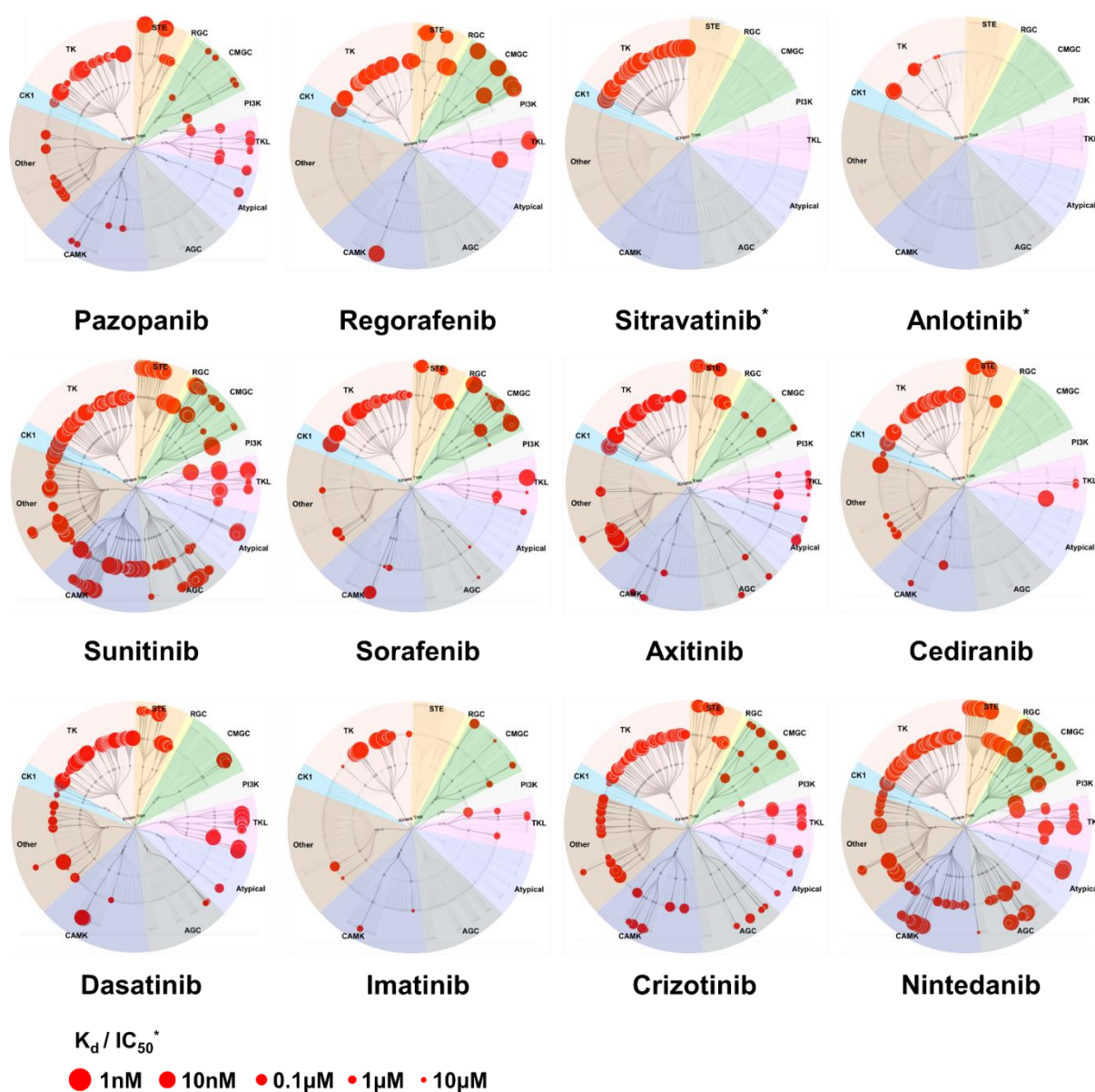


Figure 1.9: Kinase selectivity maps. Kinome-wide profiling measuring the dissociation constant (K_d) or inhibitory constant (IC_{50}) of the TKIs outlined in **Table 1.3** (adapted from Wilding *et al.*, 2019). The K_d data for pazopanib, sunitinib, sorafenib, axitinib, cediranib, dasatinib, imatinib, crizotinib, and nintedanib were obtained from PMID: 22037378 (Davis *et al.*, 2011). The K_d data for regorafenib were obtained from PMID: 27734608 (Zopf *et al.*, 2016). The IC_{50} data for sitravatinib and anlotinib were obtained from PMID: 26675259 and PMID: 29446853, respectively (Patwardhan *et al.*, 2016; Xie *et al.*, 2018). AGC; Protein kinases A, G, and C, CAMK; Ca²⁺/calmodulin-dependent protein kinase, CK1; Casein kinase 1, CMGC; Cyclin-dependent kinase, mitogen-activated protein kinase, glycogen synthase kinase, and cyclin-dependent-kinase-like kinase, PI3K; Phosphoinositide 3-kinase, PMID; PubMed identifier, RGC; Receptor guanylate cyclase, STE; Sterile kinase, TK; Tyrosine kinase, TKL; Tyrosine kinase-like.

1.3.3.1 Preclinical characterisation of multi-target tyrosine kinase inhibitors

The preclinical characterisation of the multi-target, antiangiogenic TKIs listed in **Table 1.3** have mostly followed parallel drug discovery pathways starting with the identification of candidate compounds through biochemical screens of VEGFR2 kinase inhibition (Dumas *et al.*, 2005; Harris *et al.*, 2008; Hu-Lowe *et al.*, 2008; Roth *et al.*, 2009; Sun *et al.*, 2003; Wedge *et al.*, 2005; Xie *et al.*, 2018). Exceptions to this are sorafenib, imatinib, crizotinib, and dasatinib which were discovered through biochemical kinase screens to assess for potent inhibition of C-Raf, Abl kinases, MET, and Src family kinases, respectively (Buchdunger *et al.*, 1996; Lombardo *et al.*, 2004; Wilhelm *et al.*, 2004; Zou *et al.*, 2007). Additionally, the preclinical characterisation data for sitravatinib are not currently publicly available (Wilding *et al.*, 2019).

For those inhibitors discovered via VEGFR2 kinase inhibitory screens, as well as sorafenib, these multi-target TKIs have been found to potently inhibit VEGF-induced VEGFR2 autophosphorylation in human umbilical vein endothelial cells (HUVECs), with associated decreases in endothelial cell proliferation, migration, and tube formation (Gomez-Rivera *et al.*, 2007; Hilberg *et al.*, 2008; Hu-Lowe *et al.*, 2008; Kumar *et al.*, 2007; Mendel *et al.*, 2003; Roth *et al.*, 2009; Schmieder *et al.*, 2014; Wedge *et al.*, 2005; Wilhelm *et al.*, 2004; Wilhelm *et al.*, 2011; Xie *et al.*, 2018). The preclinical antiangiogenic properties of these TKIs were also found to translate into an *in vivo* setting. Treatment of murine xenograft models of various cancer types with these TKIs resulted in significant reductions in microvessel area, microvessel density, and/or qualitative tumour vascularity (Daudigeos-Dubus *et al.*, 2015; Gomez-Rivera *et al.*, 2007; Hilberg *et al.*, 2008; Hu-Lowe *et al.*, 2008; Kumar *et al.*, 2007; Liu *et al.*, 2006; Mendel *et al.*, 2003; Rössler *et al.*, 2011; Schmieder *et al.*, 2014; Wedge *et al.*, 2005; Wilhelm *et al.*, 2004; Xie *et al.*, 2018; Zhang *et al.*, 2009). Additionally, these TKIs were found to elicit antimetastatic *in vivo* effects on tumour xenograft models of various cancers with significant decreases in tumour perfusion, vascular permeability, extravasation, and/or formation of metastases. (Gril *et al.*, 2011; Hilberg *et al.*, 2008; Hu-Lowe *et al.*, 2008; Murray *et al.*, 2003; Najy *et al.*, 2012; Rössler *et al.*, 2011; Schmieder *et al.*, 2014; Yin *et al.*, 2010; Zhang *et al.*, 2009). As well as their antiangiogenic and antimetastatic attributes, these multi-target TKIs were also found to exhibit direct antitumour effects through their potent inhibition of growth-promoting

RTKs such as PDGFRs, FGFRs, and KIT (**Table 1.3; Figure 1.9**). This inhibitory capability has been extensively reported to result in reductions in proliferation and migration in various cell line models across differing cancer types, as well as reductions in bulk tumour growth in a range of xenograft models (Daudigeos-Dubus *et al.*, 2015; Gomez-Rivera *et al.*, 2007; Hilberg *et al.*, 2008; Hu-Lowe *et al.*, 2008; Kumar *et al.*, 2007; Liu *et al.*, 2006; Mendel *et al.*, 2003; Murray *et al.*, 2003; Najy *et al.*, 2012; Patwardhan *et al.*, 2016; Rössler *et al.*, 2011; Roth *et al.*, 2009; Schmieder *et al.*, 2014; Sun *et al.*, 2003; Wedge *et al.*, 2005; Wilding *et al.*, 2019; Wilhelm *et al.*, 2004; Wilhelm *et al.*, 2011; Xie *et al.*, 2018; Yin *et al.*, 2010; Zhang *et al.*, 2009; Zopf *et al.*, 2016).

Similar preclinical characterisation data has been reported with imatinib, crizotinib, and dasatinib. For instance, treatment of *in vitro* and *in vivo* preclinical models of solid and haematological malignancies with imatinib, crizotinib, or dasatinib has extensively been reported to result in antitumour and antimetastatic effects (Araujo & Logothetis, 2010; Beran *et al.*, 1998; Buchdunger *et al.*, 1996; Carroll *et al.*, 1997; Deininger *et al.*, 1997; Druker *et al.*, 1996; Heinrich *et al.*, 2000; Lombardo *et al.*, 2004; O'Hare *et al.*, 2005; Shah *et al.*, 2006; Tuveson *et al.*, 2001; Zou *et al.*, 2007). Additionally, crizotinib has also been shown to have antiangiogenic properties in both *in vitro* and *in vivo* models. For example, in HUVEC and human microvascular endothelial cells (HMVECs), crizotinib was found to inhibit HGF-stimulated MET phosphorylation and endothelial tube formation (Zou *et al.*, 2007). This effect was translated into an *in vivo* effect where crizotinib treatment reduced microvessel area in MET-dependent murine xenografts of glioblastoma, lung, and gastric cancers (Wilding *et al.*, 2019; Zou *et al.*, 2007).

Building on the promising anticancer properties of these targeted therapies in a variety of preclinical cancer models, the effectiveness of multi-target TKIs in the context of STS has been extensively evaluated in a number of preclinical and clinical studies.

1.3.3.2 Pazopanib

As stated previously, pazopanib is the first, and currently only TKI, that is approved for the treatment of a broad range of advanced, non-adipocytic, non-GIST STS subtypes, following disease progression on chemotherapy (**Figure 1.8; Table 1.2**). Pazopanib is an orally bioavailable, multi-target, type I TKI that is often described as an

antiangiogenic therapy through its inhibition of VEGFR-mediated angiogenesis but is also thought to have direct antitumour effect through its inhibition of growth-promoting RTKs such as PDGFR, FGFR, and KIT (**Table 1.3; Figure 1.9**) (Roskoski Jr., 2016). Pazopanib was firstly approved for use in advanced renal cell carcinoma before going on to be evaluated preclinically and clinically for use in advanced STS (Cella & Beaumont, 2016; Lee *et al.*, 2019). The skeletal formula structure of pazopanib is shown in **Figure 1.10**.

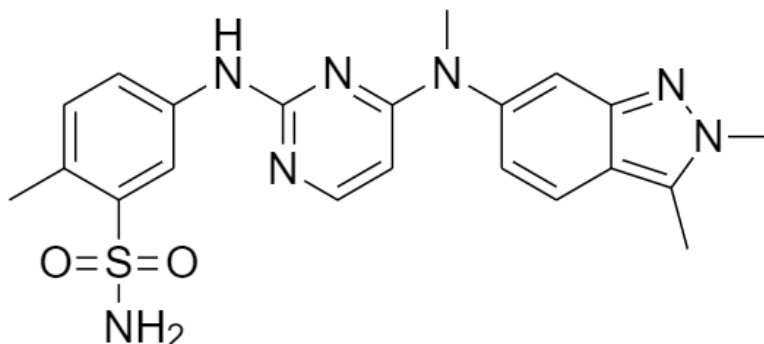


Figure 1.10: Skeletal formula structure of pazopanib. Figure was created using ChemOffice+ Cloud (PerkinElmer).

1.3.3.2.1 Preclinical evaluation of pazopanib in soft tissue sarcoma

The vast majority of preclinical cell models of STS have been shown to be relatively resistant to pazopanib treatment *in vitro* (Becker *et al.*, 2016; Teicher *et al.*, 2015; Wong *et al.*, 2016). However, pazopanib has shown potent antiproliferative effects in cell line and patient-derived cell models within certain subtypes of STS including malignant rhabdoid tumour, leiomyosarcoma, synovial sarcoma, clear cell sarcoma, and intimal sarcoma (Fleuren *et al.*, 2017; Hosaka *et al.*, 2012; Lanzi *et al.*, 2019; Outani *et al.*, 2014; Qiao *et al.*, 2017; Sanada *et al.*, 2019; Teicher *et al.*, 2015; Vyse *et al.*, 2018; Wong *et al.*, 2016). These antiproliferative effects were almost universally concurrent with decreases in PDGFR α and Akt phosphorylation, with blockade of the MAPK and MET pathways also occasionally reported (Fleuren *et al.*, 2017; Hosaka *et al.*, 2012; Lanzi *et al.*, 2019; Outani *et al.*, 2014; Wong *et al.*, 2016). Furthermore, the antiproliferative effects of pazopanib were found to be primarily cytostatic, rather than cytotoxic, with many publications reporting pazopanib-induced cell cycle arrest, thereby suppressing *in vitro* cell growth, but with no significant concurrent increases in apoptosis (Hosaka *et al.*, 2012; Outani *et al.*, 2014).

Despite limited pazopanib-sensitive *in vitro* models of STS, pazopanib has far greater antitumour activity within *in vivo* xenograft models of STS. This is putatively regarded as being due to the supplementary antiangiogenic effects of pazopanib *in vivo*, in addition to the inhibitor's antiproliferative properties (Fleuren *et al.*, 2017). For instance, pazopanib has been shown to significantly stall or regress the growth of a range of STS subtype cell line or patient-derived xenograft models, including intimal sarcoma, liposarcoma, undifferentiated pleomorphic sarcoma, and synovial sarcoma (Becker *et al.*, 2016; Fleuren *et al.*, 2017; Hosaka *et al.*, 2012; Igarashi *et al.*, 2017; Igarashi *et al.*, 2019; Kawaguchi *et al.*, 2019; Kiyuna *et al.*, 2018; Lanzi *et al.*, 2019; Li *et al.*, 2014). Within these sensitive xenograft models, commonly reported histological changes associated with pazopanib treatment included significant reductions in microvessel density, total vascularity, and mitotic activity, with concurrent significant increases in apoptosis and tumour necrosis (Fleuren *et al.*, 2017; Igarashi *et al.*, 2017; Igarashi *et al.*, 2019; Kiyuna *et al.*, 2018; Li *et al.*, 2014). However, the efficacy of pazopanib in these xenograft models appears to be model- and subtype-specific. This is because several studies in further xenograft models of liposarcoma and undifferentiated pleomorphic sarcoma, as well as in models of follicular dendritic cell sarcoma, rhabdomyosarcoma, Ewing sarcoma, and solitary fibrous tumour subtypes, have reported robust resistance to pazopanib treatment (Becker *et al.*, 2016; Keir *et al.*, 2012; Miyake *et al.*, 2019; Oshiro *et al.*, 2019; Stacchiotti *et al.*, 2014).

1.3.3.2.2 Clinical evaluation of pazopanib in soft tissue sarcoma

The first study of note was a phase II study of pazopanib in patients with advanced STS conducted by the European Organisation for Research and Treatment of Cancer (EORTC) (Sleijfer *et al.*, 2009). Patients were stratified into four cohorts based on histology: liposarcoma, leiomyosarcoma, synovial sarcoma, and "Other". An initial accrual of 17 patients for each cohort were treated with 800 mg pazopanib *omni die* (OD – once daily) until consent withdrawal, toxicity, or disease progression. The OD dose of 800 mg pazopanib is the standard dosing regimen for this TKI as determined by Hurwitz *et al.* in a pan-cancer phase I trial that found that steady-state exposure was achieved at ≥ 800 mg OD (Hurwitz *et al.*, 2009). The EORTC phase II study was expanded to at least 37 patients (and max. 41 patients) in each cohort if 4/17 of the

initial enrolment experienced non-progressive disease after 12 weeks of pazopanib treatment (progression-free rate (PFR) at 12 weeks \geq 24%) (Sleijfer *et al.*, 2009). All of the histological cohorts reached the 12-week PFR endpoint for increased enrolment, except for the liposarcoma cohort that only reached 3/17 patients showing non-progression. Therefore, further enrolment to the liposarcoma cohort was terminated. Within the expanded cohorts, the PFRs at 12 weeks for leiomyosarcoma, synovial sarcoma, and “Other” were 44%, 49%, and 39%, respectively (**Table 1.4**) (Sleijfer *et al.*, 2009).

These PFRs met the primary endpoint of the study which was set at 11/37 patients (30%) showing non-progression after 12 weeks of pazopanib. Additionally, the progression-free survival (PFS) and OS rates of these three non-adipocytic cohorts were increased when compared to historical controls for these histological subtypes (**Table 1.4**) (Van Glabbeke *et al.*, 2002). These clinical results indicated that further clinical evaluation of pazopanib in these STS cohorts was warranted.

Based on the findings of the EORTC phase II trial, pazopanib activity in non-adipocytic, advanced STS was evaluated in the placebo-controlled, phase III PALETTE study (Van der Graaf *et al.*, 2012). The PALETTE study was a multicentre, international clinical trial that randomly allocated 369 STS patients 2:1 to either receive 800 mg pazopanib OD or placebo until consent withdrawal, toxicity, or disease progression. Enrolled patients were TKI treatment-naïve with advanced STS that had progressed despite previous chemotherapy. The primary endpoint of the study was PFS and, after a median follow-up of 25 months, a statistically significant improvement in median PFS (mPFS) was reported in the pazopanib arm compared to the placebo arm (mPFS: 4.6 vs. 1.6 months, $p < 0.0001$) (**Table 1.4**). This significant elongation in PFS was, however, not translated into a significant mOS benefit in patients treated with pazopanib compared to placebo (mOS: 12.5 vs. 10.7 months, $p = 0.25$) (**Table 1.4**) (Van der Graaf *et al.*, 2012). Based on the findings of the PALETTE phase III trial, pazopanib was approved for use in advanced, non-adipocytic, non-GIST STS following disease progression with previous lines of chemotherapy.

In addition to these seminal studies, other clinical evaluations of pazopanib effect in STS have been undertaken. Firstly, several post-hoc analyses of the PALETTE phase III trial have been reported. Using only the Japanese cohort ($n=47$) of the PALETTE

trial, Kawai *et al.* reported that the safety and efficacy of pazopanib in the Japanese subpopulation was similar to those observed in the global population (**Table 1.4**) (Kawai *et al.*, 2016). Furthermore, and in conjunction with data from the EORTC phase II trial, Benson *et al.* reported that pazopanib efficacy in uterine sarcoma was broadly similar to non-uterine sarcomas when compared to placebo (**Table 1.4**) (Benson *et al.*, 2016).

In separate phase II clinical trials or prospective/retrospective case series of specific STS subtypes, pazopanib was found to have effective activity and manageable toxicities in patients with solitary fibrous tumour, alveolar soft part sarcoma, dermatofibrosarcoma protuberans, extraskeletal myxoid chondrosarcoma, desmoplastic small round cell tumour, and desmoid tumour (**Table 1.4**) (Delyon *et al.*, 2021; Frezza *et al.*, 2014; Kim *et al.*, 2019; Martín-Broto *et al.*, 2019; Martín-Broto *et al.*, 2020; Maruzzo *et al.*, 2015; Menegaz *et al.*, 2018; Stacchiotti *et al.*, 2014; Stacchiotti *et al.*, 2018; Stacchiotti *et al.*, 2019; Toulmonde *et al.*, 2019; Urakawa *et al.*, 2020). Furthermore, in vascular sarcomas such as angiosarcoma, epithelioid haemangioendothelioma, and intimal sarcomas, pazopanib was reported to show promising clinical activity (**Table 1.4**) (Kollár *et al.*, 2016). However, in retrospective case series of other specific subtypes such as epithelioid sarcoma, the antitumour activity of pazopanib was limited, indicating that pazopanib may not be a worthwhile treatment in these STS subtypes (**Table 1.4**) (Frezza *et al.*, 2018).

Additionally, clinical trials of pazopanib in the geriatric population, as well as those patients that are not candidates for cytotoxic chemotherapy, have corroborated the findings of effective pazopanib activity in STS as described in the EORTC and PALETTE trials. Firstly, the SPIRE retrospective study, conducted in a compassionate use setting, demonstrated that pazopanib had activity and tolerable toxicities in heavily pre-treated patients diagnosed with a broad range of advanced, non-adipocytic STS subtypes (**Table 1.4**) (Gelderblom *et al.*, 2017). In a further phase II clinical study in geriatric patients (age: ≥60 years), pazopanib was found to be non-inferior to gold-standard doxorubicin treatment in elderly STS patients but with decreased incidences in neutropenia (**Table 1.4**). Additionally, in a study conducted in patients that are not suitable for cytotoxic chemotherapy due to age or co-morbidities, pazopanib was found to have suitable activity and toxicity profiles, nominating this therapy for use in a first-line setting for patients with negligible chemotherapeutic options (**Table 1.4**) (Hirbe *et*

et al., 2020). This highlights the potential of pazopanib as a first-line therapeutic option in elderly patients, as well as non-geriatric patients not suitable for cytotoxic chemotherapy, where standard anthracycline cytotoxic chemotherapy would not be appropriate due to heightened toxicity issues (**Table 1.4; Figure 1.8**) (Grünwald *et al.*, 2020).

Furthermore, despite the exclusion of liposarcoma from the approved indications for pazopanib, the utility of pazopanib for this relatively common STS subtype remains controversial. Firstly, despite the termination of the liposarcoma cohort in the EORTC phase II trial, two patients that had initially been categorised into one of the other 3 cohorts were later found on central histopathology review to have liposarcoma (Sleijfer *et al.*, 2009). Both of these patients had met the 12-week PFR endpoint for the study and, therefore, the overall 12-week PFR in the liposarcoma arm was actually 26% (compared to the originally reported 18%). This revised percentage would have surpassed the threshold for expanding the liposarcoma cohort (Sleijfer *et al.*, 2009). Additionally, a phase II study of pazopanib in advanced liposarcoma reported a 12-week PFR of 68% and, after 24 weeks, 44% of patients experienced tumour control (combined PR and stable disease (SD)) (Samuels *et al.*, 2017). The study also reported a mPFS and mOS of 4.4 and 12.6 months, respectively, which are comparable with the survival data observed for the cohorts in the PALETTE study (**Table 1.4**) (Samuels *et al.*, 2017). In a further phase II clinical trial of pazopanib in advanced liposarcoma, the study reported pazopanib activity in well-differentiated and dedifferentiated liposarcoma (12-week PFR: 43%, mPFS: 3.5 months, mOS: 16.4 months) but not in myxoid or round-cell liposarcoma (12-week PFR: 13%, mPFS: 2.0 months, mOS: 22.3 months) (**Table 1.4**) (Valverde *et al.*, 2016). Furthermore, Nakano *et al.* has also reported some promising activity of pazopanib in liposarcoma patients that warrants further evaluation (Nakano *et al.*, 2015). Conversely, a number of studies have corroborated the decreased pazopanib activity in liposarcoma compared to non-adipocytic STS subtypes as was initially reported in the EORTC phase II trial (**Table 1.4**) (Nakamura *et al.*, 2016; Yoo *et al.*, 2015). Therefore, further evaluation of pazopanib utility and activity in liposarcoma is warranted, especially within the individual subtypes of liposarcoma (Chamberlain *et al.*, 2019; Lee *et al.*, 2019).

More recent studies of pazopanib activity in advanced, non-resectable STS are in the context of combination therapy alongside cytotoxic chemotherapies such as

gemcitabine, topotecan (Hycamtin[®]), doxorubicin, ifosfamide, and paclitaxel (Taxol[®]) (Pautier *et al.*, 2020; Pink *et al.*, 2021; Schmoll *et al.*, 2021; Schulte *et al.*, 2021; Somaiah *et al.*, 2021; Weiss *et al.*, 2020). Data from these clinical evaluations have been mixed. On the one hand, several combinations have been reported as having high rates of severe toxicities, such as topotecan and pazopanib, thereby making them unsuitable for use (Schulte *et al.*, 2021). Conversely, other combinations, such as gemcitabine and pazopanib, have displayed acceptable toxicity profiles with improved responses in STS patients when compared to pazopanib monotherapy, as well as other gemcitabine-based chemotherapeutic combinations (Schmoll *et al.*, 2021; Schulte *et al.*, 2021; Somaiah *et al.*, 2021). Therefore, further clinical evaluation is required into the combinatorial efficacy and safety of concurrent pazopanib and cytotoxic chemotherapy in the treatment of STS patients.

A major clinical hurdle in the utilisation of pazopanib in STS is the issue of drug resistance. Clinical experience with pazopanib therapy in STS has shown that patients either have intrinsic resistance to pazopanib or develop an acquired resistance after an initial response to therapy (Lee *et al.*, 2019). As opposed to GIST treatment paradigms, where the underlying pathology, response to targeted therapy, and resistance mechanisms are relatively well-understood leading to the development of several lines of approved targeted therapy, the mechanisms of multi-target TKI action and drug resistance in the remainder of STS are poorly understood (Lee *et al.*, 2019). This therefore limits our ability to develop treatment strategies that can be used to effectively treat pazopanib-resistant STS. Additionally, there are currently no clinically validated biomarkers for determining which patients are more likely to display an increased clinical benefit to pazopanib over those patients that are likely to have intrinsic resistance (Lee *et al.*, 2019). Due to the lack of OS benefit observed with pazopanib therapy in STS, the clinical efficacy and cost-effectiveness of pazopanib therapy in STS is limited and, for these reasons, the National Health Service (NHS) funding for pazopanib therapy by the Cancer Drugs Fund was terminated in 2015 (Lee *et al.*, 2016).

Therefore, there is an unmet clinical need to develop a greater understanding of the underlying biology of STS resistance mechanisms in response to pazopanib therapy. This increased knowledge will help guide the development of future potential

therapeutic regimens for STS treatment that can be utilised to effectively treat pazopanib-resistant STS.

Table 1.4: Clinical evaluations of pazopanib activity in non-GIST STS.							
TKI	Study	Study type	Patient #	Therapy regimen	Subtypes (n)	Response	Survival
Pazopanib	NCT00753688; Van der Graaf <i>et al.</i> , 2012	Placebo-controlled phase III trial	369	2:1 randomisation to pazopanib 800 mg OD or placebo	LMS (165) SS (44) Other (160)	PR: 6% SD: 67% PD: 23%	mPFS: 4.6 vs. 1.6 months in placebo (p < 0.0001) mOS: 12.5 vs. 10.7 months in placebo (p = 0.25)
					LMS (42)	PR: 2%	mPFS: 3.0 months mOS: 11.8 months PFR at 12 weeks: 44%
	NCT00297258; Sleijfer <i>et al.</i> , 2009	Single-arm phase II trial	142	Pazopanib 800 mg OD	SS (38)	PR: 13%	mPFS: 5.4 months mOS: 10.3 months PFR at 12 weeks: 49%
					LPS (19)	PR: 0%	mPFS: 2.7 months mOS: 6.6 months PFR at 12 weeks: 26%
					Other (43)	PR: 7%	mPFS: 3.0 months mOS: 10.0 months PFR at 12 weeks: 39%
	NCT01861951; Grünwald <i>et al.</i> , 2020	Double-arm phase II trial	120	2:1 pazopanib 800 mg OD or Doxorubicin 75 mg/m ² triweekly	LMS (34) UPS (23) LPS (18) Other (45)	Paz/Dox CR: 1%/0% Paz/Dox PR: 11%/15% Paz/Dox SD: 51%/39% Paz/Dox PD: 37%/46%	mPFS: 4.4 (Paz) vs. 5.3 months (Dox) (p = n/a) mOS: 12.3 (Paz) vs. 14.3 months (Dox) (p = 0.74)
					UPS (22)	CR/PR: 2%/7% (9%)	
	NCT02300545; Hirbe <i>et al.</i> , 2020	Single-arm phase II trial	56	Pazopanib 800 mg OD	LMS (21) LPS (2) Other (11)	SD: 50% PD: 29% n/a: 13%	mPFS: 3.7 months mOS: 14.2 months
	NCT02066285; Martín-Broto <i>et al.</i> , 2019	Single-arm phase II trial	36	Pazopanib 800 mg OD	SFT (malignant-dedifferentiated) (36)	RECIST/Choi PR: 6%/51% RECIST/Choi SD: 60%/26% RECIST/Choi PD: 34%/23%	mPFS: 5.6 months mOS: Not reached OSR at 24 months: 73%
	NCT02066285; Martín-Broto <i>et al.</i> , 2020	Single-arm phase II trial	31	Pazopanib 800 mg OD	SFT (typical) (31)	PR: 58% SD: 39% PD: 3%	mPFS: 12.1 months mOS: 49.8 months
	NCT02066285; Stacchiotti <i>et al.</i> , 2019	Single-arm phase II trial	26	Pazopanib 800 mg OD	ESMC (23)	PR: 18% SD: 73% PD: 9%	mPFS: 19.0 months mOS: Not reached
	NCT02113826; Kim <i>et al.</i> , 2019	Single-arm phase II trial	6	Pazopanib 800 mg OD	ASPS (6)	PR: 17% SD: 83%	mPFS: 5.5 months mOS: Not reached
					ASPS (5)	RECIST/Choi PR: 20%/60% RECIST/Choi SD: 40%/0% RECIST/Choi PD: 40%/40%	mPFS: 15.6 months mOS: Not reached
	Urakawa <i>et al.</i> , 2020	Single-arm phase II trial	8	Pazopanib 800 mg OD	ES (2)	RECIST/Choi PR: 0%/50% RECIST/Choi SD: 50%/50% RECIST/Choi PD: 50%/0%	mPFS: 4.9 months mOS: Not reached
				CCS (1)	RECIST/Choi PR: 0%/0% RECIST/Choi SD: 0%/0% RECIST/Choi PD: 100%/100%	mPFS: 10.3 months mOS: 23.2 months	
NCT01876082; Toulmonde <i>et al.</i> , 2019	Single-arm phase II trial	48	Pazopanib 800 mg OD	DT (48)	PR: 37% SD: 59% PD: 4%	mPFS: Not reached PFR at 24 months: 67% mOS: Not reached OSR at 24 months: 97%	
NCT01059656; Delyon <i>et al.</i> , 2021	Single-arm phase II trial	23	Pazopanib 800 mg OD	DFSP (23)	ORR: 30% PR: 9% SD: 55% PD: 36%	n/a	

Pazopanib	NCT01692496; Valverde <i>et al.</i> , 2016	Single-arm phase II trial	52	Pazopanib 800 mg OD	WDLPS/DDLPS (37)	n/a	mPFS: 3.5 months mOS: 16.4 months PFR at 12 weeks: 43%
					Myxoid/Round-cell LPS (15)	n/a	mPFS: 2.0 months mOS: 22.3 months PFR at 12 weeks: 13%
	NCT01506595; Samuels <i>et al.</i> , 2017	Single-arm phase II trial	41	Pazopanib 800 mg OD	LPS (41)	PR: 2% SD: 42% PD: 66%	mPFS: 4.4 months mOS: 12.6 months PFR at 12 weeks: 68%
	Maruzzo <i>et al.</i> , 2015	Prospective case series	13	Pazopanib 800 mg OD	SFT (13)	RECIST/Choi PR: 9%/46% RECIST/Choi SD: 73%/36% RECIST/Choi PD: 18%/18%	mPFS: 4.7 months mOS: 13.3 months
	Nakano <i>et al.</i> , 2015	Retrospective case series	47	Pazopanib 800 mg OD	LMS (9) SS (9) LPS (7) Other (22)	Overall ORR: 11% PALETTE-eligible: 11% PALETTE-ineligible ORR: 11%	Overall PFS: 4.3 months mPFS: 4.5 (PALETTE-eligible) vs. 2.9 months (PALETTE- ineligible) (p = 0.15) Overall mOS: 9.6 months mOS: 10.7 (PALETTE-eligible) vs. 7.8 months (PALETTE- ineligible) (p = 0.55)
	Nakamura <i>et al.</i> , 2016	Retrospective case series	156	Pazopanib 800 mg OD	LPS (33)	PR: 0% SD: 27% PD: 39% n/a: 33%	mPFS: 1.8 months mOS: 7.3 months
					UPS (30)	PR: 10% SD: 63% PD: 13% n/a: 13%	mPFS: 3.5 months mOS: 9.5 months
					LMS (21)	PR: 0% SD: 57% PD: 29% n/a: 14%	mPFS: 4.3 months mOS: 20.1 months
					SS (18)	PR: 11% SD: 56% PD: 22% n/a: 11%	mPFS: 3.8 months mOS: 10.6 months
					Other (54)	PR: 15% SD: 44% PD: 20% n/a: 20%	mPFS: 3.4 months mOS: 7.2 months
	Yoo <i>et al.</i> , 2015	Retrospective case series	43	Pazopanib 800 mg OD	LMS (9) AS (6) UPS (5) Other (23)	PR: 17% SD: 44% PD: 39%	mPFS: 5.0 months mOS: 8.2 months
	Kawai <i>et al.</i> , 2016	Retrospective case series	47	Pazopanib 800 mg OD	LMS (13) UPS (8) SS (5) Other (21)	PR: 16% SD: 65% PD: 19%	mPFS: 5.7 vs. 1.6 months in placebo (p < 0.01) mOS: 15.4 vs. 14.9 months in placebo (p = 0.69)
Gelderblom <i>et al.</i> , 2017	Retrospective case series	211	Pazopanib 800 mg OD	LMS (87) SS (24) NOS (19) Other (81)	Observed CBR: 46%	mPFS: 3.0 months mOS: 11.1 months	
Frezza <i>et al.</i> , 2014	Retrospective case series	9	Pazopanib 800 mg OD	DSRCT (9)	PR: 22% SD: 56% PD: 22%	mPFS: 9.2 months mOS: 15.4 months	

Pazopanib	Benson <i>et al.</i> , 2016	Retrospective case series	44	Pazopanib 800 mg OD	Uterine (44)	PR: 11% SD: 57% PD: 32%	mPFS: 3.0 (uterine) vs. 4.5 months (non-uterine) (p = n/a) mOS: 17.5 (uterine) vs. 11.0 months (non-uterine) (p = 0.35)
	Stacchiotti <i>et al.</i> , 2018	Retrospective case series	30	Pazopanib 800 mg OD	ASPS (30)	CR/PR: 3%/24% (27%) SD: 59% PD: 14%	mPFS: 13.6 months mOS: Not reached
	Frezza <i>et al.</i> , 2018	Retrospective case series	18	Pazopanib 800 mg OD	ES (18)	PR: 0% SD: 50% PD: 50%	mPFS: 3.0 months mOS: 14.0 months
	Kollár <i>et al.</i> , 2017	Retrospective case series	52	Pazopanib 800 mg OD	AS (40)	CR/PR: 0%/20% (20%) SD: 18% PD: 58% n/a: 2%	mPFS: 3.0 months mOS: 9.9 months
					EHE (10)	CR/PR: 10%/10% (20%) SD: 40% PD: 30% n/a: 10%	mPFS: 26.3 months mOS: 26.3 months
					Intimal (2)	CR/PR: 0%/100% (100%) SD: 0% PD: 0%	n/a
	Menegaz <i>et al.</i> , 2018	Retrospective case series	29	Pazopanib 800 mg OD	DSRCT (29)	CR/PR: 3%/3% (6%) SD: 55% PD: 38%	mPFS: 5.6 months mOS: 15.7 months
	Stacchiotti <i>et al.</i> , 2014	Retrospective case series	6	Pazopanib 800 mg OD	SFT (6)	RECIST/Choi PR: 0%/17% RECIST/Choi SD: 50%/33% RECIST/Choi PD: 50%/50%	mPFS: 3.0 months mOS: n/a

AS; Angiosarcoma, ASPS; Alveolar soft part sarcoma, CCS; Clear cell sarcoma, CR; Complete response, DDLPS; Dedifferentiated liposarcoma, DFSP; Dermatofibrosarcoma protuberans, Dox; Doxorubicin, DSRCT; Desmoplastic small round cell tumour, EHE; Epithelioid haemangioendothelioma, ES; Epithelioid sarcoma, ESMC; Extraskeletal myxoid chondrosarcoma, LMS; Leiomyosarcoma, LPS; Liposarcoma, mOS; Median overall survival, mPFS; Median progression-free survival, n/a; Not available, NCT; National Clinical Trial, NOS; Not otherwise specified, OD; Omni die (Once daily), OSR; Overall survival rate, ORR; Objective response rate, Paz; Pazopanib, PD; Progressive disease, PFR; Progression-free rate, PR; Partial response, RECIST; Response evaluation criteria in solid tumours, SD; Stable disease, SFT; Solitary fibrous tumour, SS; Synovial sarcoma, STS; Soft tissue sarcoma, TKI; Tyrosine kinase inhibitor, UPS; Undifferentiated pleomorphic sarcoma, WDLPS; Well-differentiated liposarcoma (adapted from Lee *et al.*, 2019).

1.3.3.3 Regorafenib

Regorafenib is another multi-target TKI from the same family as pazopanib that strongly inhibits many of the same targets and is currently undergoing clinical evaluation for use in advanced STS (Attia *et al.*, 2017; Marrari *et al.*, 2020; Mir *et al.*, 2016; Penel *et al.*, 2020; Riedel *et al.*, 2020; Stacchiotti *et al.*, 2021) (**Table 1.3; Figure 1.9**). As with pazopanib, regorafenib has previously been approved for use in non-STs cancer types, namely advanced hepatocellular carcinoma and colorectal cancer (Goel, 2018; Liu *et al.*, 2019). Additionally, regorafenib has been approved for use in advanced GIST following disease progression on imatinib and sunitinib therapies (Ferraro & Zalcborg, 2014). In addition to these advanced cancer types, regorafenib has also been undergoing preclinical and clinical assessment of efficacy in non-GIST STS. Regorafenib is a type II TKI and the skeletal formula structure of regorafenib is shown in **Figure 1.11** (Roskoski Jr., 2016).

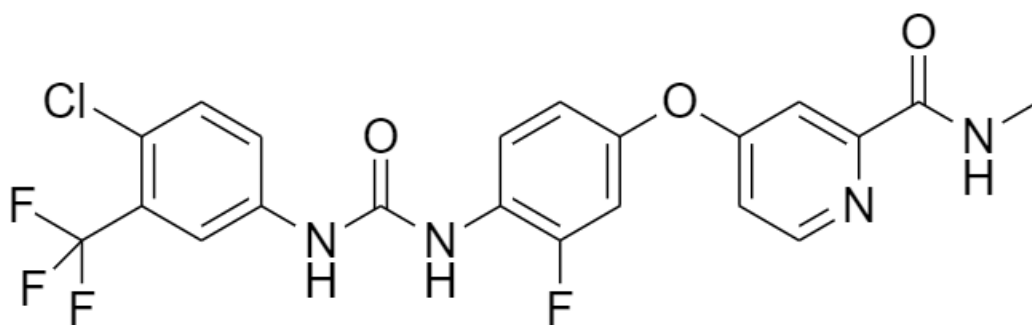


Figure 1.11: Skeletal formula structure of regorafenib. Figure was created using ChemOffice+ Cloud (PerkinElmer).

Within the preclinical setting, regorafenib has shown promising results in STS models of leiomyosarcoma, malignant rhabdoid tumour, and solitary fibrous tumour. For instance, regorafenib has been shown to significantly reduce proliferation in malignant rhabdoid tumour and leiomyosarcoma cell line models (Daudigeos-Dubus *et al.*, 2015; Teicher *et al.*, 2015). Furthermore, regorafenib was reported to have the greatest antitumour effect in a xenograft model of solitary fibrous tumour when compared to a panel comprising antiangiogenic TKIs and bevacizumab – a humanised therapeutic antibody that blocks VEGF binding to VEGFR (Stacchiotti *et al.*, 2014; Wilding *et al.*, 2019). The greater effect of regorafenib compared to the other therapies assessed was attributed to a concurrent decrease in both PDGFR β and VEGFR2 phosphorylation in the xenograft tumours 4 weeks after treatment with regorafenib. In contrast, the remainder of the antiangiogenic therapies inhibited only one or neither of

these targets, thereby explaining the reduced efficacy of these therapies compared to regorafenib (Stacchiotti *et al.*, 2014).

As discussed previously with pazopanib, antiangiogenic multi-target TKIs have been reported as having clinically meaningful activity in the treatment of advanced STS (Van der Graaf *et al.*, 2012). With pazopanib showing improved PFS but not an OS benefit in STS, regorafenib has undergone clinical trial evaluation in order to potentially provide necessary alternative options for treating advanced STS (Grothey *et al.*, 2020; Mir *et al.*, 2016; Van der Graaf *et al.*, 2012). The utilisation of regorafenib in STS was evaluated in the randomised, placebo-controlled phase II REGOSARC trial (**Table 1.5**). (Mir *et al.*, 2016). The trial recruited adult patients with advanced STS of various subtypes that had undergone previous chemotherapeutic treatments with anthracycline-based therapy. These patients were randomised 1:1 to receive either placebo or 160 mg regorafenib once daily and then stratified into one of four cohorts based on histological subtype; liposarcoma, leiomyosarcoma, synovial sarcoma, or “Other”. The study found that regorafenib significantly prolonged mPFS in patients with non-adipocytic STS relative to placebo (mPFS: 4.0 vs. 1.0 months; $p < 0.0001$ [pooled analysis of leiomyosarcoma, synovial sarcoma, and “Other” cohorts]) (Grothey *et al.*, 2020; Mir *et al.*, 2016). Conversely, but similarly to pazopanib, regorafenib failed to improve PFS in liposarcoma compared to placebo (mPFS: 1.0 vs. 1.7 months, $p = 0.70$) (**Table 1.5**) (Mir *et al.*, 2016). Additionally, as seen with pazopanib, regorafenib efficacy in prolonging mPFS did not translate into an OS benefit (**Table 1.5**) (mOS: 13.4 vs. 9.0 months; $p = 0.059$ [pooled analysis of leiomyosarcoma, synovial sarcoma, and “Other” cohorts]) (Mir *et al.*, 2016; Van der Graaf *et al.*, 2012). These results were corroborated in an updated analysis of the REGOSARC trial that confirmed the prolonged mPFS benefit with regorafenib but concurrently reported a nonsignificant difference in OS between patients treated with regorafenib compared to placebo (Brodowicz *et al.*, 2018). However, both studies also state that this could be partially explained due to the high rate of patient crossover from placebo to regorafenib upon disease progression (Brodowicz *et al.*, 2018; Mir *et al.*, 2016).

A subsequent analysis on a fifth cohort of the REGOSARC trial focussing on pazopanib-pre-treated, advanced, non-adipocytic sarcomas supported the findings of the originating REGOSARC study, with regorafenib treatment significantly increasing mPFS when compared to placebo (mPFS: 2.1 vs. 1.1 months, $p < 0.01$) (**Table 1.5**)

(Penel *et al.*, 2020). Interestingly, and despite treatment cross-over, the study also observed a clinically relevant mOS benefit with regorafenib treatment compared to placebo (mOS: 17.8 vs. 8.2 months, $p = 0.07$) (**Table 1.5**) (Penel *et al.*, 2020). However, the authors note that the trial was not designed to demonstrate an mOS benefit due to treatment cross-over and limited sample size (Penel *et al.*, 2020). The results of this REGOSARC analysis highlights the potential of regorafenib use in pazopanib-refractory, non-adipocytic, advanced STS and therefore further clinical evaluation of regorafenib use in pazopanib-resistant STS is warranted (Penel *et al.*, 2020). These results also suggest that regorafenib and pazopanib, despite having very similar selectivity profiles, operate via differing mechanisms of action in advanced STS.

A separate phase II study of regorafenib conducted in advanced, pre-treated STS also observed regorafenib activity in patients with a clinical benefit rate (CBR) of 62% and mPFS and mOS comparable to those observed in the REGOSARC trial for non-adipocytic STS (mPFS: 3.8 months, mOS: 14.8 months) (**Table 1.5**) (Marrari *et al.*, 2020). Additionally, and in further corroboration to the liposarcoma results reported in REGOSARC, the placebo-controlled phase II SARC024 trial described no mPFS benefit (mPFS: 1.9 vs. 2.1 months, $p = 0.62$) or mOS benefit (mOS: 6.5 vs. 4.9 months, $p = 0.28$) in liposarcoma patients treated with regorafenib compared to placebo (**Table 1.5**) (Riedel *et al.*, 2020). Despite this, the SARC024 trial has elucidated the potential activity of regorafenib in patients with advanced soft tissue Ewing sarcoma. In a single-arm, phase II sub-study of the SARC024 trial, composed of both bone and soft tissue Ewing sarcoma (bone: 12 patients, soft tissue: 18 patients), patients treated with regorafenib had a mPFS of 3.6 months and 73% were progression-free after 8 weeks, thereby meeting the sub-study's primary 8-week PFS endpoint (**Table 1.5**) (Attia *et al.*, 2017). Further analysis into the soft tissue Ewing sarcoma cohort within this trial will further clarify the potential activity of regorafenib within this STS subtype. Furthermore, another instance of subtype-specific regorafenib efficacy was observed in patients with solitary fibrous tumour (Stacchiotti *et al.*, 2021). This recent study showed that regorafenib induced a CBR of 78%, with a mPFS and mOS of 3.7 and 15.7 months, respectively (**Table 1.5**) (Stacchiotti *et al.*, 2021).

The clinical data discussed shows that regorafenib may have efficacy in treating a broad range of non-adipocytic STS subtypes, as well as specific subtypes such as

Ewing sarcoma and solitary fibrous tumour (Attia *et al.*, 2017; Mir *et al.*, 2016; Stacchiotti *et al.*, 2021). Furthermore, analysis by Penel *et al.* of the REGOSARC trial has highlighted the potential efficacy of second-line regorafenib in pazopanib-refractory, advanced STS (Penel *et al.*, 2020). However, the REGOSARC trial also describes increasing rates of disease progression over the course of 9 months with regorafenib therapy (PFR at 9 months: leiomyosarcoma = 18%, synovial sarcoma = 38%, “Other” = 27%) (Mir *et al.*, 2016). Additionally, the publication by Penel *et al.* reported that all pazopanib-refractory patients had experienced disease progression with regorafenib therapy by the time of analysis, with a median follow-up of 27.2 months (Penel *et al.*, 2020). This further highlights the continuous issue of drug resistance with multi-target TKI therapy and underscores the need for a greater understanding of multi-target TKI resistance mechanisms in STS.

1.3.3.4 Sitravatinib

Sitravatinib is a recently developed member of the multi-RTK inhibitor family (**Table 1.3; Figure 1.9**) and preclinical studies of sitravatinib in STS are currently limited to a solitary study. However, this study has shown that sitravatinib possesses promising preclinical activity in models of STS (Patwardhan *et al.*, 2016). Sitravatinib is proposed to be a type II TKI and the skeletal formula structure of sitravatinib is shown in **Figure 1.12** (Jiang *et al.*, 2021).

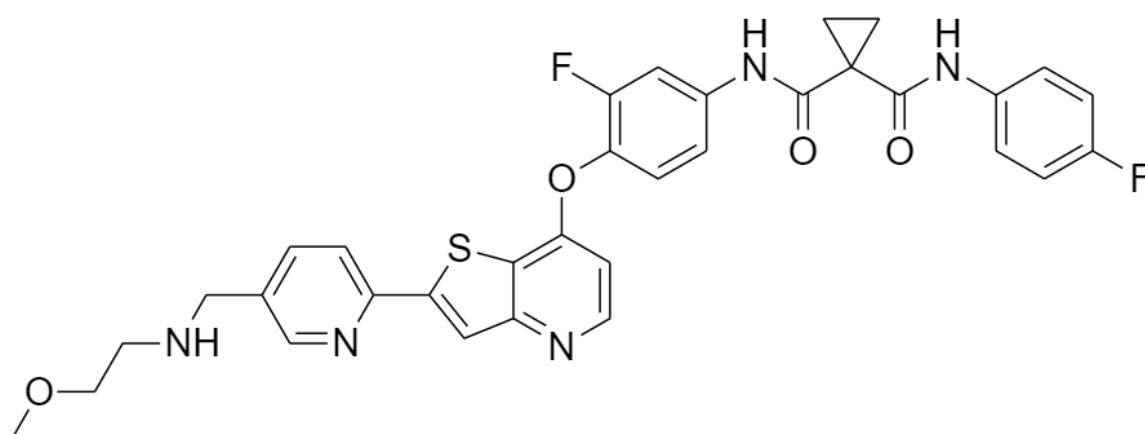


Figure 1.12: Skeletal formula structure of sitravatinib. Figure was created using ChemOffice+ Cloud (PerkinElmer).

The study by Patwardhan *et al.* reports the potent, antiproliferative properties of sitravatinib within *in vitro* cell line and *in vivo* xenograft models of liposarcoma and malignant peripheral nerve sheath tumour (Patwardhan *et al.*, 2016). In cell line

models of liposarcoma and malignant peripheral nerve sheath tumour, sitravatinib was shown to potently inhibit phosphorylation of a number of growth-promoting RTKs, namely PDGFR β , MET, and IGF1R, as well as blockading downstream Akt signalling, at low nanomolar concentrations (Patwardhan *et al.*, 2016). When compared to other broad-spectrum TKIs such as pazopanib, crizotinib, and imatinib, the authors found that sitravatinib had a superior antiproliferative effect in the liposarcoma and malignant peripheral nerve sheath tumour cell lines. Immunoblotting revealed sitravatinib potently and concurrently inhibited multiple RTKs compared to the other three TKIs. Combination therapy of crizotinib and imatinib phenocopied the increased antiproliferative effects seen with sitravatinib monotherapy, with simultaneous inhibition of MET, PDGFR β , and downstream Akt signalling. By utilising siRNA-mediated RTK knockdown, the study determined that the increased potency observed with sitravatinib is due to the concurrent inhibition of multiple RTKs, which the other evaluated TKIs only block individually (Patwardhan *et al.*, 2016). The superior *in vitro* antiproliferative properties of sitravatinib translated into an *in vivo* effect, with sitravatinib significantly suppressing tumour growth, with increased inhibition of RTK and PI3K/Akt pathways, in xenograft models compared to imatinib and crizotinib (Patwardhan *et al.*, 2016).

The promising results observed in this preclinical study, especially the potent activity towards models of liposarcoma, have led to the commencement of clinical evaluations of sitravatinib in advanced STS, with a particular emphasis on liposarcoma (**Table 1.5**) (Ingham *et al.*, 2017; Oza *et al.*, 2021). The prominence of liposarcoma within the clinical study of sitravatinib in advanced STS is of high importance as there are currently no targeted therapies approved for use in this relatively common STS subtype. In a single-arm, phase II clinical trial of sitravatinib in 29 patients with either well-differentiated or dedifferentiated liposarcoma that had progressed on previous chemotherapy, 41% of patients were progression-free at 12 weeks, which met the primary endpoint for activity in this study (Oza *et al.*, 2021). This primary endpoint was based upon historical controls that stated a 12-week PFR of $\geq 40\%$ was considered promising therapeutic activity (Oza *et al.*, 2021; Van Glabbeke *et al.*, 2002). The study concluded that sitravatinib had superior clinical activity in liposarcoma than was observed in the EORTC phase II trial of pazopanib and that sitravatinib warranted further clinical evaluation in this STS subtype that currently lacks targeted treatment

options (**Table 1.4-1.5**) (Oza *et al.*, 2021; Sleijfer *et al.*, 2009). However, comparing the two clinical trials shows that the mPFS are identical (mPFS: 2.7 months), with sitravatinib showing negligible improvement in ORR when compared to pazopanib (ORR: pazopanib = 0%, sitravatinib = 3%) (**Table 1.4-1.5**) (Oza *et al.*, 2021; Sleijfer *et al.*, 2009). Therefore, this current clinical trial of sitravatinib in liposarcoma actually appears to show very similar levels of clinical activity to those observed with pazopanib in the EORTC phase II clinical trial (Oza *et al.*, 2021; Sleijfer *et al.*, 2009). Further results from this trial are eagerly awaited in order to fully determine whether sitravatinib has superior therapeutic activity in liposarcoma compared to pazopanib and whether this activity of sitravatinib in liposarcoma is clinically meaningful. Additionally, the clinical trial conducted by Oza *et al.* once again underlined the ubiquitous problem of TKI resistance with 76% of patients progressing on sitravatinib therapy, therefore further highlighting the importance of understanding mechanisms of multi-target TKI resistance in STS (Oza *et al.*, 2021).

1.3.3.5 Anlotinib

Anlotinib (also known as catequentinib) is a recently developed multi-target TKI and, as such, preclinical studies in STS are currently limited (Wilding *et al.*, 2019). Anlotinib is proposed to be a type II TKI and the skeletal formula structure of anlotinib is shown in **Figure 1.13** (Xie *et al.*, 2018).

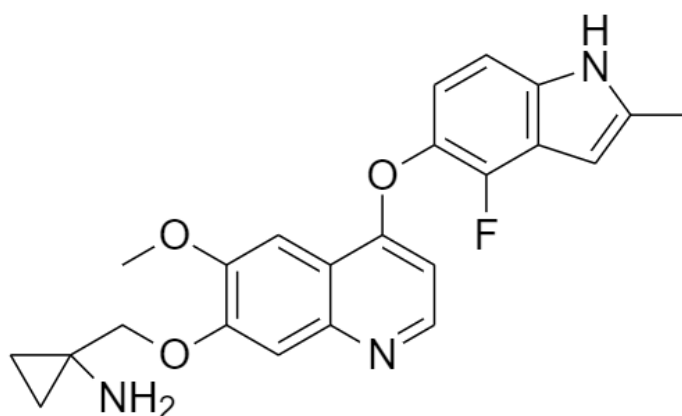


Figure 1.13: Skeletal formula structure of anlotinib. Figure was created using ChemOffice+ Cloud (PerkinElmer).

In a preclinical study of synovial sarcoma in both cell line and xenograft models, anlotinib was found to significantly inhibit cell proliferation and tumour growth compared to controls (Tang *et al.*, 2019). Within the synovial sarcoma cell line model,

microarray profiling found that anlotinib significantly reduced the expression of *GINS1*, a subunit of the GINS DNA replication complex required for replication initiation, when compared to control (Tang *et al.*, 2019). The study further reported that expression of *GINS1* in synovial sarcomas is associated with a poorer prognosis in synovial sarcoma patients when compared to *GINS1*-negative synovial sarcoma patients. In the same cell line model of synovial sarcoma, shRNA-mediated knockdown of *GINS1* was found to phenocopy the antiproliferative and pro-apoptotic effects of anlotinib. The study concludes by stating that the downregulation of downstream *GINS1* expression in response to anlotinib treatment was important in achieving anlotinib's antitumour effect and nominates *GINS1* as a novel target for future cancer therapeutics in synovial sarcoma (Tang *et al.*, 2019). However, the study does not describe the inhibitory mechanism of anlotinib that results in downstream *GINS1* gene downregulation (Tang *et al.*, 2019). In a further preclinical study of anlotinib in STS, anlotinib was found to significantly inhibit tumour growth of undifferentiated pleomorphic sarcoma xenografts in a dose-dependent manner, when compared to vehicle control (Wang *et al.*, 2020). Histological analysis of tumours treated with anlotinib revealed significantly increased necrosis and apoptosis, with concurrent decreases in cellular proliferation, CD31 expression, and microvessel density, when compared to control. These results therefore highlighted the antiproliferative and antiangiogenic properties of anlotinib in a xenograft model of undifferentiated pleomorphic sarcoma (Wang *et al.*, 2020).

Clinical evaluations of anlotinib in advanced STS have shown very promising results in phase II trials demonstrating a clinically meaningful activity in a broad range of TKI-treatment naïve STS who had progressed on previous chemotherapy. In the ALTER0203 phase II clinical trial conducted by Chi *et al.*, anlotinib was shown to significantly improve mPFS when compared to placebo, in a heterogeneous mix of STS subtypes (mPFS: 6.3 vs. 1.5 months, $p < 0.0001$) (**Table 1.5**) (Chi *et al.*, 2018; Tang *et al.*, 2019). Additionally, the study found significant increases in DCR and ORR in patients treated with anlotinib compared to placebo (DCR: 56% vs. 23%, $p < 0.0001$, ORR: 10% vs. 1%) (Chi *et al.*, 2018) (**Table 1.5**). This activity has been corroborated by a number of single-arm phase II trials and retrospective case series, in both heterogeneous or subtype-specific cohorts (**Table 1.5**) (Chi *et al.*, 2018; Huang *et al.*, 2021; Li *et al.*, 2021; Tian *et al.*, 2020). Notably, the retrospective study conducted by Li *et al.* focussed on a cohort of liposarcoma patients and, therefore, anlotinib activity

in this subtype nominates another potential treatment in this currently hard-to-treat STS subtype (**Table 1.5**) (Li *et al.*, 2021).

Based on the findings of the ALTER0203 phase II trial, the phase III APROMISS clinical trial was initiated (Van Tine *et al.*, 2021). The APROMISS trial is being conducted in patients diagnosed with advanced synovial sarcoma, leiomyosarcoma, or alveolar soft part sarcoma, and is comparing the activity of anlotinib to intravenous dacarbazine chemotherapy (**Table 1.5**) (Van Tine *et al.*, 2021). Additionally, a further indication for a second cohort of leiomyosarcoma patients is being undertaken where anlotinib activity is being compared to placebo rather than intravenous dacarbazine. At present, only the results of the synovial sarcoma cohort have been reported with the leiomyosarcoma and alveolar soft part sarcoma cohorts either currently undergoing recruitment or analysis (**Table 1.5**) (Van Tine *et al.*, 2021). Synovial sarcoma patients were randomised 2:1 to either receive 12 mg anlotinib OD or dacarbazine 1g/m² triweekly with a primary endpoint of the study being PFS. The study reported that anlotinib had a significantly improved mPFS when compared to dacarbazine (mPFS: 2.9 vs. 1.6 months, $p < 0.01$) with a 12-month PFR of 27% (**Table 1.5**) (Van Tine *et al.*, 2021). The study therefore reports anlotinib as a clinically meaningful treatment option with some activity in patients with advanced synovial sarcoma (Van Tine *et al.*, 2021).

The clinical trial results of anlotinib in a variety of STS subtypes have demonstrated that anlotinib has clinically meaningful activity in advanced STS, including liposarcoma. Further results of the APROMISS phase III clinical trial for the leiomyosarcoma and alveolar soft part sarcoma cohorts are highly anticipated and may guide future approval for this multi-target TKI in STS.

Table 1.5: Clinical evaluations of regorafenib, sitravatinib, and anlotinib activity in non-GIST STS.								
TKI	Study	Study type	Patient #	Therapy regimen	Subtypes (n)	Response	Survival	
Regorafenib	NCT01900743; Mir <i>et al.</i> , 2016	Placebo-controlled phase II trial	182	1:1 randomisation to regorafenib 160 mg OD or placebo	LMS (56)	PR: 0% SD: 86% PD: 11% n/a: 3%	mPFS: 3.7 vs. 1.8 months in placebo (p < 0.01) mOS: 21.0 vs. 9.1 months in placebo (p = 0.056)	
					LPS (43)	PR: 0% SD: 45% PD: 55%	mPFS: 1.1 vs. 1.7 months in placebo (p = 0.70) mOS: 4.7 vs. 8.8 months in placebo (p = 0.21)	
					SS (27)	PR: 8% SD: 77% PD: 15%	mPFS: 5.6 vs. 1.0 months in placebo (p < 0.0001) mOS: 13.4 vs. 6.7 months in placebo (p = 0.79)	
					Other (56)	PR: 11% SD: 67% PD: 22% n/a: 3%	mPFS: 2.9 vs. 1.0 months in placebo (p < 0.01) mOS: 12.1 vs. 9.5 months in placebo (p = 0.37)	
	NCT01900743; Penel <i>et al.</i> , 2020	Placebo-controlled phase II trial	37	1:1 randomisation to regorafenib 160 mg OD or placebo	LMS (24) UPS (6) Other (7)	PR: 0% SD: 72% PD: 28%	mPFS: 2.1 vs. 1.1 months in placebo (p < 0.01) mOS: 17.8 vs. 8.2 months in placebo (p = 0.07)	
	NCT02048371; Riedel <i>et al.</i> , 2020	Placebo-controlled phase II trial	48	1:1 randomisation to regorafenib 160 mg OD or placebo	LPS (48)	No responses observed with regorafenib	mPFS: 1.9 vs. 2.1 months in placebo (p = 0.62) mOS: 6.5 vs. 4.9 months in placebo (p = 0.28)	
	NCT02307500; Marrari <i>et al.</i> , 2020	Single-arm phase II trial	21	Regorafenib 160 mg OD	LMS (13) SS (5) ASPS (2) AS (1)	PR: 5% SD: 57% PD: 24% n/a	mPFS: 3.8 months mOS: 14.8 months	
NCT02048371; Attia <i>et al.</i> , 2017	Single-arm phase II trial	30	Regorafenib 160 mg OD	Ewing sarcoma (30)	PR: 10% SD: 60% PD: 23% n/a: 6%	mPFS: 3.6 months mOS: n/a PFS at 8 weeks: 73%		
Stacchiotti <i>et al.</i> , 2021	Single-arm phase II trial	18	Regorafenib 160 mg OD	SFT (18)	RECIST/Choi PR: 7%/43% RECIST/Choi SD: 71%/36% RECIST/Choi PD: 21%/21%	mPFS: 3.7 months mOS: 15.7 months		
Sitratvatnib	NCT02978859; Oza <i>et al.</i> , 2021; Ingham <i>et al.</i> , 2017	Single-arm phase II trial	29	Sitratvatnib 120-150 mg OD	LPS (29)	ORR: 3%	mPFS: 2.7 months mOS: n/a PFR at 12 weeks: 41%	

Anlotinib	NCT03016819; Van Tine <i>et al.</i> , 2021	Double-arm phase III trial	79	2:1 randomisation to anlotinib 12 mg OD or dacarbazine 1 g/m ² triweekly	SS (79)	n/a	mPFS: 2.9 (Anlo) vs. 1.6 months (Dac) (p < 0.01) mOS: n/a PFR at 12 months: 27%
	NCT02449343; Chi <i>et al.</i> , 2018; Tang <i>et al.</i> , 2019	Placebo-controlled phase II trial	233	2:1 randomisation to anlotinib 12 mg OD or placebo	SS (57) ASPS (56) LMS (41) Other (79)	ORR: 10% DCR: 56%	mPFS: 6.3 vs. 1.5 months in placebo (p < 0.0001) mOS: n/a
	NCT01878448; Chi <i>et al.</i> , 2018	Single-arm phase II trial	166	Anlotinib 12 mg OD	SS (47) LMS (26) UPS (19) FS (18) LPS (13) Other (43)	PR: 13% SD: 61% PD: 26%	mPFS: 5.6 months mOS: 12.0 months PFR at 12 weeks: 68%
	NCT03792542; Huang <i>et al.</i> , 2021	Single-arm phase II trial	29	Anlotinib 12 mg OD	LPS (8) UPS (5) FS (5) SS (4) Other (7)	PR: 4% SD: 92% PD: 4%	mPFS: Not reached mOS: n/a
	Tian <i>et al.</i> , 2020	Retrospective case series	29	Anlotinib 12 mg OD	SS (7) UPS (5) LMS (3) LPS (2) Other (12)	PR: 14% SD: 41% PD: 45%	mPFS: 6.0 months mOS: n/a
	Li <i>et al.</i> , 2021	Retrospective case series	17	Anlotinib 12 mg OD	LPS (17)	PR: 0% SD: 65% PD: 35%	mPFS: 6.4 months mOS: 13.0 months PFR at 24 weeks: 59%
Anlo; Anlotinib, AS; Angiosarcoma, ASPs; Alveolar soft part sarcoma, Dac; Dacarbazine, DCR; Disease control rate, FS; Fibrosarcoma, LMS; Leiomyosarcoma, LPS; Liposarcoma, mOS; Median overall survival, mPFS; Median progression-free survival, n/a; Not available, NCT; National Clinical Trial, OD; Omni die (once daily), ORR; Objective/overall response rate, PD; Progressive disease, PFR; Progression-free rate, PR; Partial response, RECIST; Response evaluation criteria in solid tumours, SD; Stable disease, SFT; Solitary fibrous tumour, SS; Synovial sarcoma, TKI; Tyrosine kinase inhibitor, UPS; Undifferentiated pleomorphic sarcoma (adapted from Wilding <i>et al.</i> , 2019).							

1.3.3.6 Landscape of multi-target tyrosine kinase inhibitors in soft tissue sarcoma

As well as the four TKIs discussed above, a variety of other multi-target TKIs have been clinically evaluated for use in STS, with some showing efficacy in specific subtypes or tumours with specific, underlying biological characteristics. This sub-chapter will discuss these clinical evaluations by focussing on the multi-target TKIs sunitinib, imatinib, sorafenib, axitinib, dasatinib, cediranib, nintedanib, and crizotinib (**Table 1.6**).

Sunitinib was one of the earliest multi-target TKIs to undergo phase II clinical trial evaluation within STS (George *et al.*, 2009; NCT00474994). Unfortunately, this phase II trial reported that sunitinib had inconclusive or modest activity in a heterogeneous cohort of STS subtypes (**Table 1.6**) (George *et al.*, 2009). Despite this lack of overall activity, subtype-specific analysis of this heterogeneous STS trial found that sunitinib activity was more pronounced and potentially warranted further evaluation in specific subtypes such as desmoplastic small round cell tumour and solitary fibrous tumour (George *et al.*, 2009; NCT00474994) (**Table 1.6**). Furthermore, in a single-arm, phase II trial conducted by Jo *et al.* on a cohort of advanced desmoid tumour, sunitinib was found to possess promising antitumour activity in this locally aggressive neoplasm (**Table 1.6**) (Jo *et al.*, 2014).

Similarly, imatinib was inactive in a heterogeneous cohort of advanced STS in a single-arm, phase II multicentre trial (Chugh *et al.*, 2009; NCT00031915). However, in specific subtypes such as dermatofibrosarcoma protuberans and desmoid tumour, imatinib has shown potent antitumour activity in a number of phase II clinical trials (Chugh *et al.*, 2010; Kasper *et al.*, 2017; Penel *et al.*, 2011; Rutkowski *et al.*, 2010). Within dermatofibrosarcoma protuberans, a pooled analysis of two phase II clinical trials reported a CBR of 71% and a 57% PFR at 12 months (**Table 1.6**) (Rutkowski *et al.*, 2010; NCT00084630; NCT00085475). The composite trials in this pooled analysis had to be curtailed due to slow accrual and regulatory body approval, thereby providing a targeted therapy option for this chemoresistant STS subtype (Rutkowski *et al.*, 2010). Furthermore, in a number of phase II clinical trials conducted in desmoid tumour, imatinib has shown strong activity with high rates of disease control (CBR;

84%, 92%, 42%) and progression-arrest (**Table 1.6**) (Chugh *et al.*, 2010; Kasper *et al.*, 2017; Penel *et al.*, 2011; NCT00031915; NCT00287846; NCT01137916)

In a ground-breaking phase III placebo-controlled study of sorafenib in desmoid tumour patients, Gounder *et al.* reported a significantly improved mPFS with sorafenib when compared to placebo (mPFS: Not reached vs. 11.3 months, $p < 0.001$) (**Table 1.6**) (Gounder *et al.*, 2018; NCT02066181). Additionally, sorafenib induced a durable response in a substantial number of desmoid tumour patients with 33% showing CR or PR and 55% presenting SD (**Table 1.6**) (Gounder *et al.*, 2018). These data therefore present compelling evidence for the approval of sorafenib in desmoid tumour. Furthermore, in a heterogeneous mix of STS subtypes, a single-arm, phase II study of sorafenib was found to have significant activity against angiosarcoma but minimal activity against other STS (**Table 1.6**) (Maki *et al.*, 2009; NCT00245102). However, in a subsequent phase II trial focussing on angiosarcoma, sorafenib activity was found to be disappointing, with a mPFS in the range of 1.8-3.8 months, depending on tumour location (**Table 1.6**) (Ray-Coquard *et al.*, 2012; NCT00874874). Further subsequent analyses of the same clinical trial on vascular sarcomas have elucidated the potential activity of sorafenib in small cohorts of solitary fibrous tumour and epithelioid haemangioendothelioma, thereby warranting potential further evaluation in these specific subtypes (Chevreau *et al.*, 2013; Valentin *et al.*, 2013; NCT00874874).

Further clinical trials of multi-target TKIs in solitary fibrous tumour have been conducted with varying degrees of success. On the positive side, the phase II clinical trial conducted by Stacchiotti *et al.* found that axitinib exhibited high activity in advanced solitary fibrous tumour, with a CBR of 88%, as per RECIST (**Table 1.6**) (Stacchiotti *et al.*, 2019; NCT02261207). In the same phase II trial, axitinib also showed activity in solitary fibrous tumour patients that had progressed on previous antiangiogenic treatments, such as pazopanib, highlighting the potential of axitinib use in a multi-line TKI setting (Stacchiotti *et al.*, 2019; NCT02261207). The utility of axitinib is also currently being evaluated in a phase II trial of advanced angiosarcoma, where patient enrolment has recently been completed (NCT01140737).

Conversely, the SARC009 single-arm, phase II trial of dasatinib in STS found that dasatinib efficacy in solitary fibrous tumour was limited with a PFR at 6 months of only 30% (Schuetze *et al.*, 2017; NCT00464620). Furthermore, the solitary fibrous tumour

patients were embedded within a heterogeneous mix of rare STS subtypes and, within the clinical trial analysis as a whole, dasatinib did not meet the primary endpoint of 6-month PFR of $\geq 50\%$ (**Table 1.6**) (Schuetze *et al.*, 2017; NCT00464620). This analysis corroborated the findings of an earlier evaluation of the same SARC009 phase II trial conducted upon more common advanced STS subtypes, such as liposarcoma, undifferentiated pleomorphic sarcoma, and leiomyosarcoma, where dasatinib displayed low activity in the vast majority of enrolled STS subtypes (CBR $\leq 25\%$) (**Table 1.6**) (Schuetze *et al.*, 2016; NCT00464620). Despite this, some specific subtypes did show promising activity with dasatinib therapy including undifferentiated pleomorphic sarcoma (CBR $\geq 25\%$) and alveolar soft part sarcoma (6-month PFR; 62%) that potentially warrant further clinical evaluation (Schuetze *et al.*, 2016; Schuetze *et al.*, 2017; NCT00464620).

Within alveolar soft part sarcoma, cediranib has been found to have specific activity in this rare STS subtype. The placebo-controlled CASPS phase II trial, building on the positive results from the single-arm, phase II trial conducted by Kummar *et al.* (CBR: 95%), found that cediranib significantly reduced tumour size when compared to placebo (Median percentage change in sum of diameters of target lesions: -8.3% vs. +13.4%, $p = 0.001$), which was the primary endpoint of the study (Judson *et al.*, 2019; Kummar *et al.*, 2013; NCT00942877; NCT01337401). No significant difference between cediranib and placebo were observed in mPFS or mOS but the authors postulate that this is due to treatment crossover (Judson *et al.*, 2019). An ongoing trial of cediranib in alveolar soft part sarcoma is highly anticipated in order to elucidate reliable survival outcomes (NCT01391962). The high efficacy of cediranib in alveolar soft part sarcoma is a major development in the contemporary treatment of this chemoresistant disease which has a poor prognosis and high metastatic incidence.

Unfortunately, a phase II trial comparing the efficacy of nintedanib versus ifosfamide in a heterogeneous cohort of advanced STS did not report sufficient nintedanib activity to warrant further evaluation (Schöffski *et al.*, 2021; NCT02808247). The 1:1 double-arm trial showed that nintedanib treatment resulted in inferior response rates (CBR; 50% vs. 63%, $p = 0.368$) and survival outcomes (mPFS; 2.5 months vs. 4.4 months, $p = 0.07$) compared to ifosfamide, with a 12-week PFR (36%) falling short of the expansion criteria (53%). The trial was therefore ceased for futility (Schöffski *et al.*, 2021). However, new targeted therapies are constantly being developed and a number

of other multi-target TKIs not discussed previously have recently entered into clinical evaluation for advanced STS including cabozantinib (Cabometyx®), brivanib, and apatinib (Jones *et al.*, 2019; Li *et al.*, 2018; Schöffski *et al.*, 2020)

Finally, biomarker-driven basket trials have been undertaken on cohorts harbouring particular biological “fingerprints” that suggests that they would be susceptible to targeted TKI therapy. For instance, results from the single-arm CREATE phase II trial has shown that crizotinib, a potent ALK/MET inhibitor, has clinically meaningful activity in STS subtypes possessing ALK and/or MET activation (**Table 1.6**) (Schöffski *et al.*, 2017; Schöffski *et al.*, 2018; Schöffski *et al.*, 2018; NCT01524926). This includes MET-positive alveolar soft part sarcoma and clear cell sarcoma, as well as ALK-positive inflammatory myofibroblastic tumour, where crizotinib was found to achieve high rates of disease response and control (MET-positive alveolar soft part sarcoma DCR: 91%, MET-positive clear cell sarcoma DCR: 69%, ALK-positive inflammatory myofibroblastic tumour ORR: 50%) (**Table 1.6**) (Schöffski *et al.*, 2017; Schöffski *et al.*, 2018; Schöffski *et al.*, 2018). The success of the CREATE biomarker-driven basket trial provides a good model for the future design of biomarker-driven trials in STS. It is anticipated that biomarker-driven clinical trials in STS will move treatment paradigms of STS away from one-size-fits-all approaches based on histology towards a personalised treatment strategy based on a patient’s tumour biology. This would not only benefit patients and improve responses, but also improve cost-effectiveness of treatments (Wilding *et al.*, 2019).

Table 1.6: Notable clinical evaluations of other multi-target TKIs in non-GIST STS.							
TKI	Study	Study type	Patient #	Therapy regimen	Subtypes (n)	Response	Survival
Sunitinib	NCT0047994; George <i>et al.</i> , 2009	Single-arm phase II trial	48	Sunitinib 37.5 mg OD	LMS (11) NOS (5) SS (4) Other (28)	PR: 2% SD: 20% PD: 78%	mPFS: 1.8 months mOS: n/a
	Jo <i>et al.</i> , 2014	Single-arm phase II trial	19	Sunitinib 37.5 mg OD	DT (19)	PR: 26% SD: 42% PD: 32%	PFR at 24 months: 75% OSR at 24 months: 94%
Sorafenib	NCT02066181; Gounder <i>et al.</i> , 2018	Placebo-controlled phase III trial	87	2:1 randomisation to sorafenib 400 mg OD or placebo	DT (87)	CR/PR: 2%/31% SD: 55% PD: 12%	mPFS: Not reached vs. 11.3 months in placebo (p < 0.001) mOS: n/a
	NCT00245102; Maki <i>et al.</i> , 2009	Single-arm phase II trial	147	Sorafenib 400 mg BD	LMS (42) AS (40) Other (65)	CR/PR: 1%/4% SD: 51% PD: 44%	mPFS: 3.2 months mOS: 14.3 months
	NCT00874874; Ray-Coquard <i>et al.</i> , 2012	Single-arm phase II trial	41	Sorafenib 400 mg BD	AS (41)	CR/PR: 5%/10% SD: 10% PD: 61% n/a: 15%	mPFS: 1.8-3.8 months mOS: 9.0-12.0 months
Axitinib	NCT02261207; Stacchiotti <i>et al.</i> , 2019	Single-arm phase II trial	17	Axitinib 5 mg BD	SFT (17)	RECIST/Choi PR: 6%/41% RECIST/Choi SD: 82%/35% RECIST/Choi PD: 12%/24%	mPFS: 5.1 months mOS: 25.3 months
Cediranib	NCT01337401; Judson <i>et al.</i> , 2019	Placebo-controlled phase II trial	48	2:1 randomised to cediranib 30 mg OD or placebo	ASPS (48)	PR: 11% SD: 50% PD: 39%	mPFS: 10.1 vs. 4.9 months in placebo (p = 0.28) mOS: 27.8 vs. 47.3 months in placebo (p = 0.48) PFR at 12 months: 39% vs. 34% in placebo Median % change in sum of diameters of target lesion: -8% vs. +13% in placebo (p = 0.001) Best median change in sum of diameters of target lesion: -16% vs. +1% in placebo (p < 0.0001)
	NCT00942877; Kummar <i>et al.</i> , 2013	Single-arm phase II trial	46	Cediranib 30 mg OD	ASPS (46)	PR: 35% SD: 60% PD: 5%	DCR at 24 weeks: 84%
Dasatinib	NCT00464620; Schuetze <i>et al.</i> , 2017	Single-arm phase II trial	109	Dasatinib 100 mg BD	SFT (25) ASPS (12) ES (7) Other (65)	RECIST/Choi ORR: 1%/18%	mPFS: 5.8 months mOS: 21.6 months PFR at 6 months: 48%
	NCT00464620; Schuetze <i>et al.</i> , 2016	Single-arm phase II trial	200	Dasatinib 100 mg BD	LMS (49) UPS (48) Other (103)	CBR: < 25%	mPFS: 1.9 months mOS: 8.0 months

Imatinib	NCT00031915; Chugh <i>et al.</i> , 2009	Single-arm phase II trial	190	Imatinib 300 mg BD	LPS (31) UPS (30) LMS (29) Other (100)	CBR: 15%	mPFS: 1.9 months mOS: n/a
	NCT00031915; Chugh <i>et al.</i> , 2010	Single-arm phase II trial	51	Imatinib 100-300 mg BD	DT (51)	SD: 84% PD: 10% n/a: 6%	mPFS: Not reached PFR at 2 months: 94% PFR at 4 months: 88%
	NCT00287846; Penel <i>et al.</i> , 2011	Single-arm phase II trial	40	Imatinib 400 mg OD	DT (40)	CR/PR: 3%/9% SD: 80% PD: 9%	mPFS: 25.0 months PFR at 2 years: 55% mOS: Not reached OSR at 2 years: 95%
	NCT01137916; Kasper <i>et al.</i> , 2017	Single-arm phase II trial	38	Imatinib 800 mg OD	DT (38)	PR: 18% SD: 24% PD: 42% n/a: 16%	PFR at 24 months: 45% OSR at 24 months: 100%
	NCT00085475; NCT00084630; Rutkowski <i>et al.</i> , 2010	Single-arm phase II trial	24	Imatinib 400-800 mg OD	DFSP (24)	PR: 46% SD: 25% PD: 17% n/a: 13%	mPFS: 20.4 months PFR at 12 months: 57% mOS: Not reached OSR: 88%
Crizotinib	NCT01524926; Schöffski <i>et al.</i> , 2018	Single-arm phase II trial	40	Crizotinib 250 mg BD	MET-positive ASPS (40)	PR: 3% SD: 88% PD: 10%	PFR at 24 months: 38% OSR at 24 months: 97%
	NCT01524926; Schöffski <i>et al.</i> , 2018	Single-arm phase II trial	20	Crizotinib 250 mg BD	ALK-positive IMT (12)	ORR: 50%	PFR at 12 months: 73%
					ALK-negative IMT (8)	ORR: 14%	PFR at 12 months: 54%
NCT01524926; Schöffski <i>et al.</i> , 2017	Single-arm phase II trial	26	Crizotinib 250 mg BD	MET-positive CCS (26)	PR: 4% SD: 65% PD: 31%	mPFS: 4.3 months mOS: 9.1 months	
Nintedanib	NCT02808247; Schöffski <i>et al.</i> , 2021	Double-arm phase II trial	80	1:1 randomisation to nintedanib 200 mg BD or ifosfamide 3 g/m ² triweekly	LMS (31) LPS (22) Other (27)	PR: 5% SD: 45% PD: 48% n/a 3%	mPFS: 2.5 (Nin) vs, 4.4 months (Ifos) (p = 0.07) mOS: 13.7 (Nin) vs. 24.1 months (Ifos) (p = 0.11)

ALK; Anaplastic lymphoma kinase, AS; Angiosarcoma, ASPs; Alveolar soft part sarcoma, BD; Bis die, CBR; Clinical benefit rate, CCS; Clear cell sarcoma, CR; Complete response, DCR; Disease control rate, DFSP; Dermatofibrosarcoma protuberans, DT; Desmoid tumour, ES; Epithelioid sarcoma, IMT; Inflammatory myofibroblastic tumour, LMS; Leiomyosarcoma, LPS; Liposarcoma, mOS; Median overall survival, mPFS; Median progression-free survival, n/a; Not available, NCT; National Clinical Trial, NOS; Not otherwise specified, OD; Omni die (Once daily), ORR; Objective/overall response rate, OSR; Overall survival rate, PD; Progressive disease, PFR; Progression-free rate, PR; Partial response, RECIST; Response evaluation criteria in solid tumours, SD; Stable disease, SFT; Solitary fibrous tumour, SS; Synovial sarcoma, TKI; Tyrosine kinase inhibitor, UPS; Undifferentiated pleomorphic sarcoma (adapted from Wilding *et al.*, 2019).

1.3.3.7 Tyrosine kinase inhibitor resistance mechanisms in cancer

One of the main challenges in the contemporary targeted therapy of cancers, including STS, is the ubiquitous problem of drug resistance. Clinical experience with pazopanib has shown that patients either have tumours that display intrinsic resistance or develop an acquired resistance after an initial response (Lee *et al.*, 2019). Due to the similarities in molecular targets and clinical trial data, other multi-target TKIs evaluated within STS, such as regorafenib, sitravatinib, and anlotinib, are predicted to encounter similar issues. Regarding this, there are several reported mechanisms of TKI resistance that have been reported across the spectrum of cancers, including STS. This sub-chapter will discuss some of the most widely reported TKI resistance mechanisms that occur in cancer including secondary resistance mutations, tumour heterogeneity, TME alterations, metabolomics, and compensatory signalling pathways.

The first is secondary resistance mutations that arise on the targeted kinase. These mutations result in the inability, or reduced ability, of TKI binding, and subsequent inhibition, of the oncogenic kinase. These mutations are well-documented in cancer research with notable examples being the T790M and C797S *EGFR* mutations in NSCLC in response to *EGFR* TKI therapy (Vyse & Huang, 2019). Within an STS setting, treatment of GISTs with TKIs is frequently associated with the acquisition of secondary resistance mutations. In first-line therapy, advanced GIST is treated with imatinib, and the vast majority of patients experience disease progression after approximately 2 years due to the emergence of secondary mutations in *KIT* (e.g., V654A or T670I) or *PDGFRA* (e.g., D842V) (**Table 1.2**) (Lostes-Bardaji *et al.*, 2021). Upon disease progression with imatinib, sunitinib and regorafenib are utilised as second- and third-line therapies, respectively (**Table 1.2**). This multi-line therapeutic strategy has been guided by the biological understanding of resistance mechanisms and the mechanism of TKI action in GIST (Bauer *et al.*, 2021). For instance, sunitinib has been shown to have high efficacy against the most prevalent imatinib-resistance secondary mutation V654A, whilst regorafenib is preferentially effective against imatinib/sunitinib-resistant activation loop secondary mutations (Lostes-Bardaji *et al.*, 2021; Serrano *et al.*, 2019). In the fourth-line setting, ripretinib can be employed as it has broad activity against all known, clinically relevant *KIT* and *PDGFRA* secondary mutations due to the novel switch control mechanism of action that the inhibitor

employs (Smith *et al.*, 2019) (**Table 1.2**). Similarly, avapritinib has been approved for use in GIST patients harbouring refractory *PDGFRA* exon 18 resistance mutations, most notably D842V, which renders the tumour resistant to imatinib, sunitinib, and regorafenib treatment (Heinrich *et al.*, 2020; Lostes-Bardaji *et al.*, 2021). However, continued research is needed due to the reported emergence of ripretinib and avapritinib resistance mechanisms (Bauer *et al.*, 2021; Blay *et al.*, 2020; Grunewald *et al.*, 2021). In contrast to GIST, the targets and mechanisms of action of TKIs in the vast majority of STS are not currently well understood and secondary resistance mutations in targeted molecules in response to TKI therapy have not been reported.

Secondary resistance mutations primarily arise due to the outgrowth of pre-existing, resistant, sub-clonal populations harbouring these mutations in response to TKI therapy (Grünewald *et al.*, 2020). This is due to the nature of intratumoural heterogeneity where cells of the same tumour exhibit significant differences in genetics, epigenetics, metabolomics, and/or transcription, such as differences in p53 expression, miRNA epigenetic regulation, and glycolytic metabolism (Wang *et al.*, 2019; Xiao *et al.*, 2019; Xue *et al.*, 2019). Another important consideration in terms of tumour heterogeneity is the existence of drug-tolerant persister cells (De Conti *et al.*, 2021; Grünewald *et al.*, 2020; Vallette *et al.*, 2019). These are cells without pre-existing resistance mutations but survive TKI therapy nonetheless due to their slow or non-cycling nature with additional altered metabolism, epigenetics, signalling, and/or transcription (De Conti *et al.*, 2021; Vallette *et al.*, 2019). These drug-tolerant populations of cells can then give rise to cellular progeny with genetic and/or non-genetic resistance mechanisms and lead to tumour relapse and growth (De Conti *et al.*, 2021; Vallette *et al.*, 2019). Additionally, a small fraction of a tumour is often made up of cancer stem cells which possess the potential for self-renewal and the development of *de novo* resistance mechanisms that can cause disease relapse and metastases (Ferguson *et al.*, 2021; Grünewald *et al.*, 2020). The existence of drug-tolerant and sarcoma stem cells and their promotion of drug-resistant cellular states have been reported in a number of STS subtypes (Cao *et al.*, 1998; Grünewald *et al.*, 2020; Rogers *et al.*, 2014; Vallette *et al.*, 2019). Therefore, intratumoural heterogeneity and the cellular subpopulations that exist within a tumour are important considerations in contemporary research of TKI resistance in STS.

Furthermore, the interaction between heterogeneous populations of cells within a tumour and their surrounding tumour microenvironment (TME) further increases the complexity and heterogeneity of tumours and plays an important part in the response and resistance to targeted therapies such as TKIs (Grünewald *et al.*, 2020; Ferguson *et al.*, 2021; Son *et al.*, 2017; Tan *et al.*, 2018). The TME comprises tumour cells, embedded within ECM, and the surrounding components of cellular tissues such as immune cells, vasculature, MSCs, and cancer-associated fibroblasts. The biological interplay between components of the TME significantly influences the tumourigenic behaviour and therapy response in tumour cells. For example, ECM remodelling has frequently been associated with drug resistance by promoting drug-resistant phenotypes in tumours including epithelial-mesenchymal transition induction, apoptosis evasion, and increased expression of drug efflux pumps (Henke *et al.*, 2020; Januchowski *et al.*, 2014; Son *et al.*, 2017; Winkler *et al.*, 2020). Additionally, increased ECM density can impair drug access to the tumour thereby protecting the tumour from therapeutically effective doses of treatment (Henke *et al.*, 2020; Januchowski *et al.*, 2014). Furthermore, the level of immune infiltration, vascularity, and paracrine signalling within the TME have been shown to have profound effects on tumour response to cytotoxic and targeted therapies (Ferguson *et al.*, 2021; Grünewald *et al.*, 2020; Khalaf *et al.*, 2021; Petitprez *et al.*, 2020; Son *et al.*, 2017; Tan *et al.*, 2018). Various studies have corroborated the role of the TME on therapy response and resistance in sarcomas (Bai *et al.*, 2015; Heymann *et al.*, 2019; Grünwald *et al.*, 2020). Most of these studies are primarily based on osteosarcoma and are focussed on cytotoxic chemotherapies. There is therefore an unmet need to study the effects of the TME and ECM upon targeted therapy response and resistance in STS.

A further important consideration when discussing mechanisms of resistance is drug metabolism and efflux by proteins such as cytochrome P450 (CYP450) and p-glycoprotein (Grünewald *et al.*, 2020; Mansoori *et al.*, 2017; Wilding *et al.*, 2019). For the majority of the TKIs discussed, the CYP450 pathway is the primary avenue of metabolism for removal of these compounds from the body (Wilding *et al.*, 2019). Therefore, patients with increased activity of CYP450 or those harbouring activating CYP450 polymorphisms will result in increased metabolism of TKIs, thereby reducing the activity of the TKI upon the tumour and increasing drug resistance. Similarly,

increased activation levels and activating polymorphisms in p-glycoprotein, for which the majority of TKIs discussed are also substrates, results in increased drug efflux from target tumour cells (Grünewald *et al.*, 2020; Wilding *et al.*, 2019). Therefore, high inter-patient variability has been shown in STS patients treated with TKIs, with increased activity of metabolic and/or efflux proteins having a profound effect on drug response and resistance (Wilding *et al.*, 2019). Recent discussions have focussed on employing therapeutic drug monitoring techniques to subvert the TKI resistance issues caused by increased metabolism and/or efflux (Herviou *et al.*, 2016; Wilding *et al.*, 2019). This involves maintaining the TKI plasma concentration within an effective range by altering the TKI dosage dependent on patient pharmacokinetics and temporal considerations, without administering a toxic dosage which would result in adverse side effects (Wilding *et al.*, 2019).

Finally, in response to TKI therapy, tumours have been extensively reported to alter their cellular signalling to activate compensatory signalling pathways to bypass the antitumour effects of therapy (Grünewald *et al.*, 2020; Logue & Morrison, 2012; Trusolino & Bertotti, 2012; Von Manstein *et al.*, 2013). As discussed in **Chapter 1.2.4**, there is extensive crosstalk between differing critical, intracellular signalling pathways with negative feedback loops, cross activation/inhibition, and pathway convergence. Therefore, inhibition of a specific signalling pathway can result in the activation of a bypass survival signal that circumvents the TKI-induced pathway blockade in order to elicit drug resistance and disease progression. Various mechanisms of compensatory signalling pathways have been reported in the literature. Firstly, in response to inhibition of a specific RTK, pathway redundancies can occur through the increased and/or constitutive signalling via an alternative, non-inhibited receptor. These can include other alternative RTKs, as well as other receptor types, such as integrins and transforming growth factor β receptor (TGF β R). These alternative receptors lead to the activation of the same signalling pathways previously activated by the inhibited RTK, thereby overcoming the antitumour consequence of RTK inhibition (Logue & Morrison, 2012; Niederst & Engelman, 2013; Von Manstein *et al.*, 2013). Similarly, the activity of another receptor can be enhanced that activates a distinct pro-survival signalling pathway, thereby bypassing TKI-induced signalling pathway blockade. This therefore negates the tumour's dependency upon the targeted RTK pathway, resulting in drug resistance (Logue & Morrison, 2012; Niederst *et al.*, 2013; Von Manstein *et al.*,

2013). The increased activation of compensatory RTKs and/or non-RTK receptors can be due to various reasons such as receptor amplification, increased autocrine and paracrine ligand expression, and/or positive feedback loops by hyperactivated cellular signalling nodes (Jiao *et al.*, 2018; Logue & Morrison, 2012; Trusolino & Bertotti, 2012; Von Manstein *et al.*, 2013). Furthermore, the emergence of activating mutations within critical intracellular signalling components such as N-Ras and B-Raf can also elicit bypass signalling pathways to overcome the antiproliferative effects of TKI therapy (Lanzi *et al.*, 2019; Logue & Morrison, 2012; Von Manstein *et al.*, 2013; Watanabe *et al.*, 2020).

1.3.3.7.1 Current literature of multi-target TKI resistance specific to non-GIST soft tissue sarcoma

The mechanisms of multi-target TKI resistance in non-GIST STS are poorly understood and the current literature on the topic is limited to a handful of studies. In this sub-chapter, studies evaluating mechanisms of resistance to multi-target TKIs in STS will be discussed, both in the acquired and intrinsic resistance settings.

1.3.3.7.1.1 Acquired multi-target TKI resistance in soft tissue sarcoma

The study by Yokoyama *et al.* derived two pazopanib-resistant synovial sarcoma models by exposing two relatively sensitive synovial sarcoma cell lines to chronic pazopanib exposure (Yokoyama *et al.*, 2017). Gene expression microarray analysis revealed that the acquisition of pazopanib resistance resulted in the downregulation of dual specificity phosphatase 6 (*DUSP6*) expression, a phosphatase that is known to regulate ERK1/2 activity. Through the utilisation of CRISPR knockdown of *DUSP6*, the authors confirmed that *DUSP6* downregulation results in the increased activity of ERK1/2 and subsequent resistance to pazopanib treatment in synovial sarcoma cell line models (Yokoyama *et al.*, 2017). Therefore, treatment with the MEK inhibitor trametinib was found to be effective in these cell line models. Furthermore, the study reports that dual treatment with pazopanib and low-dose trametinib significantly decreased the growth of murine synovial sarcoma tumours (Yokoyama *et al.*, 2017).

Shiozawa *et al.*, once again utilising acquired resistance synovial sarcoma cell line models generated through chronic pazopanib exposure, reported that secreted miRNA-761 levels (enclosed within extracellular vesicles) were found to be increased in resistant cells compared to parental cells. The study also found that miRNA-761 targeted proteins such as sirtuin-3 and lamin A, whose knockdown have previously been shown to confer chemotherapeutic resistance in cancer (Shiozawa *et al.*, 2018). Employing identical models in a subsequent study, Shiozawa *et al.* also reported that pazopanib-resistant synovial sarcoma secreted increased levels of extracellular vesicles containing Wnt signalling pathway components, when compared to parental cells (Shiozawa *et al.*, 2018). This corroborates with previous findings that have shown the critical nature of Wnt signalling in the growth and survival of synovial sarcoma (Baird *et al.*, 2005; Barham *et al.*, 2013).

Furthermore, the study by Wong *et al.* generated acquired resistance models of malignant rhabdoid tumour through the chronic exposure of initially sensitive A204 cells to increasing concentrations of the multi-target TKIs pazopanib, dasatinib, and sunitinib (Wong *et al.*, 2016). Within the TKI-resistant sublines, PDGFR α expression was found to be lost compared to parental cells, with subsequent signalling bypass of the downstream Akt signalling pathway. The TKI-resistant cells had thereby lost their initial PDGFR α signalling dependency and, as a result, became resistant to PDGFR α -targeting TKIs. The authors determined that targeting of the FGFR pathway – a pathway known to be activated in A204 cells – was an effective salvage therapy in this model (Wong *et al.*, 2016).

Finally, the study by Vyse *et al.* undertook a phosphoproteomic analysis upon the A204 TKI-resistant sublines described previously by Wong *et al.*, excluding the sunitinib-resistant model. This evaluation found that pazopanib-resistant cells were found to display elevated phosphorylation in cytoskeletal regulation pathways, whilst dasatinib-resistant cells showed an upregulation of IGF1R/InsR signalling activity, when compared to parental cells (Vyse *et al.*, 2018).

1.3.3.7.1.2 Intrinsic multi-target TKI resistance in soft tissue sarcoma

The study by Qiao *et al.* focussed on determining tyrosine kinases associated with intrinsic pazopanib resistance in synovial sarcoma cell lines (Qiao *et al.*, 2017). The

study determined that the 1273/99 cell line had robust intrinsic resistance to pazopanib compared to the other synovial sarcoma cell lines evaluated. Immunoblotting and subsequent siRNA evaluation found that expression of the RTKs PDGFR β , MET, and protein tyrosine kinase 2 β (PTK2B) were elevated and driving proliferation in the pazopanib-resistant 1273/99 model compared to the remaining relatively sensitive synovial sarcoma cell lines (Qiao *et al.*, 2017). Additionally, phosphoproteomic analysis conducted on the synovial sarcoma cell line panel found that the increased activity of the tyrosine kinases FGFR3, RET, VEGFR1, NTRK1, Src, ephrin A2 (EphA2), and EphA4 were correlated with pazopanib resistance (Qiao *et al.*, 2017).

The existence of activating mutations in STS with intrinsic multi-target TKI resistance has also been reported. In synovial sarcoma cell line and xenograft models with intrinsic pazopanib resistance, activating N-Ras Q61R mutations were found to be driving pazopanib resistance and could be overcome with dual pazopanib and low-dose MEK inhibition (Lanzi *et al.*, 2019). Activating Ras mutations have also been reported in STS patients with intrinsic pazopanib resistance. For instance, Saturno *et al.* described a G12V K-Ras-activating mutation in a patient diagnosed with spindle cell sarcoma that was intrinsically resistant to pazopanib therapy (Saturno *et al.*, 2021). Subsequent therapy with a pan-Raf inhibitor was found to result in significant clinical benefit and an unconfirmed PR (Saturno *et al.*, 2021).

Finally, Lanzi *et al.* also reported the overactivation of IGF1R/InsR with subsequent downstream Akt signalling in a synovial sarcoma cell line with intrinsic pazopanib resistance (Lanzi *et al.*, 2019). The authors determined that combination therapy of pazopanib and IGF1R/InsR inhibitor overcomes intrinsic pazopanib resistance in this cell line model (Lanzi *et al.*, 2019).

1.4 Hypothesis and aims

The mechanisms of multi-target TKI resistance in STS are poorly understood and this limits our ability to develop effective treatment strategies to treat multi-target TKI-resistant STS.

The hypothesis of the project is that TKI-resistant STS tumours alter their cellular signalling pathways in response to treatment to overcome the antiproliferative effects of multi-target TKIs. To address this hypothesis, the project has the following aims:

Aim 1: Derive and characterise models of acquired and intrinsic multi-target TKI resistance. Utilising patient-derived xenograft (PDX)-derived cells, immortalised cell lines, and murine xenografts, I seek to derive and characterise STS models of acquired and intrinsic multi-target TKI resistance.

Aim 2: Define signalling alterations associated with multi-target TKI resistance in STS models. Perform proteomic analysis and chemical inhibitor screens in STS models to define signalling alterations associated with multi-target TKI resistance.

Aim 3: Characterise mechanisms driving multi-target TKI resistance and develop new salvage therapies in STS. Characterise the mechanisms by which genes/proteins identified previously confer multi-target TKI resistance. Exploit this knowledge to develop new therapeutic strategies that can effectively be used to treat multi-target TKI-resistant STS.

By achieving these aims, I seek to address the gap in the current knowledge of multi-target TKI resistance mechanisms which could allow us to design future therapies for STS patients.

Chapter 2

Materials and methods

2.1 Mammalian cell culture and phenotypic assays

2.1.1 Cell culture and derivation of acquired resistance sublines

The SARC-209 cell model was generated from a patient-derived xenograft (PDX) derived from a percutaneous core needle biopsy of a post-relapse abdominal wall metastasis in a spindle cell sarcoma patient from the Royal Marsden Hospital Sarcoma Unit. Biopsied cells were implanted subcutaneously into nude mice by Champions Oncology to form a PDX. The J000104314 cell model was generated from a PDX model derived from a synovial sarcoma patient. The PDX was obtained from The Jackson Laboratory.

SARC-209 and J000104314 tumour tissue was collected from mice and minced samples were dissociated in 1x dissociation media (Dulbecco's modified Eagle medium (DMEM):Ham's F12 1:1 + 15 mM HEPES, 0.1x insulin-transferrin-selenium A (Gibco), 10 µg/mL epidermal growth factor (EGF) (Peprotech), 10 mg/mL hydrocortisone (Sigma Aldrich), 10 µM Y-27632 (LC Laboratories), 0.5 mg/mL collagenase (Sigma Aldrich), 0.1 mg/mL hyaluronidase (Sigma Aldrich), 100 units/mL DNase I (Sigma Aldrich), 5% foetal bovine serum (FBS) (Gibco), and 0.5% penicillin/streptomycin) for 2 hours at 37 °C on a rotator at 100 rpm. Cell pellet was collected, washed with phosphate-buffered saline (PBS) (spiked with 10 µM Y-27632), and centrifuged for 5 minutes at 1400 rpm. Cell pellet was resuspended in red blood cell (RBC) lysis buffer (Invitrogen) and incubated for 1 minute at room temperature. Cells were washed with PBS (spiked with 10 µM Y-27632) and centrifuged for 5 minutes at 1400 rpm. Cell pellet was resuspended in warm 0.05% trypsin/EDTA (Gibco) (spiked with 10 µM Y-27632). Cells were agitated by pipetting, incubated for 8 minutes at 37 °C, agitated again, before trypsin inactivation with Y-media (DMEM:Ham's F12 1:1 + 15 mM HEPES, 1% L-glutamine, 5 µg/mL insulin (Sigma Aldrich), 0.4 µg/mL hydrocortisone, 10 ng/mL EGF, 250 ng/mL amphotericin (ThermoFisher Scientific), 9.62 ng/mL cholera toxin (Sigma Aldrich), 5 µM Y-27632, 10% FBS, and 0.5% penicillin/streptomycin). Cells were pelleted before resuspension in a 1:1 mix of DNase solution (1 mg/mL DNase I and 10 µM Y-27632 in PBS) and Y-media, before incubation for 5 minutes at 37 °C. Cells were washed with PBS (spiked with 10 µM Y-27632) and centrifuged for 5 minutes at 1400 rpm. Cells were resuspended in Y-media and agitated through pipetting. Cells were filtered through a

70 μm filter, pelleted, and then resuspended in 1x magnetic-activated cell sorting (MACS) buffer, diluted in PBS from a stock 20x solution (20x MACS buffer; 5 g bovine serum albumin (BSA) (Sigma Aldrich), 4 mL 0.5 M EDTA (Sigma Aldrich) in 50 mL PBS), with 10 μM Y-27632. Superparamagnetic nanoparticle (MicroBead)-conjugated antibodies targeted towards mouse-specific antigens (Mouse Cell Depletion Kit, Miltenyi Biotec 130-104-694) were added and agitated by pipetting to mix. Solution was incubated on ice for 15 minutes. Further 1x MACS buffer was added to the sample solution before the sample was loaded into a 1x MACS-buffer-equilibrated QuadroMACS magnet LS column (Miltenyi Biotec). The column was washed twice with 1x MACS buffer. The magnetic column allowed non-murine cells to pass through and elute, whilst retaining antibody-bound murine cells. Eluted cells were resuspended in Y-media. PDX-derived cells were frozen in 10% dimethyl sulfoxide (DMSO) (Sigma Aldrich) in FBS plus 10 μM Y-27632. SARC-209 and J000104314 cells were cultured *in vitro* in Y-media. HEK-293T, A204, and G402 cell lines were obtained from the American Type Culture Collection (ATCC). HS-SY-II cell line was obtained from the Riken BioResource Research Center. All other cell lines were a gift from Professor Janet Shipley. Cell lines were cultured in DMEM (A204, G402, SAOS2, U2OS, HT1080, MESSA, SW684, SW872, Hs729T, RUCH3, T91-95, SW982, and HEK-293T) or Roswell Park Memorial Institute (RPMI) 1640 media (SJSA1 and RMS-YM), supplemented with 10% FBS and 0.5% penicillin/streptomycin. Cell lines were frozen in 10% DMSO in FBS. All cells were cultured in 95% air:5% CO_2 at 37 $^\circ\text{C}$. Media was replenished twice weekly.

Pazopanib, regorafenib (LC Laboratories), sitravatinib, and anlotinib (Selleck Chemicals) were used to derive acquired resistance in the A204 cell line. Cells were initially grown in media containing a tyrosine kinase inhibitor (TKI) concentration at the determined inhibitory constant (IC_{50}) values from cell viability assays. Inhibitor concentration was incremented stepwise to 1 μM , 2 μM , and 3 μM , until a final inhibitor concentration of between 3-5 μM was maintained in resistant cells. Resistance was determined using cell viability and colony formation assays. Media and inhibitors were replenished twice weekly.

2.1.2 Cell viability assay

Cells (2,000/well) were seeded into 96 well plates. After 24 hours, cells were treated with inhibitors at the indicated concentrations and incubated for 72 hours prior to cell viability measurement by CellTiter-Glo assay (Promega), following the manufacturer's recommendations. Measurements were undertaken on Victor X5 (PerkinElmer), Spark (Tecan), or FLUOstar Omega (BMG Labtech) plate readers. IC₅₀ data were generated from dose response curves using four-parameter regression fit in PRISM (Graphpad). Combination indices for combinatorial treatments were calculated using **Equation E1** (Chou, 2010).

$$\text{Equation 1: Combination index} = \left(\frac{A_x B}{A} \right) + \left(\frac{A B_x}{B} \right)$$

Equation E1: Combination index calculation. A; the IC₅₀ value of inhibitor A, B; the IC₅₀ value of inhibitor B, A_xB; the concentration of constituent inhibitor A within the IC₅₀ concentration of combination treatment AB, AB_x; the concentration of constituent inhibitor B within the IC₅₀ concentration of combination treatment AB, IC₅₀; Inhibitory constant.

Inhibitors included pazopanib, regorafenib, ponatinib, dasatinib (LC Laboratories), sitravatinib, anlotinib, infigratinib, and erdafitinib (Selleck Chemicals).

2.1.3 Temporal (27 day) cell viability assay

The initial sensitivities to sitravatinib and infigratinib (Selleck Chemicals) were evaluated in parental A204 cells (2,000/well) via cell viability assays, as per the protocol outlined previously. Using the same flask of parental A204 cells, cells (1,000,000/flask) were seeded into x2 T75 flasks. After 24 hours, x1 T75 was treated with DMSO (Sigma Aldrich) and the remaining x1 T75 was treated with 1 μM sitravatinib. Cells were allowed to grow for four weeks post-seeding in their respective treatments. Media and inhibitors were replenished twice weekly. Cells were maintained at between 70-90% confluency. After 4-, 7-, 14-, 21-, and 28-days post-seeding, cells from the x2 flasks were evaluated for temporal changes in their sensitivities to sitravatinib and infigratinib via cell viability assays, as per the protocol outlined previously.

2.1.4 Apoptosis assay

Cells (2,000/well) were seeded into 96 well plates. After 24 hours, cells were treated with inhibitors at the indicated concentrations and incubated for 24 hours prior to apoptosis measurement by Caspase-Glo 3/7 assay (Promega), following the manufacturer's recommendations. Measurements were undertaken on Victor X5 (PerkinElmer) or FLUOstar Omega (BMG Labtech) plate readers. Inhibitors included pazopanib, regorafenib, ponatinib, dasatinib (LC Laboratories), sitravatinib, anlotinib, infigratinib, and erdafitinib (Selleck Chemicals).

2.1.5 Small molecule inhibitor screen

Cells (2,000/well) were seeded into 96 well plates. After 24 hours, cells were treated with inhibitors at 0.5 μ M and incubated for 72 hours prior to cell viability measurement by CellTiter-Glo assay (Promega), following the manufacturer's recommendations. Measurements were undertaken on Victor X5 plate readers (PerkinElmer). A list of the small molecule inhibitors utilised along with their primary target and supplier is presented in **Table 1.2**. Data was clustered two-way based on Euclidean distance using the Perseus software (Tyanova *et al.*, 2016).

Small molecule inhibitor	Primary target(s)	Supplier
Axitinib *	Broad spectrum: RTKs	LC Laboratories
Cabozantinib *	Broad spectrum: RTKs	LC Laboratories
Cediranib	Broad spectrum: RTKs	LC Laboratories
Foretinib	Broad spectrum: RTKs	LC Laboratories
Imatinib	Broad spectrum: RTKs, Abl1	LC Laboratories
Lenvatinib	Broad spectrum: RTKs	LC Laboratories
Nintedanib *	Broad spectrum: RTKs	LC Laboratories
Pazopanib	Broad spectrum: RTKs	LC Laboratories
Ponatinib	Broad spectrum: RTKs, Abl1	LC Laboratories
Regorafenib	Broad spectrum: RTKs	LC Laboratories
Sitravatinib ***	Broad spectrum: RTKs	Selleck Chemicals
Sorafenib	Broad spectrum: RTKs, C-Raf, B-Raf	LC Laboratories
Sunitinib	Broad spectrum: RTKs	LC Laboratories
Vandetanib	Broad spectrum: RTKs	LC Laboratories
Entrectinib	NTRK1/2/3, ROS1, ALK	Selleck Chemicals
GW441756	NTRK1	Selleck Chemicals
Ceritinib	ALK	Selleck Chemicals
Crizotinib	ALK, MET	LC Laboratories
NVP-TAE684	ALK	Selleck Chemicals
Osimertinib (AZD-9291)	EGFR	Selleck Chemicals
EAI045	EGFR	Selleck Chemicals
Erlotinib	EGFR	LC Laboratories
Gefitinib	EGFR	LC Laboratories
Lapatinib	EGFR, HER2	LC Laboratories
Neratinib	EGFR, HER2	LC Laboratories

Infigratinib (BGJ-398)	FGFR1/2/3	Selleck Chemicals
Erdafitinib (JNJ-42756493) **	FGFR1/2/3/4	Selleck Chemicals
Linsitinib	IGF1R	LC Laboratories
NVP-AEW541	IGF1R, InsR	Selleck Chemicals
Cilengitide trifluoroacetate	Integrins $\alpha\beta3$, $\alpha\beta5$	Selleck Chemicals
Bosutinib	Src, Abl1	LC Laboratories
Dasatinib	Src, Abl1, Broad spectrum: RTKs	LC Laboratories
Nilotinib *	Bcr-Abl1	LC Laboratories
Saracatinib	Src	Selleck Chemicals
PF562271	FAK	Selleck Chemicals
TAE226	FAK	Selleck Chemicals
BI-2536	PLK1	Selleck Chemicals
BX-795	PDPK1	Sigma Aldrich
Dactolisib (BEZ235)	PI3K, mTOR	LC Laboratories
Rapamycin (Sirolimus)	mTOR	LC Laboratories
Binimetinib	MEK1/2	LC Laboratories
Trametinib	MEK1/2	LC Laboratories
Dabrafenib	B-Raf V600E	Selleck Chemicals
Adezmapimod (SB203580)	p38 MAPK	Selleck Chemicals
SP600125	JNK1/2/3	Selleck Chemicals
Capivasertib (AZD-5363)	Akt1/2/3	Selleck Chemicals
MK2206	Akt1/2/3	Selleck Chemicals
Momelotinib	JAK1/2	Selleck Chemicals
Niclosamide	STAT3	Selleck Chemicals
SH-4-54	STATs	Selleck Chemicals
Galunisertib	TGF β R1	Selleck Chemicals
BMS345541	IKK1/2	Sigma Aldrich
Alisertib	Aurora A	Selleck Chemicals
Rabusertib (LY2603618)	Chk1	Selleck Chemicals
MK8776	Chk1	Selleck Chemicals
Palbociclib	CDK4/6	Selleck Chemicals
Silmitasertib	CK2	Selleck Chemicals
Talazoparib	PARP	Selleck Chemicals
Rucaparib	PARP	Selleck Chemicals
XAV-939	Tankyrase	Selleck Chemicals
Navitoclax	Bcl-2, Bcl-w, Bcl-xL	Selleck Chemicals
GSK126	EZH2	Selleck Chemicals
JQ1	BET bromodomains	Selleck Chemicals
Luminespib (NVP-AUY922)	Hsp90	LC Laboratories

ADP; Adenosine diphosphate, ALK; Anaplastic lymphoma kinase, Bcl-(2/xL); B-cell lymphoma (2/extra large) protein; Bcl-w; Bcl-2-like protein 2, Bcr; Breakpoint cluster region protein, BET; Bromo- and extra-terminal domain, CDK(4/6); Cyclin-dependent kinase (4/6); Chk1; Checkpoint kinase 1, CK2; Casein kinase 2, EGFR; Epidermal growth factor, EZH2; Enhancer of zeste homolog 2, FAK; Focal adhesion kinase, FGFR(1/2/3/4); Fibroblast growth factor receptor (1/2/3/4), HER2; Human epidermal growth factor receptor 2, Hsp90; Heat shock protein 90, IGF1R; Insulin-like growth factor 1 receptor, IKK(1/2); I κ B kinase (1/2), InsR; Insulin receptor, JAK(1/2); Janus kinase (1/2), JNK(1/2/3); c-Jun N-terminal kinase (1/2/3), MAPK; Mitogen-activated protein kinase, MEK; Mitogen-activated protein kinase kinase, mTOR; Mechanistic target of rapamycin, N-terminal; Amino-terminal, NTRK(1/2/3); Neurotrophic tyrosine kinase receptor (1/2/3) PARP; Poly (ADP-ribose) polymerase, PDPK1; Phosphoinositide-dependent protein kinase 1, PI3K; Phosphoinositide 3-kinase, PLK1; Polo-like kinase 1, (B/C)-Raf; Rapidly accelerated fibrosarcoma, RTK; Receptor tyrosine kinase, STAT(3); Signal transducer and activator of transcription (3), TGF β R1; Transforming growth factor β receptor 1. (* = SARC-209/J000104134 screens only, ** = A204/G402 screens only, *** = Screen utilised in **Figure 4.6A** only.

2.1.6 Tyrosine kinase inhibitor sequential treatment assay

Cells (500/well) were seeded into x13 sets of black-walled 96 well plates. After 24 hours, one plate set was fixed with 10% neutral-buffered formalin solution (Sigma Aldrich) and stored at 4 °C. The remaining plate sets were treated with DMSO (Sigma Aldrich) or 1 μ M of inhibitor for a period of two weeks (**Table 2.2**). After a period of two weeks, the administered inhibitor was continued or altered as per the protocol outlined

in **Table 2.2** before undergoing a further two weeks of treatment. After this secondary period of two weeks, the administered inhibitor was continued or altered as per the protocol outlined in **Table 2.2** before undergoing a final two weeks of treatment. Formalin fixing of plate sets was repeated twice weekly for the duration of the 6-week assay. Media and inhibitors were replenished every 72 hours. Fixed cells were stained with Hoescht 33342 (R & D Systems) for 10 minutes at 37 °C, followed by PBS washes. Direct cell count was undertaken using a Celigo Image Cytometer (Nexcelcom BioScience). Cell count for a particular inhibitor sequence was ceased upon both technical replicates reaching overconfluency. Inhibitors used include pazopanib, regorafenib, ponatinib (LC Laboratories), sitravatinib, anlotinib, infigratinib, and erdafitinib (Selleck Chemicals).

Table 2.2: Protocol schedule for 6-week TKI sequential treatment assay.			
	2 weeks	2 weeks	2 weeks
	1	2	3
Sequential treatments	P/R/S/A	Paz	
		Reg	
		Sit	
		Anlo	
		Pon	
		Inf	Inf
			P/R/S/A
			Inf + P/R/S/A
			Pon
		Erda	Erda
			P/R/S/A
			Erda + P/R/S/A
Pon			
Monotherapies	DMSO	DMSO	DMSO
	Paz	Paz	Paz
	Reg	Reg	Reg
	Sit	Sit	Sit
	Anlo	Anlo	Anlo
	Inf	Inf	Inf
	Erda	Erda	Erda
	Pon	Pon	Pon
Dual	Inf + P/R/S/A	Inf + P/R/S/A	Inf + P/R/S/A
	Erda + P/R/S/A	Erda + P/R/S/A	Erda + P/R/S/A
DMSO; Dimethyl sulfoxide, Erda; Erdafitinib, Inf; Infigratinib, P/R/S/A; Pazopanib (Paz), regorafenib (Reg), sitravatinib (Sit), or anlotinib (Anlo), Pon; Ponatinib, TKI; Tyrosine kinase inhibitor.			

2.1.7 Growth curve assay

Cells (1,000/well) were seeded into x14 black-walled 96 well plates. After 24 hours, one plate was fixed with 10% neutral-buffered formalin solution (Sigma Aldrich) and stored at 4 °C. Formalin fixing was repeated once daily upon a single plate for the duration of the 14-day assay. Media was replenished every 72 hours. After 14 days, cells were stained with Hoescht 33342 (R & D Systems) for 10 minutes at 37 °C, followed by PBS washes. Direct cell count was undertaken using a Celigo Image Cytometer (Nexcelcom BioScience).

2.1.8 Colony formation assay

Cells (10,000/well) were seeded into 6 well plates. After 24 hours, cells were treated with inhibitors at the indicated concentrations for a duration of 2 weeks. Media and inhibitors were replenished every 72 hours. After 2 weeks, cells were fixed using Carnoy's fixative (3:1 methanol:acetic acid) and stained with 1% crystal violet solution (Sigma Aldrich). Plates were digitally imaged using ChemiDoc Touch Imaging System (Bio-Rad) or G-Box Chemi-XX6 (Syngene) imagers. Densitometry analysis was performed using the ImageJ software program (National Institutes of Health). Inhibitors used include pazopanib, regorafenib, ponatinib, dasatinib (LC Laboratories), sitravatinib, anlotinib, infigratinib, and erdafitinib (Selleck Chemicals).

2.1.9 Xenograft assay

Harvested SARC-209-originating PDX tumours were cut into 3x3x3 mm³ pieces and implanted into the left flank of 5-6 week old female NCR nude mice aged. Mice were from the ICR Sutton breeding unit. Tumour size and body weight were measured twice a week. Tumour size was measured using calipers with volume calculated using **Equation E2**.

$$\text{Equation E2: Tumour volume} = \frac{L \times W^2}{2}$$

Equation E2: Tumour volume calculation. L; length of tumour, W; width of tumour.

Body weight was measured using a weighing balance. Sample sizes were decided to ensure a minimum of 5 mice, with the maximum number being 10. Mice (n=19) with tumours over 250 mm³ were randomly allocated into different treatments and treated daily p.o. with vehicle (80 mM sodium citrate pH 3.0) (n=9) or 30 mg/kg dasatinib (n=10) (LC Laboratories). Dasatinib and vehicle treatments were made up by the same member of staff at the Biological Services Unit (BSU) at the ICR. Experiment was undertaken by licenced staff at the BSU. The BSU follows the regulations and ethics as set out in the Animals (Scientific Procedures) Act 1986 (ASPA). The ICR, and those undertaking the work at the BSU, carry the requisite licences to permit animal studies, namely the establishment, project, and personal licences. Mice with tumour volume over 500 mm³ at the start of treatment (n=1 vehicle), mice whose tumours were erroneously slow-growing (relative to majority of tumours) prior to the start of treatment (n=2 vehicle), or mice whose tumour spontaneously and erroneously regressed between adjacent timepoints indicating poor measurements (n=1 vehicle) were removed from the final analysis. Neither the measurements nor the analyses were blinded. Final analysis included mice (n=15) consisting of vehicle-treated (n=5) and dasatinib-treated (n=10). Mice were sacrificed once tumours exceeded 1000 mm³. Upon sacrifice, tumour samples (both fixed and frozen) were taken for downstream analysis. Outcomes measurements were survival data and tumour volume. Statistical analyses undertaken are stated within the figure legend. Reporting of mouse study was undertaken in accordance with the ARRIVE guidelines 2.0 (Percie du Sert *et al.*, 2020).

2.2 Molecular biology techniques

2.2.1 Retroviral plasmid production and transduction

Retroviruses were produced using HEK-293T cells with the pUMVC packaging plasmid and the pCMV-VSV-G envelope protein plasmid (Stewart *et al.*, 2003). The SRC constructs included pBABE-hygro empty vector (EV), pBABE-SRC-Rescue wild-type (Src^{WT}), pBABE-SRC-Dasatinib-resistant T338I (Src^{T338I}), and pBABE-SRC-Dominant-negative K295M (Src^{K295M}) (**Table 2.3**) (Morgenstern & Land, 1990; Stewart *et al.*, 2003; Zhang *et al.*, 2009).

Plasmid	Addgene plasmid #	Addgene reference	RRID
pUMVC	#8449	http://n2t.net/addgene:8449	Addgene_8449
pCMV-VSV-G	#8454	http://n2t.net/addgene:8454	Addgene_8454
pBABE-hygro empty vector (EV)	#1765	http://n2t.net/addgene:1765	Addgene_1765
pBABE-SRC-Rescue wild-type (Src ^{WT})	#26983	http://n2t.net/addgene:26983	Addgene_26983
pBABE-SRC-Dasatinib-resistant T338I (Src ^{T338I})	#26980	http://n2t.net/addgene:26980	Addgene_26980

EV; Empty vector; RRID; Research Resource Identifiers, Src^{T338I}; Dasatinib-resistant Src^{WT}; Wild-type (Morgenstern & Land, 1990; Stewart *et al.*, 2003; Zhang *et al.*, 2009).

The Src^{K295M} construct was engineered from pBABE-SRC-Rescue wild-type plasmid using the Q5 site-directed mutagenesis kit (New England BioLabs) and Stellar competent cells (Takara Bio), following the manufacturer's recommendations. The primers (Sigma Aldrich) that were used are displayed in **Table 2.4**.

The *CXCR1* and *CXCR2* constructs were cloned into linearised pBABE-hygro EV plasmid through amplification of the open-reading frame of *CXCR1* or *CXCR2* cDNA packaged into pMD18-T vectors (Sino Biological). Cloning was undertaken using the In-Fusion HD cloning kit, CloneAmp HiFi polymerase chain reaction (PCR) premix, NucleoSpin Gel and PCR clean-up kit, and Stellar competent cells (Takara Bio), following the manufacturer's recommendations. Sanger sequencing was undertaken using the Eurofins Genomics TubeSeq service, as per the service recommendations. The primers (Sigma Aldrich) that were used are displayed in **Table 2.4**.

Primer	Forward (5'-->3')	Reverse (5'-->3')
Src mutagenesis primers		
Src ^{K295M}	GTGGCATAATGACTCTGAAGCCC	TCTGGTGGTGCCGTTCCA
CXCR1/CXCR2 cloning primers		
CXCR1	GGCGCCGGCCGGATCCATGTCAAATA TTACAGATCCACAGATGTGGGA	CACCACACTGGGATCCTCAGAGGTTGG AAGAGACATTGACAGA
CXCR2	GGCGCCGGCCGGATCCATGGAAGATT TTAACATGGAGAGTGACAGCTT	CACCACACTGGGATCCTTAGAGAGTAG TGGAAGTGTGCCCTGA

CXCR(1/2); C-X-C motif chemokine receptor (1/2), Src^{K295M}; Dominant-negative Src, Src^{Y527F}; Constitutively-active Src.

pBABE-hygro EV was linearised using BamHI-HF restriction enzyme (New England BioLabs) and purified using the QIAquick gel extraction kit (Qiagen), following the manufacturer's recommendations.

Transduced cells were selected using 200 µg/mL hygromycin B (Invivogen) and maintained in culture with 100 µg/mL hygromycin B. Transduction was confirmed through immunoblotting or quantitative PCR (qPCR).

2.2.2 Quantitative polymerase chain reaction

Cells (350,000/well or 600,000/T25) were seeded into 6 well plates or T25 flasks. After 24 hours, cells were lysed and RNA extracted using QIAshredder and RNeasy kits (Qiagen), following the manufacturer's recommendations. For A204 TKI-resistant qPCR experiments, cells (100,000/well) were seeded into 6 well plates. After 24 hours, media was replenished with fresh media without TKI addition. After a further 72 hours, cells were lysed as per the methodology outlined above. Contaminating DNA was degraded by RQ1 RNase-free DNase (Promega) followed by cDNA synthesis utilising the SuperScript III First-Strand Synthesis kit (ThermoFisher Scientific), following the manufacturer's recommendations. qPCR was undertaken using SYBR green fluorescent dye (ThermoFisher Scientific), following the manufacturer's recommendations, on Applied Biosystems QuantStudio 6 or 7 Flex Real-Time PCR systems (ThermoFisher Scientific). PCR conditions and primers (Sigma Aldrich) that were used are displayed in **Table 2.5**. A melt curve was also undertaken post-reaction to assess primer and experiment quality.

Table 2.5: qPCR primers and conditions.			
Primer	Forward (5'-->3')	Reverse (5'-->3')	
ACTB primers			
ACTB	GACAGGATGCAGAAGGAGATCAC	TGATCCACATCTGCTGGAAGGT	
CXCL8 (IL-8) primers			
CXCL8	GCTCTGTGTGAAGGTGCAGTT	TGGCATCTTCACTGATTCTTGGGA	
CXCR1/CXCR2 primers			
CXCR1	TCCTTTTCCGCCAGGCTTACCA	GGCAGATGAAGCCAAAGGTGT	
CXCR2	CCTGTCTTACTTTTCCGAAGGAC	TTGCTGTATTGTTGCCCATGT	
Integrin primers			
ITGA2	GGGAATCAGTATTACACAACGGG	CCACAACATCTATGAGGGAAGGG	
ITGA3	TGTGGCTTGGAGTGACTGTG	TCATTGCCTCGCACGTTAGC	
ITGA6	GGCGGTGTTATGTCCTGAGTC	AATCGCCATCACAAAAGCTC	
ITGA7	TATTGACTCGGGGAAAGGTCT	CCAGCCATCACTGTTGAGG	
ITGA10	AACATCACCCACGCCTATTCC	GTTGGTAGTCACCTAAGTGGC	
ITGB1	CAAGAGAGCTGAAGACTATCCCA	TGAAGTCCGAAGTAATCCTCCT	
ITGB3	AGTAACCTGCGGATTGGCTTC	GTCACCTGGTCAGTTAGCGT	
ITGB4	GCTTCACACCTATTTCCCTGTC	GACCCAGTCCCTCGTCTTCTG	
ITGAV	AATCTTCCAATTGAGGATATCAC	AAAACAGCCAGTAGCAACAAT	
RTK primers			
PDGFRA	GACTTTTCGCCAAAGTGGAGGAG	AGCCACCGTGAGTTCAGAACGC	
FGFR1	GCACATCCAGTGGCTAAAGCAC	AGCACCTCCATCTCTTTGTCGG	
FGFR2	GTGCCGAATGAAGAACACGACC	GGCGTGTGTTATCCTCACCAG	
FGFR3	TCCATCTCTGGCTGAAGAACG	TGTTCTCCACGACGCAGGTGTA	
FGFR4	AACACCGTCAAGTTCGGCTGTC	CATCACGAGACTCCAGTGCTGA	
qPCR conditions			
Step	Temperature (°C)	Time (seconds)	Cycle(s)
1	50	120	Hold
2	95	120	Hold
3	95	15	40
4	58 (for CXCL8) & 60 (for the remainder)	60	40
ACTB; β -actin, CXCL8; Chemokine C-X-C motif ligand 8, CXCR(1/2); C-X-C motif chemokine receptor (1/2), FGFR(1/2/3/4); Fibroblast growth factor receptor (1/2/3/4), IL-8; Interleukin-8, ITG(A2/3/6/7/10/V)(B1/3/4); Integrin (α 2/3/6/7/10/V)(β 1/3/4), PDGFRA; Platelet-derived growth factor receptor α , qPCR; Quantitative polymerase chain reaction, RTK; Receptor tyrosine kinase.			

2.2.3 SS18-SSX fusion polymerase chain reaction

Cells (350,000/well) were seeded into 6 well plates. After 24 hours, cells were lysed and RNA extracted using QIAshredder and RNeasy kit (Qiagen), following the manufacturer's recommendations. Contaminating DNA was degraded by RQ1 RNase-free DNase (Promega) followed by cDNA synthesis utilising the SuperScript III First-Strand Synthesis kit (ThermoFisher Scientific), following the manufacturer's recommendations. PCR was undertaken using GoTaq DNA polymerase (Promega),

following the manufacturer's recommendations. PCR conditions and primers (Sigma Aldrich) that were used are displayed in **Table 2.6**. PCR product was loaded onto 1% agarose (Invitrogen) gel, stained with ethidium bromide (Sigma Aldrich), and digitally imaged using a Bio-Rad ChemiDoc Touch Imaging System (Bio-Rad). Samples yielding PCR products of the predicted amplicon size (108 bp) for the fusion gene were deemed positive as synovial sarcoma (Lan *et al.*, 2016). The cell line HS-SY-II, with a known *SS18-SSX1* gene fusion, was used as a positive control (Sonobe *et al.*, 1992).

Table 2.6: <i>SS18-SSX</i> fusion PCR primers and conditions.			
Primer	Forward (5'-->3')	Reverse (5'-->3')	
<i>ACTB</i> primers			
<i>ACTB</i>	GACAGGATGCAGAAGGAGATCAC	TGATCCACATCTGCTGGAAGGT	
<i>SS18-SSX</i> fusion primers			
<i>SS18-SSX1</i>	AGACCAACACAGCCTGGACCAC	ACACTCCCTTCGAATCATTTTCG	
<i>SS18-SSX2</i>	AGACCAACACAGCCTGGACCAC	GCACCTCCTCCGAATCATTTTC	
<i>SS18-SSX4</i>	AGACCAACACAGCCTGGACCAC	GCACCTCCTTCAAACCATTTTCT	
<i>ACTB</i> PCR conditions			
Step	Temperature (°C)	Time (seconds)	Cycle(s)
1	95	120	Hold
2	95	15	40
	60	15	
3	72	60	Hold
	72	300	
<i>SS18-SSX</i> fusion PCR conditions			
1	95	420	Hold
2	94	45	Annealing
	66 (annealing temperature)	45	
	72	90	
	Step 2 cycle was repeated 9 further times with annealing temperature reduced by 1 °C each cycle until 57 °C		
3	94	45	30
	56	45	
	72	90	
4	72	300	Hold

ACTB; β -actin, PCR; Polymerase chain reaction, SS18; Synovial sarcoma translocation, chromosome 18, SSX(1/2/4); Synovial sarcoma X (1/2/4) breakpoint protein.

2.2.4 Short tandem repeat analysis

Cells (350,000/well) were seeded into 6 well plates. After 24 hours, cells were lysed and DNA extracted using DNeasy blood and tissue kits (Qiagen), following the manufacturer's recommendations. Human Cell Line Authentication via short tandem repeat (STR)/DNA profiling was undertaken using the Eurofins Genomics Cell Line Authentication service, as per the service recommendations.

2.3 Protein analysis techniques

2.3.1 Immunoblotting

Cells (350,000/well) were seeded into 6 well plates. After 24 hours, cells were treated with inhibitors at the indicated concentrations and/or durations. If no inhibitor or cytokine treatment indicated, cells were lysed 24 hours post-seeding. For 6-hour and 72-hour A204 TKI-resistant experiments, cells (350,000/well or 300,000/flask, respectively) were seeded into 6 well plates or T25 flasks, respectively. After 24 hours, cells were treated with DMSO (Sigma Aldrich) and incubated for a further 6 or 72 hours. For serum-starved conditions for interleukin-8 (IL-8) (Peprotech) stimulation experiments, cells (250,000/well) were seeded into 6 well plates. After 24 hours, media was replenished with serum-free media, following several PBS washes, and serum-starved overnight. Cells were then treated with IL-8 at the indicated concentration and duration. After the indicated time period post treatment, cells were lysed in radioimmunoprecipitation assay (RIPA) buffer (50 mM Tris.Cl pH 7.6, 150 mM NaCl, 1% IGEPAL CA-630 (NP-40) (Sigma Aldrich), 0.1% sodium dodecyl sulfate (SDS) (Sigma Aldrich), and 0.5% sodium deoxycholate (Sigma Aldrich)), supplemented with Halt™ protease and phosphatase inhibitors and EDTA #78442 (ThermoFisher Scientific) at 4 °C. Protein quantification was undertaken using a Pierce bicinchoninic acid (BCA) assay kit (ThermoFisher Scientific), as per the manufacturer's recommendations. Lysates were loaded onto NuPAGE Novex 4-12% Bis-Tris gels (Invitrogen), followed by blotting onto iBlot polyvinylidene fluoride (PVDF) membranes (Invitrogen). Membranes were blocked for 4-5 hours at room temperature with either 5% dried skimmed milk (Marvel) (for total protein) or 5% BSA (Sigma Aldrich) (for phosphoprotein) in 1x tris-buffered saline (TBS) with 0.1% Tween 20 (TBST) (Sigma Aldrich). Blots were subsequently incubated with primary antibodies (diluted in the respective blocking agent) at 4 °C overnight. Membranes were then washed at room temperature with 3 x 10 minutes of TBST incubation. Following this, membranes were incubated at room temperature with horseradish peroxidase (HRP)-conjugated secondary antibodies (diluted in 5% dried skimmed milk) for 1 hour. Membranes were subsequently washed for a further 3 x 10 minutes of TBST incubation at room temperature. Primary and secondary antibodies utilised within this thesis are outlined in **Table 2.7** with associated dilutions. Immunoreactive bands were visualised by

SuperSignal West Pico PLUS chemiluminescence substrate (ThermoFisher Scientific) and the blots were digitally imaged using ChemiDoc Touch Imaging System (Bio-Rad) or G-Box Chemi-XX6 (Syngene) imagers. Blots were analysed using Image Lab (Bio-Rad) and GNU image manipulation program (GIMP). Inhibitors used include pazopanib, regorafenib, ponatinib, dasatinib, cabozantinib, neratinib, crizotinib (LC Laboratories), sitravatinib, anlotinib, infigratinib, erdafitinib, cilengitide trifluoroacetate, NVP-AEW541, osimertinib, and NVP-TAE684 (Selleck Chemicals).

Table 2.7: Primary and secondary antibodies utilised for immunoblotting with associated dilutions.		
Antibody	Dilution	Supplier and catalogue number
Primary antibodies		
anti-pSTAT3 (Y705) D3A7 (Rabbit)	1:1000	Cell Signalling Technology (#9145)
anti-STAT3 α D1A5 (Rabbit)	1:1000	Cell Signalling Technology (#8768)
anti-pSrc family (Y416) (Rabbit)	1:1000	Cell Signalling Technology (#2101)
anti-Src (Rabbit)	1:1000	Cell Signalling Technology (#2108)
anti-pAkt (S473) 193H12 (Rabbit)	1:1000	Cell Signalling Technology (#4058)
anti-Akt (pan) C67E7 (Rabbit)	1:1000	Cell Signalling Technology (#4691)
anti-p44/42 MAPK (ERK1/2) (T202/Y204) D13.14.4E (Rabbit)	1:1000	Cell Signalling Technology (#4370)
anti-p44/42 MAPK (ERK1/2) 137F5 (Rabbit)	1:1000	Cell Signalling Technology (#4695)
anti-PDGFR α D1E1E (Rabbit)	1:1000	Cell Signalling Technology (#3174)
anti-FGFR1 [EPR806Y] (Rabbit)	1:1000	Abcam (ab76464)
anti- α -tubulin (Mouse)	1:5000	Sigma Aldrich (#T5168)
Secondary antibodies		
anti-Rabbit HRP-linked antibody	For total protein: 1:5000 For phosphoprotein: 1:2000	Cell Signalling Technology (#7074)
anti-Mouse HRP-linked antibody	1:5000	SignalChem (#G32-62G-1000)
ERK1/2; Extracellular signal-regulated kinase 1/2, FGFR1; Fibroblast growth factor receptor 1, HRP; Horseradish peroxidase, PDGFR α ; Platelet-derived growth factor receptor α , STAT3; Signal transducer and activator of transcription 3.		

2.3.2 Temporal (27 day) immunoblotting

Parental A204 cells (350,000/well) were seeded into 6 well plates. After 24 hours, cells were lysed for immunoblotting, as per the protocol outlined previously. Using the same flask of parental A204 cells, cells (1,000,000/flask) were seeded into x2 T75 flasks. After 24 hours, x1 T75 was treated with DMSO (Sigma Aldrich) and the remaining x1 T75 was treated with 1 μ M sitravatinib. Cells were allowed to grow for four weeks post-seeding in their respective treatments. Media and inhibitors were replenished twice weekly. Cells were maintained at between 70-90% confluency. After 4-, 7-, 14-, 21-, and 28-days post-seeding, cells from the x2 flasks were evaluated for temporal changes in protein expression and phosphorylation status via immunoblotting, as per the protocol outlined previously. This experiment was run concomitantly with the same

flasks of cells used for the temporal (27 day) cell viability assays outlined in **Chapter 2.1.3**.

2.3.3 Temporal (14 day) immunoblotting

Cells (1,000,000/flask) were seeded into x2 T75 flasks. After 24 hours, x1 T75 was treated with DMSO (Sigma Aldrich) and the remaining T75 was treated with 1 μM sitravatinib (Selleck Chemicals). Cells were allowed to grow for two weeks in their respective treatments. Media and inhibitors were replenished twice weekly. Cells were maintained at between 70-90% confluency and cells were split into T175s one-week post-seeding. After two weeks of treatments, the x2 T75 flasks were split and seeded as follows:

1. x1 6 well seedings (350,000/well) of DMSO pre-treated cells.
2. x3 6 well seedings (350,000/well) of Sit pre-treated cells.

After 24 hours, cells were treated for 6 hours as follows:

1. Well 1 (DMSO pre-treated cells): Treated with DMSO.
2. Well 2 (Sitravatinib pre-treated cells): Treated with DMSO.
3. Well 3 (Sitravatinib pre-treated cells): Treated with 1 μM sitravatinib.
4. Well 4 (Sitravatinib pre-treated cells): Treated with 1 μM infigratinib.

After 6 hours of treatment, cells were lysed for immunoblotting, as per the protocol outlined previously.

2.3.4 Phospho-receptor tyrosine kinase antibody array

Cells (1,000,000/flask) were seeded into x4 T75 flasks. After 24 hours, x2 of T75s were treated with DMSO (Sigma Aldrich) and remaining x2 T75s were treated with 1 μM sitravatinib (Selleck Chemicals). Cells were allowed to grow for two weeks in their respective treatments. Media and inhibitors were replenished twice weekly. Cells were maintained at between 70-90% confluency and cells were split into T175s one-week post-seeding. After two weeks of treatments, the x4 T75s were treated for 6 hours as follows:

1. Flask 1 (DMSO pre-treated cells): Media changed plus DMSO.
2. Flask 2 (DMSO pre-treated cells): Media changed plus 1 μM infigratinib (Selleck Chemicals).
3. Flask 3 (Sitravatinib pre-treated cells): Media changed plus 1 μM sitravatinib.
4. Flask 4 (Sitravatinib pre-treated cells): Media changed plus 1 μM infigratinib.

After 6 hours of treatment, cells were lysed and lysates collected using the Proteome Profiler Human Phospho-receptor tyrosine kinase (RTK) Array kit (R & D Systems), as per the manufacturer's recommendations. Protein quantification was undertaken using a Pierce BCA assay kit (ThermoFisher Scientific), as per the manufacturer's recommendations. Lysates were incubated and blotted onto phospho-RTK antibody arrays using the Proteome Profiler Human Phospho-RTK array kit, as per the manufacturer's recommendations. RTK arrays were digitally imaged using the G-Box Chemi-XX6 (Syngene) imager. Array was analysed using Image Lab (Bio-Rad) and GIMP.

2.3.5 Mass spectrometry

Cells (1,000,000/flask) were seeded into T175 flasks. After 24 hours, media was replenished with fresh media without TKI addition. After a further 72 hours, cells were lysed in 8 M urea (Sigma Aldrich) at 4 °C. Protein quantification was undertaken using a Pierce BCA assay kit (ThermoFisher Scientific), as per the manufacturer's recommendations. Using 600 μg total protein, lysates were prepared by reduction with dithiothreitol (Sigma Aldrich), alkylation with iodoacetamide (Sigma Aldrich), dilution with ammonium bicarbonate (Sigma Aldrich), and overnight trypsinisation with sequence grade modified trypsin (Promega). Trypsinised samples were acidified with 10% trifluoroacetic acid (Sigma Aldrich), desalted using Sep-Pak C18 Plus cartridges (Waters), and dried on a SpeedVac (Eppendorf) for 3 hours. Samples were resuspended and peptide quantification was undertaken using a Pierce BCA assay kit, as per the manufacturer's recommendations. Once quantified, samples were diluted and split into 33 μg samples and re-dried on a SpeedVac along with a reference pooled sample. Samples were frozen at -80 °C prior to mass spectrometry preparation and experimentation.

Each sample was resuspended in 100 mM tetraethylammonium bicarbonate (Sigma Aldrich) buffer and aliquots of 33 μg were labelled with 1/3rd of Tandem Mass Tag (TMT) 11-plex Isobaric Mass Tag Labelling Reagents (ThermoFisher Scientific), as per the manufacturer's recommendations.

Prior to addition to samples, TMT label reagents were equilibrated at room temperature and dissolved in liquid chromatography-mass spectrometry grade anhydrous acetonitrile (Sigma Aldrich). Individual TMT label reagents were added to individual samples and incubated for 1 hour at room temperature. Reactions were quenched by addition of 5% (w/w) hydroxylamine (Sigma Aldrich) and incubated for 15 minutes at room temperature. Individual samples were combined at equal amounts into a single sample, desalted on a Sep-Pak C18 Plus cartridge, and dried in a SpeedVac. Combined sample was then fractionated by reverse phase liquid chromatography at basic pH using UltiMate 3000 ultra-high performance liquid chromatography system (ThermoFisher Scientific). Dried sample was resuspended in 0.1% (v/v) hydroxylamine (in water) and loaded onto 2.1 x 150 mm XBridge C18, 5 μm column (Waters). Peptides were eluted at a flow rate of 200 $\mu\text{L}/\text{min}$ by 0.1% (v/v) hydroxylamine (in acetonitrile) with a linear gradient of 5-40% of 0.1% (v/v) hydroxylamine (in acetonitrile) over 45 minutes and 90 fractions were collected overall (1 fraction every 30 seconds) during the gradient elution. Every 9th fraction was pooled resulting in a total number of 10 fractions which were dried in a SpeedVac.

Dried pooled fractions were resuspended in 2% (v/v) acetonitrile, 0.1% (v/v) formic acid (ThermoFisher Scientific) and aliquots equivalent to 6 μg of peptides were analysed by liquid chromatography-tandem mass spectrometry using UltiMate 3000 RSCLnano liquid chromatography system coupled to Orbitrap Fusion Lumos (ThermoFisher Scientific) mass spectrometer. Peptides were separated on 75 μm x 50 cm Acclaim PepMap 100 C18, 3 μm column (ThermoFisher Scientific) with a linear gradient of 2-28% acetonitrile in 0.1% formic acid over a duration of 120 minutes at a flow rate of 250 nL/min. The spectra of the full mass spectrometry scan (m/z 375-1600) were acquired in the Orbitrap mass analyser at 120,000 resolution for a maximum injection time of 50 ms with an automatic gain control target value of 3e6. Up to 15 precursors were selected for tandem mass spectrometry analysis with an isolation window of 0.7 Th and the dynamic exclusion time was set to 20 seconds. Precursors were fragmented by higher-energy C-trap dissociation using a normalised

collision energy of 33% at 60,000 resolution for a maximum injection time of 120 ms with an automatic gain control target value of 1e5. Precursor ions with unassigned charge state as well as charge state of 1+, or superior to 7+, were excluded from fragmentation selection.

Acquired data were processed by Proteome Discoverer version 2.2 (ThermoFisher Scientific) and searched against the human protein database Swiss-Prot (Swiss Institute of Bioinformatics) using Mascot (Matrix Science) and Sequest HT (University of Washington) search engine with the following parameters:

- Precursor search peptide tolerance of 10 ppm.
- Mass spectrometry-3 reporter ion quantification with reporter ion mass tolerance of 0.1 Da.
- Trypsin digestion with maximum 2 miscleavages.
- Fixed modification: carbamidomethylation of cysteines, TMT label on lysine, and peptide N-terminus.
- Variable modifications: oxidation of methionine and deamidation of asparagine/glutamine.
- 1% false discovery rate threshold on peptide and protein level.

Data was filtered for master proteins with a false discovery rate (FDR) < 0.01, a minimum of 2 peptides, and no missing values. Data was then log₂ transformed and normalised by cross sample median-centring followed by within sample standardisation. Differentially expressed proteins between parental cells and x4 TKI-resistant sublines were identified by significance analysis of microarrays (SAM) 2-class unpaired tests and significance was determined at q-value < 0.01. All heatmaps were generated by unsupervised hierarchical clustering using Pearson's correlation distance. All analysis were performed in R version 4.0.2, using the packages tidyverse, samr, ComplexHeatmap, and circlize.

Chapter 3

Pazopanib-resistant soft tissue sarcomas
are vulnerable to targeting of the Src
pathway

3.1 Introduction

In order to effectively study multi-target tyrosine kinase inhibitor (TKI) resistance in soft tissue sarcoma (STS), clinically relevant disease models that recapitulate drug resistance are required. Although immortalised cell line models of STS exist and provide functional, cost-effective, and practical tools for studying this disease preclinically, questions persist about their ability to accurately recapitulate disease (Capes-Davis *et al.*, 2010; Kaur & Dufour, 2012). This is due to a variety of problems such as the perpetual culturing of cells resulting in genetic drift and genetic alterations upon continuous passaging, whereby the cell lines are no longer accurately modelling the disease (Hughes *et al.*, 2007; Kaur & Dufour, 2012). Furthermore, in some instances, genetic manipulations of the cells are undertaken in order to induce the immortalised phenotype, and this may alter the characteristics and properties of the cell models (Capes-Davis *et al.*, 2010; Kaur & Dufour, 2012).

In comparison, patient-derived and patient-derived xenograft (PDX)-derived cells are a more clinically relevant model of disease than immortalised cell lines. Low passage, patient-derived and PDX-derived models tend to maintain the cellular and molecular heterogeneity of the originating tumour and, therefore, therapy response and resistance can be more accurately modelled preclinically (Brodin *et al.*, 2019; Bruna *et al.*, 2016; Huo *et al.*, 2020; Pauli *et al.*, 2017). Notably, previous studies have highlighted the utility of patient-derived and PDX-derived models in accurately recapitulating TKI resistance *in vitro* and *in vivo*, for the express purpose of determining and evaluating novel therapeutic strategies that can be utilised to treat TKI-resistant cancers (Crystal *et al.*, 2014; Kim *et al.*, 2016; Kodack *et al.*, 2017).

In this chapter, two PDX-derived cellular models of STS were established and characterised in order to provide clinically relevant and robust models for evaluating multi-target TKI resistance in STS. These models were subjected to pharmacological screens to elucidate potential signalling pathway dependencies with the aim to identify any salvage therapies that can be utilised in the treatment of multi-target TKI-resistant STS.

3.2 Results

3.2.1 Generation of PDX-derived cell models of soft tissue sarcoma

The SARC-209 cell model was generated from a PDX that had been derived from a percutaneous core needle biopsy of a post-relapse abdominal wall metastasis from a patient diagnosed with spindle cell sarcoma (**Figure 3.1**). Generation of the PDX model from originating patient biopsy was undertaken by Champions Oncology.

The J000104314 cell model was generated from a PDX model obtained from The Jackson Laboratory (**Figure 3.1**). The PDX was generated from a surgical resection of a synovial sarcoma patient that had undergone neoadjuvant chemotherapy with cyclophosphamide and topotecan and was naïve to pazopanib therapy (**Figure 3.1**).

PDX tumour tissue was harvested and dissociated into single-cell suspensions. Following this, cell suspensions underwent mouse cell depletion to remove contaminating murine cells and retain PDX-derived human cancer cells (**Figure 3.1**). These PDX-derived cell models, termed SARC-209 and J000104314, were utilised at low-passage (< 10 passages following mouse cell depletion) for subsequent *in vitro* evaluation (**Figure 3.1**).

Short tandem repeat (STR) analysis was undertaken to record a genomic profile of the SARC-209 PDX-derived cell model (**Table 3.1**). Work is currently undergoing to generate a STR profile of the SARC-209-originating PDX in order to compare genomic profiles. This will allow for the evaluation of whether the genomic characteristics of the PDX model are being recapitulated within the SARC-209 PDX-derived cell model. STR analysis for the J000104314 PDX-derived cell model and originating PDX are also currently undergoing.

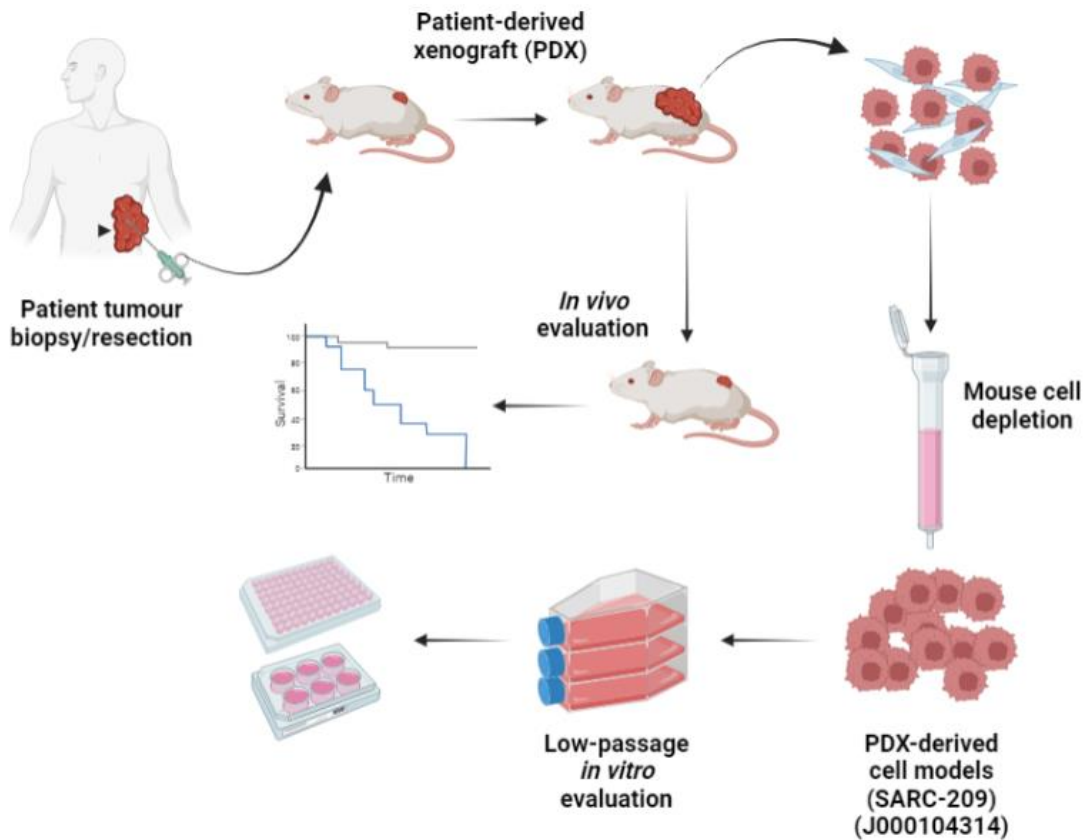


Figure 3.1: Generation of SARC-209 and J000104314 PDX-derived cell models. Patient-derived xenografts (PDX) were generated from patient tumour biopsy or surgical resection. Viable tumours were grown in PDX before being harvested and dissociated into single-cell suspensions. For *in vivo* evaluation of drug effectiveness, SARC-209-originating PDX tumours were taken and implanted into NCR nude mice. Mice were then treated with differing arms of treatment to determine survival outcomes. Single-cell suspensions underwent mouse cell depletion via magnetic cell separating columns to result in the PDX-derived cell models, SARC-209 and J000104314. PDX-derived cell models were utilised at low-passage for subsequent *in vitro* evaluation. Image was created using BioRender.

STR loci	Allele (Repeat no.)
D8S1179	9, 12
D21S11	30, 32.2
D7S820	9, 12
CSF1PO	9, 12
D3S1358	15, 16
TH01	6, 9
D13S317	11, 13
D16S539	12, 12
D2S1338	17, 24
D19S433	12, 13
vWA	14, 18
TPOX	8, 9
D18S51	16, 17
AMEL	X, X
D5S818	11, 12
FGA	20, 23

AMEL; Amelogenin, CSF1PO; Colony stimulating factor 1 receptor proto-oncogene, FGA; Fibrinogen α chain, PDX; Patient-derived xenograft, STR; Short tandem repeat, TH01; Tyrosine hydroxylase intron 1, TPOX; Thyroid peroxidase intron 10, vWA; Von Willebrand factor type A domain protein.

The SARC-209 PDX-derived cell model originated from a patient diagnosed with spindle cell sarcoma who was treated with pazopanib at the Royal Marsden Hospital Sarcoma Unit, after previous treatment with radiotherapy and chemotherapy. The patient displayed an initial long-term response to pazopanib with tumour regression/suppression for approximately 12 months before disease relapse, progression, and the development of further metastases (**Figure 3.2A**). Upon disease progression, pazopanib treatment was ceased, at which point a core needle biopsy was taken from the abdominal wall tumour and this biopsy was used to generate a PDX model. The morphology of spindle cell sarcoma was confirmed by Dr. Khin Thway, a histopathologist at the Royal Marsden Hospital Sarcoma Unit, in both the PDX and the originating patient tumour (**Figure 3.2B**). Given the clinical history of this patient, where an initial long-term response to pazopanib is followed by eventual disease progression, the SARC-209 PDX-derived cell model was predicted to have acquired resistance to pazopanib (**Figure 3.2A**).

Furthermore, the morphology of synovial sarcoma was also evaluated by histopathological analysis of the J000104314-originating PDX tumour by Dr. Khin Thway and was determined to have histopathology consistent with synovial sarcoma diagnosis (**Figure 3.2C**). Synovial sarcomas are characterised in 90% of cases by the *SS18-SSX* gene fusion (Ladanyi, 2001). To confirm the existence of the pathognomonic *SS18-SSX* gene fusion within the J000104314 PDX-derived cell model, a polymerase chain reaction (PCR) was performed to detect the fusion, using the HS-SY-II synovial sarcoma cell line as a positive control (**Figure 3.3**) (Sonobe *et al.*, 1992). This work was undertaken by Will Kerrison, a PhD student in our lab. Both the HS-SY-II and J000104314 samples displayed bands at approximately 108 bp – the expected amplicon size for the pathognomonic gene fusion – for the *SS18-SSX1* fusion, thereby molecularly confirming the diagnosis of synovial sarcoma for the J000104314 PDX-derived cell model (**Figure 3.3**).

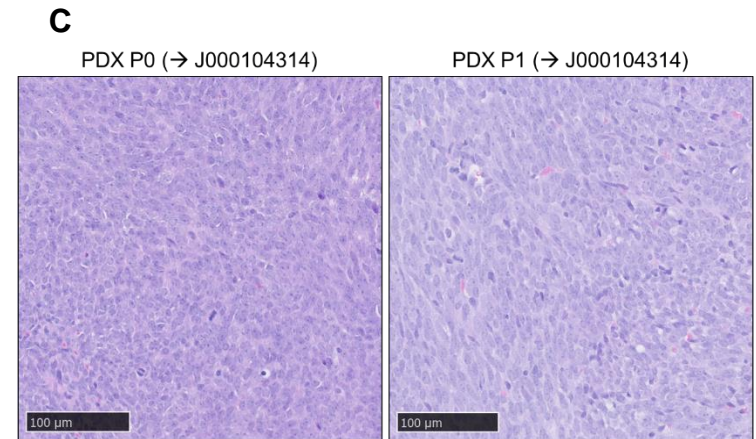
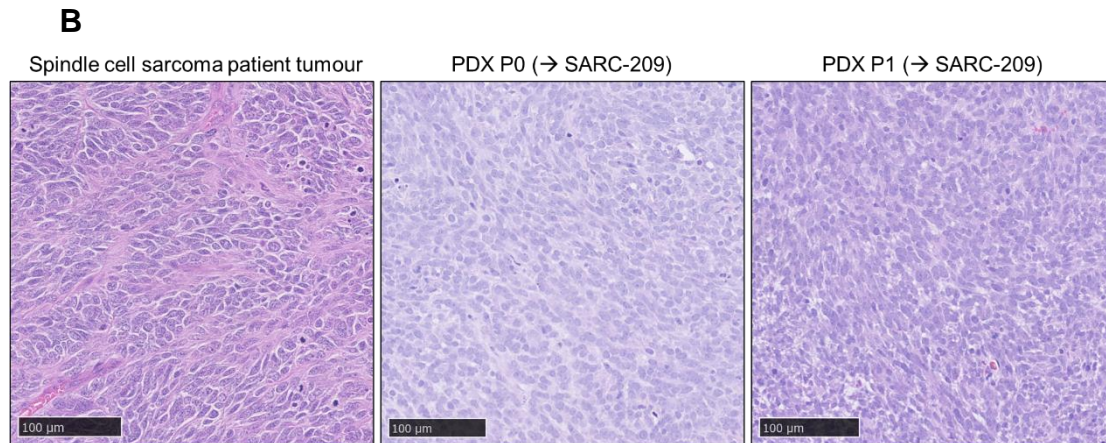
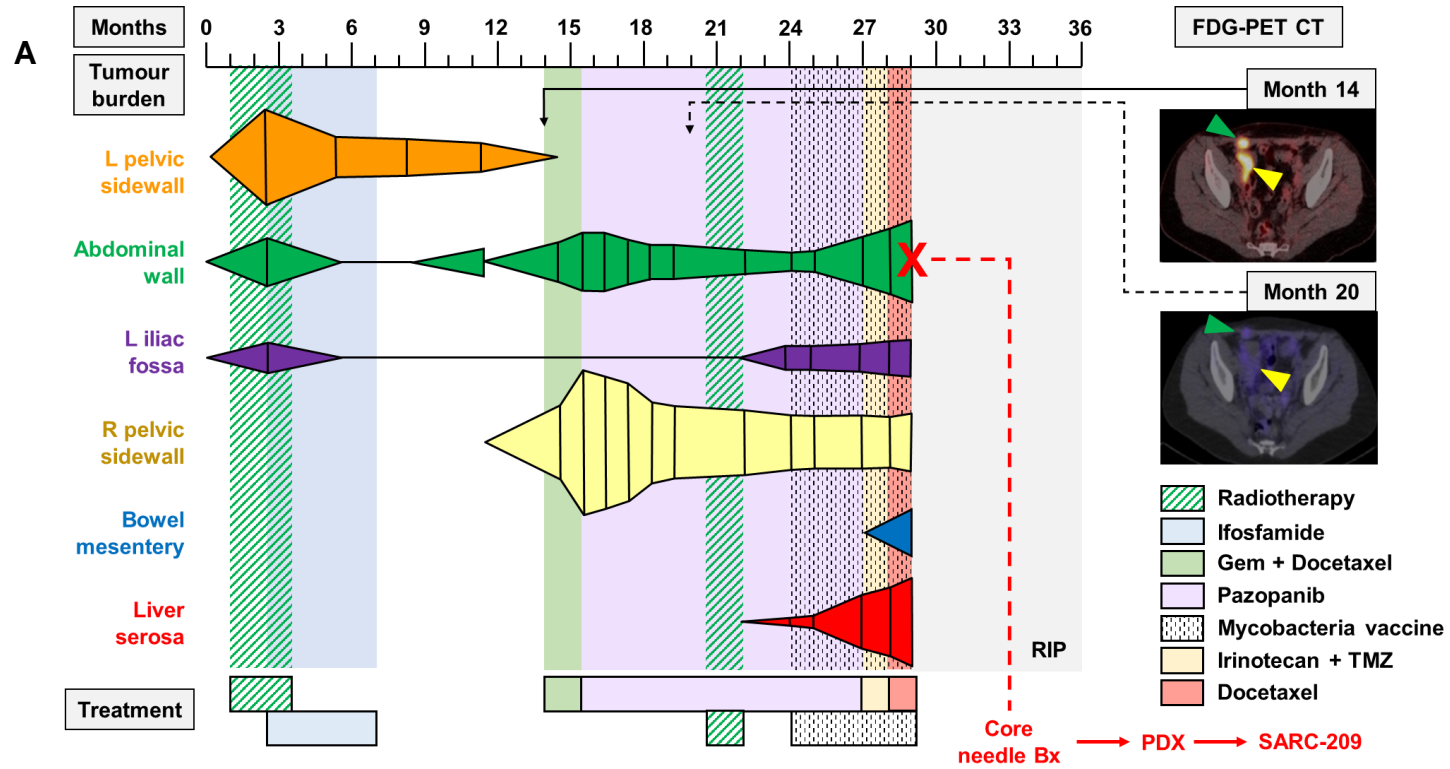


Figure 3.2: Patient clinical history and histopathological evaluation of STS subtypes. (A) Schematic overview of the clinical history of a patient with initial, long-term pazopanib response and subsequent acquisition of resistance. Schematic shows the time and location of the core-needle biopsy (Bx) that was used to derive the PDX and subsequent SARC-209 PDX-derived cell model. Schematic also shows tumour location and burden, treatment paradigm, and computerised tomography (CT) scans to show reduction in initial tumour burden observed with pazopanib therapy (green and yellow arrows). Figure was adapted from work by Dr. Alex Lee. Haematoxylin and eosin (H & E) staining of (B) originating spindle cell sarcoma patient tumour, SARC-209-originating PDX (P0 & 1), and (C) J000104314-originating PDX (P0 & 1). The scale bar shown is 100 μ m. H & E slides were used by Dr. Khin Thway to confirm histopathological diagnosis of STS subtypes. FDG-PET CT; Fluorodeoxyglucose (18 F)-positron emission tomography computerised tomography, Gem; Gemcitabine, P(0/1); Passage number (0/1), PDX; Patient-derived xenograft, RIP; Rest in peace, TMZ; Temozolamide.

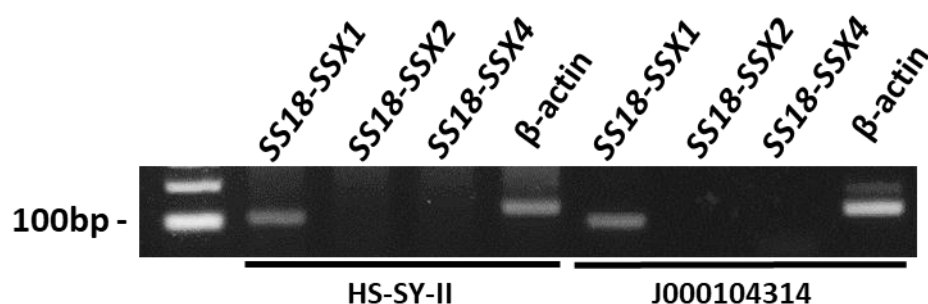


Figure 3.3: Molecular diagnosis of synovial sarcoma in the J000104314 PDX-derived cell model. PCR gel image displaying the presence of the *SS18-SSX1* translocation in the J000104314 PDX-derived cell model, with the HS-SY-II cell line acting as a positive control. Image is representative of three separate experiments (n=3). Work was undertaken by Will Kerrison. Bp; Base pairs, PCR; Polymerase chain reaction, PDX; Patient-derived xenograft, SS; Synovial sarcoma, SS18; Synovial sarcoma translocation, chromosome 18, SSX(1/2/4); Synovial sarcoma X (1/2/4) breakpoint protein.

3.2.2 SARC-209 and J000104314 PDX-derived cell models are resistant to pazopanib *in vitro*

To evaluate whether SARC-209 and J000104314 PDX-derived cell models were resistant to pazopanib treatment *in vitro*, cell viability assays were undertaken to compare pazopanib sensitivity to a known pazopanib-sensitive cell line model, A204 (Wong *et al.*, 2016). As shown in **Figure 3.4A-B**, both SARC-209 and J000104314 have significantly higher IC₅₀ values (8.22 μ M and > 10 μ M, respectively) than the known pazopanib-sensitive cell line A204 (0.56 μ M) (**Table S1**). These results indicate that SARC-209 can be utilised as an *in vitro* model for acquired pazopanib resistance. Additionally, due to its pazopanib-naïve patient history, J000104314 can be used as a model of intrinsic pazopanib resistance (**Figure 3.4A-B**).

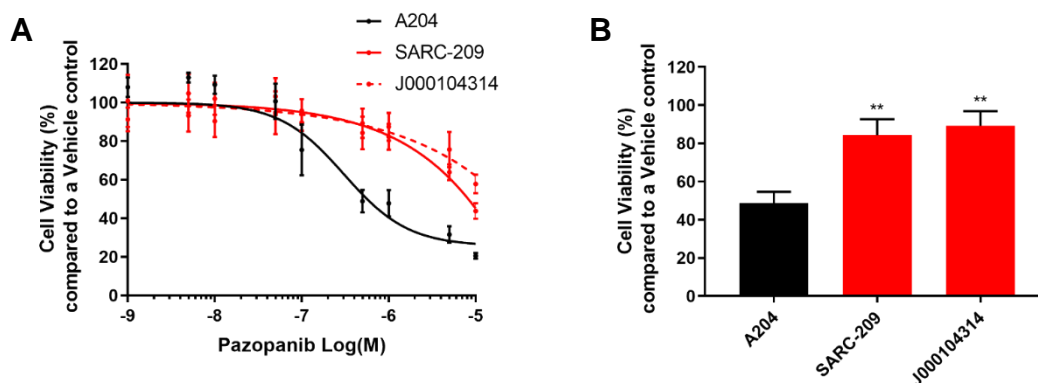


Figure 3.4: Cell viability assays to determine pazopanib sensitivity in SARC-209 and J000104314 PDX-derived cell models. (A) Cell viability assays of A204, SARC-209, and J000104314 cells treated with increasing concentrations of pazopanib to determine IC_{50} values (**Table S1**). **(B)** Bar plots displaying cell viability at 0.5 μ M pazopanib. Cell viability was normalised to DMSO control ($n=3$). Statistical analysis of IC_{50} values not possible as certain models did not reach 50% cell viability. Statistical analysis was undertaken by one-way ANOVAs with Tukey's multiple comparison tests (** = $p \leq 0.01$). Error bars represent standard deviation. ANOVA; Analysis of variance, DMSO; Dimethyl sulfoxide, IC_{50} ; Inhibitory constant, PDX; Patient-derived xenograft.

3.2.3 A small molecule inhibitor screen identifies dasatinib as an effective salvage therapy for pazopanib-resistant soft tissue sarcomas

To elucidate pathway dependencies within the PDX-derived cell models and potentially identify salvage therapies for pazopanib-resistant STS, a small molecule inhibitor screen was undertaken (**Figure 3.5 & 3.6**). SARC-209 and J000104314 PDX-derived cell models were subjected to treatment (0.5 μ M) with a panel of 62 small molecule inhibitors (**Table 2.1**) and cell viability was assessed after 72 hours (**Figure 3.5-3.6A & C**). The screen comprised mostly of kinase inhibitors that target major cellular signalling pathways associated with cancer survival and progression. Additionally, the screen also contains non-kinase inhibitors targeting heat shock protein 90 (Hsp90) (luminespib (NVP-AUY922)), STAT (niclosamide and SH-4-54), integrins (cilengitide trifluoroacetate), B-cell lymphoma 2 protein (Bcl-2) (navitoclax), EZH2 (GSK126), tankyrase (XAC-939), bromo- and extra-terminal domain (BET) bromodomain (JQ1), and poly (adenosine diphosphate(ADP)-ribose) polymerase (PARP) (rucaparib and talazoparib), which are undergoing preclinical and/or clinical assessment in cancer. Pearson's correlation analysis was performed to assess the reproducibility of biological replicates ($n=2$) within the small molecule inhibitor screens. Pearson's analysis showed strong correlation ($r^2 > 0.80$) between biological replicates for all the inhibitor screens undertaken, indicating high reproducibility (**Figure 3.6B & D**).

To identify inhibitors that have efficacy in STS models of both acquired and intrinsic pazopanib resistance, an overlap analysis of inhibitors showing efficacy ($\leq 60\%$ cell viability compared to DMSO control) in both PDX-derived cell models was conducted. As shown in **Figure 3.6E**, consistent sensitivities with the dual PI3K/mTOR inhibitor dactolisib (BEZ235), polo-like kinase 1 (PLK1) inhibitor BI-2536, BET bromodomain inhibitor JQ1, and the multi-kinase inhibitor dasatinib were observed (**Figure 3.6E; Table S2**). However, dactolisib, BI-2536, and JQ1 have been shown to be universally cytotoxic in a wide range of human cancer cell models regardless of cancer type or underlying genetics (Seashore-Ludlow *et al.*, 2015). Therefore, further investigation into these compounds was not pursued. Several inhibitors were found to be exclusively effective in only one of the PDX-derived cell models (**Table S2**). Therefore, the multi-target kinase inhibitor dasatinib was chosen for functional mechanistic investigation to understand the mechanism of dasatinib sensitivity within the PDX-derived cell models of pazopanib resistance.

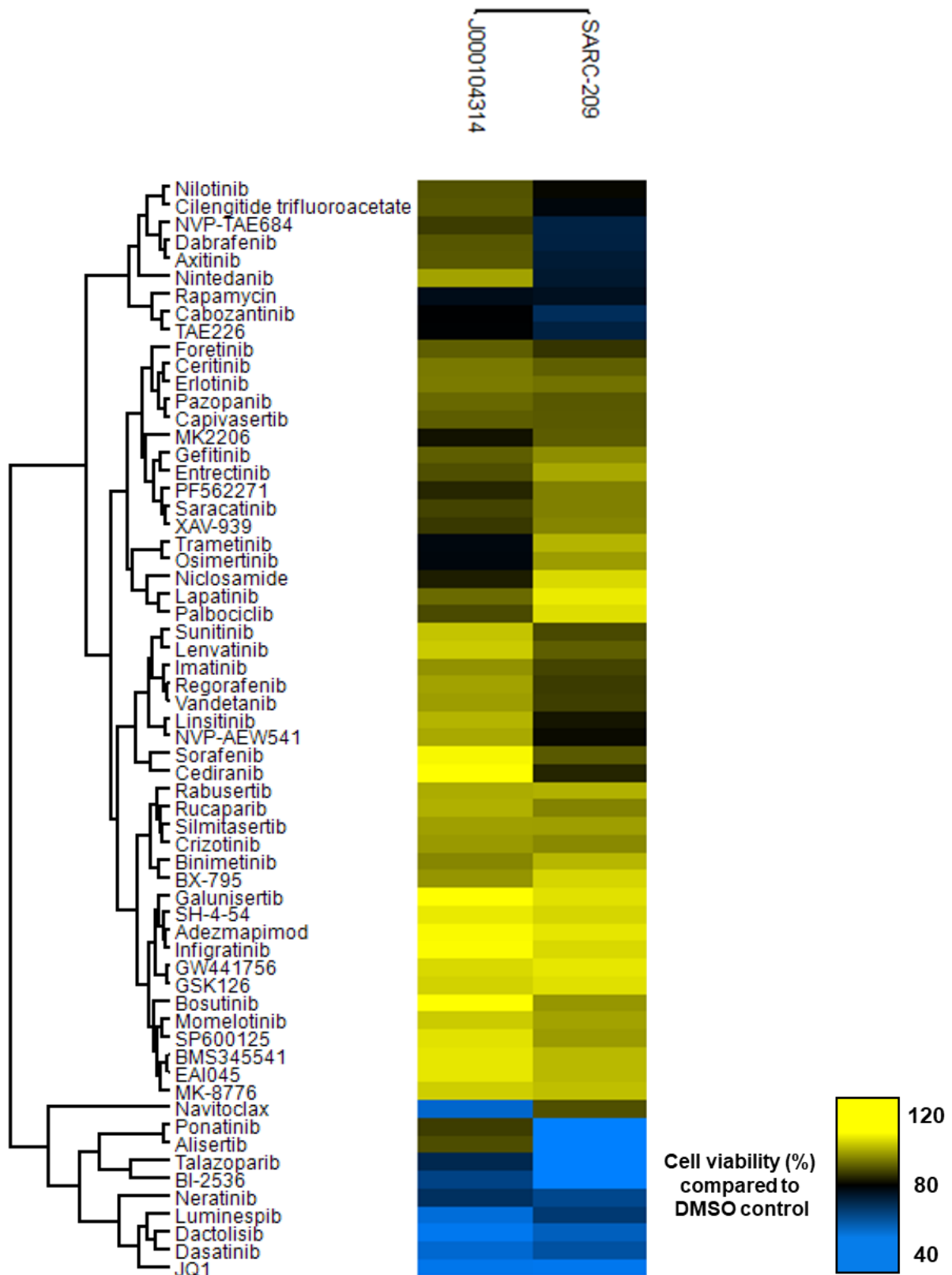


Figure 3.5: Small molecule inhibitor screens of SARC-209 and J000104314 PDX-derived cell models. Small molecule inhibitor screens of SARC-209 and J000104314 cells at an inhibitor concentration of 0.5 μM . Cell viability was normalised to DMSO control (n=2). Two-way hierarchical clustering based on Euclidean distance was performed by Perseus software (Tyanova *et al.*, 2016). DMSO; Dimethyl sulfoxide, PDX; Patient-derived xenograft.

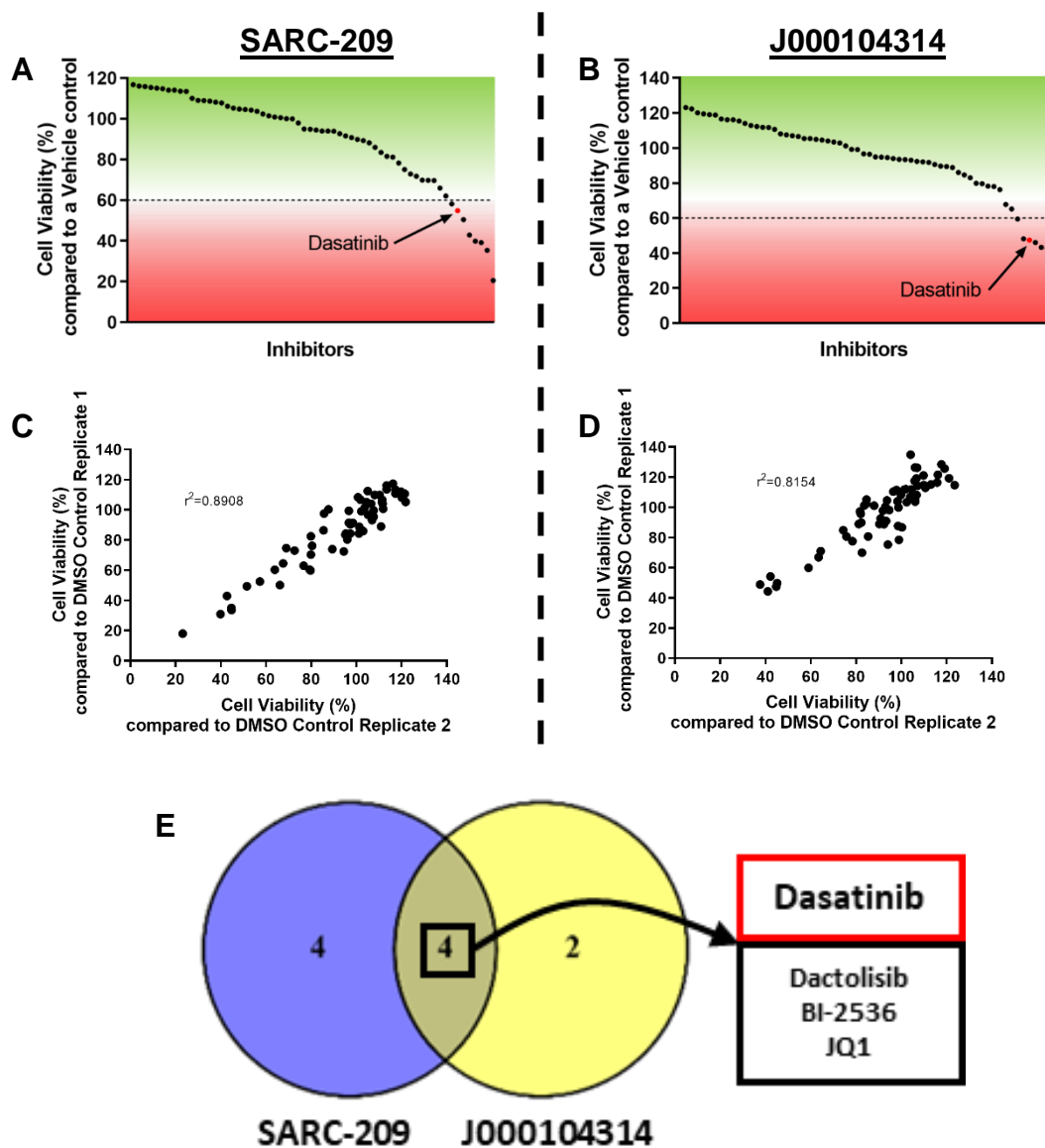


Figure 3.6: Analysis of small molecule inhibitor screens of SARC-209 and J000104314 PDX-derived cell models. Small molecule inhibitor screens of (A) SARC-209 and (B) J000104314 cells at 0.5 μM inhibitor concentration. Cell viability was normalised to DMSO control ($n=2$). X-axis represents the 62 inhibitors and is ordered by descending cell viability. Pearson's correlation analysis of biological replicates for (C) SARC-209 and (D) J000104314. Y-axes show the results of biological replicate 1 and the x-axes show the results of biological replicate 2. (E) Venn diagram showing the inhibitor overlap between effective ($\leq 60\%$ cell viability compared to DMSO control) inhibitors from small molecule inhibitor screens of pazopanib-resistant STS cell models SARC-209 and J000104314 (Table S2). DMSO; Dimethyl sulfoxide, STS; Soft tissue sarcoma.

3.2.4 Pazopanib-resistant soft tissue sarcomas are sensitive to inhibition of the Src pathway by dasatinib

To confirm enhanced dasatinib sensitivity in the pazopanib-resistant SARC-209 and J000104314 PDX-derived cell models compared to pazopanib, I undertook full dose response cell viability assays. From these assays, cell viability was significantly lower with dasatinib (SARC-209; $\text{IC}_{50} = 0.64 \mu\text{M}$, J000104314; $\text{IC}_{50} = 0.18 \mu\text{M}$) treatment

compared with pazopanib (SARC-209; $IC_{50} = 8.46 \mu\text{M}$, J000104314; $IC_{50} > 10 \mu\text{M}$) treatment (**Figure 3.7A-D; Table S3**). Consistent with the reduction in cell viability observed in these short-term assays, long-term colony formation assays found that dasatinib treatment displayed a significant decrease in colony formation compared to pazopanib treatment in both the SARC-209 and J000104314 cell models (**Figure 3.7E-H**).

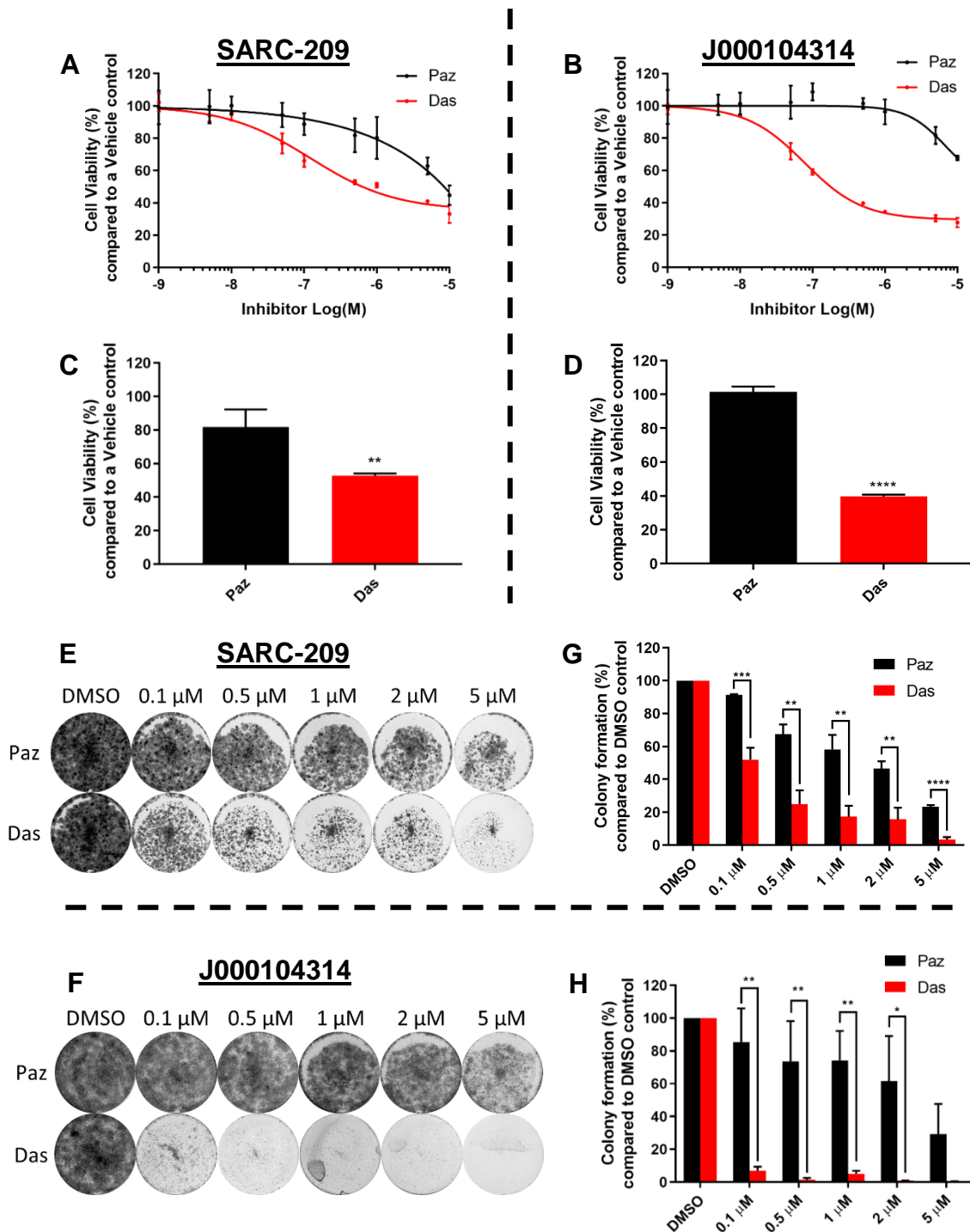


Figure 3.7: Cell viability and colony formation assays of SARC-209 and J000104314 PDX-derived cell models treated with pazopanib and dasatinib. Cell viability assays of (A) SARC-209 and (B) J000104314 cells treated with

increasing concentrations of pazopanib (Paz) and dasatinib (Das) to determine IC₅₀ values (**Table S3**). Bar plots displaying cell viability at 0.5 μ M inhibitor for **(C)** SARC-209 and **(D)** J000104314 cells. Cell viability was normalised to DMSO control (n=3). Statistical analysis of IC₅₀ values not possible as certain models did not reach 50% cell viability. Colony formation assays of **(E)** SARC-209 and **(F)** J000104314 cells treated with increasing concentrations of Paz and Das over a period of 2 weeks. Images are representative of three separate experiments (n=3). Quantification of colony formation assays was normalised to DMSO control for **(G)** SARC-209 and **(H)** J000104314. Statistical analysis was undertaken using Student's unpaired T tests (* = $p \leq 0.05$, ** = $p \leq 0.01$, *** = $p \leq 0.001$, **** = $p \leq 0.0001$). Error bars represent standard deviation. DMSO; Dimethyl sulfoxide, IC₅₀; Inhibitory constant.

Having determined the enhanced antiproliferative activity of dasatinib compared to pazopanib, I next wanted to assess for whether dasatinib had greater cytotoxicity than pazopanib in the pazopanib-resistant STS models. I therefore performed apoptosis assays evaluating caspase 3/7 cleavage to evaluate the pro-apoptotic activities of dasatinib and pazopanib treatment in the PDX-derived cell models (**Figure 3.8A-B**). Dasatinib treatment was found to significantly increase apoptosis compared to DMSO control (~2-fold enhancement) and pazopanib (~1.7- to 2-fold enhancement) treatment in both models (**Figure 3.8A-B**). Together with the cell viability and colony formation assay results, these data demonstrate that dasatinib was an effective treatment in pazopanib-resistant STS cells.

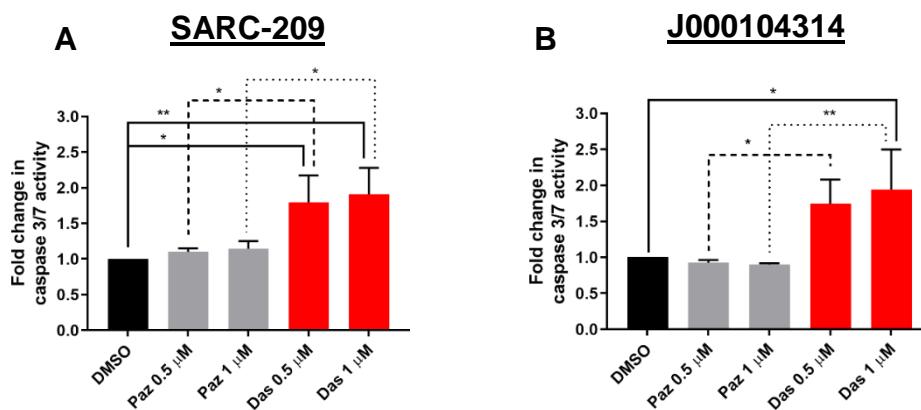


Figure 3.8: Apoptosis assays of SARC-209 and J000104314 PDX-derived cell models treated with pazopanib and dasatinib. Bar plots displaying the fold change in caspase 3/7 activity in the **(A)** SARC-209 and **(B)** J000104314 cells treated with two concentrations of pazopanib (Paz) and dasatinib (Das) for 24 hours. Fold change was normalised to DMSO control (n=3). Statistical analysis was undertaken using one-way ANOVAs with Tukey's multiple comparison tests (* = $p \leq 0.05$, ** = $p \leq 0.01$). Error bars represent standard deviation. ANOVA; Analysis of variance, DMSO; Dimethyl sulfoxide.

In order to evaluate the signalling components that are modulated upon treatment with pazopanib and dasatinib, immunoblotting of key intracellular signalling proteins Src, Akt, ERK1/2, and STAT3 was undertaken on SARC-209 and J000104314 cell models after treatment with 1 μ M pazopanib or dasatinib for 2 or 6 hours (**Figure 3.9A-B**). This allowed for the determination of signalling pathways associated with dasatinib sensitivity in pazopanib-resistant STS cells. The immunoblots show potent inhibition

of Src phosphorylation in both PDX-derived cell models with dasatinib treatment compared to DMSO and pazopanib treatment. Additionally, dasatinib treatment also resulted in a marked increase in total Src levels; a phenomenon which has previously been observed but the mechanism by which this occurs is not yet understood (**Figure 3.9A-B**) (Goc *et al.*, 2014; Konig *et al.*, 2008; Shor *et al.*, 2007). In the SARC-209 model, the only other signalling component which was altered by dasatinib treatment was a minor and transient (2 hr) reduction in ERK1/2 phosphorylation (**Figure 3.9A**). However, both Akt and ERK1/2 phosphorylation in the J000104314 model were decreased upon both 2- and 6-hour dasatinib treatment compared to DMSO and pazopanib treatment (**Figure 3.9B**). STAT3 signalling was not affected by any of the treatments. Pazopanib treatment had no noticeable effects on the phosphorylation status of any of the signalling components analysed (**Figure 3.9A-B**). Due to the common reductions in Src phosphorylation observed with dasatinib treatment in both PDX-derived cell models of pazopanib resistance, I decided to evaluate the association between dasatinib efficacy and Src signalling in pazopanib-resistant STS.

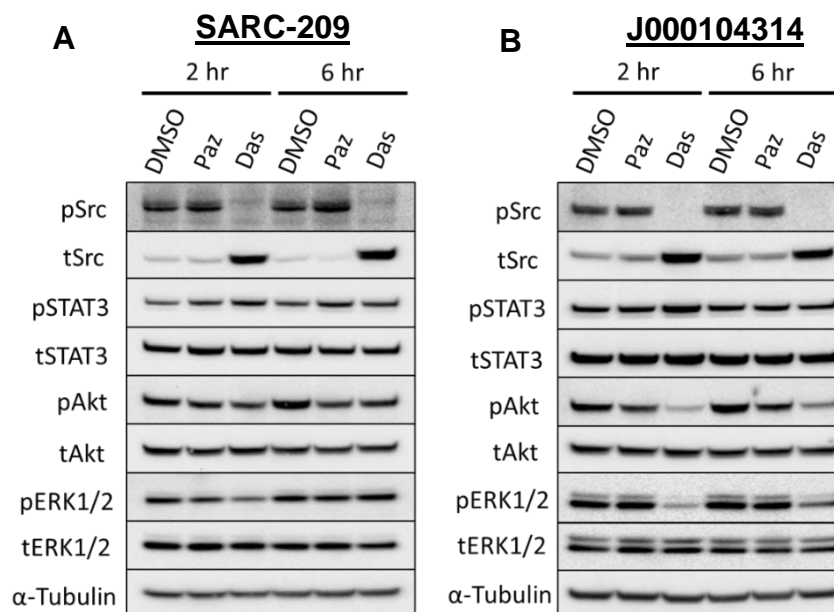


Figure 3.9: Immunoblots of SARC-209 and J000104314 PDX-derived cell models treated with pazopanib and dasatinib. Immunoblots of total levels and phosphorylation status of the major signalling proteins Src, STAT3, Akt, and ERK1/2 in the **(A)** SARC-209 and **(B)** J000104314 cells after treatment with 2 or 6 hours of DMSO, 1 μ M pazopanib (Paz), or 1 μ M dasatinib (Das). Images are representative of two separate experiments (n=2). DMSO; Dimethyl sulfoxide, ERK1/2; Extracellular signal-regulated kinase 1/2, STAT3; Signal transducer and activator of transcription 3.

As discussed in **Chapter 1.3.3**, dasatinib is a multi-target TKI with a broad spectrum of targeted kinases, including Src, Abl1, PDGFRs, KIT, and CSF1R (**Table 1.3; Figure**

1.9). Given this broad kinase inhibitory profile of dasatinib, I undertook experiments to establish whether Src is the kinase responsible for the observed sensitivity to dasatinib in the pazopanib-resistant STS models. To achieve this, a rescue experiment was performed utilising the avian Src gene harbouring the T338I gatekeeper mutation (Src^{T338I}). This mutation exchanges the gatekeeper threonine-338 residue, located at the ATP-binding site, for a hydrophobic and bulky isoleucine residue. Dasatinib binding to Src occurs at this ATP-binding site through hydrogen bonding with the amide backbone, as well as an additional hydrogen bond with the hydroxyl side chain of threonine-338. Substitution of threonine with the hydrophobic and bulkier side chain of isoleucine removes this critical hydrogen bond and also results in steric clashes with the dasatinib molecule, thereby blocking dasatinib access into the binding pocket preventing Src inhibition (Krishnamurty & Maly, 2010; Kwarcinski *et al.*, 2012). Therefore, if sensitivity is caused by dasatinib inhibition of Src, then expression of Src^{T338I} will rescue viability of the cells in the presence of dasatinib.

SARC-209 cells were stably transduced with a Src^{T338I} plasmid construct as well as empty vector (EV) and wild-type Src (Src^{WT}) controls (**Figure 3.10**). The experiment was only carried out in the SARC-209 cells due to the relative ease of viral plasmid transduction into the SARC-209 cells compared to the J000104314 cells, where transductions proved unsuccessful.

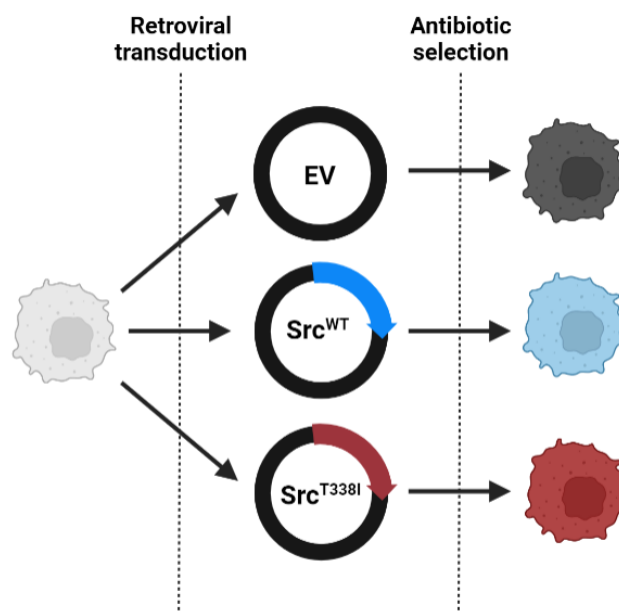


Figure 3.10: Generation of Src construct-expressing SARC-209 cells. pBABE vectors expressing wild-type avian Src (Src^{WT}), dasatinib-resistant Src with T338I mutation (Src^{T338I}) or empty vector (EV) were packaged into retrovirus via co-transfection of HEK293T cells with envelope and packaging plasmids. SARC-209 PDX-derived cell model was

retrovirally transduced with EV, Src^{WT}, and Src^{T338I} plasmids and allowed to recover from viral infection. Successfully transduced cells were selected via exposure to antibiotic (hygromycin). Image was created using BioRender.

To confirm successful viral transduction of Src constructs, immunoblotting was performed to monitor changes in phosphorylation status and total Src levels in EV-, Src^{WT}-, and Src^{T338I}-expressing SARC-209 cells in the presence of DMSO or 1 μ M dasatinib for 6 hours. Firstly, total and phosphorylation levels of Src were increased in cells with Src^{WT} and Src^{T338I} compared to EV at baseline, confirming expression of transduced Src (**Figure 3.11A**). As observed previously in the parental SARC-209 cells, dasatinib treatment resulted in the abolishment of Src phosphorylation and an increase in total Src levels in the EV and Src^{WT} cells. However, whilst the increase in total Src was still observed in the Src^{T338I} cells upon treatment with dasatinib, there was also a large increase in the phosphorylation of Src, confirming that dasatinib was unable to inhibit this mutant (**Figure 3.11A**). The increased activation of gatekeeper-mutated Src has been previously reported (Higuchi *et al.*, 2021). Consistent with my results, Higuchi *et al.* reported that dasatinib treatment of a breast cancer cell line transduced with Src^{T338I} resulted in a dose-dependent increase in Src phosphorylation. The authors postulate that binding of inhibitors to the Src molecule results in the “paradoxical activation of Src” whereby the inhibitor induces a conformational change to shift Src from an inactive conformation to an active conformation. This “conformational activation” results in the recruitment of FAK, however activation of FAK by Src remains inhibited by the bound inhibitor. However, the authors propose a model whereby dasatinib treatment of Src^{T338I}-expressing cells results in increased dasatinib-induced “conformational activation” of Src, resulting in subsequent FAK recruitment, but the reduced binding affinity of dasatinib to Src^{T338I} results in the accelerated dissociation of the molecule, removing the inhibitory block and increasing Src phosphorylation and activity (Higuchi *et al.*, 2021).

Undertaking cell viability assays in the panel of Src-expressing cells, Src^{T338I} cells were found to rescue the phenotype of dasatinib sensitivity with a significant increase in cell viability compared to EV and Src^{WT} cells (**Figure 3.11B-C; Table S4**). The rescued phenotype was also observed in colony formation assays which showed a significant decrease in colony formation upon dasatinib treatment in the EV and Src^{WT} cells but not in the Src^{T338I} cells (**Figure 3.11D-E**). The results of these rescue experiments demonstrate that the sensitivity of the pazopanib-resistant SARC-209 cells to dasatinib

was due to the inhibition of Src phosphorylation and not other kinase targets of dasatinib.

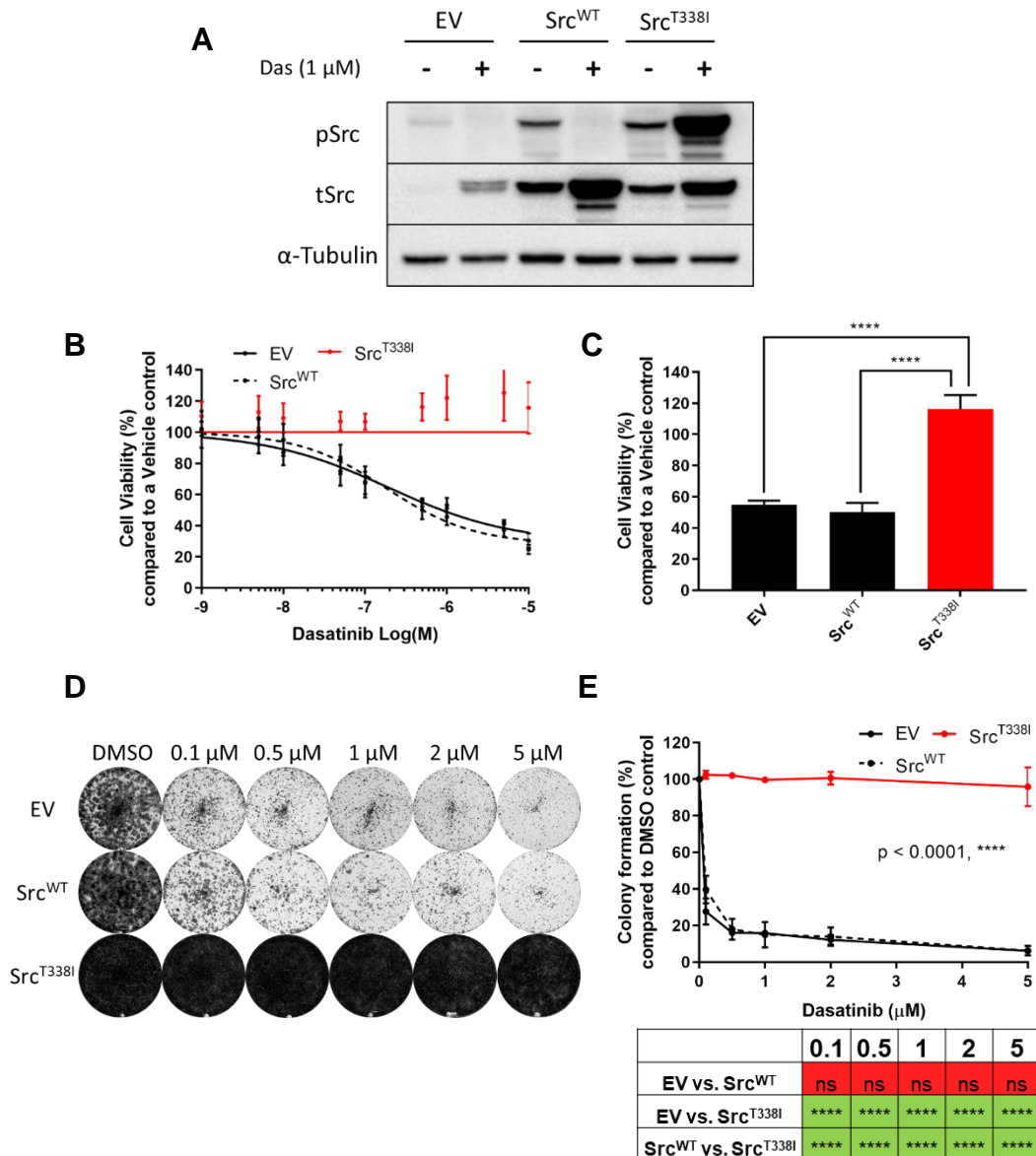


Figure 3.11: Src^{T338I} expression rescues the phenotype of dasatinib sensitivity in SARC-209 cells. (A) Immunoblot of total levels and phosphorylation status of Src in empty vector (EV), wild-type Src (Src^{WT}), and dasatinib (Das)-resistant Src (Src^{T338I}) SARC-209 cells after treatment with 6 hours of DMSO or 1 μM Das. Image is representative of two separate experiments. **(B)** Cell viability assays of EV, Src^{WT}, and Src^{T338I} SARC-209 cells treated with increasing concentrations of Das to determine IC₅₀ values (Table S4). **(C)** Bar plots displaying cell viability at 0.5 μM Das. Cell viability was normalised to DMSO control (n=3). Statistical analysis of IC₅₀ values not possible as certain models did not reach 50% cell viability. **(D)** Colony formation assays of EV, Src^{WT}, and Src^{T338I} SARC-209 cells treated with increasing concentrations of Das over a period of 2 weeks. Image is representative of three separate experiments. **(E)** Quantification of colony formation assay was normalised to DMSO control (n=3). p values corresponding to colony formation assay quantification are displayed in the adjacent table. Statistical analysis was undertaken using one-way ANOVAs with Tukey's multiple comparison tests (**** = p ≤ 0.0001). Error bars represent standard deviation. ANOVA; Analysis of variance, DMSO; Dimethyl sulfoxide, IC₅₀; Inhibitory constant.

To further establish if Src signalling is integral to the growth of pazopanib-resistant cells, genetic inactivation of Src kinase activity was undertaken to evaluate the effects on the proliferation of the SARC-209 model. This was achieved by stably transducing the cells with the Src^{K295M} plasmid construct, as per the methodology outlined in **Figure 3.10**. This mutation results in a dominant-negative, kinase-dead Src molecule. Substitution of the catalytic kinase site lysine-295 with a methionine residue leads to a catalytically inactive Src, which also exerts a dominant-negative effect on endogenous Src molecules (Destaing *et al.*, 2008).

Immunoblotting confirmed increased expression of Src in the Src^{K295M} cells, with a comparable baseline total level compared to Src^{WT} but an increase in expression relative to EV (**Figure 3.12A**). As expected, the Src^{K295M} cells had reduced basal Src phosphorylation levels compared to Src^{WT} cells and comparable levels to EV cells (**Figure 3.12A**). These results confirmed the presence of the dominant-negative phenotype. Consistent with previous results, dasatinib treatment of Src^{K295M} cells resulted in the abolishment of Src phosphorylation and a concurrent increase in total Src levels (**Figure 3.12A**).

To evaluate the effect of the Src^{K295M} mutation on pazopanib-resistant SARC-209 cell proliferation, a 2-week growth curve assay measuring the number of cells on a daily basis was undertaken. **Figure 3.12B** shows that there was a significant decrease in the number of Src^{K295M} cells compared to Src^{WT}. This result phenocopies the chemical blockade of Src signalling by dasatinib and demonstrates that Src signalling is integral to the growth of pazopanib-resistant SARC-209 cells.

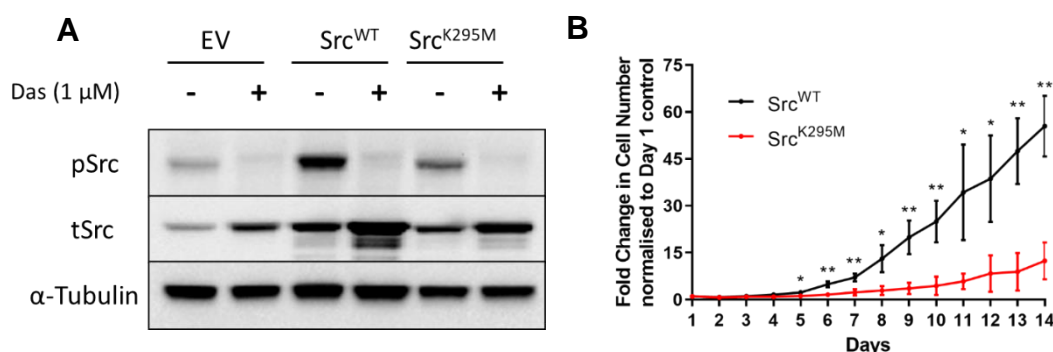


Figure 3.12: Src^{K295M} expression reduces the proliferation of SARC-209 cells. (A) Immunoblot of total levels and phosphorylation status of Src in empty vector (EV), wild-type Src (Src^{WT}), and dominant-negative Src (Src^{K295M}) SARC-209 cells after treatment with 6 hours of DMSO or 1 μM dasatinib (Das). Image is representative of two separate experiments (n=2). (B) Growth curve assays of Src^{WT} and Src^{K295M} SARC-209 cells to measure the fold change in cell number over a period of two weeks. Fold change was normalised to day 1 control (n=3). Statistical analysis was

undertaken using Student's unpaired T tests (* = $p \leq 0.05$, ** = $p \leq 0.01$). Error bars represent standard deviation. DMSO; Dimethyl sulfoxide.

To establish if dasatinib is an effective treatment for pazopanib-resistant STS *in vivo*, SARC-209-originating PDX tumour tissue was implanted into NCR nude mice to establish xenografts (**Figure 3.1**). Xenograft-bearing mice were stratified into two arms: a vehicle-treated control arm (n=5) and a dasatinib-treated arm (n=10). Mice were treated twice a week via oral gavage with either vehicle (80 mM sodium citrate, pH 3.0) or 30 mg/kg dasatinib. Mice were sacrificed once the tumour mass exceeded 1000 mm³. The Kaplan-Meier and tumour volume curves in **Figure 3.13A-B** show that there was a significant improvement in the survival of mice and a concurrent reduction in tumour volume growth in the dasatinib arm compared to the vehicle arm. This result shows that the antiproliferative phenotypes observed *in vitro* with dasatinib were translated into an antitumour effect *in vivo* (**Figure 3.10A-B**).

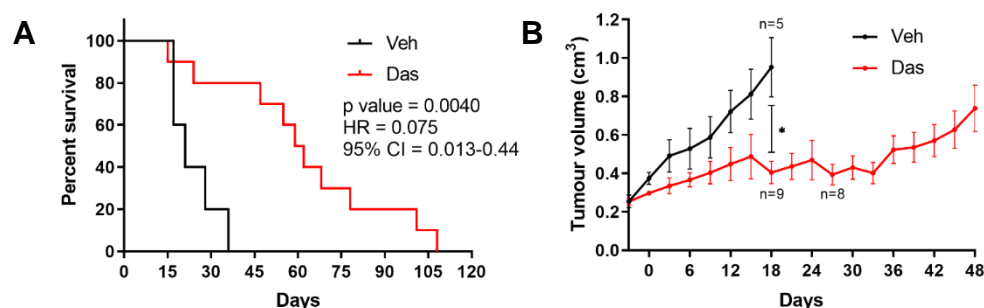


Figure 3.13: *In vivo* evaluation of dasatinib in mouse xenograft models of STS. (A) Kaplan-Meier curves of xenografts generated by implantation of mice with SARC-209-originating PDX tumours. Mice were treated twice a week via oral gavage with either vehicle (Veh) (n=5) (80 mM sodium citrate, pH 3.0) or 30 mg/kg dasatinib (Das) (n=10). Mice were sacrificed when tumour mass exceeded 1000 mm³. p value was determined by logrank Mantel-Cox test and hazard ratio (HR)/95% confidence interval (CI) of ratio was determined by Mantel-Haenszel test (** = $p \leq 0.01$). **(B)** Average tumour volume curves of SARC-209 xenografts treated with either Veh (n=5) or Das (n=10). Least squares regression between two immediately adjacent datapoints was used to calculate tumour volume for days when no measurement for a particular individual xenograft was taken. Statistical analysis was undertaken using Welch's unpaired T test (* = $p \leq 0.05$). Error bars represent the standard error of the mean.

Taken together, these results demonstrate that the TKI dasatinib is an effective treatment in pazopanib-resistant models of STS both *in vitro* and *in vivo*. Dasatinib mediates its antiproliferative effect through blockade of the Src signalling pathway; an integral pathway in the proliferation and survival of pazopanib-resistant STS cells. Therefore, these results nominate dasatinib as a candidate salvage therapy for treating pazopanib-resistant STS through targeting of the Src pathway.

3.3 Discussion

The critical intracellular signalling node Src has extensively been shown to play a prominent role in many hallmarks of tumourigenesis including proliferation, migration, and metastasis (Zhang & Yu, 2012). Additionally, numerous preclinical studies have reported the efficacy of Src inhibition in abrogating tumour growth and progression (Zhang & Yu, 2012). Notably, several publications have reported that dasatinib possesses potent antitumour activity in preclinical models of STS (Aslam *et al.*, 2014; Brodin *et al.*, 2019; Lopez-Acevedo *et al.*, 2014; Michels *et al.*, 2013; Mukaihara *et al.*, 2017; Shor *et al.*, 2007; Sievers *et al.*, 2015; Teicher *et al.*, 2015; Wong *et al.*, 2016; Yeung *et al.*, 2013; Zhang & Yu, 2012).

In a study by Brodin *et al.*, dasatinib was found to have activity in a panel of primary, patient-derived cell models of translocation-associated STS. Pharmacological screens of patient-derived cell models of alveolar rhabdomyosarcoma, synovial sarcoma, and alveolar soft part sarcoma found significant and universal activity with dasatinib therapy in the STS subtypes evaluated (Brodin *et al.*, 2019). Additionally, dasatinib has also shown potent antitumour effects in further preclinical cell and xenograft models of STS subtypes that are characterised by “simple”, pathognomonic genetic aberrations including rhabdomyosarcoma, synovial sarcoma, alveolar soft part sarcoma, and malignant rhabdoid tumour (Aslam *et al.*, 2014; Michels *et al.*, 2013; Mukaihara *et al.*, 2017; Shor *et al.*, 2007; Teicher *et al.*, 2015; Wong *et al.*, 2016; Yeung *et al.*, 2013). The reported preclinical activity of dasatinib is not just limited to “simple” STS subtypes however, with multiple studies reporting activity in “complex” subtypes such as liposarcoma, malignant peripheral nerve sheath tumour, and leiomyosarcoma (Lopez-Acevedo *et al.*, 2014; Shor *et al.*, 2007; Sievers *et al.*, 2015; Teicher *et al.*, 2015). Throughout these publications, dasatinib-induced Src inhibition is commonly shown as the causative factor in effectuating the antiproliferative and antitumour properties of dasatinib (Michels *et al.*, 2013; Mukaihara *et al.*, 2017; Shor *et al.*, 2007; Sievers *et al.*, 2015).

However, the activity of dasatinib in preclinical models of STS has not currently been successfully translated into meaningful activity in phase II clinical trials. The SARC009 trial has evaluated the efficacy of dasatinib in advanced STS. In two analyses of the SARC009 trial, dasatinib failed to meet the primary endpoint in either study (**Table 1.6**)

(Schuetze *et al.*, 2016; Schuetze *et al.*, 2017). In the first study, Schuetze *et al.* reported that dasatinib fell short of the primary endpoint of 25% clinical benefit rate (CBR) in a cohort of advanced STS (**Table 1.6**) (Schuetze *et al.*, 2016). Similarly, in a subsequent analysis on patients diagnosed with alveolar soft part sarcoma, epithelioid sarcoma, and solitary fibrous tumour, dasatinib once again failed to reach the primary endpoint of the trial ($\geq 50\%$ progression-free rate (PFR) at 6 months) (**Table 1.6**) (Schuetze *et al.*, 2017). Despite these disappointing results, dasatinib did show potential activity in a small subset of patients diagnosed with undifferentiated pleomorphic sarcoma and alveolar soft part sarcoma subtypes (Schuetze *et al.*, 2016; Schuetze *et al.*, 2017). A significant proportion of the patients enrolled onto the SARC009 trial had received previous lines of anticancer therapy however it is currently unclear if, and how many, of these patients received pazopanib. Therefore, the utility of dasatinib therapy in pazopanib-refractory STS patients has not yet been evaluated.

The data outlined in **Chapter 3.2** demonstrates that the multi-target TKI dasatinib shows both *in vitro* and *in vivo* efficacy in PDX-derived STS cell models of acquired and intrinsic pazopanib resistance. Through subjecting pazopanib-resistant models to small molecule inhibitor screens, dasatinib was proposed as a potential salvage therapy for pazopanib-resistant STS. Comparative assessment of dasatinib with pazopanib determined that dasatinib possessed superior antiproliferative and antitumour properties than pazopanib within these PDX-derived cell models, with significant decreases in cell viability and colony formation, as well as concurrent increases in apoptotic activity. Functional assessment determined that these phenotypes were mediated through the inhibition of Src phosphorylation. Through the utilisation of functional Src gatekeeper mutants, the antiproliferative effects of dasatinib were found to be as a direct consequence of Src pathway blockade. Additionally, dominant-negative Src experiments determined that Src signalling is integral to the growth and proliferation of pazopanib-resistant STS cells. Finally, the antitumour activity of dasatinib was translated into an *in vivo* effect, where dasatinib was found to significantly improve murine survival outcomes when compared to vehicle control. Therefore, these results nominate dasatinib as a candidate salvage therapy for pazopanib-resistant STS through targeting of the Src pathway. The results are consistent with previous findings by Qiao *et al.* who showed that synovial sarcoma models with pazopanib resistance exhibited increased levels of Src phosphorylation

(Qiao *et al.*, 2017). In a further phosphoproteomic analysis, Wong *et al.* also reported the upregulation of Src family kinase members in pazopanib-resistant cells (Wong *et al.*, 2016). Furthermore, Saturno *et al.* reported that utilisation of a dual Src and pan-Raf inhibitor, CCT3833, provided prolonged clinical benefit, as well as an unconfirmed partial response (PR), in a patient diagnosed with spindle cell sarcoma that had progressed on previous pazopanib therapy (Saturno *et al.*, 2021).

Dasatinib has also shown clinically meaningful activity in non-STS cancer types and is currently approved for the treatment of Philadelphia chromosome-positive acute lymphoblastic leukaemia and chronic myeloid leukaemia (Nekoukar *et al.*, 2021). These leukaemias are characterised by the expression of the oncogenic Bcr-Abl1 fusion protein, encoded on the translocated Philadelphia chromosome (t(9;22)(q34;q11)) (Kang *et al.*, 2016). The Bcr-Abl1 fusion protein is a constitutively activated tyrosine kinase that aberrantly activates downstream signalling pathways to induce tumourigenic phenotypes such as enhanced proliferation and apoptotic evasion (Kang *et al.*, 2016). Dasatinib is an effective treatment for Philadelphia chromosome-positive leukaemias due to its potent inhibition of Abl1 – in keeping with its characteristics as a multi-target TKI (as outlined in **Table 1.3**) (Davis *et al.*, 2011; Reddy & Aggarwal, 2012). Therefore, the potential importance of Abl1 inhibition by dasatinib within my models of pazopanib-resistant STS should be considered in future studies. This is especially true of the SARC-209 model which showed potent sensitivity towards another Abl1 inhibitor, the multi-target TKI ponatinib (Reddy & Aggarwal, 2012). Future work will firstly focus on whether RNAi-induced knockdown (either by siRNA or shRNA) of Src phenocopies the antiproliferative effect observed with dasatinib treatment within my cell models of pazopanib-resistant STS. Additionally, utilisation of Src-specific inhibitors, such as PP2 and SU6656, will be utilised to observe whether specific Src inhibition mimics the effects observed with dasatinib (Blake *et al.*, 2000; Hanke *et al.*, 1996; Hua *et al.*, 2019; Yu *et al.*, 2021). Building on this work, I will also study the expression levels of Abl1 before determining whether dasatinib treatment inhibits Abl1 phosphorylation within these models. Through these means I aim to fully elucidate whether Src inhibition is the sole cause of the antitumoural effects observed within the pazopanib-resistant sarcoma models, or whether Abl1 inhibition (or indeed any other signalling pathway) is also concurrently involved.

The results also highlighted the clinically relevant benefit of utilising low-passage, PDX-derived cells as surrogates in the study of drug resistance in STS. As shown in **Chapter 3.1**, the *in vitro* cell cultures derived from PDX models retained the molecular, histological, and therapeutic response characteristics of the originating tumour. Previous studies utilising patient-derived models in STS have demonstrated the clinically relevant nature of these models to predict patient response and identify effective therapies for STS patients (Brodin *et al.*, 2019; Stebbing *et al.*, 2014). The current limitations of using such models to aid personalised patient treatments is the amount of time that it takes to progress from tumour biopsy to pharmacological screens, which can often stretch into several months, by which time the patient's disease is likely to have progressed (Brodin *et al.*, 2019). However, the development of several PDX databases containing large numbers of patient-derived models of STS (e.g., Champions TumorGraft® and XenoSarc databases), as well as the development of extremely thorough pharmacological screens, hold promise for the use of patient-derived and PDX-derived models as predictive models of drug sensitivity in STS patients (Cornillie *et al.*, 2019; Schöffski *et al.*, 2019; Stebbing *et al.*, 2014; Wells *et al.*, 2021).

In relation to the data in **Chapter 3**, there are currently outstanding questions related to the mechanisms of Src signalling in pazopanib-resistant STS, and whether Src signalling is a causative factor of resistance. For instance, the upstream receptors and kinases that mediate Src activity, as well as downstream Src signalling effectors, remain to be determined in pazopanib-resistant STS.

Chapter 4

Understanding the mechanistic basis of
Src dependency in pazopanib-resistant
soft tissue sarcoma

4.1 Introduction

As shown in **Chapter 3**, pazopanib-resistant sarcoma cell lines are sensitive to targeting of the Src pathway. However, the mechanisms of Src activation and its downstream signalling in pazopanib-resistant soft tissue sarcoma (STS) are not yet understood.

Src has been identified as a central signalling node in a variety of signalling pathways that mediate numerous biological processes. For instance, Src has been shown to be a downstream effector of numerous receptor tyrosine kinases (RTKs), including platelet-derived growth factor receptors (PDGFRs), fibroblast growth factor receptors (FGFRs), and MET (as well as many others), in the transduction of proliferation, growth, and survival signals (Bromann *et al.*, 2004). Similarly, survival, migratory, and proliferation signals transduced by Src activity have been reported to be directly regulated by cytokine receptors, such as type I/II cytokine receptors, chemokine G-protein coupled receptors (GPCRs), and transforming growth factor β receptors (TGF β R) (Luttrell & Luttrell, 2004; Rane & Reddy, 2002; Zhang *et al.*, 2015). Additionally, Src signalling has extensively been shown to be an important component of integrin receptor signalling (Playford *et al.*, 2004). In response to extracellular matrix (ECM) binding to integrins, Src is recruited to an intracellular protein scaffold at the integrin interface alongside other proteins such as focal adhesion kinase (FAK) and paxillin (Playford *et al.*, 2004). The ECM-induced external signal is therefore transduced through this scaffold to induce intracellular cytoskeletal remodelling, thereby affecting migratory, metastatic, and morphological phenotypes, and the activation of survival and proliferation signals (Desgrosellier & Cheresh, 2015; Playford *et al.*, 2004).

In addition to various upstream mediators, Src is known to possess wide substrate specificity, resulting in the phosphorylation and subsequent activation of a variety of downstream effector proteins. As well as the previously discussed MAPK, PI3K/Akt, and STAT3 pathways that result in cellular phenotypes such as survival, proliferation, growth, and differentiation (**Chapter 1.2.3**), Src has also been shown to mediate Abl1, phospholipase C- γ , FAK, p130Cas, and c-Myc pathways. Further to their mitogenic consequences, these pathways also induce migration, invasion, and growth of healthy and cancerous cells (Bromann *et al.*, 2004; Yeatman, 2004).

Therefore, understanding the upstream and downstream components of Src signalling in Src-dependent, pazopanib-resistant STS will allow for the determination of further potential vulnerabilities for targeted therapy. **Chapter 4.2** will focus on the upstream mediators of Src activity in pazopanib-resistant STS. In this chapter, the role of interleukin-8 (IL-8) signalling in pazopanib-resistant STS and the association with Src signalling will be assessed. Additionally, I performed a screen of inhibitors to identify upstream regulators of Src activity in pazopanib-resistant STS.

4.2 Results

4.2.1 IL-8 signalling does not confer pazopanib resistance through autocrine signalling in soft tissue sarcoma models of pazopanib resistance

In order to determine potential mechanisms of acquired pazopanib resistance, tumour biopsies were obtained from a patient diagnosed with spindle cell sarcoma that had displayed an initial long-term response to pazopanib before acquiring resistance. Biopsies were taken from the abdominal wall metastases preceding pazopanib treatment (at which point the tumour was pazopanib sensitive) and 2 months following the cessation of pazopanib (at which point the tumour had acquired pazopanib resistance) (**Figure 4.1**).

Analysis of significant, temporal changes in gene expression between the two biopsies was undertaken by Dr. Alex Lee – a clinical PhD student working in our group. The analysis found that the inflammatory cytokines leukaemia inhibitory factor (LIF), IL-6, and IL-8 were significantly upregulated in the acquired pazopanib resistance setting compared to the pre-pazopanib tumour (**Figure 4.1**). These cytokines play critical roles in a number of biological pathways, most notably inflammation and immune response. However, through both paracrine and autocrine mechanisms, these cytokines have also been shown to promote tumour progression, metastasis, angiogenesis, and survival in a number of cancer types (Hirano, 2021; Waugh & Wilson, 2008; Zhang *et al.*, 2021).

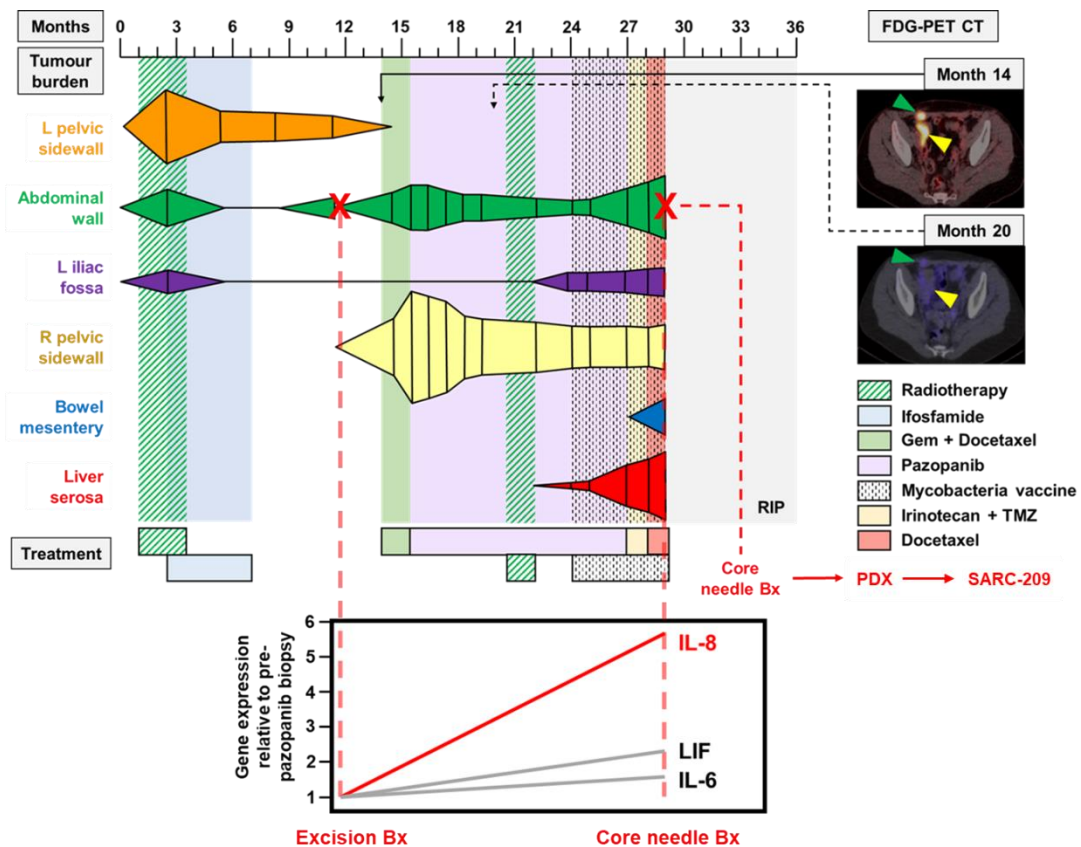


Figure 4.1: Clinical history of a STS patient with acquired pazopanib resistance and significant gene expression changes between biopsies. Schematic overview of the clinical history of a patient diagnosed with spindle cell sarcoma with an initial, long-term pazopanib response and subsequent acquisition of resistance. Schematic shows the time and location of the pre-pazopanib treatment excision biopsy and post-pazopanib treatment core needle biopsy. Schematic also shows tumour location and burden, as well as treatment paradigm. Gene expression fold change is shown for IL-8, IL-6, and LIF. Figure was adapted from work by Dr. Alex Lee. Bx; Biopsy, FDG-PET CT; Fluorodeoxyglucose (^{18}F)-positron emission tomography computerised tomography, Gem; Gemcitabine, IL-(6/8); Interleukin-(6/8), LIF; Leukaemia inhibitory factor, PDX; Patient-derived xenograft, RIP; Rest in peace, TMZ; Temozolomide.

Upregulation of these cytokines have previously been reported to confer tyrosine kinase inhibitor (TKI) resistance, as well as act as potential biomarkers, in several models of cancer including lung and prostate cancer (Fernando *et al.*, 2016; Kutikov *et al.*, 2011; Liu *et al.*, 2015; Tamura *et al.*, 2018). Similarly, high levels of IL-8 and IL-6 expression have been found to be correlated with increased tumour grade and aggressiveness, as well as being associated with an overall worse prognosis in STS patients (Highfill *et al.*, 2014; Rutkowski *et al.*, 2002).

I therefore wanted to assess whether IL-8 signalling causes pazopanib resistance in STS, and whether IL-8 signalling mediates its effects via the Src pathway in pazopanib-resistant STS. I decided to focus on IL-8 as this cytokine was shown to have a far higher expression level fold change than LIF or IL-6 in pazopanib-resistant tissue, when compared to pre-pazopanib tissue (**Figure 4.1**). However, the cytokine

measurements determined by gene expression analysis of biopsies taken from the patient could be from both tumour and/or stromal cells. It is therefore important to determine the levels of IL-8 expression in STS tumour cells.

In order to answer these questions, I firstly wanted to determine the levels of IL-8 expression within the pazopanib-resistant, PDX-derived STS cell models (SARC-209 and J000104314), as well as a panel of sarcoma cell lines. It is important to re-iterate that the SARC-209 cells were derived from a PDX generated from the same tumour biopsy as was used to determine the IL-8 gene expression levels in the pazopanib-resistant setting (**Figure 4.1**). The panel of sarcoma cell lines is outlined in **Table 4.1** and consists of varying sarcoma histological subtypes (**Table 4.1**). Furthermore, previous work by Wong *et al.* has shown that all the cell lines within the panel (with the exception of A204 and G402) are resistant to *in vitro* pazopanib treatment (Wong *et al.*, 2016).

Table 4.1: Panel of 14 sarcoma cell lines with subtype, Cellosaurus accession codes, and additional comments.

Cell line	Subtype	Cellosaurus accession code (Bairoch <i>et al.</i> , 2018)	Comments
A204	MRT	CVCL_1058	Initially misclassified as RMS (Hinson <i>et al.</i> , 2013)
G402	MRT	CVCL_1221	Initially misclassified as LMB (Brenca <i>et al.</i> , 2021)
HT1080	Fibrosarcoma	CVCL_0317	
SW684	Fibrosarcoma	CVCL_1726	
MESSA	Uterine sarcoma	CVCL_1404	
SW872	Liposarcoma	CVCL_1730	
Hs729T	eRMS	CVCL_0871	
RMS-YM	eRMS	CVCL_A792	
RUCH3	eRMS	CVCL_C541	
SW982	Synovial sarcoma	CVCL_1734	Potentially misclassified as does not contain pathognomonic SS18-SSX1/2/4 translocation (Kawano <i>et al.</i> , 2017)
SAOS2	Osteosarcoma	CVCL_0548	
U2OS	Osteosarcoma	CVCL_0042	
SJSA1	Osteosarcoma	CVCL_1697	
T91-95	aRMS	n/a (Lee <i>et al.</i> , 2003; Martins <i>et al.</i> , 2011)	T91-95 have also been described as normal fibroblast cells (Gryder <i>et al.</i> , 2017)

aRMS; Alveolar rhabdomyosarcoma, CVCL; Cellosaurus accession code, (e)RMS; (Embryonal) rhabdomyosarcoma, LMB; Leiomyoblastoma, MRT; Malignant rhabdoid tumour, SS18; Synovial sarcoma translocation chromosome 18, SSX(1/2/4); Synovial sarcoma X (1/2/4) breakpoint protein.

To determine whether the sarcoma cell models expressed IL-8, I undertook real-time quantitative polymerase chain reaction (qPCR) to assess for the levels of *CXCL8* (the gene encoding the IL-8 cytokine) mRNA (**Figure 4.2**). As a positive control for *CXCL8* expression, the cell line SW982 was used. SW982 is a synovial sarcoma cell line that is characterised by high expression of inflammatory cytokines such as IL-8 and IL-6, and, as such, is commonly used as a cellular model to study rheumatoid arthritis (Lv *et al.*, 2013; Yamazaki *et al.*, 2003). **Figure 4.2A** shows that the majority of evaluated

STS cell models express *CXCL8* mRNA to at least a quantifiable level, but expression was very heterogeneous across the panel. The data was normalised to the cell line that exhibited the median level of *CXCL8* expression, U2OS. The PDX-derived, pazopanib-resistant cells, SARC-209 and J000104314, were shown to both moderately express *CXCL8* compared to the remainder of the cell line panel.

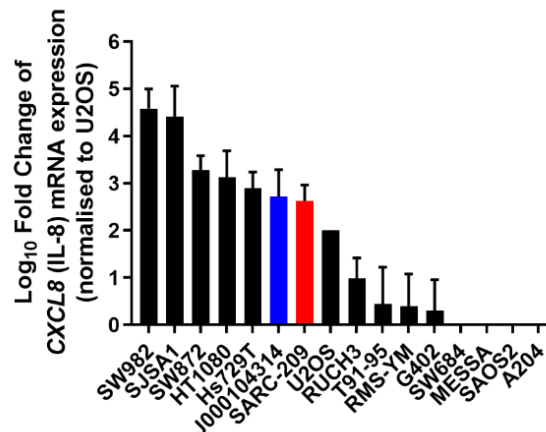


Figure 4.2: *CXCL8* (IL-8) expression levels in a panel of sarcoma cell lines and PDX-derived models. (A) qPCR data displaying the log₁₀ fold change of *CXCL8* (IL-8) mRNA, normalised to the osteosarcoma cell line U2OS (n=3). Error bars represent standard deviation. *CXCL8*; Chemokine C-X-C motif ligand 8, IL-8; Interleukin-8, mRNA; Messenger RNA, PDX; Patient-derived xenograft, qPCR; Quantitative polymerase chain reaction, RNA; Ribonucleic acid.

IL-8 mediates its intracellular effects through binding to one of two membrane-bound GPCRs, termed C-X-C motif chemokine receptor 1 (CXCR1) and CXCR2. These two receptors are highly homologous to each other and are expressed on the cell surface of immune cells, such as leukocytes and neutrophils, as well as tumour cells. Due to this expression within immune and tumour cells, the IL-8-CXCR1/2 signalling axis has been implicated in playing an important role within the tumour microenvironment to aid cancer progression (Ha *et al.*, 2017; Waugh & Wilson, 2008). Additionally, expression of CXCR1 and CXCR2 on the surface of IL-8-secreting tumour cells has been shown to result in oncogenic autocrine signalling loops, thereby driving cancer cell proliferation and migration (Brew *et al.*, 2000; Lang *et al.*, 2002; Takamori *et al.*, 2000). Autocrine signalling refers to the secretion of signalling molecules by a cell, which in turn, bind to receptors on the same cell, resulting in biological changes occurring within the cell (Doğaner *et al.*, 2016).

Therefore, having determined that the majority of sarcoma cell models express *CXCL8* to at least a quantifiable level, I wanted to determine whether the sarcoma cell models expressed *CXCR1* and/or *CXCR2* mRNA. I postulated that if the cell models were

found to express both the cytokine and receptor(s), then an autocrine signalling loop potentially driving proliferation could be at work. However, preliminary evaluation via qPCR found that none of the sarcoma cell lines within the panel expressed *CXCR1* or *CXCR2* to a readily quantifiable level (data not shown).

To confirm these preliminary findings, I wanted to create a positive cell model control for *CXCR1* and *CXCR2* expression. I therefore decided to transduce the SARC-209 PDX-derived cell model with *CXCR1*- or *CXCR2*-expressing plasmids. These plasmids were generated by inserting the open-reading frame of *CXCR1* or *CXCR2* cDNA into linearised pBABE vectors (**Figure S1-S2**). Following this, the SARC-209 cells were stably transduced with empty vector (EV)-, *CXCR1*- or *CXCR2*-expressing plasmids via retroviral infection, as outlined in **Figure 4.3A**.

To confirm the successful transduction of *CXCR1*- and *CXCR2*-expressing plasmids, I undertook qPCR analysis on the transduced SARC-209 cells to observe for *CXCR1* or *CXCR2* DNA amplification (**Figure 4.3B-C**). Consistent with preliminary results, no amplification was observed in the SARC-209 EV control (**Figure 4.3B-C**). However, SARC-209 cells transduced with the *CXCR1* plasmid were found to selectively express *CXCR1*, with no amplification of *CXCR2* (**Figure 4.3B**). The reverse is true for the SARC-209 cells transduced with the *CXCR2* plasmid (**Figure 4.3C**). As no amplification was observed in the EV control for either receptor, the reporter signal (Rn) from raw qPCR data was normalised to the Rn of the housekeeping gene, β -actin (*ACTB*). Therefore, if the gene of interest is expressed, the Rn curve will display a bell-shaped or flat-line trajectory as the Rn tends towards 0 after 40 PCR cycles. Cells not expressing the gene of interest will always display a negative drop in Rn. **Figure 4.3B-C** show that *CXCR1* and *CXCR2* were successfully transduced into the SARC-209 cells.

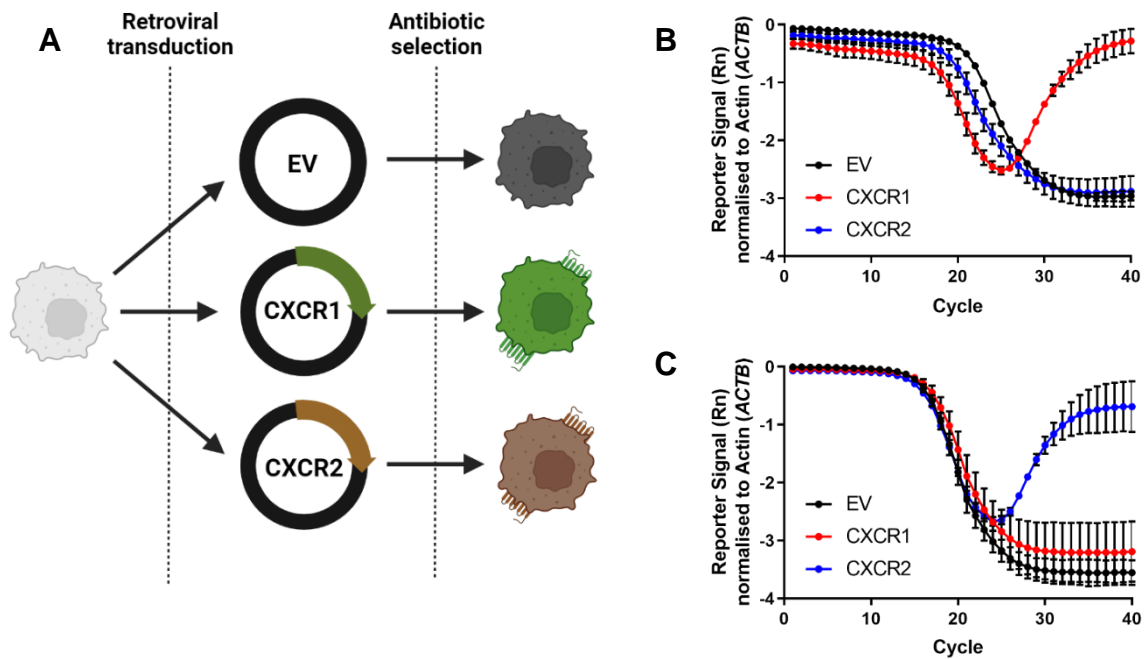


Figure 4.3: Generation of *CXCR1*- and *CXCR2*-expressing SARC-209 cells. (A) pBABE vectors expressing *CXCR1*, *CXCR2*, or empty vector (EV) were packaged into retrovirus via co-transfection of HEK293T cells with envelope and packaging plasmids. SARC-209 PDX-derived cell model was retrovirally transduced with EV, *CXCR1*, and *CXCR2* plasmids and allowed to recover from viral infection. Successfully transduced cells were selected via exposure to antibiotic (hygromycin). Image was created using BioRender. Reporter signal (Rn), normalised to β -actin (*ACTB*), of (B) *CXCR1* and (B) *CXCR2* expression in SARC-209 EV, *CXCR1*- and *CXCR2*-expressing cells. Image is representative of three separate experiments (n=3). CXCR(1/2); C-X-C motif chemokine receptor (1/2), PDX; Patient-derived xenograft.

I therefore incorporated the SARC-209 *CXCR1*- or *CXCR2*-expressing cells into the qPCR analysis of *CXCR1* and *CXCR2* expression in the panel of sarcoma cell lines and PDX-derived cell models. **Figure 4.4** shows that, consistent with the preliminary results, none of the parental sarcoma cell models evaluated expressed either receptor to a quantifiable level.

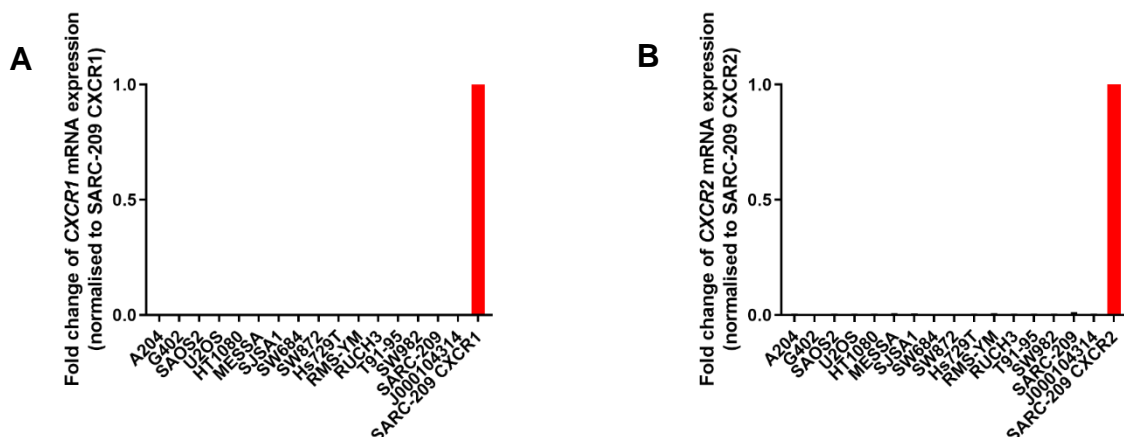


Figure 4.4: *CXCR1* and *CXCR2* expression levels in a panel of sarcoma cell lines and PDX-derived models. qPCR data displaying the relative mRNA expression of (C) *CXCR1* and (D) *CXCR2* normalised to SARC-209 *CXCR1*- and *CXCR2*-expressing cell controls, respectively (n=3). Error bars represent standard deviation. CXCR(1/2); C-X-C

motif chemokine receptor (1/2), mRNA; Messenger RNA, PDX; Patient-derived xenograft, qPCR; Quantitative polymerase chain reaction, RNA; Ribonucleic acid.

As none of the sarcoma cell models expressed *CXCR1* or *CXCR2*, it can therefore be determined that IL-8 expressed by the sarcoma cell models is not having an autocrine effect. Therefore, if the upregulation of IL-8 expression observed in the pazopanib-resistant patient tissue is associated with pazopanib resistance, it is more likely to be due to IL-8 paracrine signalling. Paracrine signalling refers to cellular signalling between nearby cells within a local microenvironment. In cancerous tissue, paracrine signalling occurs between tumour cells and cells of the surrounding tumour microenvironment (TME), such as immune cells, cancer-associated fibroblasts, and other stromal cells. In corroboration with the hypothesis of IL-8 paracrine signalling potentially driving pazopanib resistance in STS, *CXCR1* and *CXCR2* receptors are known to be ubiquitously expressed in immune cells and have been reported to be associated with the recruitment of pro-tumourigenic immune cells to the TME (Acharyya *et al.*, 2012; Najjar *et al.*, 2017; Susek *et al.*, 2018).

4.2.2 IL-8 stimulation does not affect Src pathway activity in pazopanib-resistant soft tissue sarcoma

The IL-8-*CXCR1* & *CXCR2* signalling axis has been shown to activate a variety of downstream signalling cascades, most commonly the PI3K/Akt and MAPK pathways (MacManus *et al.*, 2017; Waugh & Wilson, 2008). IL-8 signalling has also been shown to operate through the Src signalling pathway in cell line models of prostate cancer (Lee *et al.*, 2004).

The data shown in **Chapter 4.2.1** reports that due to the lack of the IL-8 receptors, *CXCR1* and *CXCR2*, IL-8 signalling cannot be an upstream mediator of Src signalling in the sarcoma cell models evaluated. However, I wanted to assess whether IL-8 could activate Src signalling in STS tumours should they express the receptor(s).

I therefore stimulated the SARC-209 *CXCR1*- and *CXCR2*-expressing cells with exogenous IL-8 and assessed for subsequent cytokine-induced signalling modulations in critical downstream effector proteins, including Akt, ERK1/2, STAT3, and Src. I performed this experiment through stimulating serum-starved SARC-209 EV, *CXCR1*- , and *CXCR2*-expressing cells with 5 minutes of 100 ng/mL IL-8. This treatment

resulted in a marked increase of Akt and ERK1/2 phosphorylation within the receptor-expressing cells but not in the EV control (**Figure 4.5**). Additionally, IL-8 stimulation of the EV cells resulted in no noticeable changes in the signalling of any of the proteins evaluated. Finally, IL-8 stimulation had no effect on the phosphorylation of Src and STAT3 in any of the cell models (**Figure 4.5**).

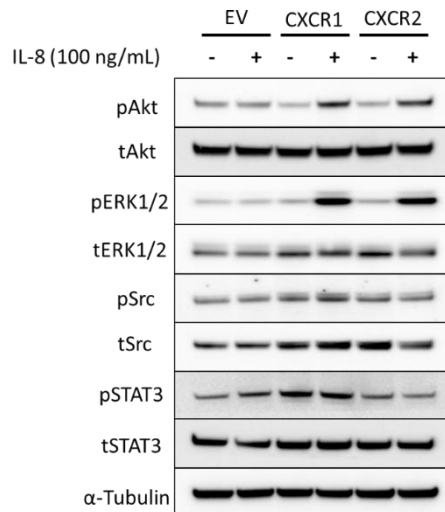


Figure 4.5: Immunoblot of exogenous IL-8 stimulation of SARC-209 CXCR1- and CXCR2-expressing cells. Immunoblot of total levels and phosphorylation status of the major signalling components Akt, ERK1/2, Src, and STAT3 in serum-starved SARC-209 empty vector (EV), CXCR1-, and CXCR2-expressing cells after stimulation with 5 minutes of exogenous IL-8. Image is representative of two separate experiments (n=2). CXCR(1/2); C-X-C motif chemokine receptor (1/2), ERK1/2; Extracellular signal-regulated kinase 1/2, IL-8; Interleukin-8, STAT3; Signal transducer and activator of transcription 3.

These data demonstrate that IL-8 does not signal via the Src pathway in STS cells expressing exogenous CXCR1 and CXCR2 receptors. Instead, the data shows that IL-8 stimulation of the CXCR1 and CXCR2 receptors activates the MAPK and Akt signalling pathways. Therefore, IL-8 does not mediate its activity via the Src pathway in pazopanib-resistant STS, even when the cells express the requisite receptors.

4.2.3 Integrin signalling is a potential upstream receptor of Src signalling in pazopanib-resistant soft tissue sarcoma

Having determined that IL-8 signalling is not an upstream mediator of Src signalling activity in my STS cell models, I wanted to evaluate a range of other receptors for their ability to activate Src signalling in pazopanib-resistant models of STS. I therefore exposed the SARC-209 pazopanib-resistant cells to a panel of 12 inhibitors that target

signalling receptors and evaluated for the ability of these inhibitors to decrease Src phosphorylation.

The 12 inhibitors (**Table 4.2**) were chosen for the following reasons:

1. They are inhibitors of specific receptor types, and/or
2. They displayed relatively high efficacy in reducing cell viability in the SARC-209 small molecule inhibitor screen (**Figure 3.6A & 4.6A**)

For the first point, infogatinib (BGJ-398), crizotinib, and Osimertinib (AZD-9291) were chosen due to their selective inhibition of FGFRs, ALK/MET, and epidermal growth factor receptor (EGFR), respectively (**Table 4.2**) (Cui *et al.*, 2011; Finlay *et al.*, 2014; Guagnano *et al.*, 2011).

For the second point, as reported in **Chapter 3**, I showed that inhibiting Src activity in the SARC-209 cells resulted in significant decreases in cell viability and proliferation. I therefore posited that inhibitors with relatively high efficacy in reducing cell viability, as determined by the inhibitor screen, could be inducing the antiproliferative effect through inhibition of the Src signalling pathway.

Of the small molecule inhibitors showing relative efficacy (< 85% cell viability compared to DMSO control) in the small molecule inhibitor screen (**Figure 4.6A**), NVP-AEW541, cilengitide trifluoroacetate, neratinib, and NVP-TAE684 are also selective inhibitors of insulin-like growth factor 1 receptor (IGF1R)/insulin receptor (InsR), integrins, EGFR/HER2, and ALK, respectively (**Table 4.2 & Figure 4.6A**) (Galkin *et al.*, 2007; García-Echeverría *et al.*, 2004; Rabindran *et al.*, 2004; Reardon *et al.*, 2008). I therefore included these inhibitors in the panel based on these combined properties (**Table 4.2**).

Finally, the multi-target TKIs cabozantinib, ponatinib, and sitravatinib, which target a broad range of RTKs including PDGFRs, FGFRs, and vascular endothelial growth factor receptors (VEGFRs), were also included (**Table 4.2**). This was due to their relatively potent activity (< 75% cell viability compared to DMSO control) upon SARC-209 cells in the small molecule inhibitor screen (**Figure 4.6A**). Pazopanib and dasatinib were also included in the screen as controls (**Table 4.2**).

Pazopanib-resistant SARC-209 cells were treated with 1 μ M for 6 hours with the small molecule inhibitors listed in **Table 4.2** (**Figure 4.6B**). As shown previously in **Figure**

3.9A, pazopanib had no effect on Src phosphorylation or total Src levels, whilst dasatinib abolished Src phosphorylation with a concurrent increase in total Src levels (**Figure 4.6B**). Furthermore, treatment with ponatinib induced an increase in total Src levels, as seen with dasatinib, but with no noticeable effect on Src phosphorylation (**Figure 4.6B**).

Interestingly, treatment of SARC-209 cells with the potent $\alpha v\beta 3$ and $\alpha v\beta 5$ integrin inhibitor cilengitide trifluoroacetate resulted in an observable decrease in Src phosphorylation (**Figure 4.6B**). The remaining inhibitors evaluated did not show any noticeable differences in either Src phosphorylation or total Src levels upon treatment (**Figure 4.6B**). Currently, only a single replicate has been undertaken for this experiment and therefore further replicates are required to confirm this finding. However, integrin signalling is an extensively reported upstream component of Src signalling and further research into the role of integrin signalling in mediating Src activity in Src-dependent, pazopanib-resistant STS is needed (Mitra & Schlaepfer, 2006; Shattil, 2005).

Table 4.2: Reference table displaying small molecule inhibitors utilised within the Src phosphorylation screen with primary target(s) and rationale for inclusion.			
Small molecule inhibitor	Figure 4.6A #	Primary target(s)	Rationale for inclusion
Pazopanib	1	Broad spectrum: RTKs	Control
Dasatinib	2	Src, Abl1, Broad spectrum: RTKs	Control
Infigratinib (BGJ-398)	3	FGFR1/2/3	Selective inhibitor
NVP-AEW541	4	IGF1R, InsR	Selective inhibitor & relative efficacy in screen (Figure 4.6A)
Cilengitide trifluoroacetate	5	Integrins $\alpha v\beta 3$, $\alpha v\beta 5$	Selective inhibitor & relative efficacy in screen (Figure 4.6A)
Neratinib	6	EGFR, HER2	Selective inhibitor & relative efficacy in screen (Figure 4.6A)
Cabozantinib	7	Broad spectrum: RTKs	Relative efficacy in screen (Figure 4.6A)
NVP-TAE684	8	ALK	Selective inhibitor & relative efficacy in screen (Figure 4.6A)
Crizotinib	9	MET, ALK	Selective inhibitor
Osimertinib (AZD-9291)	10	EGFR	Selective inhibitor
Ponatinib	11	Broad spectrum: RTKs, Abl1	Relative efficacy in screen (Figure 4.6A)
Sitravatinib	12	Broad spectrum: RTKs	Relative efficacy in screen (Figure 4.6A)

ALK; Anaplastic lymphoma kinase, EGFR; Epidermal growth factor receptor, FGFR(1/2/3); Fibroblast growth factor receptor (1/2/3), HER2; Human epidermal growth factor receptor 2, IGF1R; Insulin-like growth factor 1 receptor, InsR; Insulin receptor, n/a; Not available, RTK; Receptor tyrosine kinase.

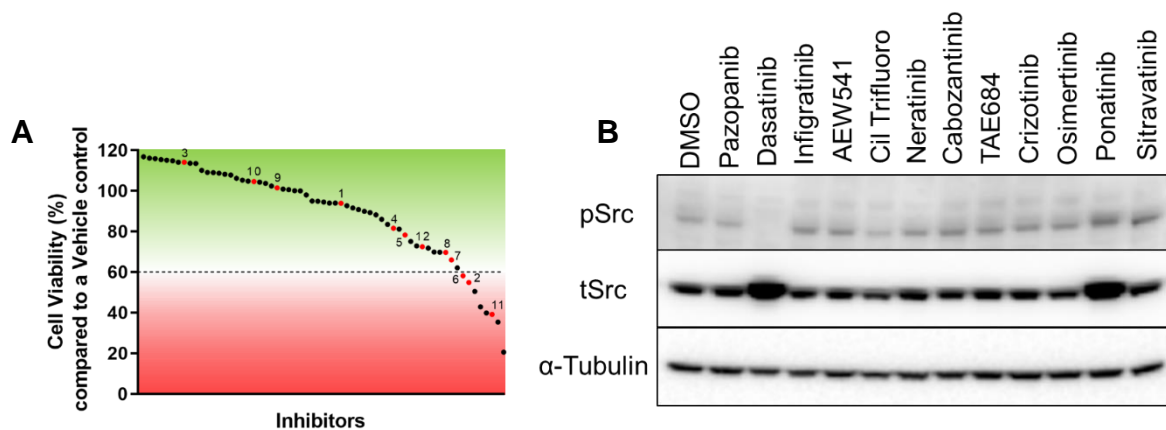


Figure 4.6: The integrin inhibitor cilengitide trifluoroacetate decreases Src phosphorylation. (A) Small molecule inhibitor screen of SARC-209 at 0.5 μ M inhibitor concentration. Selected inhibitors are labelled with red dots and numbers. Key to numerical labelling is given in **Table 4.2**. Cell viability was normalised to DMSO control (n=2). **(B)** Immunoblot of total levels and phosphorylation status of Src in the SARC-209 cells after treatment with 6 hours of DMSO or 1 μ M of the indicated small molecule inhibitor. Image is representative of a single experiment (n=1). AEW541; NVP-AEW541, Cil Trifluoro; Cilengitide trifluoroacetate, DMSO; Dimethyl sulfoxide, IC₅₀; Inhibitory constant, TAE684; NVP-TAE684.

Integrins are cellular receptors that form a critical signalling link between external signals from the ECM and resultant intracellular processes, such as cytoskeletal remodelling and the activation of pro-survival pathways (Mitra & Schlaepfer, 2006; Shattil, 2005). Integrins are composed of heterodimers of α and β subunits, whose combination determine which ECM component the integrin dimer binds (e.g., laminin, fibronectin, and collagen) (Hynes, 2002).

As this preliminary data indicates a potential link between the inhibition of integrin signalling and downstream Src activity, I wanted to evaluate whether the pazopanib-resistant, PDX-derived STS cell models expressed a number of integrin subunits, especially those targeted by cilengitide trifluoroacetate (integrins α V and β 3). To achieve this, primers were designed for a variety of integrin subunits, including *ITGAV* (α V) and *ITGB3* (β 3), in order to assess integrin mRNA expression within SARC-209 and J000104314 cell models via qPCR. The evaluated integrins are shown in **Table 4.3** and this work was performed by Valeriya Pankova, a PhD student in our lab. Currently only a single replicate has been undertaken. Unfortunately, data for *ITGA1* and *ITGB5* had to be dropped from analysis due to inconsistent results.

Table 4.3: Panel of assessed integrin subunits.	
Integrins	Gene
Integrin α 2	<i>ITGA2</i>
Integrin α 3	<i>ITGA3</i>
Integrin α 6	<i>ITGA6</i>
Integrin α 7	<i>ITGA7</i>
Integrin α 10	<i>ITGA10</i>
Integrin β 1	<i>ITGB1</i>
Integrin β 3	<i>ITGB3</i>
Integrin β 4	<i>ITGB4</i>
Integrin α V	<i>ITGAV</i>

Figure 4.7 displays the cycle threshold (Ct) which is defined as the number of cycles required for the fluorescent Rn to cross the background level threshold (**Figure 4.7**). Ct values are inversely proportional to gene expression (i.e., lower Ct value = higher gene expression; higher Ct value = lower gene expression). From previous experience, and qPCR platform guidelines, Ct values for expressed gene should fall between the range of 12 to 35 (Applied Biosystems, 2016). Ct values > 35 indicate negligible to zero expression of the target gene. Conversely, Ct values < 12 indicate contamination, poor primer design, or experimental error. Ct values that fall outside of this range should be viewed with scepticism unless subsequent biological replicates with fresh materials reproduce the findings (Applied Biosystems, 2016; Ruiz-Villalba *et al.*, 2021). The purpose of this experiment was to assess whether these two cell models express the indicated integrin subunits rather than evaluating any potential differences in integrin expression levels. **Figure 4.7** shows that both the pazopanib-resistant SARC-209 cells and J000104314 cells express a wide variety of integrin receptors, including the cilengitide trifluoroacetate-targeted integrin subunits α v and β 3 (**Figure 4.7**). To note, for integrin β 4, the Ct value was > 35 in the J000104314 cell model suggesting very low to negligible expression which can be confirmed by subsequent replicates (**Figure 4.7**).

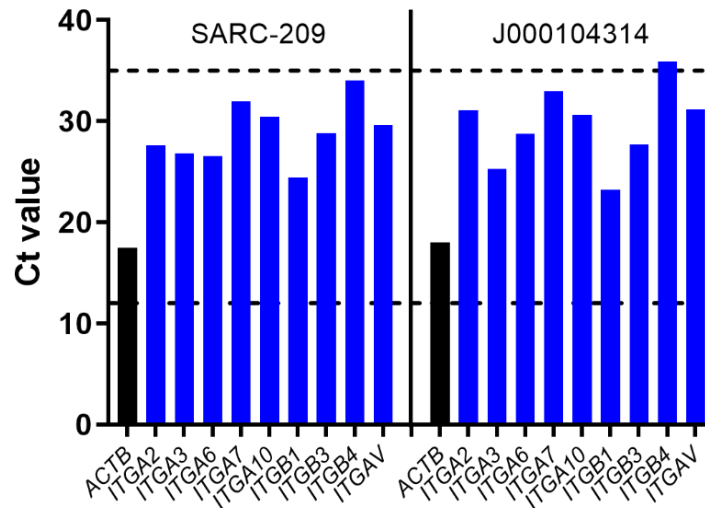


Figure 4.7: Evaluating the expression of a panel of integrin subunits in pazopanib-resistant STS models. qPCR data displaying the cycle threshold (Ct) values of integrin subunit mRNA expression (blue bars) in SARC-209 and J000104314 cells, with housekeeping gene β -actin (*ACTB*) (black bars) (n=1). Ct values are inversely proportional to gene expression (i.e., lower Ct value = higher gene expression; higher Ct value = lower gene expression). Dotted lines indicate Ct values < 12 and > 35. ITG(A2/3/6/7/10/V)(B1/3/4); Integrin (α 2/3/6/7)(β 1/3/4).

All together, these preliminary data indicate the expression of many integrin subunits, including the cilengitide trifluoroacetate-targeted subunits α v and β 3, in two cell models of pazopanib-resistant STS. Building upon this work, future research will focus on the role of the integrin signalling pathway in mediating Src activity in Src-dependent, pazopanib-resistant STS.

4.3 Discussion

In this chapter, several strategies were employed to determine the upstream mediators of Src activity in Src-dependent, pazopanib-resistant STS. The first strategy utilised previously determined molecular data from a STS patient who had developed an acquired resistance to pazopanib therapy after a prolonged initial response. These data determined that the expression of the cytokine IL-8 was significantly upregulated in the pazopanib-resistant tumour when compared to the pre-pazopanib sensitive tissue, indicating a potential association between IL-8 expression and the accrual of pazopanib resistance. Additionally, IL-8 signalling has previously been shown to be an upstream regulator of Src activity in preclinical models of cancer, and I wanted to determine whether IL-8 signalling operates via the Src pathway in pazopanib-resistant STS (Lee *et al.*, 2004).

Associations between IL-8 expression and TKI resistance have previously been shown in studies of lung cancer where increased IL-8 expression resulted in increased resistance to the TKIs erlotinib and gefitinib (Fernando *et al.*, 2016; Liu *et al.*, 2015). Similarly, other groups have reported that IL-8 expression is increased in response to chemotherapy and is associated with poor chemotherapeutic response (Collins *et al.*, 2000; Lev *et al.*, 2004; Park *et al.*, 2014). Therefore, the expression levels of *CXCL8* (IL-8) were evaluated in a panel of sarcoma cell lines and PDX-derived, pazopanib-resistant cells. The vast majority of sarcoma models (including SARC-209 and J000104314) expressed IL-8 to at least a quantifiable level, with notable heterogeneity of *CXCL8* expression observed across the panel. However, similar expression level analysis of the IL-8 receptors, *CXCR1* and *CXCR2*, found that none of the models within the sarcoma cell panel expressed these receptors. These findings indicate that IL-8 signalling does not have an autocrine effect upon sarcoma cells. Furthermore, in *CXCR1*- and *CXCR2*-expressing pazopanib-resistant STS cells, exogenous IL-8 stimulation did not affect Src activity but instead operated via MAPK and PI3K/Akt signalling pathways.

Taken together, these findings suggest that if IL-8 is linked to pazopanib resistance in STS, then it is likely to be due to paracrine effects with cells of the TME rather than an autocrine effect. Furthermore, the data shows that IL-8 is not an upstream regulator of Src activity in Src-dependent, pazopanib-resistant STS. Despite this, other publications have highlighted the role that Src activity has in the expression of IL-8 with several studies reporting that Src is a direct upstream signalling modulator of *CXCL8* (IL-8) transcription (Lin *et al.*, 2006; Trevino *et al.*, 2005). Therefore, future research will focus on the effects of Src upon downstream IL-8 expression and the subsequent potential paracrine signalling associations in pazopanib-resistant STS.

Although there are previous studies reporting the autocrine IL-8 activation of *CXCR1* and *CXCR2* receptors on the surface of tumour cells, *CXCR1* and *CXCR2* are primarily and ubiquitously expressed upon the cell surface of immune cells, as well as other cells of the TME (Brew *et al.*, 2000; Kamohara *et al.*, 2007; Susek *et al.*, 2018; Takamori *et al.*, 2000). The extensive expression of *CXCR1* and *CXCR2* within cells of the TME, combined with the data from **Chapter 4**, suggest that if IL-8 is associated with pazopanib resistance in STS then it is due to paracrine signalling by tumour-secreted IL-8 to induce TME remodelling and/or a pro-tumourigenic immune response.

Recent studies have shown that paracrine signalling by tumour-derived IL-8 promotes the recruitment of neutrophils and myeloid-derived suppressor cells into the TME, which can dampen antitumour immune response, induce targeted therapy resistance, and drive disease progression (David *et al.*, 2016; Tan *et al.*, 2018). Additionally, IL-8 paracrine signalling with TME endothelial cells has been shown to have an angiogenic and metastatic effect in the growth and dissemination of tumours (Waugh & Wilson, 2008). Therefore, future work will focus on the potential role of IL-8 paracrine signalling in mediating pazopanib-resistance in STS.

However, due to the lack of TME components within standard, two-dimensional *in vitro* monolayers, different models that incorporate the three-dimensional nature of the TME are essential in determining the role of IL-8 paracrine signalling in pazopanib-resistant STS. Although *in vivo* animal models remain the best option for accurately recapitulating tumour interactions with the TME, these models suffer from issues such as high expense and low-throughput (Fontana *et al.*, 2021). Therefore, a number of high-throughput, three-dimensional modelling techniques have been developed that can accurately reproduce the interactions between tumour cells and the TME (Fontana *et al.*, 2021; Goers *et al.*, 2014; Rodrigues *et al.*, 2021). For instance, co-culturing experiments where tumour cells are cultured alongside cells of the TME, all of which are embedded within ECM scaffolds, can provide biologically relevant models of tumour-TME interactions, and can be used to accurately evaluate the effects of paracrine signalling (Wu *et al.*, 2010; Wu & Swartz, 2014). Co-culturing experiments can be undertaken using various three-dimensional methodologies such as hydrogels, organoids/(hetero)spheroids, and microfluidic systems, which can be precisely tailored, such as altering cytokine gradients, ECM stiffness, and TME cell composition (Fontana *et al.*, 2021; Goers *et al.*, 2014; Rodrigues *et al.*, 2021; Wu *et al.*, 2010). Three-dimensional, co-cultured models have previously been shown to provide accurate models for researching tumour-TME interactions in various cancer types, including colon, gastric, and breast cancers (Dolznic *et al.*, 2011; Sun *et al.*, 2013; Phan-Lai *et al.*, 2013). Therefore, development of a three-dimensional co-culture model of pazopanib-resistant STS would provide an accurate model to determine the potential paracrine role of IL-8 signalling in mediating pazopanib resistance in STS.

Finally, this chapter also elucidated that integrin signalling is a potential upstream mediator of Src activity in pazopanib-resistant STS. In a panel of receptor inhibitors

that showed antiproliferative activity in pazopanib-resistant SARC-209 cells and/or possess selective inhibitory profiles, only cilengitide trifluoroacetate (together with dasatinib) was found to inhibit Src phosphorylation. Cilengitide trifluoroacetate is a potent inhibitor of $\alpha\beta3$ and $\alpha\beta5$ integrins and these cell surface receptors have extensively been shown to transduce extracellular signals through the Src pathway in the progression of cancer (Mitra & Schlaepfer, 2006; Shattil, 2005). Both $\alpha\beta3$ and $\alpha\beta5$ bind to ECM proteins containing the RGD (Arg-Gly-Asp) motif, such as fibronectin and vitronectin, to induce cellular responses (Kapp *et al.*, 2017). Cilengitide is a cyclic pentapeptide that contains the RGD motif and, as such, targets and inhibits certain RGD-binding integrins from binding their physiological ligands (Mas-Moruno *et al.*, 2010; Reardon *et al.*, 2008; Reardon *et al.*, 2011). Further to this, analysis of integrin subunit expression in pazopanib-resistant STS models showed that these cells express a wide variety of integrin subunits. Despite the frequent preclinical data demonstrating the role of integrins in cancer progression, clinical trials to date have been disappointing and there is an unmet need to develop novel integrin inhibitors with greater clinical efficacy (Alday-Parejo *et al.*, 2019). However, these preliminary results warrant further research into the role of integrin signalling upon Src signalling in Src-dependent, pazopanib-resistant STS. Future work to help elucidate the link between integrin and Src signalling in these models could include integrin subunit genetic knockdown/out (mediated by siRNA/shRNA and/or CRISPR), integrin activation by subunit-specific antibody/agonist stimulation, as well as incubating cells within ECM matrices (2.5 dimensional-culture) with differing compositions (e.g., RGD-based, collagen-based, laminin-based vs. plastic) (Byron *et al.*, 2009; Langhans, 2018; Shamir & Ewald, 2014; Ye *et al.*, 2012). Through these means, I can assess the downstream effects upon Src activity and subsequent changes in cellular phenotypes such as pazopanib resistance, proliferation, migration, and apoptosis.

In conclusion, the results of **Chapter 4** have shown that IL-8 does not operate via an autocrine mechanism and that IL-8 signalling is not an upstream mediator of Src activity in pazopanib-resistant STS. Furthermore, preliminary results have shown that integrins may have potential activity in mediating downstream Src signalling in Src-dependent, pazopanib-resistant STS. These initial results warrant further research into the role of integrin signalling in mediating Src signalling in pazopanib-resistant STS. Future work into determining the downstream effectors of Src activity and their effects

upon gene expression in pazopanib-resistant STS is required. Through understanding the upstream and downstream components of Src signalling in Src-dependent, pazopanib-resistant STS, this will allow for the determination of further potential vulnerabilities that could be targeted with salvage therapies.

Chapter 5

Characterisation of multi-target tyrosine
kinase inhibitor sensitivity in cell line
models of soft tissue sarcoma

5.1 Introduction

The only approved targeted therapy for the vast majority of soft tissue sarcomas (STS) in the advanced setting is the multi-target tyrosine kinase inhibitor (TKI) pazopanib. Despite regulatory body approval based on significant improvements in median progression-free survival (mPFS) versus placebo, pazopanib therapy in STS did not result in an overall survival (OS) benefit (Van der Graaf *et al.*, 2012). There is therefore an ongoing effort to develop and assess other multi-target TKIs for improved efficacy in treating advanced STS. Some inhibitors currently undergoing clinical trial evaluation in advanced STS include the TKIs regorafenib, sitravatinib, and anlotinib (**Chapter 1.3.3**) – multi-target TKIs with overlapping kinase targets to one another, as well as pazopanib (**Table 1.3**) (Davis *et al.*, 2011; Patwardhan *et al.*, 2016; Xie *et al.*, 2018; Zopf *et al.*, 2016).

However, the mechanisms of action of multi-target TKIs in the majority of STS subtypes is currently poorly understood. The antitumour activity of pazopanib, regorafenib, sitravatinib, and anlotinib are thought to be due to their antiangiogenic properties, mediated by inhibition of vascular endothelial growth factor receptor (VEGFR) receptor tyrosine kinase (RTK) signalling (**Table 1.3**) (Lee *et al.*, 2019; Wilding *et al.*, 2019). Additionally, these multi-target TKIs are also hypothesised as having direct antitumour effect through inhibition of growth-promoting RTKs such as platelet-derived growth factor receptor (PDGFR), fibroblast growth factor receptor (FGFR), and KIT (**Table 1.3**) (Lee *et al.*, 2019; Wilding *et al.*, 2019).

The data outlined in **Chapter 5** focussed on identifying STS cell line models that are sensitive to the multi-target TKIs pazopanib, regorafenib, sitravatinib, and anlotinib. Following this, the antitumour activity of these TKIs in sensitive STS cell line models was characterised, with the aim of determining their mechanisms of action. Furthermore, building on a previous study by Wong *et al.*, the antitumour effects of these multi-target TKIs in combination with selective FGFR inhibitors was investigated in order to provide potential first-line therapies with enhanced antitumour activity.

5.2 Results

5.2.1 The malignant rhabdoid tumour cell lines A204 and G402 are sensitive to multi-target tyrosine kinase inhibitors

As previously discussed in **Chapters 1.3.3** and **5.1**, pazopanib, regorafenib, sitravatinib, and anlotinib are multi-target TKIs that are either approved or undergoing clinical evaluation for use in advanced STS (Chi *et al.*, 2018; Ingham *et al.*, 2017; Mir *et al.*, 2016; Oza *et al.*, 2021; Van der Graaf *et al.*, 2012; Van Tine *et al.*, 2021). In order to determine sarcoma subtypes and cell line models that are sensitive to these TKIs *in vitro*, a panel of 14 sarcoma cell lines of varying histological subtypes (**Table 5.1**) was subjected to cell viability assays (**Figure 5.1A-E**). Only the malignant rhabdoid tumour (MRT) cell lines A204 and G402 were found to be significantly sensitive to all four of the TKIs evaluated (**Figure 5.1A-D & 5.2A-D; Table S5**).

Cell line	Subtype	Cellosaurus accession code (Bairoch <i>et al.</i> , 2018)	Comments
A204	MRT	CVCL_1058	Initially misclassified as RMS (Hinson <i>et al.</i> , 2013)
G402	MRT	CVCL_1221	Initially misclassified as LMB (Brenca <i>et al.</i> , 2021)
HT1080	Fibrosarcoma	CVCL_0317	
SW684	Fibrosarcoma	CVCL_1726	
MESSA	Uterine sarcoma	CVCL_1404	
SW872	Liposarcoma	CVCL_1730	
Hs729T	eRMS	CVCL_0871	
RMS-YM	eRMS	CVCL_A792	
RUCH3	eRMS	CVCL_C541	
SW982	Synovial sarcoma	CVCL_1734	Potentially misclassified as does not contain pathognomonic SS18-SSX1/2/4 translocation (Kawano <i>et al.</i> , 2017)
SAOS2	Osteosarcoma	CVCL_0548	
U2OS	Osteosarcoma	CVCL_0042	
SJSA1	Osteosarcoma	CVCL_1697	
T91-95	aRMS	n/a (Lee <i>et al.</i> , 2003; Martins <i>et al.</i> , 2011)	T91-95 have also been described as normal fibroblast cells (Gryder <i>et al.</i> , 2017)

aRMS; Alveolar rhabdomyosarcoma, CVCL; Cellosaurus accession code, (e)RMS; (Embryonal) rhabdomyosarcoma, LMB; Leiomyoblastoma, MRT; Malignant rhabdoid tumour, SS18; Synovial sarcoma translocation chromosome 18, SSX(1/2/4); Synovial sarcoma X (1/2/4) breakpoint protein.

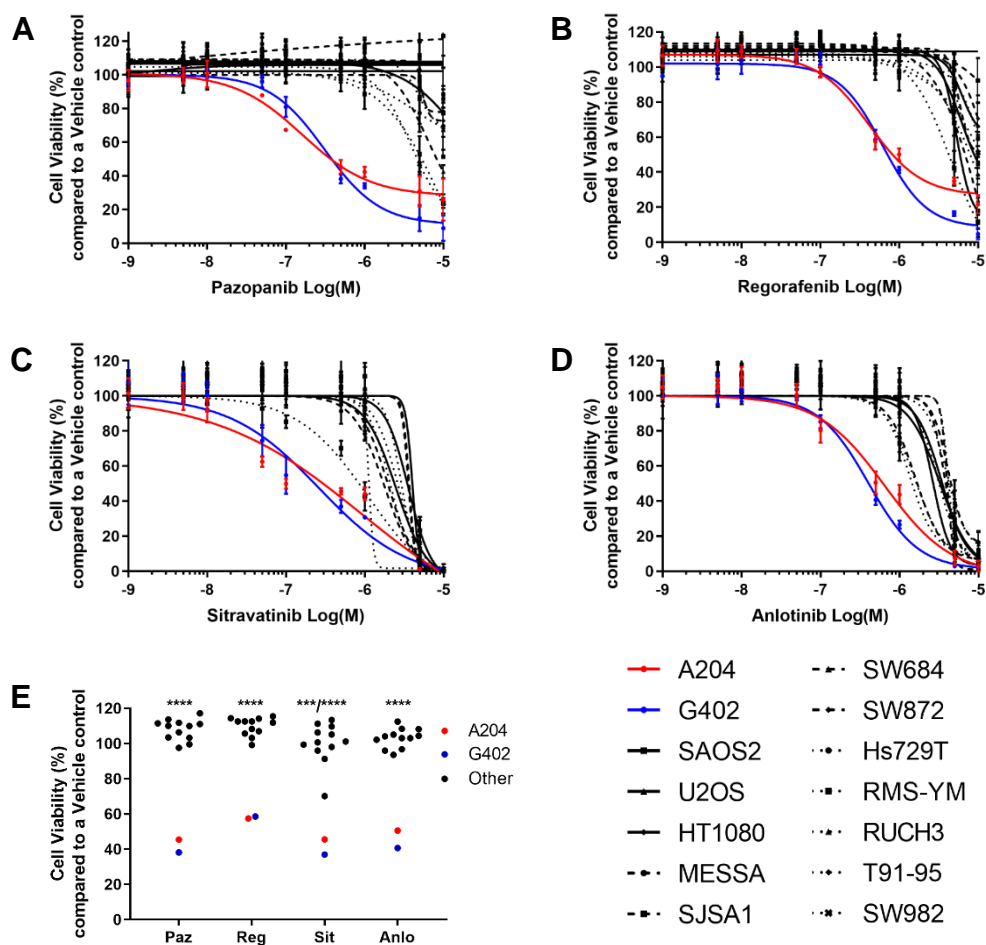


Figure 5.1: Cell viability assays of a panel of sarcoma cell lines to determine sensitivities to pazopanib, regorafenib, sitravatinib, and anlotinib. Cell viability assays of a panel of 14 sarcoma cell lines (Table 5.1) treated with increasing concentrations of (A) pazopanib (Paz), (B) regorafenib (Reg), (C) sitravatinib (Sit), or (D) anlotinib (Anlo) to determine IC_{50} values (Table S5). (E) Plot displaying cell viabilities of the sarcoma cell line panel at $0.5 \mu\text{M}$ concentration of Paz, Reg, Sit, and Anlo. Cell viability was normalised to DMSO control ($n=3$). Statistical analysis of IC_{50} values not possible as certain models did not reach 50% cell viability. Statistical analysis was undertaken by one-way ANOVAs with Tukey's multiple comparison tests (** $p \leq 0.001$, **** $p \leq 0.0001$). Error bars represent standard deviation. ANOVA; Analysis of variance, DMSO; Dimethyl sulfoxide, IC_{50} ; Inhibitory constant.

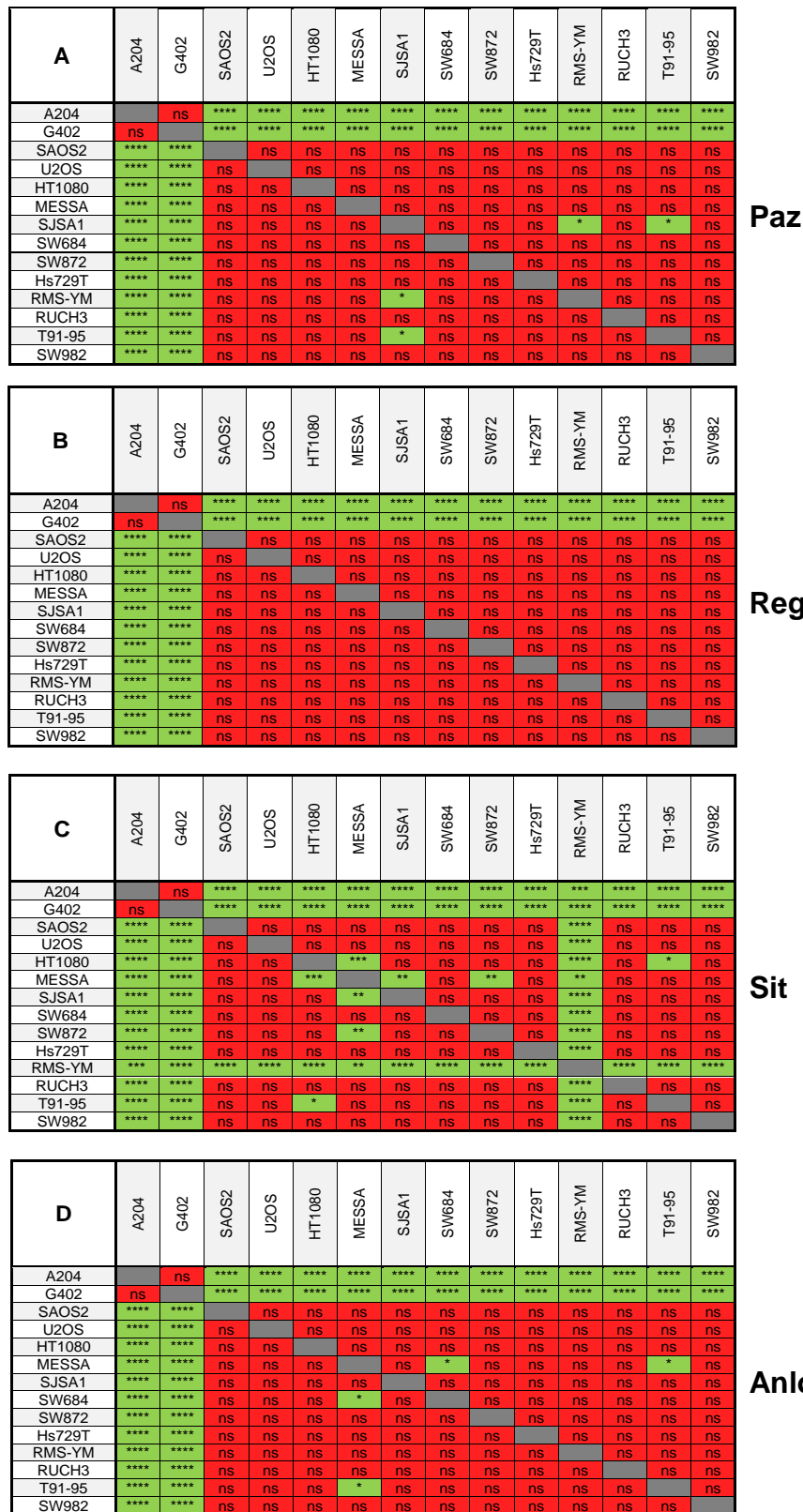


Figure 5.2: Statistical significance grids of the sarcoma cell line panel evaluating sensitivity to pazopanib, regorafenib, sitravatinib, and anlotinib. Grids displaying the statistical significance between cell viability of sarcoma cell lines treated with 0.5 μ M (A) pazopanib (Paz), (B) regorafenib (Reg), (C) sitravatinib (Sit), or (D), anlotinib (Anlo). Cell viability was normalised to DMSO control (n=3). Statistical analysis of IC₅₀ values not possible as certain models did not reach 50% cell viability. Statistical analysis was undertaken by ANOVAs with Tukey's multiple comparison tests

(* = $p \leq 0.05$, ** = $p \leq 0.01$, *** = $p \leq 0.001$, **** = $p \leq 0.0001$). ANOVA; Analysis of variance, DMSO; Dimethyl sulfoxide, IC₅₀; Inhibitory constant, ns; Non-significant.

Previous studies have shown that A204 and G402 cells are characterised by high expression of both PDGFR α and FGFR1 RTKs (Bai *et al.*, 2012; Wöhrle *et al.*, 2013; Wong *et al.*, 2016). Previous work by Wong *et al.* has also shown that PDGFR α and FGFR1 are drivers in the proliferation of both A204 and G402 cells (Wong *et al.*, 2016). Furthermore, PDGFR α and/or FGFR1 are RTKs that have previously been shown to be targets of pazopanib, regorafenib, sitravatinib, and anlotinib (Lin *et al.*, 2011; Patwardhan *et al.*, 2018; Wilding *et al.*, 2019; Wilhelm *et al.*, 2010; Wong *et al.*, 2016). I therefore wanted to assess the levels of PDGFR α and FGFR1 expression in the A204 and G402 cells, compared to the rest of the cell line panel (**Figure 5.3**). **Figure 5.3** shows that across the cell line panel, only A204 and G402 cell lines highly express both PDGFR α and FGFR1. The two MRT cell lines were therefore chosen as appropriate models to evaluate multi-target TKI sensitivity in STS, especially STS driven by PDGFR and FGFR signalling.

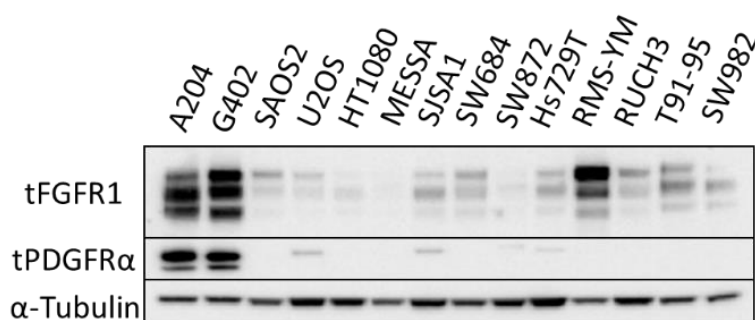


Figure 5.3: Evaluation of PDGFR α and FGFR1 expression levels in the sarcoma cell line panel. Immunoblot of basal expression profiles of the sarcoma cell line panel displaying expression of PDGFR α and FGFR1. Image is representative of two separate experiments. FGFR1; Fibroblast growth factor receptor 1, PDGFR α ; Platelet-derived growth factor receptor α .

5.2.2 Multi-target tyrosine kinase inhibitors have antiproliferative and proapoptotic activity in malignant rhabdoid tumour cell line models

Having determined that the MRT cell lines A204 and G402 are sensitive to multi-target TKI treatment in short-term cell viability assays, I wanted to determine whether these short-term effects were recapitulated in longer-term assays. Firstly, I performed long-term (2 week) colony formation assays of A204 and G402 cells treated with pazopanib, regorafenib, sitravatinib, or anlotinib. I found that treatment with the four multi-target

TKIs significantly reduced colony formation compared to DMSO control in a dose-dependent manner (Figure 5.4A-J).

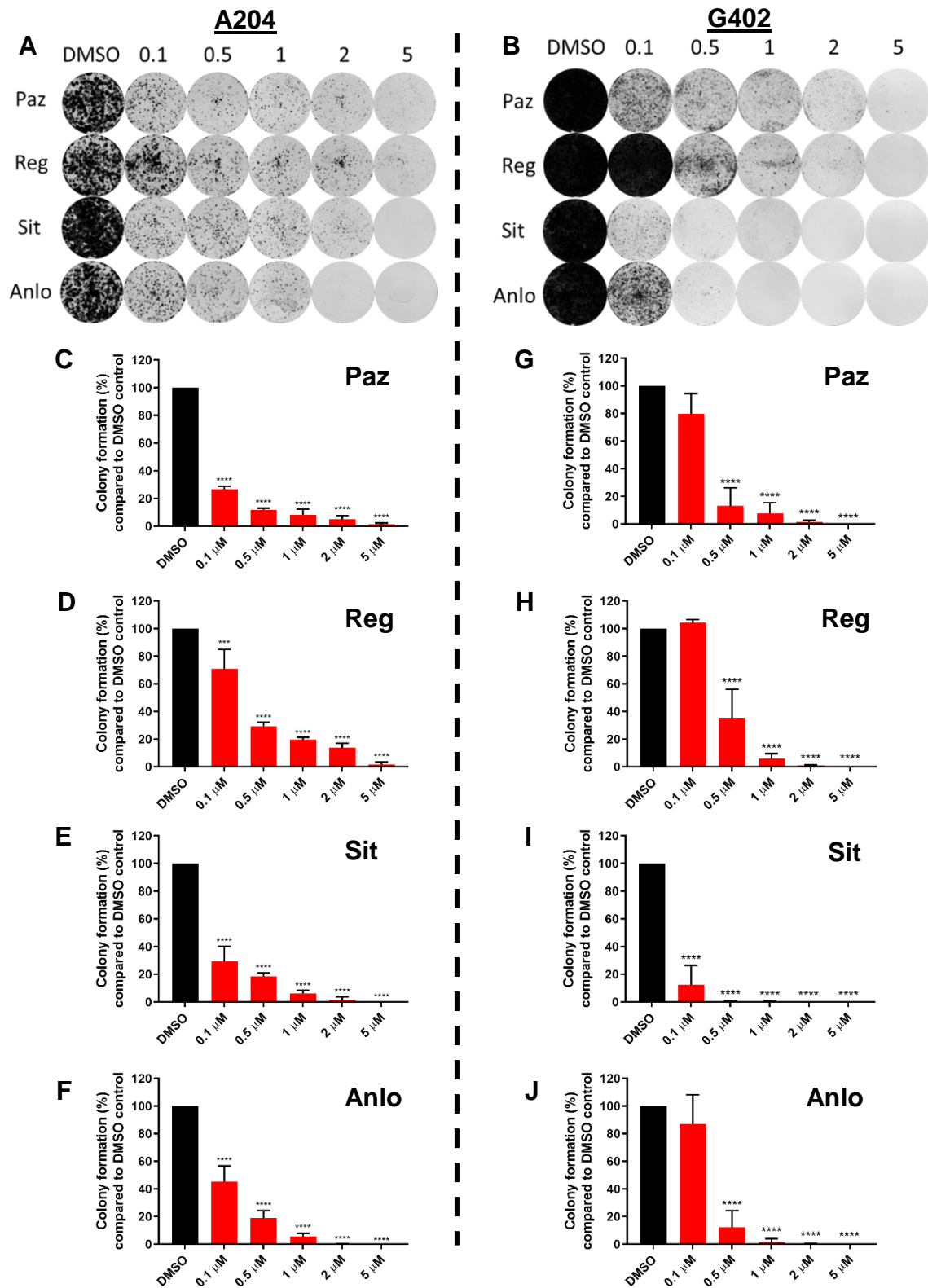


Figure 5.4: Evaluation of long-term sensitivity of A204 and G402 cells to pazopanib, regorafenib, sitravatinib, and anlotinib treatment. Colony formation assays of (A) A204 and (B) G402 cells treated with increasing concentrations of pazopanib (Paz), regorafenib (Reg), sitravatinib (Sit), or anlotinib (Anlo) over a period of 2 weeks. Images are representative of three separate experiments (n=3). Quantification of A204 colony formation assays was

normalised to DMSO control for (C) pazopanib, (D) regorafenib, (E) sitravatinib, or (F) anlotinib. Equivalent treatments in G402 cells are shown in (G-J), respectively. Statistical analysis was undertaken using one-way ANOVAs with Dunnett's multiple comparison tests (compared to DMSO) (** = $p \leq 0.01$, *** = $p \leq 0.001$, **** = $p \leq 0.0001$). Error bars represent standard deviation. ANOVA; Analysis of variance, DMSO; Dimethyl sulfoxide.

The proliferation of MRT cell lines over 6 weeks in the presence of 1 μ M multi-target TKI or DMSO treatment was also measured. I found that the multi-target TKIs significantly reduced cellular proliferation compared to DMSO treatment in both cell lines (Figure 5.5A-D). Additionally, these results highlighted significant differences between the potencies of the multi-target TKIs in repressing the growth of A204 and G402 cell lines. For instance, in the A204 model, I found that anlotinib had a significantly increased activity in impairing cellular proliferation compared to the other three TKIs (Figure 5.5A & C). In the G402 model, anlotinib and sitravatinib were found to both significantly reduce cellular proliferation when compared to pazopanib and regorafenib (Figure 5.5B & D). Finally, this experiment also illustrated that both A204 and G402 cells will eventually develop an acquired resistance to all four multi-target TKIs, albeit at different rates (Figure 5.5A-D).

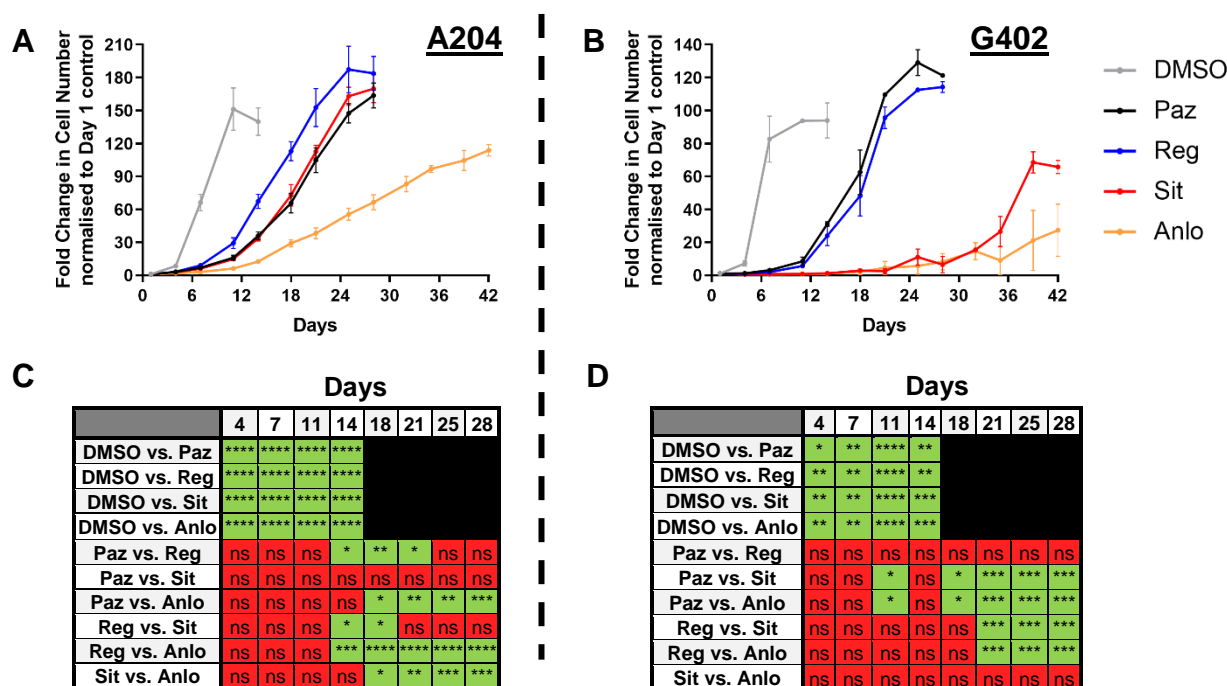


Figure 5.5: Evaluation of A204 and G402 proliferation in response to treatment by pazopanib, regorafenib, sitravatinib, and anlotinib for 6 weeks. Growth curve assays of (A) A204 and (B) G402 cells to measure the fold change in cell number of a period of six week. Cells were treated with either DMSO or 1 μ M of pazopanib (Paz), regorafenib (Reg), sitravatinib (Sit), or anlotinib (Anlo). Data collection for a specific treatment regimen was ceased once the cells had reached overconfluency within the 96 well plate and the Celigo cytometer could no longer accurately distinguish between individual cells. Fold change was normalised to day 1 control (A204; n=4, G402; n=2). Grids displaying the statistical significance between the different treatments in the (C) A204 and (D) G402 cells in the 6-week growth curve assays. Statistical analysis was undertaken using one-way ANOVAs with Tukey's multiple comparison

tests (* = $p \leq 0.05$, ** = $p \leq 0.01$, *** = $p \leq 0.001$, **** = $p \leq 0.0001$). Error bars represent standard deviation of the mean. ANOVA; Analysis of variance, DMSO; Dimethyl sulfoxide, ns; Non-significant.

Further to their antiproliferative properties, I sought to assess the pro-apoptotic capabilities of pazopanib, regorafenib, sitravatinib, and anlotinib in the A204 and G402 cell line models. To achieve this, I treated the cells with 24 hours of two differing concentrations (0.5 μM and 1 μM) of multi-target TKI before evaluating for changes in caspase 3/7 cleavage when compared to DMSO. I found that multi-target TKI treatment significantly increased apoptosis in both the A204 (0.5 μM : > 1.75-fold, 1 μM : >3-fold increase) and G402 (0.5 μM : >2.5-fold, 1 μM : >4.5-fold increase) cell lines when compared to DMSO (**Figure 5.6A-D**).

In addition, I also observed significant differences between the pro-apoptotic capabilities of the four multi-target TKIs in the evaluated cell lines. These apoptotic differences corroborated with the antiproliferative phenotypes observed in the 6-week growth curve assays shown in **Figure 5.5**. For instance, anlotinib was found to significantly increase apoptosis (0.5 μM : ~3-fold, 1 μM : ~10-fold increase relative to DMSO) in A204 cells compared to the remaining TKIs (0.5 μM : ~2-fold, 1 μM : ~4-fold increase relative to DMSO) (**Figure 5.6A & C**). Furthermore, at 1 μM concentration, anlotinib and sitravatinib were found to significantly increase apoptosis in G402 cells (~7-fold increase relative to DMSO) when compared to pazopanib and regorafenib (~5-fold increase relative to DMSO) (**Figure 5.6B & D**).

The data shown in **Figures 5.4 to 5.6** demonstrated that the MRT cell lines A204 and G402 are sensitive to pazopanib, regorafenib, sitravatinib, and anlotinib treatment, with these multi-target TKIs displaying significant antiproliferative and pro-apoptotic properties in these STS models. **Figures 5.5 & 5.6** also highlight the different potencies of the four multi-target TKIs in their antitumour activities in A204 and G402. For instance, the significantly decreased proliferation rates observed with anlotinib treatment in A204 were associated with a significantly increased apoptotic activity, when compared to the remaining TKIs evaluated. A similar phenotype was also observed in the treatment of G402 cells with sitravatinib and anlotinib.

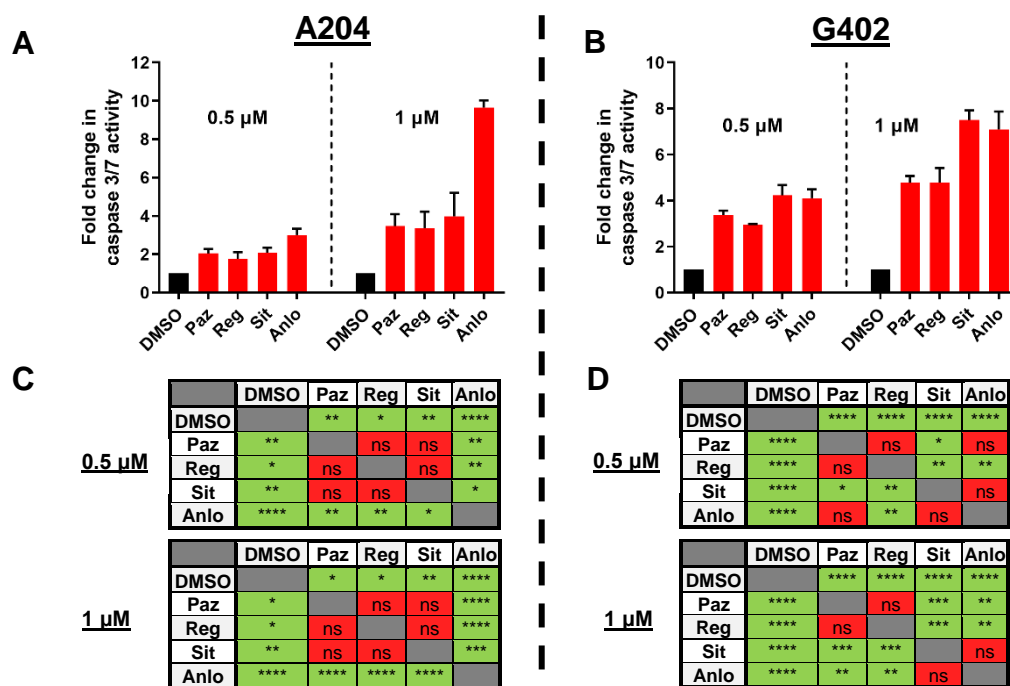


Figure 5.6: Evaluation of apoptosis levels in A204 and G402 cells in response to treatment by pazopanib, regorafenib, sitravatinib, and anlotinib. Bar plots displaying the fold change in caspase 3/7 activity in the (A) A204 and (B) G402 cells treated with two concentrations of pazopanib (Paz), regorafenib (Reg), sitravatinib (Sit), or anlotinib (Anlo) for 24 hours. Fold change was normalised to DMSO control (n=3). Grids displaying the statistical significance between the different treatments at the two different concentrations in the (C) A204 and (D) G402 cells as determined by caspase 3/7 apoptosis assays. Statistical analysis was undertaken using one-way ANOVAs with Tukey's multiple comparison tests (* = $p \leq 0.05$, ** = $p \leq 0.01$, *** = $p \leq 0.001$, **** = $p \leq 0.0001$). Error bars represent standard deviation. ANOVA; Analysis of variance, DMSO; Dimethyl sulfoxide, ns; Non-significant.

5.2.3 Evaluation of combination therapy with multi-target TKIs

Chapter 5.2.2 revealed that the four multi-target TKIs possessed differing levels of antiproliferative and pro-apoptotic potency in the A204 and G402 cell line models of MRT. I therefore assessed for whether dual treatment combinations of the TKIs had an enhanced antiproliferative effect when compared to single agent treatment. I performed this experiment by treating the MRT cell line models with dual treatment combinations of the four multi-target TKIs, as well as single agent treatments, before assessing for cell viability after 72 hours (Figure 5.7; Table S6). As shown in Figure 5.7, none of the dual treatment combinations resulted in an enhanced combinatorial effect in reducing cell viability when compared to the effects of the constituent single agents (Figure 5.7; Table S6). These results suggest that the four multi-target TKIs operate via the same or similar mechanism of action in order to exert their antiproliferative effects.

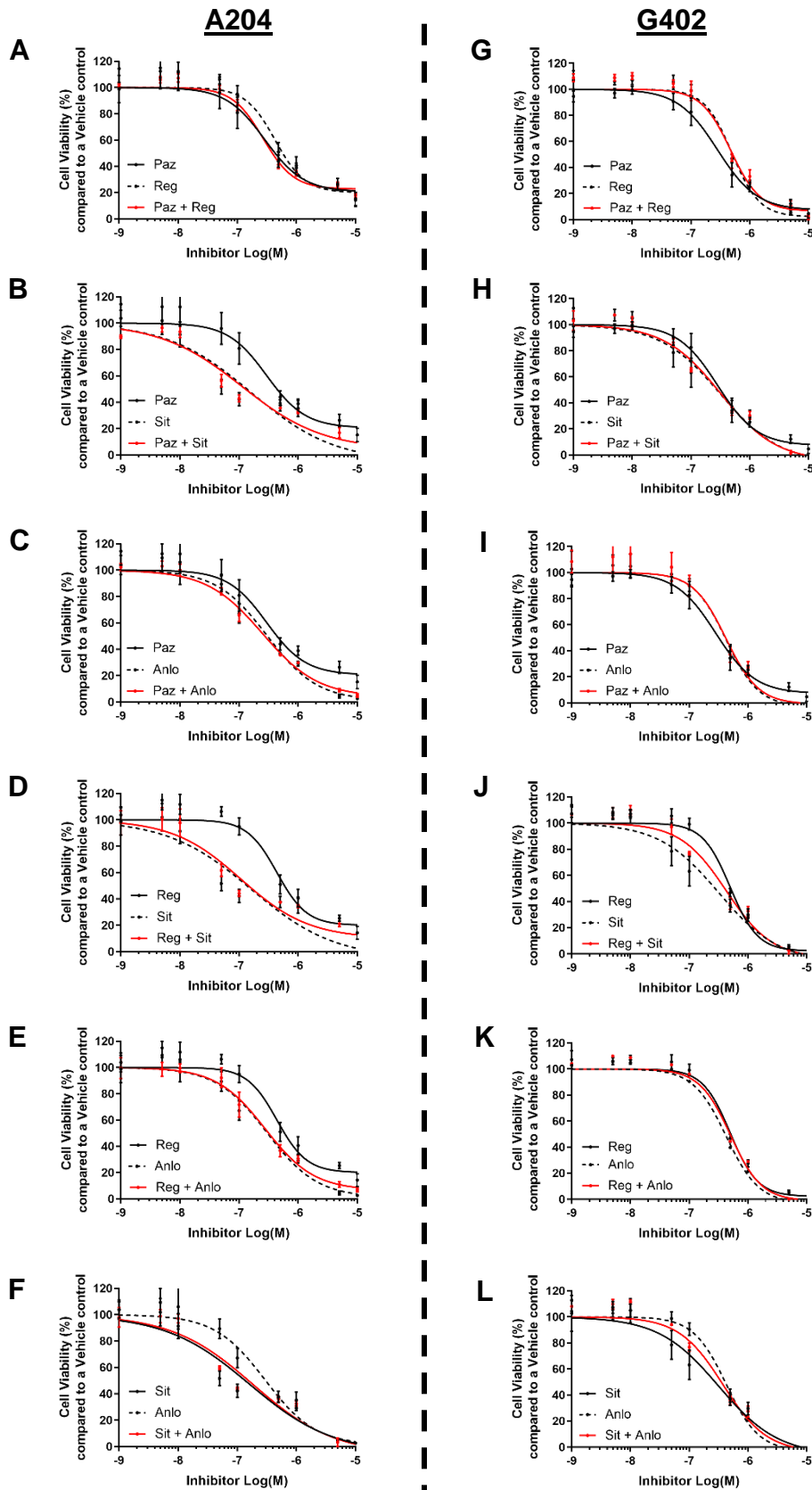


Figure 5.7: Cell viability assays evaluating the combinatorial effect of pazopanib, regorafenib, sitravatinib, and anlotinib dual treatment in A204 and G402 cells. Cell viability assays of (A-F) A204 and (G-L) G402 cells treated with increasing concentrations of the indicated multi-target TKI combinations. Dose response curves were used to

determine IC₅₀ values (**Table S6**). Cell viability was normalised to DMSO control (n=3). Error bars represent standard deviation. DMSO; Dimethyl sulfoxide, IC₅₀; Inhibitory constant, TKI; Tyrosine kinase inhibitor.

5.2.4 Multi-target TKIs potently reduce Akt phosphorylation in malignant rhabdoid tumour cell line models

As previously outlined in **Table 1.3**, pazopanib, regorafenib, sitravatinib, and anlotinib are multi-target TKIs that target a range of RTKs including PDGFRs, vascular endothelial growth factor receptors (VEGFRs), KIT, and FGFRs (Davis *et al.*, 2011; Patwardhan *et al.*, 2016; Xie *et al.*, 2018; Zopf *et al.*, 2016). Inhibition of these RTKs will result in alterations in downstream signalling pathways associated with tumour progression, such as PI3K/Akt and MAPK (Regad, 2015). Therefore, alterations in phosphorylation of major components of these pathways, namely Akt and ERK1/2, upon treatment with the four multi-target TKIs were analysed with immunoblotting (**Figure 5.8A-B**). Treatment of A204 and G402 cells with the multi-target TKIs resulted in the consistent reduction of Akt phosphorylation in a dose-dependent manner (**Figure 5.8A-B**).

Treatment with the multi-target TKIs had no noticeable effect on ERK1/2 phosphorylation at either 0.1 μ M or 1 μ M, except for a single condition. This outlying condition was 1 μ M anlotinib treatment of A204 cells which resulted in the inhibition of ERK1/2 phosphorylation. This effect was not observed at 0.1 μ M anlotinib in the A204 cells (**Figure 5.8A**).

These data indicate that pazopanib, regorafenib, sitravatinib, and anlotinib primarily exert their downstream effects through blockade of the PI3K/Akt pathway (**Figure 5.8A-B**). This is consistent with my hypothesis from the combinatorial evaluations (**Figure 5.7**) that these four multi-target TKIs employ a similar mechanism of action to exert their antiproliferative effects. Additionally, 1 μ M anlotinib has also been shown to display a supplementary ability to block MAPK signalling in the A204 cell line (**Figure 5.8A**). Significantly, the dual ability of 1 μ M anlotinib to block Akt and ERK1/2 signalling correlated with the enhanced apoptotic and antiproliferative effects of anlotinib in A204 cells (**Figure 5.5 & 5.6 & 5.8**). This is when compared to the other evaluated multi-target TKIs that only resulted in Akt blockade at the evaluated timepoints and concentrations (**Figure 5.5 & 5.6 & 5.8**).

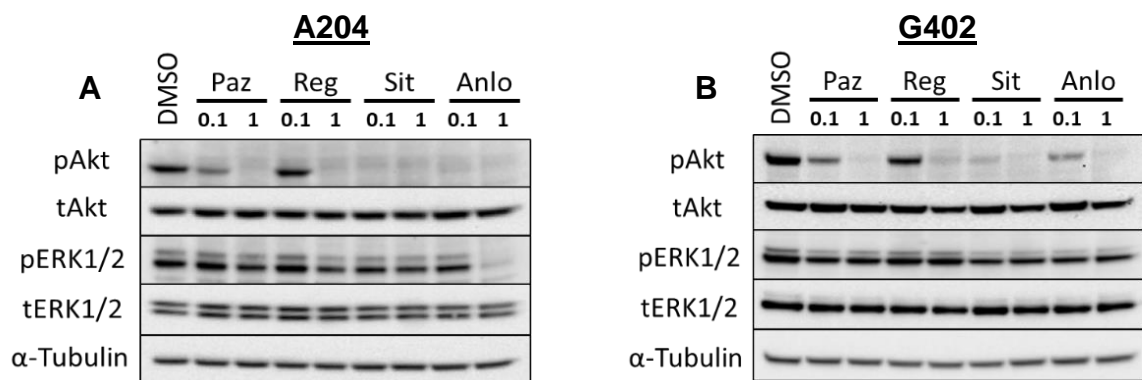


Figure 5.8: Immunoblots of A204 and G402 cells treated with two concentrations of pazopanib, regorafenib, sitravatinib, and anlotinib. Immunoblots of Akt and ERK1/2 signalling modulations in **(A)** A204 and **(B)** G402 cells after 6 hours of treatment with either 0.1 or 1 μ M pazopanib (Paz), regorafenib (Reg), sitravatinib (Sit), or anlotinib (Anlo). Images are representative of two separate experiments ($n=2$). DMSO; Dimethyl sulfoxide, ERK1/2; Extracellular signal-regulated kinase.

5.2.5 Investigation into combinatorial multi-target TKI plus FGFR inhibitor treatment strategies to provide enhanced antitumour activity

The previous study by Wong *et al.* revealed that dual inhibition of PDGFR α and FGFR1 RTKs in cell line models of MRT led to the blockade of downstream Akt and MAPK signalling, resulting in synergistic antitumour effects (Wong *et al.*, 2016). The Wong *et al.* study employed the PDGFR α -targeting sunitinib, dasatinib, and pazopanib in combination with the selective FGFR inhibitor infigratinib (BGJ-398) (Wong *et al.*, 2016).

I therefore wanted to determine whether the multi-target TKIs regorafenib, sitravatinib, and anlotinib, in combination with FGFR inhibitors, could result in a similar phenotype in the A204 and G402 cell line models. Two selective FGFR inhibitors, infigratinib and erdafitinib (JNJ-42756493) were utilised for this assessment (Guagnano *et al.*, 2011; Perera *et al.*, 2017).

A204 and G402 cells were subjected to combination therapy with one of the four multi-target TKIs (pazopanib, regorafenib, sitravatinib, or anlotinib) plus FGFR inhibitor – either infigratinib or erdafitinib – and the effects on cell viability were compared to multi-target TKI and FGFR inhibitor monotherapy (**Figure 5.9**). A204 and G402 cells were found to be relatively resistant to treatment with infigratinib monotherapy (IC_{50} : A204; 1.68 μ M, G402; 1.85 μ M) (**Figure 5.9A-H; Table S7**).

However, combination treatments of infigratinib plus multi-target TKI showed a synergistic, combinatorial effect in reducing cell viability compared to the constituent single agent treatments in both cell line models (**Figure 5.9A-H; Table S7**). This result suggests that infigratinib operates by a differing mechanism of action compared to the four multi-target TKIs.

To quantify the level of synergism, the combination indices for the IC₅₀ values were calculated using **Equation E1**, outlined in the materials and methods (Chou, 2010) (**Table 5.2**). Using this equation, for a combination to be considered synergistic, the combination index must be < 1, with the degree of synergism increasing as the value tends towards 0. **Table 5.2** shows that each of the combinations of infigratinib plus multi-target TKI resulted in high levels of synergism (combination index < 0.5).

In contrast to infigratinib monotherapy, erdafitinib monotherapy displayed potent efficacy in reducing cell viability in the A204 and G402 cell lines, with IC₅₀ values that are mostly lower than those seen with multi-target TKI monotherapy (A204 IC₅₀: 0.25 μM, G402 IC₅₀: 0.15 μM) (**Figure 5.9I-P; Table S7**). Combination treatment of erdafitinib plus multi-target TKI treatment also resulted in synergism, albeit lower than the synergism observed with infigratinib combinations (**Table 5.1**). Despite this reported synergism, the dose response curves in **Figure 5.9I-P** show that the levels of enhanced combinatorial effect compared to erdafitinib monotherapy were minimal or negligible in the combination treatments incorporating pazopanib, regorafenib, and anlotinib (**Figure 5.9I-P; Table S7**). This result indicates that erdafitinib, pazopanib, regorafenib, and anlotinib share a mechanism of action that result in the observed antiproliferative effects. However, combination treatment of erdafitinib and sitravatinib in both cell lines continued to display a strong combinatorial effect when compared to constituent monotherapies (**Figure 5.9I-P; Table S7**). This result suggests additional kinase target(s) that are inhibited by sitravatinib treatment but not with pazopanib, regorafenib, or anlotinib treatment (**Figure 5.9K & O; Table S7**).

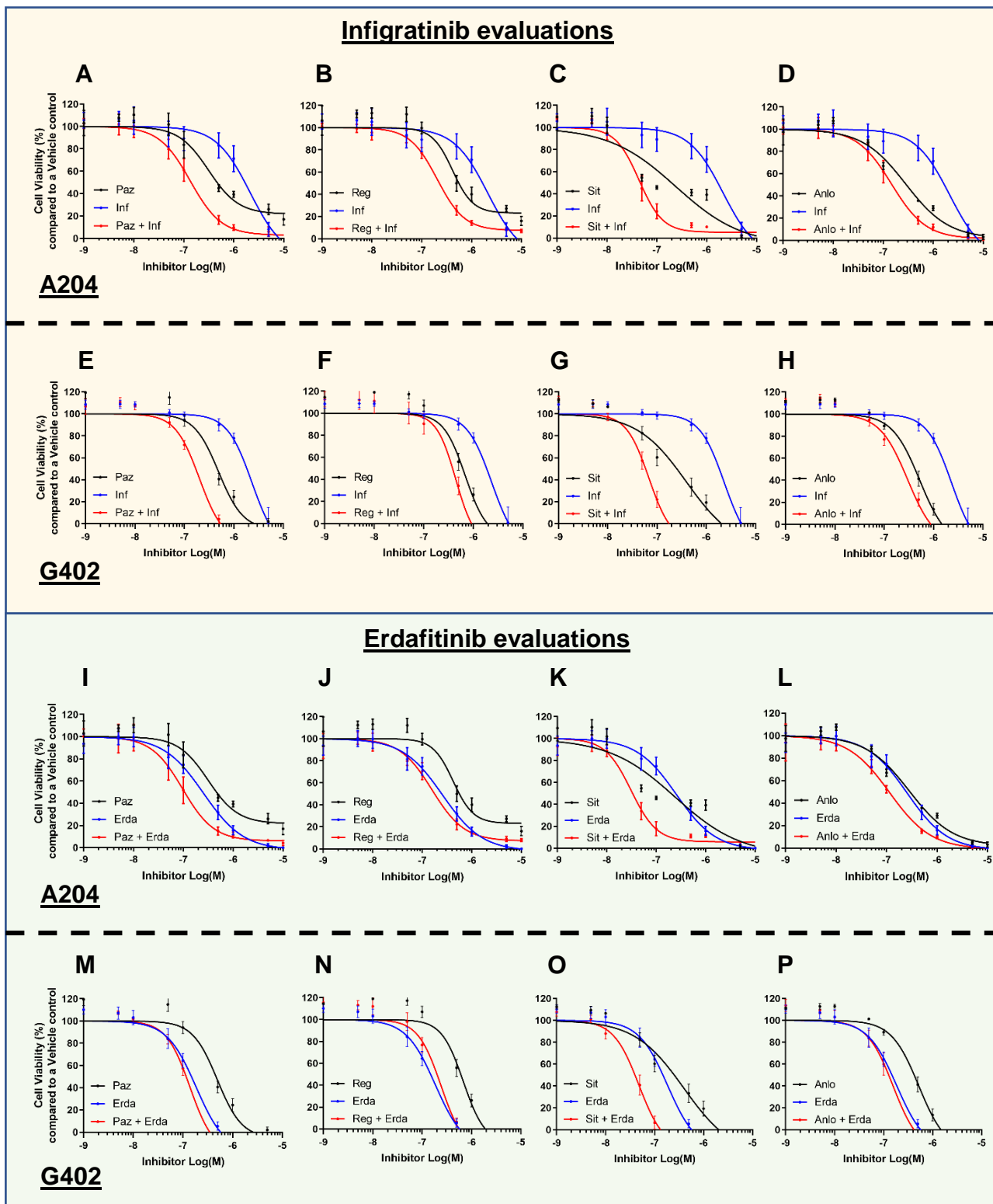


Figure 5.9: Cell viability assays evaluating the synergistic, combinatorial effect of multi-target TKI plus FGFR inhibitor treatment in A204 and G402 cells. Cell viability assays of (A-D, I-L) A204 and (E-H, M-P) G402 cells treated with increasing concentrations of multi-target TKI plus FGFR inhibitor combinations. Multi-target TKI plus infigratinib (Inf) combination efficacies evaluated in A204 cells with (A) pazopanib- (Paz), (B) regorafenib- (Reg), (C) sitravatinib- (Sit), and (D) anlotinib (Anlo)-based treatments. Equivalent combinations in G402 cells are shown in (E-H), respectively. Multi-target TKI plus erdafitinib (Erda) combination efficacies evaluated in A204 cells with (I) Paz-, (J) Reg-, (K) Sit-, and (L) Anlo-based treatments. Equivalent combinations in G402 cells are shown in (M-P), respectively. Dose response curves were used to determine IC_{50} values and combination indices (Table 5.2 & S7). Cell viability was normalised to

DMSO control (n=3). Combination indices were calculated using **Equation E1**. Error bars represent standard deviation. DMSO; Dimethyl sulfoxide, FGFR; Fibroblast growth factor receptor, IC₅₀; Inhibitory constant, TKI; Tyrosine kinase inhibitor.

Table 5.2: A204 and G402 cells treated with combinations of the TKIs pazopanib (Paz), regorafenib (Reg), sitravatinib (Sit), anlotinib (Anlo), infigratinib (Inf), and erdafitinib (Erda), with associated combination indices.

TKI treatment	A204	G402
	Combination index	Combination index
Paz + Inf	< 1 (0.20)	< 1 (0.23)
Reg + Inf	< 1 (0.27)	< 1 (0.42)
Sit + Inf	< 1 (0.13)	< 1 (0.13)
Anlo + Inf	< 1 (0.31)	< 1 (0.35)
TKI treatment		
Paz + Erda	< 1 (0.33)	< 1 (0.52)
Reg + Erda	< 1 (0.52)	< 1 (0.84)
Sit + Erda	< 1 (0.15)	< 1 (0.22)
Anlo + Erda	< 1 (0.42)	< 1 (0.58)

IC₅₀; Inhibitory constant, TKI; Tyrosine kinase inhibitor.

Building on the synergistic, antiproliferative effects observed in cell viability assays, I also wanted to evaluate whether combination treatment of the multi-target TKIs (pazopanib, regorafenib, sitravatinib, or anlotinib) plus FGFR inhibitor resulted in enhanced apoptotic activity. Assessment of caspase 3/7 activity in both the A204 and G402 cells after 24 hours of treatment (0.5 μ M and 1 μ M) showed that the combination of infigratinib plus multi-target TKI significantly enhanced apoptosis relative to monotherapy multi-target TKI (~1.5 to 3-fold enhancement) or infigratinib (~3- to 5-fold enhancement) (**Figure 5.10A-P**).

Similarly, combination of erdafitinib with multi-target TKI also significantly increased apoptosis when compared to monotherapy multi-target TKI (~1.5 to 3-fold enhancement) in the majority of treatments (**Figure 5.10A-P**). The single exception to this is with 1 μ M anlotinib treatment in A204 cells, where the significantly increased apoptotic effects of anlotinib compared to the other multi-target TKIs (**Figure 5.6A**) were found to be similar to the apoptotic effects observed with erdafitinib plus anlotinib treatment (~10- to 13-fold increase relative to DMSO) (**Figure 5.10D & H**).

Treatment of both cell lines with 1 μ M of combined erdafitinib plus multi-target TKI was not found to significantly increase apoptosis when compared to 1 μ M erdafitinib monotherapy (**Figure 5.10A-P**). At this concentration, **Figure 5.10** shows that erdafitinib monotherapy was found to consistently mirror the enhanced apoptotic effects that were seen with combination therapy of multi-target TKI plus FGFR inhibitor (~9- to 12-fold increase relative to DMSO), with marginal differences in apoptosis observed upon combination of erdafitinib plus multi-target TKI (**Figure 5.10A-P**).

Focussing on the observed enhanced pro-apoptotic activity with erdafitinib monotherapy, this FGFR inhibitor was found to significantly enhance apoptosis in both cell lines when compared to multi-target TKI (~1.5- to 3-fold enhancement) or infigratinib (~2.5- to 3.5-fold enhancement) (**Figure 5.10A-P**). The single exception to this is anlotinib treatment in A204 cells, which was found to mimic the apoptotic effects observed with erdafitinib at both concentrations (0.5 μ M; ~3-fold, 1 μ M; ~10-fold increase relative to DMSO) (**Figure 5.10D & H**).

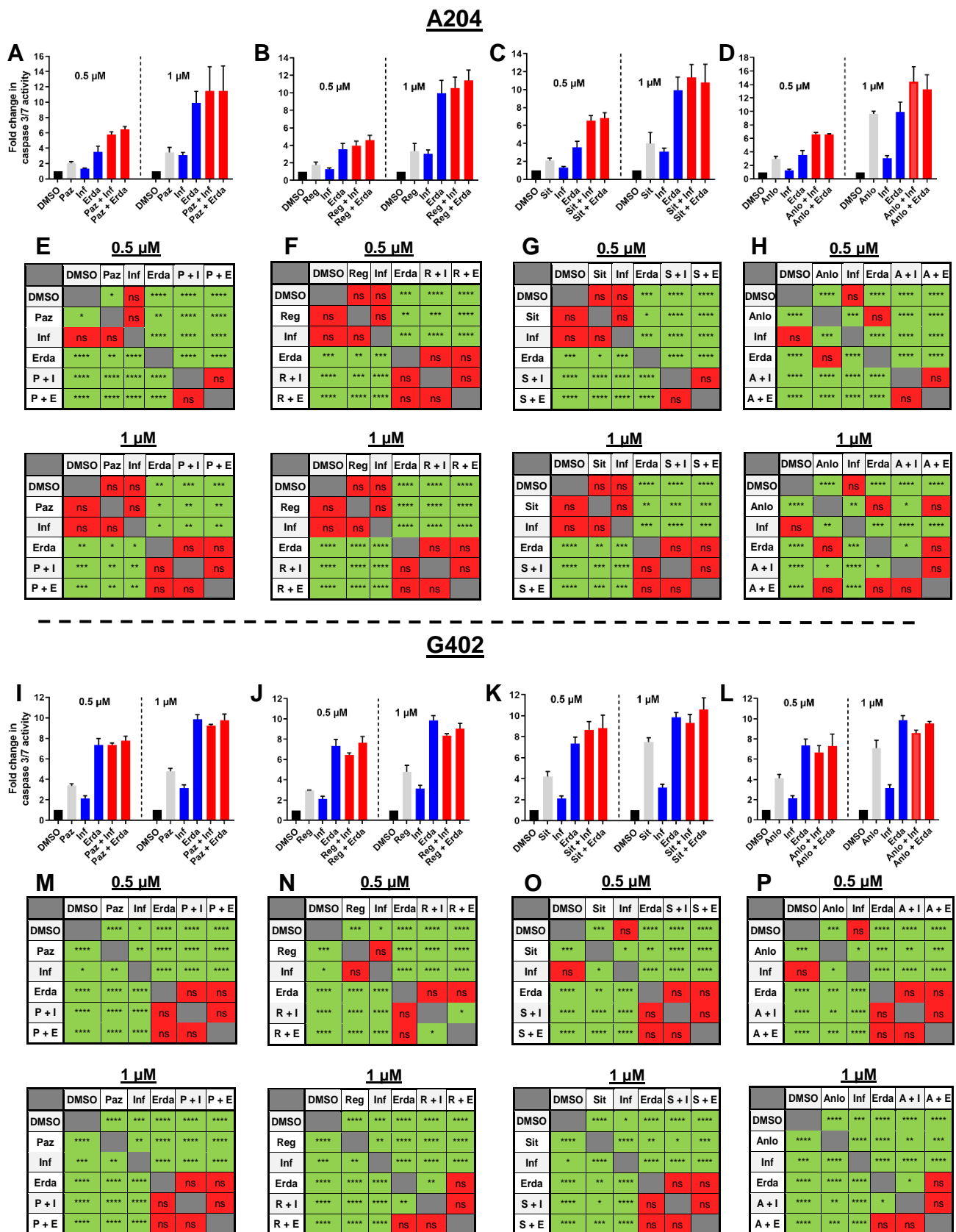


Figure 5.10: Assays evaluating changes in apoptosis levels in A204 and G402 cells upon combination therapy of multi-target TKIs plus FGFR inhibitors. Bar plots displaying the fold change in caspase 3/7 activity in the (A-H) A204 and (I-P) G402 cells treated with two concentrations of multi-target TKI and FGFR inhibitor combinations for 24 hours. Multi-target TKI plus ingefitinib (I/Inf) or erdafitinib (E/Erda) combination efficacies evaluated in A204 cells with (A) pazopanib- (P/Paz), (B) regorafenib- (R/Reg), (C) sitravatinib- (S/Sit), and (D) anlotinib (A/Anlo)-based treatments.

Equivalent combinations in G402 cells are shown in **(I-L)**. Fold change was normalised to DMSO control (n=3). Grids displaying the statistical significance between the different treatments at two different concentrations in the **(E-H)** A204 cells for **(E)** Paz-, **(F)** Reg-, **(G)** Sit-, and **(H)** Anlo-based treatments in the apoptosis assays. Equivalent statistical significance grids for G402 are shown in **(M-P)**, respectively. Statistical analysis was undertaken using one-way ANOVAs with Tukey's multiple comparison tests (* = $p \leq 0.05$, ** = $p \leq 0.01$, *** = $p \leq 0.001$, **** = $p \leq 0.0001$). Error bars represent standard deviation. ANOVA; Analysis of variance, DMSO; Dimethyl sulfoxide, FGFR; Fibroblast growth factor receptor, ns; Non-significant, TKI; Tyrosine kinase inhibitor.

These results show that dual therapy of pazopanib, regorafenib, sitravatinib, or anlotinib plus the selective FGFR inhibitor infigratinib recapitulated similar pro-apoptotic phenotypes in MRT cell lines as was observed upon dual PDGFR α and FGFR1 inhibition by Wong *et al.* (Wong *et al.*, 2016).

Furthermore, single agent erdafitinib was found to significantly enhance apoptosis levels in both A204 and G402 cells, at levels similar to combined multi-target TKI and infigratinib treatment. The work by Wong *et al.*, 2016 reported similar single agent activity with the dual PDGFR α /FGFR1 inhibitor ponatinib to what I have reported with erdafitinib (Wong *et al.*, 2016). Therefore, the effects of ponatinib upon cell viability and apoptosis were evaluated in the MRT cell lines and compared to erdafitinib, as well as dual multi-target TKI plus FGFR inhibitor therapy.

Consistent with Wong *et al.*, both the A204 and G402 cell lines were found to be extremely sensitive to ponatinib (IC₅₀: A204; 0.05 μ M, G402; 0.05 μ M), with reduced IC₅₀ values compared to multi-target TKI and infigratinib monotherapy (**Table 5.3**). Additionally, ponatinib was more potent in reducing IC₅₀ when compared to erdafitinib monotherapy (IC₅₀: A204; 0.25 μ M, G402; 0.15 μ M), as well as dual multi-target TKI plus FGFR inhibition in the majority of combinations (**Table 5.3**). Interestingly, ponatinib monotherapy was found to produce near identical IC₅₀ values when compared to sitravatinib plus FGFR inhibitor (**Table 5.3**).

Table 5.3: A204 and G402 cells treated with combinations of the TKIs pazopanib (Paz), regorafenib (Reg), sitravatinib (Sit), anlotinib (Anlo), infgratinib (Inf), erdafitinib (Erda), and ponatinib (Pon), with associated IC ₅₀ values (µM).			
TKI treatment	A204	G402	
	IC ₅₀ (µM) (± S.D.)	IC ₅₀ (µM) (± S.D.)	
Sit + Erda	0.03 (± 0.01)	0.04 (± 0.01)	IC ₅₀ < 0.10
Pon	0.05 (± 0.01)	0.05 (± 0.01)	IC ₅₀ 0.11-0.20
Sit + Inf	0.05 (± 0.01)	0.06 (± 0.01)	
Paz + Erda	0.11 (± 0.05)	0.12 (± 0.01)	IC ₅₀ 0.21-0.30
Anlo + Erda	0.11 (± 0.02)	0.13 (± 0.03)	
Paz + Inf	0.14 (± 0.04)	0.17 (± 0.02)	IC ₅₀ 0.31-1.00
Reg + Erd	0.18 (± 0.04)	0.20 (± 0.04)	
Anlo + Inf	0.15 (± 0.05)	0.24 (± 0.05)	IC ₅₀ > 1.00
Sit	0.20 (± 0.06)	0.25 (± 0.10)	
Erda	0.25 (± 0.08)	0.15 (± 0.03)	
Reg + Inf	0.23 (± 0.03)	0.38 (± 0.11)	
Anlo	0.29 (± 0.02)	0.42 (± 0.07)	
Paz	0.47 (± 0.08)	0.46 (± 0.07)	
Reg	0.56 (± 0.13)	0.61 (± 0.09)	
Inf	1.68 (± 0.28)	1.85 (± 0.50)	

IC₅₀; Inhibitory constant, S.D.; Standard deviation, TKI; Tyrosine kinase inhibitor.

In addition to the potent antiproliferative activity of ponatinib in A204 and G402 cells, ponatinib was also found to significantly induce apoptotic activity in A204 and G402 cells (**Figure 5.11A-B**). In the A204 cells, ponatinib was found to significantly increase apoptosis (0.5 µM; ~15-fold, 1 µM; ~ 40-fold increase relative to DMSO) compared to all evaluated multi-target TKI and FGFR inhibitor treatments, both monotherapy and dual therapy (**Figure 5.11A**). In the G402 cells, ponatinib was found to enhance apoptotic activity (0.5 µM; ~8.5-fold, 1 µM; ~10-fold increase relative to DMSO) to a similar level to those observed with erdafitinib monotherapy, as well as combined multi-target TKI plus FGFR inhibitor treatment (**Figure 5.11B**). Additionally, I also observed that ponatinib induced notably higher levels of apoptotic activity in the A204 cells (0.5 µM; ~15-fold, 1 µM; ~ 40-fold increase relative to DMSO) compared to the G402 cells (0.5 µM; ~8.5-fold, 1 µM; ~10-fold increase relative to DMSO) (**Figure 5.11A-B**).

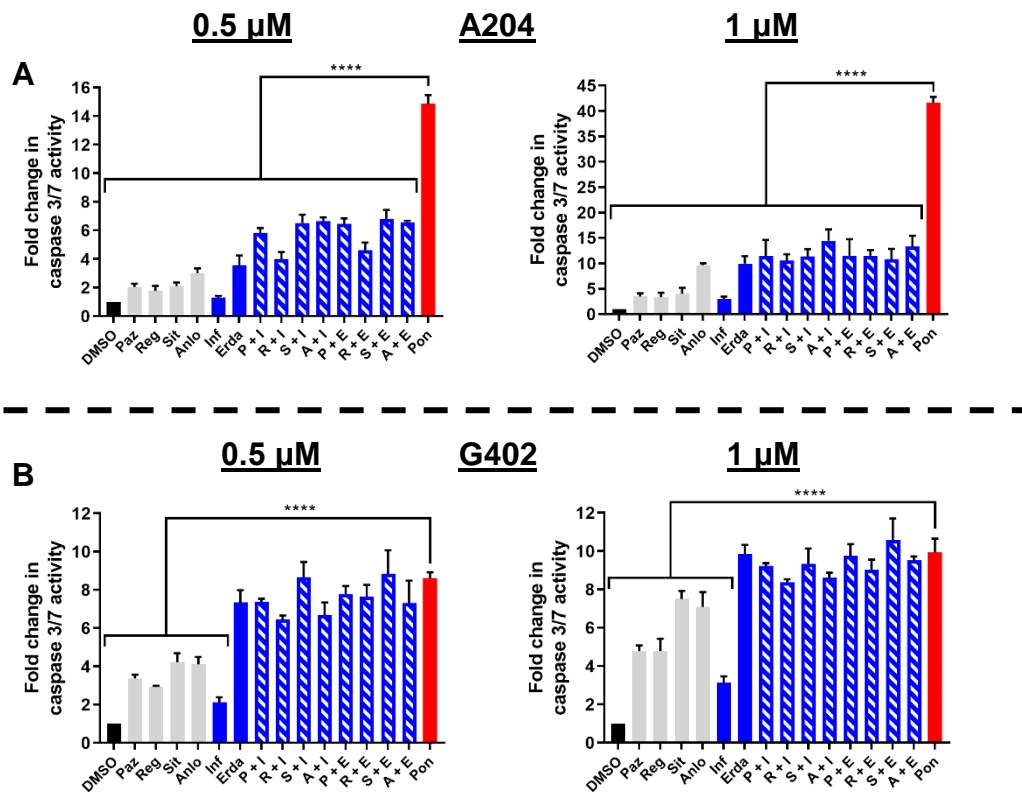


Figure 5.11: Apoptosis assays evaluating the pro-apoptotic effects of ponatinib therapy in A204 and G402 cells. Bar plots displaying the fold change in caspase 3/7 activity in the (A) A204 and (B) G402 cells treated with two concentrations of ponatinib (Pon), multi-target TKIs, and FGFR inhibitor combinations for 24 hours. Fold change was normalised to DMSO control (n=3). Statistical analysis was undertaken using one-way ANOVAs with Dunnett's multiple comparison tests (compared to Pon) (**** = $p \leq 0.0001$). Error bars represent standard deviation. A/Anlo; Anlotinib, ANOVA; Analysis of variance, DMSO; Dimethyl sulfoxide, E/Erda; Erdafitinib, FGFR; Fibroblast growth factor receptor, I/Inf; Infigratinib, P/Paz; Pazopanib, R/Reg; Regorafenib, S/Sit; Sitravatinib, TKI; Tyrosine kinase inhibitor.

To further confirm the association between enhanced cell death and the dual blockade of Akt and MAPK signalling pathways downstream of targeted RTKs that was previously reported by Wong *et al.*, immunoblotting of Akt and ERK1/2 signalling was undertaken on cells treated with combinations of multi-target TKI plus FGFR inhibitor, as well as monotherapy FGFR inhibitors and ponatinib (**Figure 5.12**). In contrast to pazopanib, regorafenib, sitravatinib, and anlotinib, the selective FGFR inhibitor infigratinib had no effect on Akt phosphorylation in either MRT cell line. However, infigratinib did instead reduce ERK1/2 phosphorylation in the A204 cell line model (**Figure 5.12A**). Interestingly, no notable change was observed in ERK1/2 phosphorylation in the G402 model with infigratinib monotherapy after 6 hours of 1 μ M treatment (**Figure 5.12B**). However, both erdafitinib and ponatinib monotherapies were found to potently inhibit both the Akt and ERK1/2 pathways in both cell lines, consistent with their enhanced pro-apoptotic and antiproliferative activities. Furthermore, combination therapy of multi-target TKI plus infigratinib resulted in the

concurrent suppression of both ERK1/2 and Akt phosphorylation (**Figure 5.12A-B**). This result is consistent with the enhanced apoptotic and antiproliferative activities observed with these combination therapies when compared to monotherapy multi-target TKI treatment.

Taken together, the results from **Chapter 5.2.5** suggest that blockade of both the Akt and MAPK pathways, caused by upstream RTK inhibition by TKIs, results in enhanced apoptotic activity and antiproliferative activity in both cell line models of MRT.

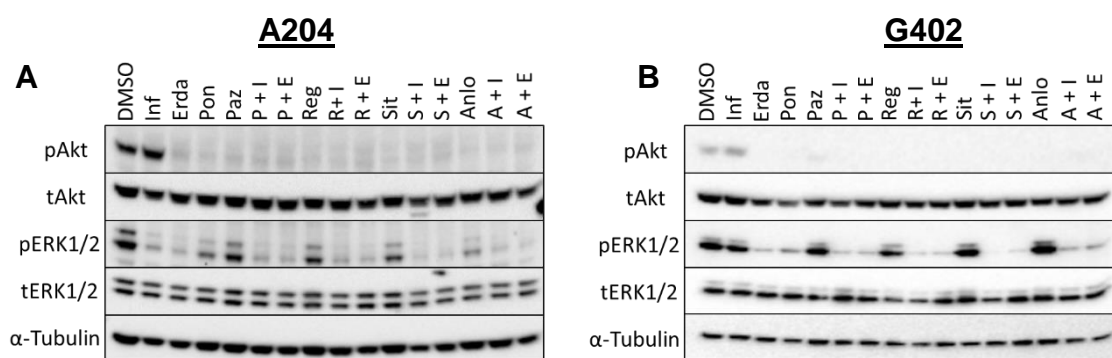


Figure 5.12: Immunoblots of A204 and G402 cells treated with monotherapies or dual therapies to assess for dual Akt and ERK1/2 signalling blockade. Immunoblots of Akt and ERK1/2 signalling modulations in **(A)** A204 and **(B)** G402 cells after 6 hours of treatment with DMSO or 1 μ M TKI. Images are representative of two separate experiments ($n=2$). A/Anlo; Anlotinib, DMSO; Dimethyl sulfoxide, E/Erda; Erdafitinib, ERK1/2; Extracellular signal-regulated kinase 1/2, I/Inf; Infigratinib, P/Paz; Pazopanib, Pon; Ponatinib, R/Reg; Regorafenib, S/Sit; Sitravatinib, TKI; Tyrosine kinase inhibitor.

5.2.6 Treatment of malignant rhabdoid tumour cells with first-line erdafitinib, ponatinib, or combination therapy suppresses the emergence of drug resistance

Although pazopanib, regorafenib, sitravatinib, and anlotinib were found to have potent antitumour activities in cell line models of MRT, **Figure 5.5** showed that cells will acquire resistance to treatment after prolonged and chronic treatment. Having determined treatment strategies with enhanced pro-apoptotic and antiproliferative properties compared to these four multi-target TKIs, I wanted to evaluate whether treating A204 cells with erdafitinib, ponatinib, or combination therapy (multi-target TKI plus FGFR inhibitor) resulted in the development of acquired resistance if treated in the first-line setting (**Figure 5.13**). I therefore treated A204 parental cells with 1 μ M of indicated treatment over 6 weeks and recorded the increase in cell number over the

course of treatment. **Figure 5.13** shows that treatment of A204 cells with combination therapies and erdafitinib monotherapy showed notably decreased cellular proliferation compared to multi-target TKI and infigratinib monotherapies (**Figure 5.13**). However, despite this prolonged antiproliferative phenotype, a small population of cells tolerate treatment and remain during the course of the 42 days of treatment, indicating potential residual disease that may give rise to subsequent drug resistance (**Figure 5.13**). On the other hand, exposure to ponatinib treatment resulted in the complete elimination of cells (**Figure 5.13**). This is consistent with previous results by Wong *et al.* who were unable to derive a ponatinib-resistant A204 subline (Wong *et al.*, 2016). Taken together, these results therefore nominate erdafitinib, ponatinib, or combination therapy (multi-target TKI plus FGFR inhibitor) as effective first-line treatments warranting further evaluation in MRT, as well as other STS driven by PDGFR and FGFR signalling.

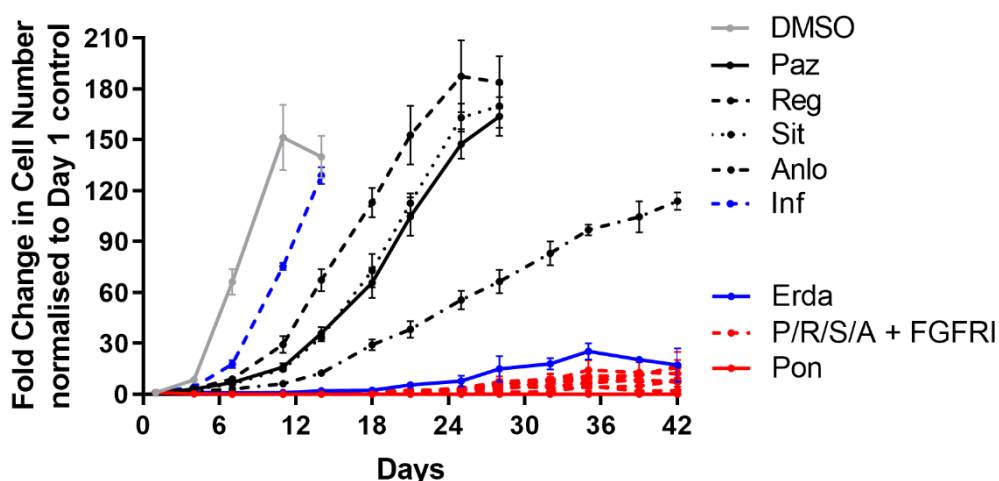


Figure 5.13: Erdafitinib, ponatinib, and combination therapies suppress the growth of TKI-resistant cells in the first-line setting. Growth curves of A204 to measure the fold change in cell number over a period of 6 weeks in cells treated with indicated treatments. Data collection for a specific treatment regimen was ceased once the cells had reached overconfluency within the 96 well plate and the Celigo cytometer could no longer accurately distinguish between individual cells. Fold change was normalised to day 1 control (n=2). Error bars represent standard error of the mean. A/Anlo; Anlotinib, Erda; Erdafitinib, FGFRi; Fibroblast growth factor inhibitor, Inf; Infigratinib, P/Paz; Pazopanib, Pon; Ponatinib, P/R/S/A; Pazopanib, Regorafenib, Sitravatinib, or Anlotinib, R/Reg; Regorafenib, S/Sit; Sitravatinib, TKI; Tyrosine kinase inhibitor.

5.3 Discussion

The work presented in **Chapter 5** shows that cell line models of MRT, a highly aggressive, paediatric STS subtype with historically dismal outcomes, are sensitive to

the multi-target TKI therapies pazopanib, regorafenib, sitravatinib, and anlotinib (Geller *et al.*, 2015). Additionally, the antitumour activity of these multi-target TKIs in the MRT cell lines was found to correlate with the downstream blockade of Akt signalling. Future work employing direct PI3K/Akt pathway inhibitors (e.g., dactolisib (BEZ235), MK2206) will focus on exploring whether Akt blockade is the causative factor resulting in the antitumour phenotypes observed with multi-target TKI treatment. The finding of pazopanib and regorafenib activity in MRT cell lines has previously been described (Daudigeos-Dubus *et al.*, 2015; Teicher *et al.*, 2015; Wong *et al.*, 2016). However, the work outlined in **Chapter 5** is the first to show the efficacy of sitravatinib and anlotinib within this STS subtype.

Chapter 5 also replicates many of the findings by Wong *et al.* but with additional multi-target TKIs, namely regorafenib, sitravatinib, and anlotinib. The Wong *et al.* study reported that dual blockade of Akt and MAPK pathways by upstream RTK inhibition in MRT cell line models resulted in enhanced apoptotic activity when compared to multi-target TKI and FGFR inhibitor monotherapy. This was determined through the treatment of MRT cells with combinations of multi-target TKIs plus the selective pan-FGFR inhibitor infgratinib, as well as dual PDGFR α /FGFR1 inhibitor single agent treatments such as ponatinib. Consistent with this study, the work presented in **Chapter 5** has replicated the association between the dual blockade of Akt and MAPK pathways and enhanced pro-apoptotic and antiproliferative effects, by employing additional multi-target TKIs and FGFR inhibitors. Future studies will work on determining whether dual Akt and MAPK blockade caused by the TKIs employed in **Chapter 5** are causing the observed enhanced antitumour effects. This will be achieved through the utilisation of inhibitors that directly target the PI3K/Akt (e.g., dactolisib) or MAPK pathways (e.g., trametinib).

The previous work by Wong *et al.* described that the multi-target TKIs pazopanib, dasatinib, and sunitinib inhibited PDGFR α phosphorylation, with downstream blockade of Akt signalling, in the A204 cell line model (Wong *et al.*, 2016). The work presented in **Chapter 5** has not yet confirmed whether the multi-target TKIs regorafenib, sitravatinib, and anlotinib inhibit PDGFR α in the A204 and G402 cell lines. However, both regorafenib and sitravatinib have previously been shown to potently target and inhibit PDGFR α (regorafenib K_d : 21 nM, sitravatinib IC_{50} : 30 nM) (**Figure 5.1; Table 1.3**) (Patwardhan *et al.*, 2016; Zopf *et al.*, 2016). Additionally, although the

inhibitory activity of anlotinib has not yet been evaluated in PDGFR α , anlotinib has been shown to be a potent inhibitor of the highly homologous PDGFR family members KIT and PDGFR β (anlotinib KIT IC₅₀: 14.8 nM, PDGFR β : 8.7-115 nM) (**Figure 5.1; Table 1.3**) (Bauer *et al.*, 2020; Lin *et al.*, 2018; Lu *et al.*, 2021; Xie *et al.*, 2018). In addition to target overlap with the multi-target TKIs evaluated in Wong *et al.*, regorafenib, sitravatinib, and anlotinib also produced similar phenotypes in terms of dose response, increased apoptosis levels, and Akt pathway blockade in the A204 cell line. I therefore hypothesise that regorafenib, sitravatinib, and anlotinib inhibit PDGFR α signalling, resulting in the downstream Akt blockade phenotype and subsequent antiproliferative and pro-apoptotic consequences, in the MRT cell line models (**Figure 5.14**). Future work will be undertaken to confirm this hypothesis. Firstly, immunoprecipitation will be undertaken to confirm the inhibition of PDGFR α by regorafenib, sitravatinib, and anlotinib. Following this, inhibitor-resistant PDGFR α mutants (e.g., T674I/M, D842V, Y288C) will be employed to determine whether the anticancer effects exerted by the multi-target TKIs can be rescued (Ip *et al.*, 2018; Weisberg *et al.*, 2010). This will allow us to confirm that inhibition of the PDGFR α /Akt signalling pathway by multi-target TKIs results in the downstream antitumour phenotypes, such as reduced cell proliferation and enhanced cell death.

Chapter 5 also shows that erdafitinib treatment results in the dual blockade of Akt and MAPK as a single agent in the MRT cell line models A204 and G402. Additionally, I found that 1 μ M anlotinib treatment also resulted in this dual blockade phenotype but only in the A204 cell line model. The dual pathway inhibition caused by erdafitinib and anlotinib phenocopies the effects observed with combination therapy of PDGFR α inhibitor plus FGFR inhibitor described by Wong *et al.*, as well as single agent PDGFR α /FGFR1 inhibitor ponatinib. I therefore postulate that erdafitinib acts as a potent dual PDGFR α /FGFR1 inhibitor in both MRT cell lines. I also hypothesise that anlotinib acts as a potent dual PDGFR α /FGFR1 inhibitor in the A204 model, with anlotinib having a reduced potency for FGFR1 inhibition in the G402 cell line. Previous studies evaluating the kinase selectivity profiles of erdafitinib and anlotinib in cell-free kinase assays support this hypothesis.

For instance, although erdafitinib is primarily described as a selective pan-FGFR inhibitor, investigation into the kinase binding activity of erdafitinib towards non-FGFR RTKs reveals a non-selective, multi-target profile (Perera *et al.*, 2017). In the study

that discovered erdafitinib by Perera *et al.*, this TKI was found to be a potent inhibitor of all four FGFRs, with K_d values of 0.24, 2.2, 1.1, and 1.4 nM for FGFR1, 2, 3, and 4, respectively (Perera *et al.*, 2017). However, the authors also reported that erdafitinib had a similar potency towards inhibiting PDGFR α (K_d : 3.4 nM) as has been previously reported with pazopanib (K_d : 4.9 nM), with both studies employing identical assays (Davis *et al.*, 2011; Perera *et al.*, 2017). Regarding anlotinib, the work by Lin *et al.* reported that this multi-target TKI was an effective inhibitor of FGFR1 activity (IC_{50} : 11.7 nM), at levels similar to PDGFR inhibition (IC_{50} : 8.7 nM), in cell-free kinase assays (Lin *et al.*, 2018).

To confirm my hypothesis that erdafitinib and anlotinib have dual inhibitory activity upon PDGFR α and FGFR1, I will employ immunoprecipitation techniques to confirm inhibition of phosphorylation of these receptors upon treatment. In addition to the inhibitor-resistant PDGFR α mutants described above, I will also employ rescue experiments utilising the FGFR1 gatekeeper mutation V561F/M in MRT cells. This will allow for the determination of the direct association of dual PDGFR α /FGFR1 inhibition and subsequent anticancer activities, including enhanced cell death and reduced proliferation. Taken together, the hypothesised mechanisms of action of the evaluated TKIs in MRT cell line models, based on the results presented in **Chapter 5** and the studies discussed above, are outlined in **Figure 5.14**.

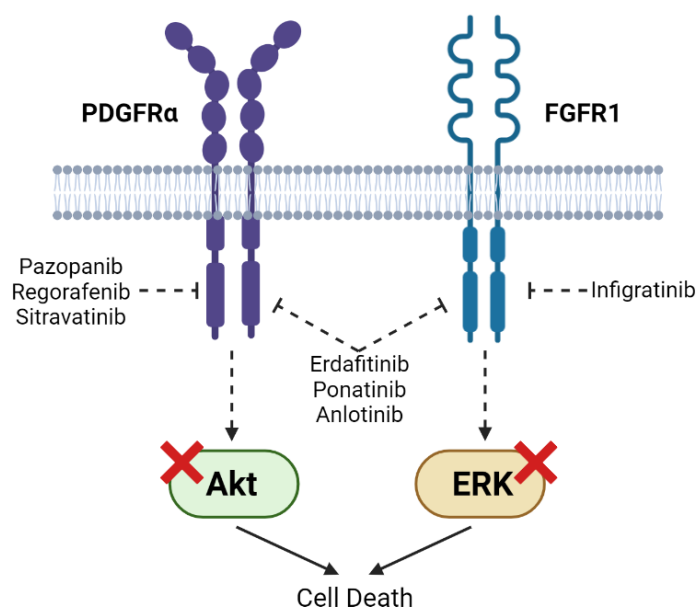


Figure 5.14: Hypothesised mechanism of action of the discussed TKIs in MRT cell line models. ERK; Extracellular signal-regulated kinase, FGFR1; Fibroblast growth factor receptor 1, PDGFR α ; Platelet-derived growth factor receptor α (adapted from Wong *et al.*, 2016). Image was created using BioRender.

The results outlined in **Chapter 5** nominate a number of therapeutic combinations whose antitumour properties are associated with concurrent blockade of Akt and MAPK signalling as effective first-line treatments in the MRT subtype of STS. However, combination therapies are often associated with clinical issues such as unacceptable toxicities and negative pharmacokinetic/dynamic interactions in patients (Lopez & Banerji, 2017). The work presented in **Chapter 5** has shown that erdafitinib and ponatinib are single agents that blockade both Akt and MAPK pathways with associated enhanced cell death in MRT cell line models, comparable or exceeding those seen with combination therapy. These data replicate the findings of Wong *et al.* for ponatinib, however the determination of erdafitinib as a dual inhibitor of Akt and MAPK signalling with potent antitumour activity in MRT models is a novel discovery.

Previous studies have shown that patients diagnosed with MRTs express both PDGFRs and FGFRs (Chauvin *et al.*, 2017; Wöhrle *et al.*, 2013; Wong *et al.*, 2016). This knowledge, coupled with the high preclinical potency observed with ponatinib and erdafitinib within **Chapter 5**, nominate erdafitinib and ponatinib as potential first-line therapeutics warranting further evaluation in this subtype of STS, as well as other STS subtypes driven by expression of PDGFR and FGFR.

In fact, erdafitinib has been undergoing clinical evaluations in patients with advanced solid tumours harbouring FGFR alterations. For instance, a phase I trial assessing the safety and pharmacokinetics/dynamics of erdafitinib in advanced solid tumours reported that the TKI had tolerability and encouraging preliminary activity in patients harbouring targetable FGFR alterations (clinical benefit rate (CBR): 42% in patients with FGFR alterations vs. 27% in all enrolled patients) (Bahleda *et al.*, 2019). Building on these promising initial results, two phase II clinical trials of erdafitinib in advanced solid tumours are actively recruiting patients whose tumours harbour FGFR alterations. The first of these (NCT03210714) focusses on paediatric malignancies (age \leq 21 years) with eligible STS subtypes including MRT, rhabdomyosarcoma, soft tissue Ewing sarcoma, as well as other STS subtypes. Similarly, in a study of adults and adolescents (age \geq 12 years) (NCT04083976), the trial is currently recruiting patients with advanced solid tumours possessing FGFR alterations, including STS subtypes, to assess the clinical utility of erdafitinib in these patients (Pant *et al.*, 2021). In addition to undergoing clinical evaluation in STS, erdafitinib has also shown preclinical activity in both cell and murine models of FGFR2-driven undifferentiated

pleomorphic sarcoma (Toulmonde *et al.*, 2020). In a study by Toulmonde *et al.*, FGFR2 expression was found to be significantly upregulated in immune-low undifferentiated pleomorphic sarcoma patients, when compared to other undifferentiated pleomorphic sarcoma patients. By utilising cell line and xenograft models derived from patient samples, the authors reported that erdafitinib selectively decreased cell viability and tumour growth in FGFR2-overexpressing, immune-low undifferentiated pleomorphic sarcoma, with concurrent inhibition of FGFR2 and downstream MAPK signalling (Toulmonde *et al.*, 2020).

Ponatinib has also been found to have extensive preclinical activity in models of STS. In addition to the previously described activity in MRT cells by Wong *et al.*, ponatinib has also been shown to have potent antiproliferative properties in cell line models of synovial sarcoma, soft tissue Ewing sarcoma, and leiomyosarcoma (Kim *et al.*, 2019; Teicher *et al.*, 2015; Wong *et al.*, 2016). Furthermore, in cellular and murine models of FGFR4-driven rhabdomyosarcoma, ponatinib reduced cell proliferation, tumour growth, and FGFR4 phosphorylation, with concurrent inductions of apoptosis and cell cycle arrest (Li *et al.*, 2013).

In addition to FGFR inhibition, the ability of ponatinib to potently inhibit members of the PDGFR RTK family was highlighted by the molecule's ability to suppress KIT-driven liposarcoma cell line proliferation in a study by Kanojia *et al.* (Kanojia *et al.*, 2017). Further to antiproliferative properties in these cell line models, ponatinib was also shown to induce cell cycle arrest and enhance apoptosis, with concurrent KIT signalling inhibition. These *in vitro* properties were found to translate into an *in vivo* effect, with ponatinib significantly suppressing tumour growth in murine KIT-driven liposarcoma xenografts, when compared to vehicle, with decreased KIT and FGFR phosphorylation (Kanojia *et al.*, 2017).

However, despite the promising preclinical activity of ponatinib in STS models, the clinical use of ponatinib is limited due to severe side effects. Ponatinib was approved by the FDA for use in patients with chronic myeloid leukaemia and Philadelphia chromosome-positive acute lymphoblastic leukaemia but was soon removed from the market due to the high rates of life-threatening arterial occlusions. The drug has since returned to the market but with black box warnings to indicate the severe side effects (Zinger *et al.*, 2020). Despite these significant problems, there are ongoing efforts to

assess strategies to employ effective ponatinib therapy whilst reducing severe side effects. These include trials utilising low-dosing regimens in heavily pre-treated GIST (NCT03171389) or encapsulating ponatinib molecules in lipid nanoparticles for more accurate drug delivery to the tumour, thereby reducing toxic off-target effects in healthy tissues (Falkenhorst *et al.*, 2020; Zinger *et al.*, 2020).

Recent articles have reported that targetable FGFR alterations occur in approximately 4% of STS, with particular subtypes, such as dedifferentiated liposarcoma, exhibiting extremely high rates (> 90%) of FGFR overactivity (Chudasama *et al.*, 2017; Napolitano *et al.*, 2021). Additionally, oncogenic PDGFR signalling has been shown to be implicated in the progression of several STS subtypes (Cornillie *et al.*, 2019; Kilvaer *et al.*, 2010). Therefore, utilising inhibitors that can simultaneously inhibit PDGFRs and FGFRs in STS, such as ponatinib (and potentially erdafitinib), could prove to be efficient strategies in the first-line setting of STS driven by PDGFRs and/or FGFRs. Additionally, the targeting of multiple growth-promoting RTKs reduces the potential of cancer cells to develop acquired resistance (Tan *et al.*, 2017).

Finally, despite the proven activity of the multi-target TKIs pazopanib, regorafenib, sitravatinib, and anlotinib in MRT cell line models of STS, **Figure 5.5** shows that these cells universally develop acquired resistance to all four TKIs. This phenomenon recapitulates the TKI-resistance phenotypes observed clinically with chronic multi-target TKI therapy in STS patients. Therefore, utilising these initially sensitive STS models, **Chapter 6** will aim to determine resistance mechanisms associated with acquired multi-target TKI resistance and elucidate potential salvage therapies that can be utilised in subsequent multi-line therapies upon the acquisition of multi-target TKI resistance in STS.

Chapter 6

Determination of effective salvage therapy regimens for multi-target TKI-resistant malignant rhabdoid tumour

6.1 Introduction

Clinical experience of treating advanced soft tissue sarcoma (STS) patients with the multi-target TKI pazopanib has shown that patients either harbour intrinsic resistance or rapidly develop an acquired resistance on treatment (Lee *et al.*, 2019). Additionally, upon disease progression with pazopanib therapy, STS patients currently have limited treatment options (Linch *et al.*, 2014). Clinical trial data has also shown that advanced STS patients invariably develop resistance towards other multi-target TKIs currently undergoing clinical evaluation in STS, such as regorafenib, sitravatinib, and anlotinib (Mir *et al.*, 2016; Oza *et al.*, 2021; Penel *et al.*, 2020; Van Tine *et al.*, 2021). The mechanisms of action of multi-target TKIs and the resultant resistance mechanisms in STS are currently poorly understood and this limits our ability to effectively treat patients with TKI-resistant STS. By increasing our understanding of the resistance mechanisms that arise in response to multi-target TKI therapies, we can design effective treatment strategies that provide new treatment options for patients with multi-target TKI-refractory STS.

In order to determine mechanisms associated with the acquisition of multi-target TKI resistance, there is a need to derive experimental models of acquired resistance in STS. The current literature reports several experimental methods that have allowed researchers to identify and evaluate underlying mechanisms that lead to the acquisition of drug resistance in cancer. These include genome-wide knockdown, knockout, and activation screens, as well as the evaluation of matched clinical biopsy samples (pre- and post-treatment) from patients that have acquired therapy resistance (Finn *et al.*, 2020; Sanson *et al.*, 2018; Wander *et al.*, 2020; Wei *et al.*, 2019).

However, the most extensively reported method of modelling acquired resistance is using cell culture models. This method typically consists of treating initially sensitive cell models with increasing concentrations of a specific therapy, thereby leading to the eventual outgrowth of drug-resistant cells. The biological differences between the sensitive, parental cells and the resistant cells can then be evaluated for their association with the acquisition of resistance. This methodology of investigating mechanisms of acquired drug resistance has frequently been shown to recapitulate clinically relevant mechanisms of acquired resistance (Engelman *et al.*, 2007; Michaelis *et al.*, 2019; Vander Velde *et al.*, 2020). For instance, the increased

expression of the drug efflux pump p-glycoprotein in drug-resistant cells compared to sensitive parental cells was first discovered in ovarian cells that had been subjected to chronic colchicine (an anti-gout corticosteroid) treatment (Juliano & Ling, 1976).

More recently, this method has also been employed in modelling acquired tyrosine kinase inhibitor (TKI) resistance in cancer. For instance, the study by Engelman *et al.* exposed gefitinib-sensitive non-small cell lung cancer (NSCLC) to increasing gefitinib concentrations over the course of 6 months, thereby deriving a gefitinib-resistant subline (Engelman *et al.*, 2007). When compared to the sensitive parental cells, the resistant subline was shown to harbour MET amplifications which resulted in gefitinib resistance through the activation of human epidermal growth factor 3 (HER3)-dependent PI3K signalling (Engelman *et al.*, 2007). Therefore, the authors concluded that MET inhibition is a potential salvage therapy in gefitinib-resistant NSCLC (Engelman *et al.*, 2007).

Similarly, the study by Vander Velde *et al.*, 2020 derived acquired resistance in an ALK-positive NSCLC cell line through chronic and escalating treatment with ALK inhibitors, such as crizotinib and ceritinib (Vander Velde *et al.*, 2020). This study reported multifactorial and cooperating resistance mechanisms driving ALK inhibitor resistance in the NSCLC model and also highlighted the emergence of collateral sensitivities. The acquired resistance model therefore allowed the authors to determine potential salvage therapies to target these collateral sensitivities and effectively treat TKI-resistant disease (Vander Velde *et al.*, 2020).

Building on the results in **Chapter 5**, **Chapter 6** reports the derivation and characterisation of TKI-resistant sublines of the initially sensitive A204 malignant rhabdoid tumour (MRT) cell line model to the multi-target TKIs pazopanib, regorafenib, sitravatinib, and anlotinib. Following the acquisition of resistance, the TKI-resistant sublines were assessed by mass spectrometry to determine proteomic alterations associated with the acquisition of multi-target TKI resistance. The TKI-resistant sublines were also subjected to small molecule inhibitor screens to elucidate potential effective salvage therapies. Building on the findings of the inhibitor screen, sequential TKI treatment strategies were evaluated for their ability to suppress or delay multi-target TKI resistance in the A204 model of MRT.

6.2 Results

6.2.1 Derivation of multi-target TKI acquired resistance in the A204 cell line

In order to model acquired multi-target TKI resistance *in vitro*, the initially sensitive A204 cells were subjected to chronic and escalating dose treatments of pazopanib, regorafenib, sitravatinib, or anlotinib (**Figure 6.1**). A204 cells were initially grown in media containing the multi-target TKI at the IC₅₀ concentrations as determined from cell viability assays (~0.5 μ M) (**Table S5**). The multi-target TKI concentration was increased stepwise once cells had proliferated to near confluency alongside minimal visible cell death. A final TKI concentration of 5 μ M was maintained in the pazopanib-, regorafenib-, and sitravatinib-resistant cells. For anlotinib, a final TKI concentration of 3 μ M was maintained as 5 μ M consistently resulted in universal cell death.

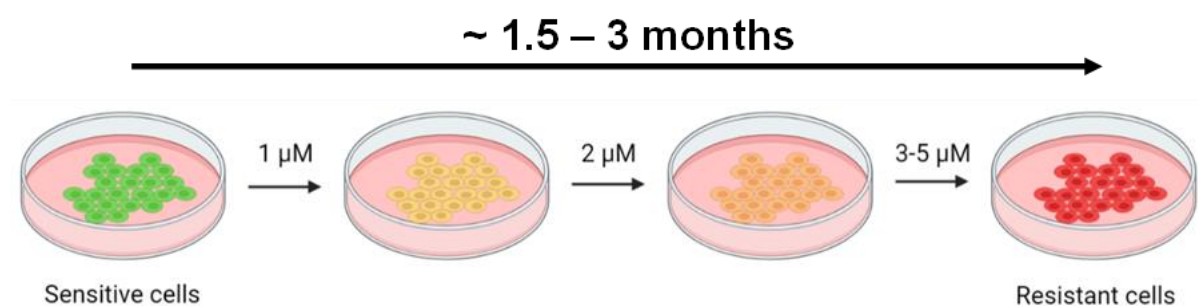


Figure 6.1: Schematic outlining the experimental process of deriving acquired multi-target TKI resistant sublines from the sensitive, parental A204 cells. Image was created using BioRender. TKI; Tyrosine kinase inhibitor.

Chronic and escalating TKI treatment resulted in the derivation of pazopanib-resistant (A204PazR), regorafenib-resistant (A204RegR), sitravatinib-resistant (A204SitR), and anlotinib-resistant (A204AnloR) A204 sublines. To confirm that the cells had developed resistance to their relative TKIs, cell viability assays and long-term colony formation assays against the respective TKIs were performed (**Figure 6.2**). The cell viability assays determined that the resistant sublines were significantly more resistant to their respective TKI than the parental A204 cells (A204PazR IC₅₀: ~7.5-fold increase, A204RegR IC₅₀: ~8-fold increase, A204SitR IC₅₀: ~8.5-fold increase, A204AnloR IC₅₀: ~3.5-fold increase) (**Figure 6.2A-H; Table S8**). Consistent with the data from these short-term assays, longer-term colony formation assays also showed significant increases in colony formation in the resistant sublines treated with their respective inhibitor, when compared to parental A204 cells (**Figure 6.2I-P**).

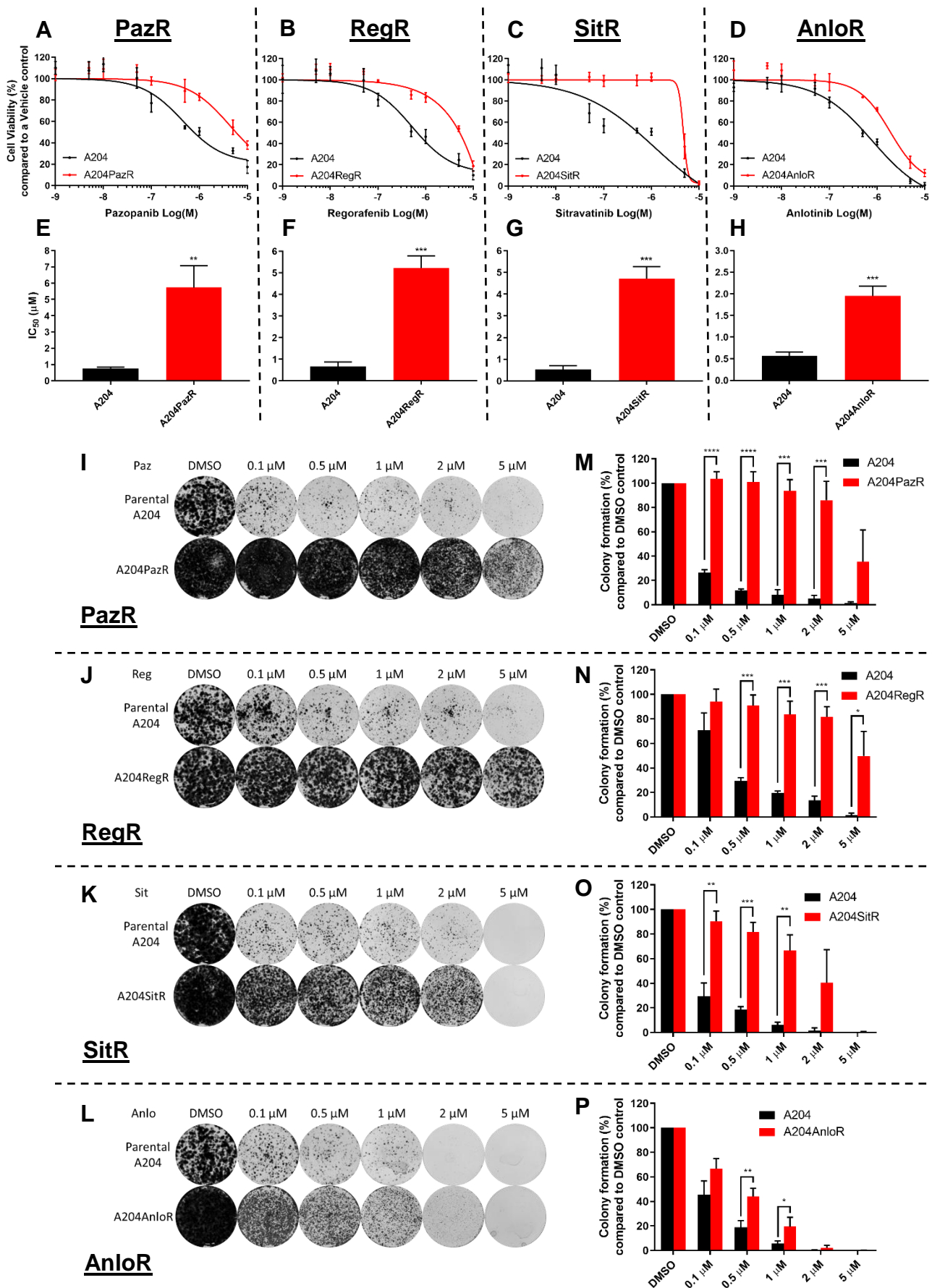


Figure 6.2: Confirmation of multi-target TKI acquired resistance in derived A204 TKI-resistant sublines. Cell viability assays of (A) A204PazR, (B) A204RegR, (C) A204SitR, and (D) A204AnloR cells treated with increasing

concentrations of their respective inhibitor to determine IC₅₀ values (**Table S8**). Bar plots displaying IC₅₀ values for **(E)** A204PazR, **(F)** A204RegR, **(G)** A204SitR, and **(H)** A204AnloR, compared to A204 parental cells. Cell viability was normalised to DMSO control (n=3). Colony formation assays of **(I)** A204PazR, **(J)** A204RegR, **(K)** A204SitR, and **(L)** A204AnloR treated with increasing concentrations of their respective inhibitor over a period of 2 weeks. Images are representative of three separate experiments (n=3). Quantification of colony formation assays was normalised to DMSO control for **(M)** A204PazR, **(N)** A204RegR, **(O)** A204SitR, and **(P)** A204AnloR. Statistical analysis was undertaken using Student's unpaired T tests (* = p ≤ 0.05, ** = p ≤ 0.01, *** = p ≤ 0.001, **** = p ≤ 0.0001). Error bars represent standard deviation. Anlo; Anlotinib, DMSO; Dimethyl sulfoxide, IC₅₀; Inhibitory constant, Paz; Pazopanib, Reg; Regorafenib, Sit; Sitravatinib, TKI; Tyrosine kinase inhibitor.

Having determined that the resistant sublines had derived acquired resistance to their respective multi-target TKIs, the resistant cells were also subjected to cell viability assays against the other three TKIs to assess whether the cells were cross-resistant (**Figure 6.3A-H**). **Figure 6.3A-H** shows that the resistant sublines were cross-resistant to all evaluated multi-target TKIs, with significantly increased resistance compared to parental cells and similar IC₅₀ levels to one another. This result suggests a shared mechanism of action between these four TKIs (**Figure 6.3A-H; Table S9**).

However, noticeable differences in the level of resistance between multi-target TKIs were observed. **Figure 6.3I-Q** shows that A204 TKI-resistant sublines had significantly increased resistance to pazopanib and regorafenib compared to sitravatinib and anlotinib. In TKI-resistant cells treated with pazopanib and regorafenib, the IC₅₀ values were in the range of 6-10 µM (**Figure 6.3I-Q; Table S9**). This was found to be significantly higher than the IC₅₀ values observed in TKI-resistant cells treated with anlotinib and sitravatinib, which were in the range of 1.5-3 µM (**Figure 6.3I-Q; Table S9**). The heatmap in **Figure 6.3Q** displays the differences in IC₅₀ values in the A204 TKI-resistant sublines.

However, if the acquired resistance to a particular inhibitor is viewed as a fold change compared to the original sensitivity of the parental A204 cells, then this pattern changes. For instance, compared to the original pazopanib sensitivity within the parental A204 cells (IC₅₀: 0.42 µM), the IC₅₀ of the TKI-resistant sublines to pazopanib (IC₅₀: 6-9 µM) has increased roughly 15- to 20-fold (**Figure 6.3R; Table S9**). Furthermore, the IC₅₀ fold change of the TKI-resistant sublines to regorafenib and sitravatinib have both increased roughly 10-fold (Regorafenib IC₅₀: 6.5-9.5 µM, Sitravatinib IC₅₀: 1.5-3 µM) when compared to the original sensitivities of the parental cells to these inhibitors (Regorafenib IC₅₀: 0.73 µM, Sitravatinib IC₅₀: 0.23 µM) (**Figure 6.3R; Table S9**). Finally, the TKI-resistant sublines showed a relatively modest fold

change in IC_{50} when treated with anlotinib, with only a roughly 3- to 4-fold increase (IC_{50} : 1.5-2.5 μ M) compared to parental A204 cells (IC_{50} : 0.57 μ M) (**Figure 6.3R; Table S9**). The heatmap in **Figure 6.3R** displays the fold differences in IC_{50} value of the TKI-resistant sublines treated with the multi-target TKIs when compared to the baseline sensitivities of the originating A204 parental cells.

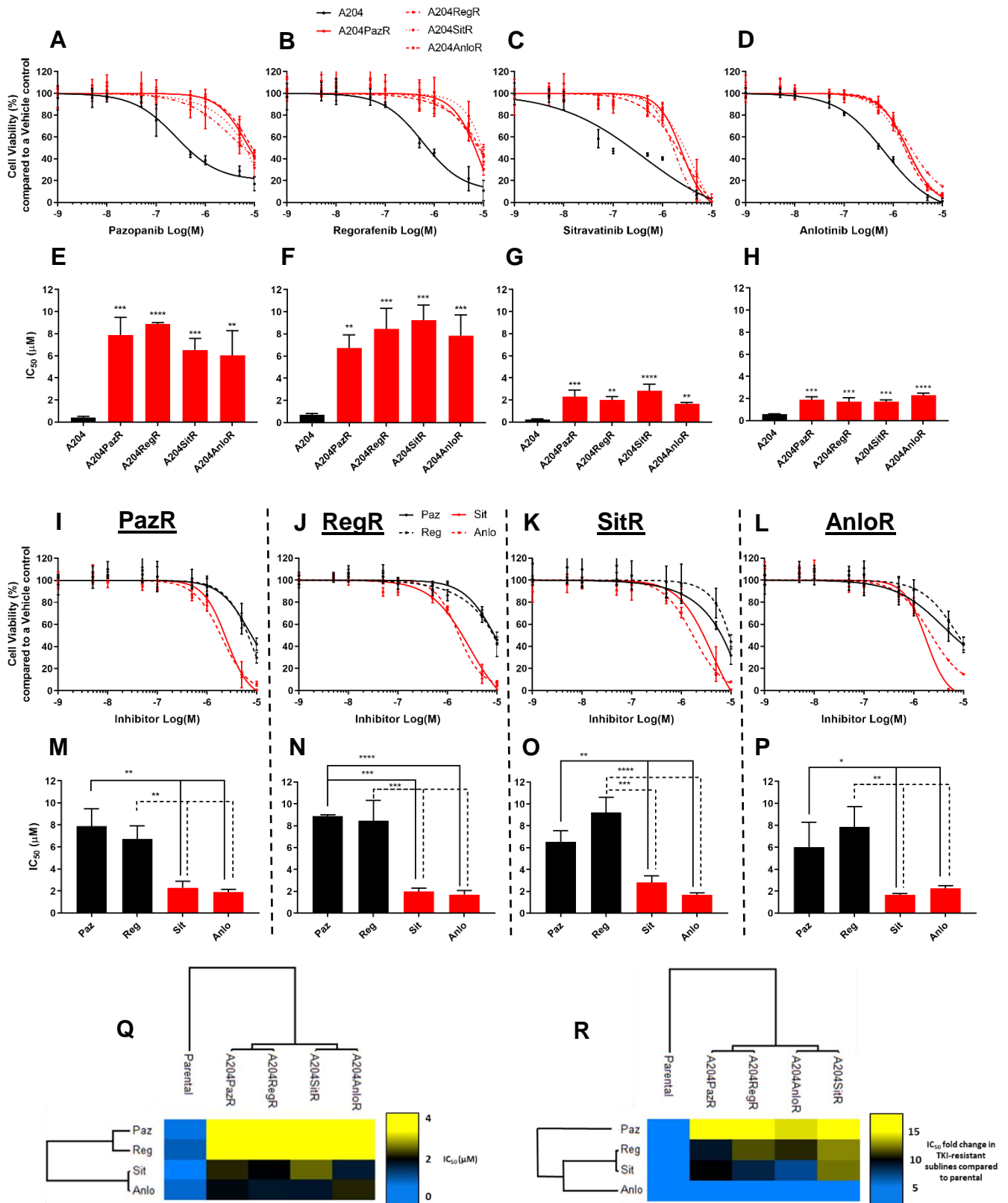


Figure 6.3: Evaluation of cross-resistance in the A204 multi-target TKI-resistant sublines. Cell viability assays of A204 multi-target TKI-resistant sublines treated with increasing concentrations of (A) pazopanib (Paz), (B) regorafenib (Reg), (C) sitravatinib (Sit), and (D) anlotinib (Anlo) to determine IC_{50} values (Table S9). Bar plots displaying IC_{50} values for (E) Paz, (F) Reg, (G) Sit, and (H) Anlo treatment in the A204 resistant sublines. Cell viability was normalised to DMSO control (n=3). Cell viability of (I) A204PazR, (J) A204RegR, (K) A204SitR, and (L) A204AnloR cells treated with increasing concentrations of Paz, Reg, Sit, or Anlo to determine IC_{50} values (Table S9). Bar plots displaying IC_{50} values for (M) A204PazR, (N) A204RegR, (O) A204SitR, and (P) A204AnloR. Cell viability was normalised to DMSO control

(n=3). The data shown in **(A-P)** are the same data but presented in different ways. **(Q)** Heatmap displaying the differences in IC₅₀ values of the A204 TKI-resistant sublines treated with the four multi-target TKIs. **(R)** Heatmap displaying the fold change in IC₅₀ values in the A204 TKI-resistant sublines treated with the four multi-target TKIs when compared to the original sensitivity in the A204 parental cells. Statistical analysis was undertaken using one-way ANOVAs with Dunnett's (compared to A204 parental) **(E-H)** or Tukey's **(M-P)** multiple comparison tests (* = p ≤ 0.05, ** = p ≤ 0.01, *** = p ≤ 0.001, **** = p ≤ 0.0001). Error bars represent standard deviation. ANOVA; Analysis of variance, DMSO; Dimethyl sulfoxide, IC₅₀; Inhibitory constant, TKI; Tyrosine kinase inhibitor.

6.2.2 Multi-target TKI-resistant A204 cells harbour reduced PDGFR α expression and Akt signalling activity

Previous work has shown that the receptor tyrosine kinases (RTKs) platelet-derived growth factor receptor α (PDGFR α) and fibroblast growth factor receptor 1 (FGFR1) are highly expressed and co-activated in the A204 cell line model (Bai *et al.*, 2012; Wong *et al.*, 2016). As these RTKs are targets of multi-target TKIs such as pazopanib, regorafenib, sitravatinib, and anlotinib, immunoblotting was undertaken to evaluate potential changes in RTK expression upon the acquisition of TKI resistance. As shown in **Figure 6.4A-B**, PDGFR α expression is notably decreased in the TKI-resistant sublines compared to parental control. Conversely, no effect upon FGFR1 expression was observed with the acquisition of multi-target TKI resistance (**Figure 6.4A-B**). These immunoblots were undertaken in the absence of inhibitor, with the cells instead treated with DMSO and cultured for 6 or 72 hours, after an initial seeding of 24 hours. **Figure 6.4B** shows that the loss of PDGFR α expression in the TKI-resistant sublines compared to parental cells was consistent in both the 6 hour and 72 hour experiments.

Following this, I wanted to investigate potential differences in the phosphorylation levels of downstream effector proteins Akt and ERK1/2 in the TKI-resistant sublines and parental A204 cells, both in the presence and absence of inhibitor. I therefore subjected the cells to 6 hours of 1 μ M of their respective inhibitor (or DMSO), after an initial seeding of 24 hours (**Figure 6.4C**). I found that baseline Akt phosphorylation was notably reduced in the TKI-resistant sublines compared to parental A204 cells. Conversely, ERK1/2 phosphorylation remained unchanged upon the acquisition of TKI resistance. Although **Figure 6.4C** shows a consistent increase in ERK1/2 phosphorylation in the A204 TKI-resistant sublines when compared to parental cells, I found that this was not a robust and reproducible phenotype in later experiments.

Finally, treatment of the TKI-resistant A204 sublines with their respective inhibitor had no noticeable effect upon either Akt or ERK1/2 phosphorylation (**Figure 6.4C**).

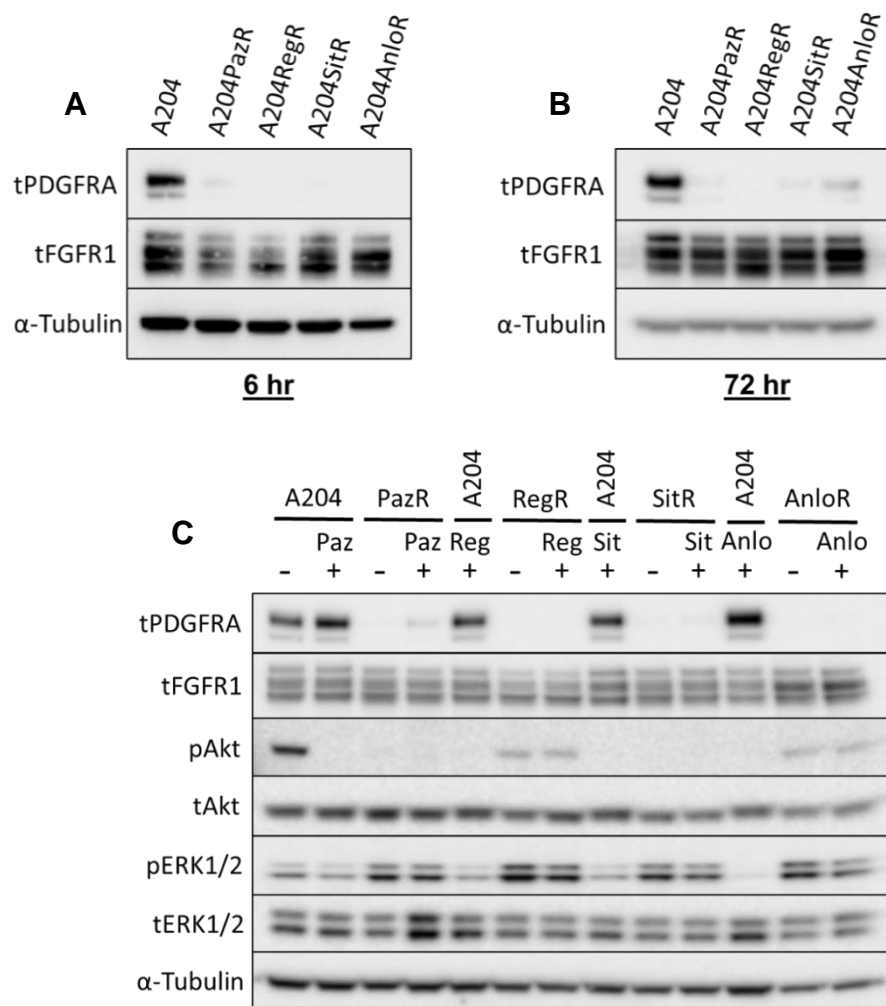


Figure 6.4: Immunoblots of A204 parental and TKI-resistant sublines to evaluate PDGFR α and FGFR1 expression and downstream effector phosphorylation profiles. Immunoblots of PDGFR α and FGFR1 expression levels in A204 parental and TKI-resistant sublines after (A) 6 hours or (B) 72 hours, after an initial 24-hour seeding period. (C) Immunoblot of PDGFR α , FGFR1, Akt, and ERK1/2 expression and/or phosphorylation levels after 6 hours of treatment with 1 μ M of indicated TKI or DMSO. Images are representative of two separate experiments (n=2). Anlo; Anlotinib, DMSO; Dimethyl sulfoxide, ERK1/2; Extracellular signal-regulated kinase 1/2, FGFR1; Fibroblast growth factor receptor 1, Paz; Pazopanib, PDGFR α ; Platelet-derived growth factor receptor α , Reg; Regorafenib, Sit; Sitravatinib, TKI; Tyrosine kinase inhibitor.

6.2.3 Proteomic analysis of A204 TKI-resistant sublines reveal common alterations associated with multi-target TKI resistance

To assess for proteomic differences that are consistently observed in TKI-resistant cells compared to parental cells, global proteomic assessment by mass spectrometry

was performed (**Figure 6.5**). This analysis allowed for the determination of proteins that are associated with multi-target TKI resistance in MRT. Subsequently, this will allow for future evaluation of whether these proteins are causative factors in the emergence of acquired TKI resistance in cell models of MRT. Cell lysates were collected from parental and TKI-resistant cells after 72 hours of culturing without inhibitor, following an initial 24 hours of seeding. Two biological replicates were collected for each of the TKI-resistant sublines and the A204 parental cells. Biological replicates were performed upon consecutive cell passages and the collected lysates were run as a single batch in the mass spectrometry machine. Running of the mass spectrometry machine was conducted by Dr. Lukas Krasny – a post-doctoral fellow within our lab – and the bioinformatic analysis was performed by Jessica Burns – a PhD student within our lab.

The analysis identified 4300 proteins across the A204 parental cells and TKI-resistant sublines. As expected, the proteomic profiles of biological replicates were found to cluster together (**Figure 6.5**). Furthermore, the proteomic profiles of the resistant sublines A204PazR, A204RegR, and A204SitR were found to cluster with one another, whilst A204AnloR clustered with the A204 parental cells (**Figure 6.5**).

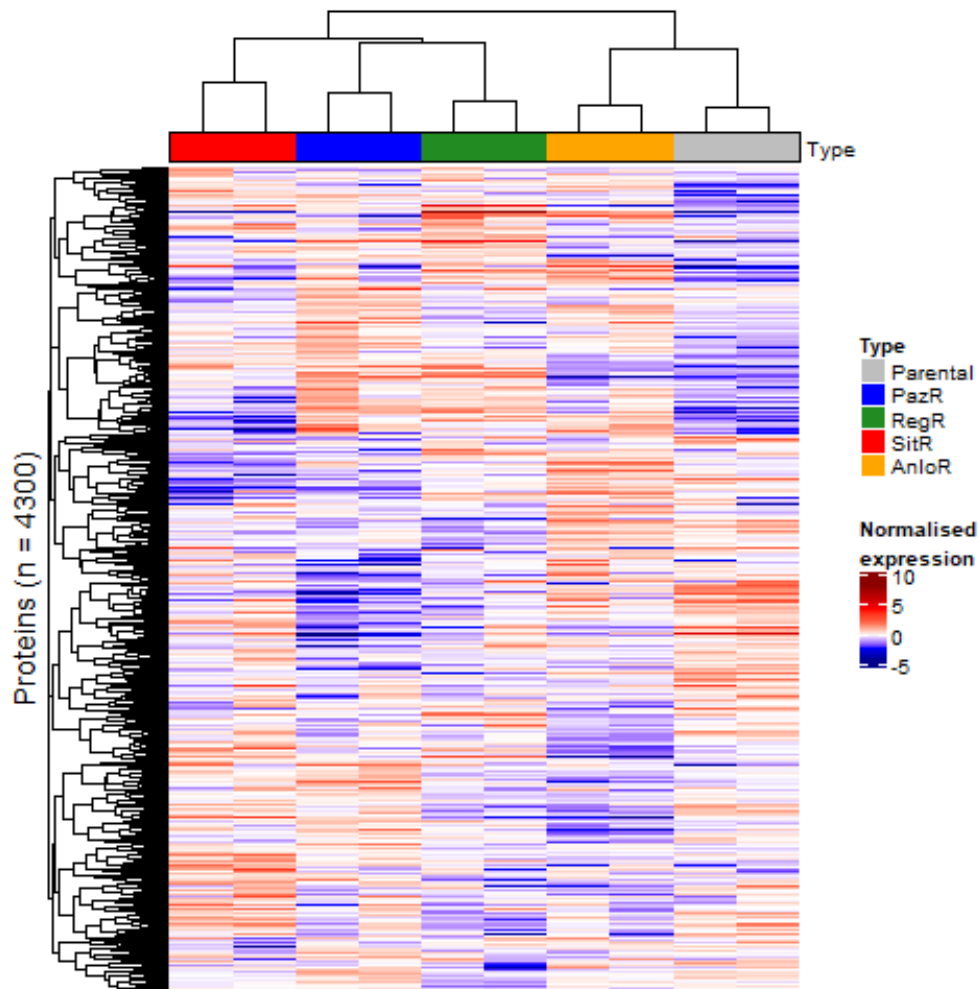


Figure 6.5: Heatmap of global proteomic analysis of A204 parental cells and TKI-resistant sublines. Data was filtered for master proteins with a false discovery rate (FDR) < 0.01, a minimum of 2 peptides, and no missing values. Data was \log_2 transformed and normalised by cross sample median-centring followed by within sample standardisation. Heatmap was generated by unsupervised hierarchical clustering using Pearson's correlation distance (n=2 biological replicates). Analysis was performed in R version 4.0.2, using the packages tidyverse, samr, ComplexHeatmap, and circlize,

Pearson's correlation was used to cluster the data and determine the reproducibility between biological replicates. Although the Pearson's correlation coefficient is relatively low in certain inter-replicate comparisons (labelled with red squares on **Figure 6.6**) (e.g., SitR; $r^2 = 0.39$), the coefficients between replicates was found to be higher than in any of the other cross-sample comparisons (**Figure 6.6**).

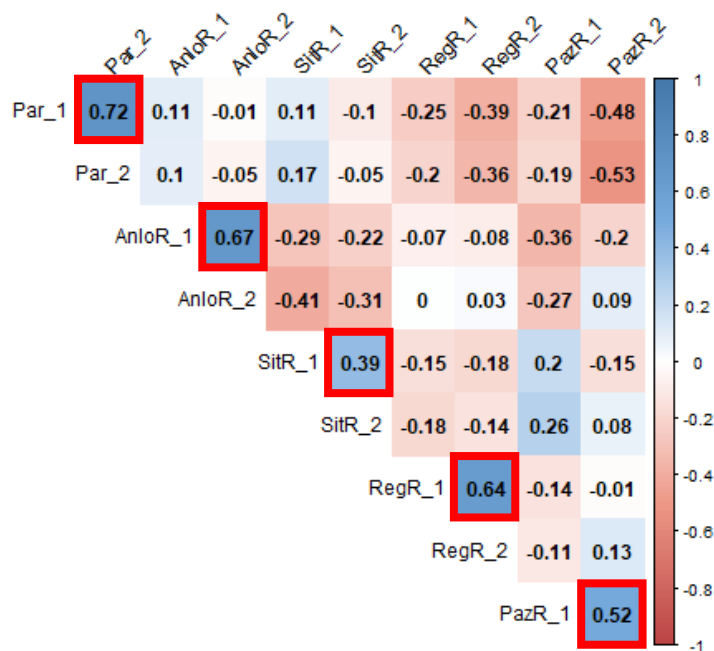


Figure 6.6: Pearson's correlation of proteomic A204 parental and TKI-resistant subline biological replicates. Values indicate Pearson's correlation coefficient (r^2). 1 indicates high positive correlation, 0 indicates no correlation, and -1 indicates high negative correlation. Analysis was performed in R version 4.0.2, using the packages tidyverse, samr, ComplexHeatmap, and circlize. AnloR; Anlotinib-resistant, Par; Parental, PazR; Pazopanib-resistant, RegR; Regorafenib-resistant, SitR; Sitravatinib-resistant.

Using the data generated in **Figure 6.5**, significance analysis of microarrays (SAM) 2-class unpaired tests identified 11 proteins whose expression was significantly (q value < 0.01) different in the TKI-resistant sublines compared to parental A204 cells (**Figure 6.7**). **Figure 6.7** shows that the 11 proteins were commonly and significantly downregulated in the TKI-resistant sublines when compared to the parental cells. To note, the analysis did not reveal any proteins that were commonly and significantly upregulated in the TKI-resistant sublines compared to parental A204 cells.

Table 6.1 outlines the general function of these proteins, as well as the central biological pathways in which they are involved. Several examples of these include proteins involved in FGF signalling (FGFBP1), purine and carbohydrate metabolism (AMPD2, CHST14, GALNT7), and Wnt signalling (FZD2). It must be noted however that CRH and FGFBP1, despite being significantly downregulated compared to parental, was still found to be highly expressed in the A204AnloR cells compared to the remaining TKI-resistant sublines. The data outlined in **Figure 6.7** warrants further evaluation into whether the downregulation of these proteins is a causative factor in the emergence of acquired multi-target TKI resistance in MRT.

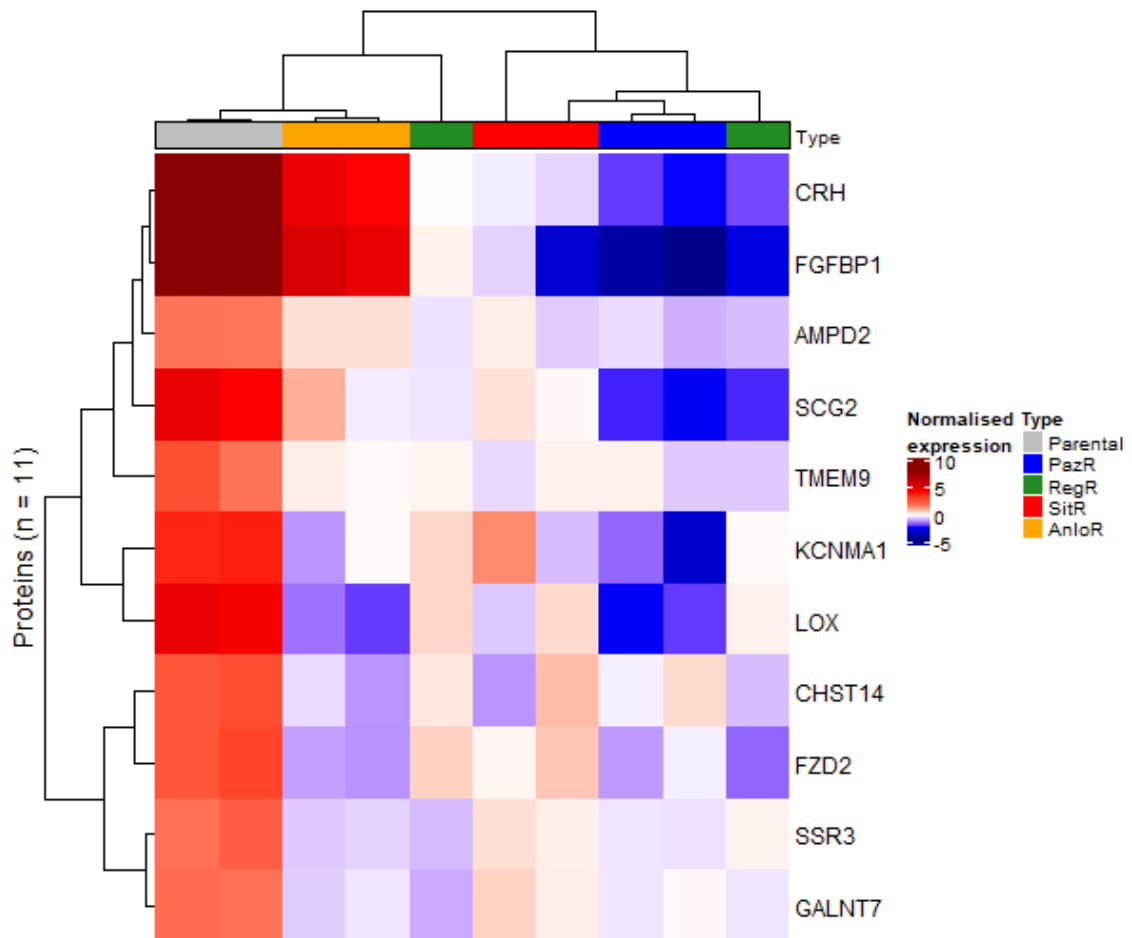


Figure 6.7: Heatmap of proteins found to be differentially expressed in multi-target TKI-resistant sublines compared to A204 parental cells. Differential protein expression was determined by comparison of TKI-resistant subline data to parental cells utilising SAM 2-class unpaired tests with significant differences of q value < 0.01. Heatmap was generated by unsupervised hierarchical clustering using Pearson's correlation distance (n=2). SAM; Significance analysis of microarrays.

Table 6.1: Differentially expressed proteins in TKI-resistant sublines compared to parental cells, with protein names, general function, and gene ontology annotations.

Gene	Protein	General function	Gene ontology annotations
<i>CRH</i>	Corticotropin releasing hormone	Neuropeptide hormone	Signalling receptor binding Neuropeptide hormone activity
<i>FGFBP1</i>	FGF binding protein 1	FGF carrier protein	FGF and heparin binding
<i>AMPD2</i>	Adenosine monophosphate deaminase 2	Purine metabolic enzyme	Deaminase activity
<i>SCG2</i>	Secretogranin II	Neuroendocrine secretory protein	Cytokine activity Chemoattractant activity
<i>TMEM9</i>	Transmembrane protein 9	Binds and facilitates assembly of ATPases	Protein assembly and function
<i>KCNMA1</i>	Potassium calcium-activated channel subfamily M α 1	Voltage-gated potassium channel	Actin binding Voltage-gated potassium channel activity
<i>LOX</i>	Lysyl oxidase	Lysyl oxidase	Copper ion binding Protein-lysine 6-oxidase activity
<i>CHST14</i>	Carbohydrate sulfotransferase 14	Sulfotransferase	Sulfotransferase activity N-acetylgalactosamine 4-O-sulfotransferase activity
<i>FZD2</i>	Frizzled class receptor 2	Wnt-pathway GPCR	GPCR activity PDZ domain binding
<i>SSR3</i>	Signal sequence receptor subunit 3	ER receptor	Protein translocation across ER
<i>GALNT7</i>	Polypeptide N-acetylgalactosaminyltransferase	Galactosyltransferase	Carbohydrate binding and metabolism Polypeptide N-acetylgalactosaminyltransferase activity

ATPase; Adenosine triphosphate hydrolase, ER; Endoplasmic reticulum, FGF; Fibroblast growth factor, GPCR; G-protein coupled receptor.

6.2.4 A small molecule inhibitor screen identifies salvage therapies for TKI-resistant malignant rhabdoid tumour

In order to elucidate pathway dependencies in the A204 TKI-resistant sublines and identify potential salvage therapies for multi-target TKI-resistant MRT, the previously described (**Chapter 3.2.3**) small molecule inhibitor screen was utilised with a number of minor variations (**Table 6.2; Figure 6.8A**). Firstly, the multi-target TKIs cabozantinib, nintedanib, nilotinib, and axitinib had not yet been incorporated into the inhibitor screen at the time of the experiment outlined in **Figure 6.8A**. Secondly, due to the potent antitumour activity observed with erdafitinib (JNJ-42756493) in **Chapter 5**, this TKI was included in the inhibitor screen shown in **Figure 6.8A**. The inhibitors utilised within this screen are outlined in **Table 6.2**.

Table 6.2: Small molecule inhibitors utilised within the A204 parental and TKI-resistant subline screens

Small molecule inhibitor	Primary target(s)
Cediranib	Broad spectrum: RTKs
Foretinib	Broad spectrum: RTKs
Imatinib	Broad spectrum: RTKs, Abl1
Lenvatinib	Broad spectrum: RTKs
Pazopanib	Broad spectrum: RTKs
Ponatinib	Broad spectrum: RTKs, Abl1
Regorafenib	Broad spectrum: RTKs
Sorafenib	Broad spectrum: RTKs, C-Raf, B-Raf
Sunitinib	Broad spectrum: RTKs
Vandetanib	Broad spectrum: RTKs
Entrectinib	NTRK1/2/3, ROS1, ALK
GW441756	NTRK1
Ceritinib	ALK
Crizotinib	ALK, MET
NVP-TAE684	ALK
Osimertinib (AZD-9291)	EGFR
EAI045	EGFR
Erlotinib	EGFR
Gefitinib	EGFR
Lapatinib	EGFR, HER2
Neratinib	EGFR, HER2
Infigratinib (BGJ-398)	FGFR1/2/3
Erdafitinib (JNJ-42756493)	FGFR1/2/3/4
Linsitinib	IGF1R
NVP-AEW541	IGF1R, InsR
Cilengitide trifluoroacetate	Integrins $\alpha\beta3$, $\alpha\beta5$
Bosutinib	Src, Abl1
Dasatinib	Src, Abl1, Broad spectrum: RTKs
Saracatinib	Src
PF562271	FAK
TAE226	FAK
BI-2536	PLK1
BX-795	PDPK1
Dactolisib (BEZ235)	PI3K, mTOR
Rapamycin (Sirolimus)	mTOR
Binimetinib	MEK1/2
Trametinib	MEK1/2
Dabrafenib	B-Raf V600E
Adezmapimod (SB203580)	p38 MAPK
SP600125	JNK1/2/3
Capivasertib (AZD-5363)	Akt1/2/3
MK2206	Akt1/2/3
Mometinib	JAK1/2
Niclosamide	STAT3
SH-4-54	STATs
Galunisertib	TGF β R1
BMS345541	IKK1/2
Alisertib	Aurora A
Rabusertib (LY2603618)	Chk1
MK8776	Chk1
Palbociclib	CDK4/6
Silmitasertib	CK2
Talazoparib	PARP
Rucaparib	PARP
XAV-939	Tankyrase
Navitoclax	Bcl-2, Bcl-w, Bcl-xL
GSK126	EZH2
JQ1	BET bromodomains
Luminespib (NVP-AUY922)	Hsp90

ADP; Adenosine diphosphate, ALK; Anaplastic lymphoma kinase, Bcl-(2/xL); B-cell lymphoma (2/extra large) protein; Bcl-w; Bcl-2-like protein 2, Bcr; Breakpoint cluster region protein, BET; Bromo- and extra-terminal domain, CDK(4/6); Cyclin-dependent kinase (4/6); Chk1; Checkpoint kinase 1, CK2; Casein kinase 2, EGFR; Epidermal growth factor, EZH2; Enhancer of zeste homolog 2, FAK; Focal adhesion kinase, FGFR(1/2/3/4); Fibroblast growth factor receptor (1/2/3/4), HER2; Human epidermal growth factor receptor 2, Hsp90; Heat shock protein 90, IGF1R; Insulin-like growth factor 1 receptor, IKK(1/2); I κ B kinase (1/2), InsR; Insulin receptor, JAK(1/2); Janus kinase (1/2), JNK(1/2/3); c-Jun N-terminal kinase (1/2/3), MAPK; Mitogen-activated protein kinase, MEK; Mitogen-activated protein kinase kinase, mTOR; Mechanistic target of rapamycin, N-terminal; Amino-terminal, NTRK(1/2/3); Neurotrophic tyrosine kinase receptor (1/2/3) PARP; Poly (ADP-ribose) polymerase, PDPK1; Phosphoinositide-dependent protein kinase 1, PI3K; Phosphoinositide 3-kinase, PLK1; Polo-like kinase 1, (B/C)-Raf; Rapidly accelerated fibrosarcoma, RTK; Receptor tyrosine kinase, STAT(3); Signal transducer and activator of transcription (3), TGF β R1; Transforming growth factor β receptor 1.

The inhibitor screens were carried out in the parental A204 cell line and the TKI-resistant sublines, with cells treated with 0.5 μ M inhibitor and cell viability assessed after 72 hours. I performed subsequent overlap analysis to evaluate the different and common sensitivities between models (**Figure 6.8A-B**). To assess the reproducibility of the small molecule inhibitor screens, Pearson's correlation analysis was performed between biological replicates (n=2). Pearson's correlation analysis reported very high correlation ($r^2 > 0.80$) for all the inhibitor screens performed, thereby confirming high reproducibility between biological replicates (**Figure 6.8C-G**).

Two-way hierarchical clustering determined that the TKI-resistant A204 cells shared similar inhibitor response profiles to one another when compared to parental A204 cells (**Figure 6.8A**). Consistent with previously described cytotoxicity in a wide variety of human cancer cell models regardless of underlying pathology, dactolisib (BEZ235) and BI-2536 were shown to be highly potent in both the parental and TKI-resistant cells (**Figure 6.8A-B**) (Seashore-Ludlow *et al.*, 2015). The screen also displayed the potent sensitivities of both the parental cells and TKI-resistant sublines to the Hsp90 inhibitor, luminespib (NVP-AUY922), thereby recapitulating the findings by Vyse *et al.* in dasatinib- and pazopanib-resistant A204 models (Vyse *et al.*, 2018).

The screen also showed that the TKI-resistant sublines became collaterally resistant to a number of inhibitors which the originating A204 parental cells were sensitive to. Collateral resistance refers to the emergence of resistance towards a particular drug that the resistant cells have not been exposed to. As shown in **Figure 6.8B**, I found that all of the TKI-resistant sublines became collaterally resistant to nine inhibitors, with eight of these being multi-target TKIs (sorafenib, sunitinib, pazopanib, imatinib, regorafenib, lenvatinib, cediranib, and dasatinib) (**Table S10**). The collateral resistance of pazopanib and regorafenib is consistent with the cross-resistance data reported in **Figure 6.3** for the TKI-resistant sublines. Furthermore, the collateral resistance to sunitinib and dasatinib in multi-target TKI-resistant A204 cells is consistent with previous work by Wong *et al.* (Wong *et al.*, 2016).

Additionally, the screen also replicated the findings by Wong *et al.* that found that TKI-resistant A204 cells retained high sensitivities towards ponatinib treatment (**Figure 6.8A-B**) (Wong *et al.*, 2016). The screen also elucidated previously undescribed vulnerabilities and collateral sensitivities. Firstly, the TKI-resistant sublines were found

to be vulnerable to erdafitinib treatment, which clustered alongside ponatinib (**Figure 6.8A-B**). Therefore, erdafitinib, as well as ponatinib, was taken forward for further evaluation in the A204 TKI-resistant sublines.

Interestingly, the inhibitor screen shows that the acquisition of sitravatinib or anlotinib resistance in the A204 cells results in the development of potent infigratinib (BGJ-398) collateral sensitivity. Collateral sensitivity is a phenomenon whereby drug-resistant cells acquire sensitivity towards a drug that the originating parental cells were resistant to (Pluchino *et al.*, 2012). In the instance of collateral sensitivity outlined in **Figure 6.8A-B**, the parental A204 cells were resistant to infigratinib treatment at 0.5 μ M concentration. However, upon acquisition of sitravatinib or anlotinib resistance, the cells become sensitive to infigratinib. Furthermore, I found that this phenotype was exclusive to cells that had become resistant to sitravatinib or anlotinib, with A204PazR and A204RegR continuing to display resistance towards infigratinib (**Figure 6.8A-B**). Therefore, infigratinib was also taken forward for further analysis in the A204 TKI-resistant sublines.

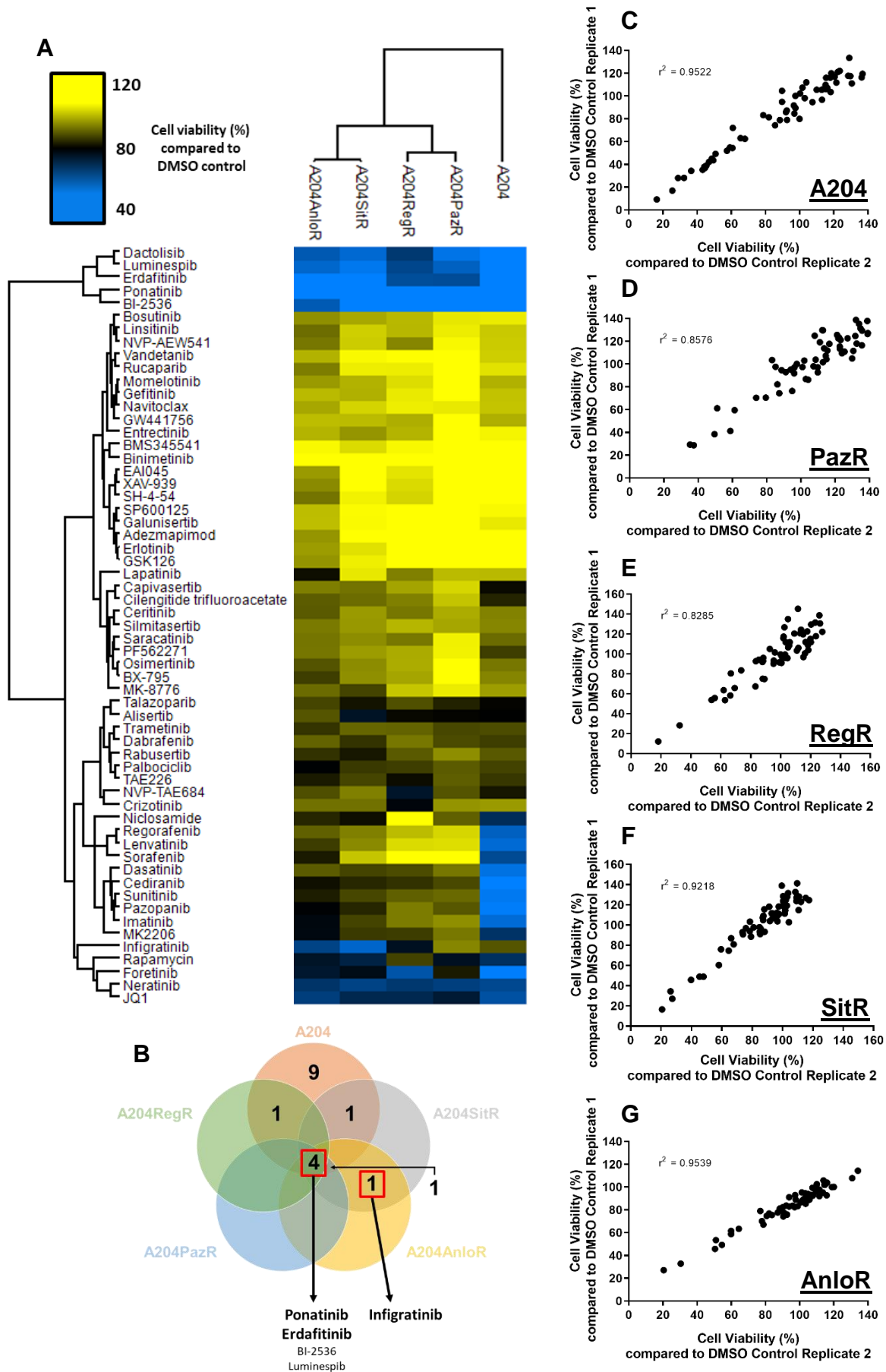


Figure 6.8: Small molecule inhibitor screens of parental A204 cells and TKI-resistant sublines. (A) Small molecule inhibitor screens of A204 and TKI-resistant sublines at an inhibitor concentration of 0.5 μ M. Cell viability was normalised to DMSO control (n=2). Two-way hierarchical clustering based on Euclidean distance was performed by

Perseus software (Tyanova *et al.*, 2016). **(B)** Venn diagram showing the inhibitor overlap between effective ($\leq 60\%$ cell viability compared to DMSO control) inhibitors from small molecule inhibitor screens of parental A204 and TKI-resistant sublines (**Table S10**). Pearson's correlation analysis of biological replicates for **(C)** A204, **(D)** A204PazR, **(E)** A204RegR, **(F)** A204SitR, and **(G)** A204AnloR. Y-axes show the results of biological replicate 1 and the x-axes show the results of biological replicate 2. DMSO; Dimethyl sulfoxide, TKI; Tyrosine kinase inhibitor.

6.2.5 Confirmation of erdafitinib and ponatinib activity in multi-target TKI-resistant A204 sublines

I firstly wanted to validate the findings of the inhibitor screen in relation to erdafitinib and ponatinib activity in the A204 TKI-resistant sublines. To achieve this, I undertook cell viability assays of the TKI-resistant sublines treated with full dose response of erdafitinib, ponatinib, or the TKI-resistant subline's respective inhibitor (e.g., either pazopanib, regorafenib, sitravatinib, or anlotinib) (**Figure 6.9A-H**). As shown in **Figure 6.9A-H**, both erdafitinib and ponatinib significantly reduced cell viability compared to the subline's respective TKI (**Table S11**).

For instance, treatment of the TKI-resistant sublines with erdafitinib resulted in an IC_{50} value that was ~4.5- to ~9-fold smaller (A204PazR: 1.22 μ M, A204RegR: 1.02 μ M, A204SitR: 0.24 μ M, A204AnloR: 0.23 μ M) than compared to treatment with the subline's respective multi-target TKI (A204PazR: 5.55 μ M, A204RegR: 7.02 μ M, A204SitR: 2.12 μ M, A204AnloR: 1.50 μ M) (**Figure 6.9A-H; Table S11**). Similarly, treatment with ponatinib resulted in IC_{50} values in the range of 0.20-0.27 μ M, which was found to be a ~26-fold decrease (for A204PazR and A204RegR) or ~9-fold decrease (for A204SitR and A204AnloR) when compared to treatment with the subline's respective multi-target TKI (**Figure 6.9A-H; Table S11**).

Following this, I wanted to evaluate whether long-term treatment of TKI-resistant sublines with erdafitinib and ponatinib could reduce the ability of cells to proliferate and form colonies. Consistent with the short-term cell viability assays, the 2-week colony formation assays displayed in **Figure 6.9I-J** showed that both erdafitinib and ponatinib significantly reduced the ability of TKI-resistant sublines to form colonies compared to DMSO (**Figure 6.9I-J**). In fact, treatment with ponatinib consistently resulted in the complete inability of cells to form colonies (**Figure 6.9I-J**).

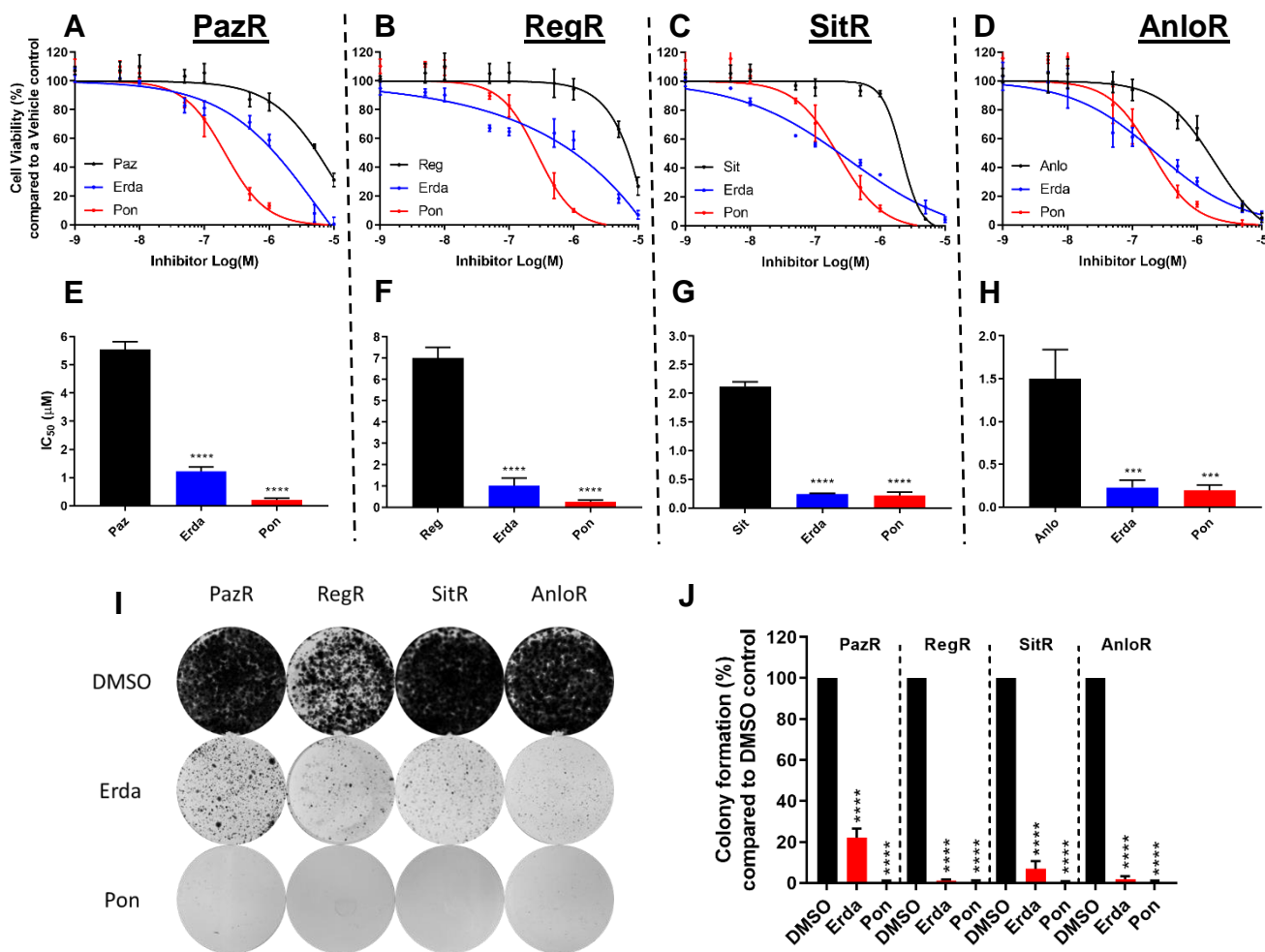


Figure 6.9: Confirmation of A204 multi-target TKI-resistant subline sensitivities to erdafitinib and ponatinib. Cell viability assays of (A) A204PazR, (B) A204RegR, (C) A204SitR, and (D) A204AnloR treated with increasing concentrations of erdafitinib (Erda), ponatinib (Pon), or their respective multi-target TKI to determine IC₅₀ values (Table S11). Bar plots displaying IC₅₀ values for (E) A204PazR, (F) A204RegR, (G) A204SitR, and (H) A204AnloR. Cell viability was normalised to DMSO control (n=3). Colony formation assays of A204 TKI-resistant sublines treated with 1 μM inhibitor over a period of 2 weeks. Image is representative of three separate experiments (n=3). (J) Quantification of colony formation assays was normalised to DMSO control. Statistical analysis was undertaken using one-way ANOVAs with Dunnett's multiple comparison tests (compared to respective multi-target TKIs for cell viability assays) (compared to DMSO for colony formation assays) (** = p ≤ 0.01, *** = p ≤ 0.001, **** = p ≤ 0.0001). Error bars represent standard deviation. Anlo; Anlotinib, ANOVA; Analysis of variance, DMSO; Dimethyl sulfoxide, IC₅₀; Inhibitory constant, Paz; Pazopanib, Reg; Regorafenib, Sit; Sitravatinib, TKI; Tyrosine kinase inhibitor.

Having determined the antiproliferative activity of these TKIs, I next evaluated whether erdafitinib and ponatinib had pro-apoptotic activity in the A204 TKI-resistant sublines. Caspase 3/7 apoptosis assays determined that treatment of the TKI-resistant sublines with their respective inhibitor did not significantly alter apoptosis levels, consistent with the resistance phenotype observed in proliferation assays (Figure 6.10A-H). However, treatment with erdafitinib and ponatinib significantly enhanced apoptosis in the majority of A204 TKI-resistant sublines, compared to both DMSO (erdafitinib: >2-fold, ponatinib: >4-fold enhancement) and the subline's respective multi-target TKI

(erdafitinib: >2-fold, ponatinib: >3-fold enhancement) (**Figure 6.10A-H**). Interestingly, although ponatinib treatment was found to significantly induce apoptosis in the A204RegR subline (>7-fold increase relative to DMSO), significant pro-apoptotic effects were not observed with erdafitinib treatment (**Figure 6.10B & F**). **Figure 6.10B** shows that treatment of A204RegR cells with erdafitinib treatment resulted in apoptotic levels similar to those observed with DMSO and regorafenib treatments (**Figure 6.10B & F**).

I next wanted to assess the effects of erdafitinib and ponatinib treatment on the activity of downstream effector proteins Akt and ERK1/2 in the A204 TKI-resistant sublines. I therefore subjected the cell models to 6 hours of 1 μ M treatment with either erdafitinib or ponatinib and subsequently evaluated for phosphorylation changes via immunoblotting. I found that both erdafitinib and ponatinib treatment suppressed ERK1/2 phosphorylation in the parental A204, A204PazR, A204SitR, and A204AnloR models, when compared to DMSO (**Figure 6.10I**).

As Akt is intrinsically suppressed in these sublines, these results are consistent with the findings of **Chapter 5** and Wong *et al.*, whereby the dual suppression of Akt and ERK1/2 pathways correlate with enhanced apoptosis in the A204 cell models (**Figure 6.10A-I**). Consistent with this, erdafitinib treatment was found to have no effect on ERK1/2 phosphorylation in the A204RegR subline, with this signalling pathway remaining highly activated in this model (**Figure 6.10I**). This phenotype corresponded with no significant increase in A204RegR apoptosis levels with erdafitinib treatment (**Figure 6.10B & F**). Interestingly, ponatinib continued to suppress ERK1/2 phosphorylation in the A204RegR subline, correlating with enhanced apoptosis.

However, whilst dual suppression of Akt and ERK1/2 may be associated with enhanced apoptosis, inhibition of ERK1/2 alongside intrinsic Akt suppression does not fully describe the antiproliferative effects observed with erdafitinib and ponatinib. This is because the inhibitor screen did not reveal activity of the MEK inhibitor trametinib in the A204 TKI-resistant sublines. If ERK1/2 inhibition was sufficient to explain the antiproliferative effects of erdafitinib and ponatinib, it would be expected that a direct MAPK pathway inhibitor, such as trametinib, would recapitulate this effect. Furthermore, erdafitinib was found to have antiproliferative effects in the A204RegR subline, despite not having an effect on ERK1/2 phosphorylation. These results

suggest that erdafitinib and ponatinib treatment are inhibiting additional, currently unknown signalling pathway(s) that are resulting in the observed antiproliferative effect. Future exploration focussing on the effects of erdafitinib and ponatinib upon additional downstream signalling pathways of RTK is warranted, such as Src, STAT3, and phospholipase C γ . Future work will also aim to determine the reason behind why erdafitinib treatment does not inhibit ERK1/2 phosphorylation in the A204RegR subline, but ponatinib continues to do so.

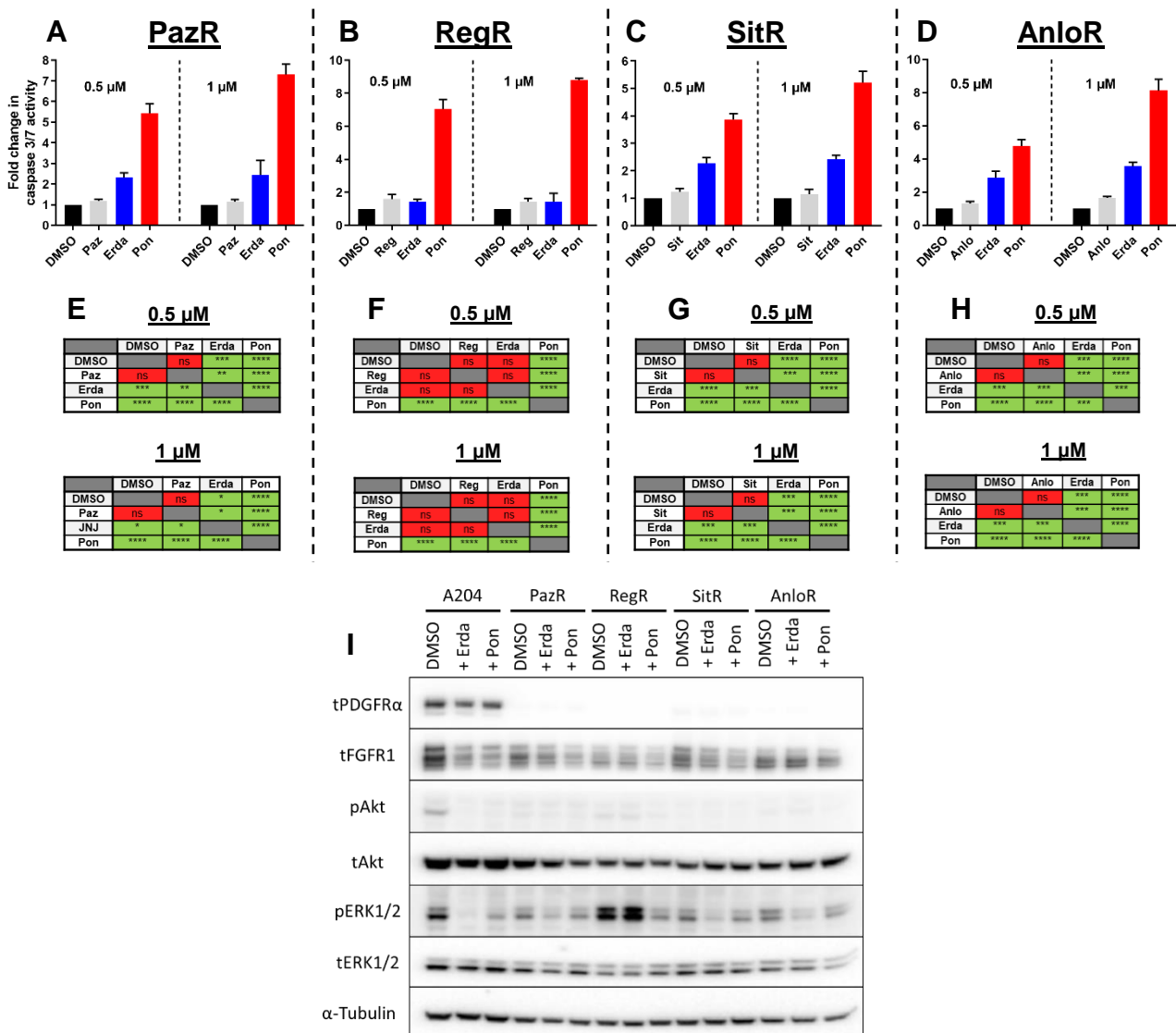


Figure 6.10: Apoptotic and signalling modulations in response to erdafitinib and ponatinib treatment of A204 TKI-resistant sublines. Bar plots displaying the fold change in caspase 3/7 activity in the (A) A204PazR, (B) A204RegR, (C) A204SitR, and (D) A204AnloR cells treated with two concentrations of erdafitinib (Erda), ponatinib (Pon), or respective multi-target TKI for 24 hours. Fold change was normalised to DMSO control (n=3). Grids displaying the statistical significance between the different treatments at two difference concentrations in the (E) A204PazR, (F) A204RegR, (G) A204SitR, and (H) A204AnloR cells in the apoptosis assays. (I) Immunoblot of PDGFR α , FGFR1, Akt, and ERK1/2 expression and/or phosphorylation levels after 6 hours of treatment with 1 μ M of indicated TKI or DMSO. Image is representative of two separate experiments (n=2). Statistical analysis was undertaken using one-way

ANOVAs with Tukey's multiple comparison tests (* = $p \leq 0.05$, ** = $p \leq 0.01$, *** = $p \leq 0.001$, **** = $p \leq 0.0001$). Error bars represent standard deviation. Anlo; Anlotinib, ANOVA; Analysis of variance, DMSO; Dimethyl sulfoxide, ERK1/2; Extracellular signal-regulated kinase 1/2, FGFR1; Fibroblast growth factor receptor 1, ns; Non-significant, Paz; Pazopanib, PDGFR α ; Platelet-derived growth factor receptor α , Reg; Regorafenib, Sit; Sitravatinib, TKI; Tyrosine kinase inhibitor.

6.2.6 Assessment of infigratinib collateral sensitivity in the multi-target TKI-resistant A204 sublines

The small molecule inhibitor screen also revealed the collateral sensitivities of A204SitR and A204AnloR sublines to the selective FGFR inhibitor infigratinib. As per **Chapter 6.2.5**, I validated the findings of the inhibitor screen by subjecting the TKI-resistant sublines to full dose response assays with infigratinib (**Figure 6.11A-B**). As shown in **Figure 6.11A-B**, I found that infigratinib treatment was significantly more effective in reducing cell viability in the A204SitR and A204AnloR sublines compared to the A204 parental cells (**Figure 6.11A-B; Table S12**). In these specific sublines, the level of sensitisation to infigratinib (A204SitR IC_{50} ; 0.39 μ M, A204AnloR; 0.63 μ M) was similar to the IC_{50} of sitravatinib (IC_{50} ; 0.23 μ M) and anlotinib (0.57 μ M) treatment in the parental A204 cells (**Table S9 & S12**).

As with erdafitinib and ponatinib evaluation in **Chapter 6.2.5**, I wanted to determine the pro-apoptotic effects of infigratinib treatment in the A204 TKI-resistant sublines and subsequently evaluate whether enhanced apoptosis correlated with dual suppression of MAPK and Akt activity (**Figure 6.11C-J**). **Figure 6.11C-J** shows that infigratinib treatment enhanced apoptosis compared to both DMSO (~2- to 3-fold enhancement) and the subline's respective multi-target TKI (~2-fold enhancement) in the A204PazR, A204SitR, and A204AnloR sublines (**Figure 6.11C-J**). Correlating with these enhanced apoptotic effects, infigratinib was found to suppress ERK1/2 phosphorylation in these sublines, resulting in concurrent Akt and ERK1/2 suppression (**Figure 6.11K**). As per the findings with erdafitinib in **Chapter 6.2.5**, apoptosis was not significantly affected by infigratinib treatment in the A204RegR subline, with no noticeable reduction in ERK1/2 phosphorylation (**Figure 6.11E, I, & K**).

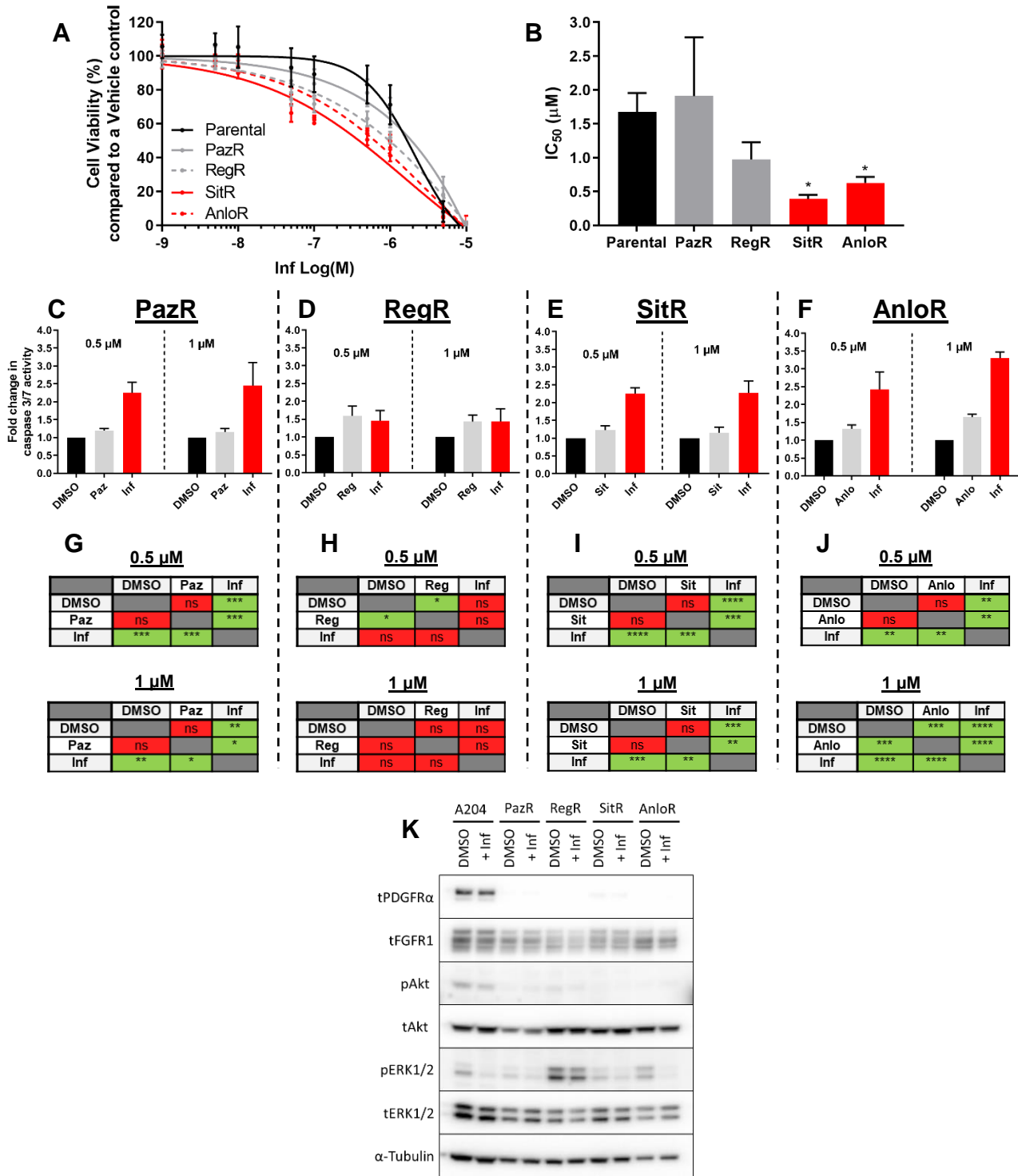


Figure 6.11: Evaluation of infigratinib activity in A204 TKI-resistant sublines. (A) Cell viability assays of A204 parental and TKI-resistant sublines treated with increasing concentrations of infigratinib (Inf) to determine IC_{50} values (Table S12). (B) Bar plot displaying IC_{50} values for A204 parental and TKI-resistant sublines. Cell viability was normalised to DMSO control ($n=3$). Bar plots displaying the fold change in caspase 3/7 activity in (C) A204PazR, (D) A204RegR, (E) A204SitR, and (F) A204AnloR treated with two concentrations of Inf for 24 hours. Fold change was normalised to DMSO control ($n=3$). Grids displaying the statistical significance between the different treatments at two different concentrations in the (G) A204PazR, (H) A204RegR, (I) A204SitR, and (J) A204AnloR cells in the apoptosis assays. (K) Immunoblots of PDGFR α , FGFR1, Akt, and ERK1/2 expression and/or phosphorylation levels after 6 hours of treatment with 1 μ M Inf or DMSO. Image is representative of two separate experiments ($n=2$). Statistical analysis

was undertaken by one-way ANOVAs with Dunnett's (cell viability) (compared to A204 parental) or Tukey's (apoptosis) multiple comparison tests (* = $p \leq 0.05$, ** = $p \leq 0.01$, *** = $p \leq 0.001$, **** = $p \leq 0.0001$). Error bars represent standard deviation. Anlo; Anlotinib, ANOVA; Analysis of variance, DMSO; Dimethyl sulfoxide, ERK1/2; Extracellular signal-regulated kinase 1/2, FGFR1; Fibroblast growth factor receptor 1, ns; Non-significant, Paz; Pazopanib, PDGFR α ; Platelet-derived growth factor receptor α , Reg; Regorafenib, Sit; Sitravatinib, TKI; Tyrosine kinase inhibitor.

As discussed in **Chapter 6.2.5**, the correlation between dual suppression of Akt and ERK1/2 phosphorylation by infigratinib treatment is not sufficient to explain the antiproliferative effects seen in the A204SitR and A204AnloR TKI-resistant sublines. As stated in **Chapter 6.2.5**, if this were the case then direct MAPK signalling inhibition by trametinib would result in similar antiproliferative effects in the A204SitR and A204AnloR TKI-resistant sublines as was observed with infigratinib treatment in the inhibitor screen. These data instead suggests that infigratinib treatment, as well as blockading the ERK1/2 pathway, is having an additional, currently unknown effect in the A204SitR and A204AnloR to produce the potent antiproliferative effects.

6.2.7 Determining the reproducibility and characteristics of selective infigratinib collateral sensitivity

The utilisation of FGFR inhibition as an effective salvage therapy in multi-target TKI-resistant STS models has previously been shown by Wong *et al.* (Wong *et al.*, 2016). Through a similar methodology of deriving acquired TKI-resistant sublines to that described in **Figure 6.1**, Wong *et al.* generated pazopanib-resistant A204 cells and subsequently found potent collateral sensitivities to infigratinib monotherapy in this pazopanib-resistant subline. However, the work presented in **Chapter 6** did not replicate the findings that pazopanib-resistant A204 are sensitive to infigratinib. However, this could be due to the stochastic nature of the development of resistant cells in response to treatment. Therefore, in order to determine the robustness and reproducibility of FGFR inhibitor collateral sensitivity in sitravatinib- and anlotinib-resistant A204 cells, I undertook sequential TKI treatment strategies, whereby administered inhibitors are changed over time. The methodology is outlined in **Figure 6.12**.

These experiments consisted of treating parental A204 cells with 14 days of 1 μ M pazopanib, regorafenib, sitravatinib, or anlotinib single agent treatment, which resulted in the acquisition of resistance and an increase in the proliferation of cells (**Figure 6.12**

& 6.13A-D). At day 14, the cells treated with a specific TKI were stratified into 5 arms – pazopanib, regorafenib, sitravatinib, anlotinib, and imfigratinib – and then treated with the indicated TKI for a further 14 days (**Figure 6.12 & 6.13A-D**). The proliferation of cells treated with a specific sequence of inhibitors was evaluated at various timepoints across the course of 28 days by direct cell count using a Celigo cytometer.

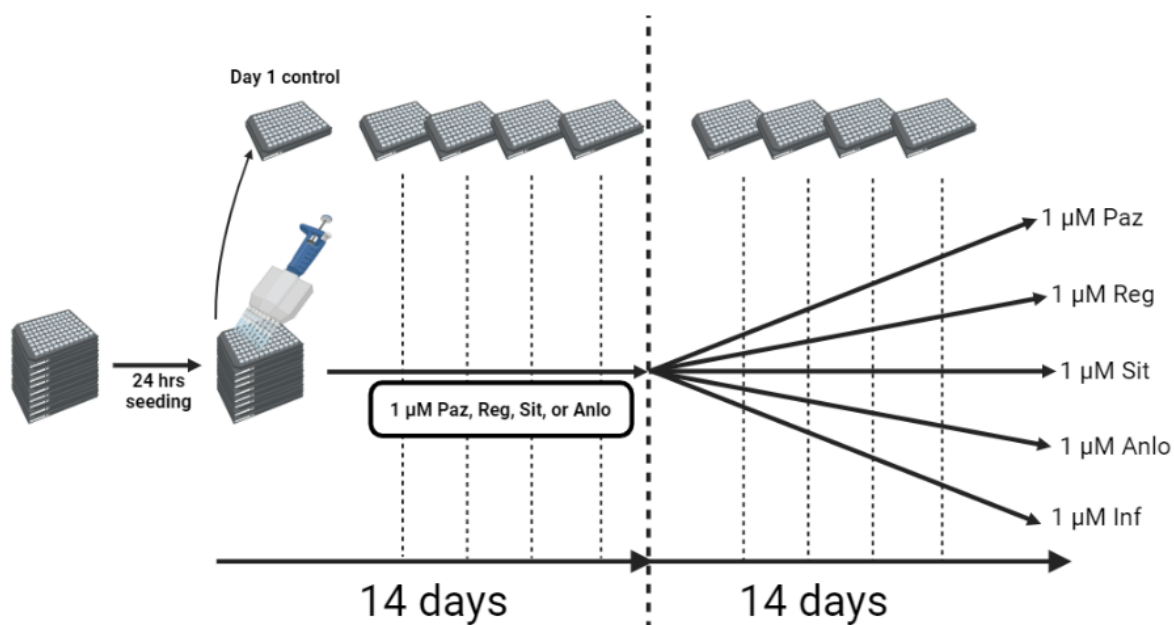


Figure 6.12: Schematic outlining methodology for sequential TKI treatment experiments. A204 cells were identically seeded for 24 hours into nine 96 well plates. After 24 hours, one plate was taken and analysed before treatment and this acts as the day 1 control for fold change normalisation. Cells within the remaining eight plates were then treated with either 1 μ M pazopanib (Paz), regorafenib (Reg), sitravatinib (Sit), or anlotinib (Anlo) for 14 days. At days 4, 7, 11, and 14, a single plate was taken and evaluated for cell growth. At day 14, the cells treated with a specific TKI were stratified into five arms – 1 μ M Paz, Reg, Sit, Anlo, or imfigratinib (Inf) – and treatment was continued for a further 14 days. At days 18, 21, 25, and 28, a single plate was taken and evaluated for cell growth. Cells were evaluated for cell growth using a Celigo cytometer. Image was created using BioRender.

As shown in **Figure 6.13A-D**, the assays confirmed that upon increased proliferation of A204 cells treated with any one of the four multi-target TKIs, switching treatment to one of the other three evaluated multi-target TKIs did not stall proliferation. This is consistent with the cross-resistance phenotype observed in the A204 TKI-resistant sublines in **Figure 6.3**.

Furthermore, **Figure 6.13A-B** also corroborates the finding that imfigratinib treatment in cells pre-treated with pazopanib or regorafenib does not notably affect cellular proliferation. Additionally, in cells pre-treated with anlotinib, imfigratinib was not found to have a long-term effect in suppressing cellular proliferation, with cells treated with imfigratinib rapidly outgrowing cells treated with continuous anlotinib (**Figure 6.13C**).

However, in A204 cells pre-treated with sitravatinib, sequential infgratinib treatment induced a robust and reproducible effect in suppressing proliferation (**Figure 6.13D**).

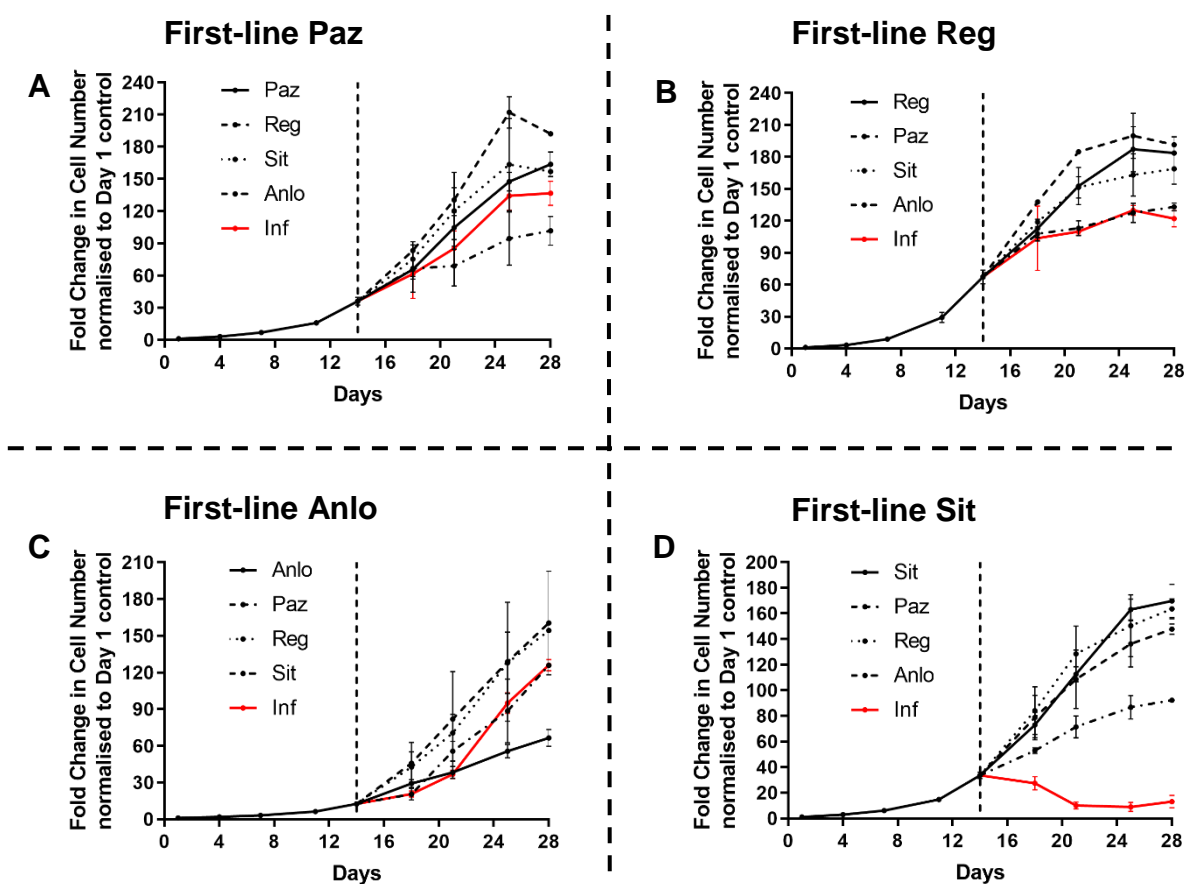


Figure 6.13: Growth curve assays evaluating infgratinib as a second-line therapy in multi-target TKI pre-treated A204 cells. Growth curve assays of A204 cells to measure the fold change in cell number over a period of 4 weeks in cells treated initially with 1 μ M (**A**) pazopanib (Paz), (**B**) regorafenib (Reg), (**C**) anlotinib (Anlo), or (**D**) sitravatinib (Sit) for 2 weeks before switching to the other multi-target TKIs indicated or infgratinib (Inf) (1 μ M). Fold change was normalised to day 1 control (n=2). Error bars represent standard error of the mean. TKI; Tyrosine kinase inhibitor.

As shown previously in **Figure 6.4**, the TKI-resistant A204 sublines harboured reduced expression of PDGFR α and suppression of Akt signalling, when compared to A204 parental cells. I therefore wanted to assess whether these phenotypes were replicated in A204 parental cells pre-treated with 14 days of sitravatinib. The A204 parental cells were treated with either DMSO or 1 μ M sitravatinib for 14 days. After 14 days of treatment, A204 cells pre-treated with sitravatinib were then further treated with either DMSO, sitravatinib, or infgratinib for 6 hours. In parallel, DMSO pre-treated A204 cells were also treated with an additional 6 hours of DMSO. Immunoblotting for PDGFR α , FGFR1, and downstream signalling proteins was subsequently performed (**Figure 6.14**).

Figure 6.14 shows that A204 cells pre-treated with 14 days of sitravatinib resulted in decreased PDGFR α expression and abrogation of Akt signalling, compared to cells pre-treated with 14 days of DMSO. Additionally, in cells pre-treated with sitravatinib, subsequent infigratinib treatment resulted in the abolishment of ERK1/2 phosphorylation, an effect not observed with DMSO or sitravatinib treatment (**Figure 6.14**). This result shows that A204 cells pre-treated with sitravatinib recapitulated the phenotypes of PDGFR α loss and decreased Akt signalling that was observed in the A204SitR TKI-resistant subline.

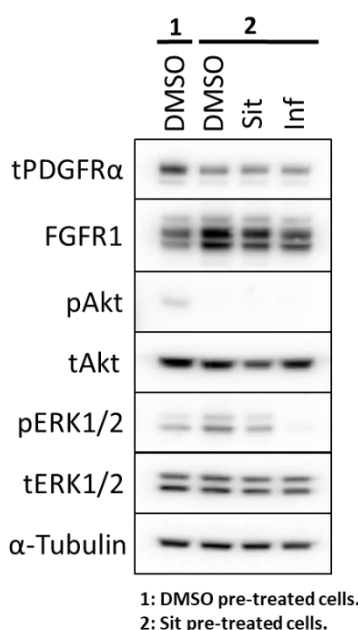


Figure 6.14: Immunoblot of A204 cells pre-treated with either DMSO or sitravatinib. Immunoblot of PDGFR α , FGFR1, Akt, and ERK1/2 expression and/or phosphorylation levels after 14 days of DMSO or 1 μ M sitravatinib (Sit) treatment. After 14 days of treatment, Sit pre-treated cells were further treated for 6 hours with DMSO or 1 μ M of indicated TKI. Similarly, after 14 days of treatment, DMSO pre-treated cells were further treated for 6 hours with DMSO. Image is representative of two separate experiments (n=2). DMSO; Dimethyl sulfoxide, ERK1/2; Extracellular signal-regulated kinase 1/2, FGFR1; Fibroblast growth factor receptor 1, Inf; Infigratinib, PDGFR α ; Platelet-derived growth factor receptor α , TKI; Tyrosine kinase inhibitor.

Previous studies have shown that collateral sensitivities can be temporal during the evolution of acquired drug resistance (Vander Velde *et al.*, 2020; Zhao *et al.*, 2016). I therefore wanted to evaluate how the collateral sensitivity towards infigratinib treatment changes over the course of acquiring sitravatinib resistance in A204 cells. The methodology of this experiment is outlined in **Figure 6.15A**.

Parental A204 cells were firstly assessed for their baseline sensitivity towards infigratinib and sitravatinib. Parental A204 cell lysates for immunoblotting were also collected. Consistent with my previous data, A204 parental cells were relatively resistant to infigratinib (IC₅₀ > 2 μ M) and sensitive to sitravatinib (IC₅₀ ~ 0.5 μ M) (**Figure**

6.15B-D). Parental A204 cells were then stratified into two arms; either treated with DMSO or 1 μM sitravatinib (**Figure 6.15A**). The two experimental arms were treated with their respective treatment for 27 days, with cell viability assessments of imfigratinib and sitravatinib sensitivities performed at days 3, 6, 13, 20, and 27 (**Figure 6.15A**). Lysates for immunoblotting were also collected on these days (**Figure 6.15A**). As expected, A204 cells pre-treated with sitravatinib became incrementally resistant to sitravatinib treatment over the course of 27 days of treatment (IC_{50} : 1.0-1.5 μM) (**Figure 6.15B & D**). Conversely, DMSO pre-treated cells remained sensitive to sitravatinib treatment over the course of 27 days of treatment (IC_{50} : \sim 0.5 μM) (**Figure 6.15B & D**).

In sitravatinib pre-treated A204 cells, imfigratinib collateral sensitivity was found to occur after only 3 days of sitravatinib treatment and remained sensitive over the course of the 27 days (IC_{50} < 0.50 μM) (**Figure 6.15C-D**). This is in contrast to DMSO pre-treated cells which remained resistant to imfigratinib (IC_{50} > 1.8 μM) throughout the 27 days (**Figure 6.15C-D**). Immunoblotting confirmed the reproducible loss of PDGFR α expression in sitravatinib pre-treated A204 cells (compared to DMSO pre-treated), with concurrent suppression of Akt signalling, and these phenotypes are retained throughout the course of the experiment (**Figure 6.15E**).

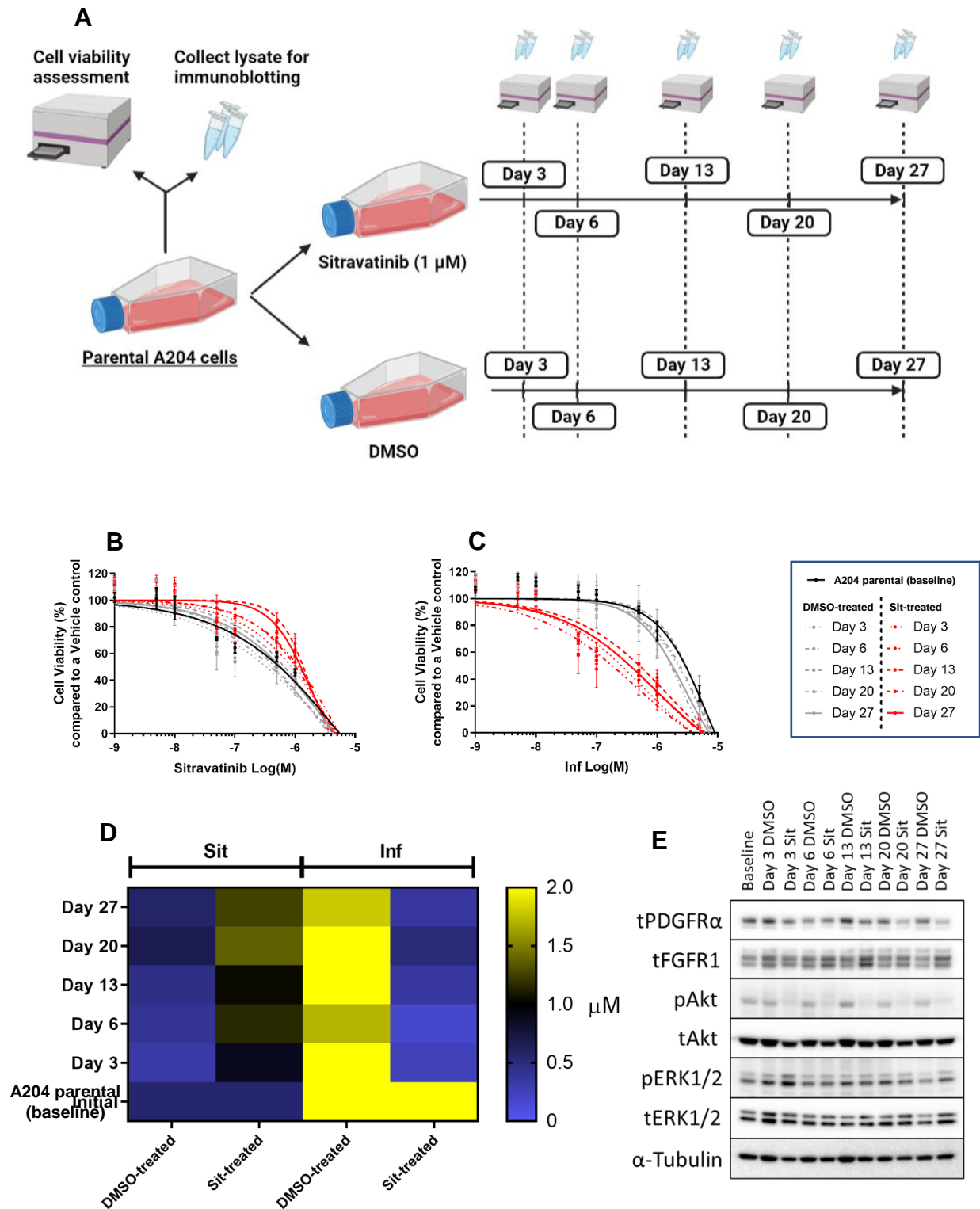


Figure 6.15: Temporal assessment of infigratinib collateral sensitivity in A204 sitravatinib pre-treated cells. (A) Schematic outlining the experimental protocol for assessing the temporal emergence of infigratinib (Inf) collateral sensitivity in sitravatinib (Sit) pre-treated A204 cells. Schematic outlines the stratification and treatment of cells, as well as the days where cell viability assessment and lysate collection were performed. Image was created using BioRender. Temporal cell viability assays of A204 parental cells pre-treated with DMSO or 1 μ M Sit over the course of 27 days and the sensitivities to **(B)** Sit or **(C)** Inf evaluated at the indicated timepoints. **(D)** Heatmap displaying the IC_{50} values for the temporal cell viability assays. **(E)** Immunoblot mapping the changes in PDGFR α , FGFR1, Akt, and ERK1/2 expression and/or phosphorylation levels in cells treated with either DMSO or 1 μ M Sit over the course of 27 days. "Baseline" refers to A204 parental cells before treatment with either DMSO or Sit. Image is representative of a single

experiment (n=1). Error bars represent standard deviation (cell viability). DMSO; Dimethyl sulfoxide, ERK1/2; Extracellular signal-regulated kinase 1/2, FGFR1; Fibroblast growth factor receptor 1, IC₅₀; Inhibitory constant, PDGFR α ; Platelet-derived growth factor receptor α , TKI; Tyrosine kinase inhibitor.

6.2.8 Investigation into the causal factors of selective infigratinib collateral sensitivity in sitravatinib-resistant cells

As infigratinib is a selective pan-FGFR inhibitor, I postulated that there could be differential expression in FGFR levels between the A204SitR cells when compared to the remaining TKI-resistant sublines and parental cells, thereby resulting in selective infigratinib collateral sensitivity in the sitravatinib-resistant cells.

I therefore decided to assess for the levels of *FGFR* mRNA expression by real-time quantitative polymerase chain reaction (qPCR) in the A204 parental cells and the TKI-resistant sublines (**Figure 6.16**). Previous studies have reported that A204 parental cell lines do not express *FGFR2* (Harttrampf *et al.*, 2021; Wöhrle *et al.*, 2013). By utilising the known *FGFR2*-expressing HS-SY-II cell line, I confirmed that the A204 cell lines and all of the TKI-resistant sublines did not express *FGFR2* to a readily quantifiable level by qPCR (data not shown) (Ishibe *et al.*, 2005). Therefore, the expression levels of *FGFR1*, 3 & 4, which are known to be expressed in A204 parental cells, were assessed by qPCR (**Figure 6.16A-C**) (Wöhrle *et al.*, 2013). The expression levels of *PDGFRA* were also assessed in the TKI-resistant A204 sublines and, consistent with the loss of PDGFR α in the TKI-resistant sublines observed by immunoblotting, found that *PDGFRA* mRNA expression was significantly reduced in the TKI-resistant cells compared to parental cells (**Figure 6.16D**). **Figure 6.16A-C** shows that the expression levels of *FGFR1*, 3, and 4 were not significantly different between any of the TKI-resistant cells or the parental cells.

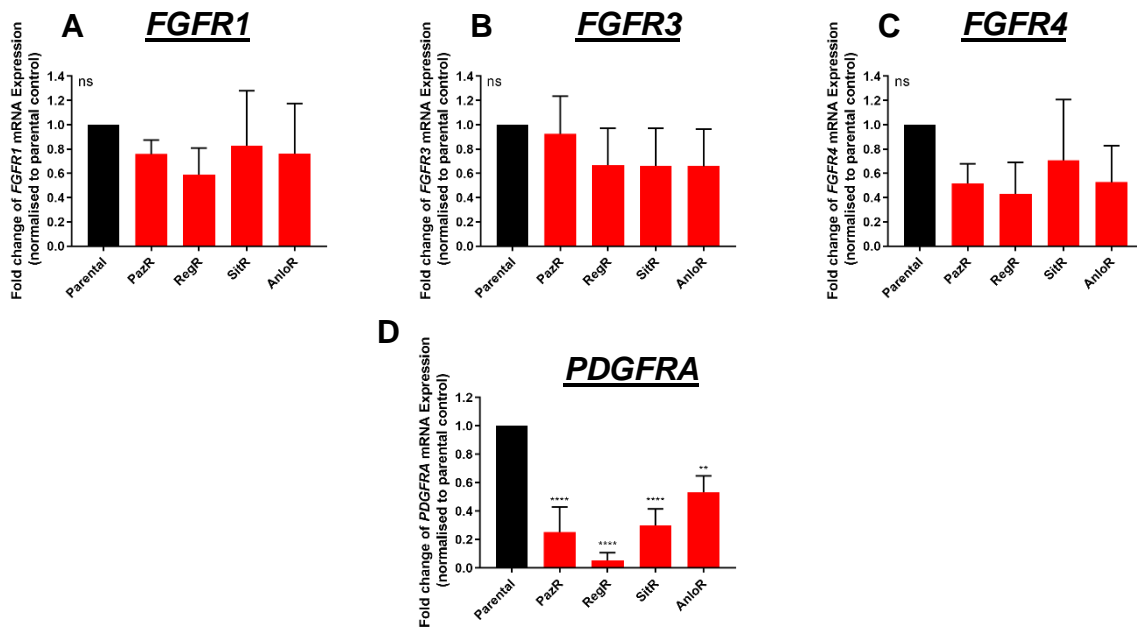


Figure 6.16: *FGFR1/3/4* and *PDGFRA* expression levels in A204 parental and TKI-resistant sublines. qPCR data displaying the fold change of (A) *FGFR1*, (B) *FGFR3*, (C) *FGFR4*, and (D) *PDGFRA* mRNA, normalised to A204 parental cells (n=3). Statistical analysis was undertaken using one-way ANOVAs with Tukey's (*FGFR1/3/4*) or Dunnett's (*PDGFRA*) (compared to parental cells) multiple comparison tests. ANOVA; Analysis of variance, *FGFR1/3/4*; Fibroblast growth factor receptor (1/3/4), mRNA; Messenger RNA, ns; Non-significant, *PDGFRA*; Platelet-derived growth factor receptor α .

Due to the lack of differential *FGFR* expression levels, I next wanted to assess for potential alterations in RTK phosphorylation levels, including FGFRs, that occur upon the acquisition of sitravatinib resistance in A204 cells, and the subsequent effects of treating these cells with infigratinib. This experiment could therefore provide a platform for further evaluation into RTK signalling pathways that are selectively rendering sitravatinib-resistant A204 cells sensitive to FGFR inhibition.

In order to evaluate phosphorylation alterations in a broad range of RTKs, including all four FGFRs, I employed a phospho-RTK antibody array. The experimental protocol is outlined in **Figure 6.17**. A204 parental cells were treated with either DMSO or 1 μ M sitravatinib for 14 days. After 14 days, the DMSO and sitravatinib pre-treated A204 cells were either subsequently treated with a further 6 hours of continued treatment (either DMSO or sitravatinib (1 μ M)) or 6 hours of 1 μ M infigratinib (**Figure 6.17**).

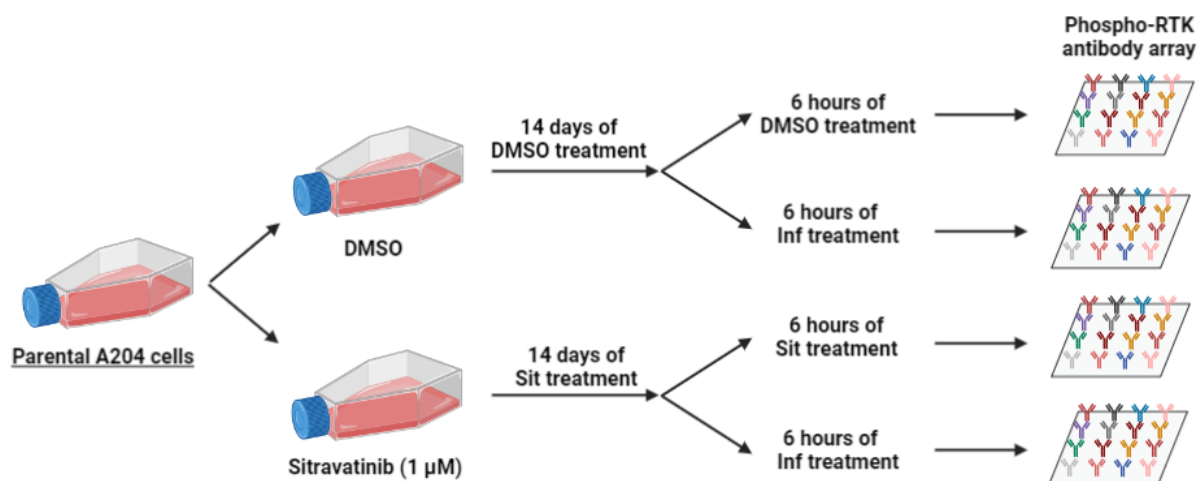


Figure 6.17: Schematic outlining the experimental protocol employed for the phospho-RTK antibody array. Parental A204 cells were treated with either DMSO or 1 μM sitravatinib (Sit) for 14 days. After 14 days of DMSO treatment, DMSO pre-treated A204 cells were treated with either DMSO or 1 μM infigratinib (Inf) treatment for 6 hours. After 14 days of Sit treatment, Sit pre-treated A204 cells were treated with either 1 μM Sit or Inf treatment for 6 hours. Lysates were collected and evaluated using phospho-RTK arrays. Image was created using BioRender. DMSO; Dimethyl sulfoxide, RTK; Receptor tyrosine kinase.

As expected, the phospho-RTK arrays showed that A204 parental cells pre-treated with sitravatinib had noticeably reduced PDGFR α phosphorylation levels compared to DMSO pre-treated cells (**Figure 6.18**), consistent with the observed reduced expression levels of PDGFR α in both sitravatinib pre-treated A204 cells and the A204SitR subline. Furthermore, corroborating previous studies employing identical phospho-RTK antibody arrays in A204 cells, FGFR phosphorylation was not observed in any of the treatment regimens (**Figure 6.18**) (Bai *et al.*, 2015).

Further phosphorylation alterations were also noted between A204 cells pre-treated with sitravatinib compared to DMSO pre-treatment. For instance, A204 cells pre-treated with sitravatinib were found to have decreased levels of discoidin domain receptor 2 (DDR2) phosphorylation compared to DMSO pre-treated cells (**Figure 6.18**). Sitravatinib has previously been shown to be a potent inhibitor of DDR2 (IC₅₀: 0.5 nM), even more so than PDGFR α (IC₅₀: 30 nM) (Patwardhan *et al.*, 2016). This result potentially indicates that a similar downregulation of DDR2 expression occurs in response to the acquisition of sitravatinib resistance as has been observed with PDGFR α . Further evaluation is warranted to determine the role of DDR2 activity in mediating collateral sensitivities in the A204 model of MRT.

Furthermore, phosphorylation of ephrin A7 (EphA7) was found to be increased in sitravatinib pre-treated A204 cells compared to DMSO pre-treated cells (**Figure 6.18**).

Additionally, infigratinib treatment was found to modestly inhibit the increased phosphorylation of EphA7 in the sitravatinib pre-treated A204 cells (**Figure 6.18**). Interestingly, previous studies have reported increased ephrin signalling acting as a mechanism of acquired resistance in both gastric and lung cancers (Amato *et al.*, 2016; Chen *et al.*, 2019; Cioce & Fazio, 2021; Koch *et al.*, 2015; Pasquale, 2010). These preliminary data outlined in **Figure 6.18** therefore also warrants further research into the role of EphA7 signalling in modulating collateral sensitivities in MRT models. Infigratinib treatment was also found to inhibit ALK phosphorylation in both the DMSO pre-treated and sitravatinib pre-treated A204 cells (**Figure 6.18**).

Interestingly, infigratinib treatment of the sitravatinib pre-treated A204 cells was found to further inhibit PDGFR α phosphorylation. Furthermore, this phenotype was not observed with infigratinib treatment of A204 cells pre-treated with DMSO (**Figure 6.18**). This implies that in sitravatinib pre-treated A204 cells, infigratinib is inhibiting any residual PDGFR α activity that remains after sitravatinib treatment-induced PDGFR α signalling loss. Further investigation into this finding will help elucidate whether this effect is the causal factor of infigratinib collateral sensitivity in sitravatinib pre-treated A204 cells, compared to A204 cells pre-treated with the other three multi-target TKIs (**Figure 6.18**).

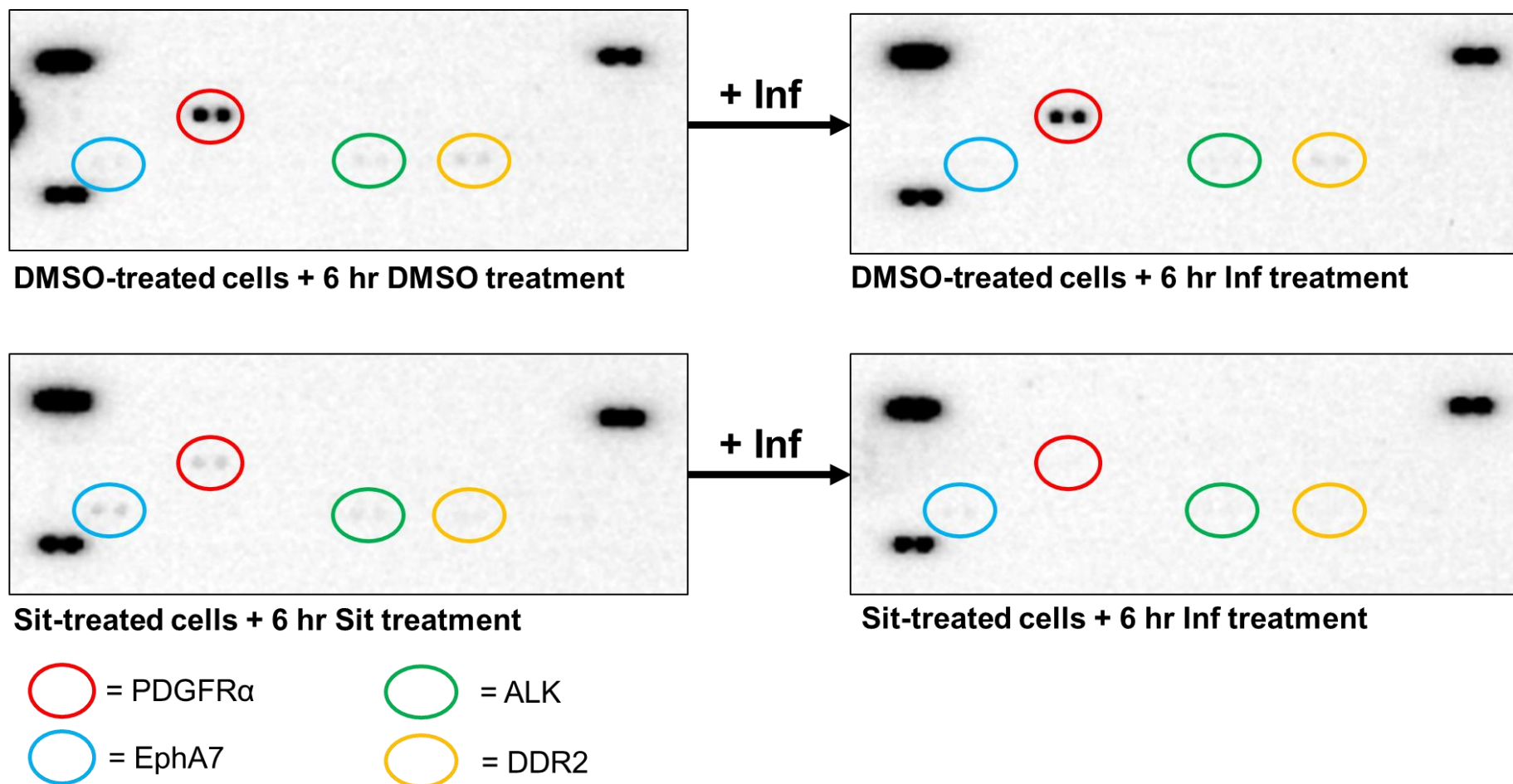


Figure 6.18: Phospho-RTK antibody array of DMSO or sitravatinib pre-treated A204 cells. Phospho-RTK array was performed upon A204 cells that had either been pre-treated with 14 days of DMSO or 1 μ M sitravatinib (Sit). After 14 days, cells were then either continued on their respective treatment (DMSO or 1 μ M Sit) for 6 hours or switched to 1 μ M infogatinib (Inf) for 6 hours. Spots in the top left/right and bottom left of the array are reference spots. RTK phosphorylation alterations of interest are circled and colour-coded. Images are representative of a single experiment (n=1). Densitometry was not performed due to the high background. ALK; Anaplastic lymphoma kinase, DDR2; Discoidin domain receptor 2, DMSO; Dimethyl sulfoxide, EphA7; Ephrin A7, PDGFR α ; Platelet-derived growth factor receptor α .

6.2.9 Sitravatinib pre-treated A204 cells and the A204SitR subline re-acquire resistance to infigratinib following longer-term and chronic infigratinib exposure

Despite the potent and reproducible collateral sensitivity observed with infigratinib treatment in sitravatinib pre-treated A204 cells, continued and chronic treatment with infigratinib resulted in the re-acquisition of infigratinib resistance (**Figure 6.19A-B**). As shown in **Figure 6.19A-B**, despite an initial regression of cell growth in sitravatinib pre-treated A204 cells and a growth plateau of approximately 11 days, longer-term exposure to infigratinib resulted in increasing proliferation after approximately 24 days of infigratinib treatment (**Figure 6.19A-B**). Furthermore, in colony formation assays conducted over the course of 2 weeks, the A204SitR TKI-resistant subline was found to be readily able to form colonies when exposed to long-term infigratinib treatment (**Figure 6.19C**). I therefore wanted to determine potential treatments that could be effectively utilised upon the re-acquisition of infigratinib resistance in sitravatinib pre-treated A204 cells in order to control cellular proliferation and subvert resistance (**Figure 6.19B**).

Based on the results outlined in **Chapters 5 & 6**, I postulated that treatment of the cells at the emergence of infigratinib resistance re-acquisition with either combination therapy of sitravatinib plus infigratinib or the single agent PDGFR α /FGFR1 inhibitor ponatinib could effectively control cell growth. I therefore treated the A204 parental cells with sitravatinib treatment for 14 days before either switching to infigratinib or continuing with sitravatinib treatment. After a further 14 days of treatment (day 28), sitravatinib pre-treated cells that were treated with second-line infigratinib were stratified into four arms of treatment – sitravatinib, infigratinib, sitravatinib plus infigratinib, or ponatinib – for a further 14 days of treatment (**Figure 6.19B**).

I found that treatment of the cells with sitravatinib at day 28 onwards mimics the effects seen if the cells were continued on infigratinib treatment, suggesting that the cells now harbour a mechanism of resistance that renders them dually resistant to both sitravatinib and infigratinib monotherapy (**Figure 6.17B**). However, treatment at day 28 with combination therapy suppressed cellular proliferation and the cell number continued to plateau. Additionally, ponatinib treatment resulted in the regression of growth, resulting in the complete lack of cells at day 42 (**Figure 6.17B**).

These results therefore nominate a potential TKI sequential treatment strategy that could be employed in the multi-line therapy of MRT, as well as potentially other STS driven by PDGFR and FGFR. The nominated sequential strategy consists of first-line sitravatinib with second-line infigratinib FGFR inhibition upon disease progression. Following re-acquisition of resistance to infigratinib, further lines of therapy such as ponatinib or combination therapy of sitravatinib plus infigratinib could be employed as effective strategies.

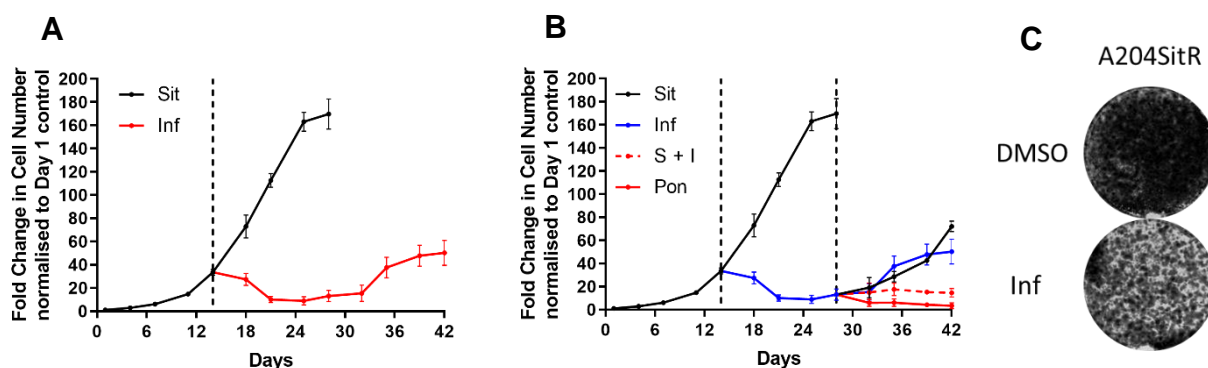


Figure 6.19: Collateral sensitivity to infigratinib is temporary and cells re-acquire resistance after prolonged exposure. (A-B) Growth curve assays of A204 parental cells to measure the fold change in cell number over a period of 6 weeks in cells treated with 1 μ M of the indicated treatments. Data collection for a specific treatment regimen was ceased once the cells had reached overconfluency within the 96 well plate and the Celigo cytometer could no longer accurately distinguish between individual cells. Fold change was normalised to day 1 control (n=2). **(C)** Colony formation assays of A204SitR TKI-resistant subline treated with 1 μ M inhibitor over a period of 2 weeks. Image is representative of three separate experiments (n=3). DMSO; Dimethyl sulfoxide, I/Inf; Infigratinib, Pon; Ponatinib, S/Sit; Sitravatinib.

6.2.10 Second-line treatment with erdafitinib and ponatinib suppresses cellular proliferation following progression on first-line multi-target TKI treatment

As I showed previously in **Figure 6.10**, and have reiterated in **Figure 6.20A**, erdafitinib notably reduced the ability of the A204SitR TKI-resistant subline to form colonies, when compared to DMSO. **Figure 6.20A** also shows that erdafitinib reduced the ability of the A204SitR cells to form colonies when compared to infigratinib treatment (**Figure 6.20A**).

I therefore wanted to evaluate whether erdafitinib was an effective second-line therapy in sitravatinib pre-treated A204 cells and whether the cells acquired resistance to erdafitinib after prolonged and chronic exposure (**Figure 6.17D**). To answer this question, I treated parental A204 cells with 14 days of sitravatinib before switching to

28 days of subsequent erdafitinib and monitoring the changes in cell number (**Figure 6.20B**). The results were then compared to sitravatinib pre-treated A204 cells that were subsequently treated with either infigratinib or continuous sitravatinib.

As shown in **Figure 6.20B**, treatment with erdafitinib mimics the initial suppressive effect seen with infigratinib up to day 31. However, at day 35 and onwards, whilst infigratinib treatment results in an increasing number of cells signifying an acquisition of treatment resistance, erdafitinib continues to suppress cellular proliferation for the remainder of the experiment (day 42). The plateau of cell number observed with erdafitinib treatment does suggest the existence of a population of drug-tolerant cells (**Figure 6.20B**). Further evaluation is warranted to explore whether the existence of these cells will eventually give rise to a drug-resistant population.

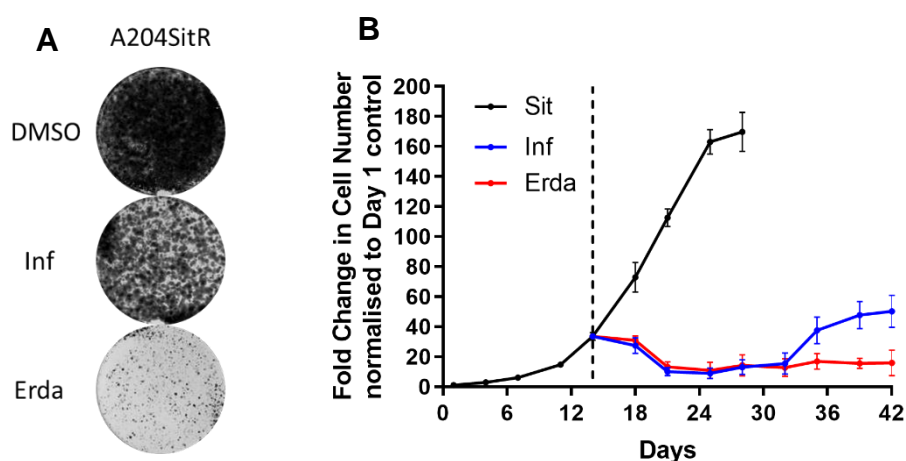


Figure 6.20: Erdafitinib is an effective second-line therapy in controlling cell growth of A204SitR and sitravatinib pre-treated A204 cells. (A-B) Growth curve assays of A204 parental cells to measure the fold change in cell number over a period of 6 weeks in cells treated with 1 μ M of the indicated treatments. Fold change was normalised to day 1 control (n=2). **(C)** Colony formation assays of A204SitR TKI-resistant subline treated with 1 μ M inhibitor over a period of 2 weeks. Image is representative of three separate experiments (n=3). **(D)** Growth curve assays of A204 parental cells to measure the fold change in cell number over a period of 6 weeks in cells treated with 1 μ M of the indicated treatments. DMSO; Dimethyl sulfoxide, Erda; Erdafitinib, Inf; Infigratinib, Pon; Ponatinib.

I next wanted to assess whether the long-term suppression of proliferation with erdafitinib was specific to A204 cells pre-treated with sitravatinib or an effect also observed in pazopanib, regorafenib, and anlotinib pre-treated A204 cells.

I therefore undertook the same experiment outlined in **Figure 6.20** but with cells pre-treated with 14 days of pazopanib, regorafenib, or anlotinib before switching to erdafitinib treatment. Due to the similar preclinical phenotypes observed with ponatinib therapy to erdafitinib in MRT cell lines and the A204 TKI-resistant sublines, the effect

of ponatinib was also assessed in pazopanib, regorafenib, sitravatinib, or anlotinib pre-treated A204 cells (**Figure 6.21A-D**).

Figure 6.21A-C shows that treatment with erdafitinib following pazopanib, regorafenib, or anlotinib pre-treatment in the A204 cells resulted in the long-term (28 days) suppression of cellular proliferation. This suppression of cell growth with second-line erdafitinib treatment was especially apparent compared to second-line treatments with multi-target TKI or infigratinib monotherapies (**Figure 6.21A-C**). As seen with the sitravatinib pre-treated A204 cells, second-line erdafitinib treatment resulted in a cell number plateau for the remainder of the experiment (42 days), again suggesting the existence of a small population of drug-tolerant persister cells (**Figure 6.21A-C**). Additionally, second-line treatment with ponatinib was found to regress cell number, with each growth curve tending towards 0 indicating that the cells are not surviving chronic and long-term treatment with ponatinib (**Figure 6.21A-D**).

Taking these results together, I further nominate erdafitinib and ponatinib as potential second-line therapies following MRT disease progression on first-line multi-target TKI therapy.

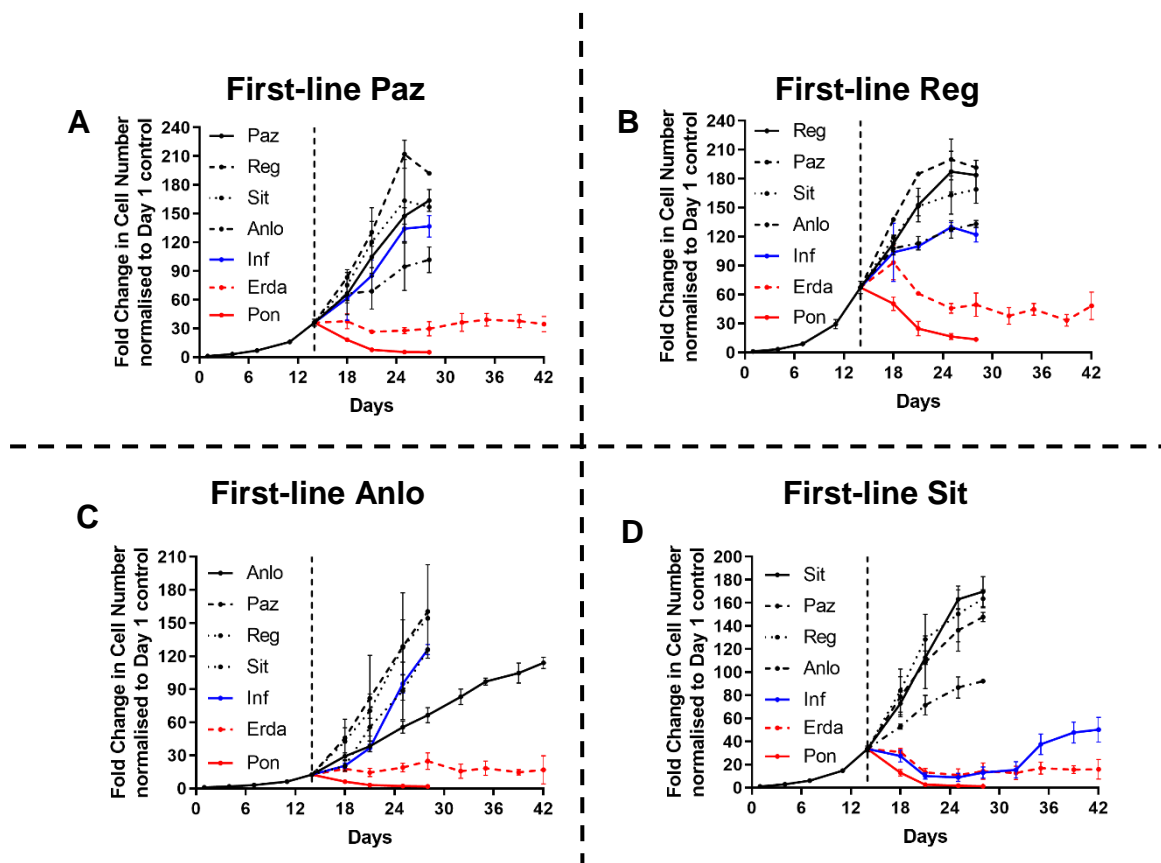


Figure 6.21: Second-line treatment with erdafitinib and ponatinib suppresses cellular proliferation following progression on first-line multi-target TKI treatment. Growth curves of A204 cells to measure the fold change in cell number over a period of 6 weeks in A204 cells pre-treated with two weeks of (A) pazopanib (Paz), (B) regorafenib (Reg), (C) anlotinib (Anlo) (D), or sitravatinib (Sit) before undergoing subsequent indicated treatment schedules. Fold change was normalised to day 1 control (n=2). Error bars represent standard error of the mean. DMSO; Dimethyl sulfoxide, Erda; Erdafitinib, Inf; Infigratinib, Pon; Ponatinib, TKI; Tyrosine kinase inhibitor.

6.3 Discussion

The work in **Chapter 6** reports the derivation of acquired TKI-resistant models of the initially sensitive A204 cell line model of MRT. This was achieved through the chronic and escalating exposure of cells to the multi-target TKIs pazopanib, regorafenib, sitravatinib, and anlotinib. In addition to resistance towards the treated inhibitor, TKI-resistant models were found to be collaterally cross-resistant to the other evaluated TKIs suggesting that pazopanib, regorafenib, sitravatinib, and anlotinib share a similar mechanism of action. Replicating the results previously seen by Wong *et al.* in sunitinib-, dasatinib-, and pazopanib-resistant A204, I found that the acquisition of regorafenib, sitravatinib, and anlotinib resistance in the A204 cells resulted in loss of PDGFR α expression and bypass of the Akt pathway. The study by Wong *et al.* determined that bypass of the Akt signalling pathway acts as a mechanism of

pazopanib resistance in A204 cells by determining that the TKI-resistant cells had lost their dependency on Akt signalling for survival. Wong *et al.* also showed that PDGFR α is regulated by SMARCB1 expression (Wong *et al.*, 2016). As the MRT subtype is highly characterised by SMARCB1 loss, Wong *et al.* found that re-expressing SMARCB1 in the A204 and G402 models resulted in reduced PDGFR α expression, showing that the oncogenic activity of PDGFR α in MRT models is regulated by SMARCB1 expression (Wong *et al.*, 2016).

Future work will focus on whether re-introducing PDGFR α expression into the multi-target TKI-resistant sublines rescues the phenotypes of TKI resistance and Akt suppression. Furthermore, direct Akt/PI3K pathway inhibitors, such as MK2206 and dactolisib, will be employed to determine whether the multi-target TKI-resistant sublines employed in my work have lost their survival dependency on Akt signalling. Through these means, I hope to elucidate the causal role of PDGFR α loss and subsequent Akt signalling suppression as a mechanism of resistance in the multi-target TKI-resistant A204 cells.

Furthermore, mass spectrometry analysis revealed several proteins that were universally downregulated in the TKI-resistant sublines compared to parental cells. Proteomic data revealed downregulation of proteins involved in such biological processes such as FGF signalling, purine and carbohydrate metabolism, and Wnt signalling, all of which have been previously shown to be associated with drug resistance in cancer (Lin *et al.*, 2019; Wood *et al.*, 1973; Zhong *et al.*, 2020; Zhou *et al.*, 2020). Future investigations into whether these downregulated proteins cause acquired TKI resistance in models of STS, primarily focussed on gene knockdown or silencing techniques within TKI sensitive cells, are required. Contrary to the data presented within **Chapter 6**, PDGFR α expression was not discovered by the proteomic analysis to be downregulated within the TKI-resistant sublines when compared to parental. This is because the analysis reported missing values within the dataset for PDGFR α expression across the samples and, as a result, PDGFR α expression was removed from subsequent analyses. This is a known limitation of the type of mass spectrometry data generation that we utilised, namely data-dependent acquisition, which only fragments the most abundant precursor ions (Beeton-Kempen, 2021). Therefore, peptides of lower abundance are missed in quantification and creates gaps within the resultant data. Data-independent acquisition, although more

expensive, complex, and time consuming, results in all precursor ions being fragmented and all peptides being included in the analysis (Beeton-Kempen, 2021). Future work utilising this approach can provide a much more complete dataset and deeper proteome coverage.

Small molecule inhibitor screens and subsequent validations in the TKI-resistant A204 sublines revealed the emergence of collateral sensitivity to the selective pan-FGFR inhibitor infigratinib in the A204SitR and A204AnloR sublines. This phenomenon was exclusive to A204 sitravatinib- and anlotinib-resistant sublines and was not observed in cells that had derived acquired pazopanib or regorafenib resistance. This is in contrast with previous work by Wong *et al.* where pazopanib-resistant A204 cells were found to be sensitive to FGFR inhibition. However, many studies have shown that the emergence of drug resistance and subsequent collateral sensitivities is an inherently stochastic phenomenon, wherein cells harbouring different mechanisms of resistance and collateral sensitivities may expand under the selective pressure of therapy in separate replicates (Dhawan *et al.*, 2017; Nichol *et al.*, 2019; Scarborough *et al.*, 2020). Therefore, the derivation of collateral sensitivities and resistance phenotypes are not necessarily reproducible despite utilising the same cell lines and inhibitors. Despite this, the work presented in **Chapter 6** revealed that infigratinib collateral sensitivity in A204 cells that had been pre-treated with sitravatinib was found to be a robust and reproducible phenotype. This result therefore provides rationale for further evaluation into employing selective FGFR inhibition as a second-line treatment strategy in MRT patients that have progressed upon sitravatinib, as well as potentially other STS driven by PDGFR and FGFR signalling.

However, **Chapter 6** also reports that prolonged and chronic treatment of the sitravatinib pre-treated A204 cells with infigratinib will eventually result in the re-acquisition of infigratinib resistance, despite an initial response and plateau of growth. Previous studies, primarily in antibiotic-resistant bacteria, have shown the applicability of drug cycling and sequential techniques in suppressing the outgrowth of drug-resistant cells (Imamovic & Sommer, 2013; Nichol *et al.*, 2015). For instance, the work by Imamovic & Sommer demonstrated that *Escherichia coli* cells initially treated with drug “A” soon become resistant and can be collaterally sensitised by drug “B” (Imamovic & Sommer, 2013). Upon subsequent acquisition of resistance to drug “B”, cycling and sequential therapies can be employed either by returning to drug “A” or a

new drug “C” that has a compatible collateral sensitivity profile. This will allow for the long-term control of cellular proliferation and resistance (Imamovic & Sommer, 2013). Imamovic & Sommer concluded that the efficacy of drug sequencing or cycling of collateral sensitivities in antibiotic-resistant bacteria can be employed in other diseases with evolutionary drug resistance mechanisms, such as cancer (Imamovic & Sommer, 2013). The hypothesis behind this strategy, incorporating the inhibitors used in **Chapter 6**, is outlined in **Figure 6.22**.

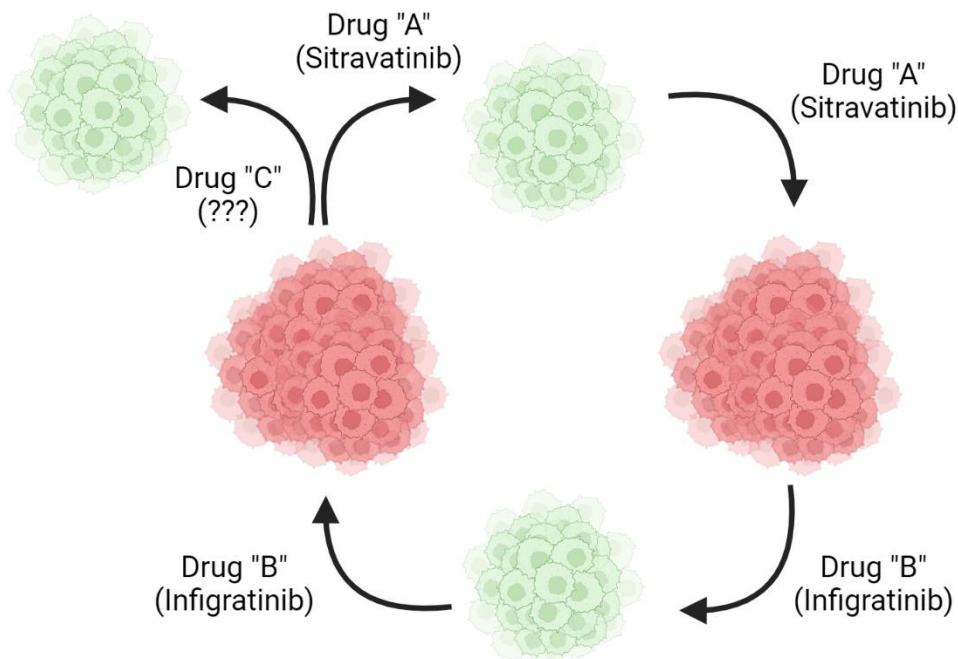


Figure 6.22: Drug cycling and sequential strategies to control disease progression through the targeting of collateral sensitivities. Image was created using BioRender.

Several studies in drug-resistant cancers and bacteria have highlighted the potential of utilising collateral sensitivity networks and sequential strategies to control disease and prevent the emergence of refractory resistance (Acar *et al.*, 2020; Nichol *et al.*, 2015). These studies state that upon the acquisition of resistance, evolutionary trade-offs occur to make cells resistant to the primary treatment but reveal collateral vulnerabilities that could be exploited therapeutically. The studies utilise a strategy termed “evolutionary steering”, which refers to the use of treatment strategies and sequences that steer cells towards a population that become collaterally susceptible to a subsequent, sequential therapy (Acar *et al.*, 2020). It is therefore feasible that upon the re-acquisition of resistance to the sequential therapy, collateral sensitivity networks and “evolutionary steering” can be re-deployed in adaptive therapies to manage and control disease in a long-term fashion.

Furthermore, recent studies have revealed the emergence of temporally-restricted windows of collateral sensitivities in ALK inhibitor-resistant NSCLC, Bcr-Abl1 inhibitor-resistant leukaemia, and chemotherapy-resistant Ewing sarcoma (Dhawan *et al.*, 2017; Scarborough *et al.*, 2020; Zhao *et al.*, 2016). These collateral sensitivities target vulnerabilities that occur during intermediate evolutionary stages of emerging drug resistance. These studies postulate that the use of sequential treatment strategies can exploit temporal collateral sensitivities that could prevent the derivation of refractory resistance and allow for the long-term management of disease.

Therefore, future research will focus on the applicability of employing drug cycling and sequential treatments to target collateral sensitivities, including temporally-restricted collateral sensitivities, in order to control progression and treatment resistance in MRT models. This approach will aim to answer outstanding questions related to the work from **Chapter 6**. These outstanding questions include whether cycling between sitravatinib and infigratinib therapies can control disease progression and resistance by exploiting collateral sensitivities in the A204 MRT model. Further to this, determining potential collateral sensitivities in sitravatinib pre-treated A204 cells that had re-acquired infigratinib resistance can provide answers to sequential therapies that can be employed in the further-line setting.

Furthermore, the reason behind the exclusive and reproducible effect observed in sitravatinib pre-treated A204 cells, compared to the other three multi-target TKI pre-treated cells, remains elusive. I hypothesise that the robust infigratinib collateral sensitivity is likely to be due to an additional and reproducible sitravatinib-induced effect which is as yet undetermined, but one which does not occur in cells treated with the other multi-target TKIs. Work presented in **Chapter 6** highlights avenues of potential research to answer this question. These include phenotypes that were observed in sitravatinib pre-treated A204 cells that weren't observed in DMSO pre-treated cells including the ability of infigratinib to inhibit residual PDGFR α activity, decreased levels of DDR2 activity, and an increase in EphA7 activity.

However, despite these outstanding questions, employment of ponatinib or combination therapy of infigratinib plus sitravatinib upon the re-acquisition of infigratinib resistance was found to control or regress cellular growth, thereby nominating these therapies in the further-line setting in this treatment paradigm

(**Figure 6.23**). It is yet to be determined whether the incorporation of erdafitinib into the subsequent treatment following infigratinib resistance re-acquisition is a viable option. However, the similar antitumour and signalling modulation phenotypes observed between erdafitinib and combination therapy/ponatinib therapy over the course of **Chapters 5** and **6** suggests that erdafitinib is likely to be effective in this multi-line treatment paradigm.

The inhibitor screens also revealed that treatment with erdafitinib and ponatinib could potentially be employed as effective salvage therapies for multi-target TKI-resistant MRT. Furthermore, following increased A204 cellular progression upon first-line multi-target TKI treatment, second-line sequential treatments with erdafitinib or ponatinib were found to result in long-term suppression of cell growth. These results therefore nominate erdafitinib and ponatinib for further evaluation as effective second-line therapies in the treatment of MRT that progress upon first-line multi-target TKI therapy, as well as other STS driven by PDGFR and FGFR activity (**Figure 6.23**).

There is a limiting caveat to the results reported in **Chapter 6**. Importantly, derivation of TKI-resistant models and subsequent evaluations were only performed within a single cell line – A204. Derivation of resistance to another model of STS driven by PDGFR α and FGFR1, G402, was being undertaken but had to be curtailed due to the initial and subsequent COVID-induced lockdowns. Upon return to laboratories, there was insufficient time to re-derive the G402 TKI-resistant sublines before submission. I therefore decided to focus on the A204 cell line for the purpose of **Chapter 6**. However, future work will focus on re-deriving the G402 TKI-resistant sublines, as well as other STS models driven by PDGFR and FGFR signalling. This will allow for the determination of whether the results described in **Chapter 6** are specific to the A204 cell line or whether the effects are consistent within other models of PDGFR- and FGFR-driven STS.

Despite this limitation, **Chapter 6** has highlighted a number of potential sequential strategies that could be employed in the long-term disease control of MRT, as well as potentially other STS driven by PDGFR and FGFR signalling (**Figure 6.23**). The nominated sequential treatment strategies are outlined in **Figure 6.23**. Further work evaluating drug cycling or sequential treatment strategies that target collateral sensitivities in the long-term disease management of STS is warranted in order to

further potentially determine novel strategies that exploit resistance-induced vulnerabilities.

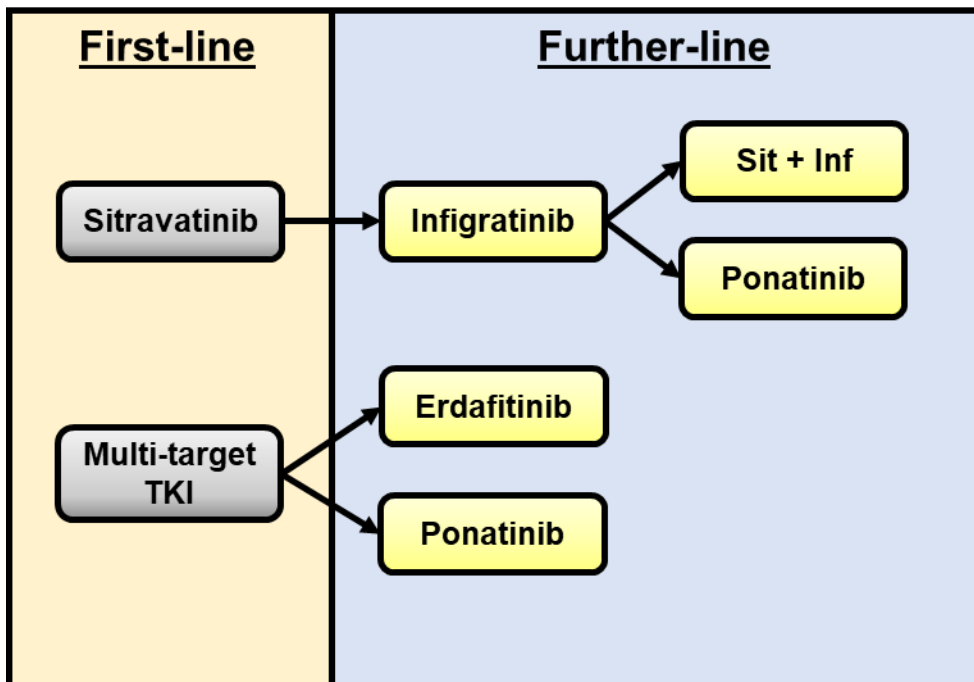


Figure 6.23: Nominated sequential treatment strategies outlined in Chapter 6 as effective long-term treatment regimens for disease control in MRT, and potentially other STS driven by PDGFR and FGFR signalling. FGFR; Fibroblast growth factor receptor, Sit; Sitravatinib, TKI; Tyrosine kinase inhibitor.

Chapter 7

Discussion

7.1 Introduction

Patients diagnosed with advanced soft tissue sarcomas (STS) currently have limited targeted therapy options, with only the multi-target tyrosine kinase inhibitor (TKI) pazopanib currently approved for use. Furthermore, clinical experience has revealed that effective pazopanib treatment is restricted by drug resistance, with patients either harbouring intrinsic resistance or developing an acquired resistance. There has therefore been a recent push to develop and evaluate further multi-target TKIs for their activity in advanced STS. However, multi-target TKIs currently undergoing clinical evaluation in STS have all shown similar problems regarding the existence or emergence of drug resistance. There is an unmet clinical need to better understand the mechanisms of multi-target TKI resistance, in order to develop more effective treatment strategies for patients with advanced STS. This chapter will place my work in the context of contemporary STS research and discuss some of the outstanding challenges for improving the efficacy of multi-target TKIs in STS patients. In addition, this chapter will also discuss a number of emerging therapeutic strategies that could soon be entering into clinical use for advanced STS patients.

7.2 Outstanding challenges for increasing the efficacy of multi-target TKI therapy in soft tissue sarcoma

The clinical efficacy of the multi-target TKI pazopanib in the treatment of advanced STS is limited and patients treated with this drug have been shown to have no significant survival benefit, when compared to placebo (Van der Graaf *et al.*, 2012). The clinical efficacy is limited as we currently have no way of determining which subsets of patients are more likely to derive a benefit from pazopanib therapy compared to patients that harbour intrinsic resistance. Additionally, STS patients will universally acquire resistance to pazopanib through resistance mechanisms that urgently need identifying to provide new therapies. These resistance mechanisms may be due to tumour heterogeneity, where subclonal resistant populations exist within an overall tumour clonal population that, upon therapeutic pressure, gives rise to

treatment-resistant disease and subsequent progression. There is therefore an urgent unmet need to develop predictive biomarkers of multi-target TKI response in STS, as well as a greater understanding of STS intratumoural heterogeneity. This sub-chapter will discuss these outstanding challenges and how my preclinical work may give rise to future avenues to overcome these hurdles.

7.2.1 Predictive biomarkers of multi-target TKI response in soft tissue sarcoma

Predictive biomarkers of targeted therapy response in cancer are invaluable tools that can help guide treatment choice for patients. They provide a means of stratifying and selecting patients for targeted therapy based on how likely they are to respond to that particular therapy (Ben-Hamo *et al.*, 2020). There are a number of validated predictive biomarkers that are currently routinely employed in the clinic (Bedard *et al.*, 2013; Ulivi, 2020). For instance, non-small cell lung cancer (NSCLC) patients harbouring epidermal growth factor receptor (*EGFR*) exon 19 or 21 mutations can be treated with *EGFR* inhibitors, which are effective therapies in this subset of patients compared to non-*EGFR* mutated NSCLC (Rosell *et al.*, 2010). Therefore, patients harbouring these predictive biomarker mutations can be specifically selected to receive effective *EGFR* inhibitor therapy, whilst patients without such mutations are spared an ineffectual therapy (Rosell *et al.*, 2010).

However, there are currently a lack of validated predictive biomarkers for multi-target TKI therapy response in STS (Lee *et al.*, 2019; Wilding *et al.*, 2019). This therefore outlines a critical unmet need to determine predictive biomarkers that allow for the prospective stratification of patients, allowing for the selection of STS patients most likely to benefit from multi-target TKI therapy. This would not only improve multi-target TKI clinical efficacy and cost-effectiveness, but also ensures that patients unlikely to respond to TKIs are not treated with ineffective therapies. This sub-chapter will discuss a number of studies that have highlighted potential predictive biomarkers of multi-target TKI therapy response in advanced STS.

In a small retrospective analysis of 18 patients with advanced STS treated with pazopanib (and 1 patient treated with sunitinib), Koehler *et al.* employed next-generation sequencing (NGS) to assess the mutational status of *TP53*. The authors reported that patients with *TP53* mutations had a significantly improved median

progression free survival (mPFS) compared to patients with wild-type *TP53* (mPFS; 3.5 vs. 2.0 months, $p = 0.036$) (Koehler *et al.*, 2016). Although a small study that requires independent validation in larger cohorts, this study highlights a promising potential biomarker predictive of pazopanib resistance in STS (Koehler *et al.*, 2016).

In a further cohort of STS patients treated with pazopanib therapy, Sleijfer *et al.* undertook baseline analysis of serum cytokine and angiogenic factors to assess their potential utility as predictive biomarkers of pazopanib response (Sleijfer *et al.*, 2012). Through analysis of 85 patients from the EORTC phase II clinical trial of pazopanib in advanced STS, low baseline plasma levels of hepatocyte growth factor (HGF) and basic nerve growth factor (bNGF) were found to be associated with a better PFS. Additionally, several further cytokine and angiogenic factors were found to correlate with increased 12-week progression-free rate (PFR) (low interleukin-12 subunit p40 (IL-12p40) and mitochondrial pyruvate carrier 3 (MPC3)) and increased overall survival (OS) (low intercellular adhesion molecule 1 (ICAM-1) and interleukin-2 receptor α (IL-2ra)). However, the authors call attention to the caveats of high false discovery rates (FDRs) (20-50%) and therefore conclude that these correlations could be false positives (Sleijfer *et al.*, 2012). Additionally, as was the case for the study by Koehler *et al.*, independent validation is required.

Predictive biomarkers of regorafenib response have also been investigated in advanced STS. Brodowicz *et al.* investigated potential predictive biomarkers for regorafenib response in patients enrolled in the REGOSARC trial (Brodowicz *et al.*, 2020). The authors assessed 134 enrolled patients and assessed for the predictive properties of 57 potential biomarkers. Unfortunately, although several promising biomarkers were found to exist within the evaluated cohort, none were found to be viable as predictive biomarkers for regorafenib response (Brodowicz *et al.*, 2020).

However, the CREATE trial has shown the utility of employing ALK and MET expression as predictive biomarkers of crizotinib response in three STS subtypes commonly associated with overactivity in these receptor tyrosine kinases (RTKs) (Schöffski *et al.*, 2017; Schöffski *et al.*, 2018; Schöffski *et al.*, 2018). The first of these is alveolar soft part sarcoma which harbour the pathognomonic *TFE3-ASPSCR1* translocation that frequently leads to MET overexpression (Jun *et al.*, 2010). Secondly, 50% of inflammatory myofibroblastic tumours are characterised by *ALK* translocations

resulting in oncogenic overactivity (Butrynski *et al.*, 2010). Finally, clear cell sarcomas are characterised by the *EWSR1-ATF1* translocation which activates the oncogenic expression of MET (Davis *et al.*, 2010). The CREATE phase II trial reported that crizotinib had clinically meaningful activity in MET-positive alveolar soft part sarcoma and clear cell sarcoma, as well as ALK-positive inflammatory myofibroblastic tumour (Schöffski *et al.*, 2017; Schöffski *et al.*, 2018; Schöffski *et al.*, 2018). Therefore, in addition to these select subtypes, ALK and MET expression could be employed as predictive biomarkers in order to stratify STS patients to select for ALK and/or MET-positive patients that are more likely to respond to crizotinib therapy.

Finally, the seminal work by Chibon *et al.* highlighted the utility of transcriptomic biomarker signatures and gene expression profiles in order to stratify STS patients (Chibon *et al.*, 2010). By designing a 67 gene transcriptomic-based risk classifier, termed CINSARC, the authors were able to stratify STS patients based on likely prognosis and predict patients at high risk of developing metastases (Chibon *et al.*, 2010). Therefore, similar gene expression-based classifiers, integrated with other potential predictive biomarkers, could be designed. These classifiers could subsequently be implemented in order to determine subgroups of STS patients harbouring specific biomarker signatures that make them more likely to respond positively to multi-target TKI therapy (Merry *et al.*, 2021). These patients can therefore be selectively treated with multi-target TKI therapy, thereby increasing clinical efficacy and cost-effectiveness of the drug.

The work presented in this thesis has shown that dasatinib therapy is an effective treatment strategy in pazopanib-resistant STS, through targeting of the Src signalling pathway, in both acquired and intrinsic resistance models. This work therefore provides rationale for determining and stratifying advanced STS patients based on levels of Src expression and activity. Future work should focus on whether Src expression can be employed as a predictive biomarker for advanced STS patients, in order to selectively stratify STS cases with relatively high Src expression that could be more effectively treated with dasatinib therapy. Similarly, this work has shown the utility of first-line erdafitinib and ponatinib in MRT cell lines driven by PDGFR α and FGFR1. My work has postulated that these two inhibitors mediate their antitumour activities in these models by concurrent inhibition of the PDGFR α and FGFR1 signalling pathways. Therefore, future work should explore whether the expression of

PDGFR and/or FGFR in STS subtypes could be employed as a potential predictive biomarker in stratifying STS cases with elevated expression of these RTKs. This could further elucidate a subset of STS patients that could be more effectively treated with either erdafitinib or ponatinib therapy.

The elucidation of predictive biomarkers for multi-target TKI response are essential in improving the efficacy of treating patients with advanced STS. Further determination of predictive biomarkers will progress our current treatment strategies away from the one-size-fits-all treatment strategy for heterogeneous STS cohorts towards a personalised medicine approach, where the right STS patient with a particular underlying pathology is treated with the right therapy.

7.2.2 Intratumoural heterogeneity and liquid biopsies

It is now well-understood that tumours are composed of a complex population of cells with varying genetics, epigenetics, and metabolomics and these differences will determine how each individual cell responds to a therapy (Vitale *et al.*, 2021). Such intratumoural heterogeneity is now an important consideration in understanding targeted therapy response and resistance. For instance, whilst the administered targeted therapy may have antitumour activity in the majority of cells within a tumour, a subpopulation of cells will harbour biological traits that confer a survival benefit. These cells will therefore out-compete the sensitive cells and lead to therapy-resistant disease. Furthermore, a large range of studies across cancer have shown that the degree of intratumoural heterogeneity positively correlates with poorer prognosis and an increase in the rate of targeted therapy resistance (Andor *et al.*, 2016; Mroz *et al.*, 2013; Patel *et al.*, 2014; Suda *et al.*, 2016).

Despite the established association between intratumoural heterogeneity and the emergence of drug resistance, studies evaluating tumour heterogeneity and drug resistance mechanisms to targeted therapy in STS are currently lacking. However, a study of rhabdomyosarcoma tumours has reported the existence of subclonal populations within heterogeneous tumours that may provide selective advantages upon therapy to result in drug-resistant populations (Chen *et al.*, 2015). This study by Chen *et al.* found that rhabdomyosarcoma patient tumours were composed primarily of a dominant clone, with typically over 80% representation. Whole-genome

sequencing determined the existence of subclonal populations that harboured additional point mutations in oncogenes including *ABL1*, *HER2*, and *KDR* (VEGFR2), which were not present in the dominant clonal population. The authors postulate that these genomic alterations, exclusive to the subclonal populations, could give rise to drug-resistant populations upon therapeutic treatment. The authors caveat this hypothesis by stating that experimental validation is required (Chen *et al.*, 2005). Furthermore, by conducting single-cell RNA sequencing, two studies focussed on Ewing sarcoma patient tumours found the existence of subclonal populations of cells with extensive alterations in terms of epigenetics, metabolomics, and transcriptomics, compared to the dominant clonal population (Aynaud *et al.*, 2020; Sheffield *et al.*, 2017). Additionally, it was reported that patients harbouring increased levels of these subclonal populations, and therefore increased tumour heterogeneity, had more aggressive disease and increased metastasis (Sheffield *et al.*, 2017). However, there is a current unmet need to evaluate the association between subclonal populations that pre-exist within heterogeneous STS tumours and the emergence of targeted therapy resistance.

The existence of drug-tolerant persister cells and cancer stem cells have also been described as important considerations when assessing intratumoural heterogeneity and therapy resistance (Cabanos & Hata, 2021). Drug-tolerant persister cells are a subpopulation of cells that are not inherently resistant to therapy, but exist in a quiescent, slowly proliferating state that renders them tolerant to therapy. These tolerant cells can subsequently give rise to drug-resistant progeny resulting in therapeutic resistance and disease relapse (Cabanos & Hata, 2021). These cells and their role in drug resistance have frequently been described in a number of cancer types, including lung and breast cancers, however studies focussed on their role in STS therapy resistance are currently lacking (Hata *et al.*, 2016; Vinogradova *et al.*, 2016). Furthermore, cancer stem cells represent a small population of tumour cells that have the capability of self-renewal and differentiation, as well as the ability to exist within a quiescent state. These properties can render cancer stem cells resistant to anticancer therapies, and these cells can promote subsequent disease relapse and progression (Cojoc *et al.*, 2015; Phi *et al.*, 2018; Yu *et al.*, 2012). Although cancer stem cells and their association with therapy resistance have frequently been reported in osteosarcoma, studies focussing on STS are currently limited to a single study

conducted in leiomyosarcoma (Fourneau *et al.*, 2019; Hatina *et al.*, 2019). In this study, Fourneau *et al.* revealed that leiomyosarcoma cell line and xenograft models that had derived an acquired resistance to PI3K/mTOR inhibition displayed significantly higher levels of cancer stem cell markers (e.g., *SOX2*, *ALDH1A2*) than the sensitive parental cells (Fourneau *et al.* 2019). The authors found that treatment of the resistant cell population with an EZH2 inhibitor resulted in the elimination of cancer stem cells and re-sensitised the overall resistant cell population to PI3K/mTOR inhibition (Fourneau *et al.*, 2019). Therefore, the existence of cancer stem cells within STS tumours are an important factor in the response to therapy and the emergence of resistance.

The work presented in this thesis revealed PDGFR α loss, and associated downstream Akt signalling suppression, as a potential mechanism of resistance in the A204 TKI-resistant sublines. This work did not determine whether this effect is due to the outgrowth of pre-existing PDGFR α -deficient subclones within the parental A204 population or whether this phenotype arose within drug-tolerant cells in response to the TKI exposure. However, previous work by Wong *et al.* with pazopanib-, sunitinib-, and dasatinib-resistant A204 cells found that PDGFR α loss was likely to be due to the survival of drug-tolerant cells that produce progeny with PDGFR α -deficiency leading to a TKI-resistant cellular population (Wong *et al.*, 2016). This therefore postulates that a similar effect has occurred within my TKI-resistant sublines. Future avenues of work, such as single cell experiments and barcoding, could look into the potential of targeting the mechanisms by which drug-tolerant cells survive multi-target TKI treatment in my employed STS models and thereby eradicate the cellular population that give rise to resistance.

In the clinic, a potential methodology to assess intratumoural heterogeneity is to employ liquid biopsies. Liquid biopsies are taken from patient blood samples and assess for circulating tumour cells (CTCs) and circulating tumour DNA/RNA (ctDNA/RNA) (Wei *et al.*, 2020). This is in contrast to the current standard of tumour assessment which is to take solid tumour biopsies. Solid tumour biopsies are the mainstay medical technique for cancer diagnosis, disease staging, and informing treatment selection. However, these are invasive procedures that can only take a snapshot of a specific area of the tumour at a specific time, thereby neglecting the temporal and spatial dynamics and heterogeneity of tumour biology. Liquid biopsies

on the other hand are non-invasive and can readily be repeated through the course of treatment. Not only does this allow for the dynamic and real-time monitoring of treatment response, but it can also evaluate temporal and spatial tumour heterogeneity, even in distant metastatic lesions. Furthermore, this technique could allow for the early detection of recurrence and therapeutic resistance (Wei *et al.*, 2020).

The use of liquid biopsies in STS however is still in its relative infancy and is primarily used for diagnostic purposes (Wei *et al.*, 2020). However, Jung *et al.* showed the utility of liquid biopsies in determining the emergence of therapy resistance in dedifferentiated liposarcoma patients treated with targeted MDM2 inhibitor therapy (Jung *et al.*, 2016). MDM2 activity results in the abrogation of p53 activity, frequently resulting in tumourigenesis. Therefore, MDM2 inhibition represents an attractive method of restoring p53 activity and controlling disease progression. However, treatment with MDM2 inhibitors has been shown preclinically to lead to the emergence of mutated p53 which results in therapeutic resistance. Through the use of liquid biopsies in dedifferentiated liposarcoma patients treated with MDM2 inhibitors, Jung *et al.* reported increasing prevalence of mutated *TP53* ctDNA that correlated with increasing tumour size and therapy resistance (Jung *et al.*, 2016).

Furthermore, studies conducted upon gastrointestinal stromal tumour (GIST) patients have reported the utility of liquid biopsies in the early detection of the emergence of secondary resistance mutations (Kang *et al.*, 2015; Wada *et al.*, 2016). For instance, Kang *et al.* analysed matched pre-treatment and post-treatment ctDNA samples obtained from liquid biopsies of GIST patients treated with imatinib (Kang *et al.*, 2015). In the post-treatment sample, the authors were able to identify the emergence of imatinib-resistant *KIT* and platelet-derived growth factor receptor α (*PDGFRA*) mutations which were found to correlate with reduced sensitivity of the tumour to imatinib treatment (Kang *et al.*, 2015). This was consistent with the findings of Wada *et al.* who were able to detect the early emergence of secondary *KIT* mutations in GIST patients that developed imatinib resistance (Wada *et al.*, 2016).

Liquid biopsies can therefore be used to accurately monitor and evaluate tumour heterogeneity and response to targeted therapies. This represents a therapeutic opportunity that could allow for the temporal monitoring of treatment response and the

implementation of reactive treatment strategies that could be employed to pre-empt significant disease progression and resistance.

7.3 Emerging therapies for the treatment of soft tissue sarcoma

Despite significant advancements in our understanding of STS pathology and the approval of a number of therapeutics to treat advanced STS, there has been marginal progress over the past two decades to increase the survival times of patients (Kasper, 2019; Lee *et al.*, 2021). There is therefore a clinically unmet need to develop novel treatments, and this sub-chapter will describe some of the emerging therapeutic strategies that could be employed in the future treatment of advanced STS. These therapeutic strategies include adaptive therapies, immunotherapies, and personalised medicine.

7.3.1 Adaptive sequential therapy and collateral sensitivity

The development of drug resistance in cancer operates via the Darwinian model of natural selection where the survival of the fittest cells in a heterogeneous tumour result in the outgrowth of drug-resistant cells and therapeutic failure (Greaves & Maley, 2012). However, the emergence of drug resistance often comes at the expense of an evolutionary trade-off whereby drug-resistant cells may become sensitive to a previously ineffective drug. This phenomenon is termed collateral sensitivity and has been extensively researched in the field of antibiotic-resistant bacteria, as well as in some cancer types (Acar *et al.*, 2020; Efferth *et al.*, 2020; Pál *et al.*, 2015; Pluchino *et al.*, 2012; Zhao *et al.*, 2016).

For instance, Imamovic & Sommer derived antibiotic-resistant *Escherichia coli* lineages to a panel of clinically relevant antibiotics (Imamovic & Sommer, 2013). Through determination of the collateral sensitivities that arose in response to resistance acquisition, the authors created a collateral sensitivity network and identified a number of collateral sensitivity cycles that could be employed to control and suppress antibiotic resistance in bacteria (Imamovic & Sommer, 2013). These

cycles operate on the basis that if a cellular population becomes resistant to drug 1, treatment can be switched to a collaterally sensitive drug 2, and then, once again switched back to drug 1 upon re-acquisition of resistance. Hypothetically, the cycle can also be a sequence of treatments where upon acquisition of resistance to drug 2, a third drug can be employed to target further collateral sensitivities, with this process continued for further-line treatments. Through this proof-of-principle study in bacteria, the authors postulate that similar adaptive drug cycling/sequential strategies, designed based on collateral sensitivity networks, could be employed in other evolutionary-driven diseases, such as drug-resistant cancers (Imamovic & Sommer, 2013).

Indeed, Dhawan *et al.* further reported the design of potential sequential drug protocols leveraging on cycling collateral sensitivities in NSCLC cell lines (Dhawan *et al.*, 2017). Through the escalating dose derivation of *in vitro* ALK inhibitor resistance in NSCLC cell lines, the authors derived a mathematical model based on pharmacological screens performed on resistant sublines. This mathematical model was able to predict which anticancer compounds, when treated in the second-line setting in response to ALK inhibitor resistance, would be the most likely treatment to induce collateral sensitivity and result in an effective salvage therapy (Dhawan *et al.*, 2017). The model further reported the design of drug cycling protocols, whereby drug sequences are employed that continuously exploit collateral sensitivities that arise in cells acquiring resistance to the preceding drug within the sequence. The authors reported 84 unique cycles of varying lengths of between 2-7 drugs. For instance, the authors highlighted the collateral sensitivity cycle of crizotinib, etoposide, paclitaxel, and luminespib (NVP-AUY922), before the cycle returns to crizotinib (Dhawan *et al.*, 2017). Despite the authors having not yet experimentally validated such cycles in their cell line models, the study reveals a notable experimental method that could be used to determine therapy cycling and sequencing strategies in cancer, including STS.

Further to the work by Dhawan *et al.*, several studies have been researching the potential of generating predictive computational models that can be used to mathematically map the emergence of collateral sensitivities in response to therapeutic resistance (Aulin *et al.*, 2021; Nichol *et al.*, 2015; Zhao *et al.*, 2016). Such predictive models would be an incredibly powerful tool that could help clinicians design treatment sequences and strategies to control therapy resistance, whereby an

administered therapy is switched upon the acquisition of resistance to a subsequent drug that induces a collateral sensitivity.

However, several studies, both in bacteria and cancer, have shown that the evolution of drug resistance is stochastic and difficult to predict (Nichol *et al.*, 2019; Scarborough *et al.*, 2020). Furthermore, the majority of studies assessing drug resistance do not take into consideration temporal considerations in the evolutionary process of acquired drug resistance. For instance, studies by Zhao *et al.* and Vander Velde *et al.* have shown the existence of temporal collateral sensitivities that exist at intermediate stages during the evolution of drug resistance in preclinical cell models of cancer (Vander Velde *et al.*, 2020; Zhao *et al.*, 2016).

The study by Zhao *et al.* describes the process of tumour evolution as a dynamic process whereby states of intermediary collateral sensitivity exist temporally during the acquisition of drug resistance (Zhao *et al.*, 2016). The authors utilised a murine-derived Philadelphia chromosome-positive acute lymphoblastic leukaemia cell line which they exposed to dose-escalating concentrations of Bcr-Abl1 inhibitors, such as bosutinib and dasatinib. Throughout the course of resistance derivation, Zhao *et al.* undertook pharmacological screens in the cells to map collateral sensitivities through the evolutionary course of resistance acquisition. The authors found that acquisition of Bcr-Abl1 inhibitor resistance resulted in the collateral sensitivity towards the multi-target TKIs crizotinib, foretinib, vandetanib, and cabozantinib, a phenotype that was found to translate into an *in vivo* murine model. However, upon the continued acquisition of increasing levels of Bcr-Abl1 inhibitor resistance, the levels of collateral sensitivity significantly decreased. Subsequently, the authors found that temporal collateral sensitivities to the multi-target TKIs were caused by the emergence of a single Abl1 point mutation (V299L) (Zhao *et al.*, 2016). Upon the continued inhibitor exposure and resultant loss of temporal collateral sensitivity, the TKI-resistant cells were found to harbour V299L compound mutations. The work by Zhao *et al.* therefore reports temporal states of collateral sensitivity that could potentially be exploited therapeutically, and which did not exist in fully Bcr-Abl1 inhibitor-resistant cells (Zhao *et al.*, 2016).

Temporal collateral sensitivities in drug-resistant cancers were also reported by Vander Velde *et al.* (Vander Velde *et al.*, 2020). In this study, an ALK-positive lung

cancer cell line was exposed to increasing concentrations of ALK inhibitor alectinib to derive a resistant subline. As EGFR and HER2 upregulation was previously found to correlate with the acquisition of ALK inhibitor resistance, the authors treated the alectinib-resistant cells with the EGFR inhibitor lapatinib throughout the course of resistance derivation. As expected, prior to alectinib exposure, parental cells were relatively resistant to lapatinib. As the cells were exposed to alectinib and evolved resistance, potent temporal collateral sensitivity to lapatinib emerged that gradually decreased as the cells became increasingly more resistant to alectinib (Vander Velde *et al.*, 2020).

Furthermore, the incorporation of drug holidays – time periods whereby treatment is ceased for a significant length of time – into adaptive treatment schedules have also been found to significantly alter collateral sensitivities in resistant cells (Dhawan *et al.*, 2017). Through the derivation of ALK inhibitor-resistant NSCLC sublines, Dhawan *et al.* found that the incorporation and length of drug holidays significantly affected collateral sensitivities in the resistant cells. For instance, temporal collateral sensitivities to lorlatinib in ceritinib-resistant cells fluctuated over the course of a 21-day drug holiday, with assessments of cell viability taking place on day 1, 3, 7, 14, and 21. Interestingly, the study also highlighted the potential of treatment strategies of the same TKI but incorporating drug holidays into the treatment schedule. This was based on the observation that alectinib-resistant cells re-acquired alectinib sensitivity after only 14 days of drug holiday (Dhawan *et al.*, 2017).

These studies therefore identify potential sequential treatment strategies that consider temporal states of collateral sensitivity, whereby upon the acquisition of intermediary levels of resistance, treatment can be switched to a collaterally sensitive drug, before the emergence of robust resistance mechanisms that attenuate any potential collateral sensitivities (Vander Velde *et al.*, 2020; Zhao *et al.*, 2016). Furthermore, the incorporation of drug holidays into treatment strategies is an important consideration within the future design of adaptive sequential therapies (Dhawan *et al.*, 2017).

Finally, a recent seminal study by Acar *et al.* has discussed the utility of “evolutionary steering” – an adaptive therapy strategy designed to control disease progression and manage the emergence of refractory resistance (Acar *et al.*, 2020). “Evolutionary steering” refers to the employment of a sequence of drugs that “steer” cellular

populations towards collaterally sensitive states, which could then be exploited by a subsequently administered drug, whilst avoiding drug-resistant states. Furthermore, adaptive therapy via “evolutionary steering” differs from other forms of adaptive therapy as the drug treated in the first-line does not even need to be the most effective drug currently available, but rather one that “steers” the population towards a more readily treatable population of cells through the emergence of collateral sensitivities (Acar *et al.*, 2020; Nichol *et al.*, 2015). This method has previously been shown to be an effective strategy in subverting and controlling antibiotic resistance in bacteria, and a recent study by Acar *et al.* has also shown utility of the method in drug-resistant cancer (Acar *et al.*, 2020; Nichol *et al.*, 2015). Within this study, gefitinib- and trametinib-resistant NSCLC were generated following chronic high-dose inhibitor treatment (Acar *et al.*, 2020). Subsequent genomic analysis revealed the existence of treatment-resistant clones with *MET* amplifications (gefitinib-treated) and *CDKN2A* loss (trametinib-resistant), both in the parental pre-treatment and the TKI-resistant populations. The study reported that the gefitinib-resistant clones harbouring *MET* amplifications were sensitive to MET inhibition by capmatinib compared to the parental cells (Acar *et al.*, 2020). These results indicate the potentiality of designing an adaptive sequencing strategy that alternates between gefitinib and capmatinib to control disease and prevent the emergence of a drug-resistant population. Similarly, the results of the study also indicated the potential utility of cycling between trametinib and palbociclib, a cyclin-dependent kinase (CDK) 4/6 inhibitor (as *CDKN2A* loss leads to CDK4/6 upregulation), in controlling disease and resistance (Acar *et al.*, 2020).

These studies in other cancer types and the work presented in this thesis may provide the platform for further evaluation of adaptive sequential therapy to target collateral sensitivities in the treatment of advanced STS. My work has shown that, similar to the work by Acar *et al.*, the development of sitravatinib resistance in the A204 cell line model of malignant rhabdoid tumour (MRT) – a paediatric STS subtype - results in a cellular population that is exquisitely sensitive to subsequent infigratinib therapy (Acar *et al.*, 2020). Building on this finding, as well as previous studies highlighting the utility of drug cycling protocols, future work will focus on whether cycles of infigratinib and sitravatinib therapy can effectively control cellular proliferation and prevent the outgrowth of resistant MRT, as well as other STS models that are driven by PDGFR and FGFR signalling (Dhawan *et al.*, 2017; Imamovic & Sommer, 2013). The

incorporation of drug holidays and the evaluation of temporal collateral sensitivities, as described by the papers discussed above, are also important future considerations in the design of evaluating collateral sensitivity drug cycles and my future work will employ such techniques (Dhawan *et al.*, 2017; Vander Velde *et al.*, 2020; Zhao *et al.*, 2016). The concept of “evolutionary steering” also opens up the potentially exciting avenue of pre-treating STS models that harbour intrinsic multi-target TKI resistance with a particular treatment in order to generate a subsequent population of cells that may be sensitive to second-line multi-target TKI therapy, as well as other second-line treatments (Acar *et al.*, 2020; Nichol *et al.*, 2015).

Adaptive therapy represents an attractive treatment strategy for the long-term control of disease through the continual targeting of collateral sensitivities that emerge in treatment-resistant cells. Therefore, rather than attempting to cure disease, cancers are treated with the aim of controlling progression and resistance, thereby avoiding the outgrowth of refractory disease. However, the majority of studies discussing such strategies are currently limited to *in vitro* and mathematical modelling studies. Additionally, studies in STS evaluating the utility of adaptive sequential therapies are currently lacking. In order to fully assess the utility of adaptive therapy in disease control for patients, *in vivo* and clinical evaluations are required.

7.3.2 Immunotherapy

The vastly improved understanding of the critical interplay that occurs between the immune system and cancer cells has resulted in the emergence of effective anticancer immunotherapies. Many anticancer immunotherapies have been approved for clinical use over the past decade, including the anti-PD-1 antibody pembrolizumab, which was approved for solid tumours with specific indications (**Table 1.2**). There has therefore been a push to determine the efficacy of immunotherapies in the treatment of advanced STS, with the majority of studies focussed on immune checkpoint inhibitors (ICIs) (**Table 1.7**). This type of immunotherapy functions by inhibiting interactions that block the stimulation of anticancer immune responses (Ramos-Casals *et al.*, 2020). The most commonly inhibited immune checkpoint interactions are those involving PD-1/PD-L1 or CTLA-4. In the former of these interactions, immunogenic cancer cells often highly express PD-L1 on their cell surface. This ligand binds to PD-1 on the

surface of a number of immune cells, most notably T lymphocytes. This interaction inactivates the T cell, with the cancer cells thereby evading T cell-mediated cell death. Similarly, CTLA-4 is expressed on the surface of T lymphocytes and inactivates the T cell when bound to either CD80 or CD86 on the surface of antigen-presenting cells. ICIs targeted towards PD-1, PD-L1, or CTLA-4 thereby release the immune blockade, resulting in the activation of T lymphocytes and a subsequent anticancer immune response (Ramos-Casals *et al.*, 2020).

Table 7.1: Immunotherapies currently undergoing clinical evaluation in STS.			
NCT identifier	Study	Treatment	Molecular target(s)
Trials with reported data			
n/a	Maki <i>et al.</i> , 2013	Ipilimumab	CTLA4
NCT02304458	Davis <i>et al.</i> , 2020	Nivolumab	PD-1
NCT02428192	Ben-Ami <i>et al.</i> , 2017	Nivolumab	PD-1
NCT02500797	D'Angelo <i>et al.</i> , 2018	Nivolumab + Ipilimumab	PD-1 + CTLA4
NCT02301039	Tawbi <i>et al.</i> , 2017; Burgess <i>et al.</i> , 2019	Pembrolizumab	PD-1
NCT03141684	Naqash <i>et al.</i> , 2021	Atezolizumab	PD-L1
NCT02815995	Somaiah <i>et al.</i> , 2020	Durvalumab + Tremelimumab	PD-L1 + CTLA4
NCT02636725	Wilky <i>et al.</i> , 2019	Pembrolizumab + Axitinib	PD-1 + TKI
NCT03396211	Chawla <i>et al.</i> , 2019	Nivolumab + Apatinib	PD-1 + TKI
NCT03851614	Ayodele <i>et al.</i> , 2021	Durvalumab + Olaparib/Cediranib	PD-L1 + PARP inhibitor/TKI
NCT01643278	D'Angelo <i>et al.</i> , 2017	Ipilimumab + Dasatinib	CTLA4 + TKI
NCT03138161	Gordon <i>et al.</i> , 2020	Ipilimumab + Nivolumab + Trabectedin	CTLA4 + PD-1 + DNA alkylator
NCT02888665	Pollack <i>et al.</i> , 2020	Pembrolizumab + Doxorubicin	PD-1 + Topoisomerase II inhibitor
NCT02406781	Italiano <i>et al.</i> , 2021	Pembrolizumab + Cyclophosphamide	PD-1 + DNA alkylator
NCT03899805	Nathenson <i>et al.</i> , 2020	Pembrolizumab + Eribulin	PD-1 + Microtubule assembly inhibitor
Ongoing trials			
NCT04784247	MSKCC phase II trial	Pembrolizumab + Lenvatinib	PD-1 + TKI
NCT04095208	CONGRATS	Nivolumab + Relatlimab	PD-1 + LAG-3
NCT03475953	REGOMUNE	Avelumab + Regorafenib	PD-L1 + TKI
NCT04874311	TRUST	Bintrafusp α + Doxorubicin	Dual PD-1/TGF β + Topoisomerase II inhibitor
ADP; Adenosine diphosphate, CTLA4; Cytotoxic T-lymphocyte-associated protein 4, DNA; Deoxyribonucleic acid, LAG3; Lymphocyte-activation gene 3, MSKCC; Memorial Sloan Kettering Cancer Centre, NCT; National Clinical Trial, PARP; Poly (ADP-ribose) polymerase, PD-1; Programmed cell death protein 1, PD-L1; Programmed death-ligand 1, TGF β ; Transforming growth factor β , TKI; Tyrosine kinase inhibitor.			

Despite their increasing use in contemporary cancer therapy, STS on the whole are relatively non-immunogenic compared to other cancer types and single agent checkpoint blockade immunotherapies in STS cohorts have reported limited activity. For instance, a pilot study conducted by Maki *et al.* assessed the utility of the anti-CTLA4 antibody ipilimumab in synovial sarcoma patients and reported no clinical benefit, with a RECIST response rate of 0% (Maki *et al.*, 2013). Similarly, monotherapy with the anti-PD-1 antibody nivolumab has repeatedly shown no clinically significant activity in a number of phase II trials performed in both paediatric and adult cohorts of heterogeneous STS subtypes (Ben-Ami *et al.*, 2017; D'Angelo *et al.*, 2018; Davis *et al.*, 2020). However, further assessment of the utility of nivolumab in combination with

ipilimumab are ongoing, with preliminary phase II data showing promising activity in certain “complex” STS subtypes, such as undifferentiated pleomorphic sarcoma and leiomyosarcoma (**Table 7.1**) (D’Angelo *et al.*, 2018; NCT02304458; NCT02428192).

Consistent with the promising results of immunotherapy in subtype-specific STS reported by D’Angelo *et al.*, certain histological subtypes have shown encouraging responses to checkpoint blockade immunotherapy (D’Angelo *et al.*, 2018). For instance, the phase II SARC028 trial of pembrolizumab monotherapy in a heterogeneous STS cohort reported limited activity, with the trial falling short of the study’s primary endpoint of 20% objective response rate (ORR) (Tawbi *et al.*, 2017). However, subtype-specific analysis of the study reported clinically meaningful activity in “complex” STS subtypes with increased mutational burden, namely undifferentiated pleomorphic sarcoma and liposarcoma (undifferentiated pleomorphic sarcoma ORR; 40%, liposarcoma ORR; 20%) (Tawbi *et al.*, 2017). Unfortunately, a subsequent analysis on an expanded SARC028 cohort of undifferentiated pleomorphic sarcoma and liposarcoma did not confirm the activity of pembrolizumab monotherapy in liposarcoma (ORR; 10%) (Burgess *et al.*, 2019). Despite this, activity of pembrolizumab in undifferentiated pleomorphic sarcoma continued to achieve the primary endpoint for efficacy (ORR; 23%) (Burgess *et al.*, 2019).

In addition to certain genetically “complex” STS, ICIs have been shown to possess clinical activity in patients with alveolar soft part sarcoma (Grisberg *et al.*, 2020). For example, in a phase II study of advanced alveolar soft part sarcoma patients treated with anti-PD-L1 atezolizumab, Naqash *et al.* described promising monotherapeutic activity with durable responses of ~16-17 months (ORR; 37%, stable disease (SD); 58%) (Grisberg *et al.*, 2020; Naqash *et al.*, 2021). Similarly, in a phase II study conducted on a heterogeneous cohort of advanced STS, anti-PD-L1 durvalumab plus anti-CTLA4 tremelimumab was found to be specifically effective in alveolar soft part sarcoma, with 90% 12-week progression-free rate (PFR) and 50% of patients displaying partial responses (PRs) (Somaiah *et al.*, 2020).

Building on the broad lack of activity within the vast majority of STS subtypes with ICI monotherapy, the combination of ICI plus other anticancer agents such as TKIs and chemotherapeutics have been evaluated (**Table 7.1**). In a phase II trial conducted on a heterogeneous STS cohort, Wilky *et al.* found that the combination of

pembrolizumab plus multi-target TKI axitinib resulted in promising preliminary activity (clinical benefit rate (CBR); 53%), with notable enhanced activity in alveolar soft part sarcoma (CBR; 72%) (Wilky *et al.*, 2019). Furthermore, a phase I trial undertaken by Chawla *et al.* in a cohort of solid malignancies, including STS, reported that combination therapy of the multi-target TKI apatinib plus nivolumab resulted in 40% of evaluable patients displaying tumour shrinkage (Chawla *et al.*, 2019). Similarly, early reports from a phase II study of leiomyosarcomas has shown the potential efficacy of combining the multi-target TKI cediranib, or PARP inhibitor olaparib, with ICI durvalumab, with 30% of patients displaying SD (Ayodele *et al.*, 2021).

Conversely, the combination modality of dasatinib plus ipilimumab in GIST and non-GIST STS had limited combinatorial efficacy in a phase Ib study (D'Angelo *et al.*, 2017). Additionally, the study also noted that dasatinib did not favourably alter the TME to synergise with concomitant immune checkpoint inhibition (D'Angelo *et al.*, 2017). This highlights the important consideration of which multi-target TKI is incorporated into combinatorial immunotherapeutic strategies, with multi-target TKIs targeting VEGF signalling within the TME postulated to play a critical factor in determining efficacy (Lee *et al.*, 2020).

The multi-target TKIs discussed within this thesis – pazopanib, regorafenib, sitravatinib, and anlotinib – are all potent inhibitors of VEGF signalling, in addition to their direct targeting of tumour growth-promoting RTKs. Previous successes with other VEGF-targeting TKIs in combination with ICIs therefore warrants further evaluation of the efficacy of pazopanib, regorafenib, sitravatinib, and anlotinib in combinatorial immunotherapeutic strategies. In fact, a preliminary case study of a single undifferentiated pleomorphic sarcoma patient treated with combination of pazopanib plus pembrolizumab resulted in very promising results, with disease regression observed over the course of 10 months (Arora *et al.*, 2020). This finding warrants further exploration in larger cohorts of STS patients to evaluate this promising activity. Additionally, a phase I/II clinical trial of regorafenib plus avelumab (REGOMUNE) is currently being undertaken in a heterogeneous cohort of advanced STS patients and the results are eagerly awaited (NCT03475953). Although the activity of regorafenib, sitravatinib, and anlotinib combinations with ICIs have not yet been reported in advanced STS, they have shown utility in immunotherapeutic combinations in other solid malignancies, such as NSCLC and colorectal cancer (Cousin *et al.*, 2021; Leal

et al., 2017; Yang *et al.*, 2020; Zhai *et al.*, 2021). Further clinical trial evaluations assessing the combinatorial efficacy of VEGFR-inhibiting multi-target TKIs plus immunotherapy in advanced STS are currently undergoing (NCT03396211; NCT04784247). There is a need for a greater understanding of the effects of multi-target TKIs upon the immune microenvironment, as well as other aspects of the TME, in addition to their direct antitumour effect. Work in our group is currently underway to create three-dimensional STS models that incorporate aspects of the TME, such as immune cells, for accurate modelling of TME-tumour interactions. Using these models, I hope to better understand the immunomodulatory effects of multi-target TKI treatment in STS and assess for the combinatorial efficacy of these TKIs plus ICIs.

Immunotherapeutic strategies incorporating chemotherapies have also elucidated potential efficacies in advanced STS. Firstly, the SAINT phase II trial examined the efficacy of a triple combination of ipilimumab, nivolumab, and topoisomerase II inhibitor trabectedin in a heterogeneous STS cohort (Gordon *et al.*, 2020). The SAINT trial reported that the triple combination elicited high levels of disease control (disease control rate (DCR; 88%), whilst maintaining safe levels of toxicities (Gordon *et al.*, 2020). Furthermore, the phase I/II trial by Pollack *et al.* assessed for the efficacy of pembrolizumab plus doxorubicin in a heterogeneous STS cohort (Pollack *et al.*, 2020). Despite the trial not meeting the predefined primary endpoint of the study (ORR; 35%), survival outcomes were favourable in relation to historical controls. In addition, Pollack *et al.* described promising disease control in more immunogenic “complex” STS subtypes, such as undifferentiated pleomorphic sarcoma (PR; 67%) and dedifferentiated liposarcoma (PR; 50%) (Pollack *et al.*, 2020). However, certain combinations of ICI and chemotherapy have been reported to lack activity in STS. For instance, an interim analysis of a phase II trial of leiomyosarcoma patients treated with eribulin – a microtubule assembly inhibitor – plus pembrolizumab did not meet the predefined primary endpoint for efficacy of 60% 12-week PFR (Nathenson *et al.*, 2020). The liposarcoma and “other” STS subtype cohorts within this phase II trial have recently finished enrolling and results are awaited (Nathenson *et al.*, 2020) (NCT03899805).

Interestingly, recent studies have shown that STS patients can be stratified based on their immunogenic profiles, as well as the existence of tertiary lymphoid structures (TLS), for enhanced responses to ICI immunotherapy (Italiano *et al.*, 2021; Petitprez

et al., 2020). In a recent study, Petitprez *et al.* reported that STS patients can be classified based on their immune profiles – immune-low, immune-high, or highly vascularised (Petitprez *et al.*, 2020). The study found that the cohort of immune-high STS patients, characterised by high B cell counts, demonstrated improved PFS and significantly increased response rate to anti-PD-1 pembrolizumab monotherapy, compared to the remainder of the cohort (ORR; 50% vs. 25%, $p = 0.026$) (Petitprez *et al.*, 2020). Additionally, the study found that the cohort of immune-high STS were characterised by the presence of TLS. TLS are ectopic aggregates of immune cells such as lymphocytes and dendritic cells that form at the tumour site as part of an immune response to disease, and their presence has correlated with favourable prognosis in solid tumours (Sautés-Fridman *et al.*, 2019). Therefore, recent immunotherapy studies have focussed on stratifying STS patients based on the presence of TLS at the tumour site. For instance, the PEMBROSARC phase II study of pembrolizumab in combination with cyclophosphamide has shown that STS patients harbouring TLS had a significantly improved response (ORR; 27%, 6-month PFR; 40%), when compared to the cohort as a whole (ORR; 2%, 6-month PFR; 4%) (Italiano *et al.*, 2021). Following the success of this trial, further immunotherapy phase II trials utilising TLS-based stratification methods (e.g., CONGRATS, REGOMUNE, TRUST) have been designed and are currently recruiting (**Table 7.1**) (NCT03475953; NCT04095208; NCT04874311).

The wave of ICI immunotherapy trials currently occurring in STS patients provide a promising future for further therapeutic options in advanced STS. Additionally, through a greater understanding of the TME of STS, patients can be more effectively stratified to enhance the efficacy of ICI immunotherapies and improve disease outcomes. In addition to ICI immunotherapies described above, vaccine and adoptive T cell transfer immunotherapies have also been undergoing clinical evaluation in STS.

7.3.2.1 Vaccine immunotherapy

Vaccine therapies in sarcoma are based on the concept of exogenously activating antigen-presenting dendritic cells to present a sarcoma-specific antigen to T cells. This therefore targets cytotoxic T cells towards the antigen-presenting tumour cells. Early studies based on this concept administered synovial sarcoma patients with synthetic

SS18-SSX fusion-derived peptide vaccines and reported encouraging preliminary results in a subset of patients (Kawaguchi *et al.*, 2012). The exogenous peptide is recognised as a foreign antigen by the immune system, thereby producing an immune response that targets synovial sarcoma cells expressing the SS18-SSX antigen (Kawaguchi *et al.*, 2012). More recently, a phase II trial conducted by Chawla *et al.* evaluated the utility of the vaccine regimen CMB305 in combination with the ICI atezolizumab in a large cohort of 89 patients with advanced synovial sarcoma or myxoid/round-cell liposarcoma (Chawla *et al.*, 2021). CMB305 targets the NY-ESO-1 antigen that is highly expressed on the cell surface of specific STS subtypes, namely synovial sarcoma (61%) and myxoid/round-cell liposarcoma (88%) (Iura *et al.*, 2017; Lai *et al.*, 2012). Additionally, expression of the NY-ESO-1 antigen outside of tumours is limited to tissues of the testes and is not expressed in other healthy tissues (Iura *et al.*, 2017). CMB305 contains a lentiviral vector (LV305) that targets and transduces dendritic cells to express NY-ESO-1 antigens at their cell surface. Additionally, CMB305 also contains a lipid agonist that activates dendritic cells. Naïve T cells bind the NY-ESO-1 antigen upon activated dendritic cells and generate tumour-specific cytotoxic T cells that can subsequently target and kill tumour cells expressing the NY-ESO-1 antigen (Albershardt *et al.*, 2016; Chawla *et al.*, 2021). Unfortunately, despite increases in anti-NY-ESO-1 immune responses, the combination of CMB305 vaccine plus atezolizumab did not significantly improve survival outcomes in patients compared to atezolizumab monotherapy (Chawla *et al.*, 2021). Despite the lack of improved survival outcomes, the trial sets a benchmark for the large-scale feasibility of such treatments in specific STS subtypes, especially within combinatorial immunotherapeutic strategies (Chawla *et al.*, 2021; NCT03450122).

7.3.2.2 Adoptive T cell immunotherapy

The use of adoptive T cell therapies has also shown early clinical promise in the treatment of advanced STS, most notably synovial sarcoma and myxoid/round cell liposarcoma. This immunotherapeutic technique utilises T cells, commonly from the patient being treated, that are genetically manipulated *ex vivo* in order to enhance their targeting of cancer cells. The modified T cells are then re-introduced into the patient to elicit their cytotoxic and immunostimulatory activity. Adoptive T cell therapies that

have shown promising efficacy in STS include engineered T cell receptor (TCR) therapy and chimeric antigen receptor T (CAR-T) therapy. These differ based on the type of antigen they can bind, with TCRs limited to antigens bound to major histocompatibility complexes (MHC) (Zhao & Cao, 2019).

7.3.2.2.1 T cell receptor therapy

In TCR therapy, the patient's own T cells are harvested and genetically altered in order to express modified TCRs at the T cell surface. These TCRs are designed to specifically target cancer-associated antigens that are presented by MHCs on the surface of tumour cells. Upon re-introduction of the modified T cells into the patient, they target antigen-presenting tumour cells, thereby eliciting a cytotoxic activity to kill the cancer cell, as well as producing an immunostimulatory response in other immune cells. This, therefore, propagates an enhanced anticancer immune response towards further cells that express the specific cancer-associated antigen (Tsimberidou *et al.*, 2021).

D'Angelo *et al.* have shown the utility of TCR therapies targeting the NY-ESO-1 antigen that is highly expressed in synovial sarcomas in a phase I trial (D'Angelo *et al.*, 2018). The utilised T cells were genetically modified to express affinity-enhanced TCRs directed towards the NY-ESO-1 antigen before being introduced into 12 synovial sarcoma patients. The study reported that the genetically-modified T cells expanded and persisted in the body for a prolonged duration (6 months), with an impressive ORR of 50% that was characterised by tumour shrinkage over the course of several months (D'Angelo *et al.*, 2018). Building on the findings of this exploratory study, D'Angelo *et al.* developed the TCR therapeutic letetresgene autoleucel (lete-cel), designed to specifically target NY-ESO-1-positive STS (D'Angelo *et al.*, 2021). The authors evaluated the efficacy of letetresgene autoleucel, following either high- or low-dose lymphodepletion, in a phase II study conducted on a cohort of myxoid/round-cell liposarcoma patients (D'Angelo *et al.*, 2021). Lymphodepletion refers to short courses of chemotherapy (in this case fludarabine plus cyclophosphamide) that are employed to kill endogenous T cells before treatment with immunotherapeutic T cells. This is performed in order to enhance the therapeutic activity, expansion, and persistence of the immunotherapy (Bechman & Maher, 2021). D'Angelo *et al.* reported clinically

meaningful activity of a single letetresgene autoleucel treatment after high dose lymphodepletion, with prolonged (2.7-10.6 months) SD of 50% and durable (1-7.8 months) ORR of 40% (D'Angelo *et al.*, 2021). Building on the promising results, a further phase II clinical trial of letetresgene autoleucel in the treatment of advanced synovial sarcomas and myxoid/round-cell liposarcomas is currently recruiting (D'Angelo *et al.*, 2020; NCT03967223). Furthermore, combinatorial trials of this immunotherapy in combination with chemotherapy, CMB305 vaccine therapy, and aldesleukin – a synthetic IL-2 mimic – in NY-ESO-1-positive sarcomas is currently undergoing (NCT03450122).

In addition to letetresgene autoleucel, the MAGE-A4-targeting TCR therapy afamitresgene autoleucel is also undergoing clinical evaluation in advanced synovial sarcomas and myxoid/round cell liposarcomas. Similarly to NY-ESO-1, MAGE-A4 is a testes antigen that is highly expressed in synovial sarcomas (82%) and myxoid/round-cell liposarcomas (68%), but not in the majority of healthy tissue (Iura *et al.*, 2017). Therefore, D'Angelo *et al.* conducted a phase II study to evaluate the efficacy of afamitresgene autoleucel in a cohort of heavily pre-treated synovial sarcoma and myxoid/round-cell liposarcoma patients (D'Angelo *et al.*, 2021). This trial found that the treatment was well tolerated with very promising response rates (ORR: 40%, SD: 44%) (D'Angelo *et al.*, 2021). Owing to the promising nature of these initial results, the trial is currently recruiting further synovial sarcoma and myxoid/round cell liposarcoma patients in an expanded cohort (NCT04044768).

7.3.2.2.2 Chimeric antigen receptor T cell therapy

CAR-T cell immunotherapy is a revolutionary method of anticancer therapy that has recently been approved for use in B-cell lymphoma and acute lymphoblastic leukaemia. In addition to their success in haematological malignancies, recent preclinical studies have shown that CAR-T cell immunotherapy also has a potential efficacy in solid tumours, including sarcoma (Marofi *et al.*, 2021; Thanindrarn *et al.*, 2020). CAR-T cells are the patient's own T cells that have been manipulated *ex vivo* in order to express synthetic CARs on the T cell surface. Upon reintroduction of the CAR-T cells into the patient, the CARs recognise and directly bind specific tumour-associated antigens on the cancer cell surface, without the need for MHCs. This direct

binding results in T cell-induced cancer cell death and subsequent immunostimulation (Feins *et al.*, 2019; Thanindratarn *et al.*, 2020). A number of recent studies have revealed the existence of several sarcoma-associated antigens that can be targeted by CAR-T cell therapy, including HER2, disialoganglioside GD2, and insulin-like growth factor 1 receptor (IGF1R) (Thanindratarn *et al.*, 2020). Utilising these sarcoma-associated antigens, several clinical trials have been completed or are actively recruiting. For instance, in a cohort of HER2-positive sarcomas, HER2-CAR-T therapy showed promising preliminary, prolonged, and non-toxic activity (NCT00902044) (Ahmed *et al.*, 2015). The authors postulate that combining CAR-T cells with other immunotherapies could result in the enhancement of CAR-T activity and persistence in STS (Ahmed *et al.*, 2015; Grünewald *et al.*, 2020). Additionally, further early-stage clinical trials utilising CAR-T cells targeted towards GD2, EGFR, or other sarcoma-associated antigens are actively recruiting STS patients (NCT02107963; NCT03618381; NCT03356782).

Although both CAR-T and TCR cells are known to face increased challenges in solid tumours compared to haematological malignancies, such as TME blocking immunotherapeutic penetration to the tumour, the identification of sarcoma-associated antigens highlights the potential value of adoptive T cell immunotherapy in STS (Thanindratarn *et al.*, 2020).

7.3.2.3 Immunotherapy and IL-8 signalling

Previous work by our group (conducted by Dr. Alex Lee) has shown that increased IL-8 levels correlated with pazopanib resistance in a patient with acquired resistance (**Figure 4.1**). This is consistent with previous studies in cellular preclinical models of lung cancer that have reported that IL-8 signalling activity confers acquired TKI resistance (Fernando *et al.*, 2016; Liu *et al.*, 2015). Furthermore, high IL-8 expression has commonly been associated with increased tumour grade and aggressiveness, as well as worse prognosis in various cancer types, including STS (Feng *et al.*, 2018; Highfill *et al.*, 2014; Rutkowski *et al.*, 2002; Tobin *et al.*, 2019). The work presented in **Chapter 4** determined that IL-8 autocrine signalling did not induce pazopanib resistance in pazopanib-resistant cell models of STS. This was because the IL-8 receptors, CXCR1 and CXCR2, were not found to be expressed in any of the

evaluated cell models. As CXCR1 and CXCR2 are known to be highly expressed on the surface of immune cells and other cells of the TME, I therefore hypothesised that if pazopanib resistance in STS is mediated by IL-8 signalling, then it is more likely to be due to paracrine signalling between the IL-8-excreting tumour cells and the surrounding TME. This hypothesis is consistent with previous studies that have shown that IL-8 paracrine signalling promotes the recruitment of immunosuppressive cells, notably myeloid-derived suppressor cells, to the TME. This activity thereby subdues antitumour immune response and T cell activity, as well as inducing targeted therapy resistance (David *et al.*, 2016; Tan *et al.*, 2018). Interestingly, the recruitment of such immunosuppressive cells into the TME by tumour-secreted IL-8 has also been shown to correlate with worse prognosis in patients treated with ICI immunotherapy (Schalper *et al.*, 2020; Yuen *et al.*, 2020).

There has therefore been recent activity to develop and assess therapeutics that abrogate the activity of the IL-8-CXCR1 & -CXCR2 pathways for improved cancer therapy. Studies have reported a number of immunotherapeutic treatments that directly target IL-8 paracrine signalling in order to abrogate chemotaxis of immunosuppressive cells to the TME (Bilusic *et al.*, 2019; Casili *et al.*, 2005). This effect thereby overcomes IL-8-induced immunosuppression, resulting in an enhanced anticancer immune response (Bilusic *et al.*, 2019; Casili *et al.*, 2005). These include reparixin (repertaxin), which is a small molecule inhibitor of CXCR1 and CXCR2, and the humanised monoclonal antibody HuMax-IL8 that directly binds free IL-8 ligand, thereby preventing receptor binding (Bilusic *et al.*, 2019; Casili *et al.*, 2005). Due to known correlation between increased IL-8 paracrine signalling and therapeutic resistance, observed by both our lab and reported in previous studies, my future work will focus on whether using anti-IL-8 signalling therapies, in combination with multi-target TKIs and/or ICIs, could potentiate the anticancer activity of the latter treatments and overcome therapeutic resistance in STS. In fact, building on a phase I clinical trial of HuMax-IL8 that reported safe toxicity profiles, a phase I/II trial of HuMax-IL8 plus nivolumab in advanced solid tumours is currently recruiting patients to assess whether HuMax-IL8 increases the anticancer activity of ICI immunotherapy (NCT03400332) (Bermejo *et al.*, 2018). Furthermore, previous studies have shown that Src signalling is a direct upstream activator of *CXCL8* (IL-8) expression (Lin *et al.*, 2006; Trevino *et al.*, 2005). Further work will therefore explore whether dasatinib, which I have shown

to be an effective treatment strategy in pazopanib-resistant STS cells, has a further collateral effect on paracrine IL-8 signalling and TME remodelling, in order to produce an anticancer immune response.

Finally, interesting work by Jin *et al.* has reported preclinical utility of employing CAR-T cells with transduced expression of CXCR1 or CXCR2 in murine models of solid tumours (Jin *et al.*, 2019). As IL-8 is frequently highly expressed in high-grade and aggressive tumours, the authors found that expressing the IL-8 receptors in CD70-targeted CAR-T cells resulted in an enhanced localisation of the cytotoxic T cells to the IL-8-secreting tumour site (Jin *et al.*, 2019). CD70 is a tumour-associated antigen that has been shown to be potential target of CAR-T cell immunotherapy in solid tumours such as glioma, ovarian, and pancreatic cancers (Akce *et al.*, 2018; Jin *et al.*, 2018; Jin *et al.*, 2019). Jin *et al.* reported that the increased localisation of CXCR1- or CXCR2-expressing CAR-T lymphocytes at the tumour site (compared to CAR-T cells lacking IL-8 receptor expression) resulted in a significantly enhanced antitumour response (Jin *et al.*, 2019).

These results therefore suggest that similar strategies employing CXCR1- or CXCR2-expressing T cell immunotherapies that target sarcoma-associated antigens (such as those discussed in **Chapter 7.3.2.2**) could potentially be effective in the treatment of STS tumours characterised by high IL-8 expression. In this way, rather than directly targeting the IL-8 signalling pathway, we could instead co-opt high IL-8 activity in STS tumours and use it to our advantage to guide immunotherapeutic cytotoxic T cells to the tumour site, thereby enhancing treatment efficacy, and potentiating a subsequent antitumour immune response.

7.3.3 Personalised medicine and MULTISARC

Personalised medicine is the ultimate goal of cancer therapy, where ‘the right drug, with the right dose, at the right time’ is administered to individual patients to achieve the best possible response (Mathur & Sutton, 2017). This does not mean that each patient is treated differently to one another, which would be economically untenable, but rather genetic, transcriptomic, clinical, and epigenomic data is integrated and subsequently evaluated in order to stratify patients to be treated with the most effective therapy.

In regard to personalised medicine in STS, Lucchesi *et al.* have reported that up to 41% of STS patients harbour potentially targetable genomic alterations (Lucchesi *et al.*, 2018). Therefore, the authors postulate that genomic profiling could be employed to determine the presence of actionable genomic alterations in STS, with the aim of tailoring personalised therapy towards targeting the oncogenic consequences of the observed genomic aberrations (Lucchesi *et al.*, 2018). Based on this hypothesis, the MULTISARC trial is a double-arm, randomised trial that will evaluate whether employment of NGS to guide therapy choice in the treatment of STS patients will improve their survival outcomes (NCT03784014). The trial will also assess whether the implementation of NGS in a large cohort is feasible without unreasonable delays. The MULTISARC trial will split STS patients 1:1 into two arms - an experimental and a standard arm. Within the experimental arm, NGS will be undertaken via exome and RNA sequencing and the results will be discussed within a multidisciplinary tumour board to provide a therapeutic decision for that patient based on their genomic profile. If a targetable genomic alteration is observed, subsequent targeted therapy will be employed based on the nature of the genetic aberration (**Table 7.2**). Conversely, the standard arm will contain patients treated with standard systemic therapy and will not be guided by NGS. The trial is currently actively recruiting, and the highly anticipated results are expected in 2024. The findings of this trial will further guide treatment strategies away from the one-size-fits-all paradigm of treating heterogeneous STS cohorts towards subtype-agnostic therapies based on molecular characteristics and underlying biology.

Targeted therapy	Targetable genomic alterations
Nilotinib	KIT, PDGFR α , CSF1R
Ceritinib	ALK, ROS1
Capmatinib	MET
Lapatinib	HER2, EGFR
Trametinib	Ras, PTPN11, NF1, MEK
Trametinib + Dabrafenib	Ras, PTPN11, NF1, MEK, B-Raf
Olaparib + Durvalumab	PDL1, PARP
Palbociclib	CDK4/6
Glasdegib	Smoothened
Futibatinib (TAS-120)	FGFR

ADP; Adenosine diphosphate, ALK; Anaplastic lymphoma kinase, CDK4/6; Cyclin-dependent kinase 4/6, CSF1R; Colony stimulating factor 1 receptor, EGFR; Epidermal growth factor receptor, FGFR; Fibroblast growth factor receptor, HER2; Human epidermal growth factor receptor 2, MEK; Mitogen-activated protein kinase kinase, NGS; Next-generation sequencing, NF1; Neurofibromin 1, PARP; Poly (ADP-ribose) polymerase, PDGFR α ; Platelet-derived growth factor receptor α , PD-L1; Programmed death-ligand 1, PTPN11; Phosphatase non-receptor type 11, Raf; Rapidly accelerated fibrosarcoma, Ras; Rat sarcoma.

7.4 Concluding remarks and future directions

There is currently only a single targeted therapy approved for the vast majority of advanced STS subtypes – the multi-target TKI pazopanib. However, clinical experience has revealed that STS patients treated with pazopanib universally encounter drug resistance, either through an intrinsic resistance or through the acquisition of resistance after prolonged treatment. Furthermore, patients treated with pazopanib were not found to live for significantly longer than if treated with placebo (Van der Graaf *et al.*, 2012). There has therefore been a recent push to clinically evaluate other multi-target TKIs for improved efficacy in the treatment of advanced STS (Wilding *et al.*, 2019). Unfortunately, findings from clinical trials have indicated that these evaluated multi-target TKIs are likely to suffer from the same drug resistance hurdles as pazopanib in the clinic (Mir *et al.*, 2016; Oza *et al.*, 2021; Van Tine *et al.*, 2021; Wilding *et al.*, 2019). Furthermore, upon disease progression with pazopanib treatment, STS patients currently lack approved salvage therapies for the effective treatment of pazopanib-resistant disease. There is therefore an unmet clinical need to better understand the resistance mechanisms of multi-target TKIs in advanced STS. This increased understanding will allow for the design of novel treatment strategies that can be employed to subvert the emergence of resistance or effectively treat TKI-resistant disease.

By employing targeted pharmacological screens, this work identified dasatinib as an effective treatment in PDX-derived models of pazopanib-resistant STS. Rescue experiments determined that dasatinib mediates its antiproliferative properties through direct inhibition of the Src signalling pathway. Additionally, Src was found to be critical to the proliferation of pazopanib-resistant STS. The activity of dasatinib also translated into an *in vivo* antitumour effect. Although dasatinib has been found to have limited clinical activity in heterogeneous cohorts of STS, the work presented in this thesis provides preclinical evidence that nominates dasatinib for future clinical evaluation as a salvage therapy in pazopanib-refractory STS (Schuetze *et al.*, 2016; Schuetze *et al.*; 2017). Additionally, future work into determining enhanced Src activity in STS patients that harbour or develop pazopanib resistance may help to select for patients that are more likely to benefit from dasatinib first-line or salvage therapy.

Building on the finding that Src signalling is critical in pazopanib-resistant STS cell models, this work aimed to elucidate upstream signalling modulators of Src, with an initial focus on IL-8 signalling. However, IL-8 was not found to be an upstream regulator of Src activity in pazopanib-resistant STS due to the absence of IL-8 autocrine signalling. Further exploration into the potential regulation of IL-8 expression by upstream Src activity and subsequent IL-8 paracrine signalling within the TME, in order to evaluate the association between Src activity, IL-8 signalling, and pazopanib resistance in STS provides an exciting avenue for future work. Preliminary work has also revealed that integrin activity may be an upstream mediator of Src activity in pazopanib-resistant STS. Future preclinical work is required to explore the link between integrin and Src signalling, as well as associated pathways, in order to understand the mechanisms of Src activity and potentially reveal further targetable vulnerabilities in pazopanib-resistant STS. It is also yet to be determined whether the activity of Src within these models is the cause of pazopanib resistance. Future work employing a matched pre-pazopanib model from the same tumour from which SARC-209 was generated (whereby the tumour was responsive to pazopanib) will hopefully aim to elucidate this outstanding question. Additionally, positive and negative genome-wide CRISPR screens could elucidate candidate genes that are associated with pazopanib resistance within the SARC-209 and the pre-pazopanib matched model. The putative model of Src mechanism in the SARC-209 cell model and the effects of dasatinib inhibition are outlined in **Figure 7.1**.

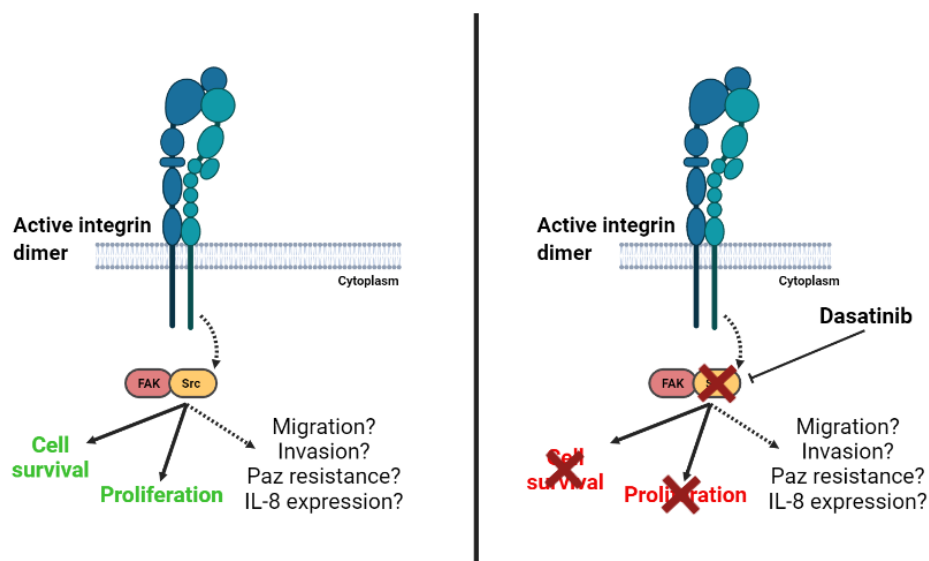


Figure 7.1: Candidate model of Src activity within the SARC-209 pazopanib-resistant STS model. Dashed lines indicate potential links that require further evaluation to be fully confirmed. Image was created using BioRender.

This work also describes a number of potential treatment strategies that could be employed to subvert or control multi-target TKI resistance in MRT, and potentially other STS driven by PDGFR and FGFR signalling. Firstly, by working with PDGFR α - and FGFR1-driven MRT cells (A204 and G402), which acquire resistance to multi-target TKI therapy after an initial sensitivity, I nominated erdafitinib and ponatinib as effective first-line therapies with potent antiproliferative and pro-apoptotic effects that result in the long-term abrogation of drug resistance. Further exploration into the *in vivo* efficacy of these treatments is required. I also derived TKI-resistant cells through the long-term exposure of A204 cells to the multi-target TKIs pazopanib, regorafenib, sitravatinib, and anlotinib. As per the findings in Wong *et al.*, the TKI-resistant sublines were found to harbour reduced expression of PDGFR α and reduced Akt signalling when compared to the parental A204 cell line. Although further evaluation is required to prove causality of these phenotypes with multi-target TKI resistance, the consistency with the work by Wong *et al.* highly implies that loss of PDGFR α expression and subsequent loss of signal dependency on the Akt pathway is a mechanism of multi-target TKI resistance in these models. The putative model of multi-target TKI resistance in the A204 TKI-resistant models is outlined in **Figure 7.2**. Future work will aim to answer these outstanding questions. Firstly I will evaluate whether re-introduction of PDGFR α expression into the TKI-resistant sublines rescues multi-target TKI sensitivity. Furthermore, I will undertake direct inhibition of the PI3K/Akt pathway in the TKI-resistant sublines and compare the effects to those seen in the parental cell line. This would be to elucidate whether the TKI-resistant sublines have indeed lost their dependency on Akt signalling for proliferation and survival.

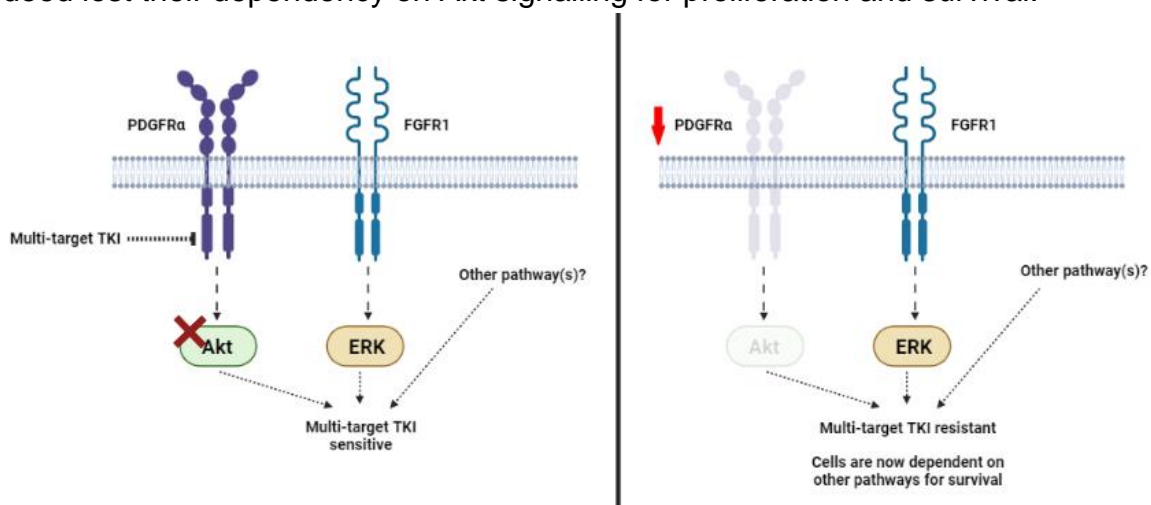


Figure 7.2: Candidate model of multi-target TKI resistance in the A204 TKI-resistant sublines. Dashed lines indicate potential links that require further evaluation to be fully confirmed. Image was created using BioRender.

Proteomic evaluation of these resistant sublines revealed a number of common alterations correlating with TKI resistance, and future work will focus on assessing the role that these changes have in the acquisition of TKI resistance. Targeted pharmacological screens and subsequent evaluations on the TKI-resistant cells revealed that erdafitinib and ponatinib, as well as their first-line efficacy, could also potentially be employed as salvage therapies in TKI-resistant STS driven by PDGFRs and FGFRs. Interestingly, the screen also revealed selective collateral sensitivity to imatinib treatment in cells with an acquired resistance to sunitinib. This nominates the possibility of employing an adaptive therapeutic approach whereby cells are pre-treated with sunitinib before switching to imatinib upon the emergence of resistance. However, outstanding questions surrounding this collateral sensitivity remain. The reason behind the selective nature of imatinib collateral sensitivity in response to sunitinib pre-treatment and resistance is not yet understood. Preliminary research has opened up avenues of future research to answer this question including imatinib inhibition of residual PDGFR α activity in sunitinib-resistant cells, as well as the potential roles of DDR2 and ephrin signalling. Furthermore, continuous treatment of sunitinib pre-treated A204 cells with imatinib results in the re-acquisition of resistance, and further modelling is required to determine potential collateral sensitivity cycles and sequences that could be employed in further lines of therapy. Through these means I hope to develop sequential or cycling strategies that leverage on the emergence of predictable collateral sensitivities that could effectively control tumour growth and provide a long-term treatment benefit for a subset of advanced STS patients.

To conclude, the following section will discuss the aims that were set out at the start of the thesis and discuss whether these have been achieved and where further work is needed.

Aim 1: Derive and characterise models of acquired and intrinsic multi-target TKI resistance. This thesis discusses the derivation and characterisation of a number of STS models of TKI-resistance. Firstly, two PDX-derived models of acquired or intrinsic pazopanib resistance were generated and subsequently utilised to determine dasatinib as an effective salvage therapy in pazopanib-resistant STS. Furthermore, the SARC-209 PDX-derived cells were used to generate mouse models for *in vivo* confirmation of dasatinib efficacy in pazopanib-resistant STS, when compared to

vehicle. Finally, using immortalised cell line models with intrinsic pazopanib sensitivity, I was able to generate four TKI-resistant sublines through chronic exposure of the parental cell line to the multi-target TKIs pazopanib, regorafenib, sitravatinib, or anlotinib.

Aim 2: Define signalling alterations associated with multi-target TKI resistance in STS models. Through proteomic evaluation of the A204 TKI-resistant sublines I have determined a number of consistent alterations that correlate with multi-target TKI resistance that warrant further future evaluation. Furthermore, and building on previous work by Wong *et al.*, this project showed that the A204 TKI-resistant sublines harboured consistent loss of PDGFR α expression and Akt signalling when compared to the sensitive parental cells. Although Src was found to be critical to cell survival and proliferation in the PDX-derived cell models of pazopanib-resistant STS (SARC-209 and J000104314), it is yet to be determined whether Src activity is the cause of pazopanib resistance within these models. Future work utilising CRISPR screens and matched pazopanib-sensitive models will aim to define signalling alterations associated with pazopanib resistance in these models.

Aim 3: Characterise mechanism driving multi-target TKI resistance and develop new salvage therapies in STS. This project has determined a number of salvage therapies and therapeutic strategies that can be utilised in multi-target TKI-resistant STS. Firstly, I found that dasatinib is an effective salvage therapy for pazopanib-resistant STS models. Secondly, the project has also discussed a number of therapeutic strategies involving infigratinib, erdafitinib, and ponatinib for the treatment of MRT. The first of these is the first-line treatment of MRT with erdafitinib or ponatinib was found to subvert the emergence of resistance. Building on this I also found that second-line treatment with erdafitinib or ponatinib following the emergence of multi-target TKI resistance was an effective strategy in controlling resistance. Finally, the project has also revealed a therapeutic regimen leveraging on collateral sensitivity whereby pre-treatment with sitravatinib results in a population of cells that are selectively sensitive to infigratinib treatment. Despite the determination of these salvage therapies and treatment regimens for multi-target TKI-resistant STS, the project currently lacks any definitive resistance mechanisms. The project has uncovered a number of associated signalling alterations with multi-target TKI but

further work (as discussed throughout the thesis) is required to fully confirm the causative role of these alterations in generating multi-target TKI resistance.

Chapter 8

Appendix

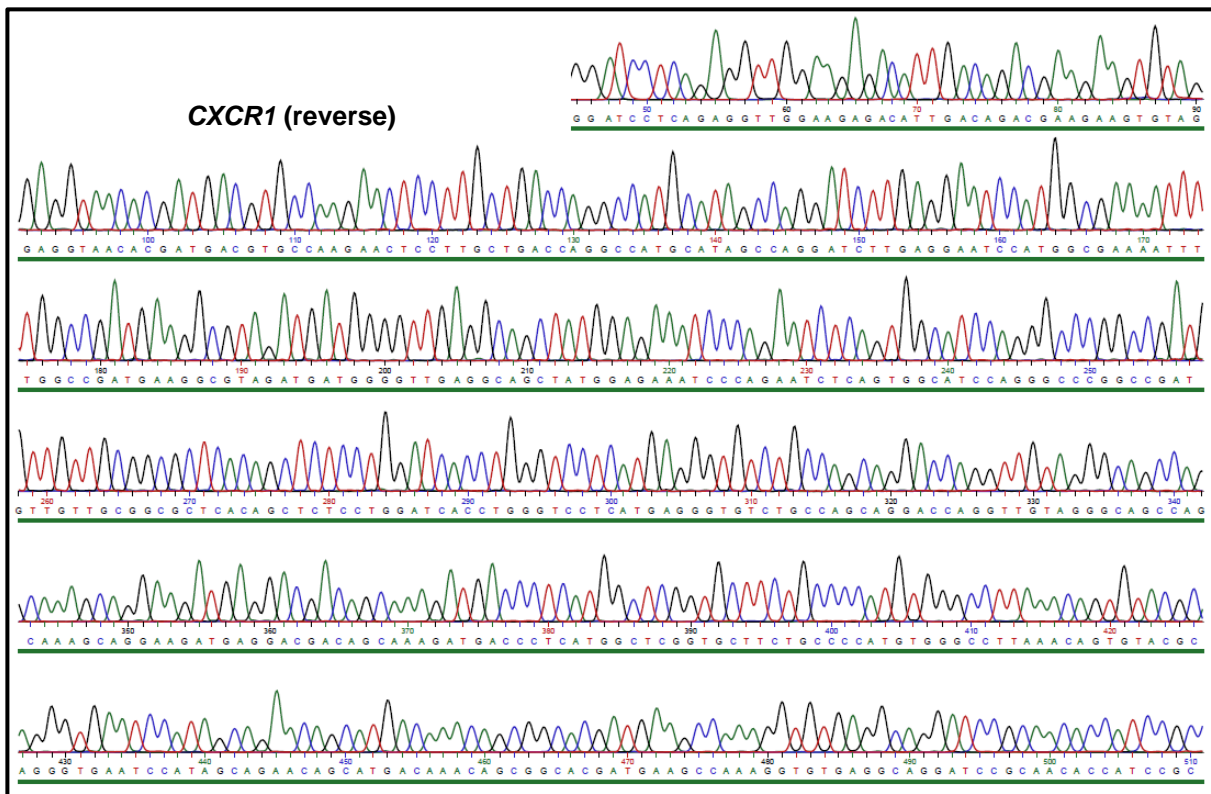
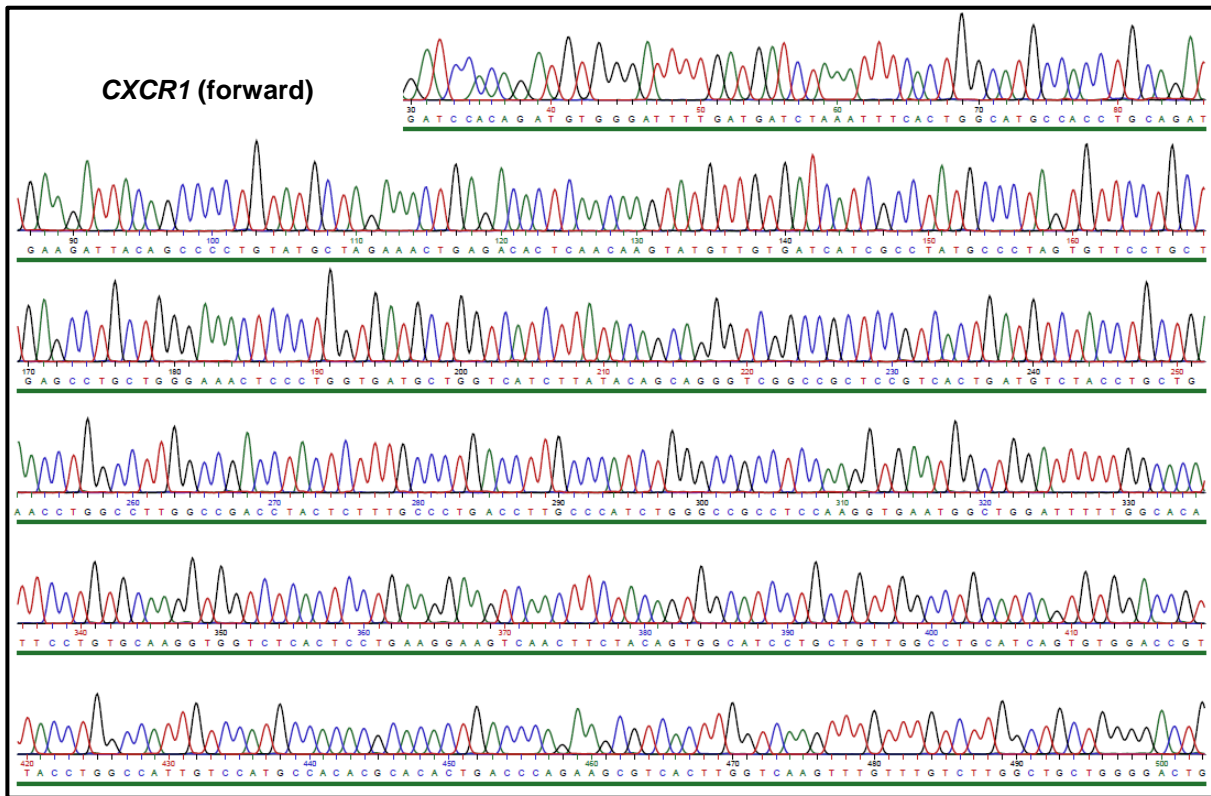


Figure S1: Genomic sequencing results of SARC-209 CXCR1-expressing cells. Genomic sequencing was undertaken using Eurofins Genomics' TubeSeq service. CXCR1; C-X-C motif chemokine receptor 1.

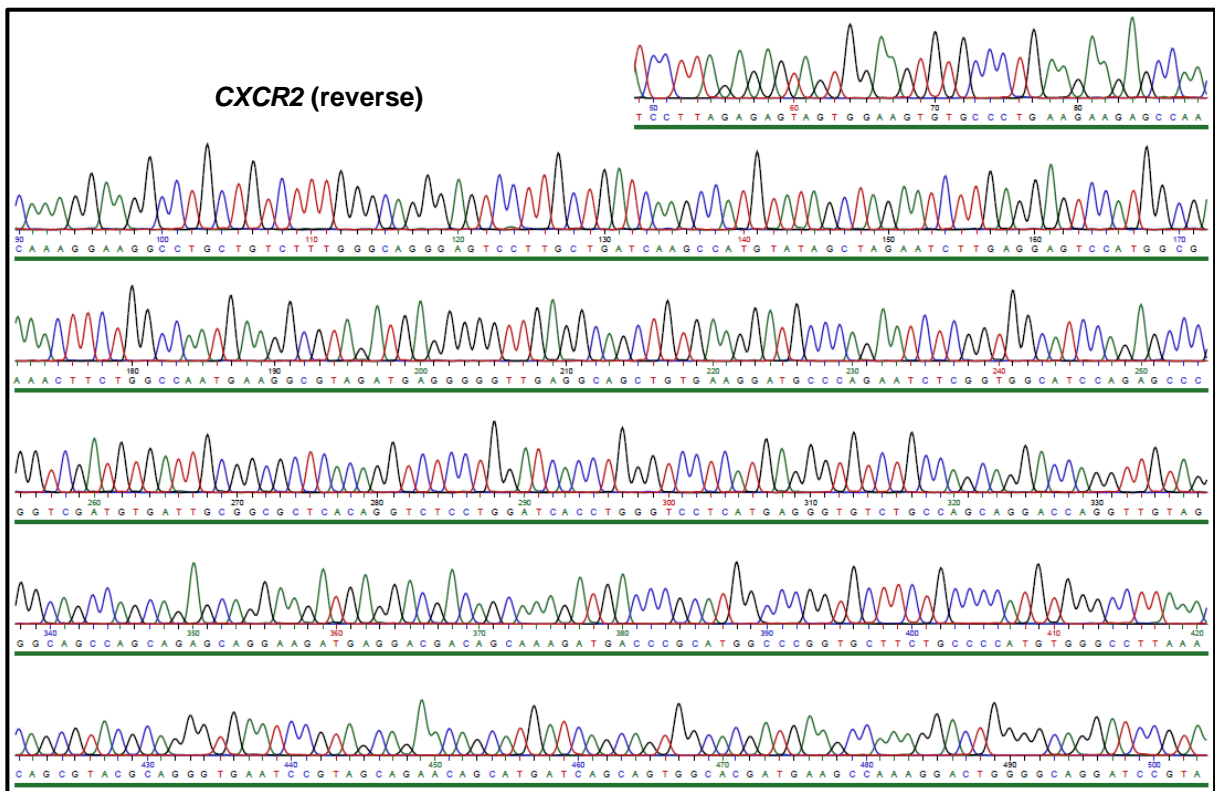
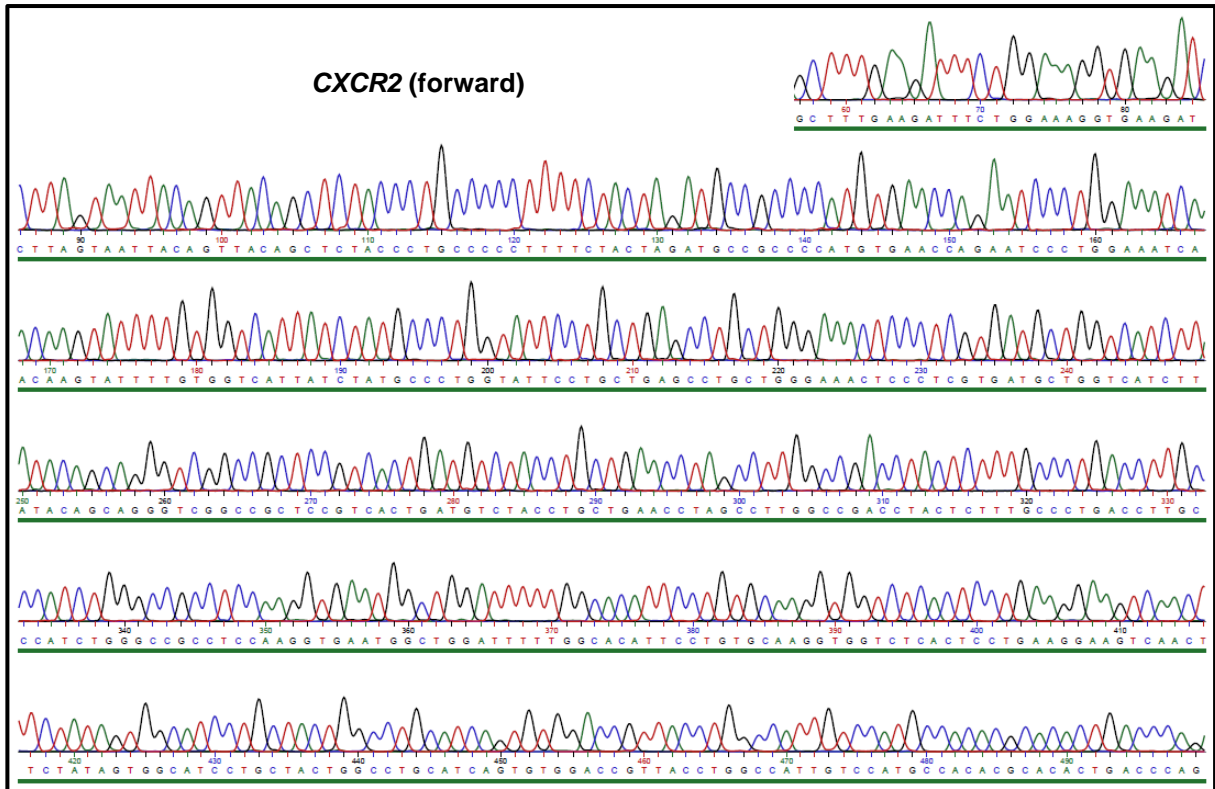


Figure S2: Genomic sequencing results of SARC-209 CXCR2-expressing cells. Genomic sequencing was undertaken using Eurofins Genomics' TubeSeq service. CXCR2; C-X-C motif chemokine receptor 2.

Table S1: A204, SARC-209, and J000104314 cells treated with pazopanib (Paz), with associated IC₅₀ (μM).

Cell model	Paz IC ₅₀ (μM) (± S.D.)
A204	0.56 (± 0.30)
SARC-209	8.22 (± 1.28)
J000104314	> 10 (n/a)

IC₅₀: Inhibitory constant, n/a; Not available, S.D.; Standard deviation, Green indicates IC₅₀ < 1 μM. Red indicates IC₅₀ > 2 μM.

Table S2: Inhibitors with ≤ 60% cell viability (compared to DMSO control) in small molecule inhibitor screens of SARC-209 and J000104314 cells.

SARC-209 (n=8)	J000104314 (n=6)
Dasatinib	Dasatinib
Dactolisib (BEZ235)	Dactolisib (BEZ235)
BI-2536	BI-2536
JQ1	JQ1
Alisertib	Navitoclax
Talazoparib	Luminespib (NVP-AUY922)
Neratinib	
Ponatinib	

DMSO; Dimethyl sulfoxide.

Table S3: SARC-209 and J000104314 cells treated with the TKIs pazopanib (Paz) and dasatinib (Das), with associated IC₅₀ values (μM).

Cell model	Paz IC ₅₀ (μM) (± S.D.)	Das IC ₅₀ (μM) (± S.D.)
SARC-209	8.46 (± 2.74)	0.64 (± 0.05)
J000104314	> 10 (n/a)	0.18 (± 0.03)

IC₅₀: Inhibitory constant, n/a; Not available, S.D.; Standard deviation, TKI; Tyrosine kinase inhibitor. Green indicates IC₅₀ < 1 μM. Red indicates IC₅₀ > 2 μM.

Table S4: EV, Src^{WT}, and Src^{T338I} cells treated with dasatinib (Das), with associated IC₅₀ values (μM).

Cell model	Das IC ₅₀ (μM) (± S.D.)
EV	0.87 (± 0.32)
Src ^{WT}	0.50 (± 0.27)
Src ^{T338I}	> 10 (n/a)

EV; Empty vector, IC₅₀: Inhibitory constant, n/a; Not available, S.D.; Standard deviation, Src^{T338I}; Dasatinib-resistant Src, Src^{WT}; Wild-type Src. Green indicates IC₅₀ < 1 μM. Red indicates IC₅₀ > 2 μM.

Table S5: Panel of 14 sarcoma cell lines treated with the TKIs pazopanib (Paz), regorafenib (Reg), sitravatinib (Sit), and anlotinib (Anlo), with associated IC₅₀ values (µM).

Cell line	Paz IC ₅₀ (µM) (± S.D.)	Reg IC ₅₀ (µM) (± S.D.)	Sit IC ₅₀ (µM) (± S.D.)	Anlo IC ₅₀ (µM) (± S.D.)
A204	0.37 (± 0.10)	0.83 (± 0.16)	0.30 (± 0.06)	0.62 (± 0.18)
G402	0.38 (± 0.05)	0.71 (± 0.06)	0.23 (± 0.10)	0.41 (± 0.41)
SAOS2	> 10 (n/a)	5.92 (± 0.09)	3.46 (± 0.69)	3.48 (± 0.65)
U2OS	> 10 (n/a)	8.97 (± 2.51)	2.38 (± 0.79)	3.27 (± 0.37)
HT1080	> 10 (n/a)	> 10 (n/a)	4.01 (± 1.37)	2.67 (± 0.93)
MESSA	> 10 (n/a)	> 10 (n/a)	1.73 (± 0.40)	3.84 (± 0.87)
SJSA1	> 10 (n/a)	> 10 (n/a)	3.66 (± 0.09)	4.02 (± 0.06)
SW684	8.26 (± 0.45)	6.89 (± 2.46)	1.95 (± 0.74)	1.68 (± 0.22)
SW872	> 10 (n/a)	> 10 (n/a)	3.57 (± 0.88)	4.50 (± 0.55)
Hs729T	> 10 (n/a)	> 10 (n/a)	2.61 (± 1.84)	4.20 (± 0.83)
RMS-YM	5.34 (± 1.50)	4.27 (± 0.93)	0.84 (± 0.17)	1.64 (± 0.50)
RUCH3	> 10 (n/a)	> 10 (n/a)	2.91 (± 1.23)	4.27 (± 0.74)
T91-95	> 10 (n/a)	7.99 (± 0.33)	2.10 (± 0.16)	1.44 (± 0.21)
SW982	4.68 (± 0.72)	> 10 (n/a)	1.13 (± 0.15)	3.18 (± 1.40)

IC₅₀: Inhibitory constant, n/a; Not available, S.D.; Standard deviation, TKI; Tyrosine kinase inhibitor. Green indicates IC₅₀ < 1 µM. Orange indicates IC₅₀ of 1-2 µM. Red indicates IC₅₀ > 2 µM.

Table S6: A204 and G402 cells treated with combinations of the TKIs pazopanib (Paz), regorafenib (Reg), sitravatinib (Sit), and anlotinib (Anlo), with associated IC₅₀ values (µM).

TKI treatment	A204	G402
	IC ₅₀ (µM) (± S.D.)	IC ₅₀ (µM) (± S.D.)
Paz	0.44 (± 0.12)	0.32 (± 0.12)
Reg	0.59 (± 0.16)	0.51 (± 0.04)
Sit	0.14 (± 0.07)	0.28 (± 0.11)
Anlo	0.30 (± 0.06)	0.41 (± 0.01)
Paz + Reg	0.39 (± 0.05)	0.51 (± 0.07)
Paz + Sit	0.13 (± 0.03)	0.29 (± 0.03)
Paz + Anlo	0.27 (± 0.03)	0.42 (± 0.09)
Reg + Sit	0.14 (± 0.05)	0.40 (± 0.05)
Reg + Anlo	0.32 (± 0.09)	0.50 (± 0.13)
Sit + Anlo	0.16 (± 0.02)	0.35 (± 0.05)

IC₅₀: Inhibitory constant, S.D.; Standard deviation, TKI; Tyrosine kinase inhibitor. Green indicates IC₅₀ < 1 µM.

Table S7: A204 and G402 cells treated with combinations of the TKIs pazopanib (Paz), regorafenib (Reg), sitravatinib (Sit), anlotinib (Anlo), ifigarginib (Inf), erdafitinib (Erda), and ponatinib (Pon), with associated IC₅₀ values (µM).

TKI treatment	A204	G402
	IC ₅₀ (µM) (± S.D.)	IC ₅₀ (µM) (± S.D.)
Paz	0.47 (± 0.08)	0.46 (± 0.07)
Reg	0.56 (± 0.13)	0.61 (± 0.09)
Sit	0.20 (± 0.06)	0.25 (± 0.10)
Anlo	0.29 (± 0.02)	0.42 (± 0.07)
Inf	1.68 (± 0.28)	1.85 (± 0.50)
Erda	0.25 (± 0.08)	0.15 (± 0.03)
Paz + Inf	0.14 (± 0.04)	0.17 (± 0.02)
Reg + Inf	0.23 (± 0.03)	0.38 (± 0.11)
Sit + Inf	0.05 (± 0.01)	0.06 (± 0.01)
Anlo + Inf	0.15 (± 0.05)	0.24 (± 0.05)
Paz + Erda	0.11 (± 0.05)	0.12 (± 0.01)
Reg + Erda	0.18 (± 0.04)	0.20 (± 0.04)
Sit + Erda	0.03 (± 0.01)	0.04 (± 0.01)
Anlo + Erda	0.11 (± 0.02)	0.13 (± 0.03)
Pon	0.05 (± 0.01)	0.05 (± 0.01)

IC₅₀: Inhibitory constant, S.D.; Standard deviation, TKI; Tyrosine kinase inhibitor. Green indicates IC₅₀ < 1 µM. Orange indicates IC₅₀ of 1-2 µM.

Table S8: A204 parental cells and TKI-resistant sublines treated with the TKIs pazopanib (Paz), regorafenib (Reg), sitravatinib (Sit), or anlotinib (Anlo), with associated IC₅₀ values (µM).

Cell model	Paz IC ₅₀ (µM) (± S.D.)	Reg IC ₅₀ (µM) (± S.D.)	Sit IC ₅₀ (µM) (± S.D.)	Anlo IC ₅₀ (µM) (± S.D.)
A204	0.77 (± 0.08)	0.67 (± 0.20)	0.54 (± 0.16)	0.57 (± 0.09)
A204PazR	5.74 (± 1.33)			
A204RegR		5.23 (± 0.57)		
A204SitR			4.71 (± 0.55)	
A204AnloR				1.95 (± 0.22)

IC₅₀; Inhibitory constant, S.D.; Standard deviation, TKI; Tyrosine kinase inhibitor. Green indicates IC₅₀ < 1 µM. Orange indicates IC₅₀ of 1-2 µM. Red indicates IC₅₀ > 2 µM.

Table S9: A204 parental cells and TKI-resistant sublines treated with the TKIs pazopanib (Paz), regorafenib (Reg), sitravatinib (Sit), and anlotinib (Anlo) to assess cross-resistance, with associated IC₅₀ values (µM).

Cell model	Paz IC ₅₀ (µM) (± S.D.)	Reg IC ₅₀ (µM) (± S.D.)	Sit IC ₅₀ (µM) (± S.D.)	Anlo IC ₅₀ (µM) (± S.D.)
A204	0.42 (± 0.08)	0.73 (± 0.09)	0.23 (± 0.06)	0.57 (± 0.04)
A204PazR	7.89 (± 1.60)	6.73 (± 1.18)	2.29 (± 0.59)	1.90 (± 0.25)
A204RegR	8.89 (± 0.11)	8.45 (± 1.89)	1.99 (± 0.31)	1.71 (± 0.37)
A204SitR	6.53 (± 1.04)	9.24 (± 1.39)	2.82 (± 0.63)	1.72 (± 0.15)
A204AnloR	6.03 (± 2.25)	7.85 (± 1.87)	1.65 (± 0.13)	2.28 (± 0.23)

IC₅₀; Inhibitory constant, S.D.; Standard deviation, TKI; Tyrosine kinase inhibitor. Green indicates IC₅₀ < 1 µM. Orange indicates IC₅₀ of 1-2 µM. Red indicates IC₅₀ > 2 µM.

Table S10: Inhibitors with ≤ 60% cell viability (compared to DMSO control) in small molecule inhibitor screens of A204 and A204 TKI-resistant sublines.

A204 (n=16)	A204PazR (n=5)	A204RegR (n=5)	A204SitR (n=7)	A204AnloR (n=6)
Ponatinib	Ponatinib	Ponatinib	Ponatinib	Ponatinib
Erdafitinib (JNJ-42756493)	Erdafitinib (JNJ-42756493)	Erdafitinib (JNJ-42756493)	Erdafitinib (JNJ-42756493)	Erdafitinib (JNJ-42756493)
Luminespib (NVP-AUY922)	Luminespib (NVP-AUY922)	Luminespib (NVP-AUY922)	Luminespib (NVP-AUY922)	Luminespib (NVP-AUY922)
BI-2536	BI-2536	BI-2536	BI-2536	BI-2536
Dactolisib (BEZ235)	Dactolisib (BEZ235)	Foretinib	Dactolisib (BEZ235)	Dactolisib (BEZ235)
Foretinib			Infgratinib (BGJ-398)	Infgratinib (BGJ-398)
Neratinib			Neratinib	
JQ1				
Dasatinib				
Cediranib				
Lenvatinib				
Regorafenib				
Imatinib				
Pazopanib				
Sunitinib				
Sorafenib				

DMSO; Dimethyl sulfoxide, TKI; Tyrosine kinase inhibitor.

Table S11: A204 TKI-resistant sublines treated with combinations of the TKIs pazopanib (Paz), regorafenib (Reg), sitravatinib (Sit), anlotinib (Anlo), erdafitinib (Erda) and ponatinib (Pon), with associated IC₅₀ values (µM).

TKI treatment	A204PazR	A204RegR	A204SitR	A204AnloR
Paz IC ₅₀ (µM) (± S.D.)	5.55 (± 0.26)			
Reg IC ₅₀ (µM) (± S.D.)		7.02 (± 0.49)		
Sit IC ₅₀ (µM) (± S.D.)			2.12 (± 0.08)	
Anlo IC ₅₀ (µM) (± S.D.)				1.50 (± 0.34)
Erda IC ₅₀ (µM) (± S.D.)	1.22 (± 0.15)	1.02 (± 0.35)	0.24 (± 0.02)	0.23 (± 0.09)
Pon IC ₅₀ (µM) (± S.D.)	0.21 (± 0.06)	0.27 (± 0.27)	0.22 (± 0.06)	0.20 (± 0.06)

IC₅₀; Inhibitory constant, S.D.; Standard deviation, TKI; Tyrosine kinase inhibitor. Green indicates IC₅₀ < 1 µM. Orange indicates IC₅₀ of 1-2 µM. Red indicates IC₅₀ > 2 µM.

TKI treatment	A204	A204PazR	A204RegR	A204SitR	A204AnloR
Inf IC₅₀ (μM)	1.68	1.91 (± 0.87)	0.98 (± 0.25)	0.39 (± 0.06)	0.63 (± 0.09)

IC₅₀; Inhibitory constant, TKI; Tyrosine kinase inhibitor. Green indicates IC₅₀ < 1 μM. Orange indicates IC₅₀ of 1-2 μM. Red indicates IC₅₀ > 2 μM.

Chapter 9

References

Acar, A, Nichol, D, Fernandez-Mateos, J, Cresswell, GD, Barozzi, I, Hong, SP, Trahearn, N, Spiteri, I, Stubbs, M, Burke, R, Stewart, A, Caravagna, G, Werner, B, Vlachogiannis, G, Maley, CC, Magnani, L, Valeri, N, Banerji, U, and Sottoriva, A, 2020, Exploiting evolutionary steering to induce collateral sensitivity in cancer, *Nat Commun.*, 11, Pg. 1923

Acharyya, S, Oskarsson, T, Vanharanta, S, Malladi, S, Kim, J, Morris, PG, Manova-Todorova, K, Leversha, M, Hogg, N, Seshan, VE, Norton, L, Brogi, E, and Massagué, J, 2012, A CXCL1 paracrine network links cancer chemoresistance and metastasis, *Cell.*, 150 (1), Pg. 165-178

Agarwal, AK, 2018, How to explain the AKT phosphorylation of downstream targets in the wake of recent findings, *Proc Natl Acad Sci USA*, 115 (27), Pg. E6099-E6100

Ahmed, N, Brawley, VS, Hedge, M, Robertson, C, Ghazi, A, Gerken, C, Liu, E, Dakhova, O, Ashoori, A, Corder, A, Gray, T, Wu, MF, Liu, H, Hicks, J, Rainusso, N, Dotti, G, Mei, Z, Grilley, B, Gee, A, Rooney, CM, Brenner, MK, Heslop, HE, Wels, WS, Wang, LL, Anderson, P, and Gottschalk, S, 2015, Human epidermal growth factor receptor 2 (HER2)-specific chimeric antigen receptor-modified T cells for the immunotherapy of HER2-positive sarcoma, *J Clin Oncol.*, 33 (15), Pg. 1688-1696

Ahmed, SBM, and Prigent, SA, 2017, Insights into the Shc family of adaptor proteins, *J Mol Signal.*, 12, Pg. 2

Akce, M, Zaidi, MY, Waller, EK, El-Rayes, BF, and Lesinski, GB, 2018, The potential of CAR T cell therapy in pancreatic cancer, *Front Immunol.*, 9, Pg. 2166

Albershardt, TC, Campbell, DJ, Parsons, AJ, Slough, MM, Ter Meulen, J, and Berglund, P, 2016, LV305, a dendritic cell-targeting integration-deficient ZVex™-based lentiviral vector encoding NY-ESO-1, induces potent anti-tumor immune response, *Mol Ther Oncolytics.*, 3, Pg. 16010

Alday-Parejo, B, Stupp, R, and Rüegg, C, 2019, Are integrins still practicable targets for anti-cancer therapy?, *Cancers (Basel).*, 11 (7), Pg. 978

Alentorn, A, Marie, Y, Carpentier, C, Boisselier, B, Giry, M, Labussière, M, Mokhtari, K, Hoang-Xuan, K, Sanson, M, Delattre, JY, and Idbaih, A, 2012, Prevalence, clinico-pathological value, and co-occurrence of PDGFRA abnormalities in diffuse gliomas, *Neuro Oncol.*, 14 (11), Pg. 1393-1403

Amato, KR, Wang, S, Tan, L, Hastings, AK, Song, W, Lovly, CM, Meador, CB, Ye, F, Lu, P, Balko, JM, Colvin, DC, Cates, JM, Pao, W, Gray, NS, and Chen, J, 2016, EPHA2 blockade overcomes acquired resistance to EGFR kinase inhibitors in lung cancer, *Cancer Res.*, 76 (2), Pg. 305-318

American Cancer Society, 2018, Risk factors for soft tissue sarcomas, <https://www.cancer.org/cancer/soft-tissue-sarcoma/causes-risks-prevention/risk-factors.html>, Last accessed [May 2020]

An, Z, Aksoy, O, Zheng, T, Fan, QW, and Weiss, WA, 2018, Epidermal growth factor receptor and EGFRvIII in glioblastoma: signaling pathways and targeted therapies, *Oncogene.*, 37 (12), Pg. 1561-1575

Andor, N, Graham, TA, Jansen, M, Xia, LC, Aktipis, CA, Petritsch, C, Ji, HP, and Maley, CC, 2016, Pan-cancer analysis of the extent and consequences of intra-tumor heterogeneity, *Nat Med.*, 22 (1), Pg. 105-113

Antonescu, CR, Suurmeijer, AJH, Zhang, L, Sung, YS, Jungbluth, AA, Travis, WD, Al-Ahmadie, H, Fletcher, CDM, and Alaggio, R, 2015, Molecular characterization of inflammatory myofibroblastic tumors with frequent ALK and ROS1 gene fusions and rare novel RET rearrangement, *Am J Surg Pathol.*, 39 (7), Pg. 957-967

Applied Biosystems, 2016, Real-time PCR: understanding Ct, <https://www.thermofisher.com/content/dam/LifeTech/Documents/PDFs/PG1503-PJ9169-CO019879-Re-brand-Real-Time-PCR-Understanding-Ct-Value-Americas-FHR.pdf>, Last accessed [October 2021]

Araujo, J, and Logothetis, C, 2010, Dasatinib: a potent SRC inhibitor in clinical development for the treatment of solid tumors, *Cancer Treat Rev.*, 36 (6), Pg. 492-500

Ardito, F, Giuliani, M, Perrone, D, Troiano, G, and Lo Muzio, L, 2017, The crucial role of protein phosphorylation in cell signaling and its use as targeted therapy (Review), *Int J Mol Med.*, 40 (2), Pg. 271-280

Arora, S, Rastogi, S, Shamim, SA, Barwad, A, and Sethi, M, 2020, Good and sustained response to pembrolizumab and pazopanib in advanced undifferentiated pleomorphic sarcoma: a case report, *Clin Sarcoma Res.*, 10, Pg. 10

Ascierto, PA, Kirkwood, JM, Grob, JJ, Simeone, E, Grimaldi, AM, Maio, M, Palmieri, G, Testori, A, Marincola, FM, and Mozzillo, N, 2012, The role of BRAF V600 mutation in melanoma, *J Transl Med.*, 10, Pg. 85

Aslam, MI, Abraham, J, Mansoor, A, Druker, BJ, Tyner, JW, and Keller, C, 2014, PDGFR β reverses EphB4 signaling in alveolar rhabdomyosarcoma, *Proc Natl Acad Sci USA*, 111 (17), Pg. 6383-6388

Attia, S, Bolejack, V, Ganjoo, KN, George, S, Agulnik, M, Rushing, DA, Loggers, ET, Livingston, MB, Wright, JA, Chawla, SP, Okuno, SH, Reinke, DK, Riedel, RF, Davis, LE, Ryan, CW, and Maki, RG, 2017, A phase II trial of regorafenib (REGO) in patients (pts) with advanced Ewing sarcoma and related tumors (EWS) of soft tissue and bone: SARC024 trial results, *J Clin Oncol.*, 35 (15), https://ascopubs.org/doi/abs/10.1200/JCO.2017.35.15_suppl.11005, Last accessed [June 2021]

Aulin, LBS, Liakopoulos, A, Van der Graaf, PH, Rozen, DE, and Van Hasselt, JGC, 2021, Design principles of collateral sensitivity-based dosing strategies, *Nat Commun.*, 12 (1), Pg. 5691

Ayraud, MM, Mirabeau, O, Gruel, N, Grossetéte, S, Boeva, V, Durand, S, Surdez, D, Saulnier, O, Zaidi, S, Gribkova, S, Fouché, A, Kairov, U, Raynal, V, Tirode, F, Grünwald, TGP, Bohec, M, Baulande, S, Janoueix-Lerosey, I, Vert, JP, Barillot, E, Delattre, O, and Zinovyev, A, 2020, Transcriptional programs define intratumoral heterogeneity of Ewing sarcoma at single-cell resolution, *Cell Rep.*, 30 (6), Pg. 1767-1779

Ayodele, O, Wang, BX, Pfister, TD, Al-Ezzi, E, Berman, H, Hansen, AR, Gupta, AA, Spreafico, A, Arones, L, Bedard, PL, Carlsson, L, Butler, MO, Haibe-Kains, B, Xu, W, Siu, LL, and Razak, ARA, 2021, A phase II, open-label, randomized trial of durvalumab (D) with Olaparib (O) or cediranib (C) in patients (pts) with leiomyosarcoma (LMS), *J Clin Oncol.*, 39 (15), https://ascopubs.org/doi/abs/10.1200/JCO.2021.39.15_suppl.11522, Last accessed [November 2021]

Bahleda, R, Italiano, A, Hierro, C, Mita, A, Cervantes, A, Chan, N, Awad, M, Calvo, E, Moreno, V, Govindan, R, Spira, A, Gonzalez, M, Zhong, B, Santiago-Walker, A, Poggesi, I, Parekh, T, Xie, H, Infante, J, and Taberero, J, 2019, Multicenter phase I study of erdafitinib (JNJ-42756493), oral pan-fibroblast growth factor receptor inhibitor, in patients with advanced or refractory solid tumors, *Clin Cancer Res.*, 25 (16), Pg. 4888-4897

Bai, C, Yang, M, Fan, Z, Li, S, Gao, T, and Fang, Z, 2015, Associations of chemo- and radio-resistant phenotypes with the gap junction, adhesion, and extracellular matrix in a three-dimensional culture model of soft sarcoma, *J Expt Clin Cancer Res.*, 34 (1), Pg. 58

Bai, Y, Li, J, Fang, B, Edwards, A, Zhang, G, Bui, M, Eschrich, S, Altiock, s, Koomen, J, Haura, EB, 2012, Phosphoproteomics identifies driver tyrosine kinases in sarcoma cell lines and tumours, *Cancer Res.*, 72 (10), Pg. 2501-2511

Baird, K, Davis, S, Antonescu, CR, Harper, UL, Walker, RL, Chen, Y, Glatfelter, AA, Duray, PH, and Meltzer, PS, 2005, Gene expression profiling of human sarcomas: insights into sarcoma biology, *Cancer Res.*, 65 (20), Pg. 9226-9235

Bairoch, A, 2018, The CellSaurus, a cell-line knowledge resource, *J BioMol Tech.*, 29 (2), Pg. 25-38

Ballinger, ML, Goode, DL, Ray-Coquard, I, James, PA, Mitchell, G, Niedermayr, E, Puri, A, Schiffman, JD, Dite, GS, Cipponi, A, Maki, RG, Brohl, AS, Myklebost, O, Stratford, EW, Lorenz, S, Ahn, SM, Ahn, JH, Kim, JE, Shanley, S, Beshay, V, Randall, RL, Judson, I, Seddon, B, Campbell, IG, Young, MA, Sarin, R, Blay, JY, O'Donoghue, SI, Thomas, DM, and International Sarcoma Kindred Study, 2016, Monogenic and polygenic determinants of sarcoma risk: an international genetic study, *Lancet Oncol.*, 17 (9), Pg. 1261-1271

Barham, W, Frump, AL, Sherrill, TP, Garcia, CB, Saito-Diaz, K, Van Saun, MN, Fingleton, B, Gleaves, L, Orton, D, Capecci, MR, Blackwell, TS, Lee, E, Yull, F, and Eid, JE, 2013, Targeting the Wnt pathway in synovial sarcoma models, *Cancer Discov.*, 3 (11), Pg. 1286-1301

Bauer, S, George, S, Von Mehren, M, and Heinrich, MC, 2021, Early and next-generation KIT/PDGFRA Kinase inhibitors and the future of treatment for advanced gastrointestinal stromal tumor, *Front Oncol.*, 11, Pg. 672500

Beadnell, TC, Nassar, KW, Rose, MM, Clark, EG, Danysh, BP, Hofmann, MC, Pozdeyev, N, and Schweppe, RE, 2018, Src-mediated regulation of the PI3K pathway in advanced papillary and anaplastic thyroid cancer, *Oncogenesis.*, 7 (2), Pg. 23

Bechman, N, and Maher, J, 2021, Lymphodepletion strategies to potentiate adoptive T-cell immunotherapy – what are we doing; where are we going?, *Expert Opin Biol Ther.*, 21 (5), Pg. 627-637

Becker, M, Graf, C, Tonak, M, Radsak, MP, Bopp, T, Bals, R, Bohle, RM, Theobald, M, Rommens, PM, Proschek, D, and Wehler, TC, 2016, Xenograft models for undifferentiated pleomorphic sarcoma not otherwise specified are essential for preclinical testing of therapeutic agents, *Oncol Lett.*, 12 (2), Pg. 1257-1264

Bedard, PL, Hansen, AR, Ratain, MJ, and Siu, LL, 2013, Tumour heterogeneity in the clinic, *Nature.*, 501 (7467), Pg. 355-364

Beeton-Kempen, N, 2021, Data-dependent vs. data-independent proteomic analysis, *Technolog Networks Proteomics & Metabolomics*, <https://www.technologynetworks.com/proteomics/lists/data-dependent-vs-data-independent-proteomic-analysis-331712>, Last accessed [January 2021]

Ben-Ami, E, Barysaukas, CM, Solomon, S, Tahlil, K, Malley, R, Hohos, M, Polson, K, Loucks, M, Severgnini, M, Patel, T, Cunningham, A, Rodig, SJ, Hodi, FS, Morgan, JA, Merriam, P, Wagner, JA, Shapiro, GI, and George, S, 2017, Immunotherapy with single agent nivolumab for advanced leiomyosarcoma of the uterus: results of a phase 2 study, *Cancer.*, 123 (17), Pg. 3285-3290

Ben-Hamo, R, Berger, AJ, Gavert, N, Miller, M, Pines, G, Oren, R, Pikarsky, E, Benes, CH, Neuman, T, Zwing, Y, Efroni, S, Getz, G, and Straussman, R, 2020, Predicting and affecting response to cancer therapy based on pathway-level biomarkers, *Nat Commun.*, 11 (1), Pg. 3296

Benjamin, RS, and Futreal, A, 2016, Are sarcomas hereditary?, *Lancet Oncol.*, 17 (9), Pg. 1179-1181

Benson, C, Ray-Coquard, I, Sleijfer, S, Litière, S, Blay, JY, Le Cesne, A, Papai, Z, Judson, I, Schöffski, P, Chawla, S, Gil, T, Piperno-Neumann, S, Marréaud, S, Dewji, MR, and Van der Graaf, WTA, 2016, Outcome of uterine sarcoma patients

treated with pazopanib: a retrospective analysis based on two European Organisation for Research and Treatment of Cancer (EORTC) Soft Tissue and Bone Sarcoma Group (STBSG) clinical trials 62043 and 62072, *Gynecol Oncol.*, 142 (1), Pg. 89-94

Beran, M, Cao, X, Estrov, Z, Jeha, S, Jin, G, O'Brien, S, Talpaz, M, Arlinghaus, RB, Lydon, NB, and Kantarjian, H, 1998, Selective inhibition of cell proliferation and BCR-ABL phosphorylation in acute lymphoblastic leukemia cells expressing Mr 190,000 BCR-ABL protein by a tyrosine kinase inhibitor (CGP-57148), *Clin Cancer Res.*, 4 (7), Pg. 1661-1672

Bermejo, IM, Jaffee, EM, Davar, D, Cardarelli, J, Williams, D, Phillips, P, Carleton, M, Zhou, M, De Henau, O, Monga, M, and Drake, CG, 2018, Phase Ib/2 study of nivolumab in combination with an anti-IL-8 monoclonal antibody, BMS-986253, in a biomarker-enriched population of patients with advanced cancer, *J Clin Oncol.*, 36 (15), https://ascopubs.org/doi/abs/10.1200/JCO.2018.36.15_suppl.TPS3109, Last accessed [November 2021]

Berndt, N, Karim, RM, and Schönbrunn, E, 2017, Advances of small molecule targeting of kinases, *Curr Opin Chem Biol.*, 39, Pg. 126-132

Berrington de Gonzalez, A, Kutsenko, A, and Rajaraman, P, 2012, Sarcoma risk after radiation exposure, *Clin Sarcoma Res.*, 2 (1), Pg. 18

Bilusic, M, Heery, CR, Collins, JM, Donahue, RN, Palena, C, Madan, RA, Karzai, F, Marté, JL, Strauss, J, Gatti-Mays, ME, Schlom, J, and Gulley, JL, 2019, Phase I trial of HuMax-IL8 (BMS-986253), an anti-IL-8 monoclonal antibody, in patients with metastatic or unresectable solid tumors, *J Immunother Cancer.*, 7 (1), Pg. 240

Blake, RA, Broome, MA, Liu, X, Wu, J, Gishizky, M, Sun, L, and Courtneidge, SA, 2000, SU6656, a selective Src family kinase inhibitor, used to probe growth factor signaling, *Mol Cell Biol.*, 20 (23), Pg. 9018-9027

Blay, JY, Sleijfer, S, Schöffski, P, Kawai, A, Brodowicz, T, Demetri, GD, and Maki, RG, 2014, International expert opinion on patient-tailored management of soft tissue sarcomas, *Eur J Cancer.*, 50 (4), Pg. 679-689

Blay, JY, Honoré, C, Stoeckle, E, Meeus, P, Jafari, M, Gouin, F, Anract, P, Ferron, G, Rochwerger, A, Ropars, M, Carrere, S, Marchal, F, Sirveaux, F, Di Marco, A, Le Nail, LR, Guiramand, J, Vaz, G, Machiavello, JC, Marco, O, Causeret, S, Gimbergues, P, Fiorenza, F, Chaigneau, L, Guillemin, F, Guilloit, JM, Dujardin, F, Spano, JP, Ruzic, JC, Michot, A, Soibinet, P, Bompas, E, Chevreau, C, Duffaud, F, Rios, M, Perrin, C, Firmin, N, Bertucci, F, Le Pechoux, C, Le Loarer, F, Collard, O, Karanian-Philippe, M, Brahmi, M, Dufresne, A, Dupré, A, Ducimetière, F, Giraud, A, Pérol, D, Toulmonde, M, Ray-Coquard, I, Italiano, A, Le Cesne, A, Penel, N, Bonvalot, S, and NETSARC/REPPS/RESOS and French Sarcoma Group-Groupe d'Etude des Tumeurs Osseuses (GSF-GETO) Networks, 2019, Surgery in reference centers improves survival of sarcoma patients: a nationwide study, *Ann Oncol.*, 30 (7), Pg. 1143-1153

Blay, JY, Serrano, C, Heinrich, MC, Zalberg, J, Bauer, S, Gelderblom, H, Schöffski, P, Jones, RL, Attia, S, D'Amato, G, Chi, P, Reichardt, P, Meade, J, Shi, K, Ruiz-Soto, R, George, S, and von Mehren, M, 2020, Ripretinib in patients with advanced gastrointestinal stromal tumours (INVICTUS): a double-blind, randomised, placebo-controlled, phase 3 trial, *Lancet Oncol.*, 21 (7), Pg. 923-934

Boczek, EE, Luo, Q, Dehling, M, Röpke, M, Mader, SL, Seidl, A, Kaila, VRI, and Buchner, J, 2019, Autophosphorylation activates c-Src kinase through global structural rearrangements, *J Biol Chem.*, 294 (35), Pg. 13186-13197

Boucher, J, Kleinridders, A, and Kahn, CR, 2014, Insulin receptor signaling in normal and insulin-resistant states, *Cold Spring Harb Perspect Biol.*, 6 (1), a009191

Bougeard, G, Renaux-Petel, M, Flaman, JM, Charbonnier, C, Fermey, P, Belotti, M, Gauthier-Villars, M, Stoppa-Lyonnet, D, Consolino, E, Brugières, L, Caron, O, Benusiglio, PR, Paillerets, BB, Bonadona, V, Bonaïti-Pellié, C, Tinat, J, Baert-Desurmont, S, and Frebourg, T, 2015, Revisiting Li-Fraumeni syndrome from TP53 mutation carriers, *J Clin Oncol.*, 33 (21), Pg. 2345-2352

Bovée, JVMG, and Hogendoorn, PCW, 2010, Molecular pathology of sarcomas: concepts and clinical implications, *Virchows Arch.*, 456 (2), Pg. 193-199

Bracken, AP, Kleine-Kohlbrecher, D, Dietrich, N, Pasini, D, Gargiulo, G, Beekman, C, Theilgaard-Mönch, K, Minucci, S, Porse, BT, Marine, JC, Hansen, KH, and Helin, K, 2007, The polycomb group proteins bind throughout the *INK4A-ARF* locus and are disassociated in senescent cells, *Genes Dev.*, 21 (5), Pg. 525-530

Braconi, C, Bracci, R, and Cellerino, R, 2008, Molecular targets in gastrointestinal stromal tumors (GIST) therapy, *Curr Cancer Drug Targets.*, 8 (5), Pg. 359-366

Brady, MS, Gaynor, JJ, and Brennan, MF, 1992, Radiation-associated Sarcoma of bone and soft tissue, *Arch Surg.*, 127 (12), Pg. 1379-1385

Brenca, M, Rossi, S, Lorenzetto, E, Piccinin, E, Piccinin, S, Rossi, FM, Guiliano, A, Dei Tos, AP, Maestro, R, and Modena, P, 2021, Correction: SMARCB1/INI1 genetic inactivation is responsible for tumorigenic properties of epithelioid sarcoma cell line VAESBJ, *Mol Cancer Ther.*, 20 (8), Pg. 1495

Brennan, B, Stiller, C, and Bourdeaut, F, 2013, Extracranial rhabdoid tumours: what we have learned so far and future directions, *Lancet Oncol.*, 14 (8), e329-336

Brew, R, Erikson, JS, West, DC, Kinsella, AR, Slavin, J, and Christmas, SE, 2000, Interleukin-8 as an autocrine growth factor for human colon carcinoma cells in vitro, *Cytokine.*, 12 (1), Pg. 78-85

Brodin, BA, Wennerberg, K, Lidbrink, E, Brosjö, O, Potdar, S, Wilson, JN, Ma, L, Moens, LN, Hesla, A, Porovic, E, Bernhardsson, E, Papakonstantinou, A, Bauer, H, Tsagkosis, P, Von Sivers, K, Wejde, J, Östling, P, Kallioniemi, O, and Stragliotto, CL, 2019, Drug sensitivity testing on patient-derived sarcoma cells predicts patient response to treatment and identifies c-Sarc inhibitors as active drugs for translocation sarcomas, *Br J Cancer.*, 120 (4), Pg. 435-443

Brodowicz, T, Mir, O, Wallet, J, Italiano, A, Blay, JY, Bertucci, F, Eisterer, W, Chevreau, C, Piperno-Neumann, S, Bompas, E, Ryckewaert, T, Liegl-Antzwager, B, Thery, J, Penel, N, Le Cesne, A, and Le Deley, MC, 2018, Efficacy and safety of regorafenib compared to placebo and to post-cross-over regorafenib in advanced non-adipocytic soft tissue sarcoma, *Eur J Cancer.*, 99, Pg. 28-26

Brodowicz, T, Liegl-Atzwanger, B, Penel, N, Mir, O, Blay, JY, Kashofer, K, Le Cesne, A, Decoupigny, E, Wallet, J, Hamacher, R, and Le Deley, MC, 2020, Assessing prognostic and predictive biomarkers of regorafenib response in patients with advanced soft tissue sarcoma: REGOSARC study, *Cancers (Basel).*, 12 (12), Pg. 3746

Broekman, F, Giovannetti, E, and Peters, GJ, 2011, Tyrosine kinase inhibitors: multi-targeted or single-targeted?, *World J Clin Oncol.*, 2 (2), Pg. 80-93

Bromann, PA, Korkava, H, and Courtneidge, SA, 2004, The interplay between Src family kinases and receptor tyrosine kinases, *Oncogene.*, 23 (48), Pg. 7957-7968

Bruna, A, Rueda, OM, Greenwood, W, Batra, AS, Callari, M, Batra, RN, Pogrebniak, K, Sandoval, J, Cassidy, JW, Tufegdzic-Vidakovic, A, Sammut, SJ, Jones, L, Provenzano, E, Baird, R, Eirew, P, Hadfield, J, Eldridge, M, McLaren-Douglas, A, Barthorpe, A, Lightfoot, H, O'Connor, MJ, Gray, J, Cortes, J, Baselga, J, Marangoni, E, Welm, AL, Aparicio, S, Serra, V, Garnett, MJ, and Caldas, C, 2016, A biobank of breast cancer explants with preserved intra-tumor heterogeneity to screen anticancer compounds, *Cell.*, 167 (1), Pg. 260-274

Buchdunger, E, Zimmermann, J, Mett, H, Meyer, T, Müller, M, Druker, BJ, and Lydon, NB, 1996, Inhibition of the Abl protein-tyrosine kinase in vitro and in vivo by a 2-phenylaminopyrimidine derivative, *Cancer Res.*, 56 (1), Pg. 100-104

Bui, NQ, Przybyl, J, Trabucco, SE, Frampton, G, Hastie, T, Van de Rijn, M, and Ganjoo, KN, 2019, A clinic-genomic analysis of soft tissue sarcoma patients reveals CDKN2A deletion as a biomarker for poor prognosis, *Clin Sarcoma Res.*, 9, Pg. 12

Burgess, MA, Bolejack, V, Schuetze, S, Van Tine, BA, Attia, S, Riedel, RF, Hu, JS, Davis, LE, Okuno, SH, Priebat, DA, Movva, S, Reed, DR, D'Angelo, SP, Lazar, AJ, Keung, EYZ, Reinke, DK, Baker, LH, Maki, RG, Patel, S, and Tawbi, HAH, 2019, Clinical activity of pembrolizumab (P) in undifferentiated pleomorphic sarcoma (UPS) and dedifferentiated/pleomorphic liposarcoma (LPS): final results of SARC028 expansion cohorts, *J Clin Oncol.*, https://ascopubs.org/doi/10.1200/JCO.2019.37.15_suppl.11015, Last accessed [November 2021]

Butrynski, JE, D'Adamo, DR, Hornick, JL, Dal Cin, P, Antonescu, CR, Jhanwar, SC, Ladanyi, M, Capelletti, M, Rodig, SJ, Ramaiya, N, Kwak, EL, Clark, JW, Wilner, KD, Christensen, JG, Jänne, PA, Maki, RG, Demetri, GD, and Shapiro, GI, 2010, Crizotinib in ALK-rearranged inflammatory myofibroblastic tumor, *N Engl J Med.*, 363 (18), Pg. 1727-1733

Byron, A, Humphries, JD, Askari, JA, Craig, SE, Mould, AP, and Humphries, MJ, 2009, Anti-integrin monoclonal antibodies, *J Cell Sci.*, 122 (Pt 22), Pg. 4009-4011

Cabanos, HF, and Hata, AN, 2021, Emerging insights into targeted therapy-tolerant persister cells in cancer, *Cancers (Basel).*, 13 (11), Pg. 2666

Cancer Research UK, 2006-2008, Childhood Cancers by Cancer Type, Average Number of New Cases per Year, Ages 0-14, Great Britain, <https://www.cancerresearchuk.org/health-professional/cancer-statistics/childrens-cancers/incidence#heading-Three>, Last accessed [May 2020]

Cancer Research UK, 2008-2010, Soft Tissue Sarcoma (All subtypes combined), Average number of new cases per year and age-specific incidence rates, UK, <https://www.cancerresearchuk.org/health-professional/cancer-statistics/statistics-by-cancer-type/soft-tissue-sarcoma/incidence#heading-One>, Last accessed [May 2020]

Cancer Research UK, 2010, Soft Tissue Sarcoma (All Subtypes Combined), Number of New Cases, UK, <https://www.cancerresearchuk.org/health-professional/cancer-statistics/statistics-by-cancer-type/soft-tissue-sarcoma/incidence#heading-Zero>, Last accessed [May 2020]

Cancer Research UK, 2015, Risks and causes, <https://www.cancerresearchuk.org/about-cancer/soft-tissue-sarcoma/risks-causes>, Last accessed [May 2020]

Cancer Research UK, 2017, Bone Sarcoma (C40-41), Number of New Cases, UK, <https://www.cancerresearchuk.org/health-professional/cancer-statistics/statistics-by-cancer-type/bone-sarcoma/incidence#heading-Zero>, Last accessed [May 2020]

Cancer Research UK, 2017, The 20 Most Common Cancers, UK, <https://www.cancerresearchuk.org/health-professional/cancer-statistics/incidence/common-cancers-compared#heading-Zero>, Last accessed [May 2020]

Cancer Research UK, 2018, Types of soft tissue sarcoma, <https://www.cancerresearchuk.org/about-cancer/soft-tissue-sarcoma/types>, Last accessed [May 2020]

Cancer Research UK, 2020, Lipoma, <https://www.cancerresearchuk.org/about-cancer/other-conditions/lipoma>, Last accessed [May 2020]

Cao, Y, O'Reilly, MS, Marshall, B, Flynn, E, Ji, RW, and Folkman, J, 1998, Expression of angiostatin cDNA in a murine fibrosarcoma suppresses primary tumor growth and produces long-term dormancy of metastases, *J Clin Invest.*, 101 (5), Pg. 1055-1063

Capes-Davis, A, Theodosopoulos, G, Atkin, I, Drexler, HG, Kohara, A, MacLeod, RAF, Masters, JR, Nakamura, Y, Reid, YA, Reddel, RR, and Freshney, RI, 2010, Check your cultures! A list of cross-contaminated or misidentified cell lines, *Int J Cancer.*, 127 (1), Pg. 1-8

Carroll, M, Ohno-Jones, S, Tamura, S, Buchdunger, E, Zimmermann, J, Lydon, NB, Gilliland, DG, and Druker, BJ, 1997, CGP 57148, a tyrosine kinase inhibitor, inhibits the growth of cells expressing BCR-ABL, TEL-ABL, and TEL-PDGFR fusion proteins, *Blood.*, 90 (12), Pg. 4947-4952

Casili, F, Bianchini, A, Gloaguen, I, Biordi, L, Alesse, E, Festuccia, C, Cavalieri, B, Strippoli, R, Cervellera, MN, Di Bitondo, R, Ferretti, E, Mainiero, F, Bizzarri, C, Colotta, F, and Bertini, R, 2005, Inhibition of interleukin-8 (CXCL8/IL-8) responses by repertaxin, a new inhibitor of the chemokine receptors CXCR1 and CXCR2, *Biochem Pharmacol.*, 69 (3), Pg. 385-394

Cella, D, and Beaumont, JL, 2016, Pazopanib in the treatment of advanced renal cell carcinoma, *Ther Adv Urol.*, 8 (1), Pg. 61-69

Cesarman, E, Damania, B, Krown, SE, Martin, J, Bower, M, and Whitby, D, 2019, Kaposi sarcoma, *Nat Rev Dis Primers.*, 5 (1), Pg. 9

Chamberlain, FE, Wilding, C, Jones, RL, and Huang, PH, 2019, Pazopanib in patients with advanced intermediate-grade or high-grade liposarcoma, *Expert Opin Invest Drugs.*, 28 (6), Pg. 505-511

Chauvin, C, Leruste, A, Tauziède-Espariat, A, Andrianteranagna, M, Surdez, D, Lescure, A, Han, ZY, Anthony, E, Richer, W, Baulande, S, Bohec, M, Zaidi, S, Aynaud, MM, Maillot, L, Masliah-Planchon, J, Cairo, S, Roman-Roman, S, Delattre, O, Del Nery, E, and Bourdeaut, F, 2017, High-throughput drug screening identifies pazopanib and clofilium tosylate as promising treatments for malignant rhabdoid tumors, *Cell Rep.*, 21 (7), Pg. 1737-1745

Chawla, SP, Chua, VS, Gordon, EM, Moradkhani, A, Kim, K, Quon, D, Wong, S, Sumner, R, Mac, V, Huang, R, Wang, K, Kim, J, Kim, B, McGinn, AN, Park, CH, Houston, S, and Sankar, N, 2019, Phase I study to evaluate the safety and efficacy of rivocecanib (apatinib) and nivolumab in patients with unresectable or metastatic cancer, *J Clin Oncol.*, https://ascopubs.org/doi/abs/10.1200/JCO.2019.37.8_suppl.18, Last accessed [November 2021]

Chawla, SP, Van Tine, BA, Pollack, SM, Ganjoo, KN, Elias, AD, Riedel, RF, Attia, S, Choy, E, Okuno, SH, Agulnik, M, Von Mehren, M, Livingston, MB, Keedy, VL, Verschraegen, CF, Philip, T, Bohac, GC, Yurasov, S, Yakovich, A, Lu, H, Chen, M, and Maki, RG, 2021, Phase II randomized study of CMB305 and atezolizumab compared with atezolizumab alone in soft-tissue sarcomas expressing NY-ESO-1, *J Clin Oncol.*, <https://ascopubs.org/doi/10.1200/JCO.20.03452>, Last accessed [November 2021]

Chen, I, Firth, B, Hopkins, L, Bougie, O, Xie, R.H., and Singh, S, 2018, Clinical characteristics differentiating uterine sarcoma and fibroids, *JSLs.*, 22 (1), Pg. e2017.00066

Chen, J, Elfiky, A, Han, M, Chen, C, and Saif, MW, 2014, The role of Src in colon cancer and its therapeutic implications, *Clin Colorectal Cancer.*, 13 (1), Pg. 5-13

Chen, L, Shern, JF, Wei, JS, Yohe, ME, Song, YK, Hurd, L, Liao, H, Catchpole, D, Skapek, SX, Barr, FG, Hawkins, DS, and Khan, J, 2015, Clonality and evolutionary history of rhabdomyosarcoma, *PLoS Genet.*, 11 (3), e1005075

Chen, R, Kim, O, Yang, J, Sato, K, Eisenmann, KM, McCarthy, J, Chen, H, and Qiu, Y, 2001, Regulation of Akt/PKB activation by tyrosine phosphorylation, *J Biol Chem.*, 276 (34), Pg. 31858-31862

Chen, Z, Liu, Z, Zhang, M, Huang, W, Li, Z, Wang, S, Zhang, C, Dong, B, Gao, J, and Shen, L, 2019, EPHA2 blockade reverses acquired resistance to afatinib induced by EPHA2-mediated MAPK pathway activation in gastric cancer cells and avator mice, *Int J Cancer.*, 145 (9), Pg. 2440-2449

Chevreau, C, Le Cesne, A, Ray-Coquard, I, Italiano, A, Cioffi, A, Isambert, N, Robin, YM, Fournier, C, Clisant, S, Chaigneau, L, Bay, JO, Bompas, E, Gauthier, E, Blay, JY, and Penel, N, 2013, Sorafenib in patients with progressive epithelioid hemangioendothelioma: a phase 2 study by the French Sarcoma Group (GSF/GETO), *Cancer.*, 119 (14), Pg. 2639-2644

Chi, Y, Fang, Z, Hong, X, Yao, Y, Sun, P, Wang, G, Du, F, Sun, Y, Wu, Q, Qu, G, Wang, S, Song, J, Yu, J, Lu, Y, Zhu, X, Niu, X, He, Z, Wang, J, Yu, H, and Cai, J, 2018, Safety and efficacy of anlotinib, a multikinase angiogenesis inhibitor, in patients with refractory metastatic soft-tissue sarcoma, *Clin Cancer Res.*, 24 (21), Pg. 5233-5238

Chi, Y, Yao, Y, Wang, S, Huang, G, Cai, Q, Shang, G, Wang, G, Qu, G, Wu, Q, Jiang, Y, Song, J, Chen, J, Zhu, X, Cai, Z, Bai, C, Lu, Y, Yu, Z, Shen, J, and Cai, J, 2018, Anlotinib for metastasis soft tissue sarcoma: a randomized, double-blind,

Chibon, F, Lagarde, P, Salas, S, Pérot, G, Brouste, V, Tirode, F, Lucchesi, C, De Reynies, A, Kauffmann, A, Bui, B, Terrier, P, Bonvalot, S, Le Cesne, A, Vince-Ranchère, D, Blay, JY, Collin, F, Guillou, L, Leroux, A, Coindre, JM, and Aurias, A, 2010, Validated prediction of clinical outcome in sarcomas and multiple types of cancer on the basis of a gene expression signature related to genome complexity, *Nat Med.*, 16 (7), Pg. 781-787

Chudasama, P, Renner, M, Straub, M, Mughal, SS, Hutter, B, Kosaloglu, Z, Schweßinger, R, Scheffler, M, Alldinger, I, Schimmack, S, Persigehl, T, Kobe, C, Jäger, D, Von Kalle, C, Schirmacher, P, Beckhaus, MK, Wolf, S, Heining, C, Gröschel, S, Wolf, J, Brors, B, Weichert, W, Glimm, H, Scholl, C, Mechtersheimer, G, Specht, K, and Fröhling, S, 2017, Targeting fibroblast growth factor receptor 1 for treatment of soft-tissue sarcoma, *Clin Cancer Res.*, 23 (4), Pg. 962-973

Chudasama, P, Mughal, SS, Sanders, MA, Hübschmann, D, Chung, I, Deeg, KI, Wong, SH, Rabe, S, Hlevnjak, M, Zapatka, M, Ernst, A, Kleinheinz, K, Schlesner, M, Sieverling, L, Klink, B, Schröck, E, Hoogenboezem, RM, Kasper, B, Heilig, CE, Egerer, G, Wolf, S, Von Kalle, C, Eils, R, Stenzinger, A, Weichert, W, Glimm, H, Gröschel, S, Kopp, HG, Omlor, G, Lehner, B, Bauer, S, Schimmack, S, Ulrich, A, Mechtersheimer, G, Rippe, K, Brors, B, Hutter, B, Renner, M, Hohenberger, P, Scholl, C, and Fröhling, S, 2018, Integrative genomic and transcriptomic analysis of leiomyosarcoma, *Nat Commun.*, 9 (1), Pg. 144

Chugh, R, Wathen, JK, Maki, RG, Benjamin, RS, Patel, SR, Meyers, PA, Priebat, DA, Reinke, DK, Thomas, DG, Keohan, ML, Samuels, BL, and Baker, LH, 2009, Phase II multicenter trial of imatinib in 10 histologic subtypes of sarcoma using a Bayesian hierarchical statistical model, *J Clin Oncol.*, 27 (19), Pg. 3148-3153

Chugh, R, Wathen, JK, Patel, SR, Maki, RG, Meyers, PA, Schuetze, SM, Priebat, DA, Thomas, DG, Jacobson, JA, Samuels, BL, Benjamin, RS, Baker, LH, and Sarcoma Alliance for Research through Collaboration (SARC), 2010, Efficacy of imatinib in aggressive fibromatosis: results of a phase II multicenter Sarcoma Alliance for Research through Collaboration (SARC) trial, *Clin Cancer Res.*, 16 (19), Pg. 4884-4891

Church, AJ, Calicchio, ML, Nardi, V, Skalova, A, Pinto, A, Dillon, DA, Gomez-Fernandez, CR, Manoj, N, Haimes, JD, Stahl, JA, Dela Cruz, FS, Tannenbaum-Dvir, S, Glade-Bender, JL, Kung, AL, DuBois, SG, Kozakewich, HP, Janeway, KA, Perez-Atayde, AR, and Harris, MH, 2018, Recurrent EML4-NTRK3 fusions in infantile fibrosarcoma and congenital mesoblastic nephroma suggest a revised testing strategy, *Mod Pathol.*, 31 (3), Pg. 463-473

Chou, TC, 2010, Drug combination studies and their synergy quantification using the Chou-Talalay method, *Cancer Res.*, 70 (2), Pg. 440-446

Ciardello, F, and Tortora, G, 2001, A novel approach in the treatment of cancer: targeting the epidermal growth factor receptor, *Clin Cancer Res.*, 7 (10), Pg. 2958-2970

Cioce, M, and Fazio, VM, 2021, EphA2 and EGFR: friends in life, partners in crime. Can EphA2 be a predictive biomarker of response to anti-EGFR agents?, *Cancers (Basel)*, 13 (4), Pg. 700

Clark, MA, Fisher, C, Judson, I, and Thomas, JM, 2005, Soft-tissue sarcomas in adults, *N Engl J Med.*, 353, Pg. 701-711

Cocco, E, Scaltriti, M, and Drilon, A, 2018, *NTRK* fusion-positive cancers and TRK inhibitor therapy, *Nat Rev Clin Oncol.*, 15 (12), Pg. 731-747

Cojoc, M, Mäbert, K, Muders, MH, and Dubrovskaja, A, 2015, A role for cancer stem cells in therapy resistance: cellular and molecular mechanisms, *Semin Cancer Biol.*, 31, Pg. 16-27

Collins, TS, Lee, LF, and Ting, JP, 2000, Paclitaxel up-regulates interleukin-8 synthesis in human lung carcinoma through an NF-kappaB- and AP-1-dependent mechanism, *Cancer Immuno Immunother.*, 49 (2), Pg. 78-84

Corless, CL, Fletcher, JA, and Heinrich, MC, 2004, Biology of gastrointestinal stromal tumors, *J Clin Oncol.*, 22 (18), Pg. 3813-3825

Corless, CL, McGreevey, L, Town, A, Schroeder, A, Bainbridge, T, Harrell, P, Fletcher, JA, and Heinrich, MC, 2004, KIT gene deletions at the intron 10-exon 11 boundary in GI stromal tumors, *J Mol Diagn.*, 6 (4), Pg. 366-370

Corless, CL, Barnett, CM, and Heinrich, MC, 2011, Gastrointestinal stromal tumours: origin and molecular oncology, *Nat Rev Cancer.*, 11 (12), Pg. 865-878

Corless, CL, 2014, Gastrointestinal stromal tumors: what do we know now?, *Mod Pathol.*, 27 (Suppl 1), S1-16

Cornillie, J, Wozniak, A, Li, H, Wang, Y, Boeckx, B, Gebreyohannes, YK, Wellens, J, Vanleeuw, U, Hompes, D, Stas, M, Sinnaeve, F, Wafa, H, Lambrechts, D, Debiec-Rychter, M, Sciot, R, and Schöffski, P, 2019, Establishment and characterization of histologically and molecularly stable soft-tissue sarcoma xenograft models for biological studies and preclinical drug testing, *Mol Cancer Ther.*, 18 (6), Pg. 1168-1178

Cornillie, J, Wozniak, A, Van Renterghem, B, Van Winkel, N, Wellens, J, Gebreyohannes, YK, Debiec-Rychter, M, Sciot, R, Hompes, D, and Schöffski, P, 2019, Assessment of the platelet-derived growth factor receptor alpha antibody olaratumab in a panel of patient-derived soft tissue sarcoma xenografts, *BMC Cancer.*, 19 (1), Pg. 724

Corte, CMD, Viscardi, G, Di Liello, R, Fasano, M, Martinelli, E, Troiani, T, Ciardiello, F, and Morgillo, F, 2018, Role and targeting of anaplastic lymphoma kinase in cancer, *Mol Cancer.*, 17 (1), Pg. 30

Cousin, S, Cantarel, C, Guegan, JP, Gomez-Roca, C, Metges, JP, Adenis, A, Pernot, S, Bellera, C, Kind, M, Auzanneau, C, Le Loarer, F, Soubeyran, I, Bessede, A, and Italiano, A, 2021, Regorafenib-avelumab combination in patients with microsatellite stable colorectal cancer (REGOMUNE): a single-arm, open-label, phase II trial, *Clin Cancer Res.*, 27 (8), Pg. 2139-2147

Crystal, AS, Shaw, AT, Sequist, LV, Friboulet, L, Niederst, MJ, Lockerman, EL, Frias, RL, Gainor, JF, Amzallag, A, Greninger, P, Lee, D, Kalsy, A, Gomez-Caraballo, M, Elamine, L, Howe, E, Hur, W, Lifshits, E, Robinson, HE, Katayama, R, Faber, AC, Awad, MM, Ramaswamy, S, Mino-Kenudson, M, Iafrate, AJ, Benes, CH, and Engelman, JA, 2014, Patient-derived models of acquired resistance can identify effective drug combinations for cancer, *Science.*, 346 (6216), Pg. 1480-1486

Cui, JJ, Tran-Dubé, M, Shen, H, Nambu, M, Kung, PP, Pairish, M, Jia, L, Meng, J, Funk, L, Botrous, I, McTigue, M, Grodsky, N, Ryan, K, Padrique, E, Alton, G, Timofeevski, S, Yamazaki, S, Li, Q, Zou, H, Christensen, J, Mroczkowski, B, Bender, S, Kania, RS, and Edwards, MP, 2011, Structure based drug design of crizotinib (PF-02341066), a potent and selective dual inhibitor mesenchymal-epithelial transition factor (c-MET) kinase and anaplastic lymphoma kinase (ALK), *J Med Chem.*, 54 (18), Pg. 6342-6363

D'Ambrosio, L, Touati, N, Blay, JY, Grignani, G, Flippot, R, Czarnecka, AM, Piperno-Neumann, S, Martín-Broto, J, Sanfilippo, R, Katz, D, Duffaud, F, Vincenzi, B, Stark, DP, Mazzeo, F, Tuchscherer, A, Chevreau, C, Sherriff, J, Estival, A, Litière, S, Sents, W, Ray-Coquard, I, Tolomeo, F, Le Cesne, A, Rutkowski, P, Stacchiotti, S, Kasper, B, Gelderblom, H, Gronchi, A, and European Organization for Research and Treatment of Cancer Soft Tissue and Bone Sarcoma Group, 2020, Doxorubicin plus dacarbazine, doxorubicin plus ifosfamide, or doxorubicin alone as a first-line treatment for advanced leiomyosarcoma: a propensity score matching analysis from the European Organization for Research and Treatment of Cancer Soft Tissue and Bone Sarcoma Group, *Cancer.*, 126 (11), Pg. 2637-2647

D'Angelo, SP, Shoushtari, AN, Keohan, ML, Dickson, MA, Gounder, MM, Chi, P, Loo, JK, Gaffney, L, Schneider, L, Patel, Z, Erinjeri, JP, Bluth, MJ, Sjoberg, A, Streicher, H, Takebe, N, Qin, LX, Antonescu, C, DeMatteo, RP, Carvajal, RD, and Tap, WD, 2017, Combined KIT and CTLA-4 blockade in patients with refractory GIST and other advanced sarcomas: a phase Ib study of dasatinib plus ipilimumab, *Clin Cancer Res.*, 23 (12), Pg. 2972-2980

D'Angelo, SP, Mahoney, MR, Van Tine, BA, Atkins, J, Milhem, MM, Jahagirdar, BN, Antonescu, CR, Horvath, E, Tap, WD, Schwartz, GK, and Streicher, H, 2018, A non-comparative multi-center randomized phase II study of nivolumab +/- ipilimumab for patients with metastatic sarcoma (Alliance A091401), *Lancet Oncol.*, 19 (3), Pg. 416-426

D'Angelo, SP, Melchiori, L, Merchant, MS, Bernstein, D, Glod, J, Kaplan, R, Grupp, S, Tap, WD, Chagin, K, Binder, GK, Basu, S, Lowther, DE, Wang, R, Bath, N, Tipping, A, Betts, G, Ramachandran, I, Navenot, JM, Zhang, H, Wells, DK, Van Winkle, E, Kari, G, Trivedi, T, Holdich, T, Pandite, L, Amado, R, and Mackall, CL, 2018, Antitumor activity associated with prolonged persistence of adoptively transferred NY-ESO-1^{c259} T cells in synovial sarcoma, *Cancer Discov.*, 8 (8), Pg. 944-957

D'Angelo, SP, Blay, JY, Chow, WA, Demetri, GD, Thistlethwaite, F, Sen, S, Razak, ARA, Haanen, JBAG, Noujaim, JC, Johnson, ML, Laetsch, TW, Chiou, VL, Pearce, L, Faitg, TH, Ji, R, Johnson, LA, Shalabi, AM, Thornton, KA, Mackall, C, and Van Tine, BA, 2020, Safety and activity of autologous T cells with enhanced NY-ESO-1-specific T-cell receptor (GSK3377794) in HLA-A*02+ previously-treated and -untreated patients with advanced metastatic/unresectable synovial sarcoma: a master protocol study design (IGNYTE-ESO), *J Clin Oncol.*, 38 (15), https://ascopubs.org/doi/10.1200/JCO.2020.38.15_suppl.TPS1571, Last accessed [November 2021]

D'Angelo, SP, Druta, M, Van Tine, BA, Liebner, DA, Schuetze, S, Hasan, AN, Holmes, AP, Huff, A, Kapoor, GS, Zajic, S, and Somaiah, N, 2021, Safety and efficacy of letresgene autoleucel (lete-cel; GSK3377794) in advanced myxoid/round cell liposarcoma (MRCLS) following high lymphodepletion (cohort 2): interim analysis, *J Clin Oncol.*, 39 (15), https://ascopubs.org/doi/abs/10.1200/JCO.2021.39.15_suppl.11521, Last accessed [November 2021]

D'Angelo, SP, Van Tine, BA, Attia, S, Blay, JY, Strauss, SJ, Morale, CMV, Razak, ARA, Van Winkle, E, Trivedi, T, Biswas, S, Williams, D, Norry, E, and Araujo, DM, 2021, SPEARHEAD-1: A phase 2 trial of afamitresgene autoleucel (formerly ADP-A2M4) in patients with advanced synovial sarcoma or myxoid/round cell liposarcoma, *J Clin Oncol.*, 39 (15), https://ascopubs.org/doi/abs/10.1200/JCO.2021.39.15_suppl.11504, Last accessed [November 2021]

Dangoor, A, Seddon, B, Gerrand, C, Grimer, R, Whelan, J, and Judson, I, 2016, UK guidelines for the management of soft tissue sarcomas, *Clin Sarcoma Res.*, 6, Pg. 20

Daudigeos-Dubus, E, Le Dret, L, Lanvers-Kaminsky, C, Bawa, O, Opolon, P, Vievard, A, Villa, I, Pagès, M, Bosq, J, Vassal, G, Zopf, D, and Georger, B, 2015, Regorafenib: antitumor activity upon mono and combination therapy in preclinical pediatric malignancy models, *PLoS One.*, 10 (11), e0142612

David, JM, Dominguez, C, Hamilton, DH, and Palena, C, 2016, The IL-8/IL-8R axis: a double agent in tumor immune resistance, *Vaccines (Basel).*, 4 (3), Pg. 22

Davies, H, Bignell, GR, Cox, C, Stephens, P, Edkins, S, Clegg, S, Teague, J, Woffendin, H, Garnett, MJ, Bottomley, W, Davis, N, Dicks, E, Ewing, R, Floyd, Y, Gray, K, Hall, S, Hawes, R, Hughes, J, Kosmidou, V, Menzies, A, Mould, C, Parker, A, Stevens, C, Watt, S, Hooper, S, Wilson, R, Jayatilake, H, Gusterson, BA, Cooper, C, Shipley, J, Hargrave, D, Pritchard-Jones, K, Maitland, N, Chenevix-Trench, G, Riggins, GJ, Bigner, DD, Palmieri, G, Cossu, A, Flanagan, A, Nicholson, A, Ho, JWC, Leung, K,

SY, Yuen, ST, Weber, BL, Seigler, HF, Darrow, TL, Paterson, H, Marais, R, Marshall, CJ, Wooster, R, Stratton, MR, and Futreal, PA, 2002, Mutations of the BRAF gene in human cancer, *Nature.*, 417 (6892), Pg. 949-954

Davis, DA, Mishra, S, Anagho, HA, Aisabor, AI, Shrestha, P, Wang, V, Takamatsu, Y, Maeda, K, Mitsuya, H, Zeldis, JB, and Yarchoan, R, 2017, Restoration of immune surface molecules in Kaposi sarcoma-associated herpes virus infected cells by lenalidomide and pomalidomide, *Oncotarget.*, 8 (31), Pg. 50342-50358

Davis, IJ, McFadden, AW, Zhang, Y, Coxon, A, Burgess, TL, Wagner, AJ, and Fisher, DE, 2010, Identification of the receptor tyrosine kinase c-Met and its ligand, hepatocyte growth factor, as therapeutic targets in clear cell sarcoma, *Cancer Res.*, 70 (2), Pg. 639-645

Davis, KL, Fox, E, Merchant, MS, Reid, JM, Kudgus, RA, Liu, X, Minard, CG, Voss, S, Berg, SL, Weigel, BJ, and Mackall, CL, 2020, Nivolumab in children and young adults with relapsed or refractory solid tumours or lymphoma (ADVL1412): a multicentre, open-label, single-arm, phase 1-2 trial, *Lancet Oncol.*, 21 (4), Pg. 541-550

Davis, MI, Hunt, JP, Herrgard, S, Ciceri, P, Wodicka, LM, Pallares, G, Hocker, M, Treiber, DK, and Zarrinkar, PP, 2011, Comprehensive analysis of kinase inhibitor selectivity, *Nat Biotechnol.*, 29 (11), Pg. 1046-1051

Deininger, MW, Goldman, JM, Lydon, N, and Melo, JV, 1997, The tyrosine kinase inhibitor CGP57148B selectively inhibits the growth of BCR-ABL-positive cells, *Blood.*, 90 (9), Pg. 3691-3698

De Conti, G, Dias, MH, and Bernards, R, 2021, Fighting drug resistance through the targeting of drug-tolerant persister cells, *Cancers (Basel).*, 13 (5), Pg. 1118

Delyon, J, Porcher, R, Battistella, M, Meyer, N, Adamski, H, Bertucci, F, Guillot, B, Jouary, T, Leccia, MT, Dalac, S, Mortier, L, Ghrieb, Z, Da Meda, L, Vicaut, E, Pedeutour, F, Mourah, S, and Lebbe, C, 2021, A multicenter phase II study of pazopanib in patients with unresectable dermatofibrosarcoma protuberans, *J Invest Dermatol.*, 141 (4), Pg. 761-769

Demetri, GD, von Mehren, M, Blanke, CD, van den Abbeele, A, Eisenberg, B, Roberts, PJ, Heinrich, MC, Tuveson, DA, Singer, S, Janicek, M, Fletcher, JA, Silverman, SG, Silberman, SL, Capdeville, R, Kiese, B, Peng, B, Dimitrijevic, S, Druker, BJ, Corless, C, Fletcher, CDM, and Joensuu, H, 2002, Efficacy and safety of imatinib mesylate in advanced gastrointestinal stromal tumors, *N Engl J Med.*, 347 (7), Pg. 472-480

Demetri, GD, van Oosterom, AT, Garrett, CR, Blackstein, ME, Shah, MH, Verweij, J, McArthur, G, Judson, IR, Heinrich, MC, Morgan, JA, Desai, J, Fletcher, CD, George, S, Bello, CL, Huang, X, Baum, CM, and Casali, PG, 2006, Efficacy and safety of sunitinib in patients with advanced gastrointestinal stromal tumour after failure of imatinib: a randomised controlled trial, *Lancet.*, 368 (9544), Pg. 1329-1338

Demetri, GD, Reichardt, P, Kang, YK, Blay, JY, Rutkowski, P, Gelderblom, H, Hohenberger, P, Leahy, M, von Mehren, M, Joensuu, H, Badalamenti, G, Blackstein, M, Le Cesne, A, Schöffski, P, Maki, RG, Bauer, S, Bui-Nguyen, B, Xu, J, Nishida, T, Chung, J, Kappeler, C, Kuss, I, Laurent, D, and Casali, PG, 2013, Efficacy and safety of regorafenib for advanced gastrointestinal stromal tumours after failure of imatinib and sunitinib (GRID): an international, multicentre, randomised, placebo-controlled, phase 3 trial, *Lancet.*, 381 (9863), Pg. 295-302

De Raedt, T, Brems, H, Wolkenstein, P, Vidaud, D, Pilotti, S, Perrone, F, Mautner, V, Frahm, S, Sciot, R, and Legius, E, 2003, Elevated risk for MPNST in *NF1* microdeletion patients, *Am J Hum Genet.*, 72 (5), Pg. 1288-1292

Desgrosellier, JS, and Cheresh, DA, 2010, Integrins in cancer: biological implications and therapeutic opportunities, *Nat Rev Cancer.*, 10 (1), Pg. 9-22

Destaing, O, Sanjay, A, Itzstein, C, Horne, WC, Toomre, D, De Camilli, P, and Baron, R, 2008, The tyrosine kinase activity of c-Src regulates actin dynamics and organization of podosomes in osteoclasts, *Mol Biol Cell.*, 19 (1), Pg. 394-404

Deyrup, AT, Lee, VK, Hill, CE, Cheuk, W, Toh, HC, Kesavan, S, Chan, EW, and Weiss, SW, 2006, Epstein-Barr virus-associated smooth muscle tumors are distinctive mesenchymal tumors reflecting multiple infection events: a clinicopathologic and molecular analysis of 29 tumors from 19 patients, *Am J Surg Pathol.*, 30 (1), Pg. 75-82

Dhawan, A, Nichol, D, Kinose, F, Abazeed, ME, Marusyk, A, Haura, EB, and Scott, JG, 2017, Collateral sensitivity networks reveal evolutionary instability and novel treatment strategies in ALK mutated non-small cell lung cancer, *Sci Rep.*, 7 (1), Pg. 1232

Dineen, SP, Roland, CL, Feig, R, May, C, Zhou, S, Demicco, E, Al Sanna, G, Ingram, D, Wang, W, Ravi, V, Guadagnolo, A, Lev, D, Pollock, RE, Hunt, K, Cormier, J, Lazar, A, Feig, B, and Torres, KE, 2015, Radiation-associated undifferentiated pleomorphic sarcoma is associated with worse clinical outcomes than sporadic lesions, *Ann Surg Oncol.*, 22 (12), Pg. 3912-3920

Doebele, RC, Davis, LE, Vaishnavi, A, Le, AT, Estrada-Bernal, A, Keysar, S, Jimeno, A, Varella-Garcia, M, Aisner, DL, Li, Y, Stephens, PJ, Morosini, D, Tuch, BB, Fernandes, M, Nanda, N, and Low, JA, 2015, An oncogenic NTRK fusion in a patient with soft-tissue sarcoma with response to the tropomyosin-related kinase inhibitor LOXO-101, *Cancer Discov.*, 5 (10), Pg. 1049-1057

Doğaner, BA, Yan, LKQ, and Youk, H, 2016, Autocrine signaling and quorum sensing: extreme ends of a common spectrum, *Trends Cell Biol.*, 26 (4), Pg. 262-271

Dolznic, H, Rupp, C, Puri, C, Haslinger, C, Schweifer, N, Wieser, E, Kerjaschki, D, and Garin-Chesa, P, 2011, Modelling colon adenocarcinomas in vitro a 3D co-culture system induces cancer-relevant pathways upon tumor cell and stromal fibroblast interaction, *Am J Pathol.*, 179 (1), Pg. 487-501

Donnez, J, Donnez, O, and Dolmans, MM, 2018, The current place of medical therapy in uterine fibroid management, *Best Pract Res Clin Obstet Gynaecol.*, 46, Pg. 57-65

Dow, DE, Cunningham, CK, and Buchanan, AM, 2014, A review of human herpesvirus 8, the Kaposi's sarcoma-associated herpesvirus, in the pediatric population, *J Pediatric Infect Dis Soc.*, 3 (1), Pg. 66-76

Downward, J, 2003, Targeting RAS signalling pathways in cancer therapy, *Nat Rev Cancer.*, 3 (1), Pg. 11-22

Drilon, A, Siena, S, Ou, SHI, Patel, M, Ahn, MJ, Lee, J, Bauer, TM, Farago, AF, Wheler, JJ, Liu, SV, Doebele, R, Giannetta, L, Cerea, G, Marrapese, G, Schirru, M, Amatu, A, Bencardino, K, Palmeri, L, Sartore-Bianchi, A, Vanzulli, A, Cresta, S, Damian, S, Duca, M, Ardini, E, Li, G, Christiansen, J, Kowalksi, K, Johnson, AD, Patel, R, Luo, D, Chow-Maneval, E, Hornby, Z, Multani, PS, Shaw, AT, and De Braud, FG, 2017, Safety and antitumor activity of the multitargeted pan-TRK, ROS1, and ALK inhibitor entrectinib: combined results from two phase I trials (ALKA-372-001 and STARTRK-1), *Cancer Discov.*, 7 (4), Pg. 400-409

Drilon, A, Laetsch, TW, Kummar, S, DuBois, SG, Lassen, UN, Demetri, GD, Nathenson, M, Doebele, RC, Farago, AF, Pappo, AS, Turpin, B, Dowlati, A, Brose, MS, Mascarenhas, L, Federman, N, Berlin, J, El-Deiry, WS, Baik, C, Deeken, J, Boni, V, Nagasubramanian, R, Taylor, M, Rudzinski, ER, Meric-Bernstam, F, Sohal, DPS, Ma, PC, Raez, LE, Hechtman, JF, Benayed, R, Ladanyi, M, Tuch, BB, Ebata, K, Cruickshank, S, Ku, NC, Cox, MC, Hawkins, DS, Hong, DS, and Hyman, DM, 2018, Efficacy of larotrectinib in TRK fusion-positive cancers in adults and children, *N Engl J Med.*, 378 (8), Pg. 731-739

Druker, BJ, Tamura, S, Buchdunger, E, Ohno, S, Segal, GM, Fanning, S, Zimmermann, J, and Lydon, NB, 1996, Effects of a selective inhibitor of the Abl tyrosine kinase on the growth of Bcr-Abl positive cells, *Nat Med.*, 2 (5), Pg. 561-566

Du, Z, and Lovly, CM, 2018, Mechanisms of receptor tyrosine kinase activation in cancer, *Mol Cancer.*, 17 (1), Pg. 58

Ducimetière, F, Lurkin, A, Ranchère-Vince, D, Decouvelaere, AV, Péoc'h, M, Istier, L, Chalabreysse, P, Muller, C, Alberti, L, Bringuier, PP, Scoazec, JY, Schott, AM, Bergeron, C, Cellier, D, Blay, JY, and Ray-Coquard, I, 2011, Incidence of sarcoma histotypes and molecular subtypes in a prospective epidemiological study with central pathology review and molecular testing, *PLoS One.*, 6 (8), e20294

Dumas, J, Boyer, S, Riedl, B, and Wilhelm, S, 2005, Fluoro substituted omega-carboxyaryl diphenyl urea for the treatment and prevention of diseases and conditions, WO2005009961A2, <https://patents.google.com/patent/WO2005009961A2/en>, Last accessed [June 2021]

Duong-Ly, KC, and Peterson, JR, 2013, The human kinome and kinase inhibition, *Curr Protoc Pharmacol.*, Chapter 2: Unit 2.9

Eaton, KW, Tooke, LS, Wainwright, LM, Judkins, AR, and Biegel, JA, 2011, Spectrum of SMARCB1/INI1 mutations in familial and sporadic rhabdoid tumors, *Pediatr Blood Cancer.*, 56 (1), Pg. 7-15

Efferth, T, Saeed, MEM, Kadioglu, O, Seo, EJ, Shirooie, S, Mbaveng, AT, Nabavi, SM, and Kuete, V, 2020, Collateral sensitivity of natural products in drug-resistant cancer cells, *Biotechnol Adv.*, 38, Pg. 107342

Emile, JF, Brahimi, S, Coindre, JM, Bringuier, PP, Monges, G, Samb, P, Doucet, L, Hostein, I, Landi, B, Buisine, MP, Neuville, A, Bouché, O, Cervera, P, Pretet, JL, Tisserand, J, Gauthier, A, Le Cesne, A, Sabourin, JC, Scoazec, JY, Bonvalot, S, Corless, CL, Heinrich, MC, Blay, JY, and Aegerter, P, 2012, Frequencies of KIT and PDGFRA mutations in the MolecGIST prospective population-based study differ from those of advanced GISTs, *Med Oncol.*, 29 (3), Pg. 1765-1772

Emmerich, D, Zemojtel, T, Hecht, J, Krawitz, P, Spielmann, M, Kühnisch, J, Kobus, K, Osswald, M, Heinrich, V, Berlien, P, Müller, U, Mautner, VF, Wimmer, K, Robinson, PN, Vingron, M, Tinschert, S, Mundlos, S, and Kolanczyk, M, 2015, Somatic neurofibromatosis type 1 (NF1) inactivation events in cutaneous neurofibromas of a single NF1 patient, *Eur J Hum Genet.*, 23 (6), Pg. 870-873

Engelman, JA, Zejnullahu, K, Mitsudomi, T, Song, Y, Hyland, C, Park, JO, Lindeman, N, Gale, CM, Zhao, X, Christensen, J, Kosaka, T, Holmes, AJ, Rogers, AM, Cappuzzo, F, Mok, T, Lee, C, Johnson, BE, Cantley, LC, and Jänne, PA, 2007, MET amplification leads to gefitinib resistance in lung cancer by activating ERBB3 signaling, *Science.*, 316 (5827), Pg. 1039-1043

Eriksson, M, Hardell, L, and Adami, HO, 1990, Exposure to dioxins as a risk factor for soft tissue sarcoma: a population-based case-control study, *J Natl Cancer Inst.*, 82 (6), Pg. 486-490

Evans, DGR, Huson, SM, and Birch, JM, 2012, Malignant peripheral nerve sheath tumours in inherited disease, *Clin Sarcoma Res.*, 2, Pg. 17

Fabbro, D, Cowan-Jacob, SW, and Moebitz, H, 2015, Ten things you should know about protein kinases: IUPHAR review 14, *Br J Pharmacol.*, 172 (11), Pg. 2675-2700

Fajer, M, Meng, Y, and Roux, B, 2017, The activation of c-Src tyrosine kinase: conformational transition pathway and free energy landscape, *J Phys Chem B.*, 121 (15), Pg. 3352-3363

Falkenhorst, J, Hamacher, R, Reichardt, P, Ivanyi, P, Kasper, B, Hohenberger, P, Hermes, B, Kostbade, K, Pink, D, Sülberg, H, Metznermacher, M, Crysandt, M, and Bauer, S, 2020, Lower-dosing ponatinib in pre-treated GIST: results of the POETIG phase II trial, *J Clin Oncol.*, 38 (15), https://ascopubs.org/doi/abs/10.1200/JCO.2020.38.15_suppl.11536, Last accessed [October 2021]

Fanelli, GN, Dal Pozzo, CA, Depetris, I, Schirripa, M, Brignola, S, Biason, P, Balistreri, M, Dal Santo, L, Lonardi, S, Munari, G, Loupakis, F, and Fassan, M, 2020, The heterogeneous clinical and pathological landscapes of metastatic Braf-mutated colorectal cancer, *Cancer Cell Int.*, 20, Pg. 30

Farid, M, and Ngeow, J, 2016, Sarcomas associated with genetic cancer predisposition syndromes: a review, *Oncologist.*, 21 (8), Pg. 1002-1013

Feins, S, Kong, W, Williams, EF, Milone, MC, and Fraietta, JA, 2019, An introduction to chimeric antigen receptor (CAR) T-cell immunotherapy for human cancer, *Am J Hematol.*, 94 (S1), S3-S9

Feng, L, Qi, Q, Wang, P, Chen, H, Chen, Z, Meng, Z, and Liu, L, 2018, Serum levels of IL-6, IL-8, and IL-10 are indicators of prognosis in pancreatic cancer, *J Int Med Res.*, 46 (12), Pg. 5228-5236

Ferguson, LP, Diaz, E, and Reya, T, 2021, The role of the microenvironment and immune system in regulating stem cell fate in cancer, *Trends Cancer.*, 7(7), Pg. 624-634

Fernando, RI, Hamilton, DH, Dominguez, C, David, JM, McCampbell, KK, and Palena, C, 2016, IL-8 signaling is involved in resistance of lung carcinoma cells to erlotinib, *Oncotarget.*, 7 (27), Pg. 42031-42044

Ferraro, D, and Zalberg, J, 2014, Regorafenib in gastrointestinal stromal tumors: clinical evidence and place in therapy, *Ther Adv Med Oncol.*, 6 (5), Pg. 222-228

Ferretti, E, and Hadjantonakis, AK, 2019, Mesoderm specification and diversification: from single cells to emergent tissues, *Curr Opin Cell Biol.*, 61, Pg. 110-116

Finlay, MRV, Anderton, M, Ashton, S, Ballard, P, Bethel, PA, Box, MR, Bradbury, RH, Brown, SJ, Butterworth, S, Campbell, A, Chorley, C, Colclough, N, Cross, DAE, Currie, GS, Grist, M, Hassall, L, Hill, GB, James, D, James, M, Kemmitt, P, Klinowska, T, Lamont, G, Lamont, SG, Martin, N, McFarland, HL, Mellor, MJ, Orme, JP, Perkins, D, Perkins, P, Richmond, G, Smith, P, Ward, RA, Waring, MJ, Whittaker, D, Wells, S, and Wrigley, GL, 2014, Discovery of a potent and selective EGFR inhibitor (AZD9291) of both sensitizing and T790M resistance mutations that spares the wild type form of the receptor, *J Med Chem.*, 57 (20), Pg. 8249-8267

Finn, KJ, Martin, SE, and Settleman, J, 2020, A single-step, high-dose selection scheme reveals distinct mechanisms of acquired resistance to oncogenic kinase inhibition in cancer cells, *Cancer Res.*, 80 (1), Pg. 79-90

Finn, RS, 2008, Targeting Src in breast cancer, *Ann Oncol.*, 19 (8), Pg. 1379-1386

Fleuren, EDG, Vlienterie, M, Van der Graaf, WTA, Hillebrandt-Roeffen, MHS, Blackburn, Ma, X, Chan, H, Magias, MC, Van Erp, A, Van Houdt, L, Cebeci, DM, Lord, CJ, Marini, KD, Vaghjiani, V, Mercer, TR, Cain, JE, Wu, J, Versleijen-Jonkers, YMH, and Daly, RJ, 2017, Phosphoproteomic profiling reveals ALK and MET as novel actionable targets across synovial sarcoma subtypes, *Cancer Res.*, 77 (16), Pg. 4279-4292

Fontana, F, Marzagalli, M, Sommariva, M, Gagliano, N, and Limonta, P, 2021, In vitro 3D cultures to model the tumor microenvironment, *Cancers (Basel).*, 13 (12), Pg. 2970

Fourneau, B, Bourdon, A, Dadone, B, Lucchesi, C, Daigle, SR, Richard, E, Laroche-Clary, A, Le Loarer, F, and Italiano, A, 2019, Identifying and targeting cancer stem cells in leiomyosarcoma: prognostic impact and role to overcome secondary resistance to PI3K/mTOR inhibition, *J Hematol Oncol.*, 12, Pg. 11

Frezza, AM, Benson, C, Judson, IR, Litiere, S, Marreaud, S, Sleijfer, S, Blay, JY, Dewji, R, Fisher, C, Van der Graaf, W, and Hayward, L, 2014, Pazopanib in advanced desmoplastic small round cell tumours: a multi-institutional experience, *Clin Sarcoma Res.*, 4, Pg. 7

Frezza, AM, Jones, RL, Lo Vullo, S, Asano, N, Lucibello, F, Ben-Ami, E, Ratan, R, Teterycz, P, Boye, K, Brahmi, M, Palmerini, E, Fedenko, A, Vincenzi, B, Brunello, A, Desar, IME, Benjamin, RS, Blay, JY, Martin-Broto, J, Casali, PG, Gelderblom, H, Grignani, G, Gronchi, A, Hall, KS, Mir, O, Rutkowski, P, Wagner, AJ, Anurova, O, Collini, P, Dei Tos, AP, Flucke, U, Hornick, JL, Lobmaier, I, Philippe, T, Picci, P, Ranchere, D, Renne, SL, Sbaraglia, M, Thway, K, Wagrodzki, M, Wang, WL, Yoshida, A, Mariani, L, Kawai, A, and Stacchiotti, S, 2018, Anthracycline, gemcitabine, and pazopanib in epithelioid sarcoma: a multi-institutional case series, *JAMA Oncol.*, 4 (9), e180219

Fukushima, T, Suzuki, S, Mashiko, M, Ohtake, T, Endo, Y, Takebayashi, Y, Sekikawa, K, Hagiwara, K, and Takenoshita, S, 2003, BRAF mutations in papillary carcinomas of the thyroid, *Oncogene.*, 22 (41), Pg. 6455-6457

Gaebler, M, Silvestri, A, Haybaeck, J, Reichardt, P, Lowery, CD, Stancato, LF, Zybarth, G, and Regenbrecht, CRA, 2017, Three-dimensional patient-derived *in vitro* sarcoma models: promising tools for improving clinical tumor management, *Front Oncol.*, 7, Pg. 203

Gajiwala, KS, Wu, JC, Christensen, J, Deshmukh, GD, Diehl, W, DiNitto, JP, English, JM, Greig, MJ, He, YA, Jacques, SL, Lunney, EA, McTigue, M, Molina, D, Quenzer, T, Welles, PA, Yu, X, Zhang, Y, Zou, A, Emmett, MR, Marshall, AG, Zhang,

HM, and Demetri, GD, 2009, KIT kinase mutants show unique mechanisms of drug resistance to imatinib and sunitinib in gastrointestinal stromal tumor patients, *Proc Natl Acad Sci USA.*, 106 (5), Pg. 1542-1547

Galkin, AV, Melnick, JS, Kim, S, Hood, TL, Li, N, Li, L, Xia, G, Steensma, R, Chopiuk, G, Jiang, J, Wan, Y, Ding, P, Liu, Y, Sun, F, Schultz, PG, Gray, NS, and Warmuth, M, 2007, Identification of NVP-TAE684, a potent, selective, and efficacious inhibitor of NPM-ALK, *Proc Natl Acad Sci USA.*, 104 (1), Pg. 270-275

Gandhi, AK, Kang, J, Havens, CG, Conklin, T, Ning, Y, Wu, L, Ito, T, Ando, H, Waldman, MF, Thakurta, A, Klippel, A, Handa, H, Daniel, TO, Schafer, PH, and Chopra, R, 2014, Immunomodulatory agents lenalidomide and pomalidomide co-stimulate T cells by inducing degradation of T cell repressors Ikaros and Aiolos via modulation of the E3 ubiquitin ligase complex CRL4^{CRBN}, *Br J Haematol.*, 164 (1), Pg. 811-821

García-Echeverría, C, Pearson, MA, Marti, A, Meyer, T, Mestan, J, Zimmermann, J, Gao, J, Brueggen, J, Capraro, HG, Cozens, R, Evans, DB, Fabbro, D, Furet, P, Porta, DG, Liebetanz, J, Martiny-Baron, G, Ruetz, S, and Hofmann, F, 2004, In vivo antitumor activity of NVP-AEW541- a novel, potent, and selective inhibitor of the IGF-IR kinase, *Cancer Cell.*, 5 (3), Pg. 231-239

Garber, JE, and Offit, K, 2005, Hereditary cancer predisposition syndromes, *J Clin Oncol.*, 23 (2), Pg. 276-292

Garje, R, An, J, Obeidat, M, Kumar, K, Yasin, HA, and Zakharia, Y, 2020, Fibroblast growth factor receptor (FGFR) inhibitors in urothelial cancer, *Oncologist.*, 25 (11), Pg. e1711-e1719

Garuti, L, Roberti, M, and Bottegoni, G, 2011, Irreversible protein kinase inhibitors, *Curr Med Chem.*, 18 (20), Pg. 2981-2994

Gasparotto, D, Rossi, S, Polano, M, Tamborini, E, Lorenzetto, E, Sbaraglia, M, Mondello, A, Massani, M, Lamon, S, Bracci, R, Mandolesi, A, Frate, E, Stanzial, F, Agaj, J, Mazzoleni, G, Piloti, S, Gronchi, A, Dei Tos, AP, and Maestro, R, 2017, Quadruple-negative GIST is a sentinel for unrecognized neurofibromatosis type 1 syndrome, *Clin Cancer Res.*, 23 (1), Pg. 273-282

Gelderblom, H, Judson, IR, Benson, C, Merimsky, O, Grignani, G, Katz, D, Freivogel, KW, Stein, D, Jobanputra, M, Mungul, A, Manson, SC, and Sanfilippo, R, 2017, Treatment patterns and clinical outcomes with pazopanib in patients with advanced soft tissue sarcomas in a compassionate use setting: results of the SPIRE study, *Acta Oncol.*, 56 (12), Pg. 1769-1775

Geller, JI, Roth, JJ, and Biegel, JA, 2015, Biology and treatment of rhabdoid tumor, *Crit Rev Oncog.*, 20 (3-4), Pg. 199-216

George, S, Merriam, P, Maki, RG, Van den Abbeele, AD, Yap, JT, Akhurst, T, Harmon, DC, Bhuchar, G, O'Mara, MM, D'Adamo, DR, Morgan, J, Schwartz, GK, Wagner, AJ, Butrynski, JE, Demetri, GD, and Keohan, ML, 2009, Multicenter phase II trial of sunitinib in the treatment of nongastrointestinal stromal tumor sarcomas, *J Clin Oncol.*, 27 (19), Pg. 3154-3160

George, S, Barysaukas, C, Serrano, C, Oduyebo, T, Rauh-Hain, JA, Del Carmen, MG, Demetri, GD, and Muto, MG, 2014, Retrospective cohort study evaluating the impact of intraperitoneal morcellation on outcomes of localized uterine leiomyosarcoma, *Cancer.*, 120 (20), Pg. 3154-3158

Gladdy, RA, Qin, LX, Moraco, N, Edgar, MA, Antonescu, CR, Alektiar, KM, Brennan, MF, and Singer, S, 2010, Do radiation-associated soft tissue sarcomas have the same prognosis as sporadic soft tissue sarcomas, *J Clin Oncol.*, 28 (12), Pg. 2064-2069

Goc, A, Al-Husein, B, Katsanevas, K, Steinbach, A, Lou, U, Sabbineni, H, DeRemer, DL, and Somanath, PR, 2014, Targeting Src-mediated Tyr216 phosphorylation and activation of GSK-3 in prostate cancer cells inhibit prostate cancer progression in vitro and in vivo, *Oncotarget.*, 5 (3), Pg. 775-787

Goel, G, 2018, Evolution of regorafenib from bench to bedside in colorectal cancer: Is it an attractive option or merely a "me too" drug?, *Cancer Manag Res.*, 10, Pg. 425-437

Goers, L, Freemont, P, and Polizzi, KM, 2014, Co-culture systems and technologies: taking synthetic biology to the next level, *J R Soc Interface.*, 11 (96), Pg. 20140065

Gomez-Rivera, F, Santillan-Gomez, AA, Younes, MN, Kim, S, Fooshee, D, Zhao, M, Jasser, SA, and Myers, JN, 2007, The tyrosine kinase inhibitor, AZD2171, inhibits vascular endothelial growth factor receptor signaling and growth of anaplastic thyroid cancer in an orthotopic nude mouse model, *Clin Cancer Res.*, 13 (15 Pt 1), Pg. 4519-4527

Gonzalez, KD, Noltner, KA, Buzin, CH, Gu, D, Wen-Fong, CY, Nguyen, VQ, Han, JH, Lowstuter, K, Longmate, J, Sommer, SS, and Weitzel, JN, 2009, Beyond Li Fraumeni syndrome: clinical characteristics of families with p53 germline mutations, *J Clin Oncol.*, 27 (8), Pg. 1250-1256

Goodson 3rd, WH, Lowe, L, Carpenter, DO, Gilbertson, M, Ali, AM, Salsamendi, ALDC, Lasfar, A, Carnero, A, Azqueta, A, Amedei, A, Charles, AK, Collins, AR, Ward, A, Salzberg, AC, Colacci, A, Olsen, AK, Berg, A, Barclay, BJ, Zhou, BP, Blanco-Aparicio, C, Bagloli, CJ, Dong, C, Mondello, C, Hsu, CW, Naus, CC, Yedjou, C, Curran, CS, Laird, DW, Koch, DC, Carlin, DJ, Felsher, DW, Roy, D, Brown, DG, Ratovitski, E, Ryan, EP, Corsini, E, Rojas, E, Moon, EY, Laconi, E, Marongiu, F, Al-Mulla, F, Chiaradonna, F, Darroudi, F, Martin, FL, Van Schooten, FJ, Goldberg, GS, Wagemaker, G, Nangami, GN, Calaf, GM, Williams, G, Wolf, GT, Koppen, G, Brunborg, G, Lyerly, HK, Krishnan H, Hamid, HA, Yasaei, H, Sone, H, Kondoh, H, Salem, HK, Hsu, HY,

Park, HH, Koturbash, I, Miousse, IR, Scovassi, AI, Klaunig, JE, Vondráček, J, Raju, J, Roman, J, Wise Sr, JP, Whitfield, JR, Woodrick, J, Christopher, JA, Ochieng, J, Martinez-Leal, JF, Weisz, J, Kravchenko, J, Sun, J, Prudhomme, KR, Narayanan, KB, Cohen-Solal, KA, Moorwood, K, Gonzalez, L, Soucek, L, Jian, L, D'Abronzio, LS, Lin, LT, Li, L, Gulliver, L, McCawley, LJ, Memeo, L, Vermeulen, L, Leyns, L, Zhang, L, Valverde, M, Khatami, M, Romano, MF, Chapellier, M, Williams, MA, Wade, M, Manjili, MH, Leonart, ME, Xia, M, Gonzalez, MJ, Karamouzis, MV, Kirsch-Volders, M, Vaccari, M, Kuemmerle, NB, Singh, N, Cruickshanks, N, Kleinstreuer, N, van Larebeke, N, Ahmed, N, Ogunkua, O, Krishnakumar, PK, Vadgama, P, Marignani, PA, Ghosh, PM, Ostrosky-Wegman, P, Thompson, PA, Dent, P, Heneberg, P, Darbre, P, Leung, PS, Nangia-Makker, P, Cheng, QS, Robey, RB, Al-Temaimi, R, Roy, R, Andrade-Vieira, R, Sinha, RK, Mehta, R, Vento, R, Di Fiore, R, Ponce-Cusi, R, Dornetshuber-Fleiss, R, Nahta, R, Castellino, RC, Palorini, R, Hamid, RA, Langie, SAS, Eltom, SE, Brooks, SA, Ryeom, S, Wise, SS, Bay, SN, Harris, SA, Papagerakis, S, Romano, S, Pavanello, S, Eriksson, S, Forte, S, Casey, SC, Luanpitpong, S, Lee, TJ, Otsuki, T, Chen, T, Massfelder, T, Sanderson, T, Guarneri, T, Hultman, T, Dormoy, V, Odero-Marah, V, Sabbisetti, V, Maguer-Satta, V, Rathmell, WK, Engström, W, Decker, WK, Bisson, WH, Rojanasakul, Y, Luqmani, Y, Chen, Z, and Hu, Z, 2015, Assessing the carcinogenic potential of low-dose exposures to chemical mixtures in the environment: the challenge ahead, *Carcinogenesis*, 36 Suppl 1 (Suppl 1), Pg. S254-296

Gordon, EM, Chua-Alcala, VS, Kim, K, Dy, PS, Paz, MK, Angel, N, Moradkhani, A, Quon, D, Wong, S, Jafari, O, and Chawla, SP, 2020, SAINT: Results of an expanded phase II study using safe amounts of ipilimumab (I), nivolumab (N), and trabectedin (T) as first-line treatment of advanced soft tissue sarcoma [NCT03138161], *J Clin Oncol*, https://ascopubs.org/doi/abs/10.1200/JCO.2020.38.15_suppl.11520, Last accessed [November 2021]

Gorfe, AA, 2010, Mechanisms of allosteric and membrane attachment in Ras GTPases: implications for anti-cancer drug discovery, *Curr Med Chem*, 17 (1), Pg. 1-9

Gounder, MM, Stacchiotti, S, Schöffski, P, Attia, S, Italiano, A, Jones, R, Demetri, GD, Blakemore, S, Clawson, A, Daigle, S, Ribich, S, Roche, M, Rodstrom, J, Ho, PTC, and Cote, GM, 2017, Phase 2 multicenter study of the EZH2 inhibitor tazemetostat in adults with INI1 negative epithelioid sarcoma (NCT02601950), *J Clin Oncol*, 35 (15), https://ascopubs.org/doi/abs/10.1200/JCO.2017.35.15_suppl.11058, Last accessed [February 2021]

Gounder, MM, Mahoney, MR, Van Tine, BA, Ravi, V, Attia, S, Deshpande, HA, Gupta, AA, Milhem, MM, Conry, RM, Movva, S, Pishvaian, MJ, Riedel, RF, Sabagh, T, Tap, WD, Horvat, N, Basch, E, Schwartz, LH, Maki, RG, Agaram, NP, Lefkowitz, RA, Mazaheri, Y, Yamashita, R, Wright, JJ, Dueck, AC, and Schwartz, GK, 2018, Sorafenib for advanced and refractory desmoid tumors, *N Engl J Med*, 379 (25), Pg. 2417-2428

Gounder, MM, Zhu, G, Roshal, L, Lis, E, Daigle, SR, Blakemore, SJ, Michaud, NR, Hameed, M, and Hollmann, TJ, 2019, Immunologic correlates of the abscopal effect in a SMARCB1/INI1-negative poorly differentiated chordoma after EZH2 inhibition and radiotherapy, *Clin Cancer Res*, 25 (7), Pg. 2064-2071

Gower, CM, Chang, MEK, and Maly, DJ, 2014, Bivalent inhibitors of protein kinases, *Crit Rev Biochem Mol Biol*, 49 (2), Pg. 102-115

Greaves, M, and Maley, CC, 2012, Clonal evolution in cancer, *Nature*, 481 (7381), Pg. 306-313

Greco, A, Roccatò, E, Miranda, C, Cleris, L, Formelli, F, and Pierotti, MA, 2001, Growth-inhibitory effect of STI571 on cells transformed by the COL1A1/PDGFB rearrangement, *Int J Cancer*, 92 (3), Pg. 354-360

Gril, B, Palmieri, D, Qian, Y, Smart, D, Ileva, L, Liewehr, DJ, Steinberg, SM, and Steeg, PS, 2011, Pazopanib reveals a role for tumor cell B-Raf in the prevention of HER2+ breast cancer brain metastasis, *Clin Cancer Res*, 17 (1), Pg. 142-153

Groisberg, R, Roszik, J, Conley, AP, Lazar, AJ, Portal, DE, Hong, DS, Naing, A, Herzog, CE, Somaiah, N, Zazour, MA, Patel, S, Brown, RE, and Subbiah, V, 2020, Genomics, morphoproteomics, and treatment patterns of patients with alveolar soft part sarcoma and response to multiple experimental therapies, *Mol Cancer Ther*, 19 (5), Pg. 1165-1172

Grothey, A, Blay, JY, Pavlakis, N, Yoshino, T, and Bruix, J, 2020, Evolving role of regorafenib for the treatment of advanced cancers, *Cancer Treat Rev*, 86, Pg. 101993

Grünwald, S, Klug, LR, Mühlenberg, T, Lategahn, J, Falkenhorst, J, Town, A, Ehrt, C, Wardelmann, E, Hartmann, W, Schildhaus, HU, Treckmann, J, Fletcher, JA, Jung, S, Czodrowski, P, Miller, S, Schmidt-Kittler, O, Rauh, D, Heinrich, MC, and Bauer, S, 2021, Resistance to avapritinib in PDGFRA-driven GIST is caused by secondary mutations in the PDGFRA kinase domain, *Cancer Discov*, 11 (1), Pg. 108-125

Grünwald, TG, Alonso, MA, Avnet, S, Banito, A, Burdach, S, Cidre-Aranaz, F, Di Pompo, G, Distel, M, Dorado-Garcia, H, Garcia-Castro, J, González-González, L, Grigoriadis, AE, Kasan, M, Koelsche, C, Krumbholz, M, Lecanda, F, Lemma, S, Longo, DL, Madrigal-Esquível, C, Morales-Molina, Á, Musa, J, Ohmura, S, Ory, B, Pereira-Silva, M, Perut, F, Rodriguez, R, Seeling, C, Al Shaaili, N, Shaabani, S, Shiavone, K, Sinha, S, Tomazou, EM, Trautmann, M, Vela, M, Versleijen-Jonkers, YM, Visgauss, J, Zalacain, M, Schober, SJ, Lissat, A, English, WR, Baldini, N, and Heymann, D, 2020, Sarcoma treatment in the era of molecular medicine, *EMBO Mol Med*, 12 (11), e111131

Grünwald, V, Karch, A, Schuler, M, Schöffski, P, Kopp, HG, Bauer, S, Kasper, B, Lindner, LH, Chemnitz, JM, Crysandt, M, Stein, A, Steffen, B, Richter, S, Egerer, G, Ivanyi, P, Zimmermann, S, Liu, X, and Kunitz, A, 2020, Randomized comparison of pazopanib and doxorubicin as first-line treatment in patients with metastatic soft tissue sarcoma age 60 years or older: results of a German intergroup study, *J Clin Oncol*, 38 (30), Pg. 3555-3564

Gryder, BE, Yohe, ME, Chou, HC, Zhang, X, Marques, J, Wachtel, M, Schaefer, B, Sen, N, Song, Y, Gualtieri, A, Pomella, S, Rota, R, Cleveland, A, Wen, X, Sindiri, S, Wei, JS, Barr, FG, Das, S, Andresson, T, Guha, R, Lal-Nag, M, Ferrer, M, Shern, JF, Zhao, K, Thomas, CJ, and Khan, J, 2017, PAX3-FOXO1 establishes myogenic super enhancers and confers BET bromodomain vulnerability, *Cancer Discov.*, 7 (8), Pg. 884-899

Guagnano, V, Furet, P, Spanka, C, Bordas, V, Le Douget, M, Stamm, C, Brueggen, J, Jensen, MR, Schnell, C, Schmid, H, Wartmann, M, Berghausen, J, Drucekes, P, Zimmerlin, A, Bussiere, D, Murray, J, and Porta, DG, 2011, Discovery of 3-(2,6-dichloro-3,5-dimethoxy-phenyl)-1-(6-[4-(4-ethyl-piperazin-1-yl)-phenylamino]-pyrimidin-4-yl)-1-methyl-urea (NVP-BGJ398), a potent and selective inhibitor of the fibroblast growth factor receptor family of receptor tyrosine kinase, *J Med Chem.*, 54 (20), Pg. 7066-7083

Guillou, L, and Aurias, A, 2010, Soft tissue sarcomas with complex genomic profiles, *Virchows Arch.*, 456 (2), Pg. 201-217

Guo, H, German, P, Bai, S, Barnes, S, Guo, W, Qi, X, Lou, H, Liang, J, Jonasch, E, Mills, GB, and Ding, Z, 2015, The PI3K/AKT pathway and renal cell carcinoma, *J Genet Genomics.*, 42 (7), Pg. 343-353

Guo, T, and Ma, S, 2021, Recent advances in the discovery of multitargeted tyrosine kinase inhibitors as anticancer agents, *Chem Med Chem.*, 16 (4), Pg. 600-620

Guo, YJ, Pan, WW, Liu, SB, Shen, ZF, Xu, Y, and Hu, LL, 2020, ERK/MAPK signalling pathway and tumorigenesis, *Exp Ther Med.*, 19 (3), Pg. 1997-2007

Gutmann, DH, Ferner, RE, Listernick, RH, Korf, BR, Wolters, PL, and Johnson, KJ, 2017, Neurofibromatosis type 1, *Nat Rev Dis Primers.*, 3, Pg. 17004

Ha, H, Debnath, B, and Neamati, N, 2017, Role of the CXCL8-CXCR1/2 axis in cancer and inflammatory diseases, *Theranostics.*, 7 (6), Pg. 1543-1588

Hanke, JH, Gardner, JP, Dow, RL, Changelian, PS, Brissette, WH, Weringer, EJ, Pollok, BA, and Connelly, PA, 1996, Discovery of a novel, potent, and Src family-selective tyrosine kinase inhibitor. Study of Lck- and FynT-dependent T cell activation, *J Biol Chem.*, 271 (2), Pg. 695-701

Hardell, L, and Eriksson, M, 1988, The association between soft tissue sarcomas and exposure to phenoxyacetic acids. A new case-referent study, *Cancer.*, 62 (3), Pg. 652-656

Harris, PA, Bolor, A, Cheung, M, Kumar, R, Crosby, RM, Davis-Ward, RG, Epperly, AH, Hinkle, KW, Hunter 3rd, RN, Johnson, JH, Knick, VB, Laudeman, CP, Luttrell, DK, Mook, RA, Nolte, RT, Rudolph, SK, Szewczyk, JR, Truesdale, AT, Veal, JM, Wang, L, and Stafford, JA, 2008, Discovery of 5-[[4-[(2,3-dimethyl-2H-indazol-6-yl)methylamino]-2-pyrimidinyl]amino]-2-methyl-benzenesulfonamide (pazopanib), a novel and potent vascular endothelial growth factor receptor inhibitor, *J Med Chem.*, 51 (15), Pg. 4632-4640

Harris, RE, 2016, *Global Epidemiology of Cancer*, Jones and Bartlett Learning, Burlington (MA) (USA), <https://www.jblearning.com/health-sciences-professions/health/specialized-epidemiology/productdetails/9781284034455>, Last accessed [May 2020]

Harrison, PT, Vyse, S, and Huang, PH, 2020, Rare epidermal growth factor receptor (EGFR) mutations in non-small cell lung cancer, *Semin Cancer Biol.*, 61, Pg. 167-179

Harttrampf, AC, Da Costa, MEM, Renoult, A, Daudigeos-Dubus, E, and Geoerger, B, 2021, Histone deacetylase inhibitor Panobinostat induces antitumor activity in epithelioid sarcoma and rhabdoid tumor by growth factor receptor modulation, *BMC Cancer.*, 21 (1), Pg. 833

Hata, AN, Niederst, MJ, Archibald, HL, Gomez-Caraballo, M, Siddiqui, FM, Mulvey, HE, Maruvka, YE, Ji, F, Bhang, HC, Radhakrishna, VK, Siravegna, G, Hu, H, Raoof, S, Lockerman, E, Kalsy, A, Lee, D, Keating, CL, Ruddy, DA, Damon, LJ, Crystal, AS, Costa, C, Piotrowska, Z, Bardelli, A, Iafrate, AJ, Sadreyev, RI, Stegmeier, F, Getz, G, Sequist, LV, Faber, AC, and Engelman, JA, 2016, Tumor cells can follow distinct evolutionary paths to become resistant to epidermal growth factor receptor inhibitor, *Nat Med.*, 22 (3), Pg. 262-269

Hatina, J, Kripnerova, M, Houfkova, K, Pesta, M, Kuncova, J, Sana, J, Slaby, O, and Rodríguez, R, 2019, Sarcoma stem cell heterogeneity, *Adv Exp Med Biol.*, 1123, Pg. 95-118

Hatzimarkou, A, Filippou, D, Papadopoulos, V, Filippou, G, Rizos, S, and Skandalakis, P, 2006, Desmoid tumor in Gardner's syndrome presented as acute abdomen, *World J Surg Oncol.*, 4, Pg. 18

Hay, ED, 2005, The mesenchymal cell, its role in the embryo, and the remarkable signaling mechanisms that create it, *Dev Dyn.*, 233 (3), Pg. 706-720

Heinrich, MC, Griffith, DJ, Druker, BJ, Wait, CL, Ott, KA, and Zigler, AJ, 2000, Inhibition of c-kit receptor tyrosine kinase activity by STI 571, a selective tyrosine kinase inhibitor, *Blood.*, 96 (3), Pg. 925-932

Heinrich, MC, Jones, RL, von Mehren, M, Schöffski, P, Serrano, C, Kang, YK, Cassier, PA, Mir, O, Eskens, F, Tap, WD, Rutkowski, P, Chawla, SP, Trent, J, Tugnait, M, Evans, EK, Lauz, T, Zhou, T, Roche, M, Wolf, BB, Bauer, S, and George,

- S, 2020, Avapritinib in advanced PDGFRA D842V-mutant gastrointestinal stromal tumour (NAVIGATOR): a multicentre, open-label, phase 1 trial, *Lancet Oncol.*, 21 (7), Pg. 935-946
- Helsten, T, Elkin, S, Arthur, E, Tomson, BN, Carter, J, and Kurzrock, R, 2016, The FGFR landscape in cancer: analysis of 4,853 tumors by next-generation sequencing, *Clin Cancer Res.*, 22 (1), Pg. 259-267
- Henke, E, Nandigama, R, and Ergün, S, 2020, Extracellular matrix in the tumour microenvironment and its impact on cancer therapy, *Front Mol Biosci.*, 6, Pg. 160
- Herviou, P, Thivat, E, Richard, D, Roche, L, Dohou, J, Pouget, M, Eschalier, A, Durando, X, and Authier, N, 2016, Therapeutic drug monitoring and tyrosine kinase inhibitors, *Oncol Lett.*, 12 (2), Pg. 1223-1232
- Heymann, MF, Lézot, F, and Heymann, D, 2019, The contribution of immune infiltrates and the local environment in the pathogenesis of osteosarcoma, *Cell Immunol.*, 343, Pg. 103711
- Hibi, K, Takahashi, T, Sekido, Y, Ueda, R, Hida, T, Ariyoshi, Y, Takagi, H, and Takahashi, T, 1991, Coexpression of the stem cell factor and the c-kit genes in small-cell lung cancer, *Oncogene.*, 6 (12), Pg. 2291-2296
- Highfill, SL, Cui, Y, Giles, AJ, Smith, JP, Zhang, H, Morse, E, Kaplan, RN, and Mackall, CL, 2014, Disruption of CXCR2-mediated MDSC tumor trafficking enhances anti-PD1 efficacy, *Sci Transl Med.*, 6 (237), Pg. 237ra67
- Higuchi, M, Ishiyama, K, Maruoka, M, Kanamori, R, Takaori-Kondon, A, and Watanabe, N, 2021, Paradoxical activation of c-Src as a drug-resistant mechanism, *Cell Rep.*, 34 (12), Pg. 108876
- Hilberg, F, Roth, GJ, Krssak, M, Kautschitsch, S, Sommergruber, W, Tontsch-Grunt, U, Garin-Chesa, P, Bader, G, Zoepfel, A, Quant, J, Heckel, A, and Rettig, WJ, 2008, BIBF 1120: triple angiokinase inhibitor with sustained receptor blockade and good antitumor efficacy, *Cancer Res.*, 68 (12), Pg. 4774-4782
- Hinson, ARP, Jones, R, Crose, LES, Belyea, BC, Barr, FG, and Linardic, CM, 2013, Human rhabdomyosarcoma cell lines for rhabdomyosarcoma research: utility and pitfalls, *Front Oncol.*, 3, Pg. 183
- Hirano, T, 2021, IL-6 in inflammation, autoimmunity and cancer, *Int Immunol.*, 33 (3), Pg. 127-148
- Hirbe, AC, Eulo, V, Moon, CI, Luo, J, Myles, S, Seetharam, M, Toeniskoetter, J, Kershner, T, Haarberg, S, Agulnik, M, Monga, V, Milhem, M, Parkes, A, Robinson, S, Okuno, S, Attia, S, and Van Tine, BA, 2020, A phase II study of pazopanib as front-line therapy in patients with non-resectable or metastatic soft-tissue sarcomas who are not candidates for chemotherapy, *Eur J Cancer.*, 137, Pg. 1-9
- Hirsch, FR, Varella-Garcia, M, and Cappuzzo, 2009, Predictive value of EGFR and HER2 overexpression in advanced non-small-cell lung cancer, *Oncogene.*, 28 Suppl 1, S32-S37
- Hobbs, GA, Der, CJ, and Rossman, KL, 2016, RAS isoforms and mutations in cancer at a glance, *J Cell Sci.*, 129 (7), Pg. 1287-1292
- Hoefkens, F, Dehandschutter, C, Somville, J, Meijnders, P, and Van Gestel, D, 2016, Soft tissue sarcoma of the extremities: pending questions on surgery and radiotherapy, *Radiat Oncol.*, 11 (1), Pg. 136
- Holderfield, M, Deuker, MM, McCormick, F, and McMahon, M, 2014, Targeting RAF kinases for cancer therapy: BRAF-mutated melanoma and beyond, *Nat Rev Cancer.*, 14 (7), Pg. 455-467
- Holland, AJ, and Cleveland, DW, 2012, Chromoanagenesis and cancer: mechanisms and consequences of localized, complex chromosomal rearrangements, *Nat Med.*, 18 (11), Pg. 1630-1638
- Hornick, JL, Dal Cin, P, and Fletcher, CDM, 2009, Loss of INI1 expression is characteristic of both conventional and proximal-type epithelioid sarcoma, *Am J Surg Pathol.*, 33 (4), Pg. 542-550
- Hosaka, S, Horiuchi, K, Yoda, M, Nakayama, R, Tohmonda, T, Susa, M, Nakamura, M, Chiba, K, Toyama, Y, and Morioka, H, 2012, A novel multi-kinase inhibitor pazopanib suppresses growth of synovial sarcoma cells through inhibition of the PI3K-AKT pathway, *J Orthop Res.*, 30 (9), Pg. 1493-1498
- Hua, TNM, Kim, MK, Vo, VTA, Choi, JW, Choi, JH, Kim, HW, Cha, SK, Park, KS, and Jeong, Y, 2019, Inhibition of oncogenic Src induces FABP4-mediated lipolysis via PPAR γ activation exerting cancer growth suppression, *EBioMedicine.*, 41, Pg. 134-145
- Huang, X, Ye, Z, Li, T, Wei, Y, Wang, S, Liu, Y, and Chen, J, 2021, A phase II study of anlotinib in the first-line treatment of locally advanced or metastatic soft tissue sarcoma, *J Clin Oncol.*, 39 (15), https://ascopubs.org/doi/abs/10.1200/JCO.2021.39.15_suppl.e23531, Last accessed [October 2021]
- Hughes, P, Marshall, D, Reid, Y, Parkes, H, and Gelber, C, 2007, The costs of using unauthenticated, over-passaged cell lines: how much more data do we need?, *Biotechniques.*, 43 (5), Pg. 575; 577-578; 581-582 passim.
- Hu-Lowe, DD, Zou, HY, Grazzini, ML, Hallin, ME, Wickman, GR, Amundson, K, Chen, JH, Rewolinski, DA, Yamazaki, S, Wu, EY, McTigue, MA, Murray, BW, Kania, RS, O'Connor, P, Shalinsky, DR, and Bender, SL, 2008, Nonclinical

antiangiogenesis and antitumor activities of axitinib (AG-013736), an oral, potent, and selective inhibitor of vascular endothelial growth factor receptor tyrosine kinases 1, 2, 3, *Clin Cancer Res.*, 14 (22), Pg. 7272-7283

Humphrey, SJ, James, DE, and Mann, M, 2015, Protein phosphorylation: a major switch mechanism for metabolic regulation, *Trends Endocrinol Metab.*, 26 (12), Pg. 676-687

Hung, GY, Yen, CC, Horng, JL, Liu, CY, Chen, WM, Chen, TH, and Liu, CL, 2015, Incidences of primary soft tissue sarcoma diagnosed on extremities and trunk wall: a population-based study in Taiwan, *Medicine (Baltimore)*, 94 (41), e1696

Huo, KG, D'Arcangelo, E, and Tsao, MS, 2020, Patient-derived cell line, xenograft and organoid models in lung cancer therapy, *Transl Lung Cancer Res.*, 9 (5), Pg. 2214-2232

Hurwitz, HI, Dowlati, A, Saini, S, Savage, S, Suttle, AB, Gibson, DM, Hodge, JP, Merkle, EM, and Pandite, L, 2009, Phase I trial of pazopanib in patients with advanced cancer, *Clin Cancer Res.*, 15 (12), Pg. 4220-4227

Hyman, D, Kummar, S, Farago, A, Geoerger, B, Mau-Sorensen, M, Taylor, M, Garralda, E, Nagasubramanian, R, Natheson, M, Song, L, Capra, M, Jorgensen, M, Ho, A, Shukla, N, Smith, S, Huang, X, Tuch, B, Ku, N, Laetsch, TW, Drilon, A, and Hong, D, 2019, Abstract CT127: Phase I and expanded access experience of LOXO-195 (BAY 2731954), a selective next-generation TRK inhibitor (TRKi), *Cancer Res.*, 79 (13 Suppl), Abstract nr CT127

Hynes, RO, 2002, Integrins: bidirectional, allosteric signaling machines, *Cell.*, 110 (6), Pg. 673-687

Ibrahim, A, and Chopra, S, 2020, Succinate dehydrogenase-deficient gastrointestinal stromal tumors, *Arch Pathol Lab Med.*, 144 (5), Pg. 655-660

Igarashi, K, Kawaguchi, K, Murakami, T, Kiyuna, T, Miyake, K, Singh, AS, Nelson, SD, Dry, SM, Li, Y, Yamamoto, N, Hayashi, K, Kimura, H, Miwa, S, Tsuchiya, H, Eilber, FC, and Hoffman, RM, 2017, High efficacy of pazopanib on an undifferentiated spindle-cell sarcoma resistant to first-line therapy is identified with a patient-derived orthotopic xenograft (PDOX) nude mouse model, *J Cell Biochem.*, 118 (9), Pg. 2739-2743

Igarashi, K, Kawaguchi, K, Kiyuna, T, Miyake, K, Miyake, M, Nelson, SD, Russell, TA, Dry, SM, Li, Y, Yamamoto, N, Hayashi, K, Kimura, H, Miwa, S, Higuchi, T, Singh, SR, Tsuchiya, H, and Hoffman, RM, 2019, Pazopanib regresses a doxorubicin-resistant synovial sarcoma in a patient-derived orthotopic xenograft mouse model, *Tissue Cell.*, 58, Pg. 107-111

Imamovic, L, and Sommer, MOA, 2013, Use of collateral sensitivity networks to design drug cycling protocols that avoid resistance development, *Sci Transl Med.*, 5 (204), Pg. 204ra132

In, GK, Hu, JS, and Tseng, WW, 2017, Treatment of advanced, metastatic soft tissue sarcoma: latest evidence and clinical considerations, *Ther Adv Med Oncol.*, 9 (8), Pg. 533-550

Indio, V, Astolfi, A, Tarantino, G, Urbini, M, Patterson, J, Nannini, M, Saponara, M, Gatto, L, Santini, D, Do Valle, IF, Castellani, G, Remondini, D, Fiorentino, M, Von Mehren, M, Brandi, G, Biasco, G, Heinrich, MC, and Pantaleo, MA, 2018, Integrated molecular characterization of gastrointestinal stromal tumors (GIST) harboring the rare D842V mutation in *PDGFRA* gene, *Int J Mol Sci.*, 19 (3), Pg. 732

Ingham, M, Lee, SM, Patwardhan, P, Choy, E, Chen, I, Singh-Kandah, S, Taiclet, L, and Schwartz, GK, 2017, Phase 2 trial of the novel multi-receptor tyrosine kinase inhibitor sitravatinib in well-differentiated/dedifferentiated liposarcoma, *J Clin Oncol.*, 35 (15), https://ascopubs.org/doi/abs/10.1200/JCO.2017.35.15_suppl.TPS11082, Last accessed [March 2021]

International Association of Cancer Registries (IACR), 2019, International Agency for Research on Cancer, Lyon (France), ICD-O-3.2, http://www.iacr.com.fr/index.php?option=com_content&view=article&id=149:icd-o-3-2&catid=80&Itemid=545, Last accessed [May 2020]

Ip, CKM, Ng, PKS, Jeong, KJ, Shao, SH, Ju, Z, Leonard, PG, Hua, X, Vellano, CP, Woessner, R, Sahni, N, Scott, KL, and Mills, GB, 2018, Neomorphic *PDGFRA* extracellular domain driver mutations are resistant to *PDGFRA* targeted therapies, *Nat Commun.*, 9, Pg. 4583

Irby, RB, and Yeatman, TJ, 2000, Role of Src expression and activation in human cancer, *Oncogene.*, 19 (49), Pg. 5636-5642

Ishibe, T, Nakayama, T, Okamoto, T, Aoyama, T, Nishijo, K, Shibata, KR, Shima, Y, Nagayama, S, Katagiri, T, Nakamura, Y, Nakamura, T, and Toguchida, J, 2005, Disruption of fibroblast growth factor signal pathway inhibits the growth of synovial sarcomas: potential application of signal inhibitors to molecular target therapy, *Clin Cancer Res.*, 11 (7), Pg. 2702-2712

Italiano, A, 2020, Targeting epigenetics in sarcoma through EZH2 inhibition, *J Hematol Oncol.*, 13, Pg. 33

Italiano, A, Bessede, A, Bompas, E, Piperno-Neumann, S, Chevreau, C, Penel, N, Bertucci, F, Toulmonde, M, Bellera, CA, Guegan, JP, Sautes-Fridman, C, Bougouïn, A, Cantarel, C, Le Loarer, F, Blay, JY, and Fridman, WH, 2021, PD1 inhibition in soft-tissue sarcomas with tertiary lymphoid structures: a multicenter phase II trial, *J Clin Oncol.*, 39 (15), https://ascopubs.org/doi/abs/10.1200/JCO.2021.39.15_suppl.11507, Last accessed [November 2021]

Ito, T, Yamamura, M, Hirai, T, Ishikawa, T, Kanda, T, Nakai, T, Ohkouchi, M, Hashikura, Y, Isozaki, K, and Hirota, S, 2014, Gastrointestinal stromal tumors with exon 8 c-kit gene mutation might occur at extragastric sites and have metastasis-prone nature, *Int J Clin Exp Pathol.*, 7 (11), Pg. 8024-8031

Lura, K, Kohashi, K, Ishii, T, Maekawa, A, Bekki, H, Otsuka, H, Yamada, Y, Yamamoto, H, Matsumoto, Y, Iwamoto, Y, and Oda, Y, 2017, MAGEA4 expression in bone and soft tissue tumors: its utility as a target for immunotherapy and diagnostic marker combined with NY-ESO-1, *Virchows Arch.*, 471 (3), Pg. 383-392

Jamison, DT, Feachem, RG, Makgoba, MW, Bos, ER, Baingana, FK, Hofman, KJ, and Rogo, KO, 2006, Disease and Mortality in Sub-Saharan Africa, The International Bank for Reconstruction and Development/The World Bank, 2nd ed, Washington (DC) (USA), <http://documents.worldbank.org/curated/en/431831468211449561/Disease-and-Mortality-in-Sub-Saharan-Africa-second-edition>, Last accessed [May 2020]

Janku, F, Yap, TA, and Meric-Bernstam, F, 2018, Targeting the PI3K pathway in cancer: are we making headway?, *Nat Rev Clin Oncol.*, 15 (5), Pg. 273-291

Januchowski, R, Zawierucha, P, Ruciński, M, Nowicki, M, and Zabel, M, 2014, Extracellular matrix proteins expression profiling in chemoresistant variants of the A2780 ovarian cancer cell line, *Biomed Res Int.*, 2014, Pg. 365867

Jayakody, N, Harris, EC, and Coggon, D, 2015, Phenoxy herbicides, soft tissue sarcoma and non-hodgkin lymphoma: a systematic review of evidence form cohort and case-control studies, *Br Med Bull.*, 114 (1), Pg. 75-94

Jiang, T, Wang, G, Liu, Y, Feng, L, Wang, M, Liu, J, Chen, Y, and Ouyang, L, 2021, Development of small-molecule tropomyosin receptor kinase (TRK) inhibitors for *NTRK* fusion cancers, *Acta Pharm Sin B.*, 11 (2), Pg. 355-372

Jiao, Q, Bi, L, Ren, Y, Song, S, Wang, Q, and Wang, YS, 2018, Advances in studies of tyrosine kinase inhibitors and their acquired resistance, *Mol Cancer.*, 17 (1), Pg. 36

Jin, L, Ge, H, Long, Y, Yang, C, Chang, YE, Mu, L, Sayour, EJ, De Leon, G, Wang, QJ, Yang, JC, Kubilis, PS, Bao, H, Xia, S, Lu, D, Kong, Y, Hu, L, Shang, Y, Jiang, C, Nie, J, Li, S, Gu, Y, Sun, J, Mitchell, DA, Lin, Z, and Huang, J, 2018, CD70, a novel target of CAR T-cell therapy for gliomas, *Neuro Oncol.*, 20 (1), Pg. 55-65

Jin, L, Tao, H, Karachi, A, Long, Y, Hou, AY, Na, M, Dyson, KA, Grippin, AJ, Deleyrolle, LP, Zhang, W, Rajon, DA, Wang, QJ, Yang, JC, Kresak, JL, Sayour, EJ, Rahman, M, Bova, FJ, Lin, Z, Mitchell, DA, and Huang, J, 2019, CXCR1- or CXCR2-modified CAR T cells co-opt IL-8 for maximal antitumor efficacy in solid tumors, *Nat Commun.*, 10 (1), Pg. 4016

Jo, JC, Hong, YS, Kim, KP, Lee, JL, Lee, J, Park, YS, Kim, SY, Ryu, JS, Lee, JS, and Kim, TW, 2014, A prospective multicenter phase II study of sunitinib in patients with advanced aggressive fibromatosis, *Invest New Drugs.*, 32 (2), Pg. 369-376

Joensuu, H, Rutkowski, P, Nishida, T, Steigen, SE, Brabec, P, Plank, L, Nilsson, B, Braconi, C, Bordoni, A, Magnusson, MK, Sufliarsky, J, Federico, M, Jonasson, JG, Hostein, I, Bringuier, PP, and Emile, JF, 2015, KIT and PDGFRA mutations and the risk of GI stromal tumor recurrence, *J Clin Oncol.*, 33 (6), Pg. 634-642

Johnson, CN, Ha, AS, Chen, E, and Davidson, D, 2018, Lipomatous soft-tissue tumors, *J Am Acad Orthop Surg.*, 26 (22), Pg. 779-788

Jones, RL, Ratain, MJ, O'Dwyer, PJ, Siu, LL, Jassem, J, Medioni, J, DeJonge, M, Rudin, C, Sawyer, M, Khayat, D, Awada, A, De Vos-Geelen, JMPGM, Evans, TRJ, Obel, J, Brockstein, B, DeGreve, J, Baurain, JF, Maki, R, D'Adamo, D, Dickson, M, Undevia, S, Geary, D, Janisch, L, Bedard, PL, Razak, ARA, Kristeleit, R, Vitfell-Rasmussen, J, Walters, I, Kaye, SB, and Schwartz, G, 2019, Phase II randomised discontinuation trial of brivanib in patients with advanced solid tumours, *Eur J Cancer.*, 120, Pg. 132-139

Jones, SE, Fleuren, EDG, Frankum, J, Konde, A, Williamson, CT, Krastev, DB, Pemberton, HN, Campbell, J, Gulati, A, Elliott, R, Menon, M, Sefe, JL, Brough, R, Pettitt, SJ, Niedzwiedz, W, Van Der Graaf, WTA, Shipley, J, Ashworth, A, and Lord, CJ, 2017, ATR is a therapeutic target in synovial sarcoma, *Cancer Res.*, 77 (24), Pg. 7014-7026

Judson, I, Bulusu, R, Seddon, B, Dangoor, A, Wong, N, and Mudan, S, 2017, UK clinical practice guidelines for the management of gastrointestinal stromal tumours (GIST), *Clin Sarcoma Res.*, 7, Pg. 6

Judson, I, Morden, JP, Kilburn, L, Leahy, M, Benson, C, Bhadri, V, Campbell-Hewson, Q, Cubedo, R, Dangoor, A, Fox, L, Hennig, I, Jarman, K, Joubert, W, Kernaghan, S, Pousa, AL, McNeil, C, Seddon, B, Snowdon, C, Tattersall, M, Toms, C, Trufero, JM, and Bliss, JM, 2019, Cediranib in patients with alveolar soft-part sarcoma (CASPS): a double-blind, placebo-controlled, randomised, phase 2 trial, *Lancet Oncol.*, 20 (7), Pg. 1023-1034

Juliano, RL, and Ling, V, 1976, A surface glycoprotein modulating drug permeability in Chinese hamster ovary cell mutants, *Biochim Biophys Acta.*, 455 (1), Pg. 152-162

Jun, HJ, Lee, J, Lim, DH, Park, JO, Ahn, G, Seo, SW, Sung, KS, Lim, DH, Yoo, KH, and Choi, YL, 2010, Expression of MET in alveolar soft part sarcoma, *Med Oncol.*, 27 (2), Pg. 459-465

Jung, J, Lee, JS, Dickson, MA, Schwartz, GK, Le Cesne, A, Varga, A, Bahleda, R, Wagner, AJ, Choy, E, De Jonge, MJ, Light, M, Rowley, S, Macé, S, and Watters, J, 2016, TP53 mutations emerge with HDM2 inhibitor SAR4-5838 treatment in de-differentiated liposarcoma, *Nat Commun.*, 7, Pg. 12609

Kadoch, C, and Crabtree, GR, 2013, Reversible disruption of mSWI/SNF (BAF) complexes by the SS18-SSX oncogenic fusion in synovial sarcoma, *Cell*, 153 (1), Pg. 71-85

Kalimuthu, SN, and Chetty, R, 2016, Gene of the month: SMARCB1, *J Clin Pathol.*, 69, Pg. 484-489

Kamohara, H, Takahashi, M, Ishiko, T, Ogawa, M, and Baba, H, 2007, Induction of interleukin-8 (CXCL-8) by tumour necrosis factor-alpha and leukemia inhibitory factor in pancreatic carcinoma cells: impact of CXCL-8 as an autocrine growth factor, *Int J Oncol.*, 31 (3), Pg. 627-632

Kang, G, Bae, BN, Sohn, BS, Pyo, JS, Kang, GH, and Kim, KM, 2015, Detection of KIT and PDGFRA mutations in the plasma of patients with gastrointestinal stromal tumor, *Target Oncol.*, 10 (4), Pg. 597-601

Kang, ZJ, Liu, YF, Xu, LZ, Long, ZJ, Huang, D, Yang, Y, Liu, B, Feng, JX, Pan, YJ, Yan, JS, and Liu, Q, 2016, The Philadelphia chromosome in leukemogenesis, *Chin J Cancer.*, 35, Pg. 48

Kanojia, D, Garg, M, Martinez, J, Anand, MT, Luty, SB, Doan, NB, Said, JW, Forscher, C, Tyner, JW, and Koeffler, HP, 2017, Kinase profiling of liposarcomas using RNAi and drug screening assays identified druggable targets, *J Hematol Oncol.*, 10 (1), Pg. 173

Kapp, TG, Rechenmacher, F, Neubauer, S, Maltsev, OV, Cavalcanti-Adam, EA, Zarka, R, Reuning, U, Notni, J, Wester, HJ, Mas-Moruno, C, Spatz, J, Geiger, B, and Kessler, H, 2017, A comprehensive evaluation of the activity and selectivity profile of ligands for RGD-binding integrins, *Sci Rep.*, 7, Pg. 39805

Karlsson, P, Holmberg, E, Samuelsson, A, Johansson, KA, and Wallgren, A, 1998, Soft tissue sarcoma after treatment for breast cancer – A Swedish population-based study, *Eur J Cancer.*, 34 (13), Pg. 2068-2075

Kasper, B, 2019, The challenge of finding new therapeutic avenues in soft tissue sarcomas, *Clin Sarcoma Res.*, 9, Pg. 5

Kasper, B, Sleijfer, S, Litière, S, Marreaud, S, Verweij, J, Hodge, RA, Bauer, S, Kerst, JM, and Van Der Graaf, WTA, 2014, Long-term responders and survivors on pazopanib for advanced soft tissue sarcomas: subanalysis of two European Organisation for Research and Treatment of Cancer (EORTC) clinical trials 62043 and 62072, *Ann Oncol.*, 25 (3), Pg. 719-724

Kasper, B, Gruenwald, V, Reichardt, P, Bauer, S, Rauch, G, Limplrecht, R, Sommer, M, Dimitrakopoulou-Strauss, A, Pilz, L, Haller, F, and Hohenberger, P, 2017, Imatinib induces sustained progression arrest in RECIST progressive desmoid tumours: Final results of a phase II study of the German Interdisciplinary Sarcoma Group (GISG), *Eur J Cancer.*, 76, Pg. 60-67

Kaur, G, and Dufour, JM, 2012, Cell lines: valuable tools or useless artifacts, *Spermatogenesis.*, 2 (1), Pg. 1-5

Kawaguchi, K, Igarashi, K, Miyake, K, Kiyuna, T, Miyake, M, Singh, AS, Chmielowski, B, Nelson, SD, Russell, TA, Dry, SM, Li, Y, Unno, M, Singh, SR, Eilber, FC, and Hoffman, RM, 2019, Patterns of sensitivity to a panel of drugs are highly individualised for undifferentiated/unclassified soft tissue sarcoma (USTS) in patient-derived orthotopic xenograft (PDOX) nude-mouse models, *J Drug Target.*, 27 (2), Pg. 211-216

Kawaguchi, S, Tsukahara, T, Ida, K, Kimura, S, Murase, M, Kano, M, Emori, M, Nagoya, S, Kaya, M, Torigoe, T, Ueda, E, Takahashi, A, Ishii, T, Tatezaki, SI, Toguchida, J, Tsuchiya, H, Osanai, T, Sugita, T, Sugiura, H, Ieguchi, M, Ihara, K, Hamada, KI, Kakizaki, H, Morii, T, Yasuda, T, Tanizawa, T, Ogose, A, Yabe, H, Yamashita, T, Sato, N, and Wada, T, 2012, SYT-SSX breakpoint peptide vaccines in patients with synovial sarcoma: a study from the Japanese Musculoskeletal oncology group, *Cancer Sci.*, 103 (9), Pg. 1625-1630

Kawai, A, Araki, N, Hiraga, H, Sugiura, H, Matsumine, A, Ozaki, T, Ueda, T, Ishii, T, Esaki, T, Machida, M, and Fukasawa, N, 2016, A randomized, double-blind, placebo-controlled, Phase III study of pazopanib in patients with soft tissue sarcoma: results from the Japanese subgroup, *Jpn J Clin Oncol.*, 46 (3), Pg. 248-253

Kawano, S, Grassian, AR, Tsuda, M, Knutson, SK, Warholc, NM, Kuznetsov, G, Xu, S, Xiao, Y, Pollock, RM, Smith, JJ, Kuntz, KW, Ribich, S, Minoshima, Y, Matsui, J, Copeland, RA, Tanaka, S, and Keilhack, H, 2017, Correction: Preclinical evidence of anti-tumor activity induced by EZH2 inhibition in human models of synovial sarcoma, *PLoS One.*, 12 (1), e0170539

Keir, ST, Morton, CL, Wu, J, Kurmasheva, RT, Houghton, PJ, and Smith, MA, 2012, Initial testing of the multitargeted kinase inhibitor pazopanib by the Pediatric Preclinical Testing Program, *Pediatr Blood Cancer.*, 59 (3), Pg. 586-588

Kentsis, A, Reed, C, Rice, KL, Sanda, T, Rodig, SJ, Tholouli, E, Christie, A, Valk, PJM, Delwel, R, Ngo, V, Kutok, JL, Dahlberg, SE, Moreau, LA, Byers, RJ, Christensen, JG, Vande Woude, G, Licht, JD, Kung, AL, Staudt, LM, and Look, AT, 2012, Autocrine activation of the MET receptor tyrosine kinase in acute myeloid leukemia, *Nat Med.*, 18 (7), Pg. 1118-1122

Khalaf, K, Hana, D, Chou, JTT, Singh, C, Mackiewicz, A, and Kaczmarek, M, 2021, Aspects of the tumor microenvironment involved in immune resistance and drug resistance, *Front Immunol.*, 12, Pg. 656364

Kia, SK, Gorski, MM, Giannakopoulos, S, and Verrijzer, CP, 2008, SWI/SNF mediates polycomb eviction and epigenetic reprogramming of the INK4b-ARF-INK4a locus, *Mol Cell Biol.*, 28 (10), Pg. 3457-3464

Killian, JK, Miettinen, M, Walker, RL, Wang, Y, Zhu, YJ, Waterfall, JJ, Noyes, N, Retnakumar, P, Yang, Z, Smith Jr., WI, Killian, MS, Lau, CC, Pineda, M, Walling, J, Stevenson, H, Smith, C, Wang, Z, Lasota, J, Kim, SY, Boikos, SA, Helman, LJ, and Meltzer, PS, 2014, Recurrent epimutation of SDHC in gastrointestinal stromal tumors, *Sci Transl Med.*, 6 (268), Pg. 268ra177

Kilvaer, TK, Valkov, A, Sorbye, SW, Donnem, T, Smeland, E, Bremnes, RM, and Busund, LT, 2010, Platelet-derived growth factors in non-GIST soft-tissue sarcomas identify a subgroup of patients with wide resection margins and poor disease-specific survival, *Sarcoma.*, 2010, Pg. 751304

Kim, HK, Kim, SY, Lee, SJ, Kang, M, Kim, ST, Jang, J, Rath, O, Schueler, J, Lee, DW, Park, WY, Kim, SJ, Park, SH, and Lee, J, 2016, BEZ235 (PIK3/mTOR inhibitor) overcomes pazopanib resistance in patient-derived refractory soft tissue sarcoma cells., *Transl Oncol.*, 9 (3), Pg. 197-202

Kim, J, Kim, HS, Shim, JJ, Lee, J, Kim, AY, and Kim, J, 2019, Critical role of the fibroblast growth factor signalling pathway in Ewing's sarcoma octamer-binding transcription factor 4-mediated cell proliferation and tumorigenesis, *FEBS J.*, 286 (22), Pg. 4443-4472

Kim, KH, and Roberts, CWM, 2015, Mechanisms by which SMARCB1 loss drives rhabdoid tumor growth, *Cancer Genet.*, 207 (9), Pg. 365-372

Kim, LC, Song, L, and Haura, EB, 2009, Src kinases as therapeutic targets for cancer, *Nat Rev Clin Oncol.*, 6 (10), Pg. 587-595

Kim, M, Kim, TM, Keam, B, Kim, YJ, Paeng, JC, Moon, KC, Kim, DW, and Heo, DS, 2019, A phase II trial of pazopanib in patients with metastatic alveolar soft part sarcoma, *Oncologist.*, 24 (1), Pg. 20-e29

Kiyuna, T, Murakami, T, Tome, Y, Igarashi, K, Kawaguchi, K, Miyake, K, Miyake, M, Li, Y, Nelson, SD, Dry, SM, Singh, AS, Russell, TA, Singh, SR, Kanaya, F, Eilber, FC, and Hoffman, RM, 2018, Doxorubicin-resistant pleomorphic liposarcoma with PDGFRA gene amplification is targeted and regressed by pazopanib in a patient-derived orthotopic xenograft mouse model, *Tissue Cell.*, 53, Pg. 30-36

Koch, H, Del Castillo Busto, ME, Kramer, K, Médard, G, and Kuster, B, 2015, Chemical proteomics uncovers EPHA2 as a mechanism of acquired resistance to small molecule EGFR kinase inhibition, *J Proteome Res.*, 14 (6), Pg. 2617-2625

Kodack, DP, Farago, AF, Dastur, A, Held, MA, Dardaei, L, Friboulet, L, Von Flotow, F, Damon, LJ, Lee, D, Parks, M, Dicecca, R, Greenberg, M, Kattermann, KE, Riley, AK, Fintelmann, FJ, Rizzo, C, Piotrowska, Z, Shaw, AT, Gainor, JF, Sequist, LV, Niederst, MJ, Engelman, JA, and Benes, CH, 2017, Primary patient-derived cancer cells and their potential for personalized cancer patient care, *Cell Rep.*, 21 (11), Pg. 3298-3309

Koehler, K, Liebner, D, and Chen, JL, 2016, TP53 mutational status is predictive of pazopanib response in advanced sarcomas, *Ann Oncol.*, 27 (3), Pg. 539-543

Kohashi, K, Yamamoto, H, Kumagai, R, Yamada, Y, Hotokebuchi, Y, Taguchi, T, Iwamoto, Y, and Oda, Y, 2014, Differential microRNA expression profiles between malignant rhabdoid tumor and epithelioid sarcoma: miR193a-5p is suggested to downregulate SMARCB1 mRNA expression, *Mod Pathol.*, 27 (6), Pg. 832-839

Kollár, A, Jones, RL, Stacchiotti, S, Gelderblom, H, Guida, M, Grignani, G, Steeghs, N, Safwat, A, Katz, D, Duffaud, F, Sleijfer, S, Van der Graaf, WT, Touati, N, Litière, S, Marreaud, S, Gronchi, A, and Kasper, B, 2017, Pazopanib in advanced vascular sarcomas: an EORTC Soft Tissue and Bone Sarcoma Group (STBSG) retrospective analysis, *Acta Oncol.*, 56 (1), Pg. 88-92

Konig, H, Copland, M, Chu, S, Jove, R, Holyoake, TL, and Bhatia, R, 2008, Effects of dasatinib on SRC kinase activity and downstream intracellular signaling in primitive chronic myelogenous leukemia hematopoietic cells, *Cancer Res.*, 68 (23), Pg. 9624-9633

Krishnamurty, R, and Maly, DJ, 2010, Biochemical mechanisms of resistance to small-molecule protein kinase inhibitors, *ACS Chem Biol.*, 5 (1), Pg. 121-138

Krystal, GW, Hines, SJ, and Organ, CP, 1996, Autocrine growth of small cell lung cancer mediated by coexpression of c-kit and stem cell factor, *Cancer Res.*, 56 (2), Pg. 370-376

Kumar, R, Knick, VB, Rudolph, SK, Johnson, JH, Crosby, RM, Crouthamel, MC, Hopper, TM, Miller, CG, Harrington, LE, Onori, JA, Mullin, RJ, Gilmer, TM, Truesdale, AT, Epperly, AH, Bolor, A, Stafford, JA, Luttrell, DK, and Cheung, M, 2007, Pharmacokinetic-pharmacodynamic correlation from mouse to human with pazopanib, a multikinase angiogenesis inhibitor with potent antitumor and antiangiogenic activity, *Mol Cancer Ther.*, 6 (7), Pg. 2012-2021

Kummar, S, Allen, D, Monks, A, Polley, EC, Hose, CD, Ivy, SP, Turkbey, IB, Lawrence, S, Kinders, RJ, Choyke, P, Simon, R, Steinberg, SM, Doroshov, JH, and Helman, L, 2013, Cediranib for metastatic alveolar soft part sarcoma, *J Clin Oncol.*, 31 (18), Pg. 2296-2302

Kutikov, A, Makhov, P, Golovine, K, Canter, DJ, Sirohi, M, Street, R, Simhan, J, Uzzo, RG, and Kolenko, VM, 2011, Interleukin-6: a potential biomarker of resistance to multitargeted receptor tyrosine kinase inhibitors in castration-resistant prostate cancer, *Urology.*, 78 (4), Pg. 968

Kwarcinski, FE, Fox, CC, Steffey, ME, and Soellner, MB, 2012, Irreversible inhibitors of c-Src kinase that target a nonconserved cysteine, *ACS Chem Biol.*, 7 (11), Pg. 1910-1917

Ladanyi, M, 2001, Fusions of the SYT and SSX genes in synovial sarcoma, *Oncogene*, 20 (40), Pg. 5755-5762

Lai, JP, Rosenborg, AZ, Miettinen, MM, and Lee, CCR, 2012, NY-ESO-1 expression in sarcoma: a diagnostic marker and immunotherapy target, *Oncoimmunology.*, 1 (8), Pg. 1409-1410

Lamouille, S, Xu, J, and Derynck, R, 2014, Molecular mechanisms of epithelial-mesenchymal transition, *Nat Rev Mol Cell Biol.*, 15 (3), Pg. 178-196

Lan, T, Chen, H, Xiong, B, Zhou, T, Peng, R, Chen, M, Ye, F, Yao, J, He, X, Wang, Y, and Zhang, H, 2016, Primary pleuropulmonary and mediastinal synovial sarcoma: a clinicopathologic and molecular study of 26 genetically confirmed cases in the largest institution of southwest China, *Diagn Pathol.*, 11, Pg. 62

Lang, K, Niggemann, B, Zanker, KS, and Entschladen, 2002, Signal processing in migrating T24 human bladder carcinoma cells: role of the autocrine interleukin-8 loop, *Int J Cancer.*, 99 (5), Pg. 673-680

Langhans, SA, 2018, Three-dimensional in vitro cell culture models in drug discovery and drug repositioning, *Front Pharmacol.*, 9, Pg. 6

Lanzi, C, Dal Bo, L, Favini, E, Tortoreto, M, Beretta, GL, Arrighetti, N, Zaffaroni, N, and Cassinelli, G, 2019, Overactive IGF1/Insulin receptors and NRASQ61R mutation drive mechanisms of resistance to pazopanib and define rational combination strategies to treat synovial sarcoma, *Cancers (Basel).*, 11 (3), Pg. 408

Lauper, JM, Krause, A, Vaughan, TL, and Monnat Jr, RJ, 2013, Spectrum and risk of neoplasia in Werner Syndrome: A systematic review, *PLoS One*, e59709

Lavoie, H, Gagnon, J, and Therrien, M, 2020, ERK signalling: a master regulator of cell behaviour, life and fate, *Nat Rev Mol Cell Biol.*, 21 (10), 607-632

Le, DT, Uram, JN, Wang, H, Bartlett, BR, Kemberling, H, Eyring, AD, Skora, AD, Lubber, BS, Azad, NS, Laheru, D, Biedrzycki, B, Donehower, RC, Zaheer, A, Fisher, GA, Crocenzi, TS, Lee, JJ, Duffy, SM, Goldberg, RM, De La Chapelle, A, Koshiji, M, Bhajee, F, Huebner, T, Hruban, RH, Wood, LD, Cuka, N, Pardoll, DM, Papadopoulos, N, Kinzler, KW, Zhou, S, Cornish, TC, Taube, JM, Anders, RA, Eshleman, JR, Vogelstein, B, and Diaz Jr., LA, 2015, PD-1 blockade in tumors with mismatch-repair deficiency, *N Engl J Med.*, 372 (26), Pg. 2509-2520

Le, DT, Durham, JN, Smith, KN, Wang, H, Bartlett, BR, Aulakh, LK, Lu, S, Kemberling, H, Wilt, C, Lubber, BS, Wong, F, Azad, NS, Rucki, AA, Laheru, D, Donehower, R, Zaheer, A, Fisher, GA, Crocenzi, TS, Lee, JJ, Greten, TF, Duffy, AG, Ciombor, KK, Eyring, AD, Lam, BH, Joe, A, Kang, SP, Holdhoff, M, Danilova, L, Cope, L, Meyer, C, Zhou, S, Goldberg, RM, Armstrong, DK, Bever, KM, Fader, AN, Taube, J, Housseau, F, Spetzler, D, Xiao, N, Pardoll, DM, Papadopoulos, N, Kinzler, KW, Eshleman, JR, Vogelstein, B, Anders, RA, and Diaz Jr., 2017, Mismatch repair deficiency predicts response of solid tumors to PD-1 blockade, *Science.*, 357 (6349), Pg. 409-413

Leal, TA, Horn, L, Velastegui, K, Christensen, J, Chen, I, and Spira, A, 2017, PS02.08 Evidence of clinical activity of sitravatinib in combination with nivolumab in NSCLC patients progressing on prior checkpoint inhibitor therapy, *J Thorac Oncol.*, 12 (11), S1567

Ledda, F, and Paratcha, G, 2007, Negative regulation of receptor tyrosine kinase (RTK) signaling: a developing field, *Biomark Insights.*, 2, Pg. 45-58

Lee, A, Judson, I, and Huang, P, 2016, Identifying the molecular determinants of pazopanib response in advanced soft tissue sarcoma, http://sarcomahelp.org/research/pazopanib.html#tpm2_1, Last accessed [October 2021]

Lee, ATJ, Jones, RL, and Huang, PH, 2019, Pazopanib in advanced soft tissue sarcomas, *Signal Transduct Target Ther.*, 4, Pg. 16

Lee, DW, Kim, HS, and Han, I, 2021, Actual long-term survival after resection of stage III soft tissue sarcoma, *BMC Cancer.*, 21 (1), Pg. 21

Lee, J, Kosowicz, JG, and Ambinder, RF, 2017, Unveiling Kaposi sarcoma viral antigens, *Oncotarget.*, 8 (31), Pg. 50325-50326

Lee, LF, Louie, MC, Desai, SJ, Yang, J, Chen, HW, Evans, CP, and Kung, HJ, 2004, Interleukin-8 confers androgen-independent growth and migration of LNCaP: differential effects of tyrosine kinases Src and FAK, *Oncogene.*, 23 (12), Pg. 2197-2205

Lee, WS, Yang, H, Chon, HJ, and Kim, C, 2020, Combination of anti-angiogenic therapy and immune checkpoint blockade normalizes vascular-immune crosstalk to potentiate cancer immunity, *Exp Mol Med.*, 52 (9), Pg. 1475-1485

Lee, YF, John, M, Edwards, S, Clark, J, Flohr, P, Maillard, K, Edema, M, Baker, L, Mangham, DC, Grimer, R, Wooster, R, Thomas, JM, Fisher, C, Judson, I, and Cooper, CS, 2003, Molecular classification of synovial sarcomas, leiomyosarcomas and malignant fibrous histiocytomas by gene expression profiling, *Br J Cancer.*, 88 (4), Pg. 510-515

Le Loarer, F, Zhang, L, Fletcher, CD, Ribeiro, A, Singer, S, Italiano, A, Neuville, A, Houlier, A, Chibon, F, Coindre, JM, and Antonescu, CR, 2014, Consistent SMARCB1 homozygous deletions in epithelioid sarcoma and in a subset of myoepithelial carcinomas can be reliably detected by FISH in archival materials, *Genes Chromosomes Cancer.*, 53 (6), Pg. 475-486

Lemmon, MA, and Schlessinger, J, 2010, Cell signaling by receptor tyrosine kinases, *Cell.*, 141 (7), Pg. 1117-1134

- Lev, DC, Onn, A, Melinkova, VO, Miller, C, Stone, V, Ruiz, M, McGary, EC, Ananthaswamy, HN, Price, JE, and Bar-Eli, M, 2004, Exposure of melanoma cells to dacarbazine results in enhanced tumor growth and metastasis in vivo, *J Clin Oncol.*, 22 (11), Pg. 2092-2100
- Li, F, Liao, Z, Zhang, C, Zhao, J, Xing, R, Teng, S, Zhang, J, Yang, Y, and Yang, J, 2018, Apatinib as targeted therapy for sarcoma, *Oncotarget.*, 9 (36), Pg. 24548-24560
- Li, FP, Fletcher, JA, Heinrich, MC, Garber, JE, Sallan, SE, Curiel-Lewandrowski, C, Duensing, A, Van de Rijn, M, Schnipper, LE, and Demetri, GD, 2005, Familial gastrointestinal stromal tumor syndrome: phenotypic and molecular features in a kindred, *J Clin Oncol.*, 23 (12), Pg. 2735-2743
- Li, H, Wozniak, A, Sciort, R, Cornillie, J, Wellens, J, Van Looy, T, Vanleeuw, U, Stas, M, Hompes, D, Debiec-Rychter, M, and Schöffski, P, 2014, Pazopanib, a receptor tyrosine kinase inhibitor, suppresses tumour growth through angiogenesis in dedifferentiated liposarcoma xenograft models, *Transl Oncol.*, 7 (6), Pg. 665-671
- Li, J, Mulvihill, TS, Li, L, Barrott, JJ, Nelson, ML, Wagner, L, Lock, IC, Pozner, A, Lambert, SL, Ozenberger, BB, Ward, MB, Grossmann, AH, Liu, T, Banito, A, Cairns, BR, and Jones, KB, 2021, A role for SMARCB1 in synovial sarcomagenesis reveals that SS18-SSX induces canonical BAF destruction, *Cancer Discov.*, candisc.1219.2020
- Li, SQ, Cheuk, AT, Shern, JF, Song, YK, Hurd, L, Liao, H, Wei, JS, and Khan, J, 2013, Targeting wild-type and mutationally activated FGFR4 in rhabdomyosarcoma with the inhibitor ponatinib (AP24534), *PLoS One.*, 8 (10), e76551
- Li, ZK, Liu, J, Deng, YT, and Jiang, Y, 2021, Efficacy and safety of anlotinib in patients with unresectable or metastatic well-differentiated/dedifferentiated liposarcoma: a single-center retrospective study, *Anticancer Drugs.*, 32 (2), Pg. 210-214
- Lim, J, Poulin, NM, and Nielsen, TO, 2015, New strategies in sarcoma: linking genomic and immunotherapy approaches to molecular subtype, *Clin Cancer Res.*, 21 (21), Pg. 4753-4759
- Lima, NC, Atkinson, E, Bunney, TD, Katan, M, and Huang, PH, 2020, Targeting the Src pathway enhances the efficacy of selective FGFR3 inhibitors in urothelial cancers with FGFR3 alterations, *Int J Mol Sci.*, 21 (9), Pg. 3214
- Lin, B, Song, X, Yang, D, Bai, D, Yao, Y, and Lu, N, 2018, Anlotinib inhibits angiogenesis via suppressing the activation of VEGFR2, PDGFR β , and FGFR1, *Gene.*, 654, Pg. 77-86
- Lin, CH, Cheng, HW, Hsu, MJ, Chen, MC, Lin, CC, and Chen, BC, 2006, c-Src mediates thrombin-induced NF-kappaB activation and IL-8/CXCL8 expression in lung epithelial cells, *J Immunol.*, 177 (5), Pg. 3427-3438
- Lin, J, Xia, L, Liang, J, Han, Y, Wang, H, Oyang, L, Tan, S, Tian, Y, Rao, S, Chen, X, Tang, Y, Su, M, Luo, X, Wang, Y, Wang, H, Zhou, Y, and Liao, Q, 2019, The roles of glucose metabolic reprogramming in chemo- and radio-resistance, *J Expt Clin Cancer Res.*, 38 (1), Pg. 218
- Linch, M, Miah, AB, Thway, K, Judson, IR, and Benson, C, 2014, Systemic treatment of soft-tissue sarcoma-gold standard and novel therapies, *Nat Rev Clin Oncol.*, 11 (4), Pg. 187-202
- Liu, L, Cao, Y, Chen, C, Zhang, X, McNabola, A, Wilkie, D, Wilhelm, S, Lynch, M, and Carter, C, 2006, Sorafenib blocks the RAF/MEK/ERK pathway, inhibits tumor angiogenesis, and induces tumor cell apoptosis in hepatocellular carcinoma model PLC/PRF/5, *Cancer Res.*, 66 (24), Pg. 11851-11858
- Liu, S, Du, Y, Ma, H, Liang, Q, Zhu, X, and Tian, J, 2019, Preclinical comparison of regorafenib and sorafenib efficacy for hepatocellular carcinoma using multimodality molecular imaging, *Cancer Lett.*, 453, Pg. 74-83
- Liu, YN, Chang, TH, Tsai, MF, Wu, SG, Tsai, TH, Chen, HY, Yu, SL, Yang, JC, and Shih, JY, 2015, IL-8 confers resistance to EGFR inhibitors by inducing stem cell properties in lung cancer, *Oncotarget.*, 6 (12), Pg. 10415-104314
- Logue, JS, and Morrison, DK, 2012, Complexity in the signaling network: insights from the use of targeted inhibitors in cancer therapy, *Genes Dev.*, 26 (7), Pg. 641-650
- Lombardo, LJ, Lee, FY, Chen, P, Norris, D, Barrish, JC, Behnia, K, Castaneda, S, Cornelius, LAM, Das, J, Dowsyko, AM, Fairchild, C, Hunt, JT, Inigo, I, Johnston, K, Kamath, A, Kan, D, Klei, H, Marathe, P, Pang, S, Peterson, R, Pitt, S, Schieven, GL, Schmidt, RJ, Tokarski, J, Wein, ML, Wityak, J, and Borzilleri, RM, 2004, Discovery of N-(2-chloro-6-methyl-phenyl)-2-(6-(4-(2-hydroxyethyl)-piperazin-1-yl)-2-methylpyrimidin-4-ylamino)thiazole-5-carboxamide (BMS-354825), a dual Src/Abl kinase inhibitor with potent antitumor activity in preclinical assays, *J Med Chem.*, 47 (27), Pg. 6658-6661
- Lopez, JS, and Banerji, U, 2017, Combine and conquer: challenges for targeted therapy combinations in early phase trials, *Nat Rev Clin Oncol.*, 14 (1), Pg. 57-66
- Lopez-Acevedo, M, Grace, L, Teoh, D, Whitaker, R, Adams, DJ, Jia, J, Nixon, AB, and Secord, AA, 2014, Dasatinib (BMS-35482) potentiates the activity of gemcitabine and docetaxel in uterine leiomyosarcoma cell lines, *Gynecol Oncol Res Pract.*, 1, Pg. 2
- Lostes-Bardaji, MJ, García-Illescas, D, Valverde, C, and Serrano, C, 2021, Ripretinib in gastrointestinal stromal tumor: the long-awaited step forward, *Ther Adv Med Oncol.*, 13, 1758835920986498

Lovly, CM, and Shaw, AT, 2014, Molecular pathways: resistance to kinase inhibitors and implications for therapeutic strategies, *Clin Cancer Res.*, 20 (9), Pg. 2249-2256

Lu, C, Zhang, Q, Zhang, H, Li, X, Jiang, Q, and Yao, J, 2021, A small molecular multi-targeting tyrosine kinase inhibitor, anlotinib, inhibits pathological ocular neovascularization, *Biomed Pharmacother.*, 138, Pg. 111493

Lu, Y, Yu, Q, Liu, JH, Zhang, J, Wang, H, Koul, D, McMurray, JS, Fang, X, Yung, WKA, Siminovitch, KA, and Mills, GB, 2003, Src family protein-tyrosine kinases alter the function of PTEN to regulate phosphatidylinositol 3-kinase/AKT cascades, *J Biol Chem.*, 278 (41), Pg. 40057-40066

Lucchesi, C, Khalifa, E, Laizet, Y, Soubeyran, I, Mathoulin-Pelissier, S, Chomienne, C, and Italiano, A, 2018, Targetable alterations in adult patients with soft-tissue sarcomas: insights for personalized therapy, *JAMA Oncol.*, 4 (10), Pg. 1398-1404

Luttrell, DK, and Luttrell, LM, 2004, Not so strange bedfellows: G-protein-coupled receptors and Src family kinases, *Oncogene.*, 23 (48), Pg. 7969-7978

Lv, F, Song, LJ, Wang, XH, Qiu, F, and Li, XF, 2013, The role of Act1, a NF- κ B-activating protein, in IL-6 and IL-8 levels induced by IL-17 stimulation in SW982 cells, *Pharm Biol.*, 51 (11), Pg. 1444-1450

MacCord, K, 2012, Mesenchyme, Embryo Project Encyclopedia, ISSN: 1940-5030, <http://embryo.asu.edu/handle/10776/3941>, Last accessed [May 2020]

MacManus, CF, Pettigrew, J, Seaton, A, Wilson, C, Maxwell, PJ, Berlinger, S, Purcell, C, McGurk, M, Johnston, PG, and Waugh, DJJ, 2007, Interleukin-8 signaling promotes translational regulation of cyclin D in androgen-independent prostate cancer cells, *Mol Cancer Res.*, 5 (7), Pg. 737-748

Madsen, RR, Vanhaesebroeck, B, and Semple, RK, 2018, Cancer-associated PIK3CA mutations in overgrowth disorders, *Trends Mol Med.*, 24 (10), Pg. 856-870

Maki, RG, D'Adamo, DR, Keohan, ML, Saulle, M, Schuetze, SM, Undevia, SD, Livingston, MB, Cooney, MM, Hensley, ML, Mita, MM, Takimoto, CH, Kraft, AS, Elias, AD, Brockstein, B, Blachère, NE, Edgar, MA, Schwartz, LH, Qin, LX, Antonescu, CR, and Schwartz, GK, 2009, Phase II study of sorafenib in patients with metastatic or recurrent sarcomas, *J Clin Oncol.*, 27 (19), Pg. 3133-3140

Maki, RG, Jungbluth, AA, Gnjjatic, S, Schwartz, GK, D'Adamo, DR, Keohan, ML, Wagner, MJ, Scheu, K, Chiu, R, Ritter, E, Kachel, J, Lowy, I, Old, LJ, and Ritter, G, 2013, A pilot study of anti-CTLA4 antibody ipilimumab in patients with synovial sarcoma, *Sarcoma.*, 2013, Pg. 168145

Malkin, D, 2011, Li-Fraumeni Syndrome, *Genes Cancer.*, 2 (4), Pg. 475-484

Manning, BD, and Toker, A, 2017, AKT/PKB signaling: navigating the network, *Cell.*, 169 (3), Pg. 381-405

Mansoori, B, Mohammadi, A, Davudian, S, Shirjang, S, and Baradaran, B, 2017, The different mechanisms of cancer drug resistance: a brief review, *Adv Pharm Bull.*, 7 (3), Pg. 339-348

Marabelle, A, Fakih, M, Lopez, J, Shah, M, Shapira-Frommer, R, Nakagawa, K, Chung, HC, Kindler, HL, Lopez-Martin, JA, Miller Jr., WH, Italiano, A, Kao, S, Piha-Paul, SA, Delord, JP, McWilliams, RR, Fabrizio, DA, Aurora-Garg, D, Xu, L, Jin, F, Norwood, K, and Bang, YJ, 2020, Association of tumour mutational burden with outcomes in patients with advanced solid tumours treated with pembrolizumab: prospective biomarker analysis of the multicohort, open-label, phase 2 KEYNOTE-158 study, *Lancet Oncol.*, 21 (10), Pg. 1353-1365

Mariño-Enríquez, A, and Bovée, JVMG, 2016, Molecular pathogenesis and diagnostic, prognostic and predictive molecular markers in sarcoma, *Surg Pathol Clin.*, 9 (3), Pg. 457-473

Marlin, MC, and Li, G, 2015, Biogenesis and function of the NGF/TrkA signaling endosome, *Int Rev Cell Mol Biol.*, 314, Pg. 239-257

Marofi, F, Motavalli, R, Safonov, VA, Thangavelu, L, Yumashev, AV, Alexander, M, Shomali, N, Chartrand, MS, Pathak, Y, Jarahian, M, Izadi, S, Hassanzadeh, A, Shirafkan, N, Tahmasebi, S, and Khiavi, FM, 2021, CAR T cells in solid tumors: challenges and opportunities, *Stem Cell Res Ther.*, 12 (1), Pg. 81

Marrari, A, Bertuzzi, A, Bozzarelli, S, Gennaro, N, Giordano, L, Quagliuolo, V, De Sanctis, R, Sala, S, Balzarini, L, and Santoro, A, 2020, Activity of regorafenib in advanced pretreated soft tissue sarcoma: results of a single-center phase II study, *Medicine (Baltimore).*, 99 (26), e20719

Martín-Broto, J, Stacchiotti, S, Lopez-Pousa, A, Redondo, A, Bernabeu, D, De Alava, E, Casali, PG, Italiano, A, Gutierrez, A, Moura, DS, Peña-Chilet, M, Diaz-Martin, J, Biscuola, M, Taron, M, Collini, P, Ranchere-Vince, D, Del Muro, XG, Grignani, G, Dumont, S, Martinez-Trufero, J, Palmerini, E, Hindi, N, Sebio, A, Dopazo, J, Dei Tos, AP, Le Cesne, A, Blay, JY, and Cruz, J, 2019, Pazopanib for treatment of advanced malignant and dedifferentiated solitary fibrous tumour: a multicentre, single-arm, phase 2 trial, *Lancet Oncol.*, 20 (1), Pg. 134-144

Martín-Broto, J, Cruz, J, Penel, N, Le Cesne, A, Hindi, N, Luna, P, Moura, DS, Bernabeu, D, De Alava, E, Lopez-Guerrero, JA, Dopazo, J, Peña-Chilet, M, Gutierrez, A, Collini, P, Karanian, M, Redondo, A, Lopez-Pousa, A, Grignani, G, Diaz-

- Martin, J, Marcilla, D, Fernandez-Serra, A, Gonzalez-Aguilera, C, Casali, PG, Blay, JY, and Stacchiotti, S, 2020, Pazopanib for treatment of typical solitary fibrous tumours: a multicentre, single-arm, phase 2 trial, *Lancet Oncol.*, 21 (3), Pg. 456-466
- Martín-Broto, J, Reichardt, P, Jones, RL, and Stacchiotti, S, 2020, Different approaches to advanced soft tissue sarcomas depending on treatment line, goal of therapy, and histological subtype, *Expert Rev Anticancer Ther.*, 20 (Sup1), Pg. 15-28
- Martín-Broto, J, Mondaza-Hernandez, JL, Moura, DS, and Hindi, N, 2021, A comprehensive review on solitary fibrous tumor: new insights for new horizons, *Cancers (Basel).*, 13 (12), Pg. 2913
- Martínez, PT, Navaias, PL, and Lietha, D, 2020, FAK structure and regulation by membrane interactions and force in focal adhesions, *Biomolecules.*, 10 (2), Pg. 179
- Martins, AS, Olmos, D, Missiaglia, E, and Shipley, J, 2011, Targeting the insulin-like growth factor pathway in rhabdomyosarcomas: rationale and future perspectives, *Sarcoma.*, 2011, Pg. 209736
- Maruzzo, M, Martin-Liberal, J, Messiou, C, Miah, A, Thway, K, Alvarado, R, Judson, I, and Benson, C, 2015, Pazopanib as first line treatment for solitary fibrous tumours: the Royal Marsden Hospital experience, *Clin Sarcoma Res.*, 5, Pg. 5
- Mas-Moruno, C, Rechenmacher, F, and Kessler, H, 2010, Cilengitide: the first anti-angiogenic small molecule drug candidate design, synthesis and clinical evaluation, *Anticancer Agents Med Chem.*, 10 (10), Pg. 753-768
- Mastboom, MJL, Hoek, DM, Bovée, JVMG, Van de Sande, MAJ, and Suzhai, K, 2019, Does CSF1 overexpression or rearrangement influence biological behaviour in tenosynovial giant cell tumours of the knee?, *Histopathology.*, 74 (2), Pg. 332-340
- Mathur, S, and Sutton, J, 2017, Personalised medicine could transform healthcare, *Biomed Rep.*, 7 (1), Pg. 3-5
- Maurer, G, Tarkowski, B, and Baccharini, M, 2011, Raf kinases in cancer-roles and therapeutic opportunities, *Oncogene.*, 30 (32), Pg. 3477-3488
- McArthur, GA, Demetri, GD, van Oosterom, A, Heinrich, MC, Debiec-Rychter, M, Corless, CL, Nikolova, Z, Dimitrijevic, S, and Fletcher, JA, 2005, Molecular and clinical analysis of locally advanced dermatofibrosarcoma protuberans treated with imatinib: imatinib target exploration consortium study B2225, *J Clin Oncol.*, 23 (4), Pg. 866-873
- McKay, MM, and Morrison, DK, 2007, Integrating signals from RTKs to ERK/MAPK, *Oncogene.*, 26 (22), Pg. 113-121
- Medves, S, and Demoulin, JB, 2012, Tyrosine kinase gene fusions in cancer: translating mechanisms into targeted therapies, *J Cell Mol Med.*, 16 (2), Pg. 237-248
- Mello, SS, and Attardi, LD, 2018, Deciphering p53 signaling in tumor suppression, *Curr Opin Cell Biol.*, 51, Pg. 65-72
- Mendel, DB, Laird, AD, Xin, X, Louie, SG, Christensen, JG, Li, G, Schreck, RE, Abrams, TJ, Ngai, TJ, Lee, LB, Murray, LJ, Carver, J, Chan, E, Moss, KG, Haznedar, JO, Sukbuntherng, J, Blake, RA, Sun, L, Tang, C, Miller, T, Shirazian, S, McMahon, G, and Cherrington, JM, 2003, In vivo antitumor activity of SU11248, a novel tyrosine kinase inhibitor targeting vascular endothelial growth factor and platelet-derived growth factor receptors: determination of a pharmacokinetic/pharmacodynamic relationship, *Clin Cancer Res.*, 9 (1), Pg. 327-337
- Mendoza, MC, Er, EE, and Blenis, J, 2011, The Ras-ERK and PI3K-mTOR pathways: cross-talk and compensation, *Trends Biochem Sci.*, 36 (6), Pg. 320-328
- Menegaz, BA, Cuglievan, B, Benson, J, Camacho, P, Lamhamedi-Cherradi, SE, Leung, CH, Warneke, CL, Huh, W, Subbiah, V, Benjamin, RS, Patel, S, Daw, N, Hayes-Jordan, A, and Ludwig, JA, 2018, Clinical activity of pazopanib in patients with advanced desmoplastic small round cell tumor, *Oncologist.*, 23 (3), Pg. 360-366
- Menge, F, Jakob, J, Kasper, B, Smakic, A, Gaiser, T, and Hohenberger, P, 2018, Clinical presentation of gastrointestinal stromal tumors, *Visc Med.*, 34 (5), Pg. 335-340
- Merry, E, Thway, K, Jones, RL, and Huang, PH, 2021, Predictive and prognostic transcriptomic biomarkers in soft tissue sarcomas, *NPJ Precis Oncol.*, 5 (1), Pg. 17
- Michaelis, M, Wass, MN, and Cintatl, J, 2019, Drug-adapted cancer cell lines as preclinical models of acquired resistance, *Cancer Drug Resist.*, 2, Pg. 447-456
- Michels, S, Trautmann, M, Sievers, E, Kindler, D, Huss, S, Renner, M, Friedrichs, N, Kirfel, J, Steiner, S, Endl, E, Wurst, P, Heukamp, L, Penzel, R, Larsson, O, Kawai, A, Tanaka, S, Sonobe, H, Schirmacher, P, Mechttersheimer, G, Wardelmann, E, Büttner, R, and Hartmann, W, 2013, SRC signaling is crucial in the growth of synovial sarcoma cells, *Cancer Res.*, 73 (8), Pg. 2518-2528
- Milella, M, Falcone, I, Conciatori, F, Incani, UC, Del Curatolo, A, Inzerilli, N, Nuzzo, CMA, Vaccaro, V, Vari, S, Cognetti, F, and Ciuffreda, L, 2015, PTEN: Multiple functions in human malignant tumors, *Front Oncol.*, 5, Pg. 24

Mir, O, Domont, J, Cioffi, A, Bonvalot, S, Boulet, B, Le Pechoux, C, Terrier, P, Spielmann, M, and Le Cesne, A, 2011, Feasibility of metronomic oral cyclophosphamide plus prednisolone in elderly patients with inoperable or metastatic soft tissue sarcoma, *Eur J Cancer.*, 47 (4), Pg. 515-519

Mir, O, Brodowicz, T, Italiano, A, Wallet, J, Blay, JY, Bertucci, F, Chevreau, C, Piperno-Neumann, S, Bompas, E, Salas, S, Perrin, C, Delcambre, C, Liegl-Atzwanger, B, Toulmonde, M, Dumont, S, Ray-Coquard, I, Clisant, S, Taieb, S, Guillemet, C, Rios, M, Collard, O, Bozec, L, Cupissol, D, Saada-Bouzid, E, Lemaignan, C, Eisterer, W, Isambert, N, Chaigneau, L, Le Cesne, A, and Penel, N, 2016, Safety and efficacy of regorafenib in patients with advanced soft tissue sarcoma (REGOSARC): a randomised, double-blind, placebo-controlled, phase 2 trial, *Lancet Oncol.*, 17 (12), Pg. 1732-1742

Miranda, C, Nucifora, M, Molinari, F, Conca, E, Anania, MC, Bordoni, A, Saletti, P, Mazzucchelli, L, Pilotti, S, Pierotti, MA, Tamborini, E, Greco, A, and Frattini, M, 2012, KRAS and BRAF mutations predict primary resistance to imatinib in gastrointestinal stromal tumors, *Clin Cancer Res.*, 18 (6), Pg. 1769-1776

Mito, JK, Mitra, D, and Doyle, LA, 2019, Radiation-associated sarcomas: an update on clinical, histological, and molecular features, *Surg Pathol Clin.*, 12 (1), Pg. 139-148

Mitra, SK, and Schlaepfer, DD, 2006, Integrin-regulated FAK-Src signaling in normal and cancer cells, *Curr Opin Cell Biol.*, 18(5), Pg. 516-523

Mittal, P, and Roberts, CWM, 2020, The SWI/SNF complex in cancer – biology, biomarkers and therapy, *Nat Rev Clin Oncol.*, 17 (7), Pg. 435-448

Miyake, K, Higuchi, T, Oshiro, H, Zhang, Z, Sugisawa, N, Park, JH, Razmjooei, S, Katsuya, Y, Barangi, M, Li, Y, Nelson, SD, Murakami, T, Homma, Y, Hiroshima, Y, Matsuyama, R, Bouvet, M, Chawla, SP, Singh, SR, Endo, I, and Hoffman, RM, 2019, The combination of gemcitabine and docetaxel arrests a doxorubicin-resistant dedifferentiated liposarcoma in a patient-derived orthotopic xenograft model, *Biomed Pharmacother.*, 117, Pg. 109093

Morgenstern, JP, and Land, H, 1990, Advanced mammalian gene transfer: high titre retroviral vectors with multiple drug selection markers and a complementary helper-free packaging cell line, *Nucleic Acids Res.*, 18 (12), Pg. 3587-3596

Mroz, EA, Tward, AD, Pickering, CR, Myers, JN, Ferris, RL, and Rocco, JW, 2013, High intratumor genetic heterogeneity is related to worse outcome in patients with head and neck squamous cell carcinoma, *Cancer.*, 119 (16), Pg. 3034-3042

Mukaihara, K, Tanabe, Y, Kubota, D, Akaike, K, Hayashi, T, Mogushi, K, Hosoya, M, Sato, S, Kobayashi, E, Okubo, T, Kim, Y, Kohsaka, S, Saito, T, Kaneko, K, and Suehara, Y, 2017, Cabozantinib and dastinib exert anti-tumor activity in alveolar soft part sarcoma, *PLoS One.*, 12 (9), e0185321

Murray, LJ, Abrams, TJ, Long, KR, Ngai, TJ, Olson, LM, Hong, W, Keast, PK, Brassard, JA, O'Farrell, AM, Cherrington, JM, and Pryer, NK, 2003, SU11248 inhibits tumor growth and CSF-1R-dependent osteolysis in an experimental breast cancer bone metastasis model, *Clin Exp Metastasis.*, 20 (8), Pg. 757-766

Najy, AJ, Jung, YS, Won, JJ, Conley-LaComb, MK, Saliganan, A, Kim, CJ, Heath, E, Cher, ML, Bonfil, RD, and Kim, HRC, 2012, Cediranib inhibits both the intraosseous growth of PDGF D-positive prostate cancer cells and the associated bone reaction, *Prostate.*, 72 (12), Pg. 1328-1338

Nakamura, IT, Kohsaka, S, Ikegami, M, Ikeuchi, H, Ueno, T, Li, K, Beyett, TS, Koyama, T, Shimizu, T, Yamamoto, N, Takahashi, F, Takahashi, K, Eck, MJ, and Mano, H, 2021, Comprehensive functional evaluation of variants of fibroblast growth factor receptor genes in cancer, *NPJ Precis Oncol.*, 5 (1), Pg. 66

Nakamura, T, Matsumine, A, Kawai, A, Araki, N, Goto, T, Yonemoto, T, Sugiura, H, Nishida, Y, Hiraga, H, Honoki, K, Yasuda, T, Boku, S, Sudo, A, and Ueda, T, 2016, The clinical outcome of pazopanib treatment in Japanese patients with relapsed soft tissue sarcoma: A Japanese Musculoskeletal Oncology Group (JMOG) study, *Cancer.*, 122 (9), Pg. 1408-1416

Nakano, K, Motoi, N, Inagaki, L, Tomomatsu, J, Gokita, T, Ae, K, Tanizawa, T, Shimoji, T, Matsumoto, S, and Takahashi, S, 2015, Differences in the responses to pazopanib and the prognoses of soft tissue sarcomas by their histological eligibility for the PALETTE study, *Jpn J Clin Oncol.*, 45 (5), Pg. 449-455

Napolitano, A, Ostler, AE, Jones, RL, and Huang, PH, 2021, Fibroblast growth factor receptor (FGFR) signaling in GIST and soft tissue sarcomas, *Cells.*, 10 (6), Pg. 1533

Naqash, AR, Coyne, GHO, Moore, N, Sharon, E, Takebe, N, Fino, KK, Ferry-Galow, KV, Hu, JS, Van Tine, BA, Burgess, MA, Read, WL, Riedel, RF, George, S, Glod, J, Conley, AP, Foster, JC, Fogli, LK, Parchment, RE, Doroshow, JH, and Chen, AP, 2021, Phase II study of atezolizumab in advanced alveolar soft part sarcoma, *J Clin Oncol.*, 39 (15), https://ascopubs.org/doi/abs/10.1200/JCO.2021.39.15_suppl.11519, Last accessed [November 2021]

Najjar, YG, Rayman, P, Jia, X, Pavicic Jr., PG, Rini, BI, Tannenbaum, C, Ko, J, Haywood, S, Cohen, P, Hamilton, T, Diaz-Montero, CM, and Finke, J, 2017, Myeloid-derived suppressor cell subset accumulation in renal cell carcinoma parenchyma is associated with intratumoral expression of IL1 β , IL8, CXCL5, and Mip-1 α , *Clin Cancer Res.*, 23 (9), Pg. 2346-2355

Nathenson, M, Choy, E, Carr, ND, Hibbard, HD, Mazzola, E, Catalano, PJ, Thornton, KA, Morgan, JA, Cote, GM, Merriam, P, Wagner, AJ, Demetri, GD, and George, S, 2020, Phase II study of eribulin and pembrolizumab in patients (pts) with

metastatic soft tissue sarcomas (STS): report of LMS cohort, *J Clin Oncol.*, https://ascopubs.org/doi/abs/10.1200/JCO.2020.38.15_suppl.11559, Last accessed [November 2021]

National Cancer Intelligence Network, 2013, Bone and Soft Tissue Sarcomas: UK Incidence and Survival: 1996 to 2010 Volume 2, <http://www.ncin.org.uk/home>, Last accessed [May 2020]

Navid, S, Fan, C, Flores-Villanueva, PO, Generali, D, and Li, Y, 2020, The fibroblast growth factor receptors in breast cancer: from oncogenesis to better treatments, *Int J Mol Sci.*, 21 (6), Pg. 2011

NCT00031915, National Cancer Institute (NCI), 2013, Imatinib mesylate in treating patients with advanced soft tissue sarcoma or bone sarcoma, <https://clinicaltrials.gov/ct2/show/NCT00031915>, Last accessed [January 2021]

NCT00075218, Pfizer, 2009, A study to assess the safety and efficacy of SU11248 in patients with gastrointestinal stromal tumor (GIST), <https://clinicaltrials.gov/ct2/show/NCT00075218>, Last accessed [January 2021]

NCT00084630, National Cancer Institute (NCI), 2013, Imatinib mesylate in treating patients with locally recurrent or metastatic dermatofibrosarcoma protuberans, <https://clinicaltrials.gov/ct2/show/NCT00084630>, Last accessed [January 2021]

NCT00085475, European Organisation for Research and Treatment of Cancer (EORTC), 2012, Imatinib mesylate in treating patients with locally advanced or metastatic dermatofibrosarcoma protuberans or giant cell fibroblastoma, <https://clinicaltrials.gov/ct2/show/NCT00085475>, Last accessed [January 2021]

NCT00122473, Dermatologic Cooperative Oncology Group, 2011, Imatinib in dermatofibrosarcoma protuberans (DFSP), <https://www.clinicaltrials.gov/ct2/show/NCT00122473>, Last accessed [January 2021]

NCT00245102, National Cancer Institute (NCI), 2014, Sorafenib in treating patients with metastatic, locally advanced, or recurrent sarcoma, <https://clinicaltrials.gov/ct2/show/NCT00245102>, Last accessed [October 2021]

NCT00287846, UNICANCER, 2016, Imatinib mesylate in treating patients with recurrent or refractory fibromatosis, <https://clinicaltrials.gov/ct2/show/NCT00287846>, Last accessed [January 2021]

NCT00297258, GlaxoSmithKline, 2016, Pazopanib in patients with relapsed or refractory soft tissue sarcoma, <https://clinicaltrials.gov/ct2/show/NCT00297258>, Last accessed [September 2021]

NCT00464620, Sarcoma Alliance for Research through Collaboration, 2018, Trial of dasatinib in advanced sarcomas, <https://clinicaltrials.gov/ct2/show/NCT00464620>, Last accessed [January 2021]

NCT00474994, Memorial Sloan Kettering Cancer Center, 2016, Sunitinib in treating patients with metastatic, locally advanced, or locally recurrent sarcomas, <https://clinicaltrials.gov/ct2/show/NCT00474994>, Last accessed [January 2021]

NCT00753688, GlaxoSmithKline, 2013, Pazopanib versus placebo in patients with soft tissue sarcoma whose disease has progressed during or following prior therapy (PALETTE), <https://clinicaltrials.gov/ct2/show/NCT00753688>, Last accessed [January 2021]

NCT00874874, Centre Oscar Lambret, 2009, Sorafenib in treating patients with angiosarcoma that is locally advanced, metastatic, or unable to be removed by surgery, <https://clinicaltrials.gov/ct2/show/NCT00874874>, Last accessed [January 2021]

NCT00902044, Baylor College of Medicine, 2021, Her2 chimeric antigen receptor expressing T cells in advanced sarcoma, <https://clinicaltrials.gov/ct2/show/NCT00902044>, Last accessed [October 2021]

NCT00942877, National Cancer Institute (NCI), 2021, Phase II study of cediranib (AZD2171) in patients with alveolar soft part sarcoma, <https://clinicaltrials.gov/ct2/show/NCT00942877>, Last accessed [January 2021]

NCT01059656, Assistance Publique – Hôpitaux de Paris, 2016, Phase II pazopanib study in advanced dermatofibrosarcomas (DFSP-PAZO), <https://clinicaltrials.gov/ct2/show/NCT01059656>, Last accessed [September 2021]

NCT01137916, Heidelberg University, 2017, Study to evaluate imatinib in desmoid tumors, <https://clinicaltrials.gov/ct2/show/NCT01137916>, Last accessed [January 2021]

NCT01140737, Sheffield Teaching Hospitals NHS Foundation Trust, 2021, A study of axitinib in patients with advanced angiosarcoma and other soft tissue sarcomas (Axi-STS), <https://www.clinicaltrials.gov/ct2/show/NCT01140737>, Last accessed [October 2021]

NCT01271712, Bayer, 2020, Study of regorafenib as a 3rd-line or beyond treatment for gastrointestinal stromal tumors (GIST) (GRID), <https://clinicaltrials.gov/ct2/show/NCT01271712>, Last accessed [January 2021]

NCT01337401, Institute of Cancer Research, United Kingdom, 2019, A trial of cediranib in the treatment of patients with alveolar soft part sarcoma (CASPS) (CASPS), <https://clinicaltrials.gov/ct2/show/NCT01337401>, Last accessed [January 2021]

NCT01391962, National Cancer Institute (NCI), 2021, Sunitinib or cediranib for alveolar soft part sarcoma, <https://www.clinicaltrials.gov/ct2/show/NCT01391962>, Last accessed [October 2021]

NCT01495598, National Cancer Institute (NCI), 2020, Pomalidomide for Kaposi Sarcoma in people with or without HIV, <https://clinicaltrials.gov/ct2/show/NCT01495598>, Last accessed [January 2021]

NCT01506595, Vector Oncology, 2017, Study of pazopanib in the treatment of surgically unresectable or metastatic liposarcoma, Study of pazopanib in the treatment of surgically unresectable or metastatic liposarcoma, <https://clinicaltrials.gov/ct2/show/NCT01506596>, Last accessed [September 2021]

NCT01524926, European Organisation for Research and Treatment of Cancer – EORTC, CREATE: Cross-tumoral phase 2 with crizotinib (CREATE), 2020, <https://clinicaltrials.gov/ct2/show/NCT01524926>, Last accessed [January 2021]

NCT01643278, National Cancer Institute (NCI), 2017, Dasatinib and ipilimumab in treating patients with gastrointestinal stromal tumors or other sarcomas that cannot be removed by surgery or are metastatic, <https://clinicaltrials.gov/ct2/show/NCT01643278>, Last accessed [November 2021]

NCT01692496, Grupo Espanol de Investigacion en Sarcomas, 2020, Activity and tolerability of pazopanib in advanced and/or metastatic liposarcoma. A phase II clinical trial, <https://clinicaltrials.gov/ct2/show/NCT01692496>, Last accessed [September 2021]

NCT01861951, Hannover Medical School, 2017, A trial comparing two medications as first treatment in elderly patients with metastatic or advanced soft tissue sarcoma (EPAZ), <https://clinicaltrials.gov/ct2/show/NCT01861951>, Last accessed [September 2021]

NCT01876082, Institut Bergonié, Pazopanib efficacy and tolerance in desmoid tumors (DESMOPAZ), <https://clinicaltrials.gov/ct2/show/NCT01876082>, Last accessed [September 2021]

NCT01876511, Sidney Kimmel Comprehensive Cancer Center at John Hopkins, 2020, Study of MK-3475 in patients with microsatellite unstable (MSI) tumors (cohorts A, B, and C), <https://clinicaltrials.gov/ct2/show/NCT01876511>, Last accessed [May 2021]

NCT01878448, Chia Tai Tianqing Pharmaceutical Group Co., Ltd., 2019, A phase II study of anlotinib in STS patients (ALTN/STS), <https://clinicaltrials.gov/ct2/show/NCT01878448>, Last accessed [January 2021]

NCT01900743, Bayer, 2018, Phase II study of regorafenib in metastatic soft tissue sarcoma (REGO-SARC), <https://clinicaltrials.gov/ct2/show/NCT01900743>, Last accessed [January 2021]

NCT02048371, Sarcoma Alliance for Research through Collaboration, 2020, SARC024: A blanket protocol to study oral regorafenib in patients with selected sarcoma subtypes, <https://clinicaltrials.gov/ct2/show/NCT02048371>, Last accessed [June 2021]

NCT02066181, National Cancer Institute (NCI), 2021, Sorafenib tosylate in treating patients with desmoid tumors or aggressive fibromatosis, <https://clinicaltrials.gov/ct2/show/NCT02066181>, Last accessed [January 2021]

NCT02066285, Grupo Espanol de Investigacion en Sarcomas, 2021, Trial of pazopanib in patients with solitary fibrous tumor and extraskelatal myxoid chondrosarcoma, <https://clinicaltrials.gov/ct2/show/NCT02066285>, Last accessed [September 2021]

NCT02097810, Hoffmann-La Roche, 2020, Study of oral RXDX-101 in adult patients with locally advanced or metastatic cancer targeting NTRK1, NTRK2, NTRK3, ROS1, or ALK molecular alterations. (STARTRK-1), <https://clinicaltrials.gov/ct2/show/NCT02097810>, Last accessed [January 2021]

NCT02107963, National Cancer Institute (NCI), 2021, A phase I trial of T cells expressing an Anti-GD2 chimeric antigen receptor in children and young adults with GD2+ solid tumors, <https://clinicaltrials.gov/ct2/show/NCT02107963>, Last accessed [October 2021]

NCT02113826, Seoul National University Hospital, 2017, Pazopanib for metastatic alveolar soft part sarcoma, <https://clinicaltrials.gov/ct2/show/NCT02113826>, Last accessed [September 2021]

NCT02122913, Bayer, 2020, A study to test the safety of the investigational drug Larotrectinib in adults that may treat cancer, <https://clinicaltrials.gov/ct2/show/NCT02122913>, Last accessed [January 2021]

NCT02261207, Fondazione IRCCS Istituto Nazionale dei Tumori, Milano, 2014, Phase II study on axitinib in advanced solitary fibrous tumor, <https://clinicaltrials.gov/ct2/show/NCT02261207>, Last accessed [January 2021]

NCT02300545, Washington University School of Medicine, 2020, Pazopanib as front-line therapy in patients with non-resectable or metastatic soft tissue sarcomas who are not candidates for chemotherapy, <https://clinicaltrials.gov/ct2/show/NCT02300545>, Last accessed [September 2021]

NCT02301039, 2020, SARC028: A phase II study of the Anti-PD1 antibody pembrolizumab (MK-3475) in patients with advanced sarcomas, <https://clinicaltrials.gov/ct2/show/NCT02301039>, Last accessed [November 2021]

NCT02304458, National Cancer Institute (NCI), 2021, Nivolumab with or without ipilimumab in treating younger patients with recurrent or refractory solid tumors or sarcomas, <https://clinicaltrials.gov/ct2/show/NCT02304458>, Last accessed [November 2021]

NCT02307500, Istituto Clinico Humanitas, 2020, Regorafenib in patients with metastatic solid tumors who have progressed after standard therapy (RESOUND), <https://clinicaltrials.gov/ct2/show/NCT02307500>, Last accessed [October 2021]

NCT02371369, Daiichi Sankyo Inc., 2020, Phase 3 study of pexidartinib for pigmented villonodular synovitis (PVNS) or giant cell tumor of the tendon sheath (GCT-TS) (ENLIVEN), <https://clinicaltrials.gov/ct2/show/NCT02371369>, Last accessed [January 2021]

NCT02406781, Institut Bergonié, 2021, Combination of MK3475 and metronomic cyclophosphamide in patients with advanced sarcomas: multicentre phase II trial (PEMBROSARC), <https://clinicaltrials.gov/ct2/show/NCT02406781>, Last accessed [November 2021]

NCT02428192, National Cancer Institute (NCI), 2021, Nivolumab alone or in combination with ipilimumab in treating patients with advanced uterine leiomyosarcoma, <https://clinicaltrials.gov/ct2/show/NCT02428192>, Last accessed [November 2021]

NCT02449343, Chia Tai Tianqing Pharmaceutical Group Co. Ltd., Study of anlotinib in patients with soft tissue sarcoma (STS) (ALTER0203), <https://clinicaltrials.gov/ct2/show/NCT02449343>, Last accessed [October 2021]

NCT02500797, National Cancer Institute (NCI), Nivolumab with or without ipilimumab in treating patients with metastatic sarcoma that cannot be removed by surgery, <https://clinicaltrials.gov/ct2/show/NCT02500797>, Last accessed [November 2021]

NCT02508532, Blueprint Medicines Corporation, 2020, (NAVIGATOR) Study of BLU-285 in patients with gastrointestinal stromal tumors (GIST) and other relapsed and refractory solid tumors, <https://clinicaltrials.gov/ct2/show/NCT02508532>, Last accessed [January 2021]

NCT02568267, Hoffmann-La Roche, 2020, Basket study of entrectinib (RXDX-101) for the treatment of patients with solid tumors harboring NTRK 1/2/3 (Trk A/B/C), ROS1, or ALK gene rearrangements (Fusions) (STARTRK-2), <https://clinicaltrials.gov/ct2/show/NCT02568267>, Last accessed [January 2021]

NCT02576431, Bayer, 2020, A study to test the effect of the drug larotrectinib in adults and children with NTRK-fusion positive solid tumors (NAVIGATE), <https://clinicaltrials.gov/ct2/show/NCT02576431>, Last accessed [January 2021]

NCT02601950, Epizyme Inc., 2020, A phase II, multicenter study of the EZH2 inhibitor tazemetostat in adult subjects with INI1-negative tumors or relapsed/refractory synovial sarcoma, <https://clinicaltrials.gov/ct2/show/NCT02601950>, Last accessed [January 2021]

NCT02628067, Merck Sharp & Dohme Corp., 2021, Study of Pembrolizumab (MK-3475) in participants with advanced solid tumors (MK-3475-158/KEYNOTE-158), <https://clinicaltrials.gov/ct2/show/NCT02628067>, Last accessed [May 2021]

NCT02636725, Jonathan Trent, MD, PhD, 2021, Axitinib and pembrolizumab in subjects with advanced alveolar soft part sarcoma and other soft tissue sarcomas, <https://clinicaltrials.gov/ct2/show/NCT02636725>, Last accessed [November 2021]

NCT02637687, Bayer, 2020, A study to test the safety and efficacy of the drug larotrectinib for the treatment of tumors with NTRK-fusion in children (SCOUT), <https://clinicaltrials.gov/ct2/show/NCT02637687>, Last accessed [January 2021]

NCT02808247, European Organisation for Research and Treatment of Cancer – EORTC, 2021, Ph II nintedanib vs. ifosfamide in soft tissue sarcoma (ANITA), <https://clinicaltrials.gov/ct2/show/NCT02808247>, Last accessed [October 2021]

NCT02815995, M.D. Anderson Cancer Center, Multi-arm study to test the efficacy of immunotherapeutic agents in multiple sarcoma subtypes, <https://clinicaltrials.gov/ct2/show/NCT02815995>, Last accessed [November 2021]

NCT02888665, Fred Hutchinson Cancer Research Center, 2021, Pembrolizumab and doxorubicin hydrochloride in treating patients with sarcoma that is metastatic or cannot be removed by surgery, <https://clinicaltrials.gov/ct2/show/NCT02888665>, Last accessed [November 2021]

NCT02978859, Mirati Therapeutics Inc., 2021, Sitravatinib in advanced liposarcoma and other soft tissue sarcomas, <https://clinicaltrials.gov/ct2/show/NCT02978859>, Last accessed [October 2021]

NCT03016819, Advenchen Laboratories LLC, 2021, Phase III trial of anlotinib, catequentinib in advanced alveolar soft part sarcoma, leiomyosarcoma, synovial sarcoma (APROMISS) (APROMISS), <https://clinicaltrials.gov/ct2/show/NCT03016819>, Last accessed [October 2021]

NCT03138161, Sarcoma Oncology Research Center, LLC, 2021, SAINT: Trabectedin, ipilimumab and nivolumab as first line treatment for advanced soft tissue sarcoma, <https://clinicaltrials.gov/ct2/show/NCT03138161>, Last accessed [November 2021]

NCT03141684, National Cancer Institute (NCI), Testing atezolizumab and bevacizumab in people with advanced alveolar soft part sarcoma, <https://clinicaltrials.gov/ct2/show/NCT03141684>, Last accessed [November 2021]

NCT03171389, Sebastian Bauer, Universität Duisberg-Essen, 2017, POETIG trial – ponatinib after resistance to imatinib in GIST (POETIG), <https://clinicaltrials.gov/ct2/show/NCT03171389>, Last accessed [October 2021]

NCT03210714, National Cancer Institute (NCI), 2021, Erdafitinib in treating patients with relapsed or refractory advanced solid tumors, non-hodgkin lymphoma, or histiocytic disorders with FGFR mutations (a pediatric MATCH treatment trial), <https://clinicaltrials.gov/ct2/show/NCT03210714>, Last accessed [October 2021]

NCT03215511, Bayer, 2021, A study to test the safety of the investigational drug selitrectinib in children and adults that may treat cancer, <https://clinicaltrials.gov/ct2/show/NCT03215511>, Last accessed [February 2021]

NCT03353753, Deciphera Pharmaceuticals LLC, 2019, Phase 3 study of DCC-2618 vs placebo in advanced GIST patients who have been treated with prior anticancer therapies (Invictus), <https://clinicaltrials.gov/ct2/show/NCT03353753>, Last accessed [January 2021]

NCT03356782, Shenzhen Geno-Immune Medical Institute, 2020, Safety and efficacy of 4th generation safety-engineered CAR T cells targeting sarcomas, <https://clinicaltrials.gov/ct2/show/NCT03356782>, Last accessed [October 2021]

NCT03396211, Elevar Therapeutics, Study to evaluate apatinib (also known as rivoceranib) plus nivolumab in patients with unresectable or metastatic cancer, <https://clinicaltrials.gov/ct2/show/NCT03396211>, Last accessed [November 2021]

NCT03400332, Bristol-Myers Squibb, 2021, A study of BMS-986253 in combination with nivolumab or nivolumab plus ipilimumab in advanced cancers, <https://clinicaltrials.gov/ct2/show/NCT03400332>, Last accessed [November 2021]

NCT03450122, M.D. Anderson Cancer Center, 2021, Modified T cells, chemotherapy, and aldesleukin with or without LV305 and CMB305 in treating participants with advanced or recurrent sarcoma, <https://clinicaltrials.gov/ct2/show/NCT03450122>, Last accessed [November 2021]

NCT03475953, Institut Bergonié, A phase I/II study of regorafenib plus avelumab in solid tumors (REGOMUNE), <https://clinicaltrials.gov/ct2/show/NCT03475953>, Last accessed [November 2021]

NCT03618381, Seattle Children's Hospital, 2021, EGFR806 CAR T Cell Immunotherapy for recurrent/refractory solid tumors in children and young adults, <https://clinicaltrials.gov/ct2/show/NCT03618381>, Last accessed [October 2021]

NCT03784014, Institut National de la Sante Et de la Recherche Medicale, France, 2020, Molecular profiling of advanced soft-tissue sarcomas (MULTISARC), <https://clinicaltrials.gov/ct2/show/NCT03784014>, Last accessed [November 2021]

NCT03792542, Second Affiliated Hospital, School of Medicine, Zhejiang University, 2019, Anlotinib hydrochloride for advanced soft tissue sarcoma patients who do not receive chemotherapy, <https://clinicaltrials.gov/ct2/show/NCT03792542>, Last accessed [October 2021]

NCT03851614, University Health Network, Toronto, 2021, Basket combination study of inhibitors of DNA damage response, angiogenesis and programmed death ligand 1 in patients with advanced solid tumors (DAPPER), <https://clinicaltrials.gov/ct2/show/NCT03851614>, Last accessed [November 2021]

NCT03899805, Dana-Farber Cancer Institute, 2021, A phase II study of eribulin and pembrolizumab in soft tissue sarcomas, <https://clinicaltrials.gov/ct2/show/NCT03899805>, Last accessed [November 2021]

NCT03967223, GlaxoSmithKline, 2021, Master protocol to assess the safety and antitumor activity of genetically engineered T cells in NY-ESO-1 and/or LAGE-1a positive solid tumors (IGNYTE-ESO), <https://clinicaltrials.gov/ct2/show/NCT03967223>, Last accessed [November 2021]

NCT04044768, Adaptimmune, 2021, Spearhead 1 study in subjects with advanced synovial sarcoma or myxoid/round cell liposarcoma, <https://clinicaltrials.gov/ct2/show/NCT04044768>, Last accessed [November 2021]

NCT04083976, Janssen Research & Development, LLC, 2021, A study of erdafitinib in participants with advanced solid tumors and fibroblast growth factor receptor (FGFR) gene alterations, <https://www.clinicaltrials.gov/ct2/show/NCT04083976>, Last accessed [October 2021]

NCT04095208, Institut Bergonié, 2020, Combination of nivolumab plus relatlimab in patients with advanced or metastatic soft-tissue sarcoma: a proof-of-concept randomized phase II study (CONGRATS), <https://clinicaltrials.gov/ct2/show/NCT04095208>, Last accessed [November 2021]

NCT04784247, Memorial Sloan Kettering Cancer Center, 2021, Lenvatinib and pembrolizumab in people with advanced soft tissue sarcoma, <https://clinicaltrials.gov/ct2/show/NCT04784247>, Last accessed [November 2021]

NCT04874311, Institut Bergonié, 2021, Bintrafusp alfa and doxorubicin hydrochloride in treating patients with advanced sarcoma (TRUST), <https://clinicaltrials.gov/ct2/show/NCT04874311>, Last accessed [November 2021]

Nekoukar, Z, Moghimi, M, and Salehifar, E, 2021, A narrative review on adverse effects of dasatinib with a focus on pharmacotherapy of dasatinib-induced pulmonary toxicities, *Blood Res.*, 56 (4), Pg. 229-242

NHS, 2019, Soft tissue sarcomas, <https://www.nhs.uk/conditions/soft-tissue-sarcoma/>, Last accessed [May 2020]

Nichol, D, Jeavons, P, Fletcher, AG, Bonomo, RA, Maini, PK, Paul, JL, Gatenby, RA, Anderson, ARA, and Scott, JG, 2015, Steering evolution with sequential therapy to prevent the emergence of bacterial antibiotic resistance, *PLoS Comput Biol.*, 11 (9), e1004493

Nichol, D, Rutter, J, Bryant, C, Hujer, AM, Lek, S, Adams, MD, Jeavons, P, Anderson, ARA, Bonomo, RA, and Scott, JG, 2019, Antibiotic collateral sensitivity is contingent on the repeatability of evolution, *Nat Commun.*, 10, Pg. 334

Nichols, KE, Malkin, D, Garber, JE, Fraumeni Jr, JF, and Li, FP, 2001, Germ-line p53 mutations predispose to a wide spectrum of early-onset cancers, *Cancer Epidemiol Biomarkers Prev.*, 10 (2), Pg. 83-87

Niederst, MJ, and Engelman, JA, 2013, Bypass mechanisms of resistance to receptor tyrosine kinase inhibition in lung cancer, *Sci Signal.*, 6 (294), re6

Nishi, H, Shaytan, A, and Panchenko, AR, 2014, Physicochemical mechanisms of protein regulation by phosphorylation, *Front Genet.*, 5, Pg. 270

Nishida, T, Tsujimoto, M, Takahashi, T, Hirota, S, Blay, JY, and Wataya-Kaneda, M, 2016, Gastrointestinal stromal tumors in Japanese patients with neurofibromatosis type I, *J Gastroenterol.*, 51, Pg. 571-578

Nobre, SP, Hensley, ML, So, M, Zhou, QC, Iasonos, A, Leitao Jr, MM, Ducie, J, Chiang, S, Mueller, JJ, Abu-Rustum, NR, and Zivanovic, O, 2021, The impact of tumor fragmentation in patients with stage I uterine leiomyosarcoma on patterns of recurrence and oncologic outcome, *Gynecol Oncol.*, 160 (1), Pg. 99-105

Noujaim, J, Thway, K, Fisher, C, and Jones, RL, 2015, Dermatofibrosarcoma protuberans: from translocation to targeted therapy, *Cancer Biol Med.*, 12 (4), Pg. 375-384

O'Donnell, PW, Griffin, AM, Eward, WC, Sternheim, A, White, LM, Wunder, JS, and Ferguson, PC, 2013, Can experience observers differentiate between lipoma and well-differentiated liposarcoma using only MRI?, *Sarcoma.*, 982784

Ognjanovic, S, Olivier, M, Bergemann, TL, and Hainaut, P, 2012, Sarcomas in TP53 germline mutation carriers: a review of the IARC TP53 database, *Cancer.*, 118 (5), Pg. 1387-1396

O'Hare, T, Walters, DK, Stoffregen, EP, Jia, T, Manley, PW, Mestan, J, Cowan-Jacob, SW, Lee, FY, Heinrich, MC, Deininger, MWN, and Druker, BJ, 2005, In vitro activity of Bcr-Abl inhibitors AMN107 and BMS-354825 against clinically relevant imatinib-resistant Abl kinase domain mutants, *Cancer Res.*, 65 (11), Pg. 4500-4505

Oppelt, PJ, Hirbe, AC, and Van Tine, BA, 2017, Gastrointestinal stromal tumors (GISTs): point mutations matter in management, a review, *J Gastrointest Oncol.*, 8 (3), Pg. 466-473

Ornitz, DM, and Itoh, N, 2015, The fibroblast growth factor signaling pathway, *Wiley Interdiscip Rev Dev Biol.*, 4 (3), Pg. 215-266

Oshiro, H, Tome, Y, Kiyuna, T, Miyake, K, Kawaguchi, K, Higuchi, T, Miyake, M, Zang, Z, Razmjooei, S, Barangi, M, Wangsiricharoen, S, Nelson, SD, Li, Y, Bouvet, M, Singh, SR, Kanaya, F, and Hoffman, RM, 2019, Temozolomide targets and arrests a doxorubicin-resistant follicular dendritic-cell sarcoma patient-derived orthotopic xenograft mouse model, *Tissue Cell.*, 58, Pg. 17-23

Outani, H, Tanaka, T, Wakamatsu, T, Imura, Y, Hamada, K, Araki, N, Itoh, K, Yoshikawa, H, and Naka, N, 2014, Establishment of a novel clear cell sarcoma cell line (Hewga-CCS), and investigation of the antitumor effects of pazopanib on Hewga-CCS, *BMC Cancer.*, 14, Pg. 455

Oza, J, Doshi, S, Lee, SM, Van Tine, BA, Choy, E, Oppelt, PJ, Singh-Kandah, SV, Hernandez, S, Singer, Z, Balaji, S, Franks, L, Ingham, M, and Schwartz, GK, 2021, A phase II trial of sitravatinib, a multireceptor tyrosine kinase inhibitor, in patients with advanced well-differentiated/dedifferentiated liposarcoma, *J Clin Oncol.*, 39 (15), https://ascopubs.org/doi/abs/10.1200/JCO.2021.39.15_suppl.11513, Last accessed [October 2021]

Pál, C, Papp, B, and Lázár, V, 2015, Collateral sensitivity of antibiotic-resistant microbes, *Trends Microbiol.*, 23 (7), Pg. 401-407

Palmerini, E, Longhi, A, Donati, DM, and Staals, EL, 2020, Pexidartinib for the treatment of adult patients with symptomatic tenosynovial giant cell tumor: safety and efficacy, *Expert Rev Anticancer Ther.*, 20 (6), Pg. 441-445

Pant, S, Tabernero, J, Massard, C, Iyer, G, Witt, O, Doi, T, Qin, S, Lu-Emerson, C, Hargrave, DR, García-Corbacho, J, Little, SM, Xia, Q, Santiago-Walker, AE, Moy, C, Hammond, C, Sweiti, H, and Schuler, MH, 2021, A phase II open-label study in adult and adolescent patients (pts) with advanced solid tumors harboring fibroblast growth factor receptor (FGFR) gene alterations, *J Clin Oncol.*, 39 (3), https://ascopubs.org/doi/abs/10.1200/JCO.2021.39.3_suppl.TPS480, Last accessed [October 2021]

Papp, G, Krausz, T, Stricker, TP, Szendrői, M, and Sági, Z, 2014, SMARCB1 expression in epithelioid sarcoma is regulated by miR-206, miR-381, and miR-671-5p on both mRNA and protein levels, *Genes Chromosomes Cancer.*, 53 (2), Pg. 168-176

Parikh, RC, Lorenzo, M, Hess, LM, Candrilli, SD, Nicol, S, and Kaye, JA, 2018, Treatment patterns and survival among older adults in the United States with advanced soft-tissue sarcomas, *Clin Sarcoma Res.*, 8, Pg. 8

Park, SY, Han, J, Kim, JB, Yang, MG, Kim, YJ, Lim, HJ, An, SY, and Kim, JH, 2014, Interleukin-8 is related to poor chemotherapeutic response and tumourigenicity in hepatocellular carcinoma, *Eur J Cancer.*, 50 (2), Pg. 341-350

Pasquale, EB, 2010, Eph receptors and ephrins in cancer: bidirectional signaling and beyond, *Nat Rev Cancer.*, 10 (3), Pg. 165-180

Patel, AP, Tirosch, I, Trombetta, JJ, Shalek, AK, Gillespie, SM, Wakimoto, H, Cahill, DP, Nahed, BV, Curry, WT, Martuza, RL, Louis, DN, Rozenblatt-Rosen, O, Suvà, ML, Regev, and Bernstein, BE, 2014, Single-cell RNA-seq highlights intratumoral heterogeneity in primary glioblastoma, *Science.*, 344 (6190), Pg. 1396-1401

Patwardhan, PP, Ivy, KS, Musi, E, de Stanchina, E, and Schwartz, GK, 2016, Significant blockade of multiple receptor tyrosine kinases by MGCD516 (Sitravatinib), a novel small molecule inhibitor, shows potent anti-tumor activity in preclinical models of sarcoma, *Oncotarget.*, 7 (4), Pg. 4093-4109

Paul, MK, and Mukhopadhyay, AK, 2004, Tyrosine kinase – role and significance in cancer, *Int J Med Sci.*, 1 (2), Pg. 101-115

Pauli, C, Hopkins, BD, Prandi, D, Shaw, R, Fedrizzi, T, Sboner, A, Sailer, V, Augello, M, Puca, L, Rosati, R, McNary, TJ, Churakova, Y, Cheung, C, Triscott, J, Pisapia, D, Rao, R, Mosquera, JM, Robinson, B, Faltas, BM, Emerling, BE, Gadi, VK, Bernard, B, Elemento, O, Beltran, H, Demichelis, F, Kemp, CJ, Grandori, C, Cantley, LC, and Rubin, MA, 2017, Personalized in vitro and in vivo cancer models to guide precision medicine, *Cancer Discov.*, 7 (5), Pg. 462-477

Pautier, P, Penel, N, Ray-Coquard, I, Italiano, A, Bompas, E, Delcambre, C, Bay, JO, Bertucci, F, Delaye, J, Chevreau, C, Cupissol, D, Bozec, L, Eymard, JC, Saada, E, Isambert, N, Guillemet, C, Rios, M, Piperno-Neumann, S, Chenuc, G, and Duffaud, F, 2020, A phase II of gemcitabine combined with pazopanib followed by pazopanib maintenance, as second-line treatment in patients with advanced leiomyosarcomas: a unicancer French Sarcoma Group study (LMS03 study), 2020, *Eur J Cancer.*, 125, Pg. 31-37

Penel, N, Le Cesne, A, Bui, BN, Perol, D, Brain, EG, Ray-Coquard, I, Guillemet, C, Chevreau, C, Cupissol, D, Chabaud, S, Jimenez, M, Duffaud, F, Piperno-Neumann, S, Mignot, L, and Blay, JY, 2011, Imatinib for progressive and recurrent aggressive fibromatosis (desmoid tumors): an FNCLCC/French Sarcoma Group phase II trial with a long-term follow-up, *Ann Oncol.*, 22 (2), Pg. 452-457

Penel, N, Mir, O, Wallet, J, Ray-Coquard, I, Le Cesne, A, Italiano, A, Salas, S, Delcambre, C, Bompas, E, Bertucci, F, Saada-Bouزيد, E, Chaigneau, L, Chevreau, C, Brodowicz, T, Decoupigny, E, Vasneymortier, M, Laroche, L, Taieb, S, Le Deley, MC, and Blay, JY, 2020, A double-blind placebo-controlled randomized phase II trial assessing the activity and safety of regorafenib in non-adipocytic sarcoma patients previously treated with both chemotherapy and pazopanib, *Eur J Cancer.*, 126, Pg. 45-55

Percie du Sert, N, Hurst, V, Ahluwalia, A, Alam, S, Avey, MT, Baker, M, Browne, WJ, Clark, A, Cuthill, IC, Dirnagl, U, Emerson, M, Garner, P, Holgate, ST, Howells, DW, Karp, NA, Lazic, SE, Lidster, K, MacCallum, CJ, Macleod, M, Pearl, EJ, Petersen, OH, Rawle, F, Reynolds, P, Rooney, K, Sena, ES, Silberberg, SD, Steckler, T, and Würbel, H, 2020, The ARRIVE guidelines 2.0: updated guidelines for reporting animal research, *PLoS Biol.*, 18 (7), e3000410

Perera, TPS, Jovcheva, E, Mevellec, L, Vialard, J, De Lange, D, Verhulst, T, Paulussen, C, Van De Ven, K, King, P, Freyne, E, Rees, DC, Squires, M, Saxty, G, Page, M, Murray, CW, Gilissen, R, Ward, G, Thompson, NT, Newell, DR, Cheng, N, Xie, L, Yang, J, Platero, SJ, Karkera, JD, Moy, C, Angibaud, P, Laquerre, S, and Lorenzi, MV, 2017, Discovery and pharmacological characterization of JNJ-42756493 (Erdafitinib), a functionally selective small-molecule FGFR family inhibitor, *Mol Cancer Ther.*, 16 (6), Pg. 1010-1020

Pergolizzi, G, Kuhaudomlarp, S, Kalita, E, and Field, RA, 2017, Glycan phosphorylases in multi-enzyme synthetic processes, *Protein Pept Lett.*, 24 (8), Pg. 696-709

Pérot, G, Soubeyran, I, Ribeiro, A, Bonhomme, B, Savagner, F, Boutet-Bouzamondo, N, Hostein, I, Bonichon, F, Godbert, Y, and Chibon, F, 2014, Identification of a recurrent STRN/ALK fusion in thyroid carcinomas, *PLoS One.*, 9 (1), e87170

Petitprez, F, de Reyniès, A, Keung, EZ, Chen, TWW, Sun, CM, Calderaro, J, Jeng, YM, Hsiao, LP, Lacroix, L, Bougouïn, A, Moreira, M, Lacroix, G, Natario, I, Adam, J, Lucchesi, C, Laizet, YH, Toulmonde, M, Burgess, MA, Bolejack, V, Reinke, D, Wani, KM, Wang, WL, Lazar, AJ, Roland, CL, Wargo, JA, Italiano, A, Sautès-Fridman, C, Tawbi, HA, and Fridman, WH, 2020, B cells are associated with survival and immunotherapy response in sarcoma, *Nature.*, 577 (7791), Pg. 556-560

Phan-Lai, V, Florczyk, SJ, Kievit, FM, Wang, K, Gad, E, Disis, ML, and Zhang, M, 2013, Three-dimensional scaffolds to evaluate tumor associated fibroblast-mediated suppression of breast tumor specific T cells, *Biomacromolecules.*, 14 (5), Pg. 1330-1337

Phi, LTH, Sari, IN, Yang, YG, Lee, SH, Jun, N, Kim, KS, Lee, YK, and Kwon, HY, 2018, Cancer stem cells (CSCs) in drug resistance and their therapeutic implications in cancer treatment, *Stem Cells Int.*, 2018, Pg. 5416923

Pink, D, Andreou, D, Bauer, S, Brodowicz, T, Kasper, B, Reichardt, P, Richter, S, Lindner, LH, Szkandera, J, Grünwald, V, Kebenko, M, Kirchner, M, and Hohenberger, P, 2021, Treatment of angiosarcoma with pazopanib and paclitaxel: results of the EVA (evaluation of Votrient in angiosarcoma) phase II trial of the German Interdisciplinary Sarcoma Group (GISG-06), *Cancers (Basel).*, 13 (6), Pg. 1223

Playford, MP, and Schaller, MD, 2004, The interplay between Src and integrins in normal and tumor biology, *Oncogene.*, 23 (48), Pg. 7928-7946

Pluchino, KM, Hall, MD, Goldsborough, AS, Callaghan, R, and Gottesman, MM, 2012, Collateral sensitivity as a strategy against cancer multidrug resistance, *Drug Resist Updat.*, 15 (1-2), Pg. 98-195

Polizzotto, MN, Uldrick, TS, Wyvill, KM, Aleman, K, Peer, CJ, Bevans, M, Sereti, I, Maldarelli, F, Whitby, D, Marshall, V, Goncalves, PH, Khetani, V, Figg, WD, Steinberg, SM, Zeldis, JB, Yarchoan, R, 2016, Pomalidomide for symptomatic Kaposi's sarcoma in people with and without HIV infection: a phase I/II study, *J Clin Oncol.*, 34 (34), Pg. 4125-4131

Pollack, SM, Redman, MW, Baker, KK, Wagner, MJ, Schroeder, BA, Loggers, ET, Trieselmann, K, Copeland, VC, Zhang, S, Black, G, McDonnell, S, Gregory, J, Johnson, R, Moore, R, Jones, RL, and Cranmer, LD, 2020, Assessment of doxorubicin and pembrolizumab in patients with advanced anthracycline-naïve sarcoma, *JAMA Oncol.*, 6 (11), Pg. 1-5

Prior, IA, Lewis, PD, and Mattos, C, 2012, A comprehensive survey of Ras mutations in cancer, *Cancer Res.*, 72 (10), Pg. 2457-2467

Przybyl, J, Sciort, R, Rutkowski, P, Siedlecki, JA, Vanspauwen, V, Samson, I, and Debiec-Rychter, M, 2012, Recurrent and novel SS18-SSX fusion transcripts in synovial sarcoma: description of three new cases, *Tumour Bio.*, 33 (6), Pg. 2245-2253

Qiao, Z, Shiozawa, K, and Kondo, T, 2017, Proteomic approach toward determining the molecular background of pazopanib resistance in synovial sarcoma, *Oncotarget.*, 8 (65), Pg. 109587-109595

Rabindran, SK, Discafani, CM, Rosfjord, EC, Baxter, M, Floyd, MB, Golas, J, Hallett, WA, Johnson, BD, Nilakantan, R, Overbeek, E, Reich, MF, Shen, R, Shi, X, Tsou, HR, Wang, YF, and Wissner, A, 2004, Antitumor activity of HKI-272, an orally active, irreversible inhibitor of the HER-2 tyrosine kinase, *Cancer Res.*, 64 (11), Pg. 3958-3965

Ramos-Casals, M, Brahmer, JR, Callahan, MK, Flores-Chávez, A, Keegan, N, Khamashta, MA, Lambotte, O, Mariette, X, Prat, A, and Suárez-Almazor, 2020, Immune-related adverse events of checkpoint inhibitors, *Nat Rev Dis Primers.*, 6 (1), Pg. 38

Rane, SG, and Reddy, EP, 2002, JAKs, STATs, and Src kinases in hematopoiesis, *Oncogene.*, 21 (21), Pg. 3334-3358

Ratner, N, and Miller, SJ, 2015, A RASopathy gene commonly mutated in cancer: the neurofibromatosis type 1 tumour suppressor, *Nat Rev Cancer.*, 15 (5), Pg. 290-301

Ray-Coquard, I, Italiano, A, Bompas, E, Le Cesne, A, Robin, YM, Chevreau, C, Bay, JO, Bousquet, G, Piperno-Neumann, S, Isambert, N, Lemaître, L, Fournier, C, Gauthier, E, Collard, O, Cupissol, D, Clisant, S, Blay, JY, Penel, N, and French Sarcoma Group (GSF/GETO), 2012, Sorafenib for patients with advanced angiosarcoma: a phase II trial from the French Sarcoma Group (GSF/GETO), *Oncologist.*, 17 (2), Pg. 260-266

RCOG, 2019, Morcellation for myomectomy or hysterectomy, <https://www.rcog.org.uk/globalassets/documents/patients/patient-information-leaflets/gynaecology/pi-morcellation-for-myomectomy-or-hysterectomy.pdf>, Last accessed [May 2020]

Reardon, DA, Nabors, LB, Stupp, R, and Mikkelsen, T, 2008, Cilengitide: an integrin-targeting arginine-glycine-aspartic acid peptide with promising activity for glioblastoma multiforme, *Expert Opin Investig Drugs.*, 17 (8), Pg. 1225-1235

Reardon, DA, Neyns, B, Weller, M, Tonn, JC, Nabors, LB, and Stupp, R, 2011, Cilengitide: an RGD pentapeptide $\alpha v\beta 3$ and $\alpha v\beta 5$ integrin inhibitor in development for glioblastoma and other malignancies, *Future Oncol.*, 7 (3), Pg. 339-354

Reddy, EP, and Aggarwal, AK, 2012, The ins and outs of Bcr-Abl inhibition, *Genes Cancer.*, 3 (5-6), Pg. 447-454

Regad, T, 2015, Targeting RTK signaling pathways in cancer, *Cancers (Basel).*, 7 (3), Pg. 1758-1784

Riedel, RF, Ballman, KV, Lu, Y, Attia, S, Loggers, ET, Ganjoo, KN, Livingston, MB, Chow, W, Wright, J, Ward, JH, Rushing, D, Okuno, SH, Reed, DR, Liebner, DA, Keedy, VL, Mascarenhas, L, Davis, LE, Ryan, C, Reinke, DK, and Maki, RG, 2020, A randomized, double-blind, placebo-controlled, phase II study of regorafenib versus placebo in advanced/metastatic, treatment-refractory liposarcoma: results from the SARC024 study, *Oncologist.*, 25 (11), e1655-e1662

Riggins, RB, DeBerry, RM, Toosarvandani, MD, and Bouton, AH, 2003, Src-dependent association of Cas a p85 phosphatidylinositol 3'-kinase in v-crk-transformed cells, *Mol Cancer Res.*, 1 (6), Pg. 428-437

Roberts, PJ, and Der, CJ, 2007, Targeting the Raf-MEK-ERK mitogen-activated protein kinase cascade for the treatment of cancer, *Oncogene.*, 26 (22), Pg. 3291-3310

Robinson, DR, Wu, YM, and Lin, SF, 2000, The protein tyrosine kinase family of the human genome, *Oncogene.*, 19 (49), Pg. 5548-5557

Rodrigues, J, Heinrich, MA, Teixeira, LM, and Prakash, J, 2021, 3D in vitro (r)evolution: unveiling tumor-stroma interactions, *Trends Cancer.*, 7 (3), Pg. 249-264

Rogers, MS, Novak, K, Zurakowski, D, Cryan, LM, Blois, A, Lifshits, E, Bø, TH, Oyan, AM, Bender, ER, Lampa, M, Kang, SY, Naxerova, K, Kalland, KH, Straume, O, Akslen, LA, Watnick, RS, Folkman, J, and Naumov, GN, 2014, Spontaneous reversion of the angiogenic phenotype to a nonangiogenic and dormant state in human tumours, *Mol Cancer Res.*, 12 (5), Pg. 754-764

- Rössler, J, Monnet, Y, Farace, F, Opolon, P, Daudigeos-Dubus, E, Bourredjem, A, Vassal, G, and Geoerger, B, 2011, The selective VEGFR1-3 inhibitor axitinib (AG-013736) shows antitumor activity in human neuroblastoma xenografts, *Int J Cancer.*, 128 (11), Pg. 2748-2758
- Rhomberg, W, 1998, Exposure to polymeric materials in vascular soft-tissue sarcomas, *Int Arch Occup Environ Health.*, 71 (5), Pg. 343-347
- Romei, C, Ciampi, R, Casella, F, Tacito, A, Torregrossa, L, Ugolini, C, Basolo, F, Materazzi, G, Vitti, P, and Elisei, R, 2018, RET mutation heterogeneity in primary advanced medullary thyroid cancers and their metastases, *Oncotarget.*, 9 (11), Pg. 9875-9884
- Rosell, R, Moran, T, Cardenal, F, Porta, R, Viteri, S, Molina, MA, Benlloch, S, and Taron, M, 2010, Predictive biomarkers in the management of EGFR mutant lung cancer, *Ann N Y Acad Sci.*, 1210, Pg. 45-52
- Rosell, R, Chaib, I, and Santaripa, M, 2020, Targeting MET amplification in EGFR-mutant non-small-cell lung cancer, *Lancet Respir Med.*, 8 (11), Pg. 1068-1070
- Roskoski Jr., R, 2005, Signaling by Kit protein-tyrosine kinases – the stem cell factor receptor, *Biochem Biophys Res Commun.*, 337 (1), Pg. 1-13
- Roskoski Jr, R, 2005, Structure and regulation of Kit protein-tyrosine kinase—the stem cell factor receptor, *Biochem Biophys Res Commun.*, 338 (3), Pg. 1307-1315
- Roskoski Jr, R, 2016, Classification of small molecule protein kinase inhibitors based upon the structures of their drug-enzyme complexes, *Pharmacol Res.*, 103, Pg. 26-48
- Roth, GJ, Heckel, A, Colbatzky, F, Handschuh, S, Kley, J, Lehmann-Lintz, T, Lotz, R, Tontsch-Grunt, U, Walter, R, and Hilberg, F, 2009, Design, synthesis, and evaluation of indolinones as triple angiokinase inhibitors and the discovery of a highly specific 6-methoxycarbonyl-substituted indolinone (BIBF 1120), *J Med Chem.*, 52 (14), Pg. 4466-4480
- Roy, S, Vega, MV, and Harmer, NJ, 2019, Carbohydrate kinases: a conserved mechanism across differing folds, *Catalysts.*, 9 (1), Pg. 29
- Ruiz-Villalba, A, Ruijter, JM, and Van den Hoff, MJB, 2021, Use and misuse of C_q in qPCR data analysis and reporting, *Life (Basel).*, 11 (6), Pg. 496
- Rutkowski, P, Kaminska, J, Kowalska, M, Ruka, W, and Steffen, J, 2002, Cytokine serum levels in soft tissue sarcoma patients: correlations with clinico-pathological features and prognosis, *Int J Cancer.*, 100 (4), Pg. 463-471
- Rutkowski, P, Van Glabbeke, M, Rankin, CJ, Ruka, W, Rubin, BP, Debiec-Rychter, M, Lazar, A, Gelderblom, H, Sciot, R, Lopez-Terrada, D, Hohenberger, P, Van Oosterom, AT, Schuetze, SM, European Organisation for Research and Treatment of Cancer Soft Tissue/Bone Sarcoma Group, and Southwest Oncology Group, 2010, Imatinib mesylate in advanced dermatofibrosarcoma protuberans: pooled analysis of two phase II clinical trials, *J Clin Oncol.*, 28 (10), Pg. 1772-1779
- Rutter, J, Winge, DR, and Schiffman, JD, 2010, Succinate dehydrogenase – assembly, regulation and role in human disease, *Mitochondrion.*, 10 (4), Pg. 393-401
- Ryu, HH, Kang, M, Park, J, Park, SH, and Lee, YS, 2019, Enriched expression of NF1 in inhibitory neurons in both mouse and human brain, *Mol Brain.*, 12 (1), Pg. 60
- Samuels, BL, Chawla, SP, Somaiah, N, Staddon, AP, Skubitz, KM, Milhem, MM, Kaiser, PE, Portnoy, DC, Priebat, DA, Walker, MS, and Stepanski, EJ, 2017, Results of a prospective phase 2 study of pazopanib in patients with advanced intermediate-grade or high-grade liposarcoma, *Cancer.*, 123 (23), Pg. 4640-4647
- Sanada, TJ, Sakao, S, Naito, A, Ishibashi-Ueda, H, Suga, M, Shoji, H, Miwa, H, Suda, R, Iwasawa, S, Tada, Y, Ishida, K, Tanabe, N, and Tatsumi, K, 2019, Characterization of pulmonary intimal sarcoma cells isolated from a surgical specimen: in vitro and in vivo study, *PLoS One.*, 14 (3), e0214654
- Sangkhatat, S, 2015, Current management of pediatric soft tissue sarcomas, *World J Clin Pediatr.*, 4 (4), Pg. 94-105
- Sannino, G, Marchetto, A, Kirchner, T, and Grünwald, TGP, 2017, Epithelial-to-mesenchymal and mesenchymal-to-epithelial transition in mesenchymal tumors: a paradox in sarcomas?, *Cancer Res.*, 77 (17), Pg. 4556-4561
- Sanson, KR, Hanna, RE, Hegde, M, Donovan, KF, Strand, C, Sullender, ME, Vaimberg, EW, Goodale, A, Root, DE, Piccioni, F, and Doench, JG, 2018, Optimized libraries for CRISPR-Cas9 genetic screens with multiple modalities, *Nat Commun.*, 9 (1), Pg. 5416
- Santoro, M, Moccia, M, Federico, G, and Carlomagno, F, 2020, RET gene fusions in malignancies of the thyroid and other tissues, *Genes (Basel).*, 11 (4), Pg. 424
- Sápi, Z, Papp, G, Szendrői, M, Pápai, Z, Plótár, V, Krausz, T, and Fletcher, CDM, 2016, Epigenetic regulation of SMARCB1 by miR-206, -381, and -671-5p is evident in a variety of SMARCB1 immunonegative soft tissue sarcomas, while miR-765 appears specific for epithelioid sarcoma. A miRNA study of 223 soft tissue sarcomas, *Genes Chromosomes Cancer.*, 55 (10), Pg. 786-802

Saturno, G, Lopes, F, Niculescu-Duvaz, I, Niculescu-Duvaz, D, Zambon, A, Davies, L, Johnson, L, Preece, N, Lee, N, Viros, A, Holovanchuk, D, Pedersen, M, McLeary, R, Lorigan, P, Dhomen, N, Fisher, C, Banerji, U, Dean, E, Krebs, MG, Gore, M, Larkin, J, Marais, R, and Springer, C, 2021, The paradox-breaking panRAF plus SRC family kinase inhibitor, CCT3833, is effective in mutant KRAS-driven cancers, *Ann Oncol.*, 32 (2), Pg. 269-278

Sautés-Fridman, C, Petitprez, F, Calderaro, J, and Fridman, WH, 2019, Tertiary lymphoid structures in the era of cancer immunotherapy, *Nat Rev Cancer.*, 19 (6), Pg. 307-325

Scarborough, JA, McClure, E, Anderson, P, Dhawan, A, Durmaz, A, Lessnick, SL, Hitomi, M, and Scott, JG, 2020, Identifying states of collateral sensitivity during the evolution of therapeutic resistance in Ewing's sarcoma, *iScience*, 23 (7), Pg. 101293

Schaefer, IM, Mariño-Enriquez, A, and Fletcher, JA, 2017, What is new in Gastrointestinal stromal tumor?, *Adv Anat Pathol.*, 24 (5), Pg. 259-267

Schaefer, IM, Cote, GM, and Hornick, JL, 2018, Contemporary sarcoma diagnosis, genetics, and genomics, *J Clin Oncol.*, 36 (2), Pg. 101-110

Schalper, KA, Carleton, M, Zhou, M, Chen, T, Feng, Y, Huang, SP, Walsh, AM, Baxi, V, Pandya, D, Baradet, T, Locke, D, Wu, Q, Reilly, TP, Phillips, P, Nagineni, V, Gianino, N, Gu, J, Zhao, H, Perez-Gracia, JL, Sanmamed, MF, and Melero, I, 2020, Elevated serum interleukin-8 is associated with enhanced intratumor neutrophils and reduced clinical benefit of immune-checkpoint inhibitors, *Nat Med.*, 26 (5), Pg. 688-692

Schmieder, R, Hoffmann, J, Becker, M, Bhargava, A, Müller, T, Kahmann, N, Ellinghaus, P, Adams, R, Rosenthal, A, Thierauch, KH, Scholz, A, Wilhelm, SM, and Zopf, D, 2014, Regorafenib (BAY 73-4506): antitumor and antimetastatic activities in preclinical models of colorectal cancer, *Int J Cancer.*, 135 (6), Pg. 1487-1496

Schmoll, HJ, Lindner, LH, Reichardt, P, Heißner, K, Kopp, HG, Kessler, T, Mayer-Steinacker, R, Rüssel, J, Egerer, G, Crysandt, M, Kasper, B, Niederwieser, D, Kunitz, A, Eigendorff, E, Petersen, I, Steighardt, J, Cygon, F, Meinert, F, and Stein, A, 2021, Efficacy of pazopanib with or without gemcitabine in patients with anthracycline- and/or ifosfamide-refractory soft tissue sarcoma: final results of the PAPAGEMO Phase 2 randomized clinical trial, *JAMA Oncol.*, 7 (2), Pg. 255-262

Schneider, JW, and Dittmer, DP, 2017, Diagnosis and treatment of Kaposi Sarcoma, *Am J Clin Dermatol.*, 18 (4), Pg. 529-539

Schöffski, P, Wozniak, A, Stacchiotti, S, Rutkowski, P, Blay, JY, Lindner, LH, Strauss, SJ, Anthony, A, Duffaud, F, Richter, S, Grünwald, V, Leahy, MG, Reichardt, P, Sufliarsky, J, Van der Graaf, WTA, Sciot, R, Debiec-Rychter, M, Van Cann, T, Marréaud, S, Lia, M, Raveloarivahy, T, Collette, L, and Bauer, S, 2017, Activity and safety of crizotinib in patients with advanced clear-cell sarcoma with MET alterations: European Organisation for Research and Treatment of Cancer phase II trial 90101 'CREATE', *Ann Oncol.*, 28 (12), Pg. 3000-3008

Schöffski, P, Sufliarsky, J, Gelderblom, H, Blay, JY, Strauss, SJ, Stacchiotti, S, Rutkowski, P, Lindner, LH, Leahy, MG, Italiano, A, Isambert, N, Debiec-Rychter, M, Sciot, R, Van Cann, T, Marréaud, S, Nzokiranteve, A, Collette, S, and Wozniak, A, 2018, Crizotinib in patients with advanced, inoperable inflammatory myofibroblastic tumours with and without anaplastic lymphoma kinase gene alterations (European Organisation for Research and Treatment of Cancer 90101 CREATE): a multicentre, single-drug, prospective, non-randomised phase 2 trial, *Lancet Respir Med.*, 6 (6), Pg. 431-441

Schöffski, P, Wozniak, A, Kasper, B, Aamdal, S, Leahy, MG, Rutkowski, P, Bauer, S, Gelderblom, H, Italiano, A, Lindner, LH, Hennig, I, Strauss, S, Zakotnik, B, Anthony, A, Albiges, L, Blay, JY, Reichardt, P, Sufliarsky, J, Van der Graaf, WTA, Debiec-Rychter, M, Sciot, R, Van Cann, T, Marréaud, S, Raveloarivahy, T, Collette, S, and Stacchiotti, S, 2018, Activity and safety of crizotinib in patients with alveolar soft part sarcoma with rearrangement of TFE3: European Organization for Research and Treatment of Cancer (EORTC) phase II trial 90101 'CREATE', *Ann Oncol.*, 29 (3), Pg. 758-765

Schöffski, P, Van Renterghem, B, Cornillie, J, Wang, Y, Gebreyohannes, YK, Lee, CJ, Wellens, J, Vanleeuw, U, Nysen, M, Hompes, D, Stas, M, Sinnaeve, F, Wafa, H, Topal, B, Verbelen, T, Debiec-Rychter, M, Sciot, R, and Wozniak, A, 2019, XenoSarC: A comprehensive platform of patient-derived xenograft (PDX) models of soft tissue sarcoma (STS) for early drug testing, *J Glob Oncol.*, 5 (37), <https://ascopubs.org/doi/abs/10.1200/JGO.2019.5.suppl.37>, Last accessed [October 2021]

Schöffski, P, Blay, JY, and Ray-Coquard, I, 2020, Cabozantinib as an emerging treatment for sarcoma, *Curr Opin Oncol.*, 32 (4), Pg. 321-331

Schöffski, P, Toulmonde, M, Estival, A, Marquina, G, Dudzisz-Śledź, M, Brahmi, M, Steeghs, N, Karavasili, V, De Haan, J, Wozniak, A, Cousin, S, Domènech, M, Bovée, J, VMG, Charon-Barra, C, Marreaud, S, Litière, S, De Meulemeester, L, Olungu, C, and Gelderblom, H, 2021, Randomised phase 2 study comparing the efficacy and safety of the oral tyrosine kinase inhibitor nintedanib with single agent ifosfamide in patients with advanced, inoperable, metastatic soft tissue sarcoma after failure of first-line chemotherapy: EORTC-1506-STBSG "ANITA", *Eur J Cancer.*, 152, Pg. 26-40

Schuetze, SM, Wathen, JK, Lucas, DR, Choy, E, Samuels, BL, Staddon, AP, Ganjoo, KN, Von Mehren, M, Chow, WA, Loeb, DM, Tawbi, HA, Rushing, DA, Patel, SR, Thomas, DG, Chugh, R, Reinke, DK, and Baker, LH, 2016, SARC009: Phase 2 study of dasatinib in patients with previously treated, high-grade, advanced sarcoma, *Cancer.*, 122 (6), Pg. 868-874

Schuetze, SM, Bolejack, V, Choy, E, Ganjoo, KN, Staddon, AP, Chow, WA, Tawbi, HA, Samuels, BL, Patel, SR, Von Mehren, M, D'Amato, G, Leu, KM, Loeb, DM, Forscher, CA, Milhem, MM, Rushing, DA, Lucas, DR, Chugh, R, Reinke, DK, and

Baker, LH, 2017, Phase 2 study of dasatinib in patients with alveolar soft part sarcoma, chondrosarcoma, chordoma, epithelioid sarcoma, or solitary fibrous tumor, *Cancer.*, 123 (1), Pg. 90-97

Schulte, B, Mohindra, N, Milhem, M, Attia, S, Robinson, S, Monga, V, Hirbe, AC, Oppelt, P, Charlson, J, Helenowski, I, Abbinanti, S, Cehic, R, Okuno, S, Van Tine, BA, and Agulnik, M, 2021, Phase II study of pazopanib with oral topotecan in patients with metastatic and non-resectable soft tissue and bone sarcomas, *Br J Cancer.*, 125 (4), Pg. 528-533

Schwartz, PA, and Murray, BW, 2011, Protein kinase biochemistry and drug discovery, *Bioorg Chem.*, 39 (5-6), Pg. 192-210

Seashore-Ludlow, B, Rees, MG, Cheah, JH, Cokol, M, Price, EV, Coletti, ME, Jones, V, Bodycombe, NE, Soule, CK, Gould, J, Alexander, B, Li, A, Montgomery, P, Wawer, MJ, Kuru, N, Kotz, JD, Hon, CSY, Munoz, B, Liefeld, T, Dančík, V, Bittker, JA, Palmer, M, Bradner, JE, Shamji, AF, Clemons, PA, and Schreiber, SL, 2015, Harnessing connectivity in a large-scale small-molecule sensitivity dataset, *Cancer Discov.*, 5 (11), Pg. 1210-1223

Ségaliny, AI, Tellez-Gabriel, M, Heymann, MF, and Heymann, D, 2015, Receptor tyrosine kinases: characterisation, mechanism of action and therapeutic interests for bone cancers, *J Bone Oncol.*, 4 (1), Pg. 1-12

Selvaggi, G, Novello, S, Torri, V, Leonardo, E, De Giuli, P, Borasio, P, Mossetti, C, Ardisson, F, Lausi, P, and Scagliotti, GV, 2004, Epidermal growth factor receptor overexpression correlates with a poor prognosis in completely resected non-small-cell lung cancer, *Ann Oncol.*, 15 (1), Pg. 28-32

Serrano, C, Mariño-Enríquez, A, Tao, DL, Ketzer, J, Eilers, G, Zhu, M, Yu, C, Mannan, AM, Rubin, BP, Demetri, GD, Raut, CP, Presnell, A, McKinley, A, Heinrich, MC, Czaplinski, JT, Sicinska, E, Bauer, S, George, S, and Fletcher, JA, 2019, Complementary activity of tyrosine kinase inhibitors against secondary kit mutations in imatinib-resistant gastrointestinal stromal tumours, *Br J Cancer.*, 120 (6), Pg. 612-620

Setty, BA, Jinesh, GG, Arnold, M, Pettersson, F, Cheng, CG, Cen, L, Yoder, SJ, Teer, JK, Flores, ER, Reed, DR, and Brohl, AS, 2020, The genomic landscape of undifferentiated embryonal sarcoma of the liver is typified by C19MC structural rearrangement and overexpression combined with TP53 mutation or loss, *PLoS Genet.*, 16 (4), e1008642

Shah, NP, Lee, FY, Luo, R, Jiang, Y, Donker, M, and Akin, C, 2006, Dasatinib (BMS-354825) inhibits KITD816V, an imatinib-resistant activating mutation that triggers neoplastic growth in most patients with systemic mastocytosis, *Blood.*, 108 (1), Pg. 286-291

Shamir, ER, and Ewald, AJ, 2014, Three-dimensional organotypic culture: experimental models of mammalian biology and disease, *Nat Rev Mol Cell Biol.*, 15 (10), Pg. 647-664

Shannon-Lowe, C, and Rickinson, A, 2019, The global landscape of EBV-associated tumors, *Front Oncol.*, 9, Pg. 713

Shattil, SJ, 2005, Integrins and Src: dynamic duo of adhesion signaling, *Trends Cell Biol.*, 15 (8), Pg. 399-403

Sheffield, NC, Pierron, G, Klughammer, J, Datlinger, P, Schönegger, A, Schuster, M, Hadler, J, Surdez, D, Guillemot, D, Lapouble, E, Freneaux, P, Champigneulle, J, Bouvier, R, Walder, D, Ambros, IM, Hutter, C, Sorz, E, Amaral, AT, De Álava, E, Schallmoser, K, Strunk, D, Rinner, B, Liegl-Atzwanger, B, Huppertz, B, Leithner, A, De Pinieux, G, Terrier, P, Laurence, V, Michon, J, Ladenstein, R, Holter, W, Windhager, R, Dirksen, U, Ambros, PF, Delattre, O, Kovar, H, Bock, C, and Tomazou, EM, 2017, DNA methylation heterogeneity defines a disease spectrum in Ewing sarcoma, *Nat Med.*, 23 (3), Pg. 386-395

Shiozawa, K, Shuting, J, Yoshioka, Y, Ochiya, T, and Kondo, T, 2018, Extracellular vesicle-encapsulated microRNA-761 enhances pazopanib resistance in synovial sarcoma, *Biochem Biophys Res Commun.*, 495 (1), Pg. 1322-1327

Shiozawa, K, Yoshioka, Y, Qiao, Z, Shuting, J, Ochiya, T, and Kondo, T, 2018, Pazopanib-induced changes in protein expression signatures of extracellular vesicles in synovial sarcoma, *Biochem Biophys Res Commun.*, 506 (3), Pg. 723-730

Shor, AC, Keschman, EA, Lee, FY, Muro-Cacho, C, Letson, GD, Trent, JC, Pledger, WJ, and Jove, R, 2007, Dasatinib inhibits migration and invasion in diverse human sarcoma cell lines and induces apoptosis in bone sarcoma cells dependent on SRC kinase for survival, *Cancer Res.*, 67 (6), Pg. 2800-2808

Sievers, E, Trautmann, M, Kindler, D, Huss, S, Gruenewald, I, Dirksen, U, Renner, M, Mechttersheimer, G, Pedeutour, F, Aman, P, Nishio, J, Schildhaus, HU, Kirfel, J, Schirmacher, P, Wardelmann, E, Buettner, R, and Hartmann, W, 2015, SRC inhibition represents a potential therapeutic strategy in liposarcoma, 137 (11), Pg. 2578-2588

Simon, MP, Navarro, M, Roux, D, and Pouyssegur, J, 2001, Structural and functional analysis of a chimeric protein COL1A1-PDGFB generated by the translocation t(17;22)(q22;q13.1) in dermatofibrosarcoma protuberans, *Oncogene.*, 20 (23), Pg. 2965-2975

Sjöblom, T, Shimizu, A, O'Brien, KP, Pietras, K, Dal Cin, P, Buchdunger, E, Dumanski, JP, Ostman, A, and Heldin, CH, 2001, Growth inhibition of dermatofibrosarcoma protuberans tumors by the platelet-derived growth factor receptor antagonist STI571 through induction of apoptosis, *Cancer Res.*, 61 (15), Pg. 5778-5783

Skapek, SX, Ferrari, A, Gupta, AA, Lupo, PJ, Butler, E, Shipley, J, Barr, FG, and Hawkins, DS, 2019, Rhabdomyosarcoma, *Nat Rev Dis Primers.*, 5 (1), Pg. 1

Sleijffer, S, Ray-Coquard, I, Papai, Z, Le Cesne, A, Scurr, M, Schöffski, P, Collin, F, Pandite, L, Marreaud, S, De Brauwier, A, Van Glabbeke, M, Verweij, J, and Blay, JY, 2009, Pazopanib, a multikinase angiogenesis inhibitor, in patients with relapsed or refractory advanced soft tissue sarcoma: a phase II study from the European organisation for research and treatment of cancer-soft tissue and bone sarcoma group (EORTC study 62043), *J Clin Oncol.*, 27 (19), Pg. 3126-3132

Sleijffer, S, Gorlia, T, Lamers, C, Burger, H, Blay, JY, Le Cesne, A, Scurr, M, Pandite, L, Marreaud, S, and Hohenberger, P, 2012, Cytokine and angiogenic factors associated with efficacy and toxicity of pazopanib in advanced soft-tissue sarcoma: an EORTC-STBSG study, *Br J Cancer.*, 107 (4), Pg. 639-645

Smith, BD, Kaufman, MD, Lu, WP, Gupta, A, Leary, CB, Wise, SC, Rutkoski, TJ, Ahn, YM, Al-Ani, G, Bulfer, SL, Caldwell, TM, Chun, L, Ensinger, CL, Hood, MM, McKinley, A, Patt, WC, Ruiz-Soto, R, Su, Y, Telikepalli, H, Town, A, Turner, BA, Vogeti, L, Vogeti, S, Yates, K, Janku, F, Razak, ARA, Rosen, O, Heinrich, MC, and Flynn, DL, 2019, Ripretinib (DCC-2618) is a switch control kinase inhibitor of a broad spectrum of oncogenic and drug-resistant KIT and PDGFRA variants, *Cancer Cell.*, 35 (5), Pg. 738-751

Smrke, A, Thway, K, Huang, PH, Jones, RL, and Hayes, AJ, 2021, Solitary fibrous tumor: molecular hallmarks and treatment for a rare sarcoma, *Future Oncol.*, fon-2021-0030

Solomon, B, Varella-Garcia, M, and Camidge, DR, 2009, ALK gene rearrangements: a new therapeutic target in a molecularly defined subset of non-small cell lung cancer, *J Thorac Oncol.*, 4 (12), Pg. 1450-1454

Somaiah, N, Conley, AP, Lin, HY, Amini, B, Sabir, SH, Araujo, DM, Benjamin, RS, Livingston, JA, Patel, S, Ratan, R, Ravi, V, Zarzour, MA, Wang, WL, Tate, T, Roland, CL, Daw, NC, Futreal, A, Lazar, AJ, Wistuba, II, and Hwu, P, 2020, A phase II multi-arm study of durvalumab and tremelimumab for advanced or metastatic sarcomas, *J Clin Oncol.*, 38 (15), https://ascopubs.org/doi/10.1200/JCO.2020.38.15_suppl.11509, Last accessed [November 2021]

Somaiah, N, Van Tine, BA, Wahlquist, AE, Milhem, MM, Hill, EG, Garrett-Mayer, E, Armeson, KE, Schuetze, SM, Meyer, CF, Reuben, DY, Elias, AD, Read, WL, Chawla, SP, and Kraft, AS, 2021, A randomized, open-label, phase 2, multicenter trial of gemcitabine with pazopanib or gemcitabine with docetaxel with advanced soft-tissue sarcoma, *Cancer.*, 127 (6), Pg. 894-904

Son, B, Lee, S, Youn, HS, Kim, EG, Kim, W, and Youn, BH, 2017, The role of tumor microenvironment in therapeutic resistance, *Oncotarget.*, 8 (3), Pg. 3933-3945

Sonobe, H, Manabe, Y, Furihata, M, Iwata, J, Oka, T, Ohtsuki, Y, Mizobuchi, H, Yamamoto, H, Kumano, O, and Abe, S, 1992, Establishment and characterization of a new human synovial sarcoma cell line, HS-SY-II, *Lab Invest.*, 67 (4), Pg. 498-505

Stacchiotti, S, Tortoreto, M, Baldi, GG, Grignani, G, Toss, A, Badalamenti, G, Cominetti, D, Morosi, C, Dei Tos, AP, Festinese, F, Fumagalli, E, Provenzano, S, Gronchi, A, Pennacchioli, E, Negri, T, Dagrada, GP, Spagnuolo, RD, Pilotti, S, Casali, PG, and Zaffaroni, N, 2014, Preclinical and clinical evidence of activity of pazopanib in solitary fibrous tumour, *Eur J Cancer.*, 50 (17), Pg. 3021-3028

Stacchiotti, S, Mir, O, Le Cesne, A, Vincenzi, B, Fedenko, A, Maki, RG, Somaiah, N, Patel, S, Brahmi, M, Blay, JY, Boye, K, Hall, KS, Gelderblom, H, Hindi, N, Martín-Broto, J, Kosela, H, Rutkowski, P, Italiano, A, Duffaud, F, Kobayashi, E, Casali, PG, Provenzano, S, and Kawai, A, 2018, Activity of pazopanib and trabectedin in advanced alveolar soft part sarcoma, *Oncologist.*, 23 (1), Pg. 62-70

Stacchiotti, S, and Van Tine, BA, 2018, Synovial sarcoma: current concepts and future perspectives, *J Clin Oncol.*, 36 (2), Pg. 180-187

Stacchiotti, S, Ferrari, S, Redondo, A, Hindi, N, Palmerini, E, Salgado, MAV, Frezza, AM, Casali, PG, Gutierrez, A, Lopez-Pousa, A, Grignani, G, Italiano, A, Le Cesne, A, Dumont, S, Blay, JY, Penel, N, Bernabeu, D, De Alava, E, Karanian, M, Morosi, C, Bricch, S, Dagrada, GP, Vallacchi, V, Castelli, C, Brenca, M, Racanelli, D, Maestro, R, Collini, P, Cruz, J, and Martín-Broto, J, 2019, Pazopanib for treatment of advanced extraskeletal myxoid chondrosarcoma: a multicentre, single-arm, phase 2 trial, *Lancet Oncol.*, 20 (9), Pg. 1252-1262

Stacchiotti, S, Schöffski, P, Jones, R, Agulnik, M, Villalobos, VM, Jahan, TM, Chen, TWW, Italiano, A, Demetri, GD, Cote, GM, Chugh, R, Attia, S, Gupta, AA, Loggers, ET, van Tine, B, Sierra, L, Yang, J, Rajarethinam, A, and Gounder, MM, 2019, Safety and efficacy of tazemetostat, a first-in-class EZH2 inhibitor, in patients (pts) with epithelioid sarcoma (ES) (NCT02601950), *J Clin Oncol.*, 37 (15), https://ascopubs.org/doi/abs/10.1200/JCO.2019.37.15_suppl.11003, Last accessed [July 2020]

Stacchiotti, S, Simeone, N, Lo Vullo, S, Morosi, C, Greco, FG, Gronchi, A, Barisella, M, Collini, P, Zaffaroni, N, Dagrada, GP, Frezza, AM, Mariani, L, and Casali, PG, 2019, Activity of axitinib in progressive advanced solitary fibrous tumour: results from an exploratory, investigator-driven phase 2 clinical study, *Eur J Cancer.*, 106, Pg. 225-233

Stacchiotti, S, Baldi, GG, Lo Vullo, S, Morosi, C, Greco, FG, Collini, P, Barisella, M, Dagrada, G, Zaffaroni, N, Gronchi, A, Simeone, N, Mariani, L, Frezza, AM, and Casali, PG, 2021, Regorafenib (R) in advanced solitary fibrous tumor (SFT): results from an exploratory phase II clinical study, *J Clin Oncol.*, 39 (15), https://ascopubs.org/doi/abs/10.1200/JCO.2021.39.15_suppl.11558, Last accessed [October 2021]

Stebbing, J, Paz, K, Schwartz, GK, Wexler, LH, Maki, R, Pollock, RE, Morris, R, Cogen, R, Shankar, A, Blackman, G, Harding, V, Vasquez, D, Krell, J, Zacharoulis, S, Ciznadija, D, Katz, A, and Sidransky, D, 2014, Patient-derived xenografts for individualized care in advanced sarcoma, *Cancer.*, 120 (13), Pg. 2006-2015

Stewart, SA, Dykxhoorn, DM, Palliser, D, Mizuno, H, Yu, EY, An, DS, Sabatini, DM, Chen, ISY, Hahn, WC, Sharp, PA, Weinberg, RA, and Novina, CD, 2003, Lentivirus-delivered stable gene silencing by RNAi in primary cells, *RNA.*, 9 (4), Pg. 493-501

Stratakis, CA, and Carney, JA, 2009, The triad of paragangliomas, gastric stromal tumours and pulmonary chondromas (Carney triad), and the dyad of paragangliomas and gastric stromal sarcomas (Carney-Stratakis syndrome): molecular genetics and clinical implications, *J Intern Med.*, 266 (1), Pg. 43-52

Suda, K, Murakami, I, Sakai, K, Tomizawa, K, Mizuuchi, H, Sato, K, Nishio, K, and Mitsudomi, T, 2016, Heterogeneity in resistance mechanisms causes shorter duration of epidermal growth factor receptor kinase inhibitor treatment in lung cancer, *91*, Pg. 36-40

Sugiyama, MG, Fairn, GD, and Antonescu, CN, 2019, Akt-ing up just about everywhere: compartment-specific Akt activation and function in receptor tyrosine kinase signaling, *Front Cell Dev Biol.*, *7*, Pg. 70

Sullivan, LM, Folpe, AL, Pawel, BR, Judkins, AR, and Biegel, JA, 2013, Epithelioid sarcoma is associated with a high percentage of SMARCB1 deletions, *Mod Pathol.*, 26 (3), Pg. 385-392

Sun, L, Liang, C, Shirazian, S, Zhou, Y, Miller, T, Cui, J, Fukuda, JY, Chu, JY, Nematalla, A, Wang, X, Chen, H, Sistla, A, Luu, TC, Tang, F, Wei, J, and Tang, C, 2003, Discovery of 5-[5-fluoro-2-oxo-1,2-dihydroindol-(3Z)-ylidenemethyl]-2,4-dimethyl-1H-pyrrole-3-carboxylic acid (2-diethylaminoethyl)amide, a novel tyrosine kinase inhibitor targeting vascular endothelial and platelet-derived growth factor receptor tyrosine kinase, *J Med Chem.*, 46 (7), Pg. 1116-1119

Sun, P, Xu, Y, Du, X, Ning, N, Sun, H, Liang, W, and Li, R, 2013, An engineered three-dimensional gastric tumor culture model for evaluating the antitumour activity of immune cells in vitro, *Oncol Lett.*, 5 (2), Pg 489-494

Susek, KH, Karvouni, M, Alici, E, and Lundqvist, A, 2018, The role of CXC chemokine receptors 1-4 on immune cells in the tumor microenvironment, *Front Immunol.*, 9, Pg. 2159

Svejstrup, JQ, 2013, Synovial sarcoma mechanisms, a series of unfortunate events, *Cell*, 153 (1), Pg. 11-12

Takamori, H, Oades, ZG, Hoch, OC, Burger, M, and Schraufstatter, IU, 2000, Autocrine growth effect of IL-8 and GROalpha on a human pancreatic cancer cell line, Capan-1, *Pancreas.*, 21 (1), Pg. 52-56

Talevi, A, 2015, Multi-target pharmacology: possibilities and limitations of the "skeleton key approach" from a medicinal chemist perspective, *Front Pharmacol.*, 6, Pg. 205

Tamura, T, Kato, Y, Ohashi, K, Ninomiya, K, Makimoto, G, Gotoda, H, Kubo, T, Ichihara, E, Tanaka, T, Ichimura, K, Maeda, Y, Hotta, K, and Kiura, K, 2018, Potential influence of interleukin-6 on the therapeutic effect of gefitinib in patients with advanced non-small cell lung cancer harbouring EGFR mutations, *Biochem Biophys Res Commun.*, 495 (1), Pg. 360-367

Tan, AC, and Huang, PH, 2017, Kinase signaling networks, *Methods in Molecular Biology*, Vol. 1636, DOI; 10.1007/978-1-4939-7154-1, Humana Press, Springer Science + Business Media LLC, <https://www.springer.com/gp/book/9781493971527>, Last accessed [January 2021]

Tan, AC, Vyse, S, and Huang, PH, 2017, Exploiting receptor tyrosine kinase co-activation for cancer therapy, *Drug Discov Today.*, 22 (1), Pg. 72-84

Tan, HY, Wang, N, Lam, W, Guo, W, Feng, Y, and Cheng, YC, 2018, Targeting tumour microenvironment by tyrosine kinase inhibitor, *Mol Cancer.*, 17 (1), Pg. 43

Tang, L, Wang, Y, Zhang, J, Yu, W, Huang, Y, and Yao, Y, 2019, Efficacy and safety of anlotinib in advanced soft tissue sarcoma: results from one of multi-centers in a phase IIB trial (ALTER0230), *J Clin Oncol.*, 37 (15), https://ascopubs.org/doi/10.1200/JCO.2019.37.15_suppl.e22518, Last accessed [October 2021]

Tang, L, Yu, W, Wang, Y, Li, H, and Shen, Z, 2019, Anlotinib inhibits synovial sarcoma by targeting GINS1: a novel downstream target oncogene in progression of synovial sarcoma, *Clin Transl Oncol.*

Tap, WD, Gelderblom, H, Palmerini, E, Desai, J, Bauer, S, Blay, JY, Alcindor, T, Ganjoo, K, Martín-Broto, J, Ryan, CW, Thomas, DM, Peterfy, C, Healey, JH, van de Sande, M, Gelhorn, HL, Shuster, DE, Wang, Q, Yver, A, Hsu, HH, Lin, PS, Tong-Starksen, S, Stacchiotti, S, Wagner, AJ, and ENLIVEN investigators, 2019, Pexidartinib versus placebo for advanced tenosynovial giant cell tumours (ENLIVEN): A randomised phase 3 trial, *Lancet.*, 394 (10197), Pg. 478-487

Tawbi, HA, Burgess, M, Bolejack, V, Van Tine, BA, Schuetze, SM, Hu, J, D'Angelo, S, Attia, S, Riedel, RF, Priebat, DA, Movva, S, Davis, LE, Okuno, SH, Reed, DR, Crowley, J, Butterfield, LH, Salazar, R, Rodriguez-Canales, J, Lazar, AJ, Wistuba, II, Baker, LH, Maki, RG, Reinke, D, and Patel, S, 2017, Pembrolizumab in advanced soft-tissue sarcoma and bone sarcoma (SARC028): a multicentre, two-cohort, single-arm, open-label, phase 2 trial, *Lancet Oncol.*, 18 (11), Pg. 1493-1501

Taylor, BS, Barretina, J, Maki, RG, Antonescu, CR, Singer, S, and Ladanyi, M, 2011, Advances in sarcoma genomics and new therapeutic targets, *Nat Rev Cancer.*, 11 (8), Pg. 541-557

Teicher, BA, Polley, E, Kunkel, M, Evans, D, Silvers, T, Delosh, R, Laudeman, J, Ogle, C, Reinhart, R, Selby, M, Connelly, J, Harris, E, Monks, A, and Morris, J, 2015, Sarcoma cell line screen of oncology drugs and investigational agents identifies patterns associated with gene and microRNA expression, *Mol Cancer Ther.*, 14 (11), Pg. 2452-2462

Terrell, EM, and Morrison, DK, 2019, Ras-mediated activation of the Raf family kinases, *Cold Spring Harb Perspect Med.*, 9 (1), a033746

Thanindratan, P, Dean, DC, Nelson, SD, Hornicek, FJ, and Duan, Z, 2020, Chimeric antigen receptor T (CAR-T) cell immunotherapy for sarcomas: from mechanisms to potential clinical applications, *Cancer Treat Rev.*, 82, Pg. 101934

Thomas, DM, Savage, SA, and Bond, GL, 2012, Hereditary and environmental epidemiology of sarcomas, *Clin Sarcoma Res.*, 2, Pg. 13

Thomson, RJ, Moshirfar, M, and Ronquillo, Y, 2021, Tyrosine kinase inhibitors, *StatPearls [Internet].*, StatPearls Publishing, Treasure Island (FL) (USA), <https://www.ncbi.nlm.nih.gov/books/NBK563322/>, Last accessed [October 2021]

Thorpe, LM, Yuzugullu, H, and Zhao, JJ, 2015, PI3K in cancer: divergent roles of isoforms, modes of activation and therapeutic targeting, *Nat Rev Cancer.*, 15 (1), Pg. 7-24

Thway, K, Noujaim, J, Jones, RL, and Fisher, C, 2016, Dermatofibrosarcoma protuberans: pathology, genetics, and potential therapeutic strategies, *Ann Diagn Pathol.*, 25, Pg. 64-71

Tian, Z, Liu, H, Zhang, F, Li, L, Du, X, Li, C, Yang, J, and Wang, J, 2020, Retrospective review of the activity and safety of apatinib and anlotinib in patients with advanced osteosarcoma and soft tissue sarcoma, *Invest New Drugs.*, 38 (5), Pg. 1559-1569

Tobin, RP, Jordan, KR, Kapoor, P, Spongberg, E, Davis, D, Vorwald, VM, Coutts, KL, Gao, D, Smith, DE, Borgers, JSW, Robinson, S, Amato, C, Gonzalez, R, Lewis, KD, Robinson, WA, Borges, VF, and McCarter, MD, 2019, IL-6 and IL-8 are linked with myeloid-derived suppressor cell accumulation and correlate with poor clinical outcomes in melanoma patients, *Front Oncol.*, 9, Pg. 1223

Toulmonde, M, Pulido, M, Ray-Coquard, I, Andre, T, Isambert, N, Chevreau, C, Penel, N, Bompas, E, Saada, E, Bertucci, F, Lebbe, C, Le Cesne, A, Soulie, P, Piperno-Neumann, S, Sweet, S, Cecchi, F, Hembrough, T, Bellera, C, Kind, M, Crombe, A, Lucchesi, C, Le Loarer, F, Blay, JY, and Italiano, A, 2019, Pazopanib or methotrexate-vinblastine combination chemotherapy in adult patients with progressive desmoid tumours (DESMOPAZ): a non-comparative, randomised, open-label, multicentre, phase 2 study, *Lancet Oncol.*, 20 (9), Pg. 1263-1272

Toulmonde, M, Lucchesi, C, Verbeke, S, Crombe, A, Adam, J, Geneste, D, Chaire, V, Laroche-Clary, A, Perret, R, Bertucci, F, Bertolo, F, Bianchini, L, Dadone-Montaudie, B, Hembrough, T, Sweet, S, Kim, YJ, Cecchi, F, Le Loarer, F, and Italiano, A, 2020, High throughput profiling of undifferentiated pleomorphic sarcomas identifies two main subgroups with distinct immune profile, clinical outcome and sensitivity to targeted therapies, *EBioMedicine.*, 62, Pg. 103131

Trevino, JG, Summy, JM, Gray, MJ, Nilsson, MB, Lesslie, DP, Baker, CH, and Gallick, GE, 2005, Expression and activity of SRC regulate interleukin-8 expression in pancreatic adenocarcinoma cells: implications for angiogenesis, *Cancer Res.*, 65 (16), Pg. 7214-7222

Trusolino, L, and Bertotti, A, 2012, Compensatory pathways in oncogenic kinase signaling and resistance to targeted therapies: six degrees of separation, *Cancer Discov.*, 2 (10), Pg. 876-880

Tsimberidou, AM, Van Morris, K, Vo, HH, Eck, S, Lin, YF, Rivas, JM, and Andersson, BS, 2021, T-cell receptor-based therapy: an innovative therapeutic approach for solid tumors, *J Hematol Oncol.*, 14 (1), Pg. 102

Tuveson, DA, Willis, NA, Jacks, T, Griffin, JD, Singer, S, Fletcher, CD, Fletcher, JA, and Demetri, GD, 2001, STI571 inactivation of the gastrointestinal stromal tumor c-KIT oncoprotein: biological and clinical implications, *Oncogene.*, 20 (36), Pg. 5054-5058

Tyanova, S, Temu, T, Sinitcyn, P, Carlson, A, Hein, MY, Geiger, T, Mann, M, and Cox, J, 2016, The Perseus computational platform for comprehensive analysis of (prote)omics data, *Nat Methods.*, 13 (9), Pg. 731-740

Ulivi, P, 2020, Predictive biomarkers in clinical practice: state of the art and perspectives in solid tumours, *Int J Biol Markers.*, 35 (1_suppl), Pg. 16-19

Ullah, I, Subbarao, RB, and Rho, GJ, 2015, Human mesenchymal stem cells – current trends and future prospective, *Biosci Rep.*, 35 (2), e00191

Urakawa, H, Kawai, A, Goto, T, Hiraga, H, Ozaki, T, Tsuchiya, H, Nakayama, R, Naka, N, Matsumoto, Y, Kobayashi, E, Okuma, T, Kunisada, T, Ando, M, Ueda, T, and Nishida, Y, 2020, Phase II trial of pazopanib in patients with metastatic or unresectable chemoresistant sarcomas: A Japanese Musculoskeletal Oncology Group Study, *Cancer Sci.*, 111 (9), Pg. 3303-3312

Uusitalo, E, Rantanen, M, Kallionpää, RA, Pöyhönen, M, Leppävirta, J, Ylä-Outinen, H, Riccardi, VM, Pukkala, E, Pitkaniemi, J, Peltonen, S, and Peltonen, J, 2016, Distinctive cancer associations in patients with neurofibromatosis type 1, *J Clin Oncol.*, 34 (17), Pg. 1978-1986

Vaddepally, RK, Kharel, P, Pandey, R, Garje, R, and Chandra, AB, 2020, Review of indications of FDA-approved immune checkpoint inhibitors per NCCN guidelines with the level of evidence, *Cancers (Basel)*, 12 (3), Pg. 738

Valentin, T, Fournier, C, Penel, N, Bompas, E, Chaigneau, L, Isambert, N, and Chevreau, C, 2013, Sorafenib in patients with progressive malignant solitary fibrous tumors: a subgroup analysis from a phase II study of the French Sarcoma Group (GSF/GETO), *Invest New Drugs*, 31 (6), Pg. 1626-1627

Vallette, FM, Olivier, C, Lézot, F, Oliver, L, Cochonneau, D, Lalier, L, Cartron, PF, and Heymann, D, 2019, Dormant, quiescent, tolerant and persister cells: four synonyms for the same target in cancer, *Biochem Pharmacol*, 162, Pg. 169-176

Valverde, CM, Martín-Broto, J, Lopez-Martin, JA, Romagosa, C, Marquez, MPS, Carrasco, JA, Poveda, A, Bauer, S, Martinez-Trufero, J, Cruz, J, Reichardt, P, Fra, PL, Gruenwald, V, Persiva, O, Porres, DV, and Kasper, B, 2016, Phase II clinical trial evaluating the activity and tolerability of pazopanib in patients (pts) with advanced and/or metastatic liposarcoma (LPS): a joint Spanish Sarcoma Group (GEIS) and German Interdisciplinary Sarcoma Group (GISG) Study – NCT01692496, *J Clin Oncol*, 34 (15), https://ascopubs.org/doi/10.1200/JCO.2016.34.15_suppl.11039, Last accessed [September 2021]

Van der Geer, P, Wiley, S, Gish, GD, and Pawson, T, 1996, The Shc adaptor protein is highly phosphorylated at conserved, twin tyrosine residues (Y239/240) that mediate protein-protein interactions, *Curr Biol*, 6 (11), Pg. 1435-1444

Van der Graaf, WTA, Blay, JY, Chawla, SP, Kim, DW, Bui-Nguyen, B, Casali, PG, Schöffski, P, Aglietta, M, Staddon, AP, Beppu, Y, Le Cesne, A, Gelderblom, H, Judson, IR, Araki, N, Ouali, M, Marreaud, S, Hodge, R, Dewji, MR, Coens, C, Demetri, GD, Fletcher, CD, Dei Tos, AP, Hohenberger, P, and EORTC Soft Tissue and Bone Sarcoma Group: PALETTE study group, 2012, Pazopanib for metastatic soft-tissue sarcoma (PALETTE): a randomised, double-blind, placebo-controlled phase 3 trial, *Lancet*, 379 (9829), Pg. 1879-1886

Vander Velde, R, Yoon, N, Marusyk, V, Durmaz, A, Dhawan, A, Miroshnychenko, D, Lozano-Peral, D, Desai, B, Balynska, O, Poleszhuk, J, Kenian, L, Teng, M, Abazeed, M, Mian, O, Tan, AC, Haura, E, Scott, J, and Marusyk, A, 2020, Resistance to targeted therapies as a multifactorial, gradual adaptation to inhibitor specific selective pressures, *Nat Commun*, 11, Pg. 2393

Van Glabbeke, M, Verweij, J, Judson, I, Nielsen, OS, and EORTC Soft Tissue and Bone Sarcoma Group, 2002, Progression-free rate as the principal end-point for phase II trials in soft-tissue sarcomas, *Eur J Cancer*, 38 (4), Pg. 543-549

Van Tine, BA, Chawla, SP, Trent, JC, Wilky, BA, Chugh, R, Chmielowski, B, Kummar, S, Mallick, AB, Somaiah, N, Cranmer, LD, Agulnik, M, Keedy, VL, Stacchiotti, S, Vincenzi, B, Badalamenti, G, Siontis, BL, and Attia, S, 2021, A phase III study (APROMISS) of AL3818 (Catequentinib, Anlotinib) hydrochloride monotherapy in subjects with metastatic or advanced synovial sarcoma, *J Clin Oncol*, 39 (15), https://ascopubs.org/doi/abs/10.1200/JCO.2021.39.15_suppl.11505, Last accessed [October 2021]

Vinogradova, M, Gehling, VS, Gustafson, A, Arora, S, Tindell, CA, Wilson, C, Williamson, KE, Guler, GD, Gangurde, P, Manieri, W, Busby, J, Flynn, EM, Lan, F, Kim, HJ, Odate, S, Cochran, AG, Liu, Y, Wongchenko, M, Yang, Y, Cheung, TK, Maile, TM, Lau, T, Costa, M, Hegde, GV, Jackson, E, Pitti, R, Armott, D, Bailey, C, Bellon, S, Cummings, RT, Albrecht, BK, Harmange, JC, Kiefer, JR, Trojer, P, and Classon, M, 2016, An inhibitor of KDM5 demethylases reduces survival of drug-tolerant cancer cells, *Nat Chem Biol*, 12 (7), Pg. 531-538

Vitale, I, Shema, E, Loi, S, and Galluzzi, L, 2021, Intratumoral heterogeneity in cancer progression and response to immunotherapy, *Nat Med*, 27 (2), Pg. 212-224

Von Manstein, V, Yang, CM, Richter, D, Delis, N, Vafaizadeh, V, and Groner, B, 2013, Resistance of cancer cells to targeted therapies through the activation of compensatory signaling loops, *Curr Signal Transduct Ther*, 8 (3), Pg. 193-202

Vyse, S, McCarthy, F, Broncel, M, Paul, A, Wong, JP, Bhamra, A, and Huang, PH, 2018, Quantitative phosphoproteomic analysis of acquired cancer drug resistance to pazopanib and dasatinib, *J Proteomics*, 170, Pg. 130-140

Vyse, S, and Huang, PH, 2019, Targeting EGFR exon 20 insertion mutations in non-small cell lung cancer, *Signal Transduct Target Ther*, 4, Pg. 5

Vyse, S, Thway, K, Huang, PH, and Jones, RL, 2021, Next-generation sequencing for the management of sarcomas with no known driver mutations, *Curr Opin Oncol*, https://journals.lww.com/oncology/Abstract/9000/Next_generation_sequencing_for_the_management_of.99017.aspx, Last accessed [May 2021]

Wada, N, Kurokawa, Y, Takahashi, T, Hamakawa, T, Hirota, S, Naka, T, Miyazaki, Y, Makino, T, Yamasaki, M, Nakajima, K, Takiguchi, S, Mori, M, and Doki, Y, 2016, Detecting secondary C-KIT mutations in the peripheral blood of patients with imatinib-resistant gastrointestinal stromal tumor, *Oncology*, 90 (2), Pg. 112-117

Wagner, MJ, Stacey, MM, Liu, BA, and Pawson, T, 2013, Molecular mechanisms of SH2- and PTB-domain-containing proteins in receptor tyrosine kinase signaling, *Cold Spring Harb Perspect Biol*, 5 (12), a008987

Walsh, JH, Karnes, WE, Cuttitta, F, and Walker, A, 1991, Autocrine growth factors and solid tumor malignancy, *West J Med*, 155 (2), Pg. 152-163

Wander, SA, Cohen, O, Gong, X, Johnson, GN, Buendia-Buendia, JE, Lloyd, MR, Kim, D, Luo, F, Mao, P, Helvie, K, Kowalski, KJ, Nayar, U, Waks, AG, Parsons, SH, Martinez, R, Litchfield, LM, Ye, XS, Yu, C, Jansen, VM, Stille, JR, Smith, PS,

- Oakley, GJ, Chu, QS, Batist, G, Hughes, ME, Kremer, JD, Garraway, LA, Winer, EP, Tolaney, SM, Lin, NU, Buchanan, SG, and Wagle, N, 2020, The genomic landscape of intrinsic and acquired resistance to cyclin-dependent kinase 4/6 inhibitors in patients with hormone receptor-positive metastatic breast cancer, *Cancer Discov.*, 10 (8), Pg. 1174-1193
- Wang, N, Zheng, J, Chen, Z, Liu, Y, Dura, B, Kwak, M, Xavier-Ferruccio, J, Lu, YC, Zhang, M, Roden, C, Cheng, J, Krause, DS, Ding, Y, Fan, R, and Lu, J, 2019, Single-cell microRNA-mRNA co-sequencing reveals non-genetic heterogeneity and mechanisms of microRNA regulation, *Nat Commun.*, 10 (1), Pg. 95
- Wang, W, Xu, S, Yin, M, and Jin, ZG, 2015, Essential roles of Gab1 tyrosine phosphorylation in growth factor-mediated signaling and angiogenesis, *Int J Cardiol.*, 181, Pg. 180-184
- Wang, X, Wang, S, Troisi, EC, Howard, TP, Haswell, JR, Wolf, BK, Hawk, WH, Ramos, P, Oberlick, EM, Tzvetkov, EP, Ross, A, Vazquez, F, Hahn, WC, Park, PJ, and Roberts, CWM, 2019, BRD9 defines a SWI/SNF sub-complex and constitutes a specific vulnerability in malignant rhabdoid tumors, *Nat Commun.*, 10 (1), Pg. 1881
- Wang, ZM, Zhang, SL, Yang, H, Zhuang, RY, Guo, X, Tong, HX, Zhang, Y, Lu, WQ, and Zhou, YH, 2020, Efficacy and safety of anlotinib, a multikinase angiogenesis inhibitor, in combination with epirubicin in preclinical models of soft tissue sarcoma, *Cancer Med.*, 9 (10), Pg. 3344-3352
- Ward, CW, Lawrence, MC, Streltsov, VA, Adams, TE, and McKern, NM, 2007, The insulin and EGF receptor structures: new insights into ligand-induced receptor activation, *Trends Biochem Sci.*, 32 (3), Pg. 129-137
- Ward, J, and Odili, J, 2018, Dermatofibrosarcoma protuberans (DFSP) arising from a keloid scar – a case report, *JPRAS Open.*, 18, Pg. 65-69
- Watanabe, S, Shimomura, A, Kubo, T, Sekimizu, M, Seo, T, Watanabe, SI, Kawai, A, Yamamoto, N, Tamura, K, Kohno, T, Ichikawa, H, and Yoshida, A, 2020, BRAF V600E mutation is a potential therapeutic target for a small subset of synovial sarcoma, *Mod Pathol.*, 33 (9), Pg. 1660-1668
- Waugh, DJ, and Wilson, C, 2008, The interleukin-8 pathway in cancer, *Clin Cancer Res.*, 14 (21), Pg. 6735-6741
- Wedge, SR, Kendrew, J, Hennequin, LF, Valentine, PJ, Barry, ST, Brave, SR, Smith, NR, James, NH, Dukes, M, Curwen, JO, Chester, R, Jackson, JA, Boffey, SJ, Kilburn, LL, Barnett, S, Richmond, GHP, Wadsworth, PF, Walker, M, Bigley, AL, Taylor, ST, Cooper, L, Beck, S, Jürgensmeier, JM, and Ogilvie, DJ, 2005, AZD2171: a highly potent, orally bioavailable, vascular endothelial growth factor receptor-2 tyrosine kinase inhibitor for the treatment of cancer, *Cancer Res.*, 65 (10), Pg. 4389-4400
- Wei, J, Liu, X, Li, T, Xing, P, Zhang, C, and Yang, J, 2020, The new horizon of liquid biopsy in sarcoma: the potential utility of circulating tumor nucleic acids, *J Cancer.*, 11 (18), Pg. 5293-5308
- Wei, L, Lee, D, Law, CT, Zhang, MS, Shen, J, Chin, DWC, Zhang, A, Tsang, FHC, Wong, CLS, Ng, IOL, Wong, CCL, and Wong, CM, 2019, Genome-wide CRISPR/Cas9 library screening identified PHGDH as a critical driver for sorafenib resistance in HCC, 10 (1), Pg. 4681
- Weisberg, E, Choi, HG, Ray, A, Barrett, R, Zhang, J, Sim, T, Zhou, W, Seeliger, M, Cameron, M, Azam, M, Fletcher, JA, Debiec-Rychter, M, Mayeda, M, Moreno, D, Kung, AL, Janne, PA, Khosravi-Far, R, Melo, JV, Manley, PW, Adamia, S, Wu, C, Gray, N, and Griffin, JD, 2010, Discovery of a small-molecule type II inhibitor of wild-type and gatekeeper mutants of BCR-ABL, PDGFRalpha, Kit, and Src kinases: novel type II inhibitor of gatekeeper mutants, 115 (21), Pg. 4206-4216
- Weiss, AR, Chen, YL, Scharschmidt, TJ, Chi, YY, Tian, J, Black, JO, Davis, JL, Fanburg-Smith, JC, Zambrano, E, Anderson, J, Arens, R, Binitie, O, Choy, E, Davis, JW, Hayes-Jordan, A, Kao, SC, Kayton, ML, Kessel, S, Lim, R, Meyer, WH, Million, L, Okuno, SH, Ostrenga, A, Parisi, MT, Pryma, DA, Randall, RL, Rosen, MA, Schlapkohl, M, Shulkin, BL, Smith, EA, Sorger, JI, Terezakis, S, Hawkins, DS, Spunt, SL, and Wang, D, 2020, Pathological response in children and adults with large unresected intermediate-grade or high-grade soft tissue sarcoma receiving preoperative chemoradiotherapy with or without pazopanib (ARST1321): a multicentre, randomised, open-label, phase 2 trial, *Lancet Oncol.*, 21 (8), Pg. 1110-1122
- Wells, CI, Al-Ali, H, Andrews, DM, Asquith, CRM, Axtman, AD, Dikic, I, Ebner, D, Etmayer, P, Fischer, C, Frederiksen, M, Futrell, RE, Gray, NS, Hatch, SB, Knapp, S, Lücking, U, Michaelides, M, Mills, CE, Müller, S, Owen, D, Picado, A, Saikatendu, KS, Schröder, M, Stolz, A, Tellechea, M, Turunen, BJ, Vilar, S, Wang, J, Zuercher, WJ, Willson, TM, and Drewry, DH, 2021, The kinase chemogenomic set (KCGS): An open science resource for kinase vulnerability identification, *Int J Mol Sci.*, 22 (2), Pg. 566
- West, RB, Rubin, BP, Miller, MA, Subramanian, S, Kaygusuz, G, Montgomery, K, Zhu, S, Marinelli, RJ, De Luca, A, Downs-Kelly, E, Goldblum, JR, Corless, CL, Brown, PO, Gilks, CB, Nielsen, TO, Huntsman, D, and Van de Rijn, M, 2006, A landscape effect in tenosynovial giant-cell tumor from activation of CSF1 expression by a translocation in a minority of cells, *Proc Natl Acad Sci USA.*, 103 (3), Pg. 690-695
- Wheeler, DL, Iida, M, and Dunn, EF, 2009, The role of Src in solid tumors, *Oncologist.*, 14 (7), Pg. 667-678
- White, MC, Holman, DM, Boehm, JE, Peipins, LA, Grossman, M, and Henley, SJ, 2015, Age and cancer risk: A potentially modifiable relationship, *Am J Prev Med.*, 46 (3 Suppl 1), Pg S7-15

WHO, 2020, WHO Classification of Tumours Editorial Board, Soft Tissue and Bone Tumours, International Agency for Research on Cancer, WHO classification of tumours series, 5th ed, Vol. 3, Lyon (France), <https://publications.iarc.fr/588>, Last accessed [January 2021]

Widemann, BC, 2009, Current status of sporadic and neurofibromatosis type 1-associated malignant peripheral nerve sheath tumors, *Curr Oncol Rep.*, 11 (4), Pg. 322-328

Wilding, CP, Elms, ML, Judson, I, Tan, AC, Jones, RL, and Huang, PH, 2019, The landscape of tyrosine kinase inhibitors in sarcomas: looking beyond pazopanib, *Expert Rev Anticancer Ther.*, 19 (11), Pg. 971-991

Wilding, CP, Loong, HH, Huang, PH, and Jones, RL, 2020, Tropomyosin receptor kinase inhibitors in the management of sarcomas, *Curr Opin Oncol.*, 32 (4), Pg. 307-313

Wilhelm, SM, Carter, C, Tang, L, Wilkie, D, McNabola, A, Rong, H, Chen, C, Zhang, X, Vincent, P, McHugh, M, Cao, Y, Shujath, J, Gawlak, S, Eveleigh, D, Rowley, B, Liu, L, Adnane, L, Lynch, M, Auclair, D, Taylor, I, Gedrich, R, Voznesensky, A, Riedl, B, Post, LE, Bollag, G, and Trail, PA, 2004, BAY 43-9006 exhibits broad spectrum oral antitumor activity and targets the RAF/MEK/ERK pathway and receptor tyrosine kinases involved in tumor progression and angiogenesis, *Cancer Res.*, 64 (19), Pg. 7099-7109

Wilhelm, SM, Dumas, JD, Adnane, L, Lynch, M, Carter, CA, Schütz, G, Thierauch, KH, and Zopf, D, 2011, Regorafenib (BAY 73-4506): a new oral multikinase inhibitor of angiogenic, stromal and oncogenic receptor tyrosine kinases with potent preclinical antitumor activity, *Int J Cancer.*, 129 (1), Pg. 245-255

Wilky, BA, Trucco, MM, Subhawong, TK, Florou, V, Park, W, Kwon, D, Wieder, ED, Kolonias, D, Rosenberg, AE, Kerr, DA, Sfakianaki, E, Foley, M, Merchan, JR, Komanduri, KV, and Trent, JC, 2019, Axitinib plus pembrolizumab in patients with advanced sarcomas including alveolar soft part sarcoma: a single-centre, single-arm, phase 2 trial, *Lancet Oncol.*, 20 (6), Pg. 837-848

Williams, NG, Roberts, TM, and Li, P, 1992, Both p21ras and pp60v-src are required, but neither alone is sufficient, to activate the Raf-1 kinase, *Proc Natl Acad Sci USA*, 89 (7), Pg. 2922-2926

Winkler, J, Abisoye-Ogunniyan, A, Metcalf, KJ, and Werb, Z, 2020, Concepts of extracellular matrix remodelling in tumour progression and metastasis, *Nat Commun.* 11 (1), Pg. 5120

Wöhrl, S, Weiss, A, Ito, M, Kauffmann, A, Murakami, M, Jagani, Z, Thuery, A, Bauer-Probst, B, Reimann, F, Stamm, C, Pomon, A, Romanet, V, Guagnano, V, Brümmendorf, T, Sellers, WR, Hofmann, F, Roberts, CWM, and Porta, DG, 2013, Fibroblast growth factor receptors as novel therapeutic targets in SNF5-deleted malignant rhabdoid tumors, *PLoS One.*, 8 (10), e77652

Wong, JP, Todd, JR, Finetti, MA, McCarthy, F, Broncel, M, Vyse, S, Luczynski, MT, Crosier, S, Ryall, KA, Holmes, K, Payne, LS, Daley, F, Wai, P, Jenks, A, Tanos, B, Tan, AC, Natrajan, RC, Williamson, D, and Huang, PH, 2016, Dual targeting of PDGFR α and FGFR1 displays synergistic efficacy in malignant rhabdoid tumors, *Cell Rep.*, 17 (5), Pg. 1265-1275

Wood, AW, Becker, MA, Minna, JD, and Seegmiller, JE, 1973, Purine metabolism in normal thioguanine-resistant neuroblastoma, *Proc Natl Acad Sci USA.*, 70 (12), Pg 3880-3883

Wortzel, I, and Seger, R, 2011, The ERK cascade: Distinct functions within various subcellular organelles, *Genes Cancer.*, 2 (3), Pg. 195-209

Wu, MH, Huang, SB, and Lee, GB, 2010, Microfluidic cell culture systems for drug research, *Lab Chip.*, 10 (8), Pg. 939-956

Wu, M, and Swartz, MA, 2014, Modeling tumor microenvironments in vitro, *J Biomech Eng.*, 136 (2), Pg. 0210111-0210117

Wu, P, Nielsen, TE, and Clausen, MH, 2015, FDA-approved small-molecule kinase inhibitors, *Trends Pharmacol Sci.*, 36 (7), Pg. 422-439

Xiao, Z, Dai, Z, and Locasale, JW, 2019, Metabolic landscape of the tumor microenvironment at single cell resolution, *Nat Commun.*, 10 (1), Pg. 3763

Xie, C, Wan, X, Quan, H, Zheng, M, Fu, L, Li, Y, and Lou, L, 2018, Preclinical characterization of anlotinib, a highly potent and selective vascular endothelial growth factor receptor-2 inhibitor, *Cancer Sci.*, 109 (4), Pg. 1207-1219

Xu, B, Mei, J, Ji, W, Huo, Z, Bian, Z, Jiao, J, Li, X, Sun, J, and Shao, J, 2021, MicroRNAs involved in the EGFR pathway in glioblastoma, *Biomed Pharmacother.*, 134, Pg. 111115

Xue, Y, Luis, BS, and Lane, DP, 2019, Intratumour heterogeneity of p53 expression; causes and consequences, *J Pathol.*, 249 (3), Pg. 274-285

Yamazaki, T, Yokoyama, T, Akatsu, H, Tukiya, T, and Tokiwa, T, 2003, Phenotypic characterization of a human synovial sarcoma cell line, SW982, and its response to dexamethasone, *In Vitro Cell Dev Biol Anim.*, 39 (8-9), Pg. 337-339

- Yang, J, Nie, J, Ma, X, Wei, Y, Peng, Y, and Wei, X, 2019, Targeting PI3K in cancer: mechanisms and advances in clinical trials, *Mol Cancer.*, 18 (1), Pg. 26
- Yang, S, Zhang, W, Chen, Q, and Guo, Q, 2020, Clinical investigation of the efficacy and safety of anlotinib with immunotherapy in advanced non-small cell lung cancer as third-line therapy: a retrospective study, *Cancer Manag Res.*, 12, Pg. 10333-10340
- Yap, YS, McPherson, JR, Ong, CK, Rozen, SG, Teh, BT, Lee, ASG, and Callen, DF, 2014, The NF1 gene revisited – from bench to bedside, *Oncotarget.*, 5 (15), Pg. 5873-5892
- Ye, F, Kim, C, and Ginsberg, MH, 2012, Reconstruction of integrin activation, *Blood.*, 119 (1), Pg. 26-33
- Yeatman, TJ, 2004, A renaissance for Src, *Nat Rev Cancer.*, 4 (6), Pg. 470-480
- Yeung, CL, Ngo, VN, Grohar, PJ, Arnaldez, FI, Asante, A, Wan, X, Khan, J, Hewitt, SM, Khanna, C, Staudt, LM, and Helman, LJ, 2013, Loss-of-function screen in rhabdomyosarcoma identifies CRKL-YES as a critical signal for tumor growth, *Oncogene.*, 32 (47), Pg. 5429-5438
- Yin, JJ, Zhang, L, Munasinghe, J, Linnoila, RI, and Kelly, K, 2010, Cediranib/AZD2171 inhibits bone and brain metastasis in a preclinical model of advanced prostate cancer, *Cancer Res.*, 70 (21), Pg. 8662-8673
- Yin, Y, and Shen, WH, 2008, PTEN: a new guardian of the genome, *Oncogene.*, 27 (41), Pg. 5443-5453
- Yokoyama, N, Matsunobu, T, Matsumoto, Y, Fukushi, JI, Endo, M, Hatano, M, Nabeshima, A, Fukushima, S, Okada, S, and Iwamoto, Y, 2017, Activation of ERK1/2 causes pazopanib resistance via downregulation of DUSP6 in synovial sarcoma cells, *Sci Rep.*, 7, Pg.45332
- Yoo, KH, Kim, HS, Lee, SJ, Park, SH, Kim, SJ, Kim, SH, Choi, YL, Shin, KH, Cho, YJ, Lee, J, and Rha, SY, 2015, Efficacy of pazopanib monotherapy in patients who had been heavily pretreated for metastatic soft tissue sarcoma: a retrospective case series, *BMC Cancer.*, 15, Pg. 154
- Yu, X, Jin, J, Zheng, Y, Zhu, H, Xu, H, Ma, J, Lan, Q, Zhuang, Z, Chen, CC, and Li, M, 2021, GBP5 drives malignancy of glioblastoma via the Src/ERK1/2/MMP3 pathway, *Cell Death Dis.*, 12 (2), Pg. 203
- Yu, Z, Pestell, TG, Lisanti, MP, and Pestell, RG, 2012, Cancer stem cells, *Int J Biochem Cell Biol.*, 44 (12), Pg. 2144-2151
- Yuen, KC, Liu, LF, Gupta, V, Madireddi, S, Keerthiyan, S, Li, C, Rishipathak, D, Williams, P, Kadel 3rd, EE, Koeppen, H, Chen, YJ, Modrusan, Z, Grogan, JL, Bancheureau, R, Leng, N, Thastrom, AC, Shen, X, Hashimoto, K, Tayama, D, Van der Heijden, MS, Rosenborg, JE, McDermott, DF, Powles, T, Hegde, PS, Huseni, MA, and Mariathasan, S, 2020, High systemic and tumor-associated IL-8 correlates with reduced clinical benefit of PD-L1 blockade, *Nat Med.*, 26 (5), Pg. 693-698
- Zahm, SH, and Fraumeni Jr, JF, 1997, The epidemiology of soft tissue sarcoma, *Semin Oncol.*, 24 (5), Pg. 504-514
- Zambon, P, Ricci, P, Bovo, E, Casula, A, Gattolin, M, Fiore, AR, Chiosi, F, and Guzzinati, S, 2007, Sarcoma risk and dioxin emissions from incinerators and industrial plants: a population based case-control study (Italy), *Environ Health.*, 6, Pg. 19
- Zhai, C, Zhang, X, Ren, L, You, L, Pan, Q, Pan, H, and Han, W, 2021, The efficacy and safety of anlotinib combined with PD-1 antibody for third-line or further-line treatment of patients with advanced non-small-cell lung cancer, *Front Oncol.*, 10, Pg. 619010
- Zhang, C, Liu, J, Wang, J, Hu, W, and Feng, Z, 2021, The emerging role of leukemia inhibitory factor in cancer and therapy, *Pharmacol Ther.*, 221, Pg. 107754
- Zhang, H, Davies, KJA, and Forman, HJ, 2015, TGFβ1 rapidly activates Src through a non-canonical redox signaling mechanism, *Arch Biochem Biophys.*, 568, Pg. 1-7
- Zhang, L, Smith, KM, Chong, AL, Stempak, D, Yeger, H, Marrano, P, Thorer, PS, Irwin, MS, Kaplan, DR, and Baruchel, S, 2009, In vivo antitumor and antimetastatic activity of sunitinib in preclinical neuroblastoma mouse model, *Neoplasia.*, 11 (5), Pg. 426-435
- Zhang, S, and Yu, D, 2012, Targeting Src family kinases in anti-cancer therapies: turning promise into triumph, *Trends Pharmacol Sci.*, 33 (3), Pg. 122-128
- Zhang, W, and Liu, HT, 2002, MAPK signal pathways in the regulation of cell proliferation in mammalian cells, *Cell Res.*, 12 (1), Pg. 9-18
- Zhang, XHF, Wang, Q, Gerald, W, Hudis, CA, Norton, L, Smid, M, Foekens, JA, and Massagué, J, 2009, Latent bone metastasis in breast cancer tied to Src-dependent survival signals, *Cancer Cell.*, 16 (1), Pg. 67-78
- Zhao, B, Sedlak, JC, Srinivas, R, Creixell, P, Pritchard, JR, Tidor, B, Lauffenburger, DA, and Hemann, MT, 2016, Exploiting temporal collateral sensitivity in tumor clonal evolution, *Cell.*, 165 (1), Pg. 234-246
- Zhao, L, and Cao, YJ, 2019, Engineered T cell therapy for cancer in the clinic, *Front Immunol.*, 10, Pg. 2250

Zhong, Z, and Virshup, DM, 2020, Wnt signaling and drug resistance in cancer, *Mol Pharmacol.*, 97 (2), Pg. 72-89

Zhou, Y, Wu, C, Lu, G, Hu, Z, Chen, Q, and Du, X, 2020, FGF/FGFR signaling pathway involved resistance in various cancer types, *J Cancer.*, 11 (8), Pg. 2000-2007

Zopf, D, Fichtner, I, Bhargava, A, Steinke, W, Thierauch, KH, Diefenbach, K, Wilhelm, S, Hafner, FT, and Gerisch, M, 2016, Pharmacologic activity and pharmacokinetics of metabolites of regorafenib in preclinical models, *Cancer Med.*, 5 (11), Pg. 3176-3185

Zou, HY, Li, Q, Lee, JH, Arango, ME, McDonnell, SR, Yamazaki, S, Koudriakova, TB, Alton, G, Cui, JJ, Kung, PP, Nambu, MD, Los, G, Bender, SL, Mroczkowski, B, and Christensen, JG, 2007, An orally available small-molecule inhibitor of c-Met, PF-2341066, exhibits cytoreductive antitumor efficacy through antiproliferative and antiangiogenic mechanisms, *Cancer Res.*, 67 (9), Pg. 4408-4417